# PROCEEDINGS

# DEPARTMENT OF VETERINARY PATHOLOGY
# WEDNESDAY SLIDE CONFERENCE
# 2008-2009


**ARMED FORCES INSTITUTE OF PATHOLOGY**
**WASHINGTON, D.C. 20306-6000**
**2009**

**ML2009**

**Armed Forces Institute of Pathology**
**Department of Veterinary Pathology**

# WEDNESDAY SLIDE CONFERENCE
# 2008-2009

**100 Cases**
**100 Histopathology Slides**
**249 Images**

**PROCEEDINGS PREPARED BY:**
**Todd Bell, DVM**

**Chief Editor:**
**Todd O. Johnson, DVM, Diplomate ACVP**

**Copy Editor:**
**Sean Hahn**

**Layout and Copy Editor:**
**Fran Card**

**WSC Online Management and Design**
**Scott Shaffer**

**ARMED FORCES INSTITUTE OF PATHOLOGY**
**Washington, D.C. 20306-6000**
**2009**

**ML2009**

# PREFACE

The Armed Forces Institute of Pathology, Department of Veterinary Pathology has conducted a weekly slide conference during the resident training year since 12 November 1953. This ever-changing educational endeavor has evolved into the annual Wednesday Slide Conference program in which cases are presented on 25 Wednesdays throughout the academic year and distributed to 135 contributing military and civilian institutions from around the world. Many of these institutions provide structured veterinary pathology resident training programs. During the course of the training year, histopathology slides, digital images, and histories from selected cases are distributed to the participating institutions and to the Department of Veterinary Pathology at the AFIP. Following the conferences, the case diagnoses, comments, and reference listings are posted online to all participants.

This study set has been assembled in an effort to make Wednesday Slide Conference materials available to a wider circle of interested pathologists and scientists, and to further the education of veterinary pathologists and residents-in-training. The number of histopathology slides that can be reproduced from smaller lesions requires us to limit the number of participating institutions.

This set, composed of 100 cases, 100 histopathology slides and 249 digital images, was assembled from the cases studied during the 2008-2009 conference series.

For their participation and permission to use their cases in this study set, we wish to thank each institution, and especially the individuals who prepared and submitted the selected cases. We also wish to give special thanks to the American Veterinary Medical Association and the American College of Veterinary Pathologists, who are co-sponsors of the Registry of Veterinary Pathology. The C.L. Davis Foundation also provides substantial support for the Registry.

A special note of appreciation is extended to the reviewers who helped edit and review this year's individual case summaries: Todd Johnson, Bridget Lewis, Taylor Chance, Dr. Michelle Fleetwood, Sean Hahn, and Fran Card. A final note of thanks goes to the moderators, who unselfishly gave of their time and expertise to help make each conference both enjoyable and educational.

Gross images and photomicrographs were submitted by contributing institutions where indicated. Additional photomicrographs were taken by Cary Honnold and Jeremy Bearss.

**Armed Forces Institute of Pathology, Department of Veterinary Pathology**

**WEDNESDAY SLIDE CONFERENCE 2008-2009**
**Table of Contents**

| | | | | | | |
|---|---|---|---|---|---|---|
| 3 | 3104060 | CRL 2008-2 | Rabbit | *Eimeria stiedae* | Liver | 45 |
| 4 | 3105527 | N0710576 | Rat | Pituitary gland adenoma | Pituitary gland | 47 |

| Case | AFIP No. | Slide No. | Species | Condition/Etiology | Tissue | Page |
|---|---|---|---|---|---|---|
| **Conference 5** | | **8 Oct 2008** | | **Moderator: Marc Mattix** | | |
| 1 | 3105584 | HN 2516 | Swan | Highly pathogenic avian influenza virus | Cerebrum | 53 |
| 2 | 3101429 | 07-13414 | Cat | *Francisella tularensis* | Spleen | 55 |
| 3 | 3103602 | R08-148 | Goat | Capripox virus | Lung | 57 |
| 4 | 3102366 | ND 1 | Bison | *Mycoplasma bovis* | Lung | 60 |
| **Conference 6** | | **22 Oct 2008** | | **Moderator: Dr. Lauren Brinster** | | |
| 1 | 3106794 | DG0802868 | Dog | Acute respiratory distress syndrome | Lung | 63 |
| 2 | 3106804 | MK 0803123 | Macaque | Ductular carcinoma in situ (DCIS) | Mammary gland | 65 |
| 3 | 3094514 | 36005-7 | Mouse | Rhabdomyosarcoma, embryonal | Skeletal muscle | 68 |
| 4 | 3105526 | 0566-1C | Mouse | Botryomycosis; | Digits, foreleg | 71 |
| **Conference 7** | | **29 Oct 2008** | | **Moderator: Dale Dunn** | | |
| 1 | 3102259 | D07-045891 | Hawk | West Nile virus | Eye | 77 |
| 2 | 3102493 | 067-78252 | Cat | enrofloxacin induced retinal degeneration | Eye | 80 |
| 3 | 3103702 | 25623-07 | Dog | Traumatic panopthalmitis | Eye | 82 |
| 4 | 3065935 | 07RD0797 | Dog | *Onchocerca* sp. | Eye | 84 |
| **Conference 8** | | **05 Nov 2008** | | **Moderator: Dr. Matthew Starost** | | |
| 1 | 3106959 | A8-043171 | Ox | Malignant catarrhal fever | Rete mirabilis: | 87 |
| 2 | 3106254 | 06-17642 | Cat | *Cytauxzoon felis* | Kidney | 90 |
| 3 | 3106209 | G08-015746 | Chinchilla | *Listeria monocytogenes* | Liver | 93 |
| 4 | 3105935 | 07N 929 | Dog | *Trypanosoma cruzi* | Heart | 96 |
| **Case** | **AFIP No.** | **Slide No.** | **Species** | **Condition/Etiology** | **Tissue** | **Page** |
| **Conference 9** | | **12 Nov 2008** | | **Moderator: Dr. Michelle Fleetwood** | | |

| | | | | | | |
|---|---|---|---|---|---|---|
| 1 | 3105831 | SDSU-1 | Pig | *Staphlococcus hyicus* | Haired skin | 101 |
| 2 | 3107686 | 3777-3 | Harbor seal | *Clostridium difficile* | Intestine | 104 |
| 3 | 3106280 | 5512 | Cat | *Microsporum canis*. | Haired skin | 106 |
| 4 | 3075498 | 0707051 | Dog | *Cryptococcus neoformans* | Haired skin | 108 |
| **Conference 10** | | **03 Dec 2008** | | **Moderator: Dr. Richard Montali** | | |
| 1 | 3106956 | 08-956-1 | Leopard frog | Ranid herpesvirus 1 (RaHV-1) induced adenocarcinoma | Kidney | 111 |
| 2 | 3102369 | 04/3025 D | Tasmanian Devil | Malignant neuroendocrine neoplasm (Tasmanian Devil Facial Tumor Disease) | Haired skin | 113 |
| 3 | 3102636 | 60136 | Horseshoe crab | Shell disease | Carpace | 115 |
| 4 | 3102368 | GF-D90-3 | Guinea pig | *Mycobacterium tuberculosis.* | Mammary gland | 119 |
| **Conference 11** | | **10 Dec 2008** | | **Moderator: Thomas Steinbach** | | |
| 1 | 3106179 | Cat 3 | Cat | Renal adenocarcinoma | Kidney | 123 |
| 2 | 3109441 | YN06-328 | Macaque | Calcinosis circumscripta | Haired skin | 126 |
| 3 | 3109545 | S0709546 | Goat | Clostridium perfringens type D | Colon | 128 |
| 4 | 3102509 | Case 1 | Dog | *Angiostrongylus vasorum* | Lung | 131 |
| **Conference 12** | | **17 Dec 2008** | | **Moderator: Tony Alves** | | |
| 1 | 3107719 | 08-22155 | Ox | *Actinobacillus lignieresii* | Tongue | 137 |
| 2 | 3106267 | NIAH-2 | Pig | Porcine teschovirus (PTV) | Spinal cord | 140 |
| 3 | 3105581 | 0806396 | Cat | *Candida albicans* | Cecum; lymph node | 143 |
| 4 | 3106654 | V08-03243 | Ox | *Clostridium chauvoei* | Skeletal muscle | 145 |
| **Conference 13** | | **07 Jan 2009** | | **Moderator: Dr. Don Schlafer** | | |
| 1 | 3107596 | 42029 | Ox | Cotyledonary hyperplasia | Placenta | 149 |
| 2 | 3106183 | 08/14596 | Sheep | *Actinobacillus seminis* | Epididymis | 151 |
| 3 | 3103339 | Case 1 | Dog | *Brucella canis* | Testicle; Epididymis | 153 |
| 4 | 2937766 | 04-26927 | Dog | Teratoma, favor monodermal variant | Ovary | 156 |

| Case | AFIP No. | Slide No. | Species | Condition/Etiology | Tissue | Page |
|---|---|---|---|---|---|---|
| **Conference 14** | | **14 Jan 2009** | | **Moderator: Dr. Bruce Williams** | | |
| 1 | 3026964 | Case 05-2373 | Dog | *Escherichia coli* | Small intestine | 159 |
| 2 | 3106379 | G07-120059 | Mink | Aleutian mink disease (ADV) | Kidney | 161 |
| 3 | 3027307 | 06-34302 | Donkey | Nutritional myopathy | Skeletal muscle | 164 |
| 4 | 3096747 | 07-52047 | Dog | *Sparganum proliferum*. | Skeletal muscle | 166 |
| **Conference 15** | | **28 Jan 2009** | | **Moderator: Dr. Michael H. Goldschmidt** | | |
| 1 | 3102252 | T8944-07 | Cat | Feline acquired skin fragility syndrome | Haired skin | 171 |
| 2 | 3103426 | 05-3388 | Dog | Warty dyskeratoma | Haired skin | 174 |
| 3 | 3103391 | E28794 2 | Cat | Merkel cell carcinoma | Haired skin | 176 |
| 4 | 3102248 | H07-0778 | Bandicoot | Bandicoot papillomatosis carcinomatosis virus type 1 | Haired skin | 179 |
| **Conference 16** | | **04 Feb 2009** | | **Moderator: Dr. Tabitha Viner** | | |
| 1 | 3115836 | 08-0165-WSC-2 | White-faced Ibis | *Giardia* sp. | Small intestine | 183 |
| 2 | 3103629 | 07-18567 | Blue heron | *Eustrongylides* sp. | Proventriculus | 185 |
| 3 | 3102498 | 08N0017 | Fulvous whistling duck | *Mycobacterium avium* complex | Liver | 188 |
| 4 | 3102244 | BA 652/07 | Cat | feline idiopathic pulmonary fibrosis (FIPF) | Lung | 192 |
| **Conference 17** | | **11 Feb 2009** | | **Moderator: Dr. Fabio Del Piero** | | |
| 1 | 3113965 | S0 10582 | Horse | Gastrointestinal stromal tumor | Cecum | 197 |
| 2 | 3103695 | 23279-08 | Horse | Equine multinodular pulmonary fibrosis (EMPF) - Equine Herpesvirus-5 (EHV-5) | Lung | 199 |
| 3 | 3103693 | 63383-02 | Horse | *Cellulosimicrobium cellulans* | Placenta | 201 |
| 4 | 3103232 | S07-514.1 | Pig | Porcine cytomegalovirus (PCMV) | Nasal turbinate | 203 |

| Case | AFIP No. | Slide No. | Species | Condition/Etiology | Tissue | Page |
|---|---|---|---|---|---|---|
| **Conference 18** | | **25 Feb 2009** | | **Moderator: Dr. James Raymond** | | |
| 1 | 3071894 | S0704434 | Muscovy duck | Duck viral enteritis virus | Liver | 207 |
| 2 | 3103941 | N2008-0451 | Northern bobwhite | *Dispharynx nasuta* | Proventriculus | 209 |
| 3 | 3107607 | 122103-07 | House sparrow | *Atoxoplasma* spp. | Liver; spleen | 212 |
| 4 | 3075580 | UNL/VDC 2301-06 | Pig | *Brachyspira hyodysenteriae* | Colon | 215 |
| **Conference 19** | | **04 Mar 2009** | | **Moderator: Dr. Amanda Fales-Williams** | | |
| 1 | 3105599 | UFSM-2 | Ox | Bracken fern (*Pteridium aquilinum*) | Bone marrow | 217 |
| 2 | 1008-1080 | 1008-1080 | Dog | Babesia sp. | Blood smear | 223 |
| 3 | 3103707 | 07H7837A | Ox | Nutritional polioencephalomalacia (PEM) | Cerebrum | 225 |
| 4 | 3093118 | Case 1 | Dog | Uremic pneumonitis | Lung | 228 |
| **Conference 20** | | **11 Mar 2009** | | **Moderator: Dr. Yvonne Schulman** | | |
| 1 | 3102611 | 07-1158 | Dog | Gliomatosis cerebri | Brainstem | 235 |
| 2 | 3102490 | UNAM Case 1 | Dog | Oligodendroglioma, anaplastic | Cerebrum | 236 |
| 3 | 3115317 | AFIP 08 CASE 1 | Cat | Feline infectious peritonitis virus (FIP) | Kidney | 240 |
| 4 | 3102517 | 08N0486 | Dog | Meningioma, chordoid (myxoid) | Spinal cord | 241 |
| **Conference 21** | | **01 Apr 2008** | | **Moderator: Dr. Steven Weisbrode** | | |
| 1 | 3106281 | 07-1829 | Horse | Osteochondrosis | Bone | 245 |
| 2 | 3103608 | APO7-2888 | Dog | Vitamin D-resistant rickets, Type II | Bone | 247 |
| 3 | 3067227 | 07-5491 | Ox | Osteopetrosis | Bone | 252 |
| 4 | 3103199 | 0120-08 | Horse | enostosis | Bone | 253 |

The Armed Forces Institute of Pathology
Department of Veterinary Pathology

*Conference Coordinator:*
Todd M. Bell, DVM

WEDNESDAY SLIDE CONFERENCE 2008-2009

# Conference 1

3 September 2008

***Conference Moderator:***

Todd Johnson, DVM, Diplomate ACVP

## CASE I – N0803234 (AFIP 3102615)

**Signalment:** Juvenile, female Northern elephant seal, (*Mirounga angustirostris*)

**History:** The seal was found stranded in California. On physical exam, it was found to be blind and had bilateral cataracts. It spent eight months in a stranding center and was later sent to Adventure Aquarium in Camden, NJ. The seal did well, but a week after arrival it was found floating and unresponsive following administration of 4 tabs ("large dog size") of Drontal. The seal was known to be *Toxoplasma gondii* positive.

**Gross Pathology:** At necropsy, the animal had moderately decreased subcutaneous blubber thickness. The haircoat was extremely sparse and completely absent over much of the animal. There were numerous multifocal to coalescing cutaneous ulcers and erosions along the ventrum extending from the muzzle to the anus and on the ventral aspects of the fore and hind flippers. Both eyes had opaque, cataractous lenses. The teeth were covered with moderate to abundant dental calculus. A vascular anomaly involving the portal vein and caudal vena cava was identified.

**Laboratory Results:** Immunohistochemistry: *Toxoplasma gondii* antibody applied to sections of brain revealed strong positive staining of bradyzoite cysts for *Toxoplasma gondii* antigen **(Fig. 1-3)**. No definitive staining of cysts or tachyzoites was seen in the skin lesions.

**Histopathologic Description:** Within the leptomeninges and surrounding blood vessels throughout the cortex, cerebellum and brainstem, there are multifocal aggregates of lymphocytes, plasma cells and histiocytes **(Fig. 1-1)**. The surrounding parenchyma is rarefied and gliotic with neuronal chromatolysis and necrosis. Within some inflammatory foci are thin-walled tissue cysts up to 40 x 60 um that contain numerous 1-2 um elongate bradyzoites consistent with *T. gondii* **(Fig. 1-2)**. A few necrotic foci with moderate lymphohistiocytic inflammation and associated tissue cysts are observed within sections of skeletal muscle. Individual tissue cysts without associated inflammation or necrosis are present in the ovary and in the wall of a medium sized myocardial artery.

**Contributor's Morphologic Diagnosis:** Brain: meningo-encephalitis, necrotizing and lymphohistiocytic,

*Sponsored by the American Veterinary Medical Association, the American College of Veterinary Pathologists, and the C. L. Davis Foundation.

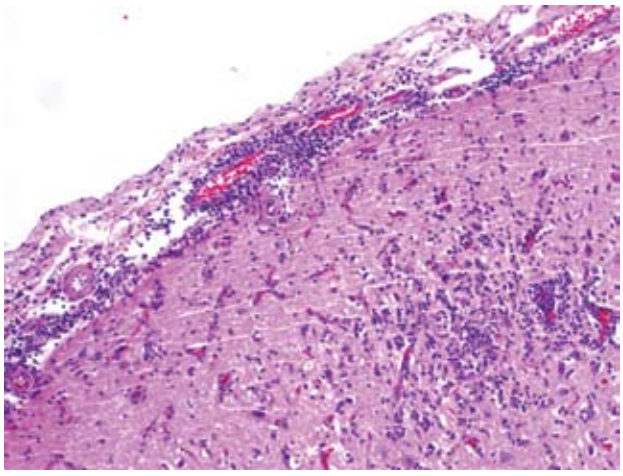

*1-1. Meninges, elephant seal. The meninges are mildly expanded by a cellular infiltrate that occasionally extends into the underlying cerebrum. (HE 200X).* *Photomicrograph courtesy of University of Pennsylvania, School of Veterinary Medicine, Laboratory of Pathology and Toxicology.*

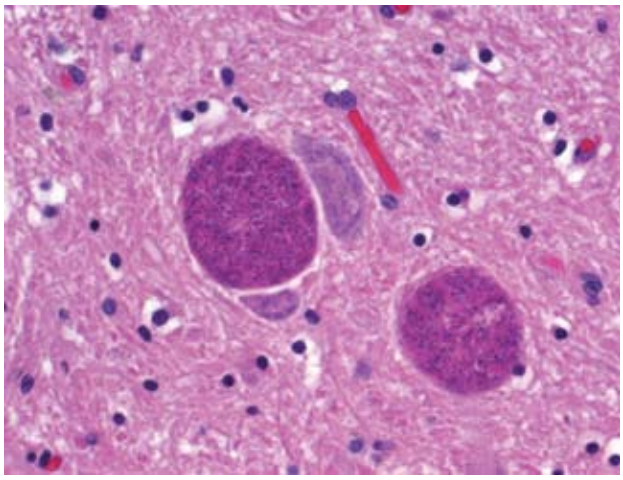

*1-2. Brainstem, elephant seal. Low numbers of protozoal cysts which contain myriad 2-4 micron bradyzoites. (HE 400X).*

multifocal, moderate to severe with intralesional protozoal cysts consistent with *T. gondii*

**Contributor's Comment:** *Toxoplasma gondii* is a coccidian parasite that is found throughout the world and infects an extensive range of intermediate hosts in which it causes both clinical and more commonly, subclinical disease.[7] Domestic and wild felids are the only known definitive hosts and also serve as intermediate hosts.

Infection occurs by ingestion of sporulated oocysts excreted in the feces of felids, by ingestion of tissues of intermediate hosts that contain encysted bradyzoites or tachyzoites, and less frequently by vertical transmission. Once ingested, sporozoites excyst and multiply in the intestinal epithelial cells as tachyzoites. Tachyzoites can either disseminate and infect cells throughout the body resulting in the necrosis and non-suppurative inflammation characteristic of toxoplasmosis, or encyst in tissues as bradyzoites. Following ingestion of tissue cysts by an intermediate host, bradyzoites will excyst, become tachyzoites, and the cycle continues.[2,6,7]

There is one report of toxoplasmosis in an elephant seal pup.[4] Microscopic lesions included multifocal non-suppurative meningoencephalitis and multiple tissue cysts with and without associated inflammation in the cerebrum. Cyst morphology was consistent with *T. gondii*, and protozoa stained positively with *T. gondii*, but not with *N. caninum*, polyclonal antibody. Focal lymphoplasmacytic inflammation was present in the brain, retina, optic nerve and renal tubules, and non-suppurative glossitis with necrosis and ulceration was also observed.[4]

Toxoplasmosis in marine mammals has recently become of particular concern since being identified as a leading cause of encephalitis and death in the threatened Southern sea otter (*Enhydra lutris nereis*).[8] Since 1951, toxoplasmosis has been reported in various species of seals, dolphins, a sea lion, a West Indian manatee, and a beluga whale.[5] Serological assays of numerous species of marine mammals suggests common and widespread exposure.[5]

It is unclear how marine mammals become infected with *T. gondii* as they rarely consume recognized intermediate hosts, and *T. gondii* is not known to parasitize fish or invertebrates. It has been proposed that infection occurs through consumption of oocysts that enter the marine environment via surface run-off or municipal sewage contaminated by cat feces.[9,11] In support of this theory, *T. gondii* oocysts have been shown to sporulate and survive in seawater for several months.[9] Laboratory experiments have shown that bivalves can concentrate *T. gondii* oocysts [9] and recently, a wild California mussel was confirmed positive for *T. gondii* [10] suggesting that invertebrate filter feeders can serve as a source of infection for marine mammals. Additionally, a type X strain of *T. gondii* that has recently been isolated in over 72% of all sea otter infections [2] was identified in the California mussel as well as in several coastal dwelling felids and canids.[10]

**AFIP Diagnosis:** Cerebrum; brainstem: Meningo-encephalitis, necrotizing, histiocytic, multifocal, mild with lymphoplasmacytic perivascular cuffing and few protozoal cysts, Northern elephant seal (*Mirounga angustirostris*), pinniped

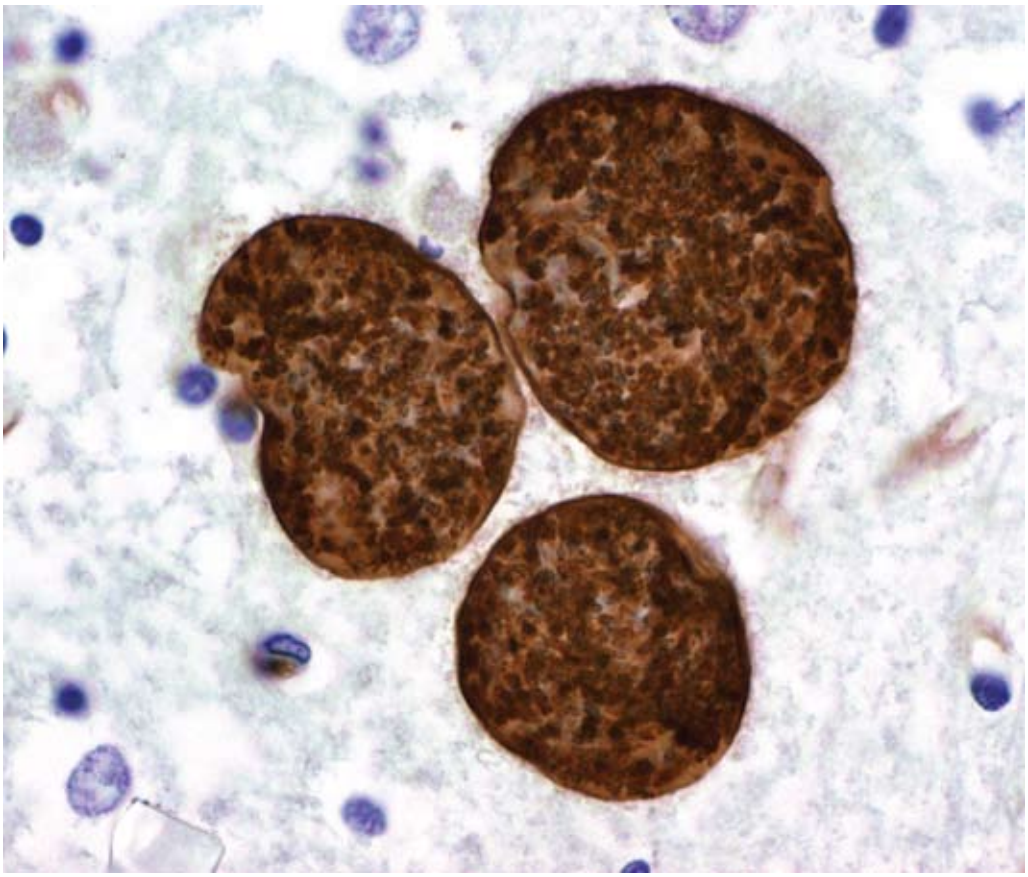

*1-3. Cerebrum, elephant seal. Protozoal cysts are strongly immunopostive for* Toxoplasma gondii. *(600X).*

*Photomicrographs courtesy of University of Pennsylvania, School of Veterinary Medicine, Laboratory of Pathology and Toxicology.*

**Conference Comment:** *Toxoplasma gondii* is a ubiquitous organism that is indiscriminate in nature, infecting all warm-blooded animals, but members of the family Felidae are the only known definitive hosts.[6] Systemic disease occurs mostly in young or immunocompromised animals, and a lack of proper macrophage function in these neonatal animals contributes directly to this outcome.[1] *Toxoplasma* can infect many different cell types, and this leads to rapid dissemination throughout the host. It can infect many different leukocytes to include macrophages, lymphocytes, and granulocytes and be carried in the bloodstream or in lymph via a cell carrier or independently in plasma.[1] *Toxoplasma* then enters a host cell by active penetration of the host cell-membrane and can contort itself in multiple ways to achieve entry into the cell. Once in the cell, the tachyzoite changes shape to form a more ovoid structure and is surrounded by a parsitophorous vacuole that protects it from the host's immune response.[7] Tachyzoites multiply with the parasitized cell, eventually killing it, with subsequent movement to adjacent cells within the resident organ resulting in the characteristic necrotizing lesion often seen with toxoplasmosis. Cell mediated immunity seems to be more important then humoral immunity, and over time animals develop a quiescent infection characterized by cysts with a thin outer wall containing numerous bradyzoites, which are more slender and less susceptible to destruction by proteolytic enzymes than tachyzoites.[1]

Numerous organ systems are affected by toxoplasmosis, with pulmonary lesions and central nervous system lesions having the highest prevalence.[1] Within the lung, lesions are characterized by necrosis of alveolar walls, bronchiolar epithelium, and the vasculature with an accompanying interstitial pneumonia with mononuclear cell invasion into the alveolar walls.[1] Multifocal necrosis within the central nervous system and accompanying non-suppurative inflammation can occur with toxoplasmosis. Microglial nodules are occasionally seen with chronicity within the parenchyma of the central nervous system.[1]

**Contributor:** University of Pennsylvania, School of Veterinary Medicine, Laboratory of Pathology and Toxicology http://www.vet.upenn.edu/departments/pathobiology/pathology

**References:**

1. Brown CC, Dale CB, Barker IK: The alimentary

system. *In:* Jubb, Kennedy, and Palmer's Pathology of Domestic Animals, ed. Maxie MG, 5th ed., vol. 2, pp. 270-272. Elsevier Limited, St. Louis, MO, 2007
2. Conrad PA, Miller MA, Kreuder C, James ER, Mazer J, Dabrtiz H, Jessup DA, Gulland F, Grigg ME: Transmission of *Toxoplasma*: Clues from the study of sea otters as sentinels of *Toxoplasma gondii* flow into the marine environment. Int J Parasitol **35**:1155-1168, 2005
3. Dubey JP: Toxoplasmosis-a waterborne zoonosis. Vet Parasitol **126**:57-72, 2004
4. Dubey JP, Lipscomb TP, Mense M: Toxoplasmosis in an elephant seal (*Mirounga angustirostris*). J Parasitol **90**:410-411, 2004
5. Dubey JP, Zarnke R, Thomas NJ, Wong SK, Van Bonn W, Briggs M, Davis JW, Ewing R, Mense M, Kwok OCH, Romand S, Thulliez P: *Toxoplasma gondii, Neospora caninum, Sarcocystis neurona* and *Sarcocystis canis*-like infections in marine animals. Vet Parasitol **116**:275-296, 2003
6. Gardiner CH, Fayer R, Dubey JP: Apicomplexa – Toxoplasma and Hammondia. *In:* An atlas of protozoan parasites in animal tissues, 2nd ed., pp. 53-56. Armed Forces Institute of Pathology, Washington, DC, 1998
7. Hill DE, Chirukandoth S, Dubey JP: Biology and epidemiology of *Toxoplasma gondii* in man and animals. Animal Health Research Reviews **6**:41-61, 2005
8. Kreuder C, Miller MA, Jessup DA, Lowenstine LJ, Harris MD, Ames JA, Carpenter TE, Conrad PA, Mazet JAK: Patterns of mortality in Southern sea otters (*Enhydra lutris nereis*) from 1998-2001. J Wildl Dis **39**:495-509, 2003
9. Lindsay DS, Collins MV, Mitchell SM, Cole RA, Flick GJ, Wetch CN, Lindquist A, Dubey JP: Sporulation and survival of *Toxoplasma gondii* oocysts in seawater. J Eukaryot Microbiol **50**:687-8, 2003
10. Lindsay DS, Collins MV, Mitchell SM, Wetch CN, Rosypal AC, Flick GJ, Zajac AM, Lindquist A, Dubey JP: Survival of *Toxoplasma gondii* oocysts in Eastern oysters (*Crassostrea virginica*). J Parasitol **90**:1054-1057, 2004
11. Miller MA, Gardner IA, Kreuder C, Paradics DM, Worcester KR, Jessup DA, Dodd E, Harris MD, Ames JA, Packham AE, Conrad PA: Coastal freshwater runoff is a risk factor for *Toxoplasma gondii* infection of southern sea otters (*Enhydra lutris nereis*). Int J Parasitol **33**:997-1006, 2002
12. Miller MA, Miller WA, Conrad PA, James ER, Melli AC, Leutenegger CM, Dabritz HA, Packham AE, Paradics DM, Harris M, Ames J, Jessup DA, Worcester K, Griggs ME: Type X *Toxoplasma gondii* in a wild mussel and terrestrial carnivores from coastal California: New linkages between terrestrial mammals, runoff and toxoplasmosis of sea otters. Int J Parasitol article in press, 2008

## CASE II – PA 4596 (AFIP 3103740)

**Signalment:** Adult, male (*Macaca fasicularis*) cynomolgus macaque

**History:** This animal had been experimentally infected with *Mycobacterium tuberculosis* 8 weeks previously and was being sacrificed as an acute control. The lesions submitted were incidental necropsy findings.

**Gross Pathology:** In the transverse and ascending colon, extending into the cecum, approximately one dozen, slender, thread-like parasites suggestive of Nematodes were noted **(Fig. 2-1)**. These ranged from 6-12 mm in length depending on their state of extension and were very darkly colored. Additionally, present primarily within the cecum were numerous circumscribed somewhat nodular areas of submucosal darkening **(Figs. 2-2, 2-3)**. Transection across several of these structures revealed cavitary areas 2-3 mm in diameter, containing small amounts of thin, dark brown fluid.

**Histopathologic Description:** Slides from multiple blocks are submitted, but are similar in appearance. Present within the submucosa are somewhat circumscribed cavitary lesions filled with a combination of necrotic debris and abundant mixed inflammatory cells, including large numbers of epithelioid macrophages, multinucleated giant cells and more peripheral lymphoplasmacytic infiltrates. Also noted centrally within these submucosal nodules are numerous metazoan parasite structures identifiable as nematodes based on the presence of an external cuticle, musculature, digestive and reproductive tracts (the latter not visible in all sections submitted) **(Figs. 2-4, 2-5, 2-6)**.

Further histological characteristics present allows identification as strongyles, including the presence of platymyarian musculature, prominent vacuolated lateral chords and characteristic intestinal tract with brush borders and iron pigment sometimes visible within intestinal cells.

**Contributor's Morphologic Diagnosis:** Typhlitis/colitis, submucosal, necrotizing and granulomatous, subacute, with numerous metazoan parasites consistent with Strongyle-type nematodes

**Contributor's Comment:** The worms present were subsequently identified by a parasitologist (DB) as *Oesophagostomum* sp. (with species identification pending). Slide mounted specimens measured 8.0 to 13.4

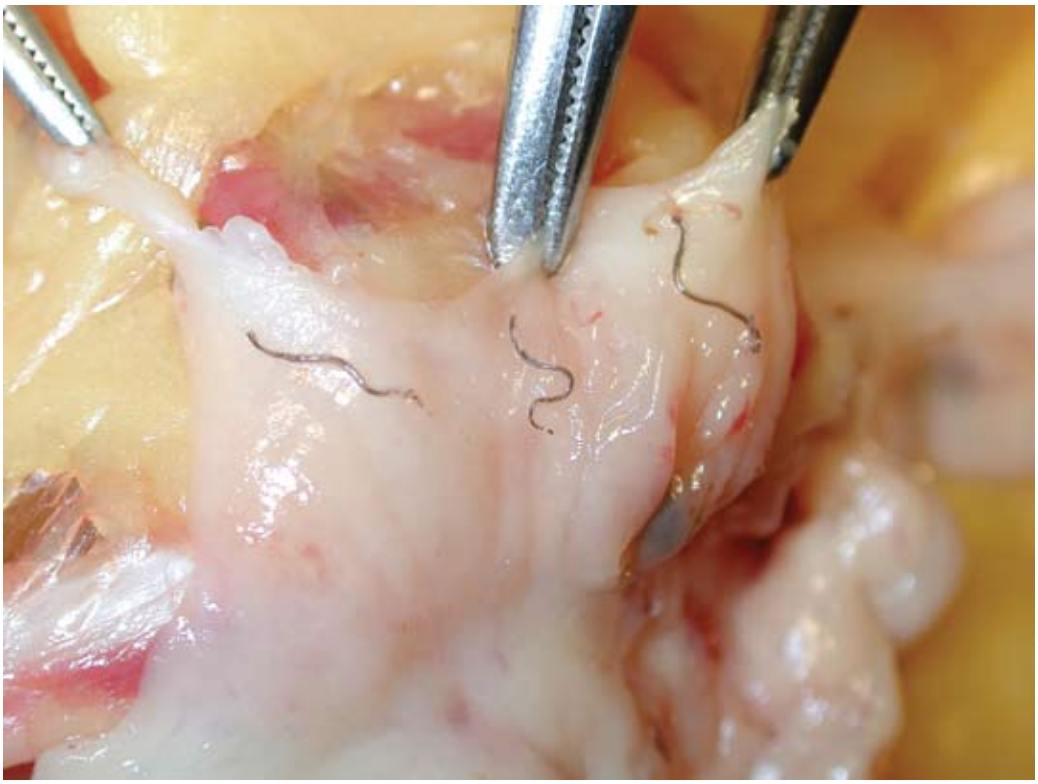

*2-1. Colon, Cynomolgus macaque. Oesophagostomum nematodes.*
*Gross photographs courtesy of the Division of Laboratory Animal Resources, University of Pittsburgh, Pittsburgh, Pennsylvania*

mm in length and possessed morphologic characteristics consistent for the subfamily Oesophagostominae within the family Strongylidae. Generic assignment to Oesophagostomum is based on specimens having a well-defined perioral corona radiata; a straight forwardly directed mouth possessing a collar with two lateral and four submedial cephalic papillae, and a deep posterior annular constriction; a transverse cervical ventral groove that extended around the body towards the dorsal side; and a dilation or inflation of the cuticle between the mouth collar and cervical ventral groove. Two leaf crowns were present: a shallow cylindrical buccal capsule, and an esophageal funnel possessing lancets. Males possessed a complex bursa with rays consistent with those described for the genera,[9] spicules of equal length, and a gubernaculum. Females had parallel uterine branches and a tail that tapered to a point, possessing a vulvar opening positioned slightly anterior to the anus.

The oesophagostomes, sometimes referred to as nodular worms, are among the most common and injurious parasites of monkeys and apes.[6] Worms characteristically produce nodules or cysts in the submucosa or muscularis of the large intestine and less frequently in ectopic sites. Although confusion exists about species identification, *apiostomum, bifurcum, aculeatum* and *stephanostomum* are recognized in the genus Oesophagostomum.[1]

Adult worms live in the lumen of the bowel in their definitive host. Eggs are passed in the feces, hatch and release larvae that mot twice to become infective. Third stage larvae, when swallowed by a new host, burrow into the submucosa of the small or large intestine, molt again to fourth stage larvae and return to the lumen of the large intestine, where they molt again to become mature worms.[2]

Seen not uncommonly in baboons, mangabeys, macaques and great apes, infestation in New World monkeys is rare. Prior to the influx of feral, recently imported Chinese macaques in recent years, the chronic, healed lesions from these parasites were occasionally recognized as discrete and circumscribed, highly mineralized nodules visible on the serosal margin of the bowel *(See submitted gross image 3)*. Such lesions generally did not demonstrate histologic evidence of residual recognizable parasite structures. The submitted case demonstrates an active nonhuman primate infection.

Oesophagostomum infestation from a variety of species is of course well recognized in numerous other animal species including pigs (*O. dentatum*), cattle (*O. radiatum*), sheep (*O. columbianus*), and several wild ruminants – in which such "nodular worm" disease may be associated with significant morbidity and mortality.[8,5]

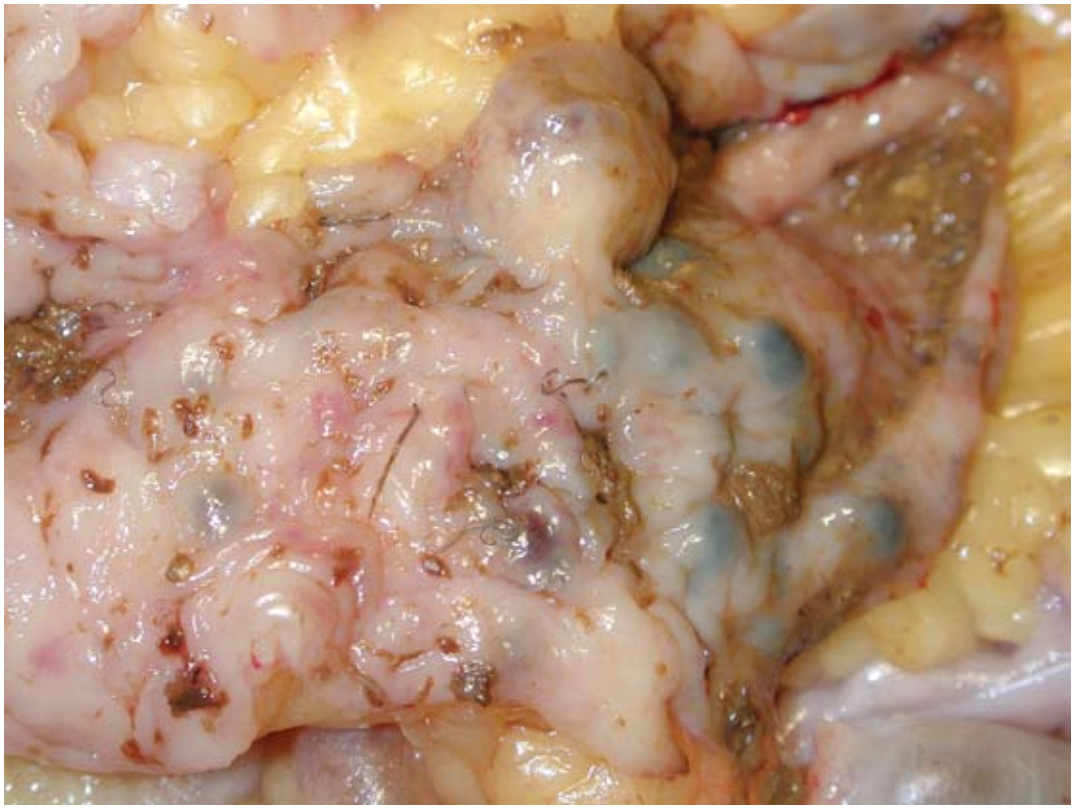

*2-2. Colon, Cynomolgus macaque. Submucosal nodules.*

*2-3. Intestinal serosa, Cynomolgus macaque. Serosal granulomatous nodules suggestive of previous infection.*

*2-4. Colon, Cynomolgus macaque (Macaca fascicularis). Granuloma centered on numerous cross sections of nematode larvae. ( HE 200X).*

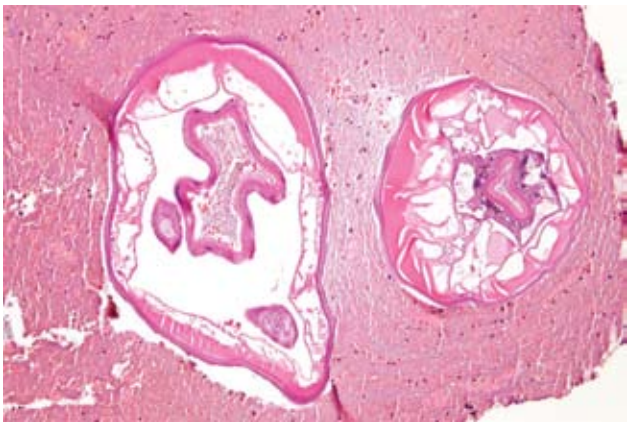

*2-5. Colon, Cynomolgus macaque ( Macaca fascicularis). Nematode larvae are characterized by a smooth cuticle, platymyarian-meromyarian musculature, prominent vacuolated lateral chords and a gastrointestinal tract lined by epithelial cell with a prominent brush border. (HE 100X).*

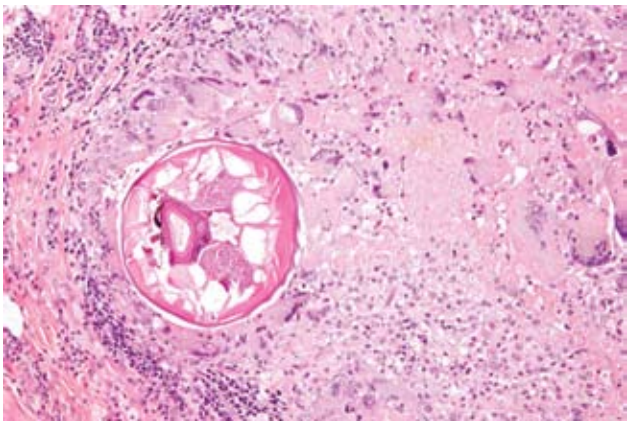

*2-6. Colon, Cynomolgus macaque (Macaca fascicularis). Nematode larvae are surrounded by numerous epithelioid macrophages and multinucleated giant cells which are bounded by lymphocytes, plasma cells and a thin fibrous capsule. (HE 200X). Photomicrographs courtesy of the Division of Laboratory Animal Resources, University of Pittsburgh, Pittsburgh, Pennsylvania*

Human Oesophagostomiasis is an infrequently described and recognized parasite infection in humans, generally caused by *Oesophagostomum bifurcum*.[3] It is a regional and very localized public health problem in Africa, but is considered common in northern Togo and Ghana.[7] Human infestation may cause localized abdominal pain and discomfort, commonly in the right lower quadrant, and this is often accompanied by epigastric or periumbilical masses.[2]

**AFIP Diagnosis:** Colon: Granulomas, multifocal, with few strongyloid nematodes, Cynomolgus macaque (*Macaca fascicularis*), primate

**Conference Comment:** There is considerable slide variation; some sections contained coalescing granulomatous inflammation centered on the nematodes but not forming distinct granulomas. The contributor did a magnificent job describing not only the identification features and life cycle of this nematode parasite, but also gave an excellent summary of comparative pathology.

For the pathologist, it is important to systematically describe nematode parasites in tissue section. One satisfactory method is to start at the outer layers and work one's way in. A brief review of the major histologic identifiable features is presented below and is based on Dr. Chris Gardiner's guidelines in *An Atlas of Metazoan Parasites in Animals Tissues*.[4]

***Cuticle:*** The cuticle is the outermost covering of a nematode, which can range in thickness from being very

prominent to almost imperceivable. Alae, which are winglike extensions of the cuticle, can also be used to identify certain nematodes.[4]

***Hypodermis:*** The hypodermis is immediately internal to the cuticle and extends into the body cavity, or pseudocoelom. Projections of the hypodermis into the pseudocoelom are called lateral chords. These chords can have many different shapes and are helpful in parasite identification.[4]

***Musculature:*** Muscle cells extend from the hypodermis into the pseudocoelom and are composed of a contractile element and a cytoplasmic element. On a normal H&E slide, the cytoplasmic portion is usually clear, and the contractile portion is bright pink to red. Muscles are categorized as being either coelomyarian or platymyarian. Coelomyarian muscles extend into the body cavity in a circular manner, whereas platymyarian muscles are often flattened against the hypodermis and do not extend into the body cavity. Coelomyarian muscles are often numerous with many present in a single section of a nematode, which explains the second portion of the muscle naming nomenclature, polymyarian (e.g., coelmyarian – polymyarian musculature). Platymyarian cells usually extend along the length of the worm and are few in number, and their arrangement is described as meromyarian.[4]

***Digestive Tract:*** Nematodes have a digestive tract composed of the following structures: a mouth, buccal cavity, esophagus, intestine, and anus. The digestive tract size is described relative to the diameter of the nematode, and thus the descriptors large, medium, and small are used. The numbers of cells lining the intestine are commonly described as either 'few multinucleate' cells or 'many uninucleate' cells. Often the intestinal cells contain pigment from digested blood or bile, and when present this can also be helpful in identifying them as intestinal cells.[4]

***Reproductive tract:*** Excluding the group of nematodes known as Rhabditoids, both males and females are represented in an active parasitic infection with females being the larger of the two sexes. Females have two genital tracts and the male nematode has one. Depending on the nematode species, some produce eggs and other produce larvae.[4]

**Contributor:** Division of Laboratory Animal Resources, University of Pittsburgh,
Pittsburgh, Pa. 15261, http://www.oorhs.pitt.edu/research/dlar.html

**References:**

1. Benirschke K, Garner FM, Jones TC: Pathology of Laboratory Animals Vol. II, pp 1648-1649. Springer-Verlag, New York NY, 1978
2. Binford CH, Connor DH: Pathology of Tropical and Extraordinary Diseases Vol. II, pp 440-445. Armed Forces Institute of Pathology, Washington, DC, 1976
3. Bogers JJ, Storey PA, Faile G, Hewitt E, Yelifari L, Polderman A, Van Marck EA: Human oesophagostomiasis: a histomorphometric study of 13 new cases in Northern Ghana. Virchows Arch **439**:21-26, 2001
4. Gardiner CH, Poynton SL: An Atlas of Metazoan Parasites in Animal Tissues, pp. 1-43. Armed Forces Institute of Pathology, Washington, DC, 1999
5. Jones TC, Hunt RD, King NW: Veterinary Pathology 6th ed. pp 612-613. William & Wilkins, Baltimore MD, 1997
6. Orihel TC, Sebold: Nematodes of the Bowel and Tissues. *In:* Pathology of Simian Primates Part II: Infectious and Parasitic Diseases, ed. Fiennes R, pp. 76-99. S. Karger, New York, NY, 1972
7. Polderman AM, Anemana SD, Asigri V: Parasitology Today **15**(4):129-30 Apr 1999
8. Soulsby EJL. Helminths, Arthropods and Protozoa of Domesticated Animals 6th ed. pp 195-200. Williams and Wilkins Company, Baltimore, MD, 1971
9. Yamaguti, S. Systema Helminthum: The Nematodes of Vertebrates Vol. III, pp. 393-397. Interscience Publishers, New York, NY, 1961

## CASE III – 06-42786 (AFIP 3102365)

**Signalment:** 5-year-old, male castrated American quarter horse (*Equus caballus*)

**History:** The horse was used for roping. This horse had moderate, recent weight loss and intermittent reluctance to work on the right hand. The horse was presented for colic and was non-responsive to sedation and anti-inflammatory medications. An abdominal mass and small intestinal distension was diagnosed by palpation and ultrasound. The horse was euthanized due to a poor prognosis.

**Gross Pathology:** The body is in poor body condition. [2/9] In the right anteriodorsal quadrant of the abdomen, a multinodular mass, approximately 60 cm in diameter and weighing ~50 pounds invades and compresses the adjacent organs. The mass is in intimate contact with and invades

the parenchyma of the right kidney, liver, and pancreas and extends into the mesentery, causing compression of the duodenum. On sectioning, the mass is firm, solid, and mottled white and pale yellow. The neoplasm effaces approximately half of the parenchyma of the right kidney and extends into the dilated renal pelvis of that kidney. Throughout the abdomen, multiple, firm, white, round nodules, ranging from 0.5 to 5 cm in diameter are attached to or embedded within the mesentery and omentum. The stomach is distended by gas and approximately 2.5 liters of cloudy, green fluid. The lungs and tracheobronchial lymph nodes are diffusely red-pink, wet, and heavy.

**Laboratory Results:** 24 mg/dl, creatinine 2.1 mg/dl. Abdominocentesis fluid: protein <2.5 g/dl.

**Histopathologic Description:** Kidney and liver: The parenchyma of both the kidney and liver is invaded by a well-demarcated, partially encapsulated, expansile and infiltrative neoplasm consisting of haphazardly arranged and densely packed sheets of polygonal to spindle-shaped (blastemal and mesenchymal) cells, and, less commonly, groups of cuboidal to columnar (epithelial) cells that form incomplete tubular structures **(Fig. 3-1)**. Sheets of cells are encapsulated by a fibrous capsule or compressed residual stroma of the kidney and are subdivided by variably thick bands of connective tissue. Cells of the blastemal component are polygonal, have indistinct cell borders, scant, pale, eosinophilic cytoplasm, and a round, hyperchromatic nucleus. The blastemal component blends with spindle-shaped (mesenchymal) cells separated by scant to moderately abundant, fibrillar, eosinophilic (collagenous) extracellular matrix. A loose, myxoid, extracellular matrix is present between spindle-shaped cells in some areas. Less commonly and usually located adjacent to collagenous stroma, cuboidal to columnar cells form tubular structures with indistinct lumens. These cells have scant eosinophilic cytoplasm and often a basally located nucleus. Blastemal and mesenchymal cells are strongly immunopositive for vimentin and are cytokeratin-negative. Approximately 40% of the spindle-shaped cells are immunopositive for desmin and all of the spindle-shaped cells are immunonegative for smooth muscle actin. The cells in the trabeculae of connective tissue between sheets of cells are faintly immunopositive for smooth muscle actin. Trichrome staining demonstrates scant collagen within the sheets of spindle-shaped cells and abundant collagen in the trabeculae between sheets of cells. The cuboidal cells forming tubules and some groups of less organized, polygonal cells are strongly immunopositive for cytokeratin and -negative or faintly -positive for vimentin. Staining with Periodic acid-Schiff demonstrates a scant, discontinuous basement membrane subjacent to some tubular structures. Mitotic figures are 8-9 per 400X field among the blastemal/ mesenchymal component. Anisokaryosis is prominent. The adjacent renal parenchyma is atrophic, with widespread loss of tubules and glomeruli and collapse of the interstitium. The hepatic parenchyma is atrophic with loss of hepatocytes and collapse of portal regions adjacent to the neoplasm.

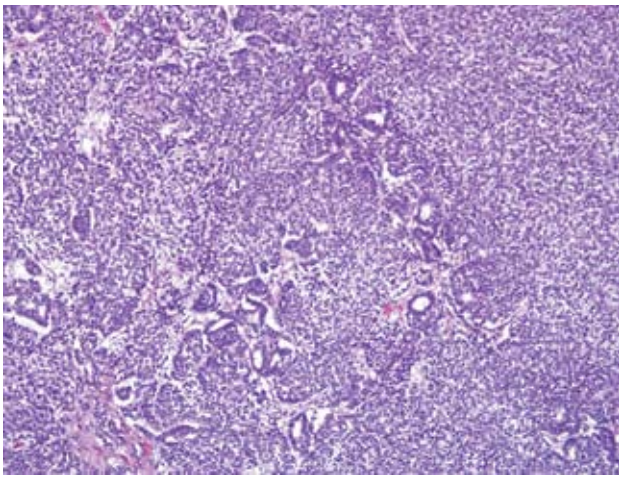

*3-1. Kidney, horse. Nephroblastoma. Effacing normal kidney architecture is a densely cellular neoplasm that occasionally forms variably sized and irregularly shaped tubules. (HE 200X).*

**Contributor's Morphologic Diagnoses:** Malignant nephroblastoma, kidney and liver

**Contributor's Comment:** Nephroblastomas (also called "embryonal nephromas" in older literature and Wilms' tumor in human beings) are theorized to arise from rests of metanephric blastema and usually develop in young animals and children.[1,7,8] Nephroblastomas are rare in horses and most other animal species, except for chickens and swine.[6,12,2,10,5,11,4] The gross and histologic features of nephroblastoma in the horse are rarely described.[6] Nephroblastomas are occasionally diagnosed in adult animals, as in the presented case in a 5-year-old horse.[5,11,4]

Nephroblastomas represent defective nephrogenesis and their component subtypes reflect the conversion of metanephric mesenchymal cells to epithelial structures that occurs during nephrogenesis.[7,8,3] The neoplasm presented here contains all three elements required for the diagnosis of a nephroblastoma: blastemal, mesenchymal, and epithelial, although not evenly represented in the presented section of kidney and in other organs. Immunohistochemical staining of the tissues from this case confirms the coexistence of mesenchymal and epithelial components

within the sheets of embryonic cells. Myofibroblastic differentiation was demonstrated by vimentin and desmin immunopositivity. Cells forming tubular structures or located adjacent to trabeculae often were immunopositive for cytokeratin. Other samples of this neoplasm from the kidney, pancreas and liver contain more of the epithelial component, consisting primarily of tubular structures; rudimentary glomeruli were not identified in examined sections from this case. The neoplasm presented here extended to anatomic structures adjacent to the right kidney, but not to the lung or more distant regions of the liver, suggesting coelomic metastasis.

Historically, nephroblastomas have been categorized according to the relative amount of each of the three cellular components, with a "triphasic nephroblastoma" containing approximately equal amounts of each of the three cell lineages.[7,8] In the neoplasm presented here, cells of all three differentiation types are identified by cytomorphology and using immunohistochemistry in varying amounts among different regions of the neoplasm. Cells that do not demonstrate cytomorphologic features of mesenchymal or epithelial differentiation, i.e., the blastemal cells, predominate in this neoplasm. In human beings, nephroblastomas that have cytologic features of anaplasia, including enlarged nuclei, hyperchromasia of nuclei, and enlarged, multipolar mitotic figures, are designated as having unfavorable histology in the currently used staging protocol.[7,9]

The genetic pathology that results in Wilms' tumor in children appears to be complex, and, in some cases, the development of Wilms' tumor in children is associated with other congenital malformations.[1,7] The protein product of the Wilms' tumor suppressor gene-1 (WT-1) is a zinc-finger DNA binding protein and an essential regulator of renal development. Inactivation of the WT1 gene is documented in a small number of Wilms' tumors in children and is believed to prevent the differentiation of primitive metanephric cells. The remaining Wilms' tumors in human beings are assumed to be due to defects in other genes, including WT3 and others. Genetic analysis was not performed on tissue from this case.

**AFIP Diagnosis:** Kidney; liver: Nephroblastoma, horse, equine

**Conference Comment:** Nephroblastoma is the most common tumor of the kidney in both the chicken and pig.[8] These tumors are less common in calves and dogs and apparently very rare in horses, cats, and sheep. This neoplasm has been found in rats exposed to different tumor producing agents.[8] Metastasis in canine tumors occurred in over 50% of the reported cases, whereas in pigs and calves metastasis is uncommon. In dogs, particularly German Shepherds, these tumors can form extramedullary, intradural spinal masses usually found between spinal cord segments T10 and L2.[8]

The typical hallmark histologic features of the nephroblastoma are loosely arranged spindle cells amongst primitive glomeruli, haphazardly arranged tubules, and densely cellular blastema.[8] Proportions of these elements vary from tumor to tumor and even within regions of the same tumor. Canine nephroblastomas have been shown to stain for human Wilms' tumor gene product C-19.

In the sections examined during conference, the blastemal component compromised the majority of neoplastic cells. The epithelial component, including rudimentary tubules was present multifocally, but glomeruloid structures were not seen. Loose mesenchymal areas were uncommon.

**Contributing Institution:** Department of Pathobiology, College of Veterinary Medicine, Auburn University, Auburn, Alabama 36849 http://www.vetmed.auburn.edu/index.pl/patho

**References:**

1. D'Angio GJ: The National Wilms Tumor Study: a 40 year perspective. Lifetime Data Anal **13**:463-470, 2007
2. Goens SD, Moore CM, Brasky KM, et al: Nephroblastomatosis and nephroblastoma in nonhuman primates. J Med Primatol **34**:165-170, 2005
3. Grieco V, Riccardi E, Belotti S, Scanziani E: Immunohistochemical study of porcine nephroblastoma. J Comp Path **134**:143-151, 2006
4. Headley SA, Saut JPE, Maiorka PC: Nephroblastoma in an adult sheep. Vet Record **159**:850-852, 2006
5. Henry CJ, Turnquist SE, Smith A, et al: Primary renal tumors in cats: 19 cases (1992-1998). J Feline Med Surg **1**:165-170, 1999
6. Jardine JE, Nesbit JW: Triphasic nephroblastoma in a horse. J Comp Pathol **114**:193-198, 1996
7. Khoury JD: Nephroblastic neoplasms. Clin Lab Med 25(2) 341-361, 2005
8. Maxie MG, Newman SJ: Nephroblastoma, Urinary system. *In:* Jubb, Kennedy, and Palmers' Pathology of Domestic Animals, 5th ed., pp. 501-503. Saunders Elsevier, Philadelphia, PA, 2007
9. Perlman EJ: Pediatric renal tumors: Practical updates for the pathologist. Pediatric Dev Pathol **8**:320-338, 2005
10. Terrell SP, Platt SR, Chrisman CL, Homer BL, de Lahunta A, Summers BA: Possible intraspinal metastasis of a canine spinal cord nephroblastoma. Vet Pathol **37**:94-97, 2000
11. Yamamoto Y, Yamada M, Nakamura K, et al: Nephroblastoma with transcoelomic metastasis in a

Japanese black bull. J Vet Med Sci **68**(8):891-893, 2006
12. Zoller M, Matz-Rensing K, Fahrion A, Kaup FJ: Malignant nephroblastoma in a common marmoset (*Callithrix jacchus*). Vet Pathol **45**:80-84, 2008

## CASE IV - 03-8246 (AFIP 3102495)

**Signalment:** 4-month-old pig

**History:** This pig was submitted with a history of sudden death.

**Gross Pathology:** There was a generalized serofibrinous pleuritis and multiple widely distributed foci of fibrinous pneumonia in both lungs. Regional lymph nodes were increased in size and hemorrhagic. Small white foci surrounded by a hyperhemic zone were disseminated in the skin.

**Laboratory Results:** *Actinobacillus suis* was isolated from the pleura, lung, skin and other organs.

**Histopathologic Description:** In the lung section submitted, there is a serofibrinous pneumonia with many necrotic leukocytes **(Figs. 4-1, 4-2)**. These lesions were multifocal and generalized in both lungs. The necrotic leukocytes appear as round cells with pyknotic nuclei, and cells with a streaming of pale basophilic chromatin, the so-called "oat cells." Small coccobacilli (gram-negative) are present in the alveolar exudate, and few bacterial emboli are present in some sections. Several capillaries are thrombosed. There is a severe fibrinous pleuritis with necrotic leukocytes similar to those in the lung lesions.

**Contributor's Morphologic Diagnosis:** Severe acute fibrinoleukocytic pleuropneumonia with many "oat cells" and the presence of intralesional coccobacilli

**Contributor's Comment:** The skin lesions observed grossly were characterized by small dermal vessels thrombosed and/or occluded by bacterial emboli (small gram-negative coccobacilli). They were infiltrated and surrounded by inflammatory cells, mainly necrotic leukocytes similar to those in the lung. Small coccobacilli were also present in the inflammatory infiltrates.

The multifocal and widespread pneumonia, and the skin lesions observed in this pig are compatible with a septicemia caused by *Actinobacillus suis*. Clinical cases of *A. suis* occur more frequently in high-health-status herds.[6] The most common manifestation of the infection is septicemia and sudden death in suckling and recently weaned pigs.[6] A disease resembling pleuropneumonia caused by *A. pleuropneumonia*, and skin lesions similar to those caused by *Erysipelothrix rhusiopathiae*, are reported in older pigs.[6]

The pneumonic lesions caused by *A. suis* can have two patterns. One of them is a focal locally extensive fibrinohemorrhagic, fibrinoleukocytic and necrotizing pneumonia or pleuropneumonia affecting the middle

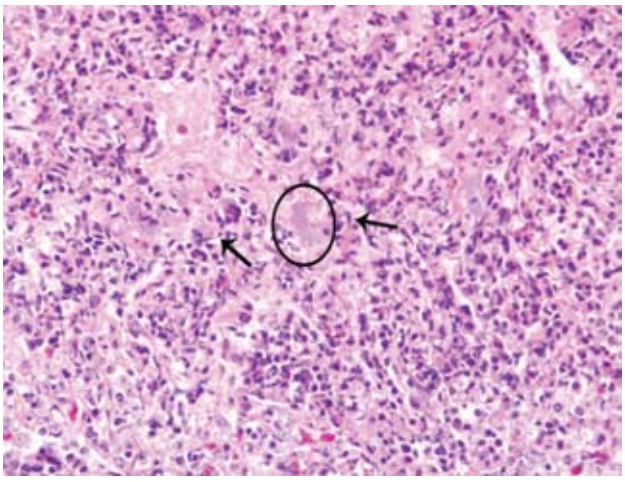

*4.1. Lung, pig. Areas of necrosis admixed with high numbers of alveolar macrophages, fewer lymphocytes and plasma cells and necrotic leukocytes with slender, elongated, streaming nuclei ("oat cells") (arrows) that often surround small colonies of 1-2 um diameter bacilli (circle). (HE 400X)*

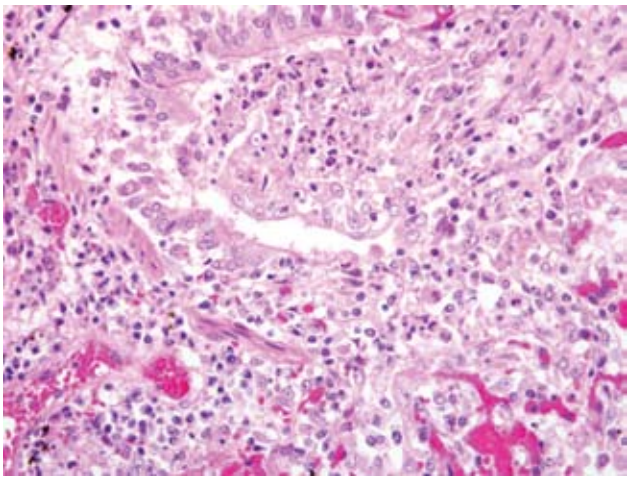

*4-2. Lung, pig. Bronchiolar epithelium is necrotic and replaced by eosinophilic cellular debris admixed with moderate numbers of histiocytes, lymphocytes, fewer plasma cell and rare neutrophils. Bronchiolar lumina often contain exudate composed of cellular and inflammatory debris. (HE 400X).*

or the caudal lung lobes, which may be unilateral or bilateral.[2] These lesions are very similar to those caused by *A. pleuropneumonia* and are probably originating from an airborne entry of the organism.[2] The other pattern is a generalized multifocal pneumonia indicating hematogenous origin. This multifocal widespread pneumonia is a common finding in cases of *A. suis* septicemia. Other lesions observed in septicemic cases are petechial hemorrhages in serosa and other organs, multifocal necrosis and inflammation in the liver, spleen, kidney and skin, splenomegaly, serofibrinous pericarditis, pleuritis and peritonitis, polyarthritis, valvular endocarditis, and rhomboid skin lesions similar to those observed incases of erysipelas.[6]

The fibrinous pneumonia with many necrotic leukocytes appearing as "oat cells" is characteristic of *A. pleuropneumonia* and *A. suis* in swine.[2] Different serotypes of *A. pleuropneumonia* produce RTX-toxins (ApxI, II and III) which are cytotoxic for the porcine neutrophils and macrophages.[2,4] Some strains of *A. suis* produce a RTX-toxin (Apx I).[6] "Oat cells" are also present in the fibrinous pneumonia caused by *Mannheimia haemolytica* in cattle, sheep and goat.[2] All serotypes of *M. haemolytica* produce a leukotoxin being a member of the RTX family of bacterial toxins.[2] These necrotic leukocytes appearing as "oat cells" are also present in the inflammatory lesions of other organs in cases of *A. Suis* septicemia.

**AFIP Diagnosis:** Lung: Pneumonia, necrotizing, histiocytic and neutrophilic, multifocal, marked, with vasculitis, necrotic leukocytes ("oat cells"), fibrin, diffuse interstitial and alveolar edema, and numerous colonies of coccobacilli, pig, porcine

**Conference Comment:** *Actinobacillus suis* is a gram-negative nonmotile, nonencapsulated aerobic and facultative anaerobic coccobacillus that is often an inhabitant of the tonsils and upper respiratory tract of pigs of any age and the vagina of clinically healthy sows.[6] *A. suis* can cause rhomboid skin lesions secondary to vasculitis, and this manifestation can be confused with erysipelas. Petechial to ecchymotic hemorrhages can occur in multiple organs to include the lung, kidney, heart, liver, spleen, and intestines. These lesions are often most pronounced in the lungs with a striking resemblance to those of pleuropneumonia. In sows, *A. suis* can cause metritis, meningitis, and abortion. Histologically, bacterial thromboemboli randomly scattered in the vasculature of the previously mentioned organs is suggestive of *A. suis*.[6]

| | | |
|---|---|---|
| Actinobacillus pleuropneumonia | Pigs | Serofibrinous pleuritis and necrotizing hemorrhagic pneumonia; caudodorsal distribution |
| Actinobacillus equuli | Horses | Common cause of suppurative embolic nephritis in foals |
| Actinobacillus lignieresii | Cattle | Glossitis and stomatitis in cattle (wooden tongue) |
| Actinobacillus seminis | Sheep | Common cause of bilateral epididymitis in rams |

[1,2,3,5]

**Contributor:** Department of Pathology and Microbiology, Faculty of Veterinary Medicine,University of Montreal, C.P. 5000, Saint-Hyacinthe, P. Quebec, Canada J2S 7C6, http://www.medvet.umontreal.ca

**References:**

1. Brown CC, Baker DC, Barker IK: Alimentary system. *In:* Jubb, Kennedy, and Palmer's Pathology of Domestic Animals, ed. Maxie MG, 5th ed., vol. 2, pp. 96-97. Elsevier Limited, St. Louis, MO, 2007
2. Caswell JL, Williams KJ: Respiratory system. *In:* Jubb, Kennedy and Palmer's Pathology of Domestic Animals, ed. Maxie MG, 5th ed., vol. 2 pp. 587-589, 601-606. Elsevier Limited, St. Louis, MO 2007
3. Foster RA, Ladds PW: Male genital system. *In:* Jubb, Kennedy and Palmer's Pathology of Domestic Animals, ed. Maxie MG, 5th ed., vol. 3 pg. 590. Elsevier Limited, St. Louis, MO 2007
4. Gottschalk M, Taylor DJ: *Actinobacillus pleuropneumonia*. *In:* Diseases of Swine, eds. Straw BE, Zimmerman JJ, D'Allaire S, Taylor DJ, 9th ed., pp. 563-576. Wiley-Blackwell, Oxford, England, 2006
5. Maxie MG, Newman SJ: Urinary system. *In:* Jubb, Kennedy and Palmer's Pathology of Domestic Animals, ed. Maxie MG, 5th ed., vol. 2, pg. 480. Elsevier Limited, St. Louis, MO, 2007
6. Taylor DJ: *Actinobacillus suis*. *In:* Diseases of Swine, ed. Straw BE, Zimmerman JJ, D'Allaire S, Taylor DJ, 9th ed., pp. 827-829. Wiley-Blackwell, Oxford, England, 2006

The Armed Forces Institute of Pathology
Department of Veterinary Pathology

*Conference Coordinator:*
Todd M. Bell, DVM

WEDNESDAY SLIDE CONFERENCE 2008-2009

# Conference 2

10 September 2008

***Conference Moderator:***

Dr. Sarah Hale, DVM, Diplomate ACVP

## CASE I – CRL 2008-1 (AFIP 3104062)

**Signalment:** Mouse (*Mus musculus*), strain unknown (homozygous for foxn1$^{nu}$), age and gender unknown

**History:** Submitted to necropsy for evaluation of scaly skin.

**Gross Pathology:** Skin over the entire body surface is hyperkeratotic, with white flakes.

**Laboratory Results:** PCR of skin surface swabs positive for *Corynebacterium bovis*.

**Histopathologic Description:** Skin (nude): The epidermis is diffusely acanthotic, approximately 3-fold thicker than normal. Abundant keratinaceous debris covers the surface (diffuse orthokeratotic hyperkeratosis) **(Fig. 1-1)**. Numerous colonies of small bacteria mix with hair and keratinaceous debris on the surface of the hyperkeratotic layer **(Fig. 1-2)**. The bacteria appear coccoid in some areas, and as short bacilli in irregular branching clusters in a few others. The dermis is diffusely mildly infiltrated by mononuclear leukocytes and a few neutrophils. Mast cells are prominent.

Brown and Brenn Gram's stain: The bacteria are Gram positive. The predominant type is short coryneforms, arranged in typical corynebacterial arrays.

**Contributor's Morphologic Diagnosis:** Dermatitis, subacute, diffuse, mild, with prominent acanthosis, hyperkeratosis and coryneform bacteria

**Contributor's Comment:** Corynebacterial hyperkeratosis, the so-called "scaly skin disease," remains fairly common, with approximately 2% of nude mice submitted to our diagnostic laboratory from non-vendor sources being confirmed with the disease.

Corynebacterial hyperkeratosis has been recognized for decades in athymic nude mice, but also occurs in SCID mice and can be experimentally reproduced in euthymic hairless mice.[1] Morbidity varies but can be high. Mortality is usually very low except in suckling mice, which can have high mortality. Immunocompetent mice, other than hairless strains, may have asymptomatic infection, but evidence suggests that infection is cleared in these mice.[2,3]

Clinical signs include hyperkeratosis, decreased activity and a wrinkled appearance which probably indicates

*Sponsored by the American Veterinary Medical Association, the American College of Veterinary Pathologists, and the C. L. Davis Foundation.

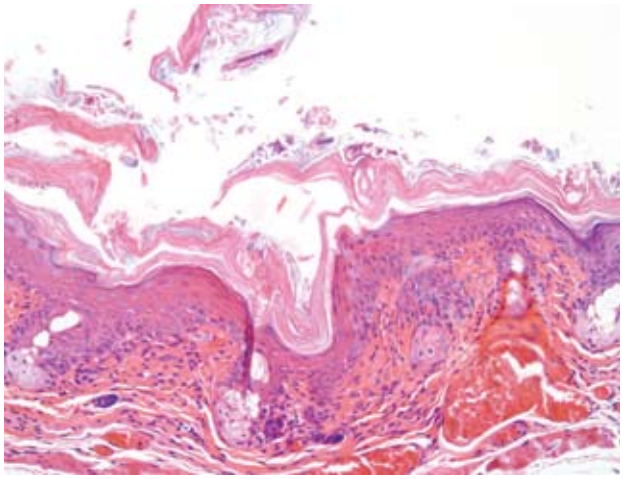

*1-1 Haired skin, mouse. Diffusely there is epidermal hyperplasia with orthokeratotic hyperkeratosis and there are scattered lymphocytes, plasma cells, histiocytes and fewer neutrophils within the superficial dermis. (HE 200X).*

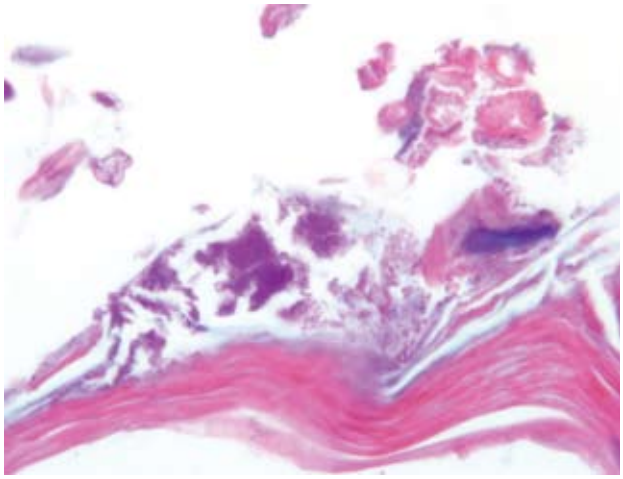

*1-2 Haired skin, mouse. Multifocally, within the stratum corneum there are few small colonies of approximately 1 micron diameter bacilli. (HE 600X).*

dehydration. Signs typically appear in susceptible mice about one week after exposure, persist for a week or more, and then usually disappear. Microscopically, the acanthosis remains after the hyperkeratosis resolves; the infection also persists. The mechanism by which *C. bovis*, a lipophilic bacterium which colonizes the stratum corneum, causes acanthosis and hyperkeratosis is unknown, as is the reason for resolution of the hyperkeratosis.

Histologic features of this case are typical. Hyperkeratosis can be difficult to assess microscopically, is transitory in this disease, and is non-specific; it may be caused by various conditions. Thus, greater diagnostic significance should be given to the acanthosis. Diffuse acanthosis, with a mild non-suppurative dermatitis and the presence of Gram-positive coryneform bacteria in the stratum corneum is sufficient for a diagnosis, although in most situations confirmation by culture and or PCR is preferred.[4] Other corynebacteria may also colonize the skin surface; our laboratory has identified *C. jeikeium, C. minutissimum* and Group F2. The latter two organisms are now included in *C. amycolatum*. None of these are thought to cause skin disease in mice.

In addition to mortality in suckling immunodeficient mice, *C. bovis* has been reported to slow xenograft growth and increase toxicity observed after chemotherapeutic agents. The mechanism of this is unknown, but the contributor speculates that it might be related to dehydration (symptomatic mice virtually always appear markedly dehydrated, conceivably due to alterations in epidermal barrier function from the diffuse skin disease). Retarded xenograft growth could also possibly be due to non-specific stimulation of host defense mechanisms such as NK cell activity. Non-specific antitumor effects have previously been described for *C. kutscheri*.[6]

Control of *C. bovis* infection is difficult. The bacterium is readily transmitted by fomites and is resistant to drying. Our diagnostic laboratory has found positive PCR samples on swabs from cage exteriors, door knobs and even tumor lines passaged as tumor fragments.

**AFIP Morphologic Diagnosis:** Skin: Hyperkeratosis, orthokeratotic, diffuse, moderate, with epidermal hyperplasia and mild subacute dermatitis

**Conference Comment:** The contributor did an excellent job of summarizing the clinical manifestations, strains affected, and histologic features of *Corynebacterium bovis* infections in mice. This comment will briefly touch on the gross and histologic features of *Corynebacterium kutscheri*, another important organism in laboratory animals.

Mice and Rats: *Corynebacterium kutscheri* is a Gram-positive, diphtheroid bacillus that is the cause of "pseudotuberculosis" in both mice and rats. The normal route of entry of *C. kutscheri* is through the oral or gastrointestinal mucosa with subsequent hematogenous spread throughout the body. An immunosuppressive event usually precedes clinical disease.[5]

Common gross findings include suppurative bronchopneumonia with randomly distributed caseopurulent nodules; raised, multifocal to coalescing caseopurulent

nodules in the heart, liver, or kidney; reactive hyperplasia in lymph nodes near an active site of infection; and pedal arthritis.[5]

On histological section, the bacteria form large colonies surrounded by abundant neutrophils and necrotic debris. Because the disease spreads via sepsis, the suppurative lesions in the lung are randomly distributed. This is an important distinguishing feature between this disease and the disease caused by *Mycoplasma pulmonis*, which is closely associated with the airways and causes bronchiectasis. The large bacterial colonies of *C. kutscheri* are pathognomonic and are described as resembling Chinese letters. Interstitial pneumonia is also commonly present in association with *C. kutscheri* infection and is characterized by hypercellular alveolar septa and pulmonary edema.[5]

Hamsters: These rodents are considered carriers of *C. kutscheri* but are typically resistant to systemic disease.[5]

**Contributing Institution:** Charles River; www.criver.com

**References:**

1. Clifford CB, Walton BJ, Reed TH, Coyle MB, White WJ, Amyx HL: Hyperkeratosis in nude mice caused by a coryneform bacterium: Microbiology, transmission, clinical signs, and pathology. Lab Anim Sci **45**:131-139, 1995
2. Gobbi A, Crippa L, Scanziani E: *Corynebacterium bovis* infection in immunocompetent hirsute mice [see comments]. Lab Anim Sci **49**:209-211, 1999
3. Gobbi A, Crippa L, Scanziani E: *Corynebacterium bovis* infection in waltzing mice [letter; comment]. Lab Anim Sci **49**:132-133, 1999
4. Kita E, Nishikawa F, Yagyu Y, Hamuro A, Oku D, Emoto M, Katsui N, Tanikawa I, Kashiba S: Nonspecific stimulation of host defense by *Corynebacterium kutscheri*. I. Antitumor effect. Nat Immun Cell Growth Regul **8**:313-324, 1989
5. Percy DH, Barthold SW: Pathology of Laboratory Rodents and Rabbits, 3rd ed., pp.72, 147-148, 192. Blackwell Publishing, Ames, Iowa, 2007
6. Russell S, Riley LK, Maddy A, Clifford CB, Russell RJ, Franklin CL, Hook RR, and Besch-Williford: CL: Identification of *Corynebacterium bovis* as the etiologic agent of hyperkeratosis in nude mice and development of a diagnostic polymerase chain reaction assay. Laboratory Animal Science **48**[4], 412, 1998 Ref Type: Abstract

## CASE II - 07-276-3 (AFIP 3102251)

**Signalment:** 10-month-old female C57BL/6 mouse (*Mus* sp.) #202, with homozygous point mutation in *Mcm4* gene ($^{Mcm4Chaos3/Chaos3}$)

**History:** The mouse was euthanized after developing an enlarged abdomen and lethargy.

**Gross Pathology:** The liver was pale brown, markedly enlarged and had rounded edges. The spleen was diffusely enlarged and also had rounded edges.

**Histopathologic Description:** Liver is diffusely hypercellular and the capsular surface has slightly irregular contour. Normal hepatic architecture is disrupted by filling of multifocal sinusoids and veins with small to moderate numbers of neoplastic cells arranged individually and in small clusters **(Fig 2-1)**. The neoplastic cells are moderately sized (2x smaller than hepatocytes), round to oval or elongate, with distinct cytoplasmic margins and a moderate amount of eosinophilic cytoplasm that occasionally contains moderate amount of green-yellow pigment (hemosiderin). Occasionally, there are RBCs within neoplastic cell cytoplasm (erythrophagocytosis). The nucleus is round to oval, often eccentrically placed and with coarsely clumped chromatin and indistinct nucleolus. There is mild anisocytosis and anisokaryosis and rare mitotic figures and binucleated cells. Other changes in the liver that are present to variable degree in submitted slides include a few small foci of hepatic lipidosis, occasional dilatation of sinusoids, rare foci of extramedullary hematopoiesis containing erythroid and granulocyte precursors and low numbers of megakaryocytes, presence of eosinophilic globular intracytoplasmic inclusions in some hepatocytes and occasional hepatocytes filled with moderate amount green-brown granular pigment.

**Laboratory Results:** Immunohistochemistry for macrophage marker Mac-2 was done using M3/38 antibody clone from Cedarlanes. The cytoplasm of intrasinusoidal neoplastic round cells was strongly positive for Mac-2 **(Fig 2-2)**.

**Contributor's Morphologic Diagnosis:**
Liver: Histiocytic sarcoma
Spleen (tissue not included): Erythroid hyperplasia, diffuse, marked

**Contributor's Comment:** Histiocytic sarcoma (HS) in mice arises from the cells of mononuclear phagocytic

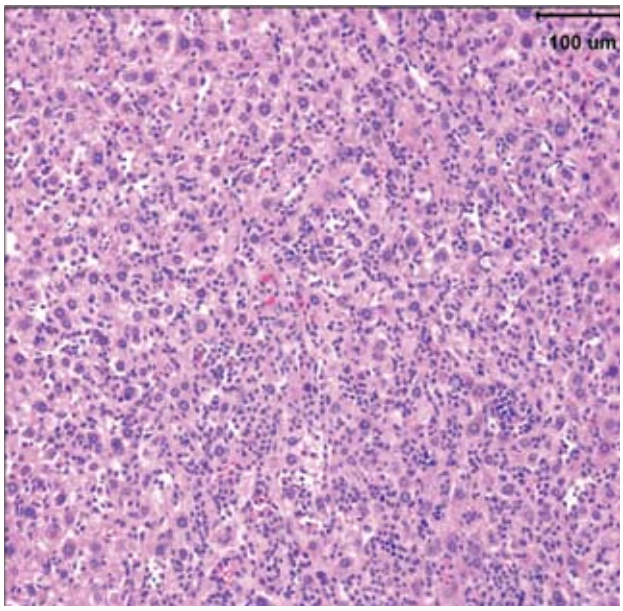


*2-1 Liver, mouse. Diffusely infiltrating and expanding the sinusoids are high numbers of round cells. Photomicrograph courtesy of Veterinary Population Medicine Department, College of Veterinary Medicine, University of Minnesota.*

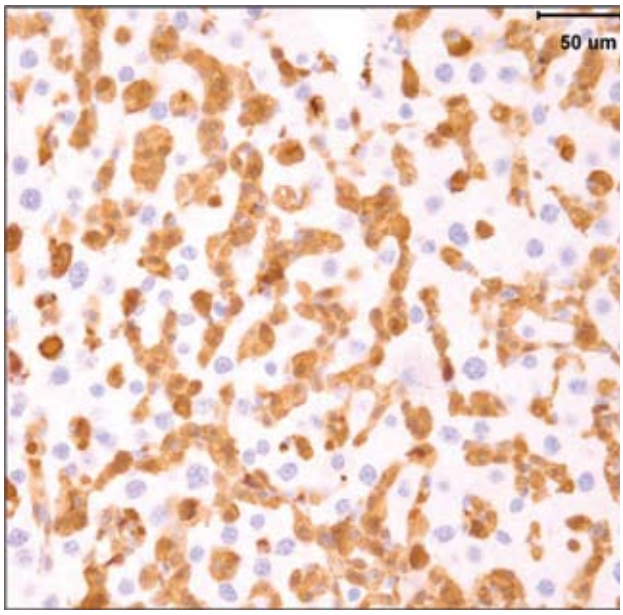


*2-2 Liver, mouse. Diffusely neoplastic cells are show strong cytoplasmic immunopositivity for Mac-2. Photomicrograph courtesy of Veterinary Population Medicine Department, College of Veterinary Medicine, University of Minnesota. DAB with hematoxylin counterstain.*

system and most commonly affects liver and uterus with less frequent involvement of spleen, lung, lymph node, ovary, kidney and bone marrow.[3,8] The incidence is dependent on strain, sex, age, nutrition, and varies from study to study[2,4] For example, HS incidence in C57BL/6 mice is higher than in most other strains of in-bred mice, and the disease in this strain occurs rarely before 12 months of age.[2,3,4] One of the highest incidences of HS has been reported by Blackwell in a study that determined effect of dietary restriction on the incidence of tumors in C57BL/6 mice.[2] HS was the most prevalent neoplasm in this study that involved almost 1000 mice over period of 3 years. Overall lifetime incidence of HS was ~30% in *ad libitum* fed C57BL/6 female mice in comparison with ~ 55% in similarly fed male mice. 40% reduction in the feed resulted in slightly decreased incidence of HS in male mice and increased HS incidence in female mice to 50%.

The gross and microscopic appearance of HS depends on organs involved. The liver involvement is the most common manifestation of HS regardless of the mouse strain.[7] The liver with HS is severely, diffusely enlarged and without focal lesions. Histologically, tumor cells are present diffusely or multifocally within sinusoids and vascular spaces. Progressive growth of neoplastic cells leads to compression of hepatic cords and hepatocyte atrophy.[3,7] Uterine involvement is strongly strain-dependent in mice: uterine HS is rare in C57BL/6 mice but common in CBA mice.[7] HS in uterus may present as diffuse thickening of both horns or as 1 to several variably sized nodules. Histologically, neoplastic histiocytic cells that infiltrate uterine wall tend to be elongated to fusiform.[3,7] Erythrophagocytosis may be associated with the neoplastic infiltrates, particularly in the liver and multinucleated giant cells may be present in some tumors.[3,7] Immunohistochemical stains that aid identification of neoplastic cells as histiocytes include Mac-2, F4/80, and lysozyme.[9]

Recent publications have linked development of HS in the liver in C57BL6/J mice with concurrent hepatic (but not splenic) extramedullary hematopoiesis (EMH) and hematologic abnormalities such as anemia.[1,5] At this point it is not clear whether HS and hepatic EMH are co-incidental lesions or if one of them leads to the other. Concurrent hematologic abnormalities may suggest genetic abnormality in myeloid stem cells.

The submitted case is from a mouse with homozygous, single base mutation in *Mcm4* gene known as Chaos3. This mutation induced high incidence of mammary adenocarcinomas in C3H mice.[7] In contrast, C57BL/6 mice with Chaos3 mutation have high prevalence of histiocytic sarcoma with shortened tumor latency of less than 12 months. Diffuse liver involvement is noted most commonly in these mice but nodular tumor infiltrates

and marked destruction of hepatic parenchyma by HS is seen occasionally. All mice with hepatic HS have extramedullary hematopoiesis in the liver and marked erythroid hyperplasia in the spleen. Some mice have intraabdominal solid masses in peripancreatic omentum and elsewhere diagnosed as HS based on presence of Mac-2 positive cells with histiocytic appearance (spindle to polygonal cells, abundant cytoplasm, and oval to indented nucleus) and neoplastic features (moderate mitotic figure rate and bizarre mitoses).

Gene complex *MCM2-7*, which includes *MCM4*, encodes protein complex that is recruited to DNA replication origins and ensures a singe initiation of DNA synthesis during S phase restricting genome replication to once per cell cycle.[7] Chaos3 mutation was first identified in the screen for chromosome instability. High incidence of tumors and short tumor latency periods in mice with *Mcm4Chaos3/Chaos3* suggests that genomic instability may have a causative role in cancer. It is not clear at this point yet whether C57BL/6 mice with *Mcm4Chaos3/Chaos3* genotype have hematologic abnormalities such as anemia concurrently with HS.

**AFIP Morphologic Diagnosis:** 1. Liver: Histiocytic sarcoma
2. Liver, hepatocytes: Microvesicular lipidosis, multifocal, moderate

**Conference Comment:** The contributor provided a thorough overview of the gross and histologic lesions of histiocytic sarcoma in mice. This brief discussion will focus on histiocytic sarcoma in rats.

In rats, the most commonly affected strain is Sprague–Dawley, and tumors are generally seen in animals over 12 months of age with no gender preference. The organs affected in rats are similar to those in mice; the most common sites are liver, lymph nodes, spleen, mediastinum, retroperitoneum, and subcutaneous tissue. Affected rats most commonly have nodules of tumor cells that displace normal organ parenchyma, whereas in the mouse liver, neoplastic cells typically infiltrate sinusoids with no distinct mass formation.[6]

Histologically, tumor cells are pleomorphic with vesicular nuclei, prominent nucleoli, and abundant cytoplasm. Multinucleate giant cells are a common component of tumors with a predominantly histiocytic makeup. Because of the variable morphology of neoplastic histiocytes, the differential diagnostic list includes various sarcomas, lymphoma and granulomatous inflammation.[6]

**Contributing Institution:** Veterinary Population Medicine Department, College of Veterinary Medicine, University of Minnesota.

**References:**

1. Barker JE, Deveau SA, Compton ST, Fancher K, Eppig JT: High incidence, early onset of histiocytic sarcomas in mice with Hertwig's anemia. Exper Hematol **33**:1118-2911, 2005
2. Blackwell BN, Bucci TJ, Hart RW, Turturro A: Longevity, body weight, and neoplasia in ad libitum-fed and diet-restricted C57BL6 mice fed NIH-31 open formula diet. Toxicol Pathol **23**:570-582, 1995
3. Frith CH: Histiocytic sarcoma, mouse. *In:* Monographs on Pathology of Laboratory Animals. Hematopoietic system, eds., Jones TC, Ward JM, Mohr U, Hunt RD, pp. 58-65. Springer-Verlag, Berlin, Heidelberg, 1990
4. Frith CH, Ward JM, Chandra M: The morphology, immunohistochemistry and incidence of hematopoietic neoplasms in mice and rats. Toxicol Pathol **21**:206-218, 1993
5. Lacroix-Triki M, Lacoste-Collin L, Jozan S, Charlet JP, Caratero C, Courtade M: Histiocytic sarcoma in C57BL/6J mice is associated with liver hematopoiesis: Review of 41 cases. Toxicol Pathol **31**:304-309, 2003
6. Percy DH, Barthold SW: Pathology of Laboratory Rodents and Rabbits, 3rd ed., pg. 116, 170-172. Blackwell Publishing, Ames, Iowa, 2007
7. Shima N, Alcaraz A, Liachko I, Buske TR, Andrews CA, Munroe RJ, Hartford SA, Tye BK, Schimenti JC: A viable allele of Mcm4 causes chromosome instability and mammary adenocarcinomas in mice. Nature Genetics **39**:93-98, 2007
8. Turusov VS: Histiocytic sarcoma. IARC Sci Publ **111**: pp. 671-680, 1994
9. Ward JM, Sheldon W: Expression of mononuclear phagocyte antigens in histiocytic sarcoma of mice. Vet Path **30**:560-565, 1993

## CASE III – 08014 (AFIP 3103042)

**Signalment:** 27-year-old, male, cynomolgus macaque (*Macaca fascicularis*), nonhuman primate

**History:** This animal arrived at Wake Forest University from Indonesia about 9 years before death. It was diagnosed with type 2 diabetes on 3/6/2008 (glucose 328 g/dL), and on the following day, became lethargic and dehydrated. Insulin treatment and supportive fluid therapy were attempted, but the animal died on 3/9/2008.

*3-1. Lung, Cynomolgus macaque. Suppurative pleuropneumonia. Photo courtesy of Animal Resources Program, Wake Forest University Health Sciences, Winston-Salem, North Carolina.*

*3-2. Lung, Cynomolgus macaque. Necrosuppurative pleuropneumonia with lymphadenitis and mediastinal edema. Photo courtesy of Animal Resources Program, Wake Forest University Health Sciences, Winston-Salem, North Carolina.*

*3-3. Lung, Cynomolgus macaque. Necrosuppurative pleuropneumonia with intralobular edema and hemorrhage. Photo courtesy of Animal Resources Program, Wake Forest University Health Sciences, Winston-Salem, North Carolina.*

**Gross Pathology:** The major gross lesion was in the lung. The entire left lung was four times larger than normal, firm, and tan to yellowish-brown, with adherence to the body wall in some areas **(Figs. 3-1, 3-2)**. Similar changes were present in the middle right lung lobe. Cut surfaces revealed suppurative exudate **(Fig. 3-3)**, and 10-20% of the parenchyma was replaced by dense fibrous connective tissue.

In addition to the pulmonary lesion, the coronary arteries were segmentally thickened by yellow plaques on the intimal surfaces (atherosclerosis).

**Laboratory Results:**

***Serum chemistry:***
Glucose, 348 mg/dL
BUN 29 mg/dL
K+ 6.2 mEq/L
Alkaline phosphatase 588 µ/L
Cholesterol 1099 mg/dL

***Hematology:***
CBC:
RBC, 6.77 x $10^5$/µL
Hematocrit, 42.3 %
Hemoglobin, 12 mg/dL
MCV, 62fl
MCHC 28.4 g/dL
Platelets 181 x $10^3$/µL
WBC 15.9 x $10^3$/µL
Neutrophils, 77% (12243)
Bands, 0
Lymphocytes 17% (2703)
Monocytes, 5% (795)
Eosinophils, 1% (159)
Basophils, 0

***Microbiology:***
Pleural fluid and a lung swab were submitted for bacterial culture. A heavy pure growth (4+) of *Corynebacterium ulcerans* was recovered.

**Histopathologic Description:** Lung: The pulmonary architecture is extensively distorted **(Fig. 3-4)** by a necrotizing inflammatory reaction composed of abundant neutrophils and protein-rich edema fluid, which fills alveoli and bronchioles. Alveolar walls are often effaced **(Fig. 3-5)** and bronchiolar epithelium is often absent. Pale perivascular spaces measuring up to 500 um in width contain fibrin and edema fluid. Vessels are variably infiltrated by neutrophils and mononuclear phagocytes, contain thrombi, and are surrounded by myriads of short bacterial rods. Similar bacterial colonies are also scattered throughout the pulmonary parenchyma

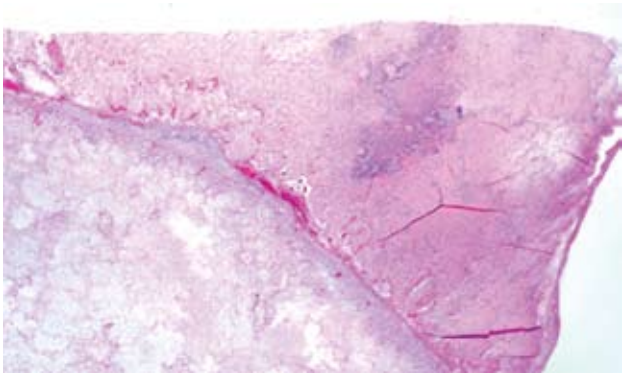

*3-4 Lung, Cynomolgus macaque. The normal lung architecture is lost and there are large coalescing areas of lytic necrosis admixed with a cellular infiltrate. (HE 40X).*

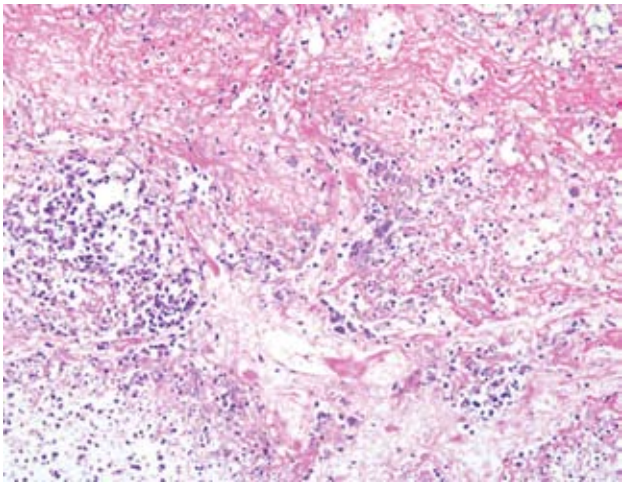

*3-5 Lung, Cynomolgus macaque. Normal lung parenchyma is necrotic and replaced by fibrin admixed with cellular and karyorrhectic debris. (HE 200X).*

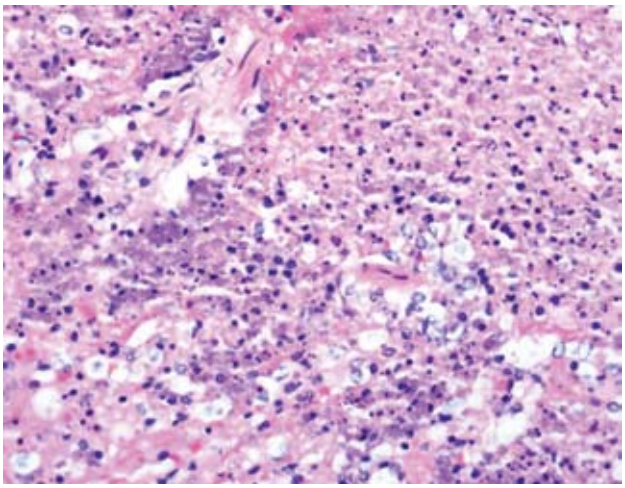

*3-6 Lung, Cynomolgus macaque. Scattered throughout the areas of necrosis there are large colonies of 1-2 micron diameter bacilli. (HE 400X).*

and subpleural space **(Fig. 3-6)**. The pleura is thickened up to 1.5 mm owing to the presence of variably mature fibrous connective tissue and suppurative inflammation. Gram staining demonstrates mats of pleomorphic Gram positive bacilli throughout the lung.

**Contributor's Morphologic Diagnosis:**
Pneumonia, diffuse, chronic, severe, fibrinosuppurative with intralesional bacteria (Etiology: *Corynebacterium ulcerans*)

**Contributor's Comment:** Corynebacteria are Gram-positive, non-motile, pleomorphic bacilli.[2] Corynebacterium ulcerans was first isolated in 1926 from a human throat lesion[4], and has since been considered a common cause of laryngitis and cutaneous granulomas in humans.[2] It has also been isolated from abscesses and causes pneumonia and mastitis in nonhuman primates.[3] It is considered a commensal of horses and cattle, although it can cause mastitis and cutaneous infections in cattle [5], and is widely distributed in soil and water. It is often isolated from non-pasteurized milk, the drinking of which has been linked to human infections.[6] Fatal pneumonia caused by *C. ulcerans* has been reported in humans and macaques.[2] A retrospective study of respiratory disease in 272 nonhuman primates (75 cynomolgus macaques, 97 rhesus macaques, 100 vervets) indicated that *C. ulcerans* and *Streptococcus pneumoniae* were major causes of winter respiratory infections in cynomolgus macaques.[3]

The pathogenicity of *C. ulcerans* is facilitated by potent exotoxins, including diphtheria toxin which inhibits protein synthesis, as well as necrotizing toxin which increases vascular permeability resulting in edema. After inhalation, *C. ulcerans* proliferates in the respiratory tract epithelium. Subsequent release of the exotoxins causes epithelial necrosis, which in turn initiates marked interstitial edema, neutrophil infiltration, and fibrinosuppurative exudation.[1]

The differential diagnosis for fibrinosuppurative broncho-pneumonia in cynomolgus macaques should include *Streptococcus pneumoniae*, *Pasteurella* spp., *Nocardia* spp., *Actinobacillus* spp., *Klebsiella* spp., and *Legionella pneumophila* as well as *Corynebacterium* sp.

**AFIP Morphologic Diagnosis:** Lung: Pleuro-pneumonia, fibrinonecrotic, diffuse, severe, with abundant coccobacilli

**Conference Comment:** Genetic analysis has revealed that *Corynebacaterium ulcerans* is a unique organism that is very closely related to *Corynebacterium diptheriae* and *Corynebacterium pseudotuberculosis*.[1]

*Corynebacterium ulcerans* can produce diphtheria toxin similar to that of *C. diphtheriae. C. diphtheriae* produces a phage-encoded A-B toxin that blocks protein synthesis. Even after vaccination with diphtheroid toxin, *C. diphtheriae* can still colonize the epithelium, and the vaccine does protect people from the harmful effects of the toxin. Release of the exotoxin in unvaccinated individuals causes necrosis of the epithelium and subsequent profuse fibrionsuppurative exudation. The settling of this exudate on the already ulcerated epithelial surface results in formation of the firm diphtheritic membrane characteristic of the disease. If the fulminant infection is stopped, the membrane may be sloughed via coughing or enzymatic digestion, and the patient can recover.[4]

**Contributing institution:** Animal Resources Program, Wake Forest University Health Sciences, Winston-Salem, NC; http://www1.wfubmc.edu/pathology/training/index.htm

**References:**

1. AFIP Wednesday slide conference 23 case # 3, 1999 http://www.afip.org/vetpath/WSC/wsc99/99wsc23.htm
2. Dessau RB, Brandtchristensen M, Jensen OJ, Tonnesen P: Pulmonary nodules due to *Corynebacterium ulcerans*. European Respiratory Journal **8**:651-653, 1995
3. Panaitescu M, Maximescu P, Michel J, Potorac E: Respiratory pathogens in non-human primates with special reference to *Corynebacterium ulcerans*. Lab Animal 11:155-157, 1977
4. McAdam AJ, Sharpe AH: Infectious Diseases. *In:* Robins and Cotran Pathologic Basis of Disease, eds. Kumar V, Abbas AK, Fausto N, 7th ed., pp. 374, Elsevier Saunders, Philadelphia, PA 2005
5. Sing A, Hogardt M, Bierschenk S, Heesemann E: Detection of differences in the nucleotide and amino acid sequences of diphtheria toxin from *Corynebacterium diphtheriae* and *Corynebacterium ulcerans* causing extrapharyngeal infections. Journal of Clinical Microbiology **41**:4848-4851, 2003
6. Wagner J, Ignatius R, Voss S, Hopfner V, Ehlers S, Funke G, Weber U, Hahn H: Infection of the skin caused by *Corynebacterium ulcerans* and mimicking classical cutaneous diphtheria. Clinical Infectious Diseases **33**:1598-1600

## CASE IV –08012 (AFIP 3103041)

**Signalment:** 7-year-old, female, African green monkey, (*Chlorocebus aethiops*) non-human primate

**History:** The animal failed to recover from sedation for routine tuberculosis testing.

**Gross Pathology:** The animal was severely dehydrated and had multiple gastric ulcerations in the fundus. Both thyroid glands were unremarkable, each weighed 0.17 g and 0.23 g.

**Laboratory Results:**

| Test | Result | Humans Reference Range[6] |
|---|---|---|
| Total Thyroxine (TT4) | 14 | 60-140 nmol/L |
| Total Triiodothyronine (TT3) | 2.3 | 1.1-2.7 nmol/L |
| Free Thyroxine (FT4) | 7 | 10-25 pmol/L |
| Free Triidothyronine (FT3) | 6.8 | 3-8 pmol/L |
| T4 Autoantibody* | 15% | N/A |
| T3 Autoantibody* | 3% | N/A |

N/A: Not Available
*: Autoantibodies to T3 and T4 are presented as the percentage of hormone binding relative to each antibody negative control

**Histopathologic Description:** Mostly lymphocytes admixed with fewer plasma cells infiltrate the interstitium diffusely, with multifocal intensification, separating and sometimes sequestering the follicles **(Fig. 4-1)**. In some instances the lymphocytes form follicles with germinal center formation (not present in all slides). The thyroid follicles range from 60-150 microns in diameter and are often devoid of colloid. The follicular epithelial cells range from cuboidal to tall columnar and are multifocally hyperplastic, forming 3-4 stratified layers, or papillary projections, into the lumina. 10 to 20 % of them are slightly shrunken, hypereosinophilic, and have deeply basophilic nuclei with condensed chromatin (apoptosis). Regularly the follicular epithelial are separated from the basement membranes by clear spaces, despite being attached to one another along their lateral sides. Sometimes the lumina are filled with sloughed cells admixed with foamy macrophages and cellular debris enmeshed in amorphous, pale eosinophilic material **(Fig. 4-2)**.

**Contributor's Morphologic Diagnosis:** Thyroiditis, diffuse, chronic, marked, lymphocytic, thyroid gland

**Contributor's Comment:** Chronic lymphocytic thyroiditis in humans and non-human primates is commonly recognized as an autoimmune disorder with a poorly understood pathogenesis. Diagnoses are made based on a thyroid test panel, clinical signs, and histologic findings. Spontaneous thyroiditis has been reported in laboratory rats, obese strains of chickens, dogs, and a cynomolgus monkey.[2,3]

Two types of autoimmune thyroiditis are described in humans, Graves' disease and Hashimoto's thyroiditis, the latter being more frequent.[3,4,6,8] In Graves' disease, the inflammation is mild, while the thyroid glands are enlarged due to proliferation of thyrocytes, resulting in follicular hyperplasia and hypertrophy. Graves' disease accounts for 50-80% of hyperthyroidism cases in humans, and results from circulating IgG antibodies that bind to and activate the G-protein-coupled thyrotropin receptor. Clinical pathological findings include decreased serum thyrotropin, elevated serum triiodothyronine (T3) and thyroxine (T4), with an increased fraction of T3 relative to T4.[1,3,6]

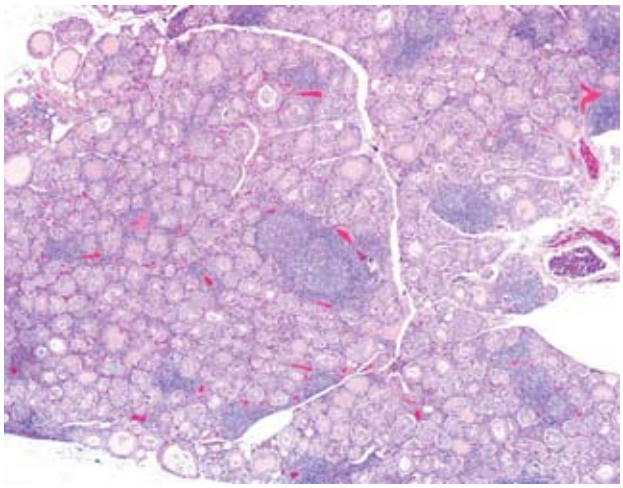

*4-1. Thyroid gland, African green monkey. Multifocally, expanding the thyroid interstitium is a cellular infiltrate that often forms lymphoid follicles with vague germinal centers. (HE 40X).*

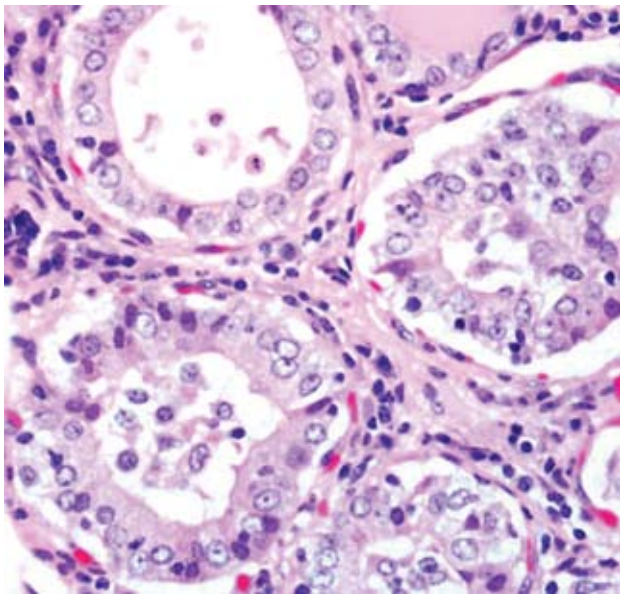

*4-2 . Thyroid gland, African green monkey. Multifocally thyroid follicles are lined by hypertrophic columnar epithelium with abundant, lightly eosinophilic, finely granular cytoplasm and often follicular lumina are devoid of colloid and contain histiocytes, lymphocytes and plasma cells. (HE 400X).*

In Hashimoto's thyroiditis, the lymphocytic infiltration is prominent, often with germinal center formation, causing enlargement of the thyroid glands and destruction of the thyroid follicles, leading to hypothyroidism. The pathogenesis of Hashimoto's thyroiditis involves a delayed hypersensitivity reaction to thyroid epitopes. Sensitization of autoreactive CD4+ T-helper cells to these initiates the immunologic events leading to thyrocyte death. The effector mechanisms include destruction of thyrocytes by CD8+ cytotoxic T cells by exocytosis of perforin/granzyme granules or engagement of the death receptor, overproduction of inflammatory cytokines by CD4+ T cells, and the binding of antithyroid antibodies (anti-TSH receptor, antithyroglobulin, and antithyroid peroxidase antibodies) followed by antibody-dependent cell-mediated cytotoxicity. Hypothyroidism usually develops gradually, although in some cases it may be preceded by transient thyrotoxicosis due to the disruption of thyroid follicles, with secondary release of thyroid hormones (hashitoxicosis).[2,3,6,8]

As there is relatively little literature on African green monkeys, normal reference ranges for humans [7] were used to confirm the presence of autoimmune thyroiditis in this case. Serum-binding assays to measure thyroxine (T4) and triiodothyronine (T3) autoantibodies revealed15% and 3% more binding of the immunoglobulin to the T4 and T3, respectively, compare to each negative control. Low TT4 and FT4 support a diagnosis of hypothyroidism, which, combined with the histological appearance, resembles Hashimoto's thyroiditis in humans. Values of thyroid stimulating hormone (TSH), autoantibodies against thyroglobulin, thyroperoxidase, or TSH receptor are not available due to the limitation of serum available for testing.

**AFIP Diagnosis:** Thyroid gland: Thyroiditis, lymphoplasmacytic, chronic, diffuse, marked, with follicular hyperplasia and colloid depletion

**Conference Comment:** Other animal species with an autoimmune thyroiditis resembling Hashimoto's disease include dogs, obese strains of chickens, nonhuman primates, and Buffalo rats. The pathogenesis of autoimmune thyroiditis in the dog is not completely understood, but it seems to stem from production of autoantibodies directed against a variety of targets in the thyroid. Autoantibodies in dogs are most commonly directed against thyroglobulin or against thyroperoxidase or other microsomal antigens; less commonly autoantigens are directed against TSH receptors, a nuclear antigen, or a second colloid antigen from thyroid follicular cells.[5]

Gross lesions in dogs with lymphocytic thyroiditis vary and include normal sized, enlarged or hypoplastic thyroid glands that may be discolored tan to off white. The classic histologic appearance is of multifocal to diffuse infiltrates of lymphocytes and plasma cells that separate thyroid

follicles and may form lymphoid nodules. Follicles are often shrunken and lined by columnar epithelial cells, which may cause nests of C cells to appear more prominent between follicles.[2]

Migration of lymphocytes and plasma cells between follicles causes follicular cells to lose their attachment to the basement membrane, and this leads to sloughing of cells into the lumen of the follicle. Lymphoid cells also migrate into the lumen, and this combination of changes leads to eventual death of the follicle. While the damage to follicles is ongoing, adjacent follicles undergo hypertrophy in an attempt to keep up with demand and in response to increased TSH secretion. Eventually the parenchyma of the thyroid gland is replaced by fibrous connective tissue. At this stage, only scant residual inflammatory cells and small, widely dispersed "end-stage" follicles with a small amount of vacuolated colloid remain.[2]

**Contributing Institution:** Animal Resources Program, Wake Forest University Health Sciences

**References:**

1. Brent GA: Graves' disease. N Engl J Med **358**:2594-605, 2008
2. Capen CC: Endocrine Glands. *In:* Jubb, Kennedy, and Palmer's Pathology of Domestic Animals, ed. Maxie MG, 5th ed., vol.3, p386. Elsevier Saunders, Philadelphia, PA, 2007
3. Caturegli P, Kimura H, Rocchi R, Rose NR: Autoimmune thyroid diseases. Curr Opin Rheumatol **19**(1):44-8, 2007
4. Guzman RE, Radi ZA: Chronic lymphocytic thyroiditis in a cynomolgus monkey (*Macaca fascicularis*). Tox Pathol **35**:296-299, 2007
5. La Perle KMD, Capen CC: Endocrine system. *In:* Pathologic Basis of Veterinary Disease, eds. McGavinMD, Zachary JF, 4th ed., pp.722. Mosby Elsevier, St. Louis, MO 2007
6. Maitra A, Abbas AK: The Endocrine System. *In:* Robbins and Cotran Pathologic Basis of Disease, eds. Kumar V, Abbas AK, Fausto N, 7th ed., pp1169-73. Elsevier Saunders, Philadelphia, PA, 2005
7. Stockigt J: Assessment of thyroid function: Towards an integrated laboratory – clinical approach. Clin Biochem Rev **24**:110-23, 2003
8. Wang SH, Baker JR: The role of apoptosis in thyroid autoimmunity. Thyroid **17**(10):975-9, 2007

**NOTES:**

The Armed Forces Institute of Pathology
Department of Veterinary Pathology

*Conference Coordinator:*
Todd M. Bell, DVM

WEDNESDAY SLIDE CONFERENCE 2008-2009

# Conference 3

17 September 2008

***Conference Moderator:***

Jennifer Chapman, DVM, Diplomate ACVP

## CASE I – AFIP Case 2 (AFIP 3103341)

**Signalment:** Tissues are from a 6-week-old, intact female, Weimaraner dog (*Canis familiaris*)

**History**: This has been going on in my kennel for about 1 year. Puppies will die sometimes with symptoms of URI and occasionally matted eyes. They have loss of appetite and thirst. For no apparent reason, it will stop and no puppies will die for several weeks. It then starts again with a lot of deaths. Adults are now vaccinated every 6 months. Puppies get Bordetella (4 wks), BA2MP (5wks), Parvo (6wks), DA2PP (7wks). It is not affecting adults, only puppies, usually between 5-7 weeks old.

**Gross Pathology:** The patient is in relatively good body condition. The eyes are markedly sunken into the orbits. There is a small amount of vomitus matted in the hair around the nose. Scattered along the ventral margins of all lung lobes are multiple to locally extensive, 2 mm to 2 cm in diameter dark red foci. These foci are slightly firm, fail to collapse and extend into the parenchyma on cross-section.

**Laboratory Results:**
***Bacteriology Results***

| | | |
|---|---|---|
| Tissue: Lung | Organism ID: | *Streptococcus canis* |
| | Organism ID: | *Pseudomonas aeruginosa* |

***Virology Results***

Tissue: Lung

| | | |
|---|---|---|
| Canine Adenovirus PCR | Positive | Canine adenovirus type [2] |
| Canine Distemper Virus PCR | Positive | Canine distemper virus |

*Sponsored by the American Veterinary Medical Association, the American College of Veterinary Pathologists, and the C. L. Davis Foundation.

***Fluorescent Antibody Staining***

| | | |
|---|---|---|
| Tissue: Lung | Positive | Canine distemper virus |
| Tissue: Intestines | Negative | Canine parvovirus |
| Tissue: Lung | Negative | TGE |
| Tissue: Intestines | Negative | Coronavirus |
| Tissue: Lung | Negative | Herpesvirus |
| Tissue: Lung | Positive | Adenovirus |

**Histopathologic Description:** Lung: The normal alveolar architecture is multifocally effaced by areas of necrosis and inflammation with bacterial cocci, viral syncytia, and viral inclusions. Within affected areas, there are coalescing aggregates of necrotic cellular debris with numerous foamy macrophages. Frequently, the macrophages contain large 7-10um diameter basophilic intranuclear inclusions and few 2-5um diameter eosinophilic intracytoplasmic inclusions. There are frequent syncytial cells that contain up to 5 nuclei. There are scattered lesser numbers of lymphocytes and neutrophils. The bacterial cocci are 1-2um in diameter and form small clusters within the area of more intense inflammation. The inflammation occasionally extends into the lumens of the adjacent bronchioles. The affected bronchioles are often lined by attenuated, ragged epithelium. Within the bronchi, the luminal epithelium is multifocally attenuated. Bronchial epithelial cells occasionally contain 5-7um in diameter oval eosinophilic intranuclear inclusion bodies. Bacterial cocci are occasionally clumped along the lumina surface. Within the less affected areas, the alveoli are flooded with small amounts of fibrin and proteinaceous fluid.

**Contributor's Morphologic Diagnosis:** Lung: Severe, multifocal to coalescing histiocytic necrotizing pneumonia with syncytial cells, intranuclear and intracytoplasmic viral inclusion bodies and bacterial cocci

**Contributor's Comment:** The cause of death of this puppy is related to respiratory failure secondary to the severe pneumonia. There is evidence of concurrent viral and bacterial infections. Most sections exhibit colonies of bacterial cocci consistent with *Streptococcus canis*, which was cultured from lung tissue collected at necropsy. The presence of intranuclear and intracytoplasmic inclusions in addition to syncytial formation is diagnostic for canine distemper virus. Morphologically, the character of some of the intranuclear inclusions was more consistent with adenovirus; additional ancillary testing confirmed a concurrent adenovirus infection in this puppy.

Individually, Canine distemper virus (CDV) is responsible for clinical disease from infection of the respiratory, gastrointestinal and central nervous systems. In uncomplicated cases, pathogenic strains cause bronchointerstitial pneumonia, gastroenteritis that can result in vomiting and diarrhea, and a non-suppurative encephalomyelitis with demyelination. The virus has a worldwide distribution and is particularly prevalent (and generally fatal) in areas where vaccination is not practiced.[4] In contrast, uncomplicated canine adenovirus-2 (CAV-2) infections are seldom fatal. CAV-2 is highly contagious and in uncomplicated cases results in transient respiratory infections characterized by high morbidity and low mortality. The most important role for CAV-2, from a pathogen standpoint, is to predispose the patient to bacterial infection, thus CAV-2 is an important etiological factor in the canine respiratory syndrome of "kennel cough." [4]

Co-infections with CDV and CAV-2 have been reported previously.[2,3,4] In fact, one retrospective study suggests that co-infections occur more frequently than were previously recognized.[3] The same study also indicated that histological examination alone is not as reliable for diagnosis of CDV and CAV-2 infections compared to coupling with ancillary virological testing, primarily because viral inclusions bodies cannot be demonstrated in all cases.[3]

Interestingly, this puppy as well as the subjects of the previous case reports [2, 4] had all been vaccinated for CDV and CAV. The development of infection and disease in the vaccinated dog may be related to vaccine failure, reversion of the vaccine strain, immune incompetence to respond to the vaccine, or perhaps infection occurred prior to vaccination.[2]

**AFIP Diagnosis:** Lung: Pneumonia, bronchointerstitial **(Fig. 1-1)**, necrotizing, multifocal to coalescing, severe, with syncytia **(Fig. 1-2)**, occasional colonies of coccobacilli, and eosinophilic intranuclear and intracytoplasmic inclusion bodies and large basophilic intranuclear inclusion bodies, etiologies consistent with canine morbillivirus and canine adenovirus type 2 **(Fig. 1-3)**

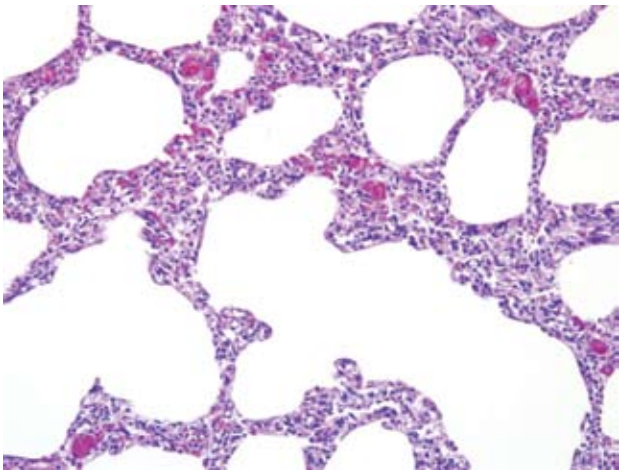

*1-1. Lung, Weimaraner. Alveolar septa are variably thicken by a cellular infiltrate and are congested. (HE 200X).*

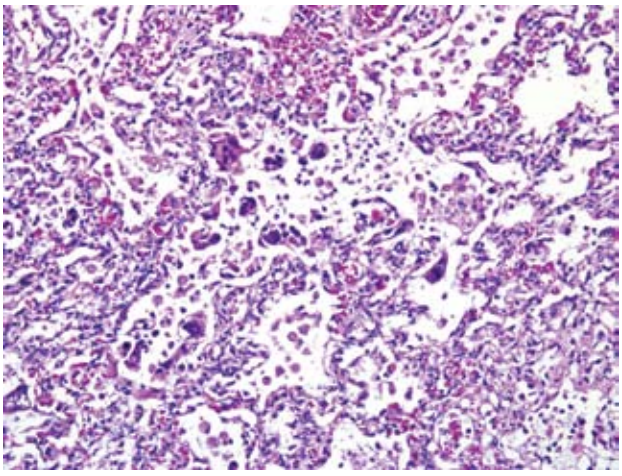

*1-2. Lung, Weimaraner. Low numbers of syncytial cells within the necrotic alveoli. (HE 200X).*

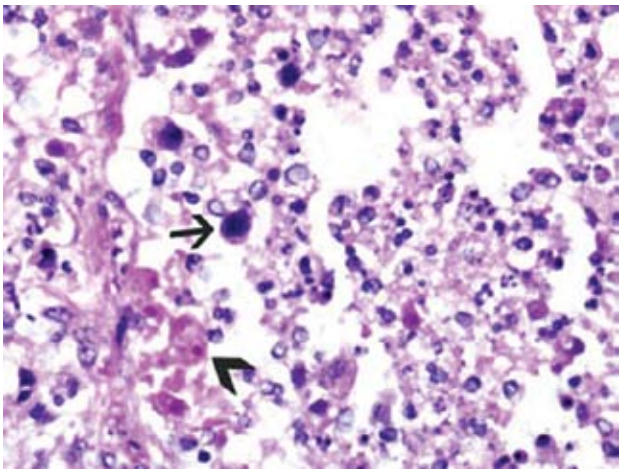

*1-3. Lung, Weimaraner. Within necrotic debris there are epithelial cells that contain large, 10-15 micron diameter, deeply basophilic intranuclear inclusion bodies (arrow). Rarely, within necrotic epithelial cells there are 6-8 micron diameter, eosinophilic intracytoplasmic inclusion bodies (arrowhead). (HE 400X).*

**Conference Comment:** Canine distemper virus (CDV), from the genus *Morbillivirus* in the family Paramyxoviridae, infects a wide range of species including canids, felids, procyonids, and mustelids, with ferrets being exquisitely sensitive to this virus. CDV is transmitted via inhalation of infected aerosols, and the virus enters macrophages within the respiratory tract within the first day of infection. The virus spreads to local lymph nodes and other lymphoid organs within 2-5 days post infection, and from there the virus uses the bloodstream to gain full access to its host. This stage of infection is critical in the development of CDV. If a strong cell mediated and humoral immune response is mounted, the virus is cleared by 14 days post infection with minimal to no viral shedding. If a partial immune response is mounted, the virus spreads to the respiratory and neurologic systems. Clinical signs may be minimal, but viral shedding due to infection of the epithelium of the respiratory tract are a sequelae. There may also be neurologic manifestations in dogs that mount a partial immune response. In dogs that mount a poor immune response, gastrointestinal, respiratory, and neurologic disease are the result with copious secretion of virus in feces, urine, and respiratory secretions.[1]

CDV is a unique virus because it is one of the few viruses that cause intranuclear and intracytoplasmic inclusions. Inclusion bodies within the central nervous system are eosinophilic and intranuclear. In other infected tissues, inclusions are usually intracytoplasmic. Inclusions are most obvious at 10-14 days post infection with waning visibility by 5-6 weeks post infection. Inclusions normally can be seen within the central nervous system after this initial 5-6 week period. Within infected cells of the respiratory tract, inclusions are most easily seen within bronchial and bronchiolar epithelial cells. Syncytia, if present, are a key diagnostic feature within affected epithelium. In acute disease, inclusions are often seen within the urinary bladder and renal pelvis transitional epithelium.[1]

**Contributing Institution:** Oklahoma Animal Disease Diagnostic Laboratory and Center for Veterinary Health Sciences, Oklahoma State University, Stillwater, OK. www.cvm.okstate.edu

**References**:
1. Caswell JL, Williams KJ: Respiratory system. *In:* Jubb, Kennedy and Palmer's Pathology of Domestic Animals, eds. Maxie ME, 5th ed., pp. 635-638. Elsevier, Philadelphia, PA, 2007
2. Chvala S, Benetka V, Mostl K, Zeugswetter F, Spergser J, Weissenbock H: Simultaneous canine distemper virus, canine adenovirus-2, and Mycoplasma cynos infection in a dog with pneumonia. Vet Pathol **44**:508-512, 2007
3. Damian M, Morales E, Salas G, Trigo FJ: Immunohistochemical detection for antigens of distemper, adenovirus and parainfluenza viruses in domestic dogs with pneumonia. J Comp Path **133**:289-293, 2005
4. Rodriguez-Tovar LE, Ramirez-Romero R, Valdez-Nava Y, Nevarez-Garza AM, Zarate-Ramos JJ, Lopes A: Combined distemper-adenoviral pneumonia in a dog. Can Vet J **48**:632-634, 2007

## CASE II – 47508 (AFIP3103923)

**Signalment:** 2-year-old, castrated male, Abyssinian cat (*Felis catus*)

**History:** The cat presented with a 2-week history of lethargy and anorexia. Echocardiography revealed pericardial effusion. The heart appeared normal. Pericardiocentesis was performed. The cat recovered normally from the procedure, but died shortly after.

**Gross Pathology:** The cat was in good nutritional condition. The pericardium contained approximately 2 ml of serosanguineous fluid with a moderate amount of fibrin loosely adhered to the epicardial surface. There was approximately 30 ml of serosanguineous pleural effusion. The abdomen contained approximately 60 ml of partially clotted blood, with blood clots adhered to a 5 x 20 mm rupture of the hepatic capsule (caused by resuscitation attempt). The spleen was enlarged, had a meaty consistency, and the cut surface showed numerous small pale grey foci, < 1 mm diameter. Mesenteric and ileocecocolic lymph nodes were moderately enlarged.

**Laboratory Results:** Analysis of the pericardial effusion revealed a nucleated cell count of less than 500 cells/µl. The cells were predominantly activated macrophages and nondegenerate neutrophils, with fewer mesothelial cells and small lymphocytes. Protein concentration was 4.8 g/dl. Based on these results the fluid was interpreted as a modified transudate.

**Histopathologic Description:** Heart: Marked vascular lesions are present in numerous small blood vessels of the left and right ventricular walls, and interventricular septum. In the free walls, the vascular changes are most prominent in the outer half of the myocardium. The vascular lesions are characterized by marked proliferation of plump spindle cells, resulting in mural thickening and luminal occlusion **(Fig. 2-1)**. Small clefts containing erythrocytes are present between the spindle cells. The spindle cells have indistinct borders and a small to moderate amount of pale eosinophilic cytoplasm. They have oval nuclei with finely stippled chromatin and one to two medium nucleoli. Mitoses are occasionally observed but are uncommon (less than 1 per 400x field). Cellular atypia is not observed. The affected vessels show occasional thrombosis **(Fig. 2-2)** and mild perivascular hemorrhages. There is mild multifocal degeneration and necrosis of myofibers, characterized by cytoplasmic hypereosinophilia and pyknosis. The epicardium is multifocally infiltrated by small numbers of lymphocytes and plasma cells, occasional siderophages, and rare neutrophils. There is hyperplasia and hypertrophy of mesothelial cells, and a small amount of fibrin is adhered to the epicardial surface multifocally.

Similar vascular lesions were present in the kidneys, lungs, pancreas, duodenum, diaphragm, cervical soft tissues, and leptomeninges. Sections from the enlarged spleen and lymph nodes revealed lymphoid hyperplasia.

Immunohistochemistry was performed on heart sections. Most spindle cells in the affected vessels showed membrane-associated expression of factor VIII-related antigen (FVIII-ra, figure 1). Fewer spindle cells showed cytoplasmic expression of smooth muscle actin (SMA, figure 2). The cells did not show expression of CD3 and CD79 **(figures 3 and 4)**.

**Contributor's Morphologic Diagnosis:** Heart, ventricular myocardium, small blood vessels: Atypical mural and occlusive spindle cell proliferation, with mild multifocal thrombosis, hemorrhage, and myocardial necrosis

**Contributor's Comment:** Histologic lesions and immunohistochemistry results are consistent with the condition recently described as feline systemic reactive angioendotheliomatosis (FSRA).

14 cases of FSRA have been described, and this appears to be a rare condition affecting exclusively domestic cats.[2,3,4,5] Similar multisystemic vascular lesions have not been described in other animal species. In all reported cases the diagnosis was obtained on post-mortem examination,

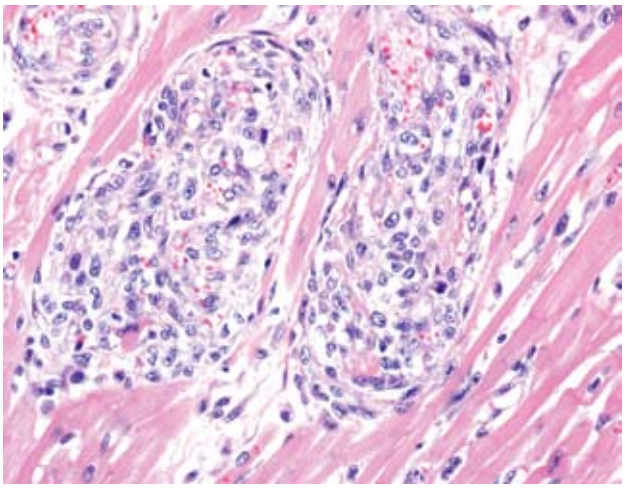

*2-1. Heart, Abyssinian, cat. Proliferations of spindle cells filling the lumina of small caliber arterioles Within the proliferation there are small slits and channels that contain few erythrocytes. (HE 400 X).*

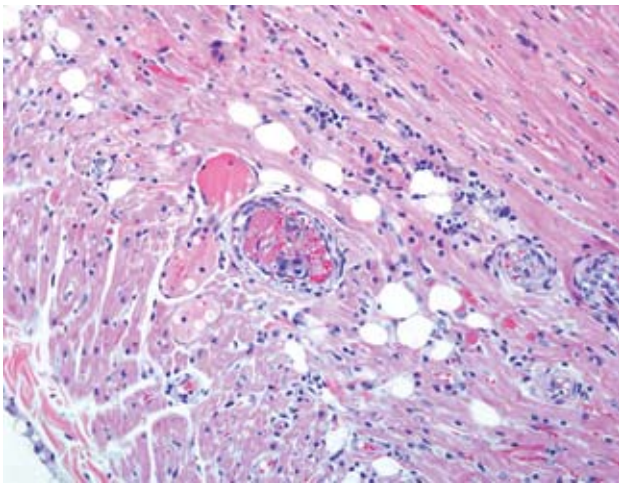

*2-2. Heart, Abyssinian, cat. Microthrombi partially or completely occlude the lumina. (HE 400X).*

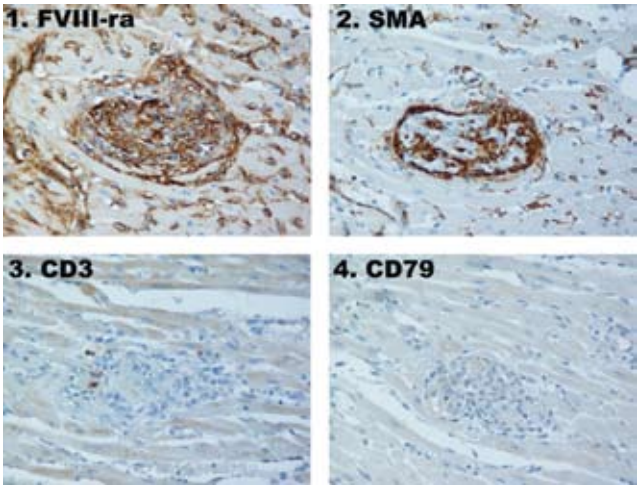


*2-3. Heart, Abyssinian, cat. The spindle cell population is immunohistochemically positive for factor VIII-ra and smooth muscle actin, but negative for CD3 and CD79.*
*Photomicrographs courtesy of Department of Pathology, The Animal Medical Center, New York, NY www.amcny.org*

after the cat died or was euthanized, usually following an acute illness. Affected cats were predominantly young adults, and males appeared more commonly affected. The clinical signs were variable, but most commonly included dyspnea, lethargy and anorexia. Gross lesions were also variable and nonspecific, but included pericardial and pleural effusion, pulmonary edema, and multifocal petechial and ecchymotic hemorrhages of various tissues. An atypical spindle cell proliferation affecting small blood vessels was always observed in the heart. Other commonly affected tissues included kidneys, spleen, lymph nodes, gastrointestinal tract, brain, meninges, eyes, and pancreas. The vascular histologic lesions described in the present case, and the immunohistochemical findings, are similar to those described in the published cases. Ultrastructural examination was described in two cats and revealed a mixture of two distinct types of spindle cells consistent with endothelial cells and pericytes.[4,5] The expression of FVIII-ra and SMA is also compatible with a mixed population composed of endothelial cells and pericytes. Based on the presence of two cell types and the lack of cellular atypia, FSRA is believed to represent a reactive proliferative process; it does not appear to be a neoplasm. While the exact cause of death was not clear in most cases, it has been suggested that heart failure probably occurs based on the consistent involvement of the heart, the evidence of perivascular ischemic myocardial necrosis, the presence of pleural and pericardial effusion, and pulmonary edema with alveolar histiocytosis in many cases.[4]

Histologically and immunohistochemically, FSRA is most similar to reactive angioendotheliomatosis (RAE), a rare human condition.[4] However, RAE in humans is a self-limiting lesion confined to the skin, while FSRA in cats is a multisystemic condition which has been associated with severe illness and death. No similar multisystemic disease has been described in humans. Other human vascular disorders characterized by mixed endothelial cell and pericyte proliferation include intravascular papillary endothelial hyperplasia, acroangiodermatitis (pseudo-Kaposi's sarcoma) glomeruloid hemangioma (POEMS syndrome), and some cases of chronic disseminated intravascular coagulation and thrombotic

thrombocytopenic purpura.[4] The pathogenesis of these lesions is complex and somewhat distinct for each disease, but possible mechanisms include an exaggerated response to thrombosis, an unusual residuum of immune-mediated vasculitis, and an exuberant angiogenesis possibly related to angiogenic cytokines and a dysfunctional endothelial regulation of coagulation and fibrinolysis.[4] In one case of FSRA, hematologic evaluation showed evidence of thrombotic thrombocytopenic purpura , but it remains unclear if this is a significant cause or mechanism in other feline cases. Some proliferative endothelial lesions in human are associated with specific infectious agents, particularly in AIDS patients.[4] Kaposi's sarcoma is caused by human herpesvirus-8, and bacillary angiomatosis is caused by *Bartonella henselae* and *B. quintana*. In the FSRA cases reported, serologic results were described for only two cats, and there was no evidence of infection by FIV, FeLV, or FIP virus. Silver stains and electron microscopy performed on the lesions from two cats did not show evidence of *Bartonella* spp. or any other infectious organisms.[4,5] The etiology and pathogenesis of FSRA remains unclear.

The term malignant angioendotheliomatosis has been used to describe intravascular angiotropic lymphoma in humans and animals. In humans, RAE has historically been confused with intravascular lymphoma. This case was not consistent with lymphoma based on cell morphology, and this was confirmed by the lack of expression of CD3 and CD79.

**AFIP Diagnosis:** Heart: Atypical endothelial proliferation (angioendotheliomatosis), multifocal, moderate, with few fibrin thrombi, rare myocardiocyte degeneration and necrosis, and minimal lymphoplasmacytic myocarditis

**Conference Comment:** The contributor's comments accurately and concisely describe the entity known as feline systemic reactive angioendotheliomatosis. A recent article in Veterinary Pathology described similar lesions in a Corriente steer that was persistently infected with bovine pestivirus (BVDV).[1] In this case, vascular lesions were seen in the heart, liver, lung, lymph nodes, kidney, adrenal gland, and brain, and consisted of glomeruloid spindle cell proliferations within arteriolar lumens. Spindle cells were immunopositive for smooth muscle actin and von-Willebrand factor and negative for CD3 and CD79a, consistent with FSRA.[1]

The pathogenesis of FSRA is still unknown, but it is hypothesized that a reactive response to thrombosis, vasculitits, or an infectious agent is the cause.[1]

**Contributing Institution:** Department of Pathology, The Animal Medical Center, New York, NY www.amcny.org

**References:**

1. Breshears, MA, Johnson BJ: Systemic reactive angioendotheliomatosis-like syndrome in a steer presumed to be persistently infected with bovine viral diarrhea virus. Vet Pathol **45**:645-649, 2008
2. Cooley AJ, Rushton SD, Porterfield ML, Tice CA: Arteriolar endothelial proliferation and microthrombosis attributed to thrombotic thrombocytopenic purpura in two cats. Vet Pathol **41**:576, 2004
3. Dunn KA, Smith KC, Blunden AS: Fatal multisystemic intravascular lesions in a cat. Vet Rec **140**:128-129, 1997
4. Fuji RN, Patton KM, Steinbach TJ, Schulman FY, Bradley GA, Brown TT, Wilson EA, Summers BA: Feline systemic reactive angioendotheliomatosis: Eight cases and literature review. Vet Pathol **42**:608-617, 2005
5. Rothwell TL, Xu FN, Wills EJ, Middleton DJ, Bow JL, Smith JS, Davies JS: Unusual multisystemic vascular lesions in a cat. Vet Pathol **22**:510-512, 1985

## CASE III – 06-47-18 (AFIP 3102492)

**Signalment:** Fingerlings (0+) (12.1 cm; 21.8 g) of Rainbow trout (*Oncorhynchus mykiss*)

**History:** Recorded mortality in previous 3 months: 7.9%, 20.7% and 4.3%. Clinical signs reported (variable): exophthalmos, cutaneous ulcers and pale gills. No treatment attempted. 12 fingerlings submitted alive for necropsy.

**Gross Pathology:** Exopthalmos, cutaneous ulcers and kidneys with multiple pale nodules (granulomas)

**Laboratory Results:** Routine bacteriology (trypticase soy) on kidneys: negative. Numerous small Gram-positive rods observed in tissue smears.

**Histopathologic Description:** A large portion of the posterior kidney parenchyma is effaced by a granulomatous infiltrate with areas of necrosis **(Fig. 3-1)**. There is loss of epithelial and hematopoietic elements. Myriads of small bacilli can be seen in macrophages, but are better seen in Gram-stained sections. The bacilli are Gram-positive **(Fig. 3-2)** and non-acid-Fast (Ziehl-Neelsen and Fite-Faraco).

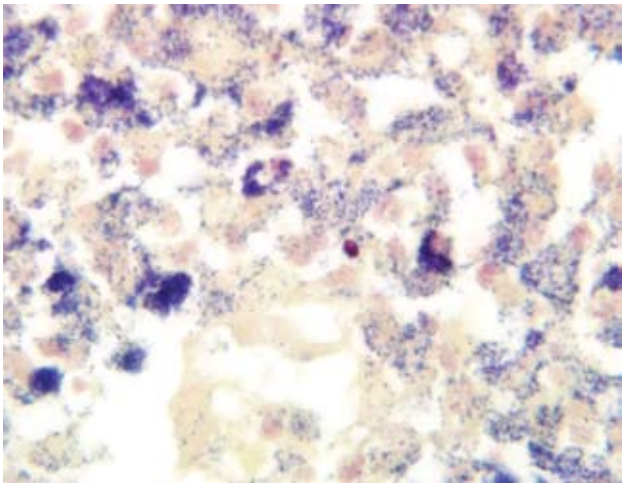

*3-1. Kidney, rainbow trout. Numerous 0.5-1 micron diameter gram positive cocci within histiocytes and extracellularly. (B&B 600X).*

**Contributor's Morphologic Diagnosis:** Kidney: Granulomatous nephritis with myriads of intra-histiocytic Gram-positive bacilli, compatible with *Renibacterium salmoninarum* (bacterial kidney disease / BKD)

**Contributor's Comment:** Based on the typical lesions and absence of growth in routine bacteriology of kidneys, bacterial kidney disease (BKD) was diagnosed. Confirmation by bacteriology (special medium) FA or ELISA was not done in this case since *Renibacterium salmoninarum* was previously identified in this particular facility; furthermore, histopathology coupled with negative results on routine bacteriology is almost pathognomonic for BKD. The two bacterium that could be confused with R. salmoninarum are *Carnobacterium (Lactobacillus) piscicola*, the agent of pseudokidney disease [1, 2], and atypical mycobacteria. *Carnobacterium piscicola* rapidly grows at 30ºC on trypticase soy or brain-heart infusion agar [1, 2], and the atypical mycobacteria are acid-fast and unevenly Gram-positive.

*Renibacterium salmoninarum*, the etiologic agent of bacterial kidney disease (BKD) is an important pathogen of salmonids, including rainbow trout. Horizontal and vertical transmission occurs. BKD is a chronic infection but stress can result in acute mortalities. There is no proven effective treatment. Prevention relies on identification of infected broodstock (asymptomatic carriers).[1, 2]

Gross lesions include dark discoloration of fish, exophthalmoses, pale gills, abdominal distension and cutaneous vesicles/ulcers, but the most consistent and typical lesion is the presence of multiple whitish nodules in the kidney (and occasionally in other viscera). Fibrinous pericarditis and large cavitations in muscle can also be seen.[2] The typical microscopic lesion is pyogranulomatous to granulomatous inflammation in the affected organ/tissue, with variable numbers of intra-histiocytic small Gram-positive rods; necrosis can be seen, and is sometimes prominent. While histopathology gives a strong presumptive diagnosis, confirmation relies on bacteriology, FA or ELISA. Bacteriology is not very practical, as *R. salmoninarum* is fastidious, very slow-growing and requires a non-commercially available medium. As mentioned previously, the only differential diagnosis is pseudokidney disease caused by *Carnobacterium (Lactobacillus) piscicola* [1]; this bacterium can be grown using routine bacteriologic techniques.

**AFIP Diagnosis:** Kidney, posterior: Nephritis, necrotizing, granulomatous, diffuse, severe, with myriad intrahistiocytic bacteria, rainbow trout (*Oncorhynchus mykiss*), piscine

**Conference Comment:** The contributor gives an excellent overview of *Renibacterium salmoniarum* infection. *Renibacterium salmoninarum* is a gram-positive, nonmotile, non-acid-fast aerobic rod which is frequently seen in pairs. This disease has only been reported in salmonids.[1] BKD generally affects grown fish over 6 months of age, which makes it a particularly harmful and economically damaging agent.[1] Several means of transmission have been reported and include water contamination, skin abrasions, or eating of contaminated foodstuffs. Once *Renibacterium salmoninarum* gains entry into a salmonid, the bacteria are taken up by macrophages and proliferate inside their new host. It is unclear how the bacteria avoid destruction within the marcophage. Stress is thought to be a precursor to clinical disease.[1]

**Contributing Institution:** Department of Pathology and Microbiology, Faculty of Veterinary Medicine, University of Montreal, C.P. 5000, Saint-Hyacinthe, P. Quebec, Canada J2S 7C6, http://www.medvet.umontreal.ca

**References:**

1. Noga EJ: Bacterial kidney disease (problem 52), Mycobacteriosis (problem 53) and miscellaneous systemic bacterial infections. *In:* Fish Disease: Diagnosis and Treatment, Noga EJ, 1st ed., pp. 153-162. Iowa State University Press, Ames, IA, 2000

2. Reimschuessel R, Ferguson HW: Kidney (Chapter Four). *In:* Systemic Pathology of Fish: A text and atlas of normal tissues in teleosts and their responses in disease, ed. Ferguson HW, 2nd ed., pp. 91-119, Scotian Press, 2006

**CASE IV - 208 0491 (AFIP 3103337)**

**Signalment:** 10-year-old, neutered male, orange tabby cat (*Felis catus*)

**History:** Generalized edema that progressed to extremities. Euthanized.

**Laboratory Results:** Immunohistochemistry – Greater than 90% of neoplastic cells had strong to weak, diffuse, intracytoplasmic labeling with both CD31 and Factor VIII markers.

**Gross Pathology:** Red to gold, serous fluid with crepitus and occasional fibrin tags extends the subcutaneous tissues of the entire body with the exception of the head. The legs and feet are edematous and swollen due to the subcutaneous fluid. The thoracic cavity contains approximately 25 ml of clear orange to pink serous fluid (specific gravity 1.022).

**Histopathologic Description:** Diffusely expanding the subcutis and multifocally infiltrating the musculature is a non-encapsulated, poorly demarcated, moderately cellular neoplasm that forms numerous clefts and variably formed channels supported by a collagenous and fibrous stroma **(Fig. 4-1)**. Cells have distinct cell borders, and are pleomorphic to spindloid. There is scant to moderate amounts of amphophilic, finely granular cytoplasm, round to oval basophilic nuclei, and finely stippled chromatin with an occasional single magenta nucleolus. There are rare mitotic figures. Moderate anisocytosis and anisokaryosis is present. Channels are filled with variable numbers of erythrocytes. There are scattered lymphohistiocytic infiltrates, multifocal areas of hemorrhage, edema, and myocyte degeneration.

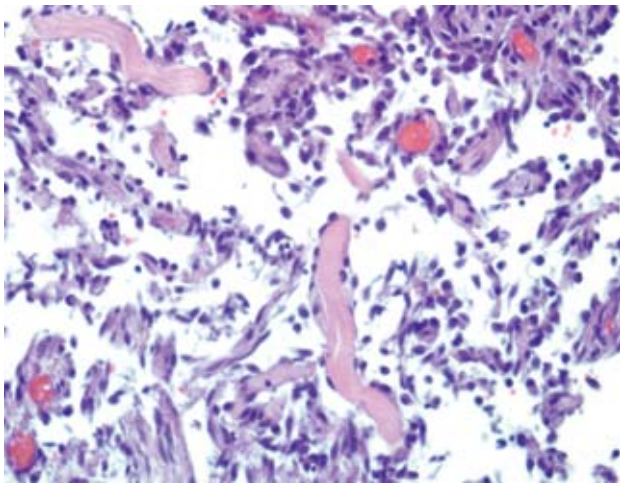

*4-1. Fibroadipose tissue and skeletal muscle, cat. Infiltrating the skeletal muscle and fibroadipose tissue is a spindle cell neoplasm that often wraps collagen bundles and forms and lines vague clefts and channels. (HE 400X).*

**Contributor's Morphologic Diagnosis:** Subcutis: Feline ventral abdominal angiosarcoma

**Contributor's Comment:** Feline abdominal angiosarcoma is a rare, malignant tumor of vascular endothelial origin, which typically only occurs in the dermis and subcutis of cats. Controversy exists as to whether the endothelial cell proliferation is of lymphatic or blood vessel origin.[2,3] The term angiosarcoma is used to avoid this confusion. Although a palpable distinct mass is usually not discernible, the neoplasm may vary in texture from gelatinous and soft to hard.[2,3] Grossly, the cut surface of the lesion may appear to have red or black discoloration and seep serosanguineous fluid.[2,3] However, in this case, widespread edema with occasional fibrin tags was the only clinical sign. There was no discernable mass. Typically, a preliminary diagnosis is established on anatomical location, clinical history, gross appearance, and histological features. Immunohistochemistry may be used to confirm the endothelial origin of the tumor using a CD31 and factor VIII antibody staining protocol.[3,4] Our case was positive for both CD31 and factor VIII. Although metastasis is rare, the prognosis is poor due to its extensive infiltrative growth and frequent recurrences.[2,3,6] The only recognized treatment is repeated surgical excision.[2] Hemangiosarcomas have also been reported in the cow, horse, pig, goat, and sheep.[4,8]

**AFIP Diagnosis:** Fibro-adipose tissue and skeletal muscle: Feline ventral abdominal angiosarcoma

**Conference Comment:** The contributor's comments accurately and concisely give a general overview of feline ventral abdominal angiosarcoma.

As noted by the contributor, there is controversy whether this neoplasm arises from blood capillary endothelium or lymphatic endothelium. Immunohistochemical staining for lymphatic vessel endothelial receptor-1 (LYVE-1), a marker unique to lymphatic endothelial cells, and the ultrastructural features are strong evidence that these neoplasms are of lymphatic origin.[1] The term 'feline abdominal lymphangiosarcoma' has been proposed.[1] These tumors form vascular clefts and cavernous channels supported by collagenous connective tissue.[5] A papilliferous growth pattern was noted in 11 of 12 cases in a retrospective study, with multifocal areas containing fusiform and polygonal cells densely packed together.[5] Differentials for this neoplasm include lymphangiomatosis

and hemangiosarcoma. Pleomorphic lymphatic endothelial cells lining vascular channels as well as blind ending trabeculae and a very aggressive, invasive growth pattern separate this neoplasm from lymphangiomatosis, which is considered a developmental disorder wherein the lymphatic system does not form proper communicating channels with the venous system.[3] Electron microscopy is useful in differentiating lymphangiosarcoma and hemangiosarcoma. Ultrastructurally, lymphatic vessels have a discontinuous basement membrane, while hemangiosarcomas have an uninterrupted basement membrane.[3] Useful immunohistochemical stains for lymphangiosarcoma include lymphatic vessel endothelial receptor-1 (LYVE-1), vascular endothelial growth factor receptor -3 (VEGFR-3), and podoplanin because they are purportedly markers unique for lymphatic endothelial cells.[1]

**Contributing Institution:** San Diego County Animal Disease Diagnostic Laboratory, 5555 Overland Avenue Bldg. #4, San Diego, CA 92123

**References:**

1. Galeotti F, Barzagli F, Vercelli A, Millanta F, Polil A, Jackson DG, Abramo F: Feline lymphangiosarcoma – definitive identification using a lymphatic vascular marker. Vet Dermatol **15**:13-18, 2004

2. Goldschmidt MH, Hendrick MJ: Tumors of Skin and Soft Tissues. *In:* Tumors in Domestic Animals, ed. Meuten DJ, 4th ed., pp.102-103. Blackwell Publishing Company, Ames, IA, 2002

3. Gross TL, Ihrke PJ, Walder EJ, Affolter VK: Mesenchymal Neoplasms and Other Tumors. *In:* Skin Diseases of the Dog and Cat, 2nd ed., pp. 748-756. Blackwell Publishing, Ames, IA, 2005

4. Ginn PE, Mansell JEKL, Rakich PM: Skin and Appendages. *In:* Pathology of Domestic Animals, ed. Maxie MG, 5th ed., pp. 767-768. Elsevier Saunders, Philadelphia, PA, 2007

5. Hinrichs U, Puhl S, Rutteman GR, Van Der Linde-Sipman JS, Van Den Ingh TSGAM: Lymphangiosarcomas in cats: a retrospective study of 12 cases. Vet Pathol **36**:164-167, 1999

6. Johannes CM, Henry CJ, Turnquist SE, et al: Hemangiosarcoma in cats: 53 cases (1992-2002). J Am Vet Med Assoc **231**(12):1851-6, 2007

7. McAbee KP, Ludwig LL, Bergman PJ, Newman SJ: Feline cutaneous hemangiosarcoma: a retrospective study of 18 cases (1998-2003). J Am Anim Hosp Assoc **41**(2):110-6, 2005

8. Schultheiss PC: A retrospective study of visceral and nonvisceral hemangiosarcoma and hemangiomas in domestic animals. J Vet Diagn Invest **16**:522-526, 2004

**NOTES:**

The Armed Forces Institute of Pathology
Department of Veterinary Pathology

*Conference Coordinator:*
Todd M. Bell, DVM

WEDNESDAY SLIDE CONFERENCE 2008-2009

# Conference 4

01 October 2008

***Conference Moderator:***

Taylor Chance, DVM, Diplomate ACVP

## CASE I – 08-0013-03 (AFIP 3102187)

**Signalment:** 18-year-old, male, pony, equine (*Equus caballus*)

**History:** This pony had a history of progressive apathy and loss of appetite. Medical treatments provided by its veterinarian failed to improve the condition. Two months after the beginning of treatment, the pony was referred to the National Veterinary School of Alfort for severe wasting, rigidity of the gait, edema of the hindlimbs and a cardiac murmur. Echocardiogram and Doppler measurements revealed a moderate aortic stenosis without apparent cardiac repercussion. The ultrasonic examination of the abdominal cavity revealed parenchymal heterogeneity of the left kidney and several voluminous abdominal masses. The patient was euthanized due to poor prognosis, poor condition, and for economical reasons. It was then submitted to necropsy.

**Gross Pathology:** A general severe amyotrophy and a mild dehydratation were noted at necropsy. Approximately 200 mL of a clear red-tinged fluid was present in the peritoneal cavity (ascites). Multiple nodules of mineralization were observed in the hepatic parenchyma accompanied by a multifocal villous perihepatitis, probably secondary to migration of strongyle larvae.

A bilateral cryptorchidism was detected with both testicles being in an intra-abdominal position. The left testicle was severely enlarged (10 x 12 x 20 cm), lobulated, white and moderately firm with foci of haemorrhage and mineralization **(Figs 1-1, 1-2)**. Another mass of similar size and consistency was detected in the left iliac region (most likely left iliac lymph node) around the left ureter and left iliac artery, and vein. Multiple white and moderately firm nodules were attached to the splenic hilus. We made a tentative gross morphologic diagnosis of seminoma with nodal and splenic (most likely by transcoelomic implantation) metastases **(Fig 1-3)**.

Multifocal endocardial mineralizations, appearing as plaques were observed in the ventricles and atria, particulary in the left side, and in the aortic intima. Mineralization was severe on the sigmoid aortic valves. Multifocal myocardial necrosis and mineralizations were suspected as well. The tracheal mucosa contained small mineralized granules, giving it an appearance of abrasive paper. Mineralizations were also observed in the renal cortex of both kidneys. As parathyroid glands were macroscopically normal, we suspected these lesions to be metastatic calcifications due to humoral hypercalcemia of

*Sponsored by the American Veterinary Medical Association, the American College of Veterinary Pathologists, and the C. L. Davis Foundation.

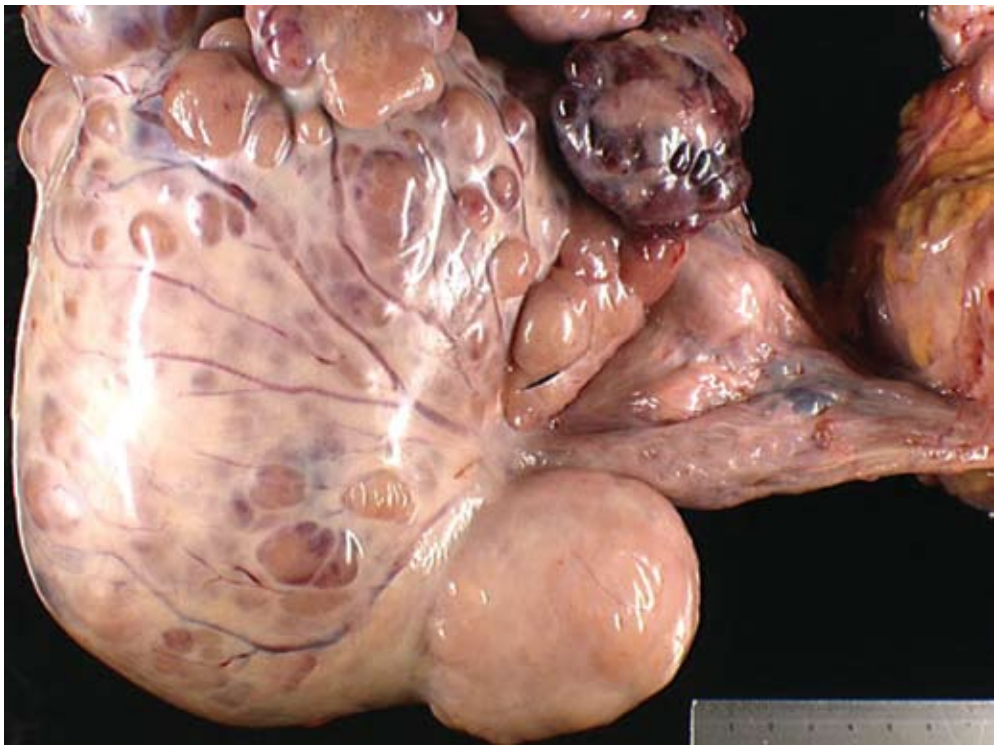

*1-1. Testicle, horse. Seminoma of the left testis.*
*Photograph courtesy of National Veterinary School of Alfort (France) ECOLE NATIONALE VETERINAIRE D'ALFORT Unité d'Histologie et d'Anatomie Pathologique 7, avenue du Général de Gaulle 94704 Maisons-Alfort Cedex France.*

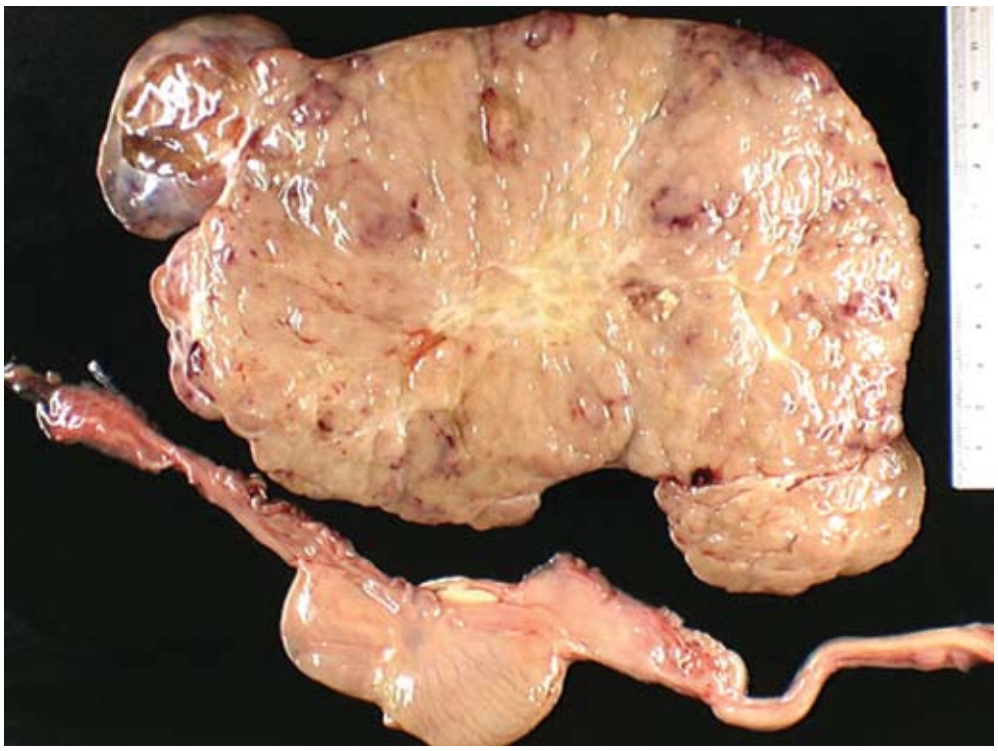

*1-2. Testicle, horse. Seminoma in left testicle (top) with hypoplastic right testicle (bottom). Note the overall conserved shape of the left testicle with its epididymis despite the massive tumoral infiltration. Foci of necrosis, haemorrhage and mineralization are present in the left testis.*
*Photograph courtesy of National Veterinary School of Alfort (France) ECOLE NATIONALE VETERINAIRE D'ALFORT Unité d'Histologie et d'Anatomie Pathologique 7, avenue du Général de Gaulle 94704 Maisons-Alfort Cedex France.*

*1-3. Spleen, horse. Metastasis of seminoma in the splenic hilus. Photograph courtesy of National Veterinary School of Alfort (France) ECOLE NATIONALE VETERINAIRE D'ALFORT Unité d'Histologie et d'Anatomie Pathologique 7, avenue du Général de Gaulle 94704 Maisons-Alfort Cedex France.*

malignancy **(Figs. 1-7, 1-8, 1-9, 1-10)** (see Contributor's Comment).

The right testicle was moderately reduced in size (6 x 3 x 3 cm) with a spongy consistency **(Fig. 1-2)**. We made a tentative gross diagnosis of testicular hypoplasia.

Subcutaneous tissue in caudoventral abdomen and hindlimbs was severely edematous. Because of tumoral involvement of the left iliac nodes and vessels, we hypothesized the acquired lymphedema was secondary to obstruction of lymph flow by the neoplasm.

**Histopathologic Description:** ***Left testicle:*** An encapsulated and well-demarcated tumoral proliferation with high cellular density infiltrates effaces the testicular parenchyma sparing some epididymal tubules (not present in all slides). Multifocally, infiltration of the testicular capsule is observed. Neoplastic cells are arranged in densely packed sheets, nests, and lobules on a fine fibrovascular stroma. Cells are non-cohesive, round, and 20 to 25 µm in diameter with indistinct cell borders. Nuclei are centrally located, large, oval, vesiculate, and contain one prominent eosinophilic nucleolus and marginalized finely reticulated chromatin. The cytoplasm is abundant, eosinophilic, and finely granular. There is marked anisocytosis/anisokaryosis and a moderately high mitotic index (2-3 mitoses per HPF). There is multifocal individual cell necrosis ("starry-sky pattern") **(Figs. 1-4, 1-5)**. Only a few lymphocytes are present between the tumoral cells. Some foci of mineralization are also observed.

***Spleen:*** The peritoneal side of the splenic capsule is infiltrated by a similar tumoral proliferation (not obvious in all slides). Intimal bodies and diffuse intimal mineralizations are prominent in some arteries.

***Right testicle:*** Testicular tubules are rarefied and separated by large bundles of a dense, mature fibrous connective tissue. They have a markedly diminished number of germinal cells and no spermatozoa with normal to mildly decreased numbers of Sertoli cells, interstitial cells and efferent ductules. Basal membranes of tubules are normal in thickness and are not obviously wrinkled. Some interstitial cells contain brown granular pigments (probably lipofuscin granules).

**Contributor's Morphologic Diagnosis:**
Left testicle: Seminoma, diffuse-type
Splenic capsule: Metastasis of seminoma
Right testicle: Testicular hypolasia

**Contributor's Comment:** This case highlights the relationship between cryptorchidism and testicular tumor development and hypoplasia.

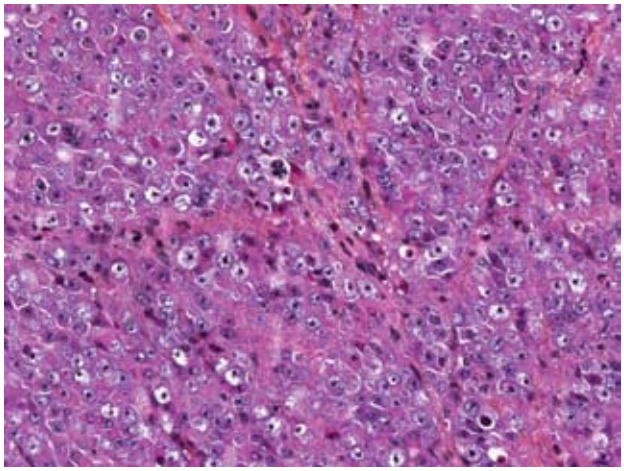

*1-4. Testicle, horse. Seminoma. Normal testicular architecture is effeced byround to polygonal cells with variably distinct cell borders, moderate amounts of eosinophilic granular cytoplasm and generally round nuclei with prominent nucleoli. Mitotic figures range from 3-5 per HPF. (Safranin 200X).* *Photomicrograph courtesy of National Veterinary School of Alfort (France) ECOLE NATIONALE VETERINAIRE D'ALFORT Unité d'Histologie et d'Anatomie Pathologique 7, avenue du Général de Gaulle 94704 Maisons-Alfort Cedex France.*

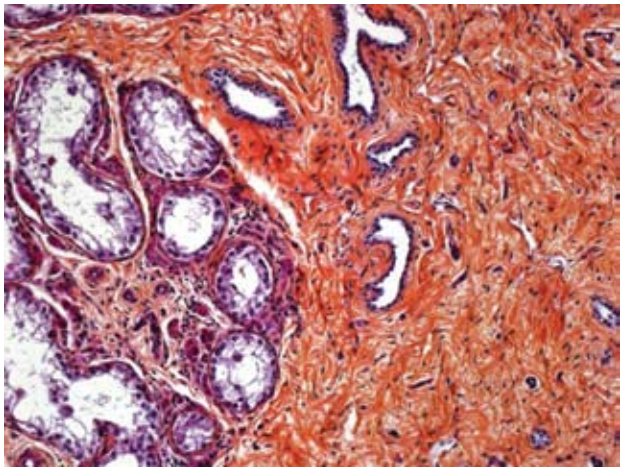

*1-6. Testicle, horse. Hypoplastic contralateral testicle characterized by few small seminiferous tubules with thickened basement membranes, decreased germinal cells, vaculated Sertoli cells, and prominent interstitial fibrosis. (Safranin 400X).* *Photomicrograph courtesy of National Veterinary School of Alfort (France) ECOLE NATIONALE VETERINAIRE D'ALFORT Unité d'Histologie et d'Anatomie Pathologique 7, avenue du Général de Gaulle 94704 Maisons-Alfort Cedex France.*

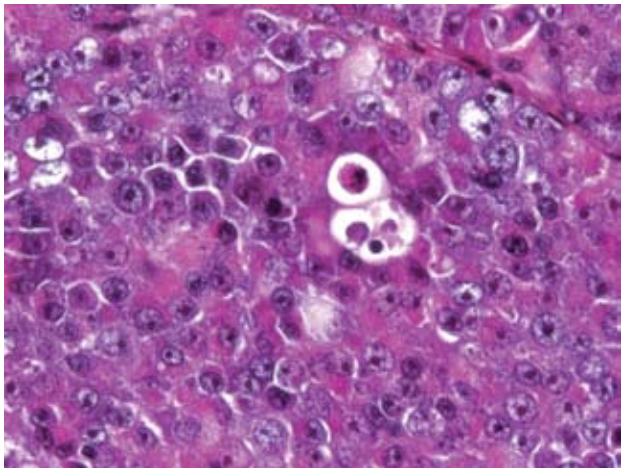

*1-5. Testicle, horse. Seminoma. Higher magnification demonstrating single cell necrosis. (Safranin 400X).* *Photograph courtesy of National Veterinary School of Alfort (France) ECOLE NATIONALE VETERINAIRE D'ALFORT Unité d'Histologie et d'Anatomie Pathologique 7, avenue du Général de Gaulle 94704 Maisons-Alfort Cedex France.*

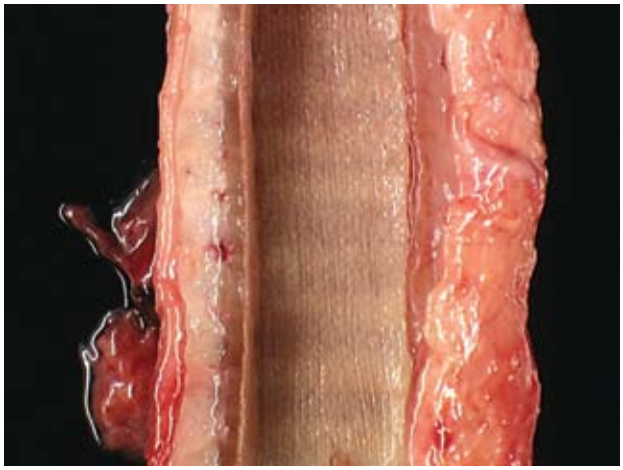

*1-7. Trachea, horse. The tracheal mucosa contains small mineralized granules, giving it an appearance of abrasive paper.* *Photograph courtesy of National Veterinary School of Alfort (France) ECOLE NATIONALE VETERINAIRE D'ALFORT Unité d'Histologie et d'Anatomie Pathologique 7, avenue du Général de Gaulle 94704 Maisons-Alfort Cedex France.*

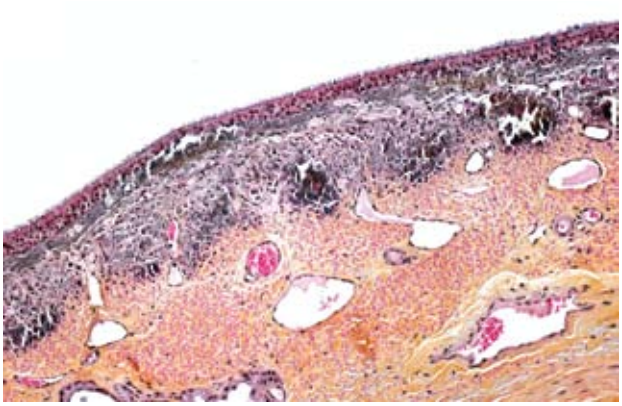

*1-8. Trachea, horse. Diffuse mineralization in the tracheal mucosa.* *Photomicrograph courtesy of National Veterinary School of Alfort (France) ECOLE NATIONALE VETERINAIRE D'ALFORT Unité d'Histologie et d'Anatomie Pathologique 7, avenue du Général de Gaulle 94704 Maisons-Alfort Cedex France.*

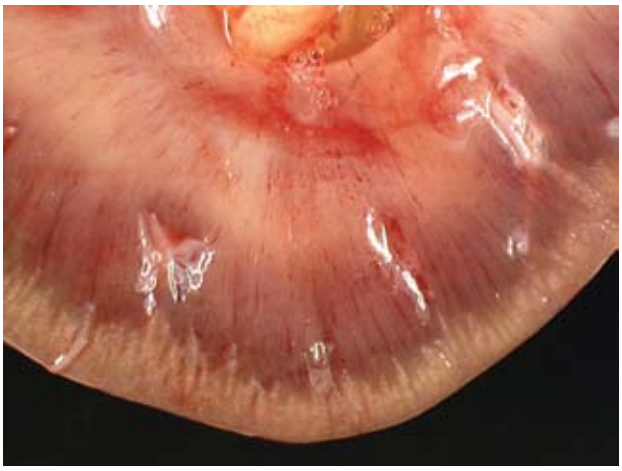

*1-10. Kidney, horse. Mineralizations in renal tubular and glomerular basement membranes (hypercalcemic nephropathy).* *Photomicrograph courtesy of National Veterinary School of Alfort (France) ECOLE NATIONALE VETERINAIRE D'ALFORT Unité d'Histologie et d'Anatomie Pathologique 7, avenue du Général de Gaulle 94704 Maisons-Alfort Cedex France.*

Primary testicular tumors may be classified as *sex-cord stromal (gonadal stromal) tumors*, which include Leydig (or interstitial) cell tumor and Sertoli cell tumor, and *germ cell tumors*, which include seminoma, embryonal carcinoma and teratoma. *Mixed germ cell-sex cord stromal tumors* are rare and include gonablastoma. Tumors derived from other testicular elements such as mesothelioma, hemangioma, fibroma and their malignant counterparts are infrequent.

Seminomas are common in canine and equine testis. They occur less frequently in the ram, buck and bull.

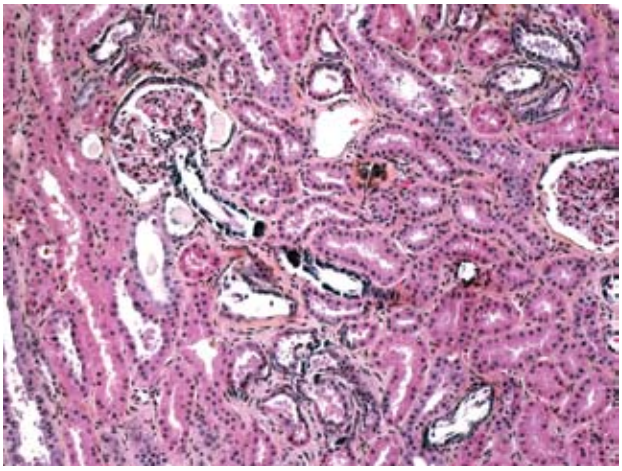

*1-9. Kidney, horse. Mineralizations in the renal cortex. Photograph courtesy of National Veterinary School of Alfort (France) ECOLE NATIONALE VETERINAIRE D'ALFORT Unité d'Histologie et d'Anatomie Pathologique 7, avenue du Général de Gaulle 94704 Maisons-Alfort Cedex France.*

This type of tumor is mostly seen in older animals and is very common in cryptorchid testicles.[2,6] Seminoma is the second most common canine testicular neoplasm and the most common testicular neoplasm in the aged stallion.[2,3,6] Clinically, this type of tumor can be recognised in horses by ultrasonic examination. A diffuse heterogeneous appearance with diffuse hypoechogenicity of the testis and ill-defined nodular regions of hyperechogenicity are characteristic of equine seminomas.[1]

Seminomas develop presumably from basal spermatogonia of the seminiferous tubules. These tumors are seldom malignant and show no hormone production; however, they tend to be locally invasive and there is no known factor to predict their metastatic potential. The actual WHO Classification of Domestic Animals does not recognize a traditional distinction between benign and malignant forms of seminomas, the term "seminoma" being applied for both. This may reflect in part the influence of human pathology where seminomas are considered malignant (see below). Because of their tendency to be locally invasive with rare metastasis in domestic animals, we should regard them as tumors of generally low malignancy; however, they are more likely to have malignant behaviour than Sertoli and Leydig cell tumors, particularly in dogs and horses.[2,6]

Seminomas are classified on their histological appearance into the intratubular type or the diffuse type. The earliest development of the tumor is intratubular. Rupture of tubules occurs and the growth becomes confluent, forming broad sheets of closely packed cells. Although

not prominent in this case, focal or diffuse accumulation of CD8-positive lymphocytes occurs in most seminomas and is a useful diagnostic feature.[2,4,6] Germ cells express vimentin in a perinuclear pattern, but no expression of neuron-specific enolase nor cytokeratin can be detected by immunohistochemistry. Tumoral cells examined by electron microscopy resemble normal germinal epithelium. A relative scarcity of cytoplasmic organelles, oval nuclei, straight cell borders and a distinct Golgi apparatus are characteristic features of seminomas.[2] Differential diagnosis on histological examination includes other round cell tumors, particularly malignant lymphoma.

Macroscopically, involved testicles are enlarged, soft to moderately firm (not as firm as Sertoli cell tumors). On cut surface, the tumor has a homogeneous glistening gray/white appearance, resembling lymphoid neoplasms.[2,6]

In humans, the actual WHO classification of germ cell tumors is more complex:

Intratubular germ cell neoplasia, unclassified (IGCNU) [2]
Other types

***Tumors of one histological type (pure forms)***
Seminoma (3)
    Cribriform, pseudoglandular and tubular variant
    Seminoma with syncytiotrophoblastic cells
Spermatocytic seminoma (3)
    Spermatocytic seminoma with sarcoma
Embryonal carcinoma (3)
Yolk sac tumor (3)
Trophoblastic tumor
    Choriocarcinoma (3)
    Trophoblastic neoplasms other than choriocarcinoma
        Monophasic choriocarcinoma
        Placental site trophoblastic tumor (1)
Teratoma (3)
    Dermoid cyst 0
    Monodermal teratoma
    Teratoma with somatic type malignancies (3)

***Tumors of more than one histological type (mixed forms)***
Mixed embryonal carcinoma and teratoma (3)
Mixed teratoma and seminoma (3)
Choriocarcinoma and teratoma/embryonal carcinoma (3)
Others

Figure 1: Human WHO classification of germ cell tumors of the testicle [9]
(0) = benign; (1) = borderline or uncertain behaviour; (2) = Carcinoma in situ or grade III intraepithelial neoplasia; (3) = malignant

Intratubular germ cell neoplasia, unclassified type (IGCNU), is equivalent to carcinoma in situ or intratubular preinvasive tumor but is different from an intratubular seminoma. It is regarded as a precursor lesion and is associated with cryptorchidism or others conditions. Although potentially present in all species, this entity has not yet been described in domestic animals except, interestingly, in horses.[8]

**Cryptorchidism** is defined as an incomplete descent of the testis and associated structures into the scrotum and is one of most common abnormalities of the male reproductive system (the most common in cats and horses). Complete testicular descent usually occurs prior to birth in most species, except in dogs. Retained testes lack spermatogenesis and fertility may be compromised. Three main stages are defined during the testicular descent: transabdominal migration phase, intra-inguinal phase and extra-inguinal migration. The regulation of descent involves the Müllerian inhibitory substance in the first phase, increased intra-abdominal pressure in the second phase, interaction of androgen, calcitonin gene-related protein, and other factors in the last stage of migration. Thus, multiple mechanisms can be responsible for cryptorchidism.

An association between testicular neoplasia and cryptorchidism is well recognized in several species, especially in dogs. Dogs with abdominally retained testes are most likely to develop Sertoli cell tumor. Seminoma is the second most common type of tumor of abdominally retained testes in the dog. In stallions, retained testicles are prone to develop into seminoma (most likely) or teratoma. Cryptorchidism also predisposes to testicular torsion in dogs and stallions, particularly if there is tumoral involvement. Cryptorchidism also occurs in boars, bulls and rams.[2,6] Table 1-1 outlines the main characteristics of cryptorchidism in domestic animals.

| Species | Predisposed breeds | Causes | Features |
|---|---|---|---|
| Cat | Mostly Persians | Unknown | Mostly unilateral with no side nor site predilection |
| Dog | Various | Autosomal recessive suspected in some breeds | Other diseases associated. Right side and inguinal location mainly |
| | Miniature Schnauzer | Persistent Müllerian duct syndrome (Müllerian duct inhibitory substance insensitivity) | Unilateral or bilateral |
| Boar | Duroc | Hereditary, recessive (several locus may be involved in Durocs) Mainly due to abnormal development of the gubernaculums | |
| Bull | Polled Hereford and Shorthorn | Hereditary | Mostly in inguinal region. Left testis twice as often affected than right |
| Ram | Polled animals | Autosomal recessive or dominant with incomplete penetrance | Mostly unilateral and involving right testis |
| Buck | Polled Saanen | Goat polled/intersex syndrome | Right testis mostly |
| Stallion | No breed predisposition | Unknown | Mainly unilateral. Left testis mostly abdominal and right testis mostly inguinal |

**Table 1-1: Main characteristics of cryptorchidism in domestic animals [2]**

*Testicular hypoplasia* is defined as testes that have failed to grow to normal size and is associated with either cryptorchidism, some intersex conditions, or as an isolated lesion. It can be unilateral or bilateral, and the affected testis can be smaller or of similar size compared to the normal testis. Etiology is often multifactorial and can have a hereditary basis. In humans and mice, a deficiency of gonadotrophins (hypogonadotrophic hypogonadism) has been associated with testicular hypoplasia. However, LH and FSH are normal and even elevated in studies concerning domestic animals. Abnormal migration of germ cells to the genital ridge in utero, development arrest, or excessive apoptosis play an important role in some forms of the condition. Histologically, there are reduced numbers, length, and/or diameter of tubules. Germ cells may be present or absent, and if present fail to produce spermatozoa. Basement membranes are not particularly wrinkled nor thickened as in testicular atrophy/degeneration.[2] Table 1-2 outlines the main causes of testicular hypoplasia in domestic animals.

| Species | Causes |
|---|---|
| Cat | Sporadic<br>Cryptorchid and tricolour/calico cats with XXY genotype (Klinefelter's syndrome) |
| Dog | Hereditary in some breeds. Cause of congenital azoospermia. Associated with cryptorchidism, XX reversal, XX syndrome and treatment of the bitch with diethylstilbestrol. |
| Bull | Multifactorial, may be hereditary in Swedish Highland breed as a recessive trait with incomplete penetrance: animals with white body and ears are highly susceptible. Most cases of hypoplasia are unilateral with the left side most often affected. |
| Ram | Sporadic, uni- or bilateral.<br>XXY syndrome reported also. Zinc deficiency implicated in some cases. |
| Buck | Goat polled/intersex syndrome<br>Sporadic forms of unknown cause in other breeds |

**Table 1-2: Main characteristics of testicular hypoplasia in domestic animals [2]**

In our case, we had the classical association of cryptorchidism with seminoma and testicular hypoplasia. Furthermore, multifocal severe mineralizations were present in the trachea, aorta, renal tubular and glomerular basement membranes (hypercalcemic nephropathy), and endocardium. A moderate hypercalcemia (precise value unknown) was communicated to attending veterinarians by the referring veterinarian. No macroscopic nor microscopic lesions were observed in the parathyroid glands. The ingestion of calcinogenic plants or nutritional imbalances has been excluded by attending clinicians. In such circumstances, the observed mineralizations may reflect a hypercalcemic state, probably induced by the seminoma as a paraneoplastic syndrome (Humoral Hypercalcemia of Malignancy). Interestingly, in human pathology, there are reports of germ cell tumors producing Parathyroid Hormone-related Peptide (PTHrP) with subsequent hypercalcemia.[5,7] To our knowledge, there is no report of paraneoplastic hypercalcemia in connection with germ cell tumors in veterinary medicine. Unfortunately, PTHrP expression could not be investigated in this case.

**AFIP Diagnosis:**

1. Left testicle: Seminoma, diffuse-type
2. Splenic capsule: Seminoma, metastatic
3. Right testicle: Hypoplasia, diffuse, severe

**Conference Comment:** A brief review of the gross and histologic appearance of common testicular tumors in dogs was discussed during the conference, and the main points of this discussion are summarized below.

| | Gross Appearance | Histologic Appearance |
|---|---|---|
| Interstitial cell tumor (Leydig cell tumor) | • small, round, well circumscribed<br>• minimal distortion of affected testicle<br>• bulge on cut section<br>• yellow to orange<br>• hemorrhagic and cystic | • large, uniform round to polygonal cells<br>• abundant eosinophilic, granular to vacuolated cytoplasm<br>• prominent lipid accumulations<br>• rare mitoses |
| Sertoli cell tumor | • well demarcated<br>• firm, white<br>• irregular, dense bands of connective tissue<br>• +/- fluid filled cysts or hemorrhage<br>• atrophy of contralateral testicle | • tall, slender to columnar cells<br>• indistinct cell borders<br>• dense, fibrous stroma<br>• may palisade along stroma<br>• patterns – diffuse and intratubular |
| Seminoma | • lobulated, irregular<br>• compresses adjacent parenchyma<br>• soft<br>• bulging, gray to white to mottled brown | • large, uniform, fairly discrete round cells<br>• scant cytoplasm<br>• occasional giant nuclei<br>• multinucleate cells<br>• mitoses common |

2

The three most common testicular neoplasms in the dog are the Sertoli cell tumor, interstitial cell tumor, and seminoma. Grossly and histologically, Sertoli cell tumors have a prominent fibrous component, while the other two tumors have only a small amount of fibrous stroma. Neoplastic Sertoli cells often palisade along tubules and are the only cells of the testes that are immunohistochemically positive for neuron-specific enolase (NSE). The interstitial cell tumor is derived from interstitial endocrine cells. Grossly, the yellow-orange color of the neoplasm reflects the high level of intracytoplasmic yellow lipochrome pigment. Histologically, neoplastic cells are round to polygonal with granular to vacuolated cytoplasm and multifocal hemorrhagic or cystic areas. Seminomas arise from germ cells and grossly appear as white-gray bulging masses. Histologically, seminomas are composed of round cells forming either a diffuse or intratubular pattern with a high mitotic rate.[2]

**Contributing Institution:** National Veterinary School of Alfort (France) www.vet-alfort.fr

**References:**

1. Beck C, Charles JA, Maclean AA: Ultrasound appearance of an equine testicular seminoma. Vet Radiol Ultrasound **42**:355-357, 2001

2. Foster RA, Ladds PW: Male genital system. *In:* Jubb, Kennedy and Palmer's Pathology of Domestic Animals, ed. Maxie MG, 5th ed., pp. 572-600. Saunders Elsevier, Edinburgh, Scotland, 2007

3. Galofaro V, Consiglio C, Rapisarda G, Marino F: Bilateral malignant seminoma with metastases in the mule: a report of two cases. Reprod Domest Anim **43**:121-123, 2008

4. Grieco V, Rondena M, Romussi S, Stefanello D, Finazzi M: Immunohistochemical characterization of the leucocytic infiltrate associated with canine seminomas. J Comp Pathol **130**:278-284, 2004

5. Looijenga LH, Oosterhuis JW: Pathogenesis of testicular germ cell tumours. Rev Reprod **4**:90-100, 1999

6. MacLachlan NJ, Kennedy PC: Tumors of the genital systems. *In:* Tumors in Domestic Animals, ed. Meuten DJ, 4th ed.pp. 561-567. Iowa State Press, Ames, IA, 2002

7. Sorscher S: Elevated parathyroid hormone-related peptide in a patient with an extragonadal germ-cell tumour and hypercalcemia. Can J Surg **47**:144, 2004

8. Veeramachaneni DN, Sawyer HR: Carcinoma in situ and seminoma in equine testis. Apmis **106**:183-185; discussion185-186, 1998

9. Woodward PJ, Heindenreich A, Looijenga LH, Oosterhuis JW, McLeod DG, Moller H, Manivel JC, Mostofi FK, Hailermariam S, Parkinson MC, Grigor K, True L, Jacobsen GK, Oliver TD, Talerman A, Kaplan GW, Ulbright TM, Sesterhenn IA, Rushton HG, Michael H, Reuter VE: Germ cell tumours. *In:* World Health Organization Classification of Tumours. Pathology and Genetics of Tumours of the Urinary System and Male Genital Organs, eds. Eble JN, Sauter G, Epstein JI Sesterhenn IA, pp. 221-249. IARC Press, Lyon, France, 2004

## CASE II – 06-0534 (AFIP 3104113)

**Signalment:** 15-year-old, female, Manx cat, (*Felis domesticus*)

**History:** Two liver masses (4-6 cm in diameter) were discovered during a regular visit to the local vet. The cat was clinically healthy.

**Gross Pathology:** None

**Laboratory Results:** None

**Histopathologic Description:** Sections of liver were partially effaced by a well-demarcated and unencapsulated mass composed of histologically normal adipose tissue and different cells of hematopoietic series. Cellular atypia and mitoses were not significant.

**Contributor's Morphologic Diagnosis:** Myelolipoma, liver

**Contributor's Comment:** Myelolipomas are rare, benign, and endocrinologically inactive tumors composed histologically of adipocytes with variable hematopoietic cells, including both mature and immature cells of the granulocytic, erythrocytic, and megakaryocytic series. They have been reported rarely in veterinary literature, particularly in the liver of cats and wild felidae; and in the spleen, adrenal gland, and spinal cord of dogs.[1,2] The vast majority of myelolipomas in humans occur within the adrenal glands, but extra-adrenal myelolipomas have been reported.[1] Feline hepatic myelolipomas are usually of no clinical significance, and they are usually diagnosed incidentally at necropsy during exploratory laparotomy or during abdominal ultrasonography. Metastasis has not been reported.[2] The pathogenesis of myelolipoma remains speculative. Theories concerning the pathogenesis include autonomous proliferation of bone marrow cells transferred during embryogenesis or metaplasia of certain mesenchymal cells triggered by various stimuli, including necrosis, infection, or stress.

When considering the differential diagnosis of hepatic myelolipomas, extramedullary proliferations of hematopoietic elements (EMH) is the primary differential. Myelolipomas are well-demarcated, discrete, single or multiple masses in any part of the liver; whereas, EMH appears as multifocal microscopic aggregates of hematopoietic cells in the perisinusoidal compartment and in portal areas. Also, hepatic EMH is usually not associated with forming discrete masses; however, severe EMH can lead to diffuse organ enlargement (hepatomegaly).

**AFIP Diagnosis:** Liver: Myelolipoma, multiple

**Conference Comment:** Myelolipomas have also been found in the adrenal glands of cattle, non-human primates, and sporadically in other various species. Histologically, these benign lesions are similar to those in

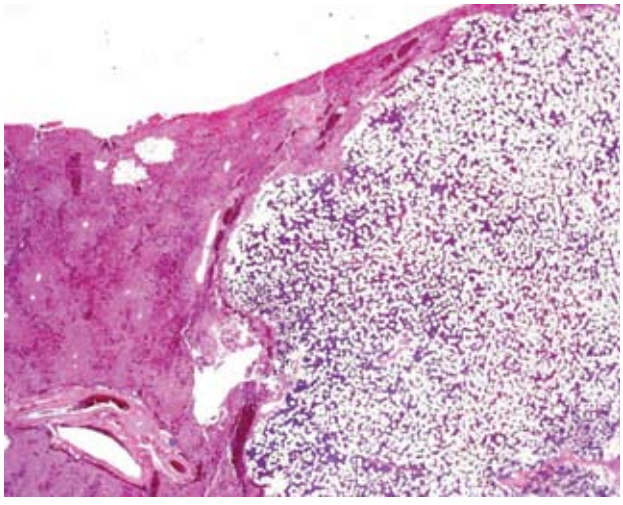

*2-1. Liver, cat. Myelolipoma. Focally, replacing and expanding normal liver architecture and compressing adjacent hepatocytes is a well circumscribed neoplasm composed of high numbers of adipocytes admixed with normal bone marrow elements. (HE 20X).*

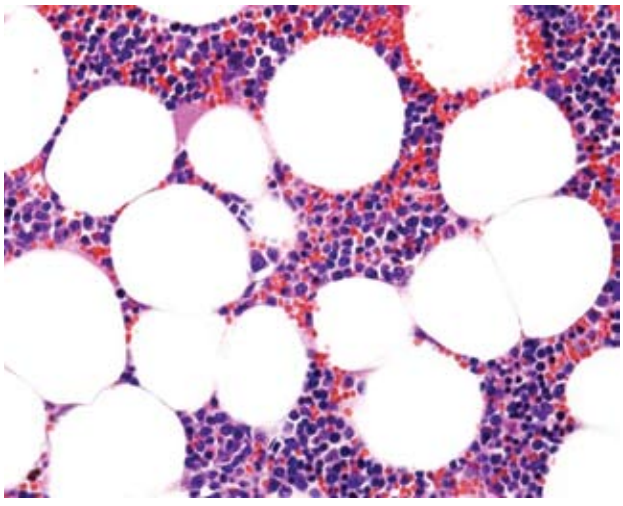

*2-2. Liver, cat. Myelolipoma. The neoplasm is composed of numerous adipocytes admixed with myeloid and erythroid precursors. (HE 400X)*

the liver and are composed of both myeloid and erythroid hematopoietic tissue admixed with well-differentiated adipocytes. Bone formation and areas of mineralization have also been observed in these tumors. Rare cases of splenic myelolipomas have also been reported. Grossly, these lesions stand out from the splenic parenchyma as a focal area of pallor. The speculative pathogenesis of this lesion is metaplastic transformation of a resident cell population regardless of location (adrenal gland, liver, and spleen).[3]

**Contributing Institution:** Egyptian Society of Comp. and Clinical Pathology, Department of Veterinary Pathology, Alexandria University, Alexandria-EGYPT

**References**:

1. Al-Rukibat RK, Bani Ismail ZA: Unusual presentation of splenic myelolipoma in a dog. Can Vet J **47**(11):1112-4. 2006
2. Capen CC: Endocrine glands. *In:* Jubb, Kennedy, and Palmer's Pathology of Domestic Animals, ed. Maxie MG, 5th ed., vol. 3, pp.415. Elsevier Limited, St. Louis, MO, 2007
3. Stalker MJ, Hayes MA: Liver and biliary system. *In:* Jubb, Kennedy, and Palmer's Pathology of Domestic Animals, ed. Maxie MG, 5th ed., vol. 2, pp. 386. Elsevier Limited, St. Louis, MO, 2007
4. Valli VEO: Hematopoietic system. *In:* Jubb, Kennedy, and Palmer's Pathology of Domestic Animals, ed. Maxie MG, 5th ed., vol. 3, pp. 289. Elsevier Limited, St. Louis, MO, 2007

## CASE III – CRL 2008-2 (AFIP 3104060)

**Signalment:** Domestic rabbit (*Oryctolagus cuniculus*), male, age and strain unknown

**History:** Clinically normal animal, incidental finding at necropsy

**Gross Pathology:** Occasional white to pale gray linear foci (0.5-1 cm diameter) in the left lateral lobe of the liver.

**Laboratory Results**: *E. cuniculi* seropositive

**Histopathologic Description:** Most portal areas and bile ducts have an infiltrate of lymphocytes, plasma cells, histiocytes and occasional heterophils. More severely affected regions have portal fibrosis, bile duct hyperplasia, and extension of the inflammation into the adjacent hepatic parenchyma. Occasionally there is marked dilation of bile ducts, with hyperplastic biliary epithelium thrown into papillary folds, and large numbers of coccidial forms in various stages of development within the biliary epithelium and free in the lumen.

**Contributor's Morphologic Diagnosis:** Liver: Cholangiohepatitis, chronic, nonsuppurative, multifocal, moderate, with bile duct proliferation and intralesional coccidia (*Eimeria stiedae*)

**Contributor's Comment:** *Eimeria stiedae* was identified using fecal centrifugation concentration.

The life cycle of *E. stiedae* is typical of *Eimeria* spp., in that all *Eimeria* are host-specific and have a direct life cycle.[2] Oocysts are not infective until sporulation, so ingestion of cecotroph feces does not result in autoinfection. Ingestion of sporulated oocysts (sporocysts) results in release (excystation) of sporozoites in the duodenum. Sporozoites invade the intestinal mucosa, are carried to the liver in the portal veins and/or lymphatics where they enter biliary epithelial cells and multiply asexually by schizogony.[5] Developing schizonts containing merozoites are evident within 3-6 days following infection, and gametogony can be identified eleven days post infection. In gametogony, the final generation merozoites form either macrogametes (female) or microgametes (male). After fertilization, macrogametes develop into oocysts, and enter the intestine through the bile, pass out of the host in the feces, and undergo sporulation. The prepatent period is 14-18 days, and oocysts may be shed in the feces for up to seven or more weeks. Oocysts of *E. stiedae* contain four sporocysts, each of which contains two sporozoites. They are ovoid to elliptical, 28-42 um by 16-25 um with a micropyle. Sporocysts are 8-10 by 17-18 um and contain a Stieda body.[5]

*Eimeria stiedae* is common in domestic rabbits throughout the world, as well as cottontail rabbits and hares.[3] It is an important cause of morbidity and mortality in commercial rabbitries (the source of this rabbit) but is rarely seen in laboratory rabbits raised according to strict barrier procedures. *E. stiedae* infections may be subclinical or manifest as clinical disease, with occasional mortality. Weanling rabbits are most often affected [4] and may exhibit anorexia, lethargy, diarrhea, abdominal enlargement due to hepatomegaly, and icterus.

At necropsy, the liver contains variable numbers of raised, linear, bosselated, yellow to gray circumscribed lesions scattered throughout the hepatic parenchyma.[4] In severe cases there is hepatomegaly, with the liver comprising up

to 20% of body weight.[5] Microscopically there is marked dilation of bile ducts, extensive portal fibrosis, and a mixed inflammatory cell infiltrate in the portal zones. In affected bile ducts, there is hyperplasia of epithelium with papillary projections, with large numbers of gametocytes and oocysts typically present in affected ducts. The characteristic histologic findings of proliferative biliary changes and coccidial organisms are essentially diagnostic for this disease.

Changes in serum chemistry seen during the acute and convalescent stages of the disease indicate significant metabolic aberrations.[4] There is some evidence that rabbits heavily infected with *E. stiedae* may have an impaired immune response.

**AFIP Diagnosis:** Liver: Cholangiohepatitis, proliferative, lymphoplasmacytic, chronic, multifocal, moderate, with intraepithelial coccidia (*Eimeria stiedae*)

**Conference Comment:** Coccidia are in the phylum Apicomplexa and are single cell, protozoal parasites. Members of the genus *Eimeria* and *Isospora* are generally host and organ specific, with lesions usually occurring in the gastrointestinal tract. These organisms also commonly infect young animals. The following is a brief, non-comprehensive list of common *Eimeria* and *Isospora* found in domestic animals. In dogs and cats, the coccidia of importance are in the genus *Cystoisospora*.[5]

| **Animal** | **Coccidia** | **Organ affected** |
|---|---|---|
| Cattle | *E. zuernii*<br>*E. bovis* | Distal small intestine<br>Distal small intestine |
| Sheep | *E. ovinoidalis*<br>*E. ashata*<br>*E. bakuensis*<br>*E. crandallis* | Terminal ileum/ cecum and colon<br>Distal small intestine<br>Distal small intestine<br>Distal small intestine |
| Goats | *E. ninakohlyakimovae*<br>*E. caprina*<br>*E. christenseni*<br>*E. arloingi* | Cecum and colon<br>Cecum and colon<br>Distal small intestine<br>Distal small intestine |
| Swine | *Isospora suis* (neonatal pigs)<br>*E. scabra* (weaners, growers)<br>*E. debliecki* (weaners, growers)<br>*E. spinosa* (weaners, growers) | Distal small intestine<br>Distal small intestine<br>Distal small intestine<br>Distal small intestine |
| Equine | *E. leuckarti* | Small intestine |
| Dogs | *C. canis*<br>*C. ohioensis complex* =<br>*(C. burrowsi, C. ohioensis,*<br>*C. neorivolta)* | Distal small intestine, large intestine<br>Distal small intestine, large intestine |
| Cats | *C. felis*<br>*C. rivolta* | Small intestine, large intestine<br>Small intestine, large intestine |
| Chickens | *E. acervulina*<br>*E. necatrix*<br>*E. tenella* | Small intestine<br>Small intestine<br>Ceca |

5

**Contributing Institution:** Charles River; www.criver.com

## References:

1. Brown CC, Baker DC, Barker IK: Alimentary system. *In:* Jubb, Kennedy, and Palmer's Pathology of Domestic Animals, ed. Maxie MG, 5th ed., vol. 2, pp.260-270. Elsevier Limited, St. Louis, MO, 2007
2. Gardiner CH, Fayer R, Dubey JP: An Atlas of Protozoan Parasites in Animal Tissues, 1st ed., pp 20-30. USDA Agricultural Research Service Agricultural Handbook Number 651, 1988
3. Levine, ND: Veterinary Protozoology, pp.178. Iowa State University Press, Ames, IA,1985
4. Percy DH, Barthold SW: Pathology of Laboratory Rodents and Rabbits, pp 288-290. Ames, IA, Blackwell Publishing, 2007
5. Schoeb TR, Cartner SC, Baker RA, Gerrity LW: Parasites of rabbits. *In:* Flynn's Parasites of Laboratory Animals, ed. Baker DG, 2nd ed., pp. 454-457. Blackwell Publishing, Oxford, UK, 2007

**CASE IV –N0710576 (AFIP 3105527)**

**Signalment:** 17-month-old, male, PLB-23 rat (*Rattus norvegicus*)

**History:** The rat is part of a research colony maintained at our research institution and was singly housed in standard rat caging. A husbandry technician noted this rat to be hunched, scruffy, lethargic and dehydrated. A large volume of blood was found in the cage with no evidence of a laceration or open wound–no obvious visible source of blood could be found grossly. The rat was dyspneic, experiencing agonal breaths and was humanely euthanized.

**Gross Pathology:** There is a large mass in the area of the pituitary gland. A large blood clot is found to fill the entire nasal cavity.

**Laboratory Results:** Microcytic, normochromic anemia, hyperglycemia, elevated liver enzymes, hyperphosphatemia and hyperkalemia. The decreased hematocrit and hemoglobin concentration are secondary to blood loss. The elevation in liver enzymes AlkP, ALT, and AST may be secondary to hypoxia or the elevated blood glucose (diabetes mellitus). The increased potassium and phosphorus are unexplained and may be due to decreased renal clearance, dehydration/shock, or tissue trauma. In addition, the blood sample was slightly hemolyzed, which may account for the elevated potassium, phosphorous and elevated liver enzymes. See detailed bloodwork results in Table 4-1.

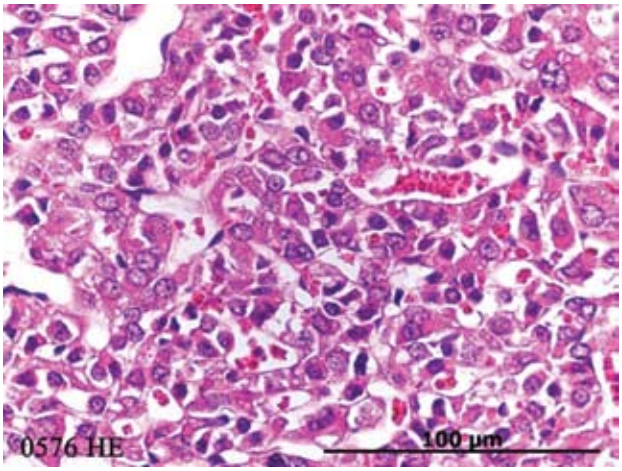


*4-1. Pituitary gland, rat. The neoplasm is composed of polygonal cells supported by a fine fibrovascular stroma; neoplastic cells have variably distinct cell borders with moderate amounts of eosinophilic finely granular cytoplasm and irregularly round to oval nuclei with finely stippled chromatin and generally one variably distinct nucleolus. (HE 400X).* *Photomicrograph courtesy of Section of Comparative Medicine, School of Medicine, Yale University New Haven, CT.*

**Table 4-1. Complete Blood Count and Serum Biochemistry Panel Results**

| Complete Blood Count | Results | Reference Range (Units) | Serum Biochemistry Panel | Results | Reference Range (Units) |
|---|---|---|---|---|---|
| Hemoglobin | 10.4 L | 11.4-19.2 g/dL | Glucose | 465 H | 60-125 mg/dL |
| Hematocrit | 28.0 L | 33-50 % | Urea Nitrogen | 22 | 9-30 mg/dL |
| WBC | 6.8 | 5.5-11 $x10^3$/uL | Creatinine | 0.5 | 0.4-1.0 mg/dL |
| RBC | 5.53 | 5.5-10.5 $x10^6$/uL | Total protein | 6.4 | 4.5-6.5 g/dL |
| MCV | 51 | Fl | Albumin | 3.2 | 2.0-6.2 g/dL |
| MCH | 18.8 | Pg | Total bilirubin | 0.1 | 0-1 mg/dL |
| MCHC | 37.1 | g/dL | Alkaline Phosphatase | 91 H | 15-45 U/L |
| Platelet Count | 634 | $x10^3$/uL | ALT | 69 H | 10-35 U/L |
| Platelet Estimate | Increased | | AST | 177 H | 10-45 U/L |
| *Differential* | | *Units* | Cholesterol | 122 | 50-250 mg/dL |
| Neutrophils | 4148 | 61% | Calcium | 12.0 | 8-12 mg/dL |
| Bands | 0 | | Phosphorous | 10.8 H | 4.2-8.5 mg/dL |
| Lymphocytes | 2448 | 36% | Sodium | 142 | 140-160 mEq/L |
| Monocytes | 136 | 2% | Potassium | 7.1 H | 4.3-5.8 mEq/L |
| Eosinophils | 68 | 1% | Chloride | 93 | 90-110 mEq/L |
| Basophils | 68 | 1% | Albumin/ Globulin Ratio | 1.0 | 0.4-1.1 |
| Polychromasia | Slight | | BUN/Creat Ratio | 44 | |
| Prothrombin Time | 13.1 | Secs | Globulin | 3.2 | 2.5-4.8 |
| PTT | 14.3 | Secs | CPK | 241 | U/L |
| Fibrinogen | 262 | Mg/dL | | | |
| D-Dimer | < 250 | Ng/mL | | | |

**Histopathologic Description:** There is a large multinodular mass (~2 cm wide) that extends from the base of the brain in the area of the pars distalis posteriorly into the cerebellum, dorsally into the overlying cerebrum and cerebellum. In addition, there is a spatially distinct section of tumor present unilaterally in the lateral ventricle in the area of the hippocampus. The neoplastic cells are arranged in solid sheets to compact cords with a fine fibrovascular stroma. There are numerous small to large cystic spaces filled with eosinophilic proteinaceous material admixed with erythrocytes. The neoplastic cells are irregularly round and contain a single predominantly vesiculate nucleus with a single prominent nucleolus and an amphophilic to slightly eosinophilic cytoplasm. Nuclear pleomorphism is high. Occasionally larger bizarre forms are observed. The third and lateral ventricles are distended and contain fibrin, edema and hemorrhage. The neoplastic cells are periodic acid-Schiff negative.

The nasal pharynx and nasal cavity are full of blood admixed with fibrin. At the level of the eyes, nasal cavity and upper molars, there is a unilateral focal area where one molar and the adjacent tissue are altered. There is a single large hair (whisker) and other cross sections of hair. The large hair extends from within the oral cavity along the medial aspect of one molar sulcus and is embedded into the overlying soft tissues of the palate. Surrounding the larger piece of hair there is a thin layer of stratified squamous epithelium and beyond this there is abundant fibrous connective tissue admixed with neutrophils, macrophages, and scattered lymphocytes and plasma cells. At the margin of the oral cavity there are greater numbers of neutrophils. There are similar inflammatory cells surrounding the smaller sections of hair. There is marked loss of bone in the subjacent maxilla. The adjacent molar occlusal surface shape is altered with the lingual aspect longer and curved toward the buccal side. There is loss of the roots and intervening bone with no visible pulp cavity. There is an inflammatory infiltrate comprised predominantly of neutrophils at the base of the root. In the ipsilateral buccal mucous tunic to the affected molar, the oral mucosa is absent and the underlying lamina propria is acutely necrotic with a large amount of fibrin and hemorrhage admixed with blood.

While the pituitary mass was considerable in size, it appears to have been an incidental finding in this animal, as the cause of impending death was respiratory failure resulting from the large blood clot within the nasal cavity. This can occur in rats because the anatomy of the oronasal cavity of rats is unique rendering them obligate nose-breathers. In rats, the soft palate is long, and the anterior opening of the esophagus, the epiglottis, and the larynx lies anterior to the nasopharyngeal opening. Therefore, an obstruction in this area would prevent a rat from being able to breathe.

**Contributor's Morphologic Diagnosis:** Pituitary Par Distalis: Carcinoma, chromophobic

**Contributor's Comment:** Pituitary tumors occur in most animal species, but occur rather frequently in laboratory rats and dogs. The classification of pituitary tumors as chromophobic, acidophilic and basophilic is based on the histologic staining characteristics of the granules they contain.[3] This traditional classification scheme is still in use, but does not categorize the functionality of the tumor and is therefore moving out of favor. Immunohistochemical demonstration of the various types of pituitary hormones contained within the tumor is another method of classification of these neoplasms and may also aid in diagnosis and prognosis.[5] The following table, extracted from Jones, et. al., demonstrates the hormones secreted and typical staining patterns of the cells of the anterior pituitary.

**Table 2. Endocrine cells and hormones of the anterior pituitary [3]**

| Cell type | Hormone | Cell characteristics |
|---|---|---|
| Somatotroph<br>(type 2 acidophil) | Growth Hormone | H&E: acidophilic granules<br>PAS: negative<br>EM: abundant, dense granules 350nm |
| Lactotroph<br>(type 1 acidophil) | Prolactin | H&E: acidophilic or chromophobic granules<br>PAS: negative<br>EM: sparse, dense granules 600-900nm |
| Gonadotroph<br>(type 2 basophil) | Follicle-stimulating Hormone<br>Leutinizing Hormone | H&E: basophilic<br>PAS: positive<br>EM: dense granules 200-250nm |

| | | |
|---|---|---|
| Thyrotroph<br>(type 1 basophil) | Thyroid-stimulating Hormone | H&E: basophilic<br>PAS: positive<br>EM: dense granules 150nm |
| Corticotroph<br>(type 3 basophil) | Adrenocorticotropic Hormone | H&E: basophilic<br>PAS: weakly positive<br>EM: variably dense granules 200-400nm<br>Cytoplasmic filaments |
| Melanotroph | Melanocyte-stimulating Hormone | H&E: basophilic<br>PAS: positive |

Most pituitary tumors are adenomas and grow by expansion thereby creating a space-occupying lesion potentially interfering with the normal function of the cells within the pituitary, hypothalamus, thalamus and other surrounding structures. The clinical signs associated with the lesion are often linked to which types of hormones are secreted. Although they occur infrequently, metastatic pituitary neoplasms have been reported in a variety of species. These lesions can produce destructive effects on the pituitary, hypothalamus and thalamus leading to a multitude of clinical signs.[3]

Even though pituitary carcinomas occur with much less frequency than pituitary adenomas in most rats, in this case the tumor invasion into the overlying brain suggests that this tumor is a carcinoma. In addition, the fact that the tumor cells had high pleomorphism with bizarre forms suggests carcinoma.

In a study by McComb, et al (1984), it was found that in rats over 24-months of age, pituitary adenomas were found in 85% of male and 79% of female SD rats. Of these tumors, 47% were prolactin (PRL)-containing and 16% were leutinizing hormone (LH)-containing adenomas. The remaining 37% were made up of tumors containing thyroid-stimulating hormone (TSH), growth hormone (GH), adrenocorticotropic hormone (ACTH) or some combination thereof, as well as immunonegative adenomas.[5] In another study done by Nagatani, et al (1987), 736 rats of various inbred strains ranging from 13 to 24 months of age were screened for pituitary tumors. Pituitary tumors were found in 284 of the 736 rats, with some rats having more than one lesion.[3] In addition to spontaneously occurring pituitary tumors, chronic estrogen treatment can induce prolactin-secreting tumor growth in the anterior pituitary of Fischer 344 rats.[8]

In dogs, ACTH-secreting tumors are the most common of the functional pituitary tumors. While these tumors can arise from the pars intermedia or the pars distalis, most commonly they are chromophobic adenomas composed of either large or small cells arising from the pars distalis. ACTH-secreting tumors frequently result in the development of adrenocortical hyperplasia and hyperfunction and cause pituitary-dependent Cushing's disease.[3]

While cats are not considered a species that commonly develops pituitary tumors, one study found that 16 out of 16 diabetic cats with insulin resistance also had pituitary adenomas manifesting as acromegaly or hyperadrenocorticism.[2]

The most frequently occurring pituitary neoplasm in horses is the adenoma of the pars intermedia leading to a variety of clinical signs including hirsutism, polyphagia, muscle wasting, hyperglycemia, and diabetes insipidus, among others.[1]

In humans, pituitary neoplasms represent approximately 10% of the intracranial tumors, the most common of which are prolactin secreting pituitary adenomas.[3,5,4] Spontaneous pituitary adenomas have also been described in parakeets and mice.[5]

**AFIP Diagnosis:** Pituitary gland, pars distalis: Adenoma **(Fig. 1)**

**Conference Comment:** Conference participants debated the differentials of adenoma and carcinoma in this case. Conference participants did not observe invasion of the overlying brain in their tissue sections. Therefore we prefer the diagnosis of adenoma based on the lack of tissue or vascular invasion and the low mitotic rate. A moderate degree of anisocytosis and anisokaryosis does not preclude the diagnosis. The AFIP Department of Neuropathology concurred with this conclusion. The neoplasm is further classified as a lactotroph adenoma based on the results of

immunohistochemical procedures performed at AFIP; the neoplasm is positive for prolactin and negative for ACTH, FSH, GH, LH, and TSH.

**Contributing Institution:** Section of Comparative Medicine, School of Medicine, Yale University
New Haven, CT

**References:**

1. Capen, CC: Endocrine glands. *In:* Jubb, Kennedy, and Palmers' Pathology of Domestic Animals, 5th ed., pp. 339-346. Saunders Elsevier, Philadelphia, PA, 2007
2. Elliot DA, Feldman EC, Koblik PD, Samii VF, Nelson RW: Prevalence of pituitary tumors among diabetic cats with insulin resistance. JAVMA **216**(11): pp. 1765-1768, 2000
3. Jones TC, Hunt RD, King NW: Veterinary Pathology, 6th ed., Williams & Wilkins, Baltimore, MD, pp. 1224-1232, 1997
4. McComb DJ, Hellmann P, Kovacs K, Scott D, Evans WS, Burdman JA, and Thorner MO: Spontaneous sparsely-granulated prolactin-producing pituitary adenomas in aging rats. Neuroendocrinology **41**:201-211, 1985
5. McComb DJ, Kovacs K, Beri J, and Zak F: Pituitary adenomas in old sprague-dawley rats: a histologic, ultrastructural, and immunocytochemical study. JNCI **19**(5): pp. 1143-1157, 1973
6. Nagatani M, Miura K, Tsuchitani M, Narama I: Relationship Between Cellular Morphology and Immunocytological Findings of Spontaneous Pituitary Tumours in the Aged Rat. J Comp Path **97**:11-20, 1987
7. Percy DH, Barthold SW: Pathology of Laboratory Rodents and Rabbits. 3rd ed., pp.108, 122, 173-174, 306. Blackwell Publishing, Ames, IA, 2007
8. Wendell DL, Platts A, Land S: Global Analysis of Gene Expression in the Estrogen Induced Pituitary Tumor of the F344 Rat. J Steroid Biochem & Mol Biology **101**:188-196, 2006

**NOTES:**

The Armed Forces Institute of Pathology
Department of Veterinary Pathology

*Conference Coordinator:*
Todd M. Bell, DVM

WEDNESDAY SLIDE CONFERENCE 2008-2009

# Conference 5

8 October 2008

*Conference Moderator:*

Marc E. Mattix, DVM, MSS, Diplomate ACVP

## CASE I – Case HN 2516 (AFIP 3105584)

**Signalment:** Whooper swan, *Cygnus cygnus*

**History:** This wild swan was found dead at the northern lake of Japan in May, 2008. The local veterinarian found the feces of this bird were influenza virus positive using a convenient test kit. The carcass was transported to our university and dissected within our P3 facility.

**Gross Pathology:** Diffusely the lungs showed severe congestive edema with edematous thickening of the pleura. Petechial hemorrhages were scattered on the pericardium and pancreas. Pericardial fluid was mildly increased and accompanied mild edematous thickening of pericardium and cardiac sac. The brain was congested.

**Laboratory Results:** Highly pathogenic avian influenza virus of H5N1 subtype was isolated from the brain, lungs, trachea, colon and pancreas of the birds. HA titers of the virus in each organ were between 32-256, and the titer of the brain was 128.

**Histopathologic Description:** Several glial nodules **(Fig. 1-1)** were scattered in the CNS. The nodules sometimes contained karyorrhexis or hyperchromatosis of nuclear wall of glial cells, rod cells, satellitosis to neuronophagia of nerve cells, and minute malacic foci. The karyorrhexis of glial cells and rod cells were also sparsely distributed throughout the CNS. The nuclei of perivascular cells (pericytes and astrocytes) were sometimes swollen, and perivascular inflammatory cell infiltration was indiscernible.

Imunohistochemistry using rabbit polyclonal antibody against highly pathogenic avian influenza virus of H5N2 subtype as primary antibody revealed viral antigens in the nuclei of astrocytes **(arrow head in Fig. 1-2 and 1-3)**, microglial cells **(arrows in Fig. 1-2)**, and nerve cells **(arrows in Fig. 1-3)** within and around the glial nodules.

Besides the brain, lymphocytic necrosis in the spleen, mild fibrinous bronchopneumonia and focal necrosis of exocrine pancreas were found with viral antigens in alveolar epithelial cells, bronchial epithelial cells and exocrine pancreatic cells. Inflammatory cell infiltration was minimal in these lesions.

**Contributor's Morphologic Diagnosis:** Nonpurulent encephalitis, diffuse, mild, influenza virus infection

**Contributor's Comment:** The threat of highly pathogenic avian influenza virus of H5N1 subtype to humans as well as domestic and wild birds is a great concern

***Sponsored by the American Veterinary Medical Association, the American College of Veterinary Pathologists, and the C. L. Davis Foundation.**

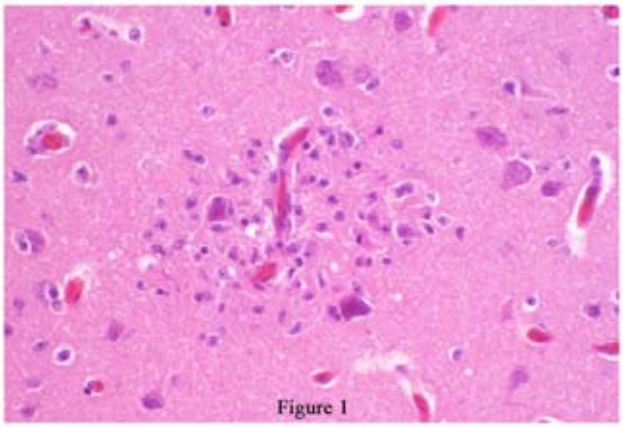
Figure 1

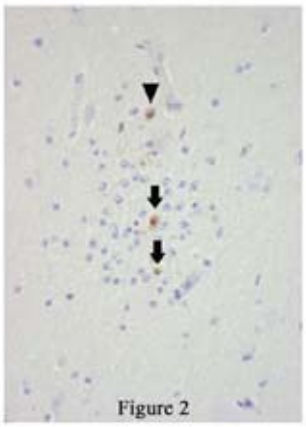
Figure 2

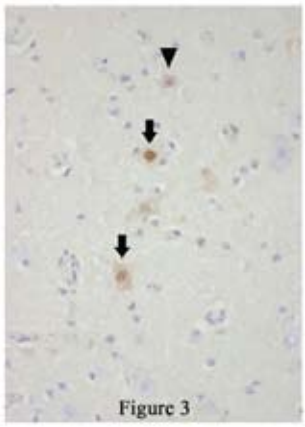
Figure 3

*1-1. Cerebrum, Whooper Swan. Glial nodules within the white matter often surround blood vessels and rare degenerate or necrotic neurons. Photomicrographs courtesy of Laboratory of Comparative Pathology, Graduate School of Veterinary Medicine, Hokkaido University, N18 W9 North, Sapporo 060-0818, Japan.*
*1-2 and 1-3. Cerebrum, Whooper Swan. Immunohistochemistry using rabbit polyclonal antibody against highly pathogenic avian influenza virus of H5N2 subtype as primary antibody revealed viral antigens in the nuclei of astrocyte (arrowhead in Fig.1-2, 1-3), microglia cells (arrows in Fig.1- 2), and nerve cells (arrows in Fig.1- 3) within and around the glial nodules. Photomicrographs courtesy of Laboratory of Comparative Pathology, Graduate School of Veterinary Medicine, Hokkaido University, N18 W9 North, Sapporo 060-0818, Japan.*

of human public health and fowl industry in worldwide magnitude.[1,10] The virus first emerged in 2003 in east and southeast Asian countries. Many human cases have been reported in Indonesia, Vietnam and China. Japan suffered the outbreaks of H5N1 infection in domestic fowl seven times from 2004 to 2007. All of these outbreaks were rapidly controlled by thorough culling. In April to May of 2008, a total of three Whooper swans were found dead in the northern lakes of Japan and highly pathogenic avian influenza viruses of H5N1 subtype were isolated from them. These birds were migrating from southern Asian countries to Siberia. The present case was one of the three cases. Genomic analysis on the isolated viruses revealed the sequence of these isolates were almost identical and were remote from those of the previous outbreaks in 2004 and 2007 in Japan.

Pathological changes of birds due to highly pathogenic avian influenza of H5N1 subtype are necrotic and hemorrhagic changes are centered in the CNS, pancreas, lungs, liver, adrenals, heart and lymphoid organs.[2-4,9,10] The CNS lesions in the present case were very mild and were at an early stage of encephalitis in comparison with previous reports on experimental or non-migratory birds.[2,4]

Birds infected with highly pathogenic avian influenza rapidly develop viremia, and then the virus infects and damages vascular endothelial cells[3,8,9] resulting in hemorrhagic and edematous changes in various organs and tissues including the skin and skeletal muscles. Necrotic and apoptotic changes of parenchymal cells of organs follow. In the CNS, the virus antigen first appears in vascular endothelial cells, then extends to astroglia and nerve cells.[8,9] In mice, the virus causes neither viremia nor endothelial damage. It invades the CNS via peripheral nerves.[5,7]

**AFIP Diagnosis:** Cerebrum: Neuronal necrosis, subacute, multifocal, mild with multiple glial nodules

**Conference Comment:** Influenza viruses are important pathogens in both humans and animals, and their ability to cross species barriers is of major concern to medical professionals. Influenza viruses are in the family *Orthomyxoviridae,* encompassing the genera *Influenza A, B, and C,* and *Thogotovirus*. Viruses from the genus influenza A infect humans, horses, pigs, seals, birds, whales, and mink; influenza B viruses infect only humans; influenza C viruses infect humans and swine; thogotoviruses are tick borne viruses found mainly in Africa, Asia, and Europe.[6]

The reservoir for influenza A is waterfowl, and the virus causes an asymptomatic infection in these species with replication in the intestinal epithelium and subsequent fecal shedding. These problematic waterfowl often spread influenza via migratory routes, and the virus has a chance to exchange genes with other novel influenza viruses during these sojourns creating a potential for a new, virulent influenza virus.[6] Swine are important intermediate hosts because they can get both influenza A and C, and thus create an environment for viral genetic rearrangement. Influenza viruses can either undergo genetic drift, (point mutation) or

genetic shift (genetic segment reassortment) to create new strains of virus. Most combinations of influenza virus are non-pathogens, but when a drift or shift occurs creating a novel, virulent virus, pandemics such as the 1918 outbreak are the result. [6]

Highly pathogenic avian influenza in chickens and turkeys, also known colloquially as fowl plague, often causes death with little to no clinical warning. If birds survive the initial stage of disease they clinically present with severe respiratory distress along with cyanosis of the unfeathered skin to include the comb and wattles. [6] In birds, unlike mammals, influenza replicates in both the respiratory and gastrointestinal tracts. Virulent strains cause viremia with resultant necrosis of lymphoid and gastrointestinal tissue, pancreatitis, myositis, and encephalitis. Petechial hemorrhages are commonly found in the digestive, respiratory and cardiac tissues because of viral damage to endothelial cells. [6]

**Contributing Institution:** http://www.vetmed.hokudai.ac.jp/

**References:**

1. Kishida N, Sakoda Y, Isoda K, Matsuda K, Eto M, Sunaga Y, Umemura T, Kida H: Pathogenicity of H5 influenza viruses in ducks. Arch Virol **150**:1383-1392, 2005
2. Kobayashi Y, Horimoto T, Kawaoka Y, Alexander DJ, Itakura C: Pathological studies of chickens experimentally infected with two highly pathogenic avian influenza viruses. Avian Pathol **25**:285-304, 1996
3. Kwon YK, Joh SJ, Kim MC, Lee YJ, Choi JG, Wee SH, Sung HW, Kwon JH, Kang MI, Kim JH: Highly pathogenic avian influenza in Magpies (*Pica pica sericea*) in South Korea. J Wildlife Dis **41**:618-623, 2005
4. Le Gall-Recule G, Briand FX, Schmitz A, Guionie O, Massin P, Jestin V: Double introduction of highly pathogenic H5N1 avian influenza virus into France in early 2006. Avian Pathol **37**:15-23, 2008.
5. Park CH, Ishinaka M, Takada A, Kida H, Kimura T, Ochiai K, Umemura T: The invasion routes of neurovirulent A/Hong Kong/483/97(H5N1) influenza virus into the central nervous system after respiratory infection in mice. Arch Vorol **147**:1425-1436, 2002
6. Matsuda K, Park CH, Sunden Y, Kimura T, Ochiai K, Kida H, Umemura T: The vagus nerve is one route of transneural invasion for intranasally inoculated influenza A virus in mice. Vet Pathol **41**:101-107, 2004
7. Murphy FA, Gibbs EPJ, Horzinek MC, Studdert MJ: *Orthomyxoviridae*. *In:* Veterinary Virology, 3rd ed., pp. 459-46. Academic Press, San Diego, California, 1999
8. Park CH, Ozaki H, Takada A, Kida H, Ochiai K, Umemura T: Primary target cells of virulent strains of type A influenza virus in chicken embryos. Avian Pathol **30**:269-272, 2001
9. Silvano FD, Yoshikawa M, Shimada A, Otsuki K, Umemura T: Enhanced neuropathogenicity of avian influenza A virus by passages through air sac and brain of chicks. J Vet Med Sci **59**:143-148, 1996
10. Teifke JP, Klopfleisch R, Globig A, Starick E, Hoffmann B, Wolf PU, Beer M, Mettenleiter TC, Harder TC: Pathology of natural infections by H5N1 highly patyogenic avian influenza virus in Mute (*Cygnus olor*) and Whooper (*Cygnus Cygnus*) swans. Vet Pathol **44**:137-143, 2007

## CASE II – Case 07-13414-(AFIP 3101429)

**Signalment:** An 8-year-old neutered male domestic short hair cat

**History:** The cat presented to the referring veterinarian with fever, lethargy and excess salivation. Another cat in the household with similar signs had died the previous night. Both cats had been ill the previous year but had recovered. Both were indoor-outdoor cats that killed and ate wildlife. A FeLV/FIV test on this cat was negative.

The referring veterinarian suspected tularemia due to positive cases in sheep in the same area the previous year.

**Gross Pathology:** The body was in good postmortem condition with good body condition. The spleen was enlarged and had pinpoint white foci throughout the parenchyma. The lungs had severe, diffuse, acute pulmonary edema; and the urinary bladder mucosa was reddened by multiple petechiae. Mesenteric lymph nodes were enlarged. The liver was slightly pale, but was considered to be grossly normal.

**Laboratory Results:** PCR for *Francisella tularensis* was positive on fresh spleen. The diagnosis was confirmed by culture in a BL-3 facility.

**Histopathologic Description:** Sections of liver and spleen were disrupted by multiple random foci of necrosis **(Figs. 2-1 and 2-2)**. Necrotic foci were composed of cellular debris admixed with moderate numbers of mononuclear cells and fewer neutrophils **(Fig. 2-3)**. Some foci were associated with hemorrhage. Brown and Hopp's tissue gram stain revealed small, gram negative coccobacilli both extracellularly and within macrophages.

Other lesions include large necrotic foci in the mesenteric lymph node similar to those seen in the liver and spleen

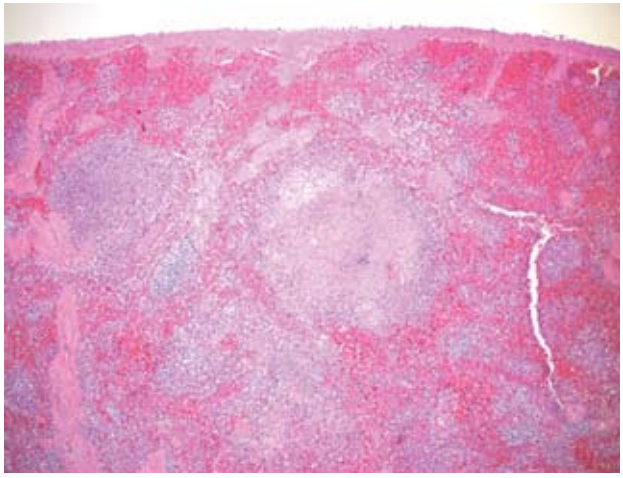

*2-1 Spleen, cat. Multifocally and randomly are variably sized foci of lytic necrosis characterized by a central eosinophilic core bounded by a cellular infiltrate. (HE 20X).*

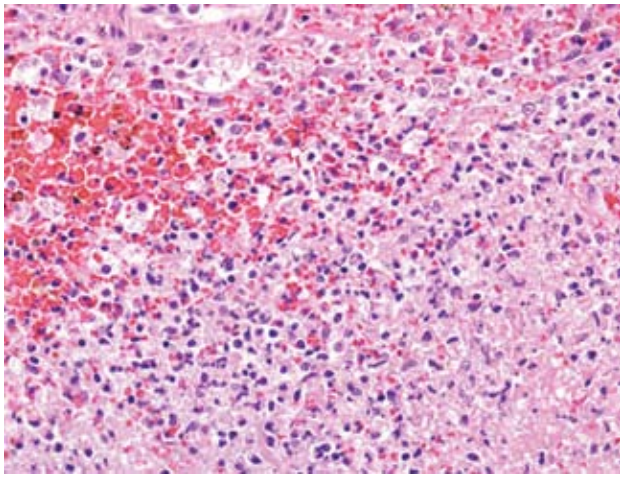

*2-2. Spleen, cat. Necrotic foci are bounded by moderate numbers of histiocytes, fewer neutrophils, lymphocytes and rare plasma cell admixed with hemorrhage and numerous erythrocytic laden macrophages (erythrophagocytosis). (HE 400X).*

and smaller foci in the lung and bone marrow.

**Contributor's Morphologic Diagnosis:** Acute multi-focal necrotizing hepatitis and splenitis, compatible with tularemia

**Contributor's Comment:** Tularemia is an often fatal septicemic disease endemic in rodents primarily in the western US but distributed worldwide. [2] The disease is caused by infection with *Francisella tularensis*, originally named *Pasteurella tularensis* but later found to be unrelated genetically to other Pasteurella species. *F. tularensis* has 4 subspecies: tularensis, holartica, mediasciatica and novidia. It is the subspecies tularensis, present only in North America, which most often causes fatal zoonotic infections in other species, especially sheep and human beings. The subspecies holartica is distributed throughout the northern hemisphere and primarily causes disease in semi-aquatic rodents such as muskrats and beavers.

The organism is a small Gram-negative rod that is a facultative intracellular bacterium. It not only lives but proliferates in macrophages.[2] Transmission is by ingestion, inhalation, direct contact with skin or mucous membranes, or by arthropods, especially ticks and deer flies. Cats and dogs are thought to be somewhat resistant; however, this cat may well have been infected by ingestion of an infected rodent. Humans may be infected by direct contact or aerosols. Sheep are infected primarily by tick infestation. [4]

Clinical signs vary depending upon route of trans-mission. In humans the most common route of transmission is by direct contact in susceptible segments of the population (hunters, butchers, farmers, etc). [3] In these patients, the most common form of the disease is ulcerglandular, characterized by systemic illness with a skin ulcer at the site of infection and swelling and drainage of local lymph nodes. The increasing concern over weaponized bacteria for biological attack has brought renewed interest in the study of forms of tularemia caused by inhalation. The typhoidal form of tularemia is characterized by fever, prostration, and absence of lymphadenopathy. The pneumonia resulting from typhoidal tularemia can be severe and fatalities may reach 35%. The disease in domestic animals may be subclinical or may manifest as fatal septicemia.[4] Clinical signs previously reported in cats with tularemia include vomiting, weight loss and anorexia. [3]

The characteristic gross lesion of miliary foci of hepatic necrosis in rodents is not always visible in other species. Multifocal splenic necrosis, as seen grossly in this case, has been previously reported in other feline cases. [3] Histologic lesions of multifocal necrosuppurative inflammation in the liver, lung, spleen, and lymph nodes is characteristic of *Francisella tularensis*, but overlaps with other septicemic organisms such as *Yersinia pestis* and *Yersinia psuedotuberculosis*.[4] If possible, animals dying with a high suspicion of tularemia (signs of septicemia in an animal from an endemic area) should be necropsied under BL-2 conditions and culture should only be attempted in BL-3 facilities due to risks to laboratory personnel. In this

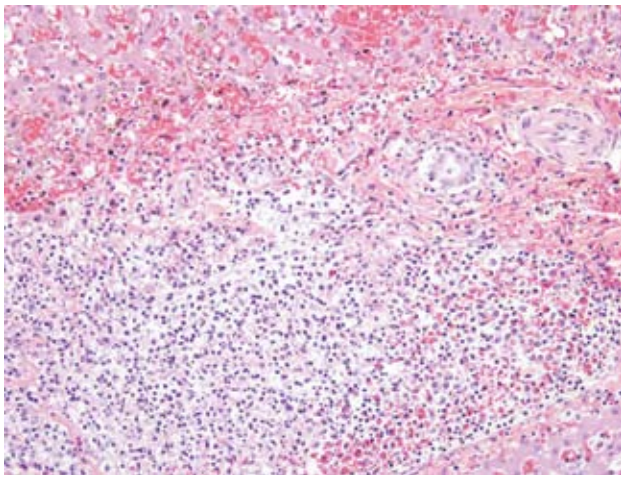

*2-3. Liver, cat. Predominately within the portal areas but also randomly, there are variably sized foci of necrosis characterized by loss of tissue architecture with replacement by high numbers of histiocytes, fewer neutrophils, lymphocytes and rare plasma cells admixed with karyorrhectic debris. (HE 400X).*

case, characteristic gross and histologic lesions along with positive PCR for *F. tularensis* allowed fresh tissues to be forwarded to an appropriate laboratory for confirmation of the diagnosis.

**AFIP Diagnosis:** Splenitis, necrotizing, random, multifocal, moderate with lymphoid depletion

**Conference Comment:** *Francisella tularensis* is a highly infectious zoonotic disease that is commonly found in the western United States. It has been reported in over 125 species of mammals, birds, reptiles, and fish. Tularemia gains access to its host by ingestion, penetration of the skin or mucous membranes, or injection by arthropods. The organism is engulfed by and multiplies within host macrophages, where it travels throughout the host via lymphatics and causes damage to vascular endothelium leading to vasculitis and thrombosis with subsequent necrotic lesions in the liver, spleen, lymph nodes, lung, and bone marrow. Cellular immunity is thought to be vital in fighting off this facultative intracellular bacteria. [1,4]

Rodents and lagomorphs are often found dead, but if found alive, they display signs of weakness and fever with lymphadenopathy. Tularemia causes a multifocal necrotizing hepatitis in rodents. Possible differential diagnoses for this lesion in rodents include Tyzzer's disease, (*Clostridium piliforme*), salmonellosis, *Listeria monocytogenes, Toxoplasma gondii, Yersinia pseudotuberculosis*, and *Yersinia enterocolitica*. [1,4]

**Contributing Institution:** Department of Veterinary Microbiology and Pathology, Washington State University, Pullman, WA (www.vetmed.wsu.edu/depts-vmp)

**References:**

1. Greene CE, DeBey BM: Tularemia. *In:* Infectious Diseases of the Dog and Cat, ed. Greene CE, 3rd ed., pp. 446-451. Saunders, St. Louis, MO, 2006
2. Sjdstedt A: Tularemia: epidemiology, physiology and clinical manifestations. Ann, NY Acad Sci **1105**:1-29, 2007
3. Tularemia. Institute for International Cooperation in Animal Biologics, The Center for Food Security and Public Health, Iowa State University, Ames, IA. www.cfsph.iastate.ed
4. Yalli VEO: Hematopoietic system. *In:* Jubb, Kennedy and Palmer's Pathology of Domestic Animals, ed. Maxie MG, 5th ed., pp. 297-298. Elsevier Limited, Edinburgh, UK, 2007

## CASE III – R08-148 (AFIP 3103602)

**Signalment:** Adult, female, crossbred goat

**History:** The owner of a goat/sheep ranch (open to the public) had previous history of contagious ecthyma (Orf). The owner's animals suffered from a pustular-like skin disorder with mortality around 50% during May to June of 2008.

**Gross Pathology:** The goat submitted for necropsy showed good nutritional condition. The skin had slightly raised, 0.5~3 cm, white to red, round papules widely spread over sparsely haired areas. The mucocutaneous junction of the muzzle, nares, conjunctiva, lingual mucosa and vaginal mucosa had variably raised nodules with occasional ulcers. The lungs were discolored with a mottled, patchy, dark purple to dark grayish red appearance. Trachea and bronchi were filled with froth and white-tinged edema fluid.

**Laboratory Results:** PCR results were positive for capripoxvirus.

**Histopathologic Description:** The mucosal membranes and skin follicles consisted of thickened, hyperplastic epithelium with ballooning degeneration, vesicle formation and necrosis, where intracytoplasmic eosinophilic inclusion bodies were clearly visible **(Figs. 3-1 and 3-2)**. The superficial epidermal layers and the

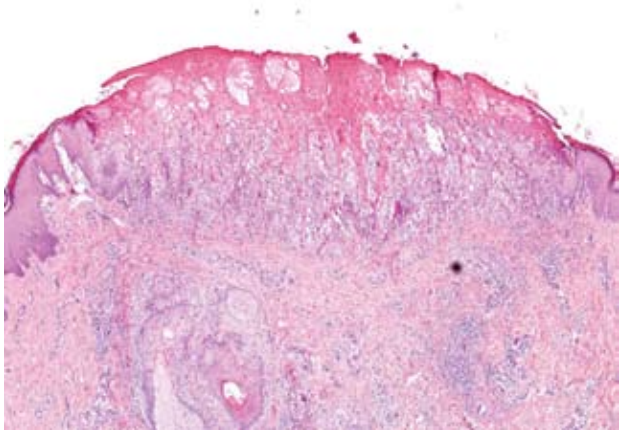

*3-1. Lip, goat. Focally extensive epidermal hyperplasia, ballooning degeneration, epidermal necrosis and intracorneal microvesicle formation. There is a moderate cellular infiltrate within the superficial dermis often surrounding adnexa. (HE 40X).*

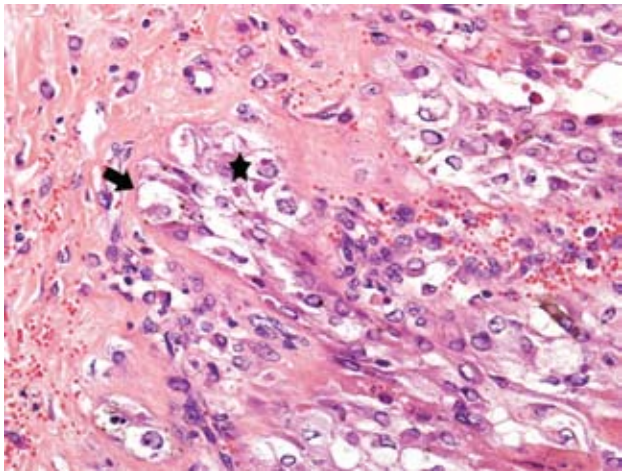

*3-2. Lip, goat. Within the stratum basale there is hydropic degeneration (arrow) and low numbers of keratinocytes containing intracytoplasmic, 5-7 um, eosinophilic intracytoplasmic inclusion bodies (star). (HE 400X).*

lingual ulcerated areas had fibrin, necrotic cellular debris, extravasated erythrocytes, and necrotic epithelium. The dermal layer was characterized by fibroplasia with a moderate infiltrate of lymphocytes, plasma cells, histiocytes, and some neutrophils. Capillaries were highly congested and some arterioles showed degeneration and perivascular infiltrates of histiocytic cells, lymphocytes, plasma cells, some neutrophils, admixed with fibroblastic cells. Intracytoplasmic eosinophilic inclusion bodies were also found in histiocytic cells and fibroblasts in the dermis in association with fibroplasia and vasculitis.

The bronchi, bronchioles, and terminal bronchioles showed varying degrees of epithelial hyperplasia, necrosis, and ballooning degeneration, with squamous metaplasia. In severely affected areas, alveolar septa were thickened as a result of pneumocyte hypertrophy. Alveolar spaces were commonly filled with fibrin, proteinaceous exudates, necrotic cellular debris, macrophages, edematous fluid with foci of alveolar septal necrosis, and septal vascular thrombi with vasculitis **(Fig. 3-3)**. Peribronchiolar and perivascular lymphocytic infiltrates were evident in some areas. Similar inclusion bodies were also detected in histiocytes, fibroblasts, epithelial cells and pneumocytes. There was lymphoid depletion along with histiocytosis in the spleen and lymph nodes, with necrosis and numerous inclusion bodies in histiocytic cells.

**Contributor's Morphologic Diagnosis:**
*Skin:* Dermatitis, hyperplasia, severe, multifocal, chronic, with vesicles, papules, ballooning degeneration, vasculitis and eosinophilic intracytoplasmic inclusion bodies

*Lung:* Bronchointerstitial pneumonia, hyperplasia, severe, multifocal, chronic, with ballooning degeneration, vasculitis, and eosinophilic intracytoplasmic inclusion bodies

**Etiology:** Capripox virus

**Contributor's Comment:** Capripoxvirus, the causative agent of sheep/goat pox, belongs to the family

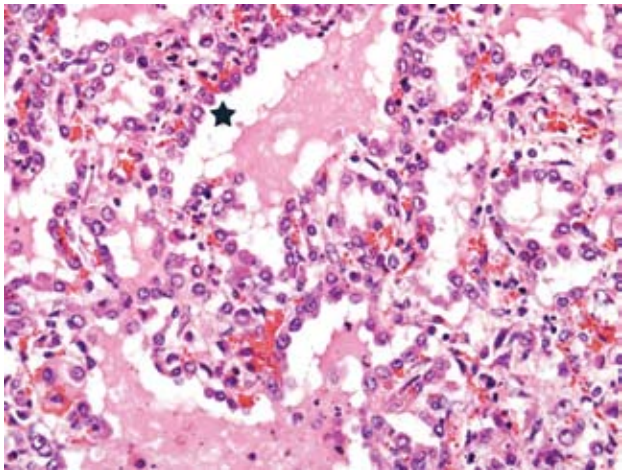

*3-3. Lung, goat. Multifocally, alveolar septa are expanded up to 5-7 times normal by predominately a lymphohistiocytic cellular infiltrate with low numbers of neutrophils and plasma cells and are lined by hypertrophied type II pneumocytes (star). The alveolar lumina contain edema, alveolar macrophages, low numbers of nondegenerate and degenerate neutrophils, and necrotic debris. (HE 400X).*

Poxviridae. It is usually more severe in goats than in sheep. All goat age groups are susceptible to the virus. The disease is endemic in Africa, the Middle East, the Indian subcontinent, and much of Asia. This disease had never been reported in Taiwan. As a result, this will be the first confirmed sheep/goat pox outbreak in Taiwan.

Clinically, infected animals can have acute to chronic disease characterized by generalized pox lesions throughout the skin and mucous membranes accompanied with persistent fever, lymphadenitis, and often a focal viral pneumonia.

The differential diagnosis should include contagious pustular dermatitis (Orf), peste des petits ruminants, and bluetongue. Orf is an endemic disease in Taiwanese goat herds.

PCR for detecting Capripox or Orf virus by the primer pair CPVS, CPVA (413 bp) and OVS, OVA (708 bp) (Zheng M. et al) respectively was employed for final diagnosis of this case. The source of the outbreak, however, is inconclusive.

**AFIP Diagnosis:** Haired skin: Dermatitis, proliferative and necrotizing, subacute, focally extensive, moderate, with intraepidermal vesicles, ballooning degeneration, intracytoplasmic eosinophilic inclusion bodies, and periadnexal and perivascular histiocytic inflammation

Lung: Pneumonia, bronchointerstitial, proliferative, subacute, multifocal, moderate, with intraepithelial intracytoplasmic eosinophilic inclusion bodies

**Conference Comment:** The family Poxviridae is divided into two subfamilies: Chordopoxvirinae which infects vertebrates, and Entomopoxvirinae which infects insects. Poxviruses are double stranded DNA viruses that cause disease in numerous living organisms. Most poxvirus virions have a characteristic brick shape and are very large viruses measuring up to 250 x 200 x 200 um, with a complex structure with lateral bodies, an outer membrane, and are sometimes enveloped. The genera of the subfamily Chordopoxvirinae include: Orthopoxvirus, Capripoxvirus, Suipoxvirus, Leporipoxvirus, Molluscipoxvirus, Yatapoxvirus, Avipoxvirus, and Parapoxvirus. This table is a brief summary of some of these viruses.

| GENUS | VIRUS | MAJOR HOSTS |
|---|---|---|
| Orthopoxvirus | Variola virus (smallpox)<br>Vaccinia virus<br>Cowpox virus<br>Camelpox virus<br>Ectromelia virus<br>Monkeypox virus<br>Seal poxvirus | Humans<br>Humans, cattle, swine, rabbits<br>Humans, cattle, cats, rats<br>Camels<br>Mice<br>Humans, non-human primates<br>Grey seals |
| Capripoxvirus | Sheeppox virus<br>Goatpox virus<br>Lumpyskin disease virus | Sheep, goats<br>Goats, sheep<br>Cattle, cape buffalo |
| Suipoxvirus | Swinepox virus | Swine |
| Leporipoxvirus | Myxoma virus | Rabbits |
| Molluscipoxvirus | Molluscum contagiosum virus | Humans, horses |
| Yatapoxvirus | Yabapox virus and tanapox virus | Humans, non-human primates |
| Avipoxvirus | Fowlpox virus | Chickens, turkeys |
| Parapoxvirus | Orf virus<br>Pseudocowpox virus<br>Bovine papular stomatitis virus | Sheep, goats, humans<br>Cattle, humans<br>Cattle, humans |

[2,4]

Poxviruses are epitheliotropic viruses, and in some instances, such as with smallpox, sheeppox, goatpox monkeypox, or ectromelia, they can cause generalized, severe, or fatal disease. Grossly, poxvirus lesions progress from an initial macule, to a papule, to a vesicle, ending in pustule and and crust formation. Histologically, poxvirus infection often causes proliferation of cells within the stratum spinosum with ballooning degeneration and eosinophilic intracytoplasmic inclusions. [2,4]

**Contributing Institution:** Division of Animal Medicine, Animal Technology Institute Taiwan, P.O. Box 23, Chunan, Miaoli, Taiwan 350.

**References:**

1. Bhanuprakash V, Indrani BK, Hosamani M, Singh RK: The current status of sheep pox disease. Comp Immunol Microbiol Infect Dis **29**:27-60, 2006
2. Ginn PE, Nasell JEKL, Rakich PM: Skin and appendages. *In:* Jubb, Kennedy and Palmer's Pathology of Domestic Animals, ed. Maxie MG, 5th ed., pp. 297-298. Elsevier Limited, Edinburgh, UK, 2007
3. Kitching RP, Hammond JM, Black DN: Studies on the major common precipitating antigen of capripoxvirus. J Gen Virol **67**:139-148, 1986
4. Murphy FA, Gibbs EPJ, Horzinek MC, Studdert MJ: Poxviridae. *In:* Veterinary Virology, 3rd ed., pp. 277-291. Academic Press, San Diego, California, 1999
5. Parthiban M, Govindarajan R, Manoharan S, Purushothaman V, Chandran NDJ, Koteeswaran A: Comparative sequence analysis of diagnostic PCR amplicons from Indian sheeppox virus. Vet Arhiv **75**:203-209, 2005
6. Zheng M, Liu Q, Jin N, Guo J, Huang X, Li H, Zhu W, Xiong Y: A duplex PCR assay for simultaneous detection and differentiation of Capripoxvirus and Orf virus. Mol Cell Probes **21**:276-81, 2007

## CASE IV – ND 1 (AFIP 3102366)

**Signalment:** 18-month-old female American bison (*Bison bison*)

**History:** The animal was sick for 10 days, gradually lost condition, developed diarrhea, and exhibited swelling in both carpal joints. Lameness led to difficulty walking. The animal eventually became recumbent and was euthanized.

**Gross Pathology:** Both lungs contained randomly distributed irregular, sometimes raised, variably sized foci of caseous necrosis. Both stifle joints were swollen, fluctuant on palpation, and, upon incision, oozed purulent to caseous exudate. There was marked inflammation of the joint capsules, synovial tissue, and tendon sheaths. There was a localized area of necrosis in the cervical musculature on the right side of the neck (injection site).

**Laboratory Results:** *Mycoplasma* spp. was cultured from lung tissue and joint exudate. This isolate was then identified as *Mycoplasma bovis* by PCR and immunohistochemistry. No other ruminant respiratory pathogens were identified in these tissues.

**Histopathologic Description:** Large areas of caseous necrosis and inflammation were noted in the pulmonary parenchyma **(Fig. 4-1)**. Affected areas were characterized by a distinct outer zone of variably dense fibrous connective tissue infiltrated with a mixture of inflammatory cells, a thinner middle zone consisting of a bilayer of activated macrophages and plasma cells (outer portion) and necrotic neutrophils (inner portion), and an expansive interior zone of caseous necrosis in which necrotic alveolar septa and bronchioles were seen. Normal lung adjacent to the outer fibrous connective tissue capsule had several areas of atelectasis, some accumulation of proteinic material within alveoli, and increased numbers of alveolar macrophages. Sections of synovium, joint capsule and tendon sheath had a marked necropurulent

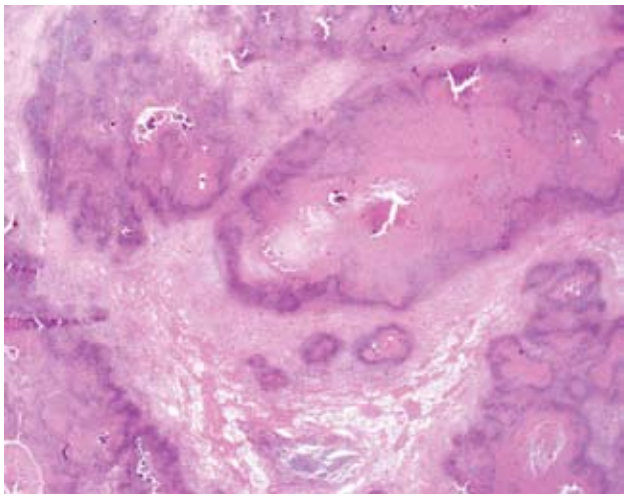

*4-1. Lung, bison. Multifocally affecting approximately 80% of the tissue section, there are large variably sized and irregularly shaped areas of lytic necrosis characterized by a deeply eosinophilic core which is often centrally mineralized and bounded by a rim of cellular infiltrate. Adjacent alveoli are compressed and atelectatic. (HE 20X).*

synovitis, arthritis, and tenosynovitis respectively.

**Contributor's Morphologic Diagnosis:** Severe, multifocal to coalescing, caseonecrotic pneumonia with bronchiectasis and atelectasis

**Contributor's Comment:** *Mycoplasma bovis*-associated disease manifests itself in a variety of ways in cattle including pneumonia and tenosynovitis, arthritis, keratoconjunctivitis, otitis media, and mastitis.[2] A condition caused by *M. bovis* characterized by chronic pneumonia and polyarthritis has been recognized in feedlot cattle.[3] Coinfection with Bovine viral diarrhea virus (BVDV), and common bovine respiratory viruses appears to occur with some frequency. Previous studies utilizing IHC to examine the pattern of bacterial colonization in *M. bovis* infected lungs described staining in bronchiolar epithelial cells, inflammatory cells, and abscessed airways (naturally infected animals), random staining in areas of both coagulative and caseous necrosis with peripheral zones of purulent to pyogranulomatous inflammation (naturally infected animals), and staining in areas of coagulative necrosis and bronchiolar epithelium (naturally infected animals) and in inflammatory cells in alveoli and septal walls (experimentally infected animals).[3] Staining patterns in naturally infected animals were consistent with the type of staining seen in this animal. The most intense staining was observed in bronchiolar epithelial cells. This pattern of staining supports the proposed pathogenesis for this condition, which is early bronchitis leading to bronchiectasis that eventually coalesces into large zones of caseous necrosis.[1] Characteristics of this case indicate that bison are susceptible to severe infections with this pathogen, and that *M. bovis* is capable of causing primary disease in this species.

**AFIP Diagnosis:** Lung: Pneumonia, necrotizing, fibrinosuppurative, diffuse, severe with interlobular edema and fibrosis

**Conference Comment:** *Mycoplasma bovis* is of significant economic importance in both the United States and Europe. It is the cause of enzootic pneumonia in young calves and a cause of chronic pneumonia and polyarthritis in adult cattle. This disease in feedlot cattle mimics shipping fever, but infected cattle are often times refractory to antimicrobial treatment with continued clinical decline. *M. bovis* is spread via genital, nasal, and mammary secretions.[1] *M. bovis* is very effective at evading the host immune response by a variety of mechanisms too in-depth to discuss here, and subsequently this organism causes chronic infections despite valiant clinical intervention.

Grossly, *M. bovis* can cause striking lesions within the respiratory tract characterized by multiple, well demarcated, caseonecrotic nodules up to a few centimeters in diameter dispersed throughout the cranioventral lung lobes. Joint lesions are characterized by a reddened and reactive synovium and serofibrinous exudate within the joint capsule.[1] Otitis media is an additional sequelae in calves to *M. bovis* infection.[1]

Histologically, acute lesions begin in the airways and progress to areas of multifocal to coalescing caseonecrotic debris often containing mineral. Early in the progression of *M. bovis* infections, leukocytes are necrotic but retain their cellular architecture and contain hypereosinophilic cytoplasm and karyorrhectic nuclei. This is characteristic for respiratory lesions caused by *M. bovis*.[1] Foci of necrosis with this distinctive gross and histologic appearance are pathognomonic for *M. bovis* in cattle.[1]

**Contributing Institution:** North Dakota State University, Veterinary Diagnostic Laboratory, 1523 Centennial Boulevard, Fargo, ND, 58105, http://www.vdl.ndsu.edu/

**References:**

1. Caswell JL, Williams KJ: Respiratory system. *In:* Jubb, Kennedy and Palmer's Pathology of Domestic Animals, ed. Maxie MG, 5th ed., pp. 611-614. Elsevier Limited, Edinburgh, UK, 2007

2. Dyer N, Hansen-Lardy L, Krogh D, Schaan L, Schamber E: An outbreak of chronic pneumonia and polyarthritis syndrome caused by *Mycoplasma bovis* in feedlot bison (*Bison bison*). J Vet Diagn Invest **20**:369-371, 2008

3. Gagea MI, Bateman KG, Shanahan RA, van Dreumel T, McEwen BJ, Carman S, Archambault M, Caswell JL: Naturally occurring *Mycoplasma bovis*-associated pneumonia and polyarthritis in feedlot beef calves. J Vet Diagn Invest **18**:29-40, 2006

**NOTES:**

The Armed Forces Institute of Pathology
Department of Veterinary Pathology

*Conference Coordinator:*
Todd M. Bell, DVM

WEDNESDAY SLIDE CONFERENCE 2008-2009

# Conference 6

22 October 2008

*Conference Moderator:*

Dr. Lauren Brinster, DVM, Diplomate ACVP

## CASE I – Case DG0802868 (AFIP 3106794)

**Signalment:** 2-year-old male beagle dog

**History:** This animal was part of an IACUC approved animal study to evaluate the pathogenesis and treatment of septic shock. The dog had been anesthetized and an intrabronchial inoculation of *Staphylococcus aureus* was placed into the right caudal lobe. The dog was sedated with fentanyl, versed and medetomidine and was mechanically ventilated via an endotracheally tube for 89 hours. Intravenous fluid administration with Normosol was provided to maintain blood pressure and hydration. Oxygen was administered to maintain adequate arterial oxygenation. After 24 hours reduced arterial oxygenation required the level of oxygen administration to be increased to 100%. The dog died after 89 hours, seven hours before the termination point for the study. The post-mortem interval was 10 hours at refrigeration temperature.

**Gross Pathology:** At necropsy this animal was well muscled with a moderate amount of body fat and in good hydration. Edema was noted in the subcutaneous tissues of the ventral neck and thorax. Approximately 500 ml of clear serosanguineous fluid was present in the abdominal cavity and approximately 400 ml of similar fluid was present in the thoracic cavity. The lungs were moderately atelectatic secondary to the presence of the pleural effusion. An area within the right caudal lobe measuring approximately 3 cm x 3 cm was noted to be pale with demarcated borders consistent with a focus of necrosis, which corresponded to the placement of the bacterial clot. All lung lobes were firm and sank in formalin. Multifocal petechial and ecchymotic hemorrhages were noted in the pancreas and mesentery. The liver, kidneys and spleen were moderately congested. The remaining organs and tissues appeared normal.

**Laboratory Results:** Samples for bacterial culture were collected from the femoral and jugular catheters, which yielded a mixed growth of Klebsiella pneumonia and *Acinetobacter baumannii*.

**Histopathologic Description:** There was a severe fibrinosuppurative bronchopneumonia. Bronchioles and alveoli contained large numbers of neutrophils admixed with moderate numbers of alveolar macrophages and fibrin. The bronchi, bronchioles and alveoli were prominently lined by homogeneous eosinophilic granular to fibrillar hyaline membranes **(Fig. 1-1)**. Degenerative cells could be identified within the hyaline membranes in areas. Respiratory epithelium was not evident lining the bronchioles.

***Sponsored by the American Veterinary Medical Association, the American College of Veterinary Pathologists, and the C. L. Davis Foundation.**

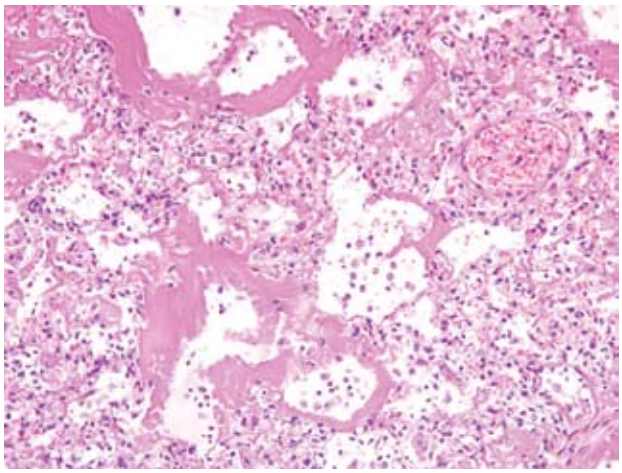

*1-1 Lung, dog. Loss of bronchiole and alveolar epithelium with replacement by variably thick, acellular, fibrillar, eosinophilic material (hyaline membranes). (HE 200X).*

**Contributor's Morphologic Diagnosis:**

1. Lung: bronchopneumonia, fibrinosuppurative, severe
2. Lung: hyaline membranes, bronchiolar and alveolar, diffuse
3. Multiple organs: bacteremia, bacterial rods

**Contributor's Comment:** The suppurative bronchopneumonia associated with intrabronchial administration of Staphylococcus aureus in this case was similar to other dogs examined on this protocol. The atypical feature of the histologic appearance of the bronchopneumonia in this case was the presence of prominent bronchiolar and alveolar hyaline membranes. Hyaline membranes may occur in a variety of disease entities where there is diffuse alveolar damage. In premature infants there is a condition termed hyaline membrane disease of the newborn or respiratory distress syndrome. Hyaline membranes are also a common feature of the Acute Respiratory Distress Syndrome (ARDS). Hyaline membranes are comprised of homogenous granular or fibrillar eosinophilic material, which line alveoli and bronchioles. They are composed of necrotic epithelial cell debris admixed with fibrin and plasma elements.[9] Immunohistochemistry studies in human tissues have demonstrated that the epithelial and endothelial components of surfactant apoprotein A, factor VIII related antigen and cytokeratin AE1/AE3 are present in hyaline membranes associated with diffuse alveolar damage.[8]

Respiratory distress syndrome in premature infants is associated with inadequate levels of pulmonary surfactant produced by type II pneumocytes.[5] Decreased levels of surfactant causes increased alveolar surface tension, which leads to atelectasis, hypoxemia and acidosis. This further causes pulmonary vasoconstriction and hypoperfusion leading to capillary endothelial damage, plasma leakage, fibrin deposition and hyaline membrane formation.

Acute respiratory distress syndrome occurs in a variety of mammalian species including man. ARDS can be due to a variety of etiologic factors such as septic shock, physiologic shock associated with trauma or burns, severe pulmonary viral infections such as SARS, inhaled toxins or irritants such as smoke, phosgene and mercury vapor, hypersensitivity to certain organic solvents and herbicides such as kerosene and paraquat, high altitude, cytotoxic drugs such as bleomycin, busulfan and methotrexate, and oxygen toxicity.[1]The common pathogenesis in these entities is the development of acute diffuse alveolar damage to the alveolar epithelium and capillary endothelium with interstitial and intraalveolar edema and fibrin exudation and the development of hyaline membranes.[6] As a response to the alveolar injury, type II epithelial cells will proliferate and resolution will either lead to recovery or given the severity of the injury may lead to pulmonary fibrosis.

In this case there were multiple interrelated contributing factors, which may have led to the development of pulmonary hyaline membranes, including septic shock, terminal gram negative sepsis, mechanical ventilation injury and oxygen toxicity. The most likely significant cause was oxygen toxicity. Oxygen toxicity has been induced and has been reported to occur in a wide variety of mammalian species. Exposure to oxygen levels of 85-100% for a prolonged period can cause oxygen toxicity. Dogs exposed to 1 atm of oxygen had an average survival time of approximately 60-80 hours.[3] Oxygen derived free radicals including superoxide, hydroxyl ion and singlet oxygen can directly injure cell membrane by causing lipid peroxidation. Additionally, there is inhibition of nucleic acid and protein synthesis and inactivation of cellular enzymes. Damage to pulmonary epithelium may also lead to decreased levels of surfactant. Oxygen toxicity can also induce CNS signs of vertigo and convulsions.[7] Ultrastructurally, studies have shown that as little as 1 to 4 hours of exposure to 100% oxygen can cause morphologic changes to type I epithelial cells with bleb formation of the cytoplasmic membranes and swelling of endothelial cells with plasma transudation.[4]

**AFIP Diagnosis:**

Lung: Pneumonia,broncho-interstitial, fibrinosuppurative, acute, diffuse, severe with bronchiolar and alveolar hyaline membranes and bacteria

**Conference Comment:** The contributor gave an excellent explanation of both the cause and pathogenesis of ARDS. Grossly, lungs with this type of insult contain lesions with greater involvement of the dorsocaudal lung fields. Despite the nature of the causative agent, diffuse alveolar damage leads to a predictable histologic pattern of progression from an acute exudative phase to a subacute proliferative phase followed by a chronic fibrosing phase.[2]

**Contributing Institution:** National Institutes of Health, Division of Veterinary Resources, Bethesda, MD 20892-5280

**References:**

1. Blennerhassett JB. Shock lung and diffuse alveolar damage pathological and pathogenetic considerations. Pathology **17(2)**:239-47, 1985
2. Caswell JL, Williams KJ: Respiratory system. *In:* Jubb, Kennedy and Palmer's Pathology of Domestic Animals, ed. Maxie MG, 5th ed., vol 2, pp.564-567. Elsevier Limited, Edinburgh, UK, 2007
3. Clark JM, Lambertsen CJ: Pulmonary oxygen toxicity: a review. Pharmacol Rev **23(2)**:37-133, 1971
4. Coalson JJ, Beller JJ, Greenfield LJ: Effects of 100 per cent oxygen ventilation on pulmonary ultrastructure and mechanics. J Pathol **104(4)**:267-73, 1971
5. Hallman M, Glumoff V, Ramet M: Surfactant in respiratory distress syndrome and lung injury. Comp Biochem Physiol A Mol Integr Physiol **129(1)**:287-94, 2001
6. Hasleton PS, Roberts TE: Adult respiratory distress syndrome- an update. Histopathology **34(4)**:285-94, 1999
7. Patel DN, Goel A,, Agarwal SB, Garg P, Lakhani KK: Oxygen toxicity. J Indian Academy of Internal Medicine **4(3)**:234-7, 2003
8. Peres SA, Parra ER, Eher E, Capelozzi VL: Nonhomogenous immunostaining of hyaline membranes in different manifestations of diffuse alveolar damage. Clinics **61(6)**:497-502, 2006
9. Scarpelli EM: Respiratory distress syndrome of the newborn. Annu Rev Med **19**:153-166,1968

## II – Case MK 0803123 (AFIP 3106804)

**Signalment:** 6-year-old male, Rhesus Macaque, (*Macaca mulatta*)

**History:** An encapsulated subcutaneous mass was noted near the right nipple. It was removed and submitted for analysis. On physical exam no other abnormalities were noted.

**Gross Pathology:** The tissue sample (biopsy) measured 1.8 x 1.5 x 1.0 cm. The mass is firm, slightly nodular and yellow to white in color. It is encapsulated in a well demarcated capsule.

**Laboratory Results:** None performed.

**Histopathologic Description:** The slide consists of a well demarcated neoplasm surrounded by a layer of smooth muscle lined by flattened epithelial cell. There are some pockets of normal glandular tissue in the surrounding soft tissue. The neoplastic nodules appear to be mostly solid with rare ductal and tubular structures. The ductal structures are lined by pleomorphic epithelial cells with loss of polarity and piling up of cells **(Figs. 2-1, 2-2)**. Some cells have clear cytoplasmic vacuoles. The nuclei have stippled chromatin with single nucleoli and are centralized in the cell. Roughly 1 mitotic figure per 40X field is seen. Multiple sections of the neoplasm fail to show invasion into surrounding soft tissue. Original tumor sections were subdivided to prepare conference slides.

**Contributor's Morphologic Diagnosis:**
Mammary Gland: ductular carcinoma in situ (DCIS)

**Contributor's Comment:** Mammary gland tumors are uncommon in macaques. It is still unclear whether the low cancer rate observed in macaques is true resistance or if insufficient lifespan studies have been conducted to see whether higher cancer rates occur in aged populations.[8] Ductular carcinoma in situ (DCIS) are neoplasms that have neoplastic cells limited to ducts. This is distinguished from lobular carcinoma in situ (LCIS) where cells extend into lobules. Occasionally it is difficult to morphologically distinguish LCIS from ductular carcinoma in situ DCIS. A potential marker to distinguish DCIS from LCIS is E-cadherin since E-cadherin protein expression is lost in LCIS, while it remains in cases of DCIS.[6,8] Differentiation between DCIS and LCIS is crucial in humans because management strategies differ greatly between the two types.[7] In humans, estrogens have been hypothesized as contributing to the formation

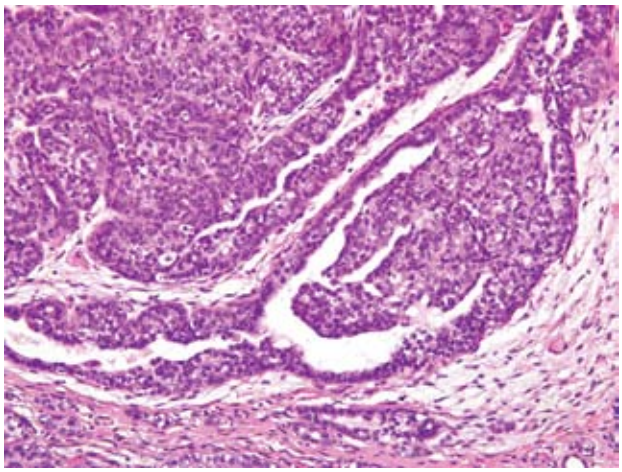

*2-1. Mammary gland, macaque. Multifocally, neoplastic cells form micropapillary projections that variably fill duct lumina. (HE 400X).*

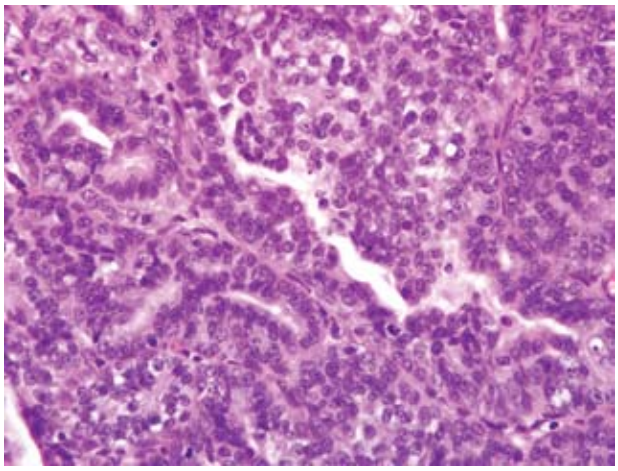

*2-2. Mammary gland, macaque. The neoplasm is composed of polygonal to cuboidal cells with variably distinct cell borders, moderate amounts of eosinophilic cytoplasm, round to oval nuclei with finely stippled chromatin and generally 1-3 nucleoli. The mitotic rate is regionally variable with up to 4-5 mitoses in some high powered field. (HE 400X).*

of mammary tumors. Estrogen stimulates the mitosis of breast epithelial cells regardless of the gender and can enhance unregulated growth of mammary tissue.[1] This particular case is interesting because it represents a mammary gland carcinoma in a male, which has been rarely reported. One report gives an incidence rate of 1.1% in a long term study of untreated animals.[8] This rate is similar to that seen in men, accounting for 0.8% of all the cases of mammary carcinoma. Most mammary carcinoma in human males is ductal in origin with the majority being invasive. Mammary gland carcinoma in men has been reported to be linked to testicular abnormalities, Klinefelter syndrome, familial history of breast cancer, infertility and breast discharge. They tend to be estrogen and progesterone receptor positive.[3]

**AFIP Diagnosis:** Mammary gland: Ductular carcinoma in-situ

**Conference Comment:** This case was reviewed in consultation with the AFIP Department of Gynecologic and Breast Pathology, who agreed with the contributor's diagnosis, and further commented that the DCIS appeared to involve a papilloma, based on the presence of papillary cores within the lesion which are lined by a monotonous proliferation of epithelial cells consistent with DCIS. They also noted the focal presence of myoepithelial cells in some of the papillary cores.

During the post conference, part of the discussion focused on general features distinguishing benign from malignant tumors. These features include pleomorphism, nuclear morphology, appearance of mitotic figures and overall mitotic rate, polarity, and invasiveness.

In malignant tumors, both cells and nuclei generally display greater variation in size and shape than do their benign counterparts. Cells can be much larger or smaller than adjacent cells, with similar variation in nuclear size. These changes are referred to as anisocytosis and anisokaryosis, respectively. In malignant tumors, nuclei often contain an abundance of DNA and stain much darker (hyperchromatic). The nuclear to cytoplasmic ratio can also approach a 1:1 ratio from the normal 1:4 to 1:6 ratio. Mitotic figures are more abundant in malignant tumors than in benign tumors. Often, malignant tumors also have "bizarre mitotic figures" forming abnormal shapes and patterns that do not resemble the normal mitotic rearrangement of chromosomes. These cells often produce multipolar spindles, which can create a highly unusual cellular appearance in relation to neighboring cells. Malignant tumors are generally faster growing neoplasms with growth occurring in a more disorganized, haphazard fashion (often referred to as loss of polarity). Malignant tumors also tend to invade surrounding tissue and metastasize to regional lymph nodes and other organ systems, whereas benign tumors stay in the location of origin. There can be a wide range of morphologic appearances within tumors depending on the specific type of tumor and the tissue involved, so these guidelines are meant as a general rule and are subject to vary from one type of neoplasm to the next.[4]

Mammary gland lesions have been reported in numerous lab animals and domestic species, and a few of the more common of these were discussed during the post-conference session. A chart listing the species discussed during this session and the changes in each species is included below. [2,5]

| Species | Mammary change | Cause |
|---|---|---|
| Rat | Fibroadenoma (S-D strain) | Increase in prolactin |
| Rabbit | Mammary dysplasia | Pituitary tumor |
| Mouse | FVB/N mice – hyperplasia of mammary glands | Proliferation of prolactin secreting cells in pars distalis |
| | Mammary tumors | Mammary tumor viruses (MMTVs) |
| Cat | Fibroepithelial hyperplasia | Progesterone administration (Ovaban other iatrogenic hormones) |
| Canine | Gynecomastia | Sertoli cell tumor |

**Contributing Institution:** National Institutes of Health, Division of Veterinary Resources, Bethesda, MD 20892-5280

**References:**

1. Clemons M, Goss P: Estrogen and the risk of breast cancer. N Engl J Med **344**:276-285, 2001
2. Foster RA, Ladd PW: Male genital system. *In:* Jubb, Kennedy and Palmer's Pathology of Domestic Animals, ed. Maxie MG, 5th ed., pp. 596-597. Elsevier, Philadelphia, Pennsylvania, 2007
3. Giordano SH, Buzdar AU, Hortobagyi GN: Breast cancer in men. Annals of Internal Medicine 137:678-687. Primatology 2001; 30:121–126
4. Kumar V, Abbas AK, Fausto N: Neoplasia. *In:* Robins and Cotran Pathologic Basis of Disease, ed. Kumar V, Abbas AK, Fausto N, 7th ed., pp. 272-276. Elsevier, Philadelphia, Pennsylvania, 2005
5. Percy DH, Barthold SW: Pathology of Laboratory Rodents and Rabbits, 3rd ed., pp.116-117, 170-171, 306. Blackwell Publishing, Ames, Iowa, 2007
6. Moll R, Mitze M, Frixen UH: Differential loss of E-cadherin expression in infiltrating ductal and lobular breast carcinomas. Am J Pathol **143**:1731–42, 1993
7. Schnitt SJ, Morrow M: Lobular carcinoma in situ: current concepts and controversies. Semin Diagn Pathol **16**:209–23, 1999
8. Wood CE, Usborne A, Tarara R, Starost MF: Hyperplastic and neoplastic lesions of the mammary gland in macaques. Vet Pathol **43**:471–483, 2006

## III – Case 36005-7 (AFIP 3094514)

**Signalment:** Adult male strain MDX mouse; *Mus musculis*; murine

**History:** The animal is submitted for necropsy for evaluation of a mass involving the right hind limb.

**Gross Pathology:** The right hind limb contains a large, firm, 2.7 cm x 2.5 cm x 2 cm, pale tan, multilobulated mass extending from the proximal hind limb to the right lateral aspect of the vertebral column. The mass involves the dorsoproximal femur and right lateral lumbar spine, and penetrates into the peritoneal cavity. No other significant gross lesions are observed.

**Laboratory Results:** N/A

**Histopathologic Description:** The skeletal and connective tissues of the proximal hind limb surrounding the femur and paralumbar region are effaced by a multinodular, highly infiltrative, and poorly demarcated neoplasm. Confluent nodules are composed of haphazardly arranged, densely cellular, interlacing bundles and streams of plump spindloid to polygonal neoplastic cells. Neoplastic cells exhibit small to moderate amounts of eosinophilic cytoplasm with variably distinct cell borders. Nuclei are large and round to oval or irregularly shaped with coarsely granular to vesicular chromatin and one to three nucleoli. There is marked anisocytosis and anisokaryosis and mitotic figures are numerous (up to eight per 40x field). Present throughout the mass are numerous multinucleated giant cells. Multinucleated cells are distributed throughout the mass and exhibit clustered nuclei with moderate to marked karyomegaly and irregularly lobular nuclei or linearly oriented row of nuclei. Also present within the mass are strap cells, racquet cells and plump polygonal cells with hypereosinophilic cytoplasm (resembling embryonal myocytes) **(Fig. 3-1)**. In multiple regions, neoplastic cells are separated by narrow bands and interconnecting septae of dense, amorphous, deeply eosinophilic matrix resembling osteoid **(Fig. 3-2)**. There are multifocal expanses of necrosis and hemorrhage within the mass.

Within the margins of the tumor adjacent to the lumbar spinal column are multiple fragments of mature cortical bone, necrotic bone, and woven bone. Focally, in association with bone fragments, are small zones of pale basophilic matrix. Along the peripheral margins of the mass, neoplastic cells envelop individualized and atrophic skeletal muscle fibers.

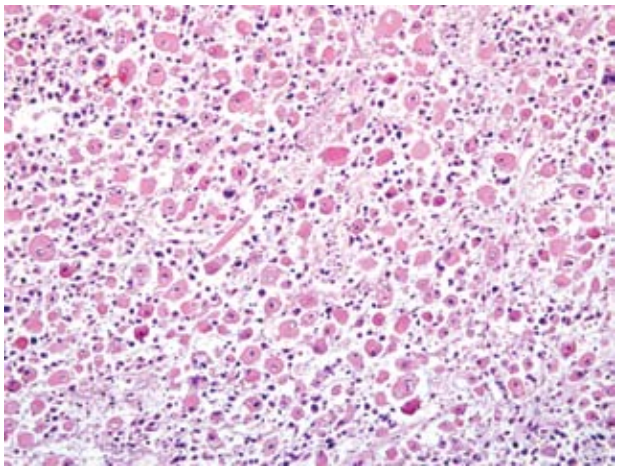

*3-1. Muscle, mouse. Within a focally extensive area there are neoplastic embryonal myofibrils characterized by abundant brightly eosinophilic cytoplasm, pleomorphic nuclei with either finely stippled or more coarsely stippled chromatin and separated by a fine fibromyxomatous matrix. (HE 200X).*

**Immunohistochemistry results for neoplastic cells (Figs. 3-3 and 3-4):**

- Vimentin: Diffuse positive cytoplasmic immunoreactivity
- Actin: Multifocal positive cytoplasmic immunoreactivity
- Myogenin: Multifocal positive nuclear immunoreactivity
- Pancytokeratin: Diffusely negative

**Contributor's Morphologic Diagnosis:** Skeletal muscle: Rhabdomyosarcoma, embryonal

**Contributor's Comment:** Skeletal muscle neoplasms are rare in both humans and animal species. In humans, rhabdomyosarcoma occurs more frequently than rhabdodmyoma and can be classified into the following categories based on histologic morphology: 1) embryonal rhabdomyosarcoma; 2) botryoid rhabdomyosarcoma; 3) alveolar rhabdomyosarcoma; and 4) pleomorphic rhabdomyosarcoma.[1] Presence of cross-striations in neoplastic cells is variable. Additional histologic types that have been described in humans include anaplastic, monomorphous round cell, spindle cell, lipid-rich/clear cell, and sclerosing rhabdomyosarcoma.[2] Differentiation of subtypes in humans is of prognostic significance, and while rhabdomyosarcomas in animals exhibit similar histomorphologic features, the rarity of these tumors in veterinary medicine hampers evaluation of the prognostic

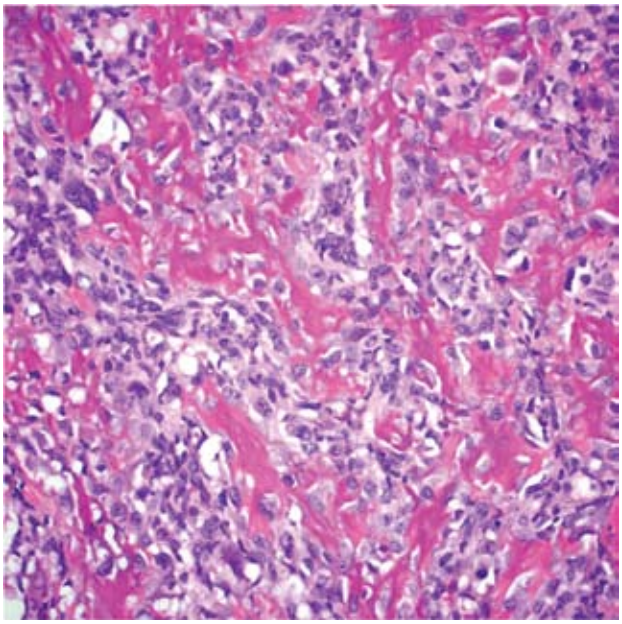

*3-2. Muscle, mouse. Neoplastic cells separate and surround osteoid in some areas (HE 400X). Photomicrograph courtesy of Comparative Molecular Pathology unit, Center for Cancer Research, National Cancer Institute Bethesda, MD.*

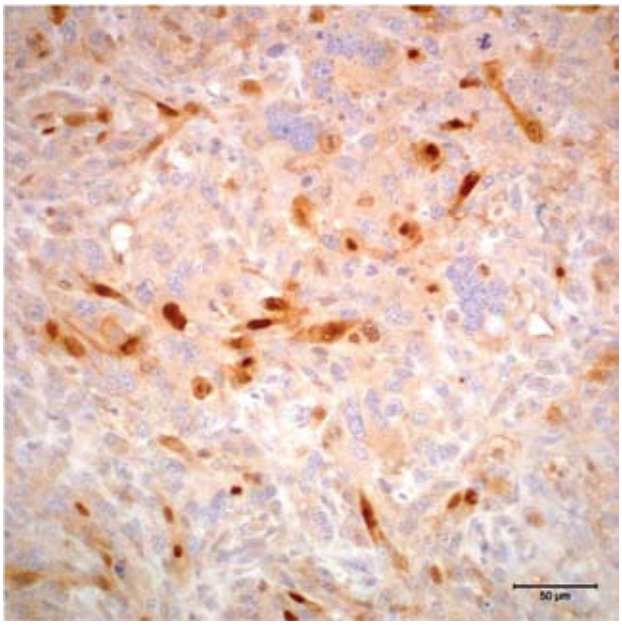

*3-3. Muscle, mouse. Multifocal nuclear immuno-positivity for myogenin. Photomicrograph courtesy of Comparative Molecular Pathology unit, Center for Cancer Research, National Cancer Institute Bethesda, MD.*

value of such sub-classification.[3]

Most skeletal muscle tumors in animals occur in dogs. Rhabdomyoma and rhabdomyosarcoma have also been reported in cats, cattle, horses, sheep, Sprague-Dawley rats, a Rhesus macaque, and a boa constrictor. In dogs, categorization of rhabdomyosarcomas has included embryonal, botryoid, alveolar, and pleomorphic subtypes, with histologic features of these subtypes in dogs paralleling those described in human cases of rhabdomyosarcoma.[3] The occurrence of laryngeal rhabdomyosarcoma and botryoid rhabdomyosarcoma of the urinary bladder are more commonly described in dogs and may represent distinct clinicopathologic entities in this species.[3]

The degree of expression of immuno-histochemical markers is influenced by the degree of differentiation of neoplastic cells, and staining is often heterogeneous within tumors.[3] Immunohistochemical markers that are described for use in the diagnosis of rhabdomyosarcoma include vimentin, desmin, actin, myoglobin, myosin, titin, myogenin, and myoD1 (myogenic determination factor). More traditionally used immunohistochemical markers, such as vimentin, actin, and myoglobin, are not specific for rhabdomyosarcoma; further, they may not be expressed in more poorly differentiated tumors.[2,11] The

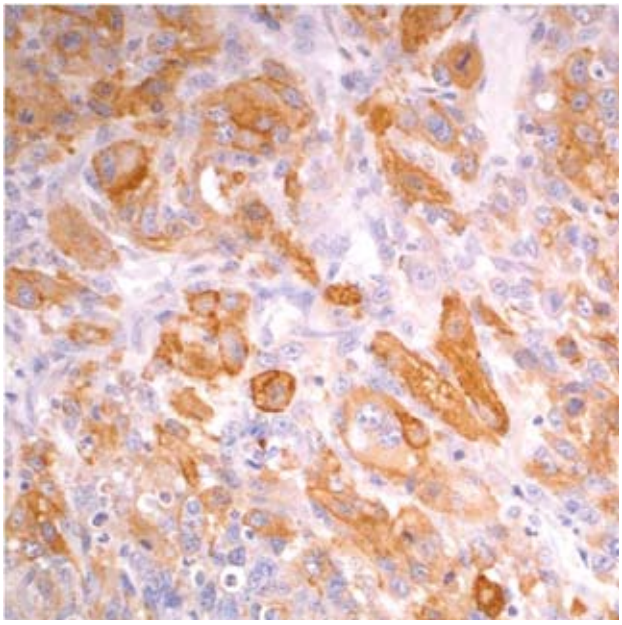

*3-4. Muscle, mouse. Multifocal cytoplasmic immuno-positivity for actin. Photomicrograph courtesy of Comparative Molecular Pathology Unit, Center for Cancer Research, National Cancer Institute Bethesda, MD.*

use of transcriptional factors, specifically myogenin and myoD1, for diagnosis of rhabdomyosarcoma has been shown to demonstrate a greater degree of specificity and sensitivity in human tumors.[2,11] Myogenin and myoD1 are preferentially expressed in the nucleus of differentiating myoblasts and are expressed earlier than desmin, muscle-specific actin, myoglobin, and myosin during skeletal muscle development and differentiation.[2,6]

Immunohistochemical analysis for myogenin expression has previously been applied in a mouse model for methylcholanthrene-induced rhabdomyosarcoma. In this model, both embryonal and pleomorphic rhabdomyosarcomas were induced.[6] Immunohistochemistry for myogenin demonstrated expression of myogenin in both pleomorphic and embryonal variants; embryonal rhabdomyosarcomas exhibited greater myogenin expression than pleomorphic types, and myogenin expression was greatest in neoplastic cells of myoblast-like morphology.[6]

Expression of myogenin and myoD1 in two canine botryoid rhabdomyosarcomas was recently evaluated.[6] In these studies, myogenin and myoD1 expression were found to be useful markers for rhabdomyosarcoma in the dog; histomorphology correlated to labeling for myogenin and myoD1. Specifically, myogenin was predominantly expressed by multinucleated cells that expressed alpha-sarcomeric actin, resembling myotubes, while myoD1 was expressed by undifferentiated mesenchymal cells.[8]

The case presented herein exhibits histo-morphologic features that are most compatible with embryonal rhabdomyosarcoma; however, some regions of the tumor are more suggestive of pleomorphic or alveolar variants, including the presence of numerous large multinucleated neoplastic cells and bundles of spindle cells. Strong and widespread positive immunohistochemical reactivity for vimentin, actin, and myogenin support the diagnosis of rhabdomyosarcoma. The majority of neoplastic cells exhibit strong cytoplasmic immunoreactivity for vimentin and actin. Cells expressing nuclear immunoreactivity for myogenin were frequently small and spindloid; myogenin expression was variably present in multinucleated neoplastic cells.

Interestingly, within the neoplastic mass and distal to the site of pathologic fracture are areas of amorphous eosinophilic matrix resembling osteoid. To our knowledge, osteoid formation within a rhabdomyosarcoma has not previously been described. The origin of this apparent osteoid matrix in this neoplasm is uncertain. No cells within the matrix exhibited immunoreactivity for actin or myogenin, which is in contrast to the majority of the neoplastic population.

Signaling morphogenetic proteins via bone has been implemented in the formation of bone by mesenchymal tissues.[4,10] Bone morphogenetic proteins (BMPs) are cytokines within the transforming growth factor-β (TGF-β) family, and signaling occurs via binding to BMP receptors.[10] While BMP expression has been documented to a variable degree in a number of sarcomas, rhabdomyosarcoma was among a subset of tumors that consistently did not show BMP expression as demonstrated by immunohistochemistry.[15]

The focal zone of osteoid formation may represent a response to bone fracture. Bone formation in muscle, referred to as myositis ossificans or myositis ossificans traumatica, is an infrequent sequelae to bone fracture or muscular trauma with hematoma formation.[1,9] Three types of myositis ossificans traumatica are described; two of these types involve the formation of new bone immediately adjacent to or connected to pre-existing bone. The third type of bone formation occurs within a region of muscle that appears to be separate from underlying bone. Theories for the pathogenesis of this type of bone formation have included escape and proliferation of periosteal osteoblasts, metaplasia of intramuscular connective tissue, or induction of osteogenic precursor cells through BMP signaling.[1] The areas of apparent osteoid formation observed in this rhabdomyosarcoma appear at some distance from the site of bone fracture and thus may be most similar to the third type of myositis ossificans traumatica.

**AFIP Diagnosis:** Skeletal muscle, hind limb: Rhabdomyosarcoma, embryonal with focal osteosarcomatous differentiation

**Conference Comments:** Conference participants noted a few areas within this neoplasm of osteoid production by neoplastic cells. The ensuing discussion then centered on whether these foci represent tumor bone, areas of osseous metaplasia, or reactive bone secondary to the pathologic fracture of the pelvis or femur. The consensus was that at least in some areas the osteoid was produced by the neoplastic mesenchymal cells. Our diagnosis of rhabdomyosarcoma reflects the predominant line of differentiation (further supported by the contributor's immunohistochemical findings), but also specifies the differentiation towards at least one additional mesenchymal cell type. Some favored the diagnosis of osteosarcoma, arguing that, by definition, if malignant mesenchymal cells are producing osteoid, the tumor is an osteosarcoma, even if other mesenchymal cell types are present.[13] We also considered a diagnosis of malignant mesenchymoma, defined as a malignant tumor consisting of at least two different neoplastic cell lines of

mesenchymal origin.[5,12] In the human literature, it has been suggested to replace the nonspecific designation of 'mesenchymoma' with a classification in one of two ways: by predominant pattern and mention the other, or by the designation as mixed mesenchymal neoplasm and specify the lines of differentiation.[7]

**Contributing Institution:** Comparative Molecular Pathology Unit, Laboratory of Cancer Biology and Genetics, Center for Cancer Research, National Cancer Institute, National Institutes of Health, 37 Convent Drive, Room 2002, Bethesda, MD 20892

**References:**

1. Beiner JM, Jokl P: Muscle contusion injury and myositis ossificans traumatica. Clin Orthop Relat Res **403S**:S110-S119, 2002
2. Cessna MH, Zhou J, Perkins SL, Tripp SR, Layfield L, Daines C, Coffin CM: Are myogenin and myoD1 expression specific for rhabdomyosarcoma? Am J Surg Pathol **25**:1150-1157, 2001
3. Cooper BJ, Valentine BA: Tumors of muscle. *In:* Tumors in Domestic Animals, ed. Meuten DJ, pp. 343-357. Iowa State Press, Ames, Iowa, 2002
4. Guo W, Gorlick R, Ladanyi M, Meyers PA, Huvos AG, Bertino JR, Healey JH: Expression of bone morphogenetic proteins and receptors in sarcomas. Clin Orthop **365**:175-183, 1999
5. Hendrick MJ, Mahaffey EA, Moore FM, Vos JH, Walder EJ: Histologic Classification of Mesenchymal Tumors of Skin and Soft Tissues of Domestic Animals, 2nd series, vol. 2, pp. 32-33. Armed Forces Institute of Pathology, Washington, DC, 1998
6. Inoue M, Wu H: mmunohistochemical detection of myogenin and p21 in mehtycholanthrene-induced mouse rhabdomyosarcoma. Int J Exp Path [87]:445-450, 2006
7. Kempson RL, Fletcher CDM, Evans HL, Hendrickson MR, Sibley RK: Atlas of Tumor Pathology, Tumors of the Soft Tissues, 3rd series, fascile 30, pp. 5. Armed Forces Institute of Pathology, Washington, DC, 1998
8. Kobayashi M, Sakai H, Hirata A, Yonemaru K, Yanai T, Watanabe K, Yamazoe K, Kudo T, Masegi T: Expression of myogenic regulating factors, myogenin and myoD, in two canine botryoid rhabdomyosarcomas. Vet Pathol **41(3)**:275-277, 2004
9. Kumar V, Abbas A, Fausto N: Cellular adaptations, cell injury, and cell death. *In:* Robbins and Kotran Pathologic Basis of Disease, ed. Kumar V, Abbas A, Fausto N, 7th ed. p. 11, Elsevier, Philadelphia, PA 2005
10. Nakamura Y, Wakitani S, Saito N, Takaoka K: Expression profiles of BMP-related molecules induced by BMP-2 or -4 in muscle-derived primary culture cells. J Bone Miner Metab **23**:426-434, 2005
11. Parham DM, Ellison DA: Rhabdomyosarcoma in adults and children. Arch Path Lab Med **130**:1454-1465, 2006
12. Pool RR, Thompson KG: Tumors of joints. *In:* Tumors in Domestic Animals, ed. Meuten DJ, 4th ed., pp. 241. Blackwell Publishing, Ames, IA, 2002
13. Thompson KG, Pool RR: Tumors of bone. *In:* Tumors in Domestic Animals, ed. Meuten DJ, 4th ed., pp. 263. Blackwell Publishing, Ames, IA, 2002
14. Vleet JFV, Valentine BA: Muscle and tendon. *In:* Pathology of Domestic Animals, ed. Maxie MG, 5th ed., pp. 272-277. Elsevier Saunders, Philadelphia, PA, 2007
15. Yoshikawa H, Rettig WJ, Lane JM, Takaoka K, Alderman E, Rup B, Rosen V, Healey JH, Juvos AG, Garin-Chesa P: Immunohistochemical detection of bone morphogenetic proteins in bone and soft-tissue sarcomas. Cancer **74(3)**:842-847, 1994

## IV – Case 0566-1C (AFIP 3105526)

**Signalment:** Four mice: 3-month-old, female MyD88-/- *mus musculus* B6/JMyD88N11F4 (*Mus musculus*)

**History:** The mice are in a full-service room, group housed, on a ventilated rack. Four mice were found with torticollis. The mice were bright, alert, responsive and in good body condition. The laboratory requested a necropsy with culture and sensitivity of the tympanic bullae. Rule outs for head tilt in mice include otitis media/interna, central nervous system disease, and necrotizing arteritis of undetermined cause.

The laboratory has had a number of mice with head tilts in the past and is interested in determining the cause in order to treat or prevent further outbreaks of disease. This is an immune-compromised line that currently is not on antibiotic prophylaxis.

**Gross Pathology:**

| | |
|---|---|
| Mice 1 – 3: | Head tilt to the left |
| Mouse 4: | Head tilt to the right |
| Mice 1 – 4: | White opaque material within the tympanic bullae |
| Mice 1, 2, 4: | Swollen right forepaw (up to 0.6 CM in maximum dimension) |
| Mouse 3: | Not foot lesions |

**Microbiology:**

| | |
|---|---|
| Mice 1 – 4: | Nasal pharynx culture |
| Mice 1 – 3: | Tympanic bulla culture |
| Mice 1, 2, 4: | Forepaw cultured |

**Laboratory Results:** Microbiology Results: Initial

| Mouse | Site | Micro # | Bacteria | AMPIC | CEPHA | CHLOR | CIPRO | ERYTH | GENTA | LINCO | PENIC | SXT |
|---|---|---|---|---|---|---|---|---|---|---|---|---|
| 1 | Foot | M0717948 | S. aureus | R | | S | | | S | S | R | S |
| 2 | Foot | M0717949 | S. aureus | R | | S | | | S | S | R | S |
| 4 | Foot | M0717950 | S. aureus | R | | S | | | S | S | R | S |
| | | | P. mirablis | S | | S | | | S | R | S | S |
| 4 | Foot | M0717951 | S. aureus | R | R | S | | | S | S | R | S |
| 1-4 | NPX | M0717952 | P. mirablis | Proteus mirabilis predominate in all the specimens from the Middle Ear, and 3 of 4 of the Nasal wash had it. | | | | | | | | |
| 1-3 | Tympanic Bullae | | | | | | | | | | | |

**Complete Antibiotic Culture and Sensitivity Profile: S = Susceptible; R = Resistant**

| Antimicrobial | Staph. aureus | Proteus mirablis |
|---|---|---|
| Amox/Clav AML | S | S |
| Ampicillin | R | S |
| Amikacin | S | S |
| Cefazolin | S | R |
| Ceftiofur | S | S |
| Cephalothin | S | S |
| Chloramphenicol | S | S |
| Ceftriaxone | S | S |
| Clindamycin | S | R |
| Doxycycline | S | R |
| Enrofloxacin | S | S |
| Gentamicin | S | S |
| Norfloxacin | S | S |
| Penicillin | R | S |
| Trimethroprim, Sulfamethoxazole | S | S |

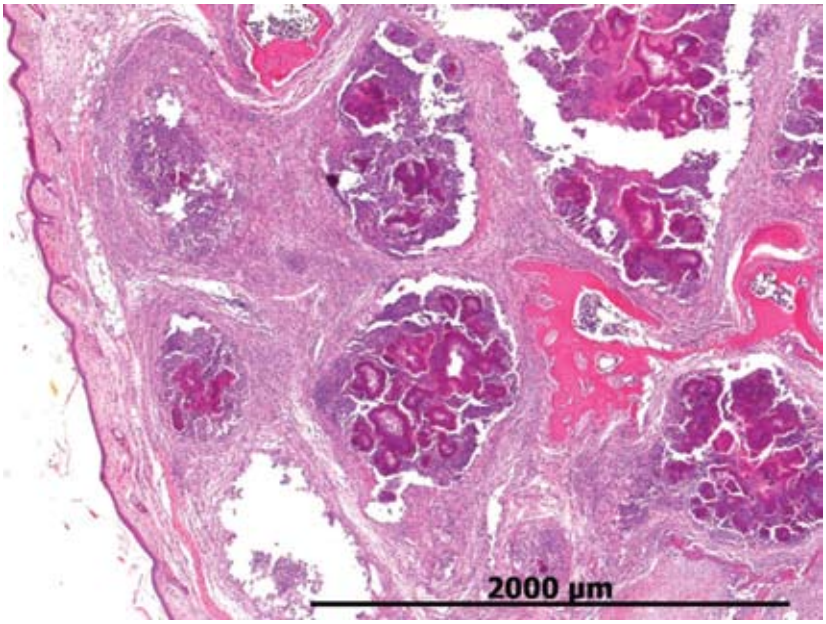


*4-1. Forepaw, mouse. Multifocal to coalescing pyogranulomas centered on bacterial colonies surrounded by brightly eosinophilic material. Photomicrograph courtesy of Section of Comparative Medicine, School of Medicine, Yale University New Haven, CT.*

**Histopathologic Description:** The forepaw is markedly expanded by numerous coalescing botryoid pyogranulomas centered on 100-200 um colonies of Gram-positive cocci, surrounded by brightly eosinophilic amorphous material (Splendore-Hoeppli) **(Figs. 4-1 and 4-2)**. These pyogranulomas contain a central core of abundant necrotic debris admixed with numerous neutrophils, surrounded by layers of epithelioid macrophages, fewer lymphocytes and plasma cells, and finally, outer layers of fibroblasts and collagen. In the adjacent tissue there is marked thinning and loss of bone of the distal phalanges. In addition, there is edema with macrophages, lymphocytes, and plasma cells within the subcutaneous tissue.

**Contributor's Morphologic Diagnosis:** Cellulitis, pyogranulomatous and necrotizing, focally extensive, subacute, severe with Splendore-Hoeppli material and large colonies of cocci

**Contributor's Comment: Myeloid differentiation f**actor 88 (MyD88) knockout mice have been shown to be deficient in the production of an innate immune response.[7,8,12] Neutrophil function is compromised due to the deletion of MyD88 from the signaling pathway of toll-like receptors (TLR). The immune response has also been shown to be delayed due to failure of proinflammatory cytokines and induction of NF-kB and MAP-kinase pathways.[1,2,12] Impairment of macrophage function, especially in the production of IL-6 and TNF-a, has been shown in response to LPS, peptidoglycan, and lipopeptides.[7,14] The model has also been shown deficient in the response to exogenous IL-1 as the production of TNF-a and IL-6 is muted.[13] The failure of a normal macrophage response also resulted in a decreased B cell response. Although the initial response to LPS in diminished, the overall deleterious effects to the animal are increased as sepsis results in hyperinflammation.[12] The decreased immune response of MyD88 knockout mice has been described in a variety of tissues, including brain [7], skin [10], and generalized infections.[12]

Reported causative agents of botryomycosis include *Staphylococcus aureus, S. hominus, S. xylosus, Pseudomonas aeruginosa, Proteus* spp*., Escherichia coli, Nocardia asteroides* and *Streptococcus intermedius*, with a variety of other aerobic and anaerobic bacterial agents implicated.[3,9,11,14,15] Immunosuppression has been suggested as a factor in increased prevalence of botryomycosis.[11,16] As described above, the MyD88 knockout mouse is deficient in the innate immune response.

Splendore-Hoeppli staining refers to the deeply eosinophilic material that surrounds the 'grains' of bacterial colonies contained centrally. The eosinophilic material is described as having a coronal appearance, which engulfs whitish purulent material associated with the colonies[3,14,15]. Necrotic tissue has also been reported to be present.[3] While Splendore-Hoeppli bodies are predominately reported to be associated with botryomycosis, numerous reports of this phenomenon in the presence of parasitic [3] or fungal infections [4,15,16] are in the literature. The eosinophilic staining component of this histologic finding has been linked to cellular debris and antigen-antibody complexes.[3,11,15] This staining

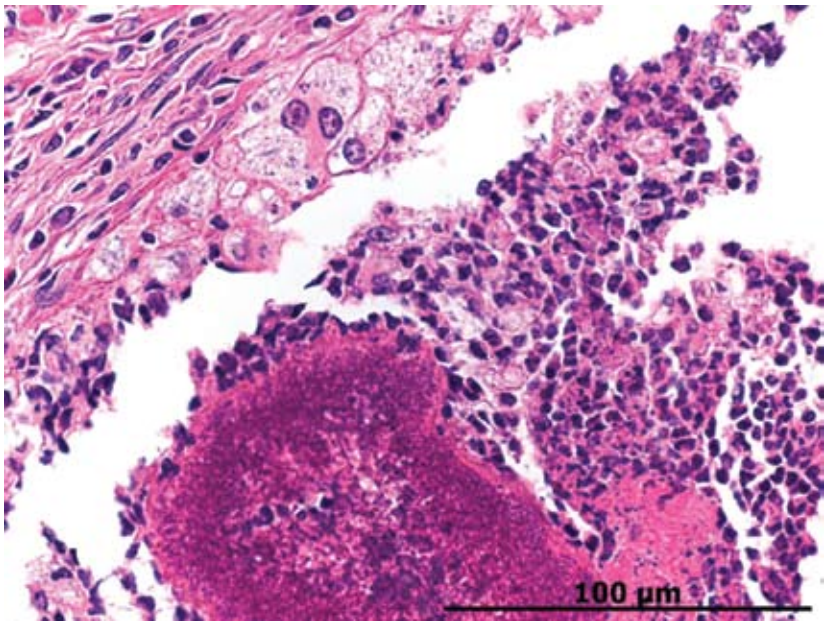


*4-2. Forepaw, mouse. The pyogranulomas are centered on bacterial colonies composed of 1-2 micron diameter cocci that are surrounded by a radiating corona of brightly eosinophilic club shaped material (Splendore-Hoeppli material) admixed with necrotic debris, neutrophils and bounded by epithelioid macrophages, lymphocytes, fibroblasts and fibrous connective tissue. Photomicrograph courtesy of Section of Comparative Medicine, School of Medicine, Yale University New Haven, CT.*

pattern has been referred to as Splendore-Hoeppli bodies, material, and phenomenon.

The lesions in the forepaw were subsequently determined to be secondary to toe-clip for identification. The colony was subsequently placed on Baytril and there were no further lesions.

**AFIP Diagnosis:** Digits, foreleg: Cellulitis, pyogranulomatous and necrotizing, subacute, focally extensive, severe with osteolysis, Splendore-Hoeppli material and large colonies of cocci

**Conference Comment:** Botryomycosis, a disease of the skin and subcutis, is caused by nonfilamentous bacteria that form grossly visible colonies that look like granules or spicules within a chronically affected lesion. This condition generally affects the skin, but it can extend into deeper tissues if left untreated. Rule outs for these lesions include actinomycotic and eumycotic mycetomas. Infections generally start after trauma to the skin or wound contamination.[6]

Botryomycosis usually manifests as a firm nodule that is ulcerated with a draining tract. The discharge often contains the previously described granules or spicules, thus suggesting botryomycosis. Histologically, this is a striking lesion with a marked pyogranulomatous response centered on bacterial colonies often encircled by Splendore-Hoeppli material. These lesions can be walled off by abundant fibrous connective tissue and can coalesce to form chains of granulomas within the subcutis and surrounding tissues.[6]

**Contributing Institution:** Section of Comparative Medicine, School of Medicine, Yale University New Haven, CT http://info.med.yale.edu/compmed/compmed/index.htm

**References:**

1. Akira S and Takeda K: Toll-like receptor signaling. Nature Reviews **4**:499-511, 2004
2. Akira S: Toll-like receptors: lessons from knockout mice. Biochem Soc Trans **28**:Part 5, 2000
3. Armed Forces Institute of Pathology: Wednesday Slide Conference, Conference 13, Case 1, AFIP #2812387, Conference Comments, 2006
4. Bersoff-Matcha Sj, Roper CC, Liapis H, and Little JR: Primary Pulmonary Botryomycosis: Case Report and Review. Clin Infec Dis **26**:620–624, 1998
5. EL van den Berk G, Noorduyn LA, van Ketel RJ, van Leeuwen J, Bemelman WA, and Prins JM: A fatal pseudo-tumour: disseminated basidiobolomycosis. BMC Infectious Diseases **6**:140, 2006
6. Ginn PE, Mansell JEKL, Rakich PM: Skin and appendages. *In:* Jubb, Kennedy and Palmer's Pathology of Domestic Animals, ed. Maxie MG, 5th ed., pp. 691. Elsevier, Philadelphia, Pennsylvania, 2007
7. Goldstein DR, Tesar BM, Akira S, and Lakkis FG: Critical role of the Toll-like receptor signal adaptor protein MyD88 in acute allograft rejection. J Clin Invest **111(10)**: 1571-1578, 2003
8. Kielian T, Phulwani NK, Esen N, Syed MM, Haney AC, McCastlain K, and Johnson J: MyD88-dependent signals are essential for the host immune response in experimental brain abscess. J Immunol **178**:4528–4537, 2007

9. Machado CR, Schubach AO, Conceição-Silva F, Quintella LP, Lourenço MCS, Carregal E, and do Valle ACF: Images in Clinical Dermatology. Dermatology **211**:303-304, 2005
10. Rodig SJ and Dorfman DM: Splendore-Hoeppli phenomenon. Arch Pathol Lab Med **125**:1515-1516, 2001
11. Schlossberg D, Pandey M, and Reddy R: The Splendore-Hoeppli phenomenon in hepatic botryomycosis. J Clin Pathol **51**:399-400, 1998
12. Sugawara I, Yamada H, Mizuno S, Takeda K, and Akira S: Mycobacterial infection in MyD88-deficient mice. Microbiol Immunol **47(11)**:841-847, 2003
13. Tohno M, Skimazu T, Aso H, Kawai Y, Saito T, and Kitazawa H. Molecular Cloning and Functional Characterization of Porcine MyD88 Essential for TLR Signaling. Cell Mol Immunol **4(5)**:369-376, 2007
14. Weighardt H, Kaiser-Moore S, Vabulas RM, Kirschning CJ, Wagner H, and Holzmann B: Cutting edge: Myeloid differentiation factor 88 deficiency improves resistance against sepsis caused by polymicrobial infection. J Immnunol **169**:2823–2827, 2002
15. Zaharopoulos P: Fine-needle aspiration cytologic diagnosis of lymphocutaneous sporotrichosis: A case report. Diag Cytopathol **20(2)**:74-77, 1998
16. Zavasky D, Samowitz W, Loftus T, Segal H, and Carroll K: Gastrointestinal zygomycotic infection caused by basidiobolus ranarum: Case report and review. Clin Infec Dis **28(6)**:1244-8, 1999

**NOTES:**

**The Armed Forces Institute of Pathology**
**Department of Veterinary Pathology**

*Conference Coordinator:*
**Todd M. Bell, DVM**

## WEDNESDAY SLIDE CONFERENCE 2008-2009

# Conference 7

**29 October 2008**

*Conference Moderator:*

Dr. Dale G. Dunn, DVM, Diplomate ACVP

### CASE I – D07-045891 (AFIP 3102259)

**Signalment:** One approximately 3-month-old female Cooper's hawk (*Accipiter cooperi*)

**History:** This animal was admitted to the Raptor Center of the University of Minnesota with neurologic signs in late August. It was emaciated and had evidence of head trauma. Funduscopic investigation revealed an "exudative" chorioretinitis. Due to the deterioration of the clinical state of the animal, and based on the funduscopic finding indicating WN disease, the animal was euthanized two days after admission.

**Gross Pathology:** The vitreous of the left eye was slightly opaque after fixation. In addition, the bird had acute bilateral leptomeningeal hemorrhages at the base of both cerebral lobes. The spleen was moderately enlarged, soft and diffusely dark red.

**Laboratory Results:** A tissue pool containing kidney, heart and brain was positive for West Nile virus (WNV) by PCR but virus isolation using Vero cells failed to detect WNV (Animal Health Diagnostic Center of Cornell University). WNV was not detected in the aqueous humor of the right eye. WNV antigen was present in the retina of the left eye (slide A), mainly in the outer nuclear layer (**Fig. 1-1**; monoclonal antibody against envelope protein epitope of WNV; clone 7H2; BioReliance, Rockville, Maryland, USA). The animal had a high WNV specific antibody titer (> 1:320) while antibodies against Saint Louis encephalitis virus were undetectable (< 1:10).

**Histopathologic Description:** Sections of two blocks representing both eyes were submitted (slide A = left eye; slide F = right eye): Right eye (slide F): Numerous capillaries of the pecten were internally lined or surrounded by predominantly plasma cells and lymphocytes and fewer macrophages **(Fig. 1-2)**. The capillaries had hyperplastic endothelial cells. Clusters of inflammatory cells were also present between lamellae of the pecten. A similar infiltrate was present in the optic disc. The retina and choroid on one side of the pecten appeared to be largely unaffected except for the deposition of a small amount of faint basophilic stringy material on the nerve fiber layer that entrapped a small number of degenerate inflammatory cells and a minimal infiltration of the nerve fiber layer by plasma cells. The choroid and retina on the other side of the pecten was significantly altered. The choroid of this segment was markedly infiltrated by plasma cells and lymphocytes. The retinal pigmented epithelial (RPE) cells overlying inflamed choroidea were degenerate with loss of their

***Sponsored by the American Veterinary Medical Association, the American College of Veterinary Pathologists, and the C. L. Davis Foundation.**

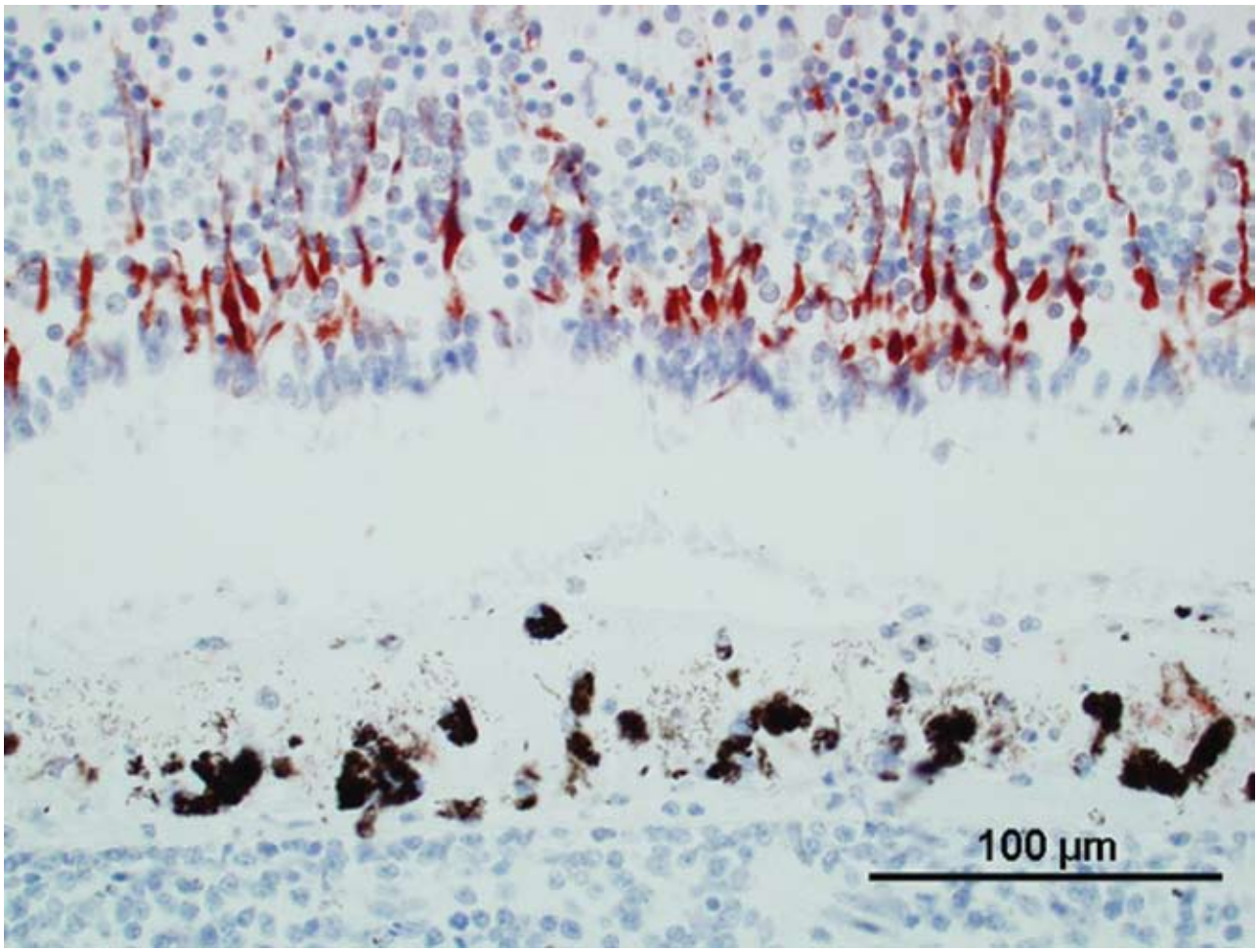


*1-1. Eye, Coopers Hawk. Multifocally with the retina there is immunohistochemical staining for WNV antigen. The WNV antigen is evident in the outer nuclear layer, cell fibers of the outer plexiform layer and inner nuclear layer. Photomicrograph courtesy of Department of Veterinary Population Medicine College of Veterinary MedicineUniversity of Minnesota 1333 Gortner Ave St. Paul, MN 55108.*

delicate processes that support the photoreceptor cells. More severely affected RPE cells were detached and individualized and assumed a plump shape. The retina was detached in these areas. Occasional small aggregates of inflammatory cells (lymphocytes and plasma cells) were present within the nerve fiber layer of this retinal segment particularly close to the pecten. Swollen axons were occasionally present within the nerve fiber layer. The iris was infiltrated by few individual plasma cells and lymphocytes. The lens was absent in some of the sections either due to a processing artifact or due to an oblique angle of the initial sectioning of the eye globe. Some sections contained adipose tissue within the area of the vitreous due to a processing artifact.

Left eye (slide A)**:** The lesions were similar to the lesions described in the right eye. The degenerate changes of the retinal pigmented epithelial cells were more widespread so that non-degenerate RPE cells were essentially absent. In addition, there was multifocal acute hemorrhage into the choroid, retina and vitreous. A group of foamy macrophages (gitter cell morphology) were present at the margin of disrupted retina in one location.

**Contributor's Morphologic Diagnosis:** Pectenitis and choroiditis, lymphoplasmacytic, chronic, marked with retinal degeneration and detachment

Acute intravitreal hemorrhage (only left eye, slide A)

**Contributor's Comment:** West Nile virus (WNV) infection is common in Cooper's hawks (and red tailed hawks).[7] The disease may be transmitted to Cooper's hawks by mosquito bites but oral infection is also

*1-2. Eye, Coopers Hawk. The pectin is expanded up to five times normal by a cellular infiltrate. (HE 40X).*

plausible since Cooper's hawks tend to prey on songbirds some of which may constitute an avian reservoir for WNV. In a subgroup of the infected Cooper's hawks, e.g., many hatch year birds, the infection results in WN disease while the majority of infected Cooper's hawks (and red tailed hawks) likely eliminate the virus rapidly without having clinical signs, similar to the situation in humans. This is evidenced by a fairly high WNV seroprevalence in apparently healthy Cooper's hawk and red tailed hawk populations.[1,6] WN disease in Cooper's hawks (and red tailed hawks) is frequently characterized by neurologic signs (e.g., "depression" and tremors) and visual impairment ultimately potentially progressing to blindness.[5] Ophthalmologic examination of hawks with WN disease frequently demonstrates opacities in the fundus of one or both eyes that is interpreted as "chorioretinitis" by clinicians.[5] The presence of funduscopic lesions in hawks may aid in establishing a diagnosis of WN disease in the living patient. Gross lesions other than emaciation are uncommon in hawks with WN disease, but may include opacities of the fundus ("chorioretinitis") of one or both eyes, myocarditis and unilateral or bilateral cerebral malacia. Histologically, pectenitis is one of the most consistent findings in Cooper's hawks with WN disease.[5,7] As in the present case, chorioditis is frequently also present and occasionally, retinal degeneration and necrosis are additional ocular lesions. Retinal pigmented epithelial cells overlying areas of chorioditis are usually degenerate as evidenced by individualization and clumping of these cells possibly leading to detachment of the retina in the respective segment. The funduscopically or grossly visible opacities in the fundus likely represent fibrin deposition on the nerve fiber layer of the retina. Lymphoplasmacytic iridocyclitis may in some cases be a minor component of the ocular lesions.

WNV may be detectable by PCR, immunohistochemistry or virus isolation in the eyes (e.g., aqueous humor) even when other organs are negative.[4,5,7] The retina may harbor only a few individual WNV antigen positive cells (e.g., ganglion cells), or in some cases entire full thickness segments of the retina overlying areas of chorioditis may be strongly WNV antigen positive. In addition, WNV-specific antibodies are usually present in the aqueous humor of infected Cooper's hawks (and red tailed hawks) with WN disease although plasma/serum titers are usually higher.[5] Hence aqueous humor may be used as substrate for detection of antibodies when plasma or serum is not available (e.g. in carcasses submitted to veterinary diagnostic laboratories).

Besides the inflammatory and degenerative lesions that were present in both eyes, one eye had evidence of trauma in the form of intravitreal hemorrhage in the present case. Trauma likely was also the cause of the macroscopically observed leptomeningeal hemorrhage.

**AFIP Diagnosis:** Eye: Pectenitis, lymphoplasmacytic, diffuse, moderate with multifocal, mild choroiditis and retinal degeneration and detachment

**Conference Comment:** West Nile virus (WNV) is a single-stranded, icosohedral, enveloped RNA virus in the family *Flaviridae*, genus *Flavirus*. WNV is mainly transmitted by mosquitoes and circulates in the environment often through a sylvatic cycle from bird to mosquito to bird. West Nile derives its name from the West Nile district of Uganda, where the virus was first discovered. WNV was first recognized in the United States in 1999 in New York after an outbreak in the local bird population.[2]

West Nile virus has a very wide host range with the major natural amplifier being crows and corvids. Birds develop a severe viremia with virus detectable in many organs in the body. This is in contrast to horses, where the virus is only found in the CNS.[3] Horses and some birds are exquisitely sensitive to WNV, and disease outbreaks are usually seen during peak mosquito season, which is the summer and fall. Mortality rate in horses can reach 50%. Gross lesions are usually absent or unspectacular, but spinal cord lesions do occur and manifest as hemorrhage and malacia of the thoracic and lumbar spinal cord. Histologically, lesions are usually present in the brainstem and thoracolumbar spinal cord and consist of a nonsuppurative encephalomyelitis, gliosis, and glial nodule formation with or without necrosis. The gray matter usually contains more severe lesions. Birds often

have lesions in the heart and liver. WNV infection is much more of a systemic disease in affected birds. Cats, dogs, cattle, and swine are susceptible to WNV, but they often have subclinical disease.[3]

**Contributing Institution:** Department of Veterinary Population Medicine, College of Veterinary Medicine, University of Minnesota, 1333 Gortner Ave, St. Paul, MN 55108, USA

**References** :

1. Hull J, Hull A, Reisen W, Fang Y, Ernst H: Variation of West Nile virus antibody prevalence in migrating and wintering hawks in central California. The Condor **108**:435-439, 2006
2. Lichtensteiger CA, Greene CE: Arthropod-Borne viral infections. *In:* Infectious Disease of the Dog and Cat, ed. Greene, 3rd ed., pp. 192-195. Saunders, Elsevier, St. Louis, MO, 2006
3. Maxie MG, Youssef S: Nervous system. *In:* Jubb, Kennedy and Palmer's Pathology of Domestic Animals, ed. Maxie MG, 5th ed., vol 1, pp.421-422. Elsevier Limited, Philadelphia, PA, 2007
4. Nemeth N, Gould D, Bowen R, Komar N: Natural and experimental West Nile virus infection in five raptor species. Jour of Wil Dis **42**:1-13, 2006
5. Pauli AM, Cruz-Martinez LA, Ponder J, Redig PT, Glaser A, Klauss G, Schoster JV, Wünschmann A: Ophthalmologic and oculopathologic findings in red-tailed hawks (*Buteo jamaicensis*) and Cooper's hawks (*Accipiter cooperi*) with naturally acquired West Nile virus infection. J Am Vet Med Assoc **231**:1240-1249, 2007
6. Stout WE, Cassini AG, Meece JK, Papp JN, Rosenfield RN, Reed KD: Serologic evidence of West Nile virus infection in three wild raptor populations. Avian Dis **49**:371-375, 2005
7. Wünschmann A, Shivers J, Bender J, Carroll L, Fuller S, Saggese M, van Wettere A, Redig P: Pathologic findings in red tailed hawks (*Buteo jamaicensis*) and Cooper's hawks (*Accipiter cooperi*) naturally infected with West Nile virus. Avian Dis **48**:570-580, 2004

## CASE II – 067-78252 (AFIP 3102493)

**Signalment:** 14-yr-old, M(n), domestic shorthair, feline

**History:** Six years prior to necropsy this animal was presented to the Ophthalmology Service of the Colorado State University Veterinary Medical Center for recent onset of blindness. The animal had been examined by a veterinarian for an abscess on the left forelimb and received a prescription for oral enrofloxacin ten days prior to ophthalmic examination. The exact dosage is unknown but was thought to be either 8mg/kg/day (1 68mg tablet per day) or 17mg/kg/day (1 68mg tablet twice daily) [It was a large fat cat]. Ophthalmic exam revealed bilateral mydriasis, lack of menace response, decreased pupillary light reflexes, diffuse tapetal hyperreflectivity, retinal vascular attenuation and non-responsive electroretinogram. A clinical diagnosis of diffuse retinal degeneration secondary to enrofloxacin retinal toxicosis was made. Six years later, the day of necropsy, the animal was found dead in the owner's yard.

**Gross Pathology:** Both eyes were grossly normal. Other findings included severe obesity, cardiomegaly (heart weight: 31 grams), severe diffuse pulmonary edema and a mildly enlarged right thyroid gland.

**Laboratory Results**: N/A

**Histopathologic Description:** Lesions are largely confined to the retina where there is a complete loss of the photoreceptor layer, outer nuclear layer, and outer plexiform layer **(Fig. 2-1)**. The inner nuclear layer is mildly disorganized and there is mild decreased cellularity—both slightly more so in the non-tapetal region. There are scattered, small amounts of pigment within the inner nuclear layer of the non-tapetal region. Additionally, there are rare, lightly eosinophilic, intranuclear inclusions within the inner nuclear layer (present in most slides but not all). Other minor changes inconsistently present in all slides are mild ciliary body cystic degeneration and mild perivascular lymphocytic iritis.

**Contributor's Morphologic Diagnosis:** Eyes: bilateral severe diffuse outer retinal atrophy

**Contributor's Comment:** The cause of death was attributed to a suspected cardiovascular event secondary to severe myocardial fibrosis (lesion not provided). The eyes were collected in hopes of documenting the histologic lesion of enrofloxacin induced retinal degeneration/atrophy, clinically diagnosed six years prior to necropsy. Given the clinical history and ocular histopathology, a diagnosis of enrofloxacin retinal toxicosis was made.

A differential diagnosis for outer retinal degeneration/atrophy in a cat includes enrofloxacin toxicity, taurine deficiency, inherited retinal atrophy, and hypertensive retinopathy.

For an excellent summary of the events associated with the appearance of enrofloxacin retinal toxicosis in the cat, and the clinical, histopathologic, and ultrastructural ocular lesions associated with oral administration of enrofloxacin at 10 times the recommended dose in an experimental setting, readers are referred to reference 2. While the current recommended dosage of 5mg/kg/day seems to have substantially decreased cases of retinal toxicosis, the authors of the same reference conclude with the following statement: "Investigation of the effects of administration of the recommended dosage of enrofloxacin on the retinas and CNS of cats is warranted."

The exact mechanism of enrofloxacin retinal toxicosis is not known; however, any fluoroquinolone or structurally related compounds should be considered potentially retinotoxic in cats.[11] Risk factors predisposing cats to enrofloxacin retinal toxicosis include large doses or plasma concentration, rapid IV infusion of the antibiotic, prolonged courses of treatment, and age.[11] In cats, the combination of methylnitrosourea and ketamine hydrochloride induces retinal degeneration, but neither drug does so individually.[10]

The retinal lesion seen in taurine deficiency usually starts centrally, hence the disease name of feline central retinal degeneration, but can progress to diffuse retinal atrophy given enough time.[5,8] Due to taurine supplementation of commercial feline diets, the disease is fairly rare now, however, it has been induced by feeding dog food to cats.[1] Affected cats may also have dilated cardiomyopathy. If recognized early enough, both vision and cardiac function can be partially restored with appropriate dietary taurine levels.

Inherited retinal atrophy, or progressive retinal atrophy, has been studied extensively in Abyssinians but has also been documented in Persians and speculated in several other cases.[3,6,9] In the Abyssinian there are two forms termed rod-cone dysplasia (autosomal dominant inheritance) and rod-cone degeneration (autosomal recessive inheritance), both of which may serve as an animal model of the human disease, retinitis pigmentosa.[6]

Hypertensive retinopathy classically includes retinal detachment, subretinal effusion/hemorrhage and retinal and choroidal vessel medial hypertrophy and/or degenerative changes, none of which was seen in this case. Affected cats usually suffer from concomitant renal disease or hyperthyroidism. Renal histology was unremarkable. The thyroid glands (right thyroid enlarged at necropsy) were not examined histologically; however, the owner indicated the animal was given a "thyroid medication" (dosage unknown) suggesting this animal may have been

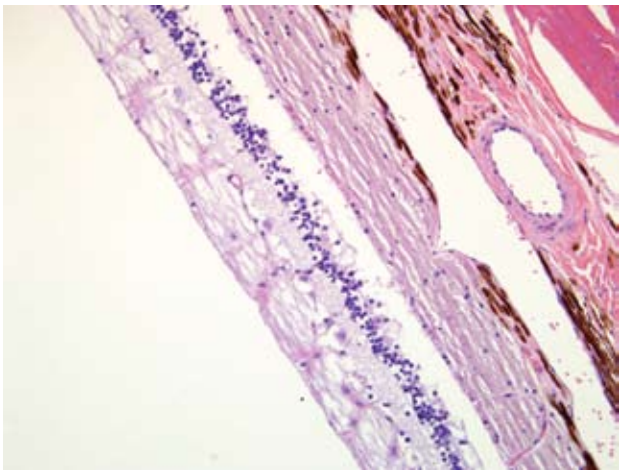

*2-1. Eye, cat. Diffusely there is retinal degeneration characterized by loss of the photoreceptor layer, outer nuclear layer, and outer plexiform layer. (HE 400 X).*

treated for hyperthyroidism. If the hyperthyroidism was appropriately controlled the cat was likely normotensive although it may have experienced hypertension prior to treatment being initiated. If hyperthyroidism was insufficiently controlled the animal may have suffered from hypertension; however, as previously mentioned the eye lacks vascular changes consistent with chronic hypertension. Hyperthyroidism may have played a role in the myocardial lesion.

Causes and significance of the sporadic intranuclear inclusions **(Fig. 2-2)** are unknown. Potential artifact or nuclear membrane invaginations were considered. To the best of our knowledge, intranuclear inclusions of the inner nuclear layer in the cat are unreported.

**AFIP Diagnosis:** Eye, retina: Degeneration and loss of photoreceptor, outer nuclear, and outer plexiform layers, diffuse, severe

**Conference Comment:** During a preconference session the moderator reviewed ocular anatomy and emphasized the importance of systematically evaluating an eye for pathologic changes. One important portion of this examination is to peruse the retina to determine if all ten layers are present and normal. The ten layers of the retina are from inside (vitreous body) to outside (choroid): 1) inner limiting membrane, 2) optic nerve fibers, 3) ganglion cell layer, 4) inner plexiform layer, 5) inner nuclear layer, 6) outer plexiform layer, 7) outer nuclear layer (cell bodies of the rods and cones), 8) outer limiting membrane, 9) photoreceptor layer, and 10) retinal pigment epithelium.[12] In this case the missing layers are the photoreceptor layer, outer nuclear layer, and outer

plexiform layer due to suspected enrofloxacin toxicity. Glaucoma is less likely in this case because degenerative changes are noted primarily in the outer layers of the retina; whereas, retinal changes associated with glaucoma primarily involve the inner layers of the retina.

Additionally, there was an active discussion during the conference regarding the few to moderate number of cells within the inner nuclear layer of the retina containing intranuclear, eosinophilic bodies. The consensus was that these "bodies" are cytoplasmic invaginations into the nuclei and should not be confused with viral inclusion bodies.

**Contributing Institution:** Colorado State University, Department of Microbiology, Immunology, Pathology and the Veterinary Diagnostic Laboratory, www.cvmbs.colostate.edu/mip and www.dlab.colostate.edu

**References:**

1. Aguirre GD: Retinal degeneration associated with the feeding of dog foods to cats. J Am Vet Med Assoc **172**:791-796, 1978
2. Ford MM, Dubielzig RR, Giuliano EA, Moore CP, Narfstrom KL: Ocular and systemic manifestations after oral administration of a high dose of enrofloxacin in cats. Am J Vet Res **68**:190-202, 2007
3. Glaze MB: Congenital and hereditary ocular abnormalities in cats. Clin Tech Small Anim Pract **20**:74-82, 2005
4. Hayes KC, Rabin AR, Berson EL: An ultrastructural study of nutritionally induced and reversed retinal degeneration in cats. Am J Pathol **78**:505-524, 1975
5. Leon A, Levick WR, Sarossy MG: Lesion topography and new histological features in feline taurine deficiency retinopathy. Exp Eye Res **61**:731-741, 1995
6. Narfstrom K: Hereditary and congenital ocular disease in the cat. J Feline Med Surg **1**:135-141, 1999
7. Pion PD, Kittleson MD, Rogers QR, Morris JG: Myocardial failure in cats associated with low plasma taurine: a reversible cardiomyopathy. Science **237**:764-768, 1987
8. Rabin AR, Hayes KC, Berson EL: Cone and rod responses in nutritionally induced retinal degeneration in the cat. Invest Ophthalmol **12**:694-704, 1973
9. Rah H, Maggs DJ, Blankenship TN, Narfstrom K, Lyons LA: Early-onset, autosomal recessive, progressive retinal atrophy in Persian cats. Invest Ophthalmol Vis Sci **46**:1742-1747, 2005
10. Schaller JP, Wyman M, Weisbrode SE, Olsen RG: Induction of retinal degeneration in cats by methylnitrosourea and ketamine hydrochloride. Vet Pathol **18**:239-247, 1981
11. Wiebe V, Hamilton P: Fluoroquinolone-induced retinal degeneration in cats. J Am Vet Med Assoc **221**:1568-1571, 2002
12. Young B, Lowe JS, Stevens A, Heath JW: Special sense organs. *In:* Wheater's Functional Histology, A Text and Color Atlas, ed. Young B, Lowe JS, Sevens A, Heath JW, 5th ed., pp. 400-413. Churchill Livingstone, Elsevier, Philadelphia, PA, 2006

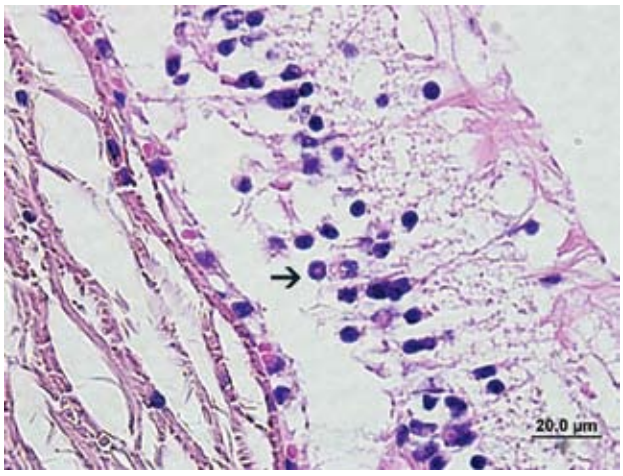


*2-2. Eye, cat. Within the degenerate outer nuclear layer there are low numbers of intranuclear cytoplasmic invaginations (arrow).* *Photomicrograph courtesy of Colorado State University Department of Microbiology, Immunology, Pathology/Veterinary Diagnostic Laboratory 1619 Campus Delivery Fort Collins, CO 8052*

## CASE III – 25623-07 (AFIP 3103702)

**Signalment:** Neutered female Pekingese dog (*Canis familiaris*), 9.5-years-old

**History:** The dog developed a right-sided corneal ulcer five months previously. The eye became cloudy five days ago, and severe periocular swelling and pain developed two days ago. The right globe was enucleated, fixed and submitted for microscopic examination.

**Gross Pathology:** NA

**Laboratory Results:** NA

**Histopathologic Description:** A perforation of the cornea is present, with debris in the defect connecting the outer aspects of the cornea and the chambers of the eye. Iridal tissue is herniated into the defect, protruding through an often fragmented Descemet's membrane, but

inflammation and hemorrhage affect both the anterior and posterior chambers and the uvea, and the inflammation extends around the periphery of the eye to involve the extra-ocular muscle. Lens liquefaction (cataractous change) is present, and neutrophils occur within the abnormal lens matrix and beneath the detaching capsule. Lenticular fibrovascular membranes are not observed. The cornea peripheral to the perforation contains embedded hemorrhage and full-thickness edema. The filtration angle is minimally visible but contains hemorrhage and debris as well. Widespread corneal ulceration is associated with a superficial infiltrate of neutrophils, and remaining corneal epithelium is undergoing squamous metaplasia and melanization. Well defined clusters of cornified material are suspended in inflammation at the surface of the cornea, along with microabscesses. Central and superficial corneal vascularization is apparent, along with localized melanin. Colonies of coccoid bacteria are most easily seen in fibrin deposits in the anterior chamber but occur throughout the eye. The iris is adhered to the posterior aspect of the cornea, and a long stretch of fibrovascular membrane extends down part of its anterior surface. Neutrophils infiltrate the iris stroma and the posterior epithelial layer is incomplete. Much of the ciliary apparatus and remaining retinal and choroidal structures are obliterated by inflammation. Neutrophils diffusely infiltrate the sclera and separate the episcleral fascia. Evidence of neovascularization and early fibroblast proliferation are seen in the latter.

**Contributor's Morphologic Diagnosis:**
Eye: Chronic suppurative panophthalmitis with corneal perforation, staphyloma, lens liquefaction and intralesional bacteria

**Contributor's Comment:** The microscopic lesions in this eye are exemplary of traumatic perforation with continued inflammation. In the absence of infection, the minimal lesions associated with canine lens trauma are characterized by breaks in the anterior lens capsule and uveitis of the anterior segment. In one study, 36/40 cases of traumatic eye injury resulted in extrusion of lens material into the anterior chamber. Of these cases, 12/14 were related to direct lens trauma. The result was endophthalmitis with or without glaucoma.

The presence of corneal perforation and associated lens inflammation point to the likelihood of a penetrating foreign body. Although the history is vague in this case, and while younger animals are more often affected, a cat claw wound was deemed most likely. These wounds cause [6] corneal and lens capsule perforation with ensuing phacoclastic uveitis. Phthisis or glaucoma resulted in 50% of the cases. Grass awns and porcupine quills are also frequently cited as sources of ocular or orbital foreign bodies in dogs.[2-4,6]

In 20 cases of lens rupture that excluded animals with intractable intraocular infection, lens-induced uveitis was characterized by capsular rupture, cataract, lymphoplasmacytic iridocyclitis, and perilenticular inflammation.[8] Moreover, capsule defects were in line with breaks in the Descemet's membrane similar to the one in this case. Even in the absence of infection, the affected lens will become invested with neutrophils, lens epithelium and/or metaplastic fibroblasts. In 13/20 cases in this study, the vitreous and posterior uvea were also inflamed. Four dogs with recent perforations had fibrinopurulent inflammation surrounding the lens.

Phacoclastic uveitis is distinguished from phacolytic uveitis in that the latter is a result of reaction to protein leakage from a cataractous lens and without other associated causes of uveal inflammation.[7] In both conditions, normal low dose tolerance to lens proteins is thought to be overwhelmed by rupture of the lens and release of high dose antigen. When lens lysis occurs, lens membrane proteins are also released, and this results in a more powerful presentation of antigens to the systemic immune system that is likely to overwhelm tolerance.

This case demonstrates the potentially catastrophic results of intraocular inflammation, which had at the time of enucleation involved every structure of the eye. Panophthalmitis, defined as inflammation of all the tunics of the eye, is much less common than endophthalmitis, defined as inflammation of the uvea, retina, and ocular cavities. The acute changes near the site of corneal rupture contrast with those inside the eye. These are of longer duration based on the presence of an anterior fibrovascular membrane, corneal vascularity, and the neovascularization at the back of the eye. Wilcock points out that many cases of traumatic lens laceration are detected by a lack of response to treatment, [8] and in his cases, the interval between injury and uveitis onset (when known) was 4-20 days.

**AFIP Diagnosis:** Eye: Panophthalmitis, fibrino-suppurative, diffuse, severe, with corneal rupture, iridal prolapse, phacoclasia, and intralesional bacteria

**Conference Comment:** This case of ocular trauma had lesions involving almost every part of the eye. The ocular anatomy's relationship to eye injury was discussed during the conference, and this review will briefly discuss anatomy of the cornea and its response to superficial ulceration.

The cornea is avascular and covered by nonkeratinized, nonpigmented stratified squamous epithelium. This thin, non-pigmented epithelium allows for clarity of vision.[9] The stroma also maintains a state of relative dehydration aided by numerous epithelial and endothelial tight junctions in combination with a Na-K-dependent ATP-ase pump in the cell membrane of the corneal endothelium.[9] Bowman's layer is just below the squamous epithelium. Bowman's layer was discussed during the conference because it is a distinctive membrane in humans, but is not distinct in mammals. Underlying Bowman's layer, and compromising 90% of the thickness of the cornea, is the corneal stroma and layers of collagen interspersed with fibroblasts. Descemet's membrane, distinct in domestic animals, lies between the corneal stroma and the corneal endothelium.[1]

The cornea is a highly specialized area of the body; therefore, it is protected from damage by numerous mechanisms including an antibacterial tear film and a physically movable barrier known as the eyelid. After damage, the cornea often quickly takes on water. Water enters from the eye's anterior aspect via lacrimal secretions and the posterior aspect via fluid from the anterior chamber. Even more water enters the cornea if the electrolyte pump is compromised because of corneal damage.

If injury to the cornea is superficial and only involves the epithelium, this defect heals by epithelial cells "sliding over" the defect, followed by mitosis after approximately 24 hours.[9] Chronic ulcers often require additional resources to heal. These resources are drawn from the epithelium of the corneoscleral junction where permanent populations of cells available for replication reside. Cells recruited from the corneoscleral junction tend to retain phenotypic characteristics of conjunctiva including pigmentation and rete ridges. This is an easy way to recognize a chronic ulcer. This is referred to as conjunctival (or cutaneous) metaplasia.

If the underlying stroma of the cornea is damaged in addition to the epithelium, rebuilding of the damaged stroma may be required before epithelial repair can occur. Within a few hours of the initial insult, neutrophils enter the wound and begin to kill bacteria, degrade damaged collagen, and stimulate fibroplasia and vascularization. Stromal cells at the edge of the defect and fibroblasts recruited from the limbus produce new stroma and cover the defect.[9] New blood vessels begin to form approximately 4 days after an extensive injury, and this ingrowth is from the limbus and progresses at a rate of about 1 mm a day. This lag time is important because superficial wounds can heal in less than 4 days without the help of vascularization. If vascularization occurs during healing, visual impairment from stromal fibroplasia is often the result.[9]

**Contributing Institution:** Department of Veterinary Pathobiology and Veterinary Medical Diagnostic Laboratory, University of Missouri, http://www.cvm.missouri.edu/vpbio/ http://www.cvm.missouri.edu/vmdl/

**References:**

1. Bacha WJ, Wood LM: Eye. *In:* Color Atlas of Veterinary Histology, ed. Bacha WJ, Wood LM, pp. 231-233. Williams & Wilkens, Media, PA, 1990
2. Brennan KE, Ihrke PJ: Grass awn migration in dogs and cats: A retrospective study of 182 cases. J Amer Vet Med Assoc **182**:1201-1204, 1983
3. Bussanich MN, Rootman J: Intraocular foreign body in a dog. Can Vet J **22**:207-210, 1981
4. Grahn BH, Szentimrey D, Pharr JW, Farrow CS, Fowler D: Ocular and orbital porcupine quills in the dogs: A review and case series. Can Vet J **36**:488-893, 1995
5. Pfleghaar S, Schäffer EH: Die linseninduzierte Uveitis (Endophthalmitis phakoanaphylactica) beim Haustier. Tierd Prax **20**:7-18, 1992
6. Spiess BM, Rühli MB, Bollinger J. Augenverletzungen durch Katzenkrallen beim Hund. Schweiz Arch Tierheilk **138**:429-433, 1996
7. Van der Woerdt A, Nasisse MP, Davidson MG: Lens-induced uveitis in dogs: 151 cases (1985-1990). J Amer Vet Med Assoc **201**:923-926, 1992
8. Wilcock BP, Peiffer RL, Jr: The pathology of lens-induced uveitis. Vet Pathol **24**:549-553, 1987
9. Wilcock BP: Eye and ear. *In:* Jubb, Kennedy and Palmer's Pathology of Domestic Animals, ed. Maxie MG, 5th ed., vol 1, pp.481-485. Elsevier Limited, Philadelphia, PA, 2007

## CASE IV – 07RD0797 (AFIP 3065935)

**Signalment:** 5-year-old male neutered Red Heeler mix, *Canis familiaris*

**History:** This was an unexpected finding. The dog had no clinical finding of parasites.

**Gross Pathology:** Gross and microscopic appearance all of the tissues of the globe appeared within normal limits including the profile and coloration of iris.

**Laboratory Results:** NA

**Histopathologic Description:** Histosections show numerous nematode adult parasites in the episclera on the superior side of the globe extending posterior to the equator of the globe **(Fig. 4-1)**. Both adult male and adult female forms are seen, and there are numerous microfilaria in the reproductive tracts of a female. The cuticular ridges are typical of *Onchocerca* in that they are circumferential so that they are seen as a series of extruding bumps on the cuticle of female worms cut in the longitudinal direction. No microfilaria are seen in the tissues. The tissue reaction is limited to fibrosis and minimal granulomatous inflammation surrounding the cavities in which the adult worms are found. There is a minimal perivascular lymphoplasmacytic inflammatory infiltrate in the episclera at sites distant from the presence of parasites. Immediately subtending the conjunctiva are numerous polymorphonuclear cells immediately adjacent to blood vessels.

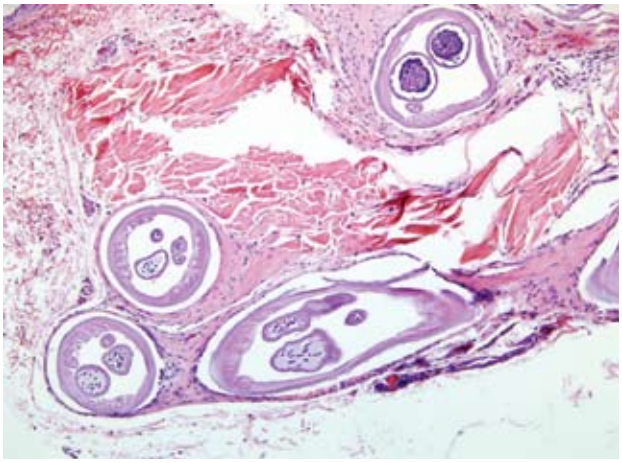

*4-1. Eye, dog. Cross and tangential sections of filarid nematodes characterized by coelomyarian –polymyarian musculature, small lateral chords, uteri containing microfilaria, and a very small intestinal tract. (HE 100X).*

**Contributor's Morphologic Diagnosis:** Episcleral fibrosis and granulomatous inflammation with intralesional *Onchocerca* filarial nematode parasites

**Contributor's Comment:** *Onchocerca* sp. are transmitted by the insect genus *Simulium* (black flies) or *Culicoides* (gnats) during a blood meal. The insect vector injests *Onchocherca* microfilaria from subcutaneous nodules of the host. The microfilaria migrate to the insect midgut, through the hemocoel to the thoracic muscles where they develop into first stage larvae. Eventually they develop into third-stage larvae and migrate to the insect's head and proboscis and are transmitted to another host. Within the vertebrate host the larvae migrate, form nodules, become adults, mate and release microfilaria that continue the cycle.

*Onchocerca* sp. has worldwide distribution and infects ungulates and humans. This tissue is from a series of 9 cases of canine ocular *onchoceriasis* we received from the Western United States (California, Nevada, Utah, Arizona) since 2004. The typical lesion is an episcleral or conjunctival nodule with lymphogranulomatous inflammation, eosinophils, plasma cells, fibrosis and granuloma formation.

Series of canine cases of episcleral *Onchocerca* infestation have been reported from Greece, Hungary, and the Western US. Controversy exists as to the *Onchocerca* species causing canine infection. The Greek and Hungarian isolates are thought to be of the same species; light microscopic study indicates morphologic similarities in U.S. versus Hungarian and Greek parasites. Many previous reports regarding Greek and Hungarian cases incriminate *O. lupi* with the dog as the definitive host. Other authors believe that aberrant migration of *O. lienalis* of cattle is responsible for American canine ocular onchocerciasis. While *O. lienalis* is considered the most likely diagnosis in the cases of American canine onchocerciasis based on widespread geographic incidence of *O. lienalis* and parasite morphology, experimental infection of dogs with *O. lienalis* has not been successful, and canine *Onchocerca* has not been found in cattle-specific locations (gastro-splenic ligament). Furthermore, although the natural host of *O. lienalis* is cattle, the worms found in dogs have been gravid, suggesting patent infection.

**AFIP Diagnosis:** Eye, episcleral connective tissue: Adult filarid nematodes, few, with mild fibrosis

**Conference Comment:** There was slide variation in the presence and severity of associated granulomatous inflammation; in most slides it was minimal. The conference discussion centered largely on the identification of this filarid nematode and the distinguishing characteristics of not only filarids but *Onchocerca* sp. Filarids are small nematodes that infect a number of different domestic animals. The majority of parasites in this group produce microfilaria, which are very distinctive larvae that when seen in the adult female are helpful in identification.[1] Dr. Chris Gardiner, the AFIP parasitology consultant, has mentioned that these larvae often are very basophilic and look like "a bag of nuclei." Filarids have coelomyarian musculature. In *Onchocerca*,

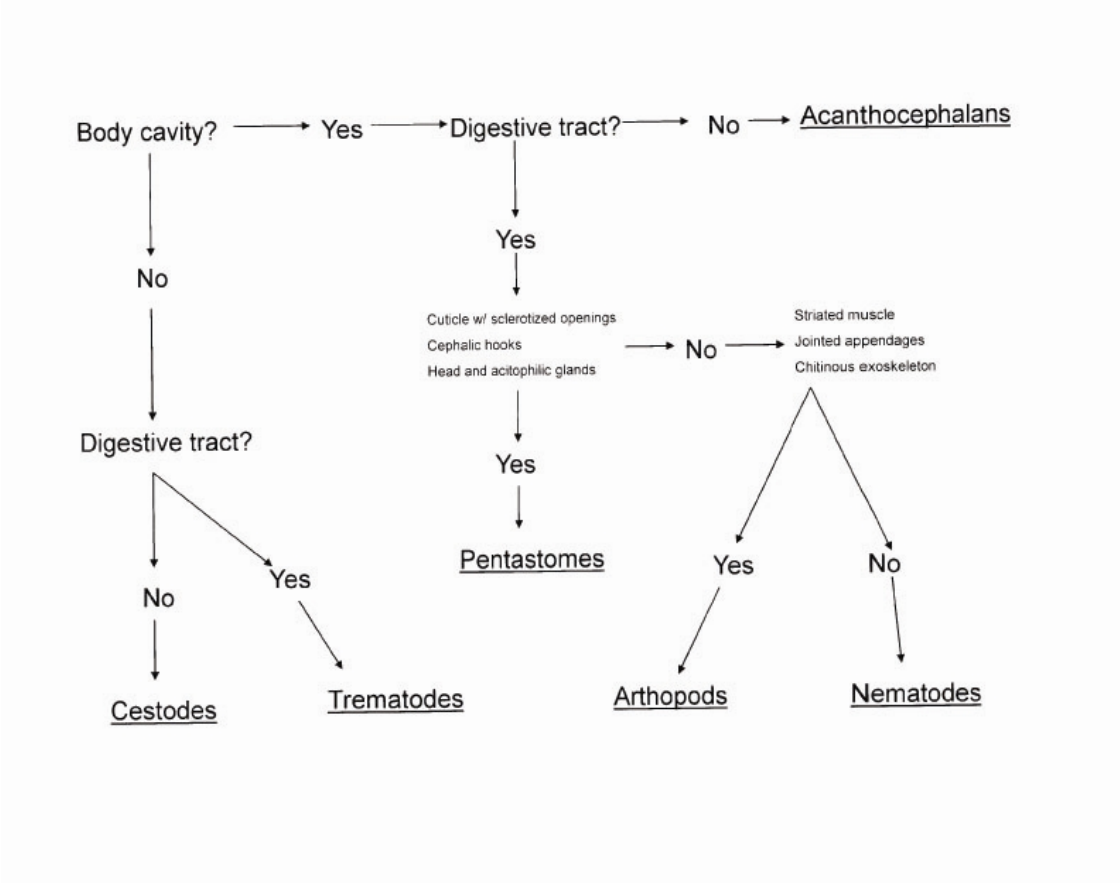


these muscles atrophy and are replaced hypodermal tissue. Even more important than microfilaria in identification of filarids is their tell-tale intestine, which is very small and a key diagnostic feature. These characteristics help differentiate *Onchocerca* sp. from the spirurid *Thelazia* sp., another common parasitic scourge of the mammalian eye.[1] The moderator also discussed various features of metazoan parasites in histologic section. A chart used by AFIP residents is included here to aid in the classification of parasites in tissue section.

**Contributing Institution:** Dept. of Pathobiological Sciences, School of Veterinary Medicine, University of Wisconsin, 2015 Linden Drive, Madison, WI 53706-1102

**References:**

1. Gardiner CH, Poynton SL: In: An Atlas of Metazoan Parasites in Animal Tissues, 2nd ed., pp. 53-56. Armed Forces Institute of Pathology, Washington, DC 1998
2. Zarfoss KM, Dubielzig RR, Eberhard ML Schmidt KS: Canine ocular onchocerciasis in the United States: Two new cases and a review of the literature. Vet Ophthal 8:51-57, 2005

The Armed Forces Institute of Pathology
Department of Veterinary Pathology

*Conference Coordinator:*
Todd M. Bell, DVM

WEDNESDAY SLIDE CONFERENCE 2008-2009

# Conference 8

5 November 2008

***Conference Moderator:***

Dr. Matthew Starost, DVM, PhD, Diplomate ACVP

## CASE I – A8-043171 (AFIP 3106959)

Signalment: 15-month-old, female, brangus (*Bos taurus x Bos indicus*)

**History:** The animal was purchased one week prior to necropsy in Texas and transported to Georgia in April 2008. In Texas, it had been in contact with exotic ruminants, including wildebeest and sheep. Initial clinical signs included keratitis, nasal discharge, and fever. When hospitalized, additional signs included cranial nerve deficits, rumen hypomotility, and generalized lymphadenopathy. A head tilt developed during the course of treatment and euthanasia was elected.

**Gross Pathology:** The carcass was in good physical condition and the uterus contained a normal, approximately 4-5 month old fetus. Eyelids contained multifocal to coalescing hyperemic foci and there was bilateral corneal opacity and turbid exudates in the anterior chambers. The nares had bilateral viscous white discharge. Turbinates were severely congested and covered by moderate amounts of fibrin. Multiple erosions on the tongue had underlying hyperemia. Mandibular, prescapular, left axillary, tracheobronchial, and mediastinal lymph nodes were severely enlarged. Parenchyma bulged from the cut surface and was hemorrhagic or had multiple small hyperplastic white nodules in the cortex and medulla. Lungs were diffusely wet and edematous and the trachea contained abundant white froth. The liver was diffusely mottled and margins were rounded.

**Laboratory Results:**
FA negative for rabies virus and *Listeria*
IFA positive for malignant catarrhal fever virus (lymph node)
PCR positive for AlHV-1 and OHV-2 malignant catarrhal fever viruses

**Histopathologic Description:** Arterial walls of the rete mirabilis are infiltrated by moderate to large numbers of lymphoid cells that accumulate predominantly at the outer margins of the tunica media and in the adventitia **(Fig. 1-1)**. Inflammatory infiltrates are predominated by lymphocytes with moderate amounts of finely granular pale eosinophilic cytoplasm and large nuclei, with marginated chromatin and prominent nucleoli **(Fig. 1-2).** Similar infiltrations are present less frequently in the subendothelial connective tissue and rarely are present transmurally. Although the severity of changes is variable between individual sections, the media of multiple arteries is expanded by amorphous eosinophilic material (fibrinoid necrosis) and foci of pyknotic debris.

**Contributor's Morphologic Diagnosis:** Severe,

*Sponsored by the American Veterinary Medical Association, the American College of Veterinary Pathologists, and the C. L. Davis Foundation.

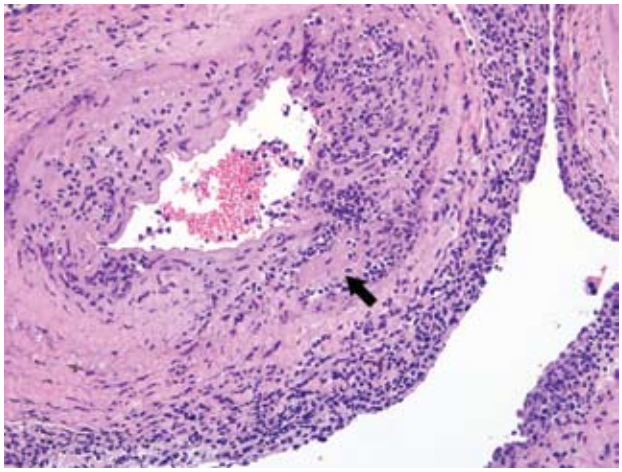

*1-1. Ox, rete mirabilis. Diffusely there is variably dense periarteriolar lymphoid proliferation with cellular infiltrate extending into and segmentally disrupting the tunica adventia, media, and intima. Focally, there is an area of fibrinoid necrosis of the tunica media characterized by brightly eosinophilic fibrillar material surrounded by moderate numbers of lymphocytes, plasma cell and histiocytes (arrow). (HE 200X).*

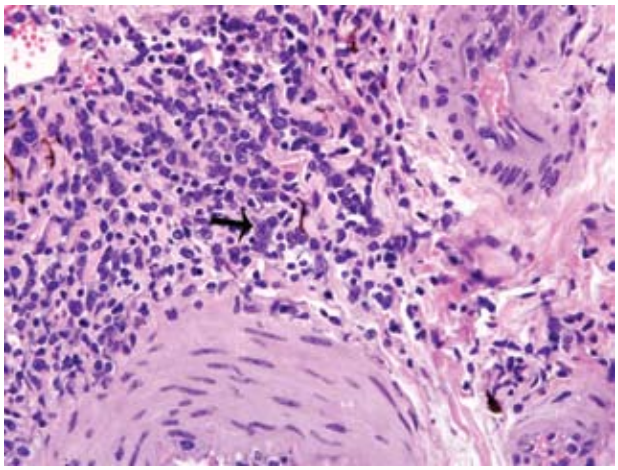

*1-2. Ox, rete mirabilis. Within periarteriolar lymphoid aggregates there are moderate numbers of lymphoblasts characterized by large vesiculate nuclei containing a prominent 5-6 micron eosinophilic nucleolus (arrow). (HE 400X).*

multifocal, lymphocytic and lymphoblastic vasculitis and perivasculitis with fibrinoid necrosis, rete mirabilis

**Contributor's Comment:** Gross and microscopic findings were consistent with malignant catarrhal fever (MCF). The predominant lesion in this heifer, severe lymphocytic and necrotizing vasculitis, was present in multiple tissues including the heart, uterus, forestomachs, abomasums, tongue, kidney, and liver. Lesions were also present in the brain and were particularly evident in the submitted rete mirabilis surrounding the pituitary. Fluorescent antibody testing performed on lymph node was positive, but does not differentiate between MCF associated viruses. PCR testing performed at the NVSL in Ames, Iowa yielded sequences compatible with both the alcelaphine and ovine forms of the MCF virus.

MCF is a pansystemic lymphoproliferative disease syndrome of certain wild and domestic artiodactylid species, occurs worldwide, and is caused by several closely related members of the *Rhadinovirus* genus of gamma-herpes viruses that exist in nature in subclinical infections in carrier ruminants.[7] Although no clinicopathologic differences exist between the diseases, four viruses are associated with MCF: 1) Alcelaphine herpesvirus 1 (AlHV-1) carried by wildebeest; 2) Ovine herpesvirus 2 (OHV-2) endemic in domestic sheep; 3) Caprine herpesvirus 2 (CpHv-2) endemic in domestic domestic goats; and 4) an undetermined virus in white-tailed deer (MCFV-WTD).(3,4) Unlike the alpha- and betaherpesvirus, the gammaherpesvirus appear to favor the establishment of latency over lytic replication in most infected cells of their natural hosts. In return for protecting their latently infected cells from immune system destruction, these reservoir hosts have evolved to being subclinical transmitters of the virus. However, a balance must exist between the immune response and the number of infected cells. Virus excretion is usually low and may occur constantly or intermittently. Animals targeted by the virus that did not co-evolve with it, as well as natural hosts with immune deficiencies, lose control over numbers of latently infected cells and develop lethal disease.[1]

First isolated and identified in 1960 from wildebeest, AlHV-1 is restricted to Africa and zoological collections where wildebeest are present.[5] OHV-2 occurs worldwide, but has never been isolated in cell culture. Natural infections can occur in goats, cattle, bison, deer, and pigs.[1,2] Clinical signs and prominent gross changes include lymphadenopathy, eyelid edema and conjunctivitis, corneal opacity and ulceration, hypopyon, oculonasal discharge, congestion of nasal mucosa, oral and esophageal erosion to ulceration, exudative dermatitis, sloughing of horns and hooves, and nervous signs. The primary microscopic lesions in ruminants with acute MCF

are lymphoid proliferation and infiltration, necrotizing vasculitis with perivascular lymphoid infiltration, and necrosis of mucosal epithelium.[3,7] In situ, PCR and immunohistochemistry studies with OHV-2 have demonstrated that the predominating infiltrating cell type is the CD8+ T-lymphocyte and that large numbers are infected. Cases of MCF are generally sporadic and the disease is not contagious among cattle by direct contact, making them dead end hosts. The incubation period is usually 2-10 weeks, but may be much longer.[3]

**AFIP Diagnosis:** Rete mirabilis: Arteritis and periarteritis, necrotizing, lymphocytic, multifocal, marked with fibrinoid necrosis

**Conference Comment:** Malignant catarrhal fever (MCF), also referred to as snotsiekte or malignant head catarrh, is an important disease in ungulates and should be included on a differential list of ulcerative, mucosal diseases in ruminants. Other differentials include: rinderpest (bovine morbillivirus), bovine viral diarrhea (bovine pestivirus), foot and mouth disease (bovine aphthovirus), bluetongue (orbivirus), bovine papular stomatitis virus (bovine parapox) and infectious bovine rhinotracheitis (bovine herpesvirus-1).

The most characteristic features of MCF are proliferation of CD8+ T-lymphocytes, vasculitis, and respiratory and gastrointestinal ulceration. The virus infects large granular lymphocytes which have T-suppressor cell and natural killer cell activity. Viral infection of these cells is thought to cause lymphoproliferation (due to suppressor dysfunction) and necrosis (due to natural killer cell dysfunction).[3] Disease progression can be as short as 1-3 days. This short clinical progression usually manifests as a hemorrhagic enteritis. Animals with less severe gastrointestinal disease often have neurologic disease combined with general debilitation and die within 10 days of disease onset.[3]

Grossly, MCF is characterized by mucosal ulceration in the upper portions of the respiratory tract, which coincides with the copious nasal discharge sometimes seen clinically. Skin lesions are often seen in sheep-associated MCF but are often overlooked during the post-mortem. Like rinderpest, esophageal erosions and ulcers are more common in the proximal third of the gastrointestinal tract. Ocular lesions include edema of the eyelids and conjunctiva and corneal opacity.[3]

The kidney may be mottled secondary to infarction or interstitial nonsuppurative nephritis. The urinary bladder can also be affected with lesions similar to those seen in the kidney, or the mucosa may be ulcerated causing hemorrhage and hematuria. As mentioned previously, lymph node as well as hemal node enlargement is prominent as a result of lymphoid hyperplasia. The spleen also contains prominent lymphoid follicles. Neurologic disease is common in subacute and chronic cases and is secondary to vasculitis.[3]

**Contributing Institution:** Department of Pathology, College of Veterinary Medicine, University of Georgia, Athens, GA 30602, http://www.vet.uga.edu/VPP/index.php

**References:**

1. Ackermann M: Pathogenesis of gamma-herpesvirus infections. Vet Micro **113**:211-222, 2006
2. Albini S, Zimmerman W, Neff F, Ehlers B, HaniH, Li H, Hussy D, Engels M, Ackermann M: Identification and quantification of ovine gammaherpesvirus 2 DNA in fresh and stored tissues of pigs with symptoms of porcine malignant catarrhal fever. J Clin Micro **42**:900-904, 2003
3. Brown CC, Baker DC, Barker IK: The Alimentary System. *In:* Jubb, Kennedy and Palmer's Pathology of Domestic Animals, ed. Maxie MG, 5th ed., vol 2, pp. 152-158. Elsevier Saunders, Philadelphia, PA, 2007
4. Li H, Dyer N, Keller J, Crawford TB: Newly recognized herpesvirus causing malignant catarrhal fever in white-tailed deer (*Odocoileus virginianus*). J Clin Micro **38**:1313-1318, 2000
5. Li H, Gailbreath K, Bender LC, West K, Keller J, Crawford TB: Evidence of three new members of malignant catarrhal fever virus group in muskox (*Ovibos moschatus*), Nubian ibex (*Capra nubiana*), and Gemsbok (*Oryx gazelle*). J Wild Dis **39**:875-880, 2003
6. Li H, Keller J, Knowles DP, Crawford TB: Recognition of another member of the malignant catarrhal fever virus group: an endemic gammaherpesvirus in domestic goats. J Gen Virol **82**:227-232, 2001
7. Simon S, Li H, O'Toole D, Crawford TB, Oaks JL: The vascular lesions of a cow and bison with sheep-associated malignant catarrhal fever contain ovine herpesvirus 2-infected CD8+ T lymphocytes. J Gen Virol **84**:2009-2013, 2003

## CASE II – 06-17642 (AFIP 3106254)

**Signalment:** A 1-year-old female domestic long hair (DLH) cat (*Felis domesticus*)

History: The cat was 5-6 weeks pregnant and died after partial abortion (aborting three of six fetuses). Fixed tissues in 10% buffered formalin and blood smears were received at Tifton Veterinary Diagnostic and Investigational Laboratory.

**Gross Pathology:** NA

**Laboratory Results:** NA

**Histopathologic Description:** Within sections of kidney, liver and spleen, veins, arterioles and arteries contained few to several foamy macrophages which occasionally partly occluded the vascular lumens **(Fig. 2-1)**. The macrophages are enlarged up to twice normal size and contained cytoplasmic schizonts with numerous 1-2 micron in diameter round to oval bluish organisms (merozoites). Similar macrophages containing protozoan schizonts were seen within several glomerular capillaries **(Fig. 2-2)**. The schizont-laden macrophages were seen attached to endothelium, at times occluding blood vessels, and were numerous especially in sections from the spleen and liver **(Figs. 2-3, 2-4)**.

Additionally, tissues (slides not submitted) from heart, lung, stomach, small intestine, ovary and urinary bladder and gall bladder were examined. In almost all examined tissues, there were similar large schizont-laden macrophages in the blood vessels. These were numerous in the sections of liver, kidney, spleen and heart. The other findings were within normal limits.

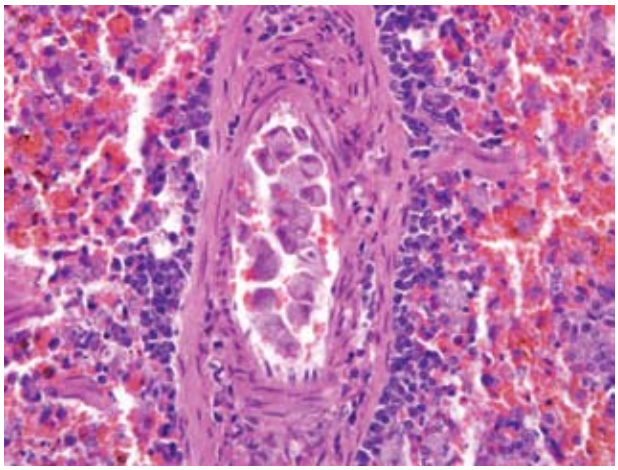

*2-1. Cat, spleen. Filling splenic vessels are numerous monocytes containing high numbers of Cytauxzoon felis schizonts. (HE 200X).*

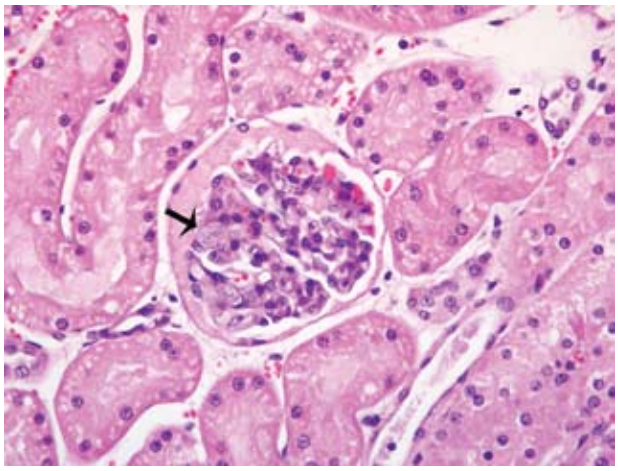

*2-2. Cat, kidney. Multifocally, within the glomerular tufts there are low numbers of monocytes containing high numbers of Cytauxzoon felis schizonts. (HE 400X).*

**Contributor's Morphologic Diagnosis:** Kidney, spleen and liver, blood vessels (veins, arteries and arterioles): Histiocytosis, diffuse, moderate with intrahistiocytic intracytoplasmic schizonts, morphology most consistent with *Cytauxzoon felis* (a Theilerial parasite)

**Contributor's Comment:** *Cytauxzoon felis* is a protozoan parasite classified in family *Theileriidae* and infects wild ungulates species in Africa including the kudu, eland and giraffe, as well as domestic and wild *Felidae* in North America.[3] The organism is believed to be transmitted from bobcat, the reservoir host, to domestic cats via a tick vector.[1] The clinical disease in domestic cat is most prevalent in the early and late summer, corresponding with the activity of its tick vector, *Dermacenter variabilis*.[4]

The infection is associated with both tissue (schizogonous) phases and an intraerythrocytic phase that correlates with the clinical phases of severe circulatory impairment and hemolytic anemia, respectively.[1] The clinical signs in domestic cats include depression, anorexia, pyrexia, dehydration, pallor, icterus, dark urine and occasionally dyspnea.[1,3]

The cat in the current case presented to the veterinarian, after partial abortion (aborting three of six fetuses) the previous night, in a near comatose stage with lethargy and mild gingival icterus. Initially, the cat had a reduced

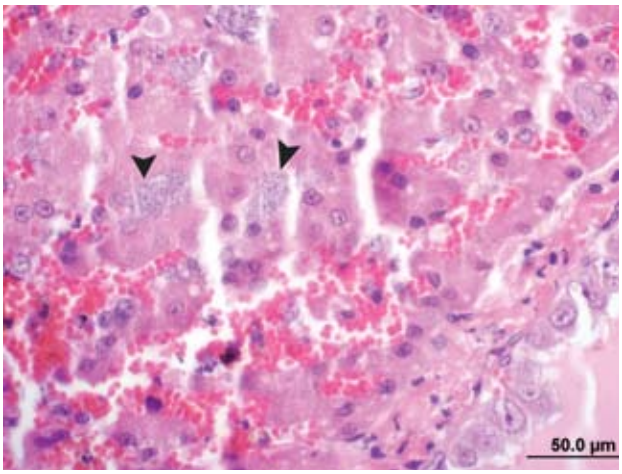


*2-3. Cat, liver. Within the hepatic vessels and hepatic sinusoids there are moderate numbers of monocytes containing high numbers of Cytauxzoon felis schizonts. Photomicrograph courtesy of University of Georgia, Tifton Veterinary Diagnostic and Investigational Laboratory, 43 Brighton Road, P.O. Box 1389, Tifton, GA 31793, USA.*

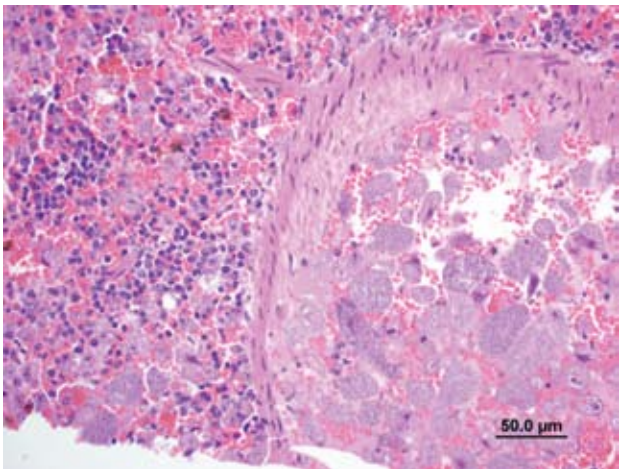


*2-4. Cat, liver. Hepatic vessels are occluded by high numbers of monocytes containing numerous Cytauxzoon felis schizonts Photomicrograph courtesy of University of Georgia, Tifton Veterinary Diagnostic and Investigational Laboratory, 43 Brighton Road, P.O. Box 1389, Tifton, GA 31793, USA.*

heart rate, which progressed to seizures, then death. A blood smear was collected immediately postmortem by cardiac puncture. Numerous schizont-laden macrophages and small round ring-shaped piroplasms in several erythrocytes were observed in the Wright-Giemsa stained smears. Generally, occasional schizont-laden macrophages may be observed on the feathered edge of blood smears in infected cats, but numbers similar to those in this case are unusual. Large numbers of schizont-laden macrophages in blood smear in the current case could be attributed to collection of blood from the heart. Because of their large size these cells are less likely to be found in peripheral circulation and are not normally found in blood smears from infected cats.[6] As in the current case, it was previously reported that high percentage of parasites are identified histologically from the spleen, liver, or lungs, suggesting sampling from these organs as the most appropriate sites for organism identification.[4] Because the tissue phase occurs prior to the erythrocytic phase, some cats can be severely ill but not have detectable parasites in their red blood cells.[1]

Three remaining fetuses were recovered at necropsy. Formalin fixed tissues from the cat and some fetal tissues (skeletal muscle, developing bone and placenta) were examined. Macrophages or piroplasms associated with the organism were not seen in fetal tissues. Whether *Cytauxzoon* infection in this cat would be incriminated for the partial abortion observed could not be ruled out.[6] The tissue schizonts are the phase that is responsible for clinical manifestation of cytauxzoonosis.[4] Clinical *Cytauxzoon felis* infection is usually fatal in domestic cats [1,4], although some infected cats survive.[1] Because of this, domestic cats (*Felis domesticus*) are regarded as accidental hosts.[6] Bobcats, thought to be the reservoir hosts, are persistently parasitemic, yet they rarely manifest marked clinical disease.[4] Rare fatal cases of cytauxzoonosis in free-ranging bobcats has been reported.[5]

**AFIP Diagnosis:** Kidney, liver, and spleen: Histiocytosis, intravascular, diffuse, moderate with intrahistiocytic schizonts, etiology consistent with *Cytauxzoon felis*

**Conference Comment:** The contributor gave a good overview of *Cytauxzoon felis* and its importance in the domestic cat. During the conference other blood parasites were discussed. With erythrocytic parasites, it is important to determine the exact location of the parasite within the erythrocyte in order to accurately identify the parasite and thus make a correct diagnosis. Included below is a non-comprehensive list of blood parasites that are important in veterinary medicine.

| Location | Parasite | Hosts |
|---|---|---|
| Intracellular parasites (within erythrocytes) | *Hemoproteus spp.*<br>*Leukocytozoon spp.*<br>*Plasmodium spp.* | Birds |
| | *Cytauxzoon felis*<br>*Babesia cati*<br>*Babesia felis* | Cats |
| | *Anaplasma marginale*<br>*Anaplasma centrale* | Cattle |
| | *Babesia bovis*<br>*Babesia bigemina* | Cattle |
| | *Theileria mutans*<br>*Theileria annulata* | Cattle |
| | *Theileria cervi* | Deer, Elk |
| | *Babesia canis*<br>*Babesia gibsoni* | Dogs |
| | *Babesia equi*<br>*Babesia caballi* | Horses |
| | *Babesia ovis*<br>*Babesia motasi* | Sheep |
| Epicellular parasites (On membrane surface of depression of erythrocytes) | *Trypanosoma johnbakeri* | Birds |
| | *Hemobartonella felis (Mycoplasma haemofelis)* | Cats |
| Epicellular parasites (On membrane surface of depression of erythrocytes) | *Hemobartonella canis (Mycoplasma haemocanis)* | Dogs |
| | *Eperythrozoon suis (Mycoplasma haemosuis)* | Pigs |
| | *Eperythrozoon wenyoni* | Cattle |
| | *Eperythrozoon sp.* | Llamas |

| | | |
|---|---|---|
| Extracellular parasites (within the plasma) | *Dipetalonema reconditum* | Dogs |
| | *Dirofilaria immitis* | Dogs (sometimes cats) |
| | *Setaria spp.* | Horses |
| | *Trypanosoma theileri* | Cattle |
| | *Trypanosoma congolense* | |
| | *Trypanosoma vivax* | Dogs |
| | *Trypanosoma cruzi* | Horses |
| | *Trypanosoma brucei* | |
| | *Trypanosoma evansi* | |

2

**Contributing Institution:** University of Georgia, College of Veterinary Medicine, Tifton Veterinary Diagnostic and Investigational Laboratory, 43 Brighton Road, (P.O. Box 1389), Tifton, GA 31793, USA

**References:**

1. Birkenheuer AJ, Le JA, Valenzisi AM, Tucker MD, Levy MG, Breitschwerdt EB: *Cytauxzoon felis* infection in cats in the Mid-Atlantic States: 34 cases (1998-2004). J Am Vet Med Assoc **228(4)**:568-71, 2006
2. Brockus CW, Andreasen CB: Erythrocytes. *In:* Duncan & Prasse's Veterinary laboratory Medicine, Clinical Pathology, eds. Latimer KS, Mahaffey EA, Prasse KW, 4th ed., pp. 19-21. Blackwell Publishing, Ames, IA, 2003
3. Maxie G: Cytauxzoonosis. *In:* Jubb, Kennedy and Palmer's Pathology of Domestic Animals, ed. Maxie MG, 5th ed., vol 3, pp. 152-158. Elsevier Saunders, Philadelphia, PA, 2007
4. Meinkoth J, Kocan AA, Whitworth L, Murphy G, Fox JC, Woods JP: Cats surviving natural infection with Cytauxzoon felis: 18 cases (1997-1998). J Vet Intern Med **(5)**:521-5, 2000
5. Nietfeld JC, Pollock C: Fatal cytauxzoonosis in a free-ranging bobcat (*Lynx rufus*). J Wildl Dis **38(3)**: 607-10, 2002
6. Weismann, JL, Woldemeskel, M, Smith, KD, Merill, A, Miller, D: Blood smear from a pregnant cat that died after partial abortion. Vet Clinc Pathol **36**:(2), 209-211, 2007

## CASE III – G08-015746 (AFIP 3106209)

**Signalment:** Adult, female, *Chinchilla lanigera*, Chinchilla

**History:** 14 of 100 adult fur-ranched chinchillas died over a one-week period. Clinical signs prior to death include listlessness, loss of balance, ataxia.

**Gross Pathology:** Six animals were submitted for postmortem, all with similar gross lesions including multiple random 1-4 mm white foci visible on the capsular surface and throughout the parenchyma of the liver **(Fig. 3-1)**; similar foci were visible through the serosa of the small intestine, cecum and colon **(Fig. 3-2)**. Cecal and colonic content was dry and inspissated.

**Laboratory Results:** Listeria monocytogenes was isolated from lung (1+) and liver (4+).

**Histopathologic Description:** Scattered throughout the liver are random multifocal areas of parenchymal necrosis and inflammation, characterized by a central zone of cellular debris, fibrin exudation and marked neutrophil infiltration, with scattered aggregates of small rod-shaped bacteria **(Fig. 3-3)**; lesser numbers of lymphocytes and histiocytes are evident around the periphery of some foci. Moderate numbers of hepatocytes, predominantly in zones 2 and 3, have one or more large clear cytoplasmic vacuoles (lipid), and there are occasional fibrin thrombi in hepatic vessels. Tissue gram stains (Brown and Brenn) reveal large numbers of gram-positive rod-shaped bacteria in the foci of necrosis **(Fig. 3-4)**.

Similar foci of mucosal to transmural necrosis are evident in sections of small intestine, cecum and colon, and there is fibrinosuppurative meningitis evident in sections of

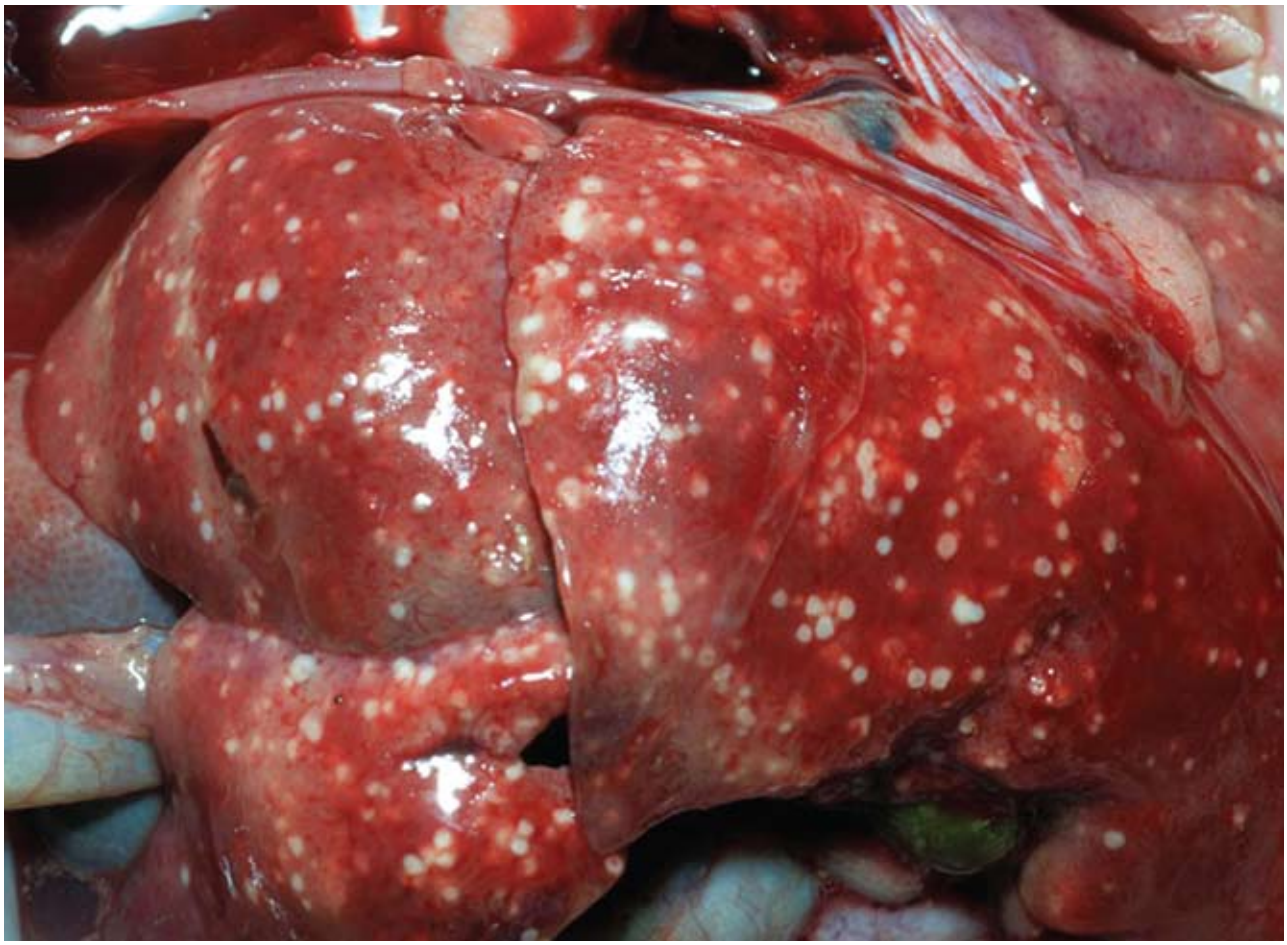

*3-1. Chinchilla, liver. Multiple random white foci visible on the capsular surface of the liver. Photograph courtesy of Animal Health Laboratory, University of Guelph, P.O. Box 3612 Guelph, Ontario CANADA N1H 6R8.*

brain (tissues not shown).

**Contributor's Morphologic Diagnosis:** Multifocal random hepatic necrosis and microabscessation with intralesional gram-positive rods, compatible with *Listeria monocytogenes* infection

**Contributor's Comment:** Listeriosis is a common disease of ranched chinchillas [2,6] first reported by MacKay et al. in 1949.[4] The disease is caused by *Listeria monocytogenes*, a facultatively anaerobic, gram-positive, rod-shaped bacterium that is considered part of the normal microbial flora in ruminants, and can persist in the environment as a plant saprophyte on decaying vegetation.[1] Listeria is also a potential pathogen, capable of causing three distinct clinical forms of disease: septicemia (principally in monogastric animals), encephalitis or abortion (principally in adult ruminants). While a wide range of animal species can be affected, chinchillas are considered highly susceptible to the visceral septicemic form of disease. Ingestion of contaminated food (such as pellets or hay contaminated with rodent, chicken or ruminant feces) can result in intestinal infection, with bloodborne dissemination to liver causing multifocal necrosis and abscessation, with subsequent septicemia and systemic spread to various organs including lymph nodes, lung, spleen, and brain.

**AFIP Diagnosis:** 1) Liver: Hepatitis, necro-suppurative, multifocal, moderate, with numerous bacilli, Chinchilla (*Chinchilla lanigera*), rodent
2) Liver, hepatocytes: Vacuolar change, lipid-type, diffuse, mild

**Conference Comment:** *Listeria monocytogenes* is an important pathogen of not only animals, but also humans, and is well known for its ability to grow in a wide temperature range to include refrigerator temperatures.

*3-2. Chinchilla, liver. Similar scattered white foci visible through the serosal surface of the cecum. Photograph courtesy of Animal Health Laboratory, University of Guelph P.O. Box 3612 Guelph, Ontario CANADA N1H 6R8.*

Because of this ability, outbreaks of food-borne listeriosis occur periodically in the United States. In veterinary medicine, it may be most notorious for its ability to grow in farm feeds, specifically silage, and cause subsequent clinical disease in cattle unlucky enough to be fed this tainted meal.[3]

*L. monocytogenes* produces a hemolytic toxin that adds to its virulence which distinguishes it from other species that are nonpathogenic. *L. monocytogenes* can also survive within macrophages and thus hide from the host immune response. A strong cell-mediated immune response by the host is essential to prevent development of clinical listeriosis.[3]

The three clinical syndromes of listeriosis—septicemia, abortion, and encephalitis— rarely overlap, thus suggesting a separate pathogenesis for each. The abortion syndrome usually occurs in ruminants in late gestation and probably gains access to the uterus and fetus via the bloodstream. The septicemic form has been reported in calves, foals, and aborted fetuses and manifests as numerous miliary microabscesses in the liver and to a lesser extent in other organs. In the encephalitic form, contaminated silage is fed to ruminants and the organism invades the oral mucosa through abrasions and enters the trigeminal nerve. The bacteria use the axon as a highway to gain entry to the brain. Listeria monocytogenes has a predilection for the brainstem and causes microabscessation that can sometimes be seen grossly. Histologically, these areas are characterized by either small aggregates of neutrophils, or more commonly small glial nodules are observed.[5]

Other domestic species rarely get listeriosis, but when they do the clinical signs and disease progression follow a similar pattern.[5]

**Contributing Institution:** Animal Health Laboratory,

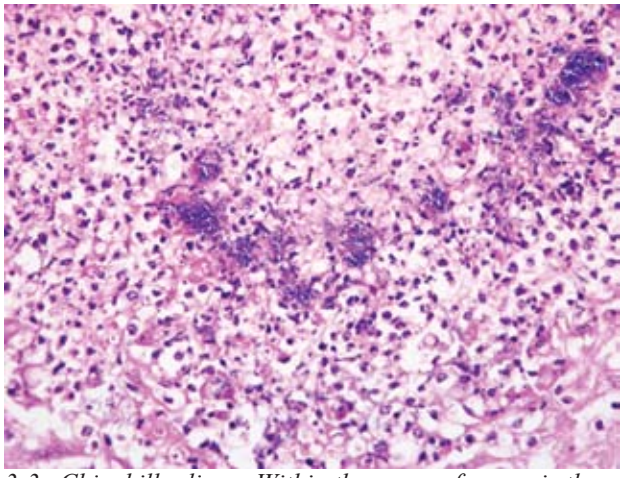

*3-3. Chinchilla, liver. Within the areas of necrosis there are numerous intrahistiocytic and extracellular bacilli. (HE 400X).*

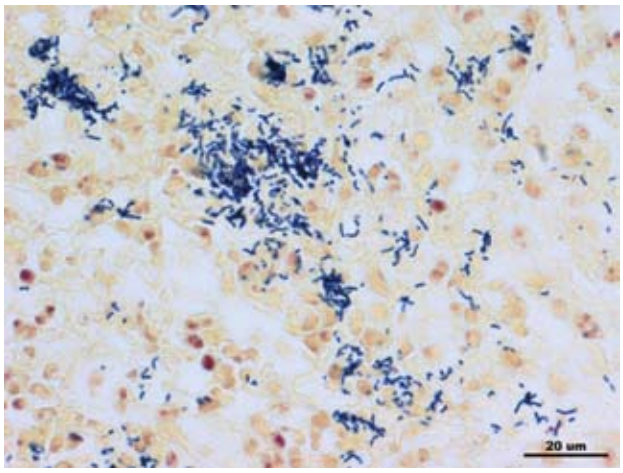


*3-4. Chinchilla, liver. Within necrotic areas there are numerous gram positive bacilli (B&B). Photomicrograph courtesy of Animal Health Laboratory, University of Guelph P.O. Box 3612 Guelph, Ontario CANADA N1H 6R8.*

University of Guelph, Guelph, Ontario, Canada http://ahl.uoguelph.ca

**References:**

1. Donnelly TM: Disease problems of chinchillas. *In:* Ferrets, Rabbits and Rodents. Clinical Medicine and Surgery, eds. Quesenberry KE, Carpenter JW, 2nd ed., pp. 255-265. Elsevier Saunders, St. Louis, MO, 2004
2. Finley GG, Long JR: An epizootic of listeriosis in chinchillas. Can Vet J **18**:164-167, 1977
3. Greene CE: Listeriosis. *In:* Infectious Diseases of the Dog and Cat, ed. Greene C, 3rd ed., pp. 311-312. Saunders, Philadelphia, PA, 2006
4. MacKay KA, Kennedy AH, Smith DLT, Bain AF: Listeria monocytogenes infection in chinchillas. *In:* Annual Report of the Ontario Veterinary College, Guelph, pp.137-145, 1949
5. Maxie MG, Youssef S: Nervous system. *In:* Jubb, Kennedy, and Palmer's Pathology of Domestic Animals, ed. Maxie, MG, 5th ed., pp. 405-408. Elsevier, Philadelphia, PA, 2007
6. Wilkerson MJ, Melendy A, Stauber E: An outbreak of listeriosis in a breeding colony of chinchillas. J Vet Diagn Invest **9**:320-323, 1997

## CASE IV – 07N 929 (AFIP 3105935)

**Signalment:** 2.5-year-old, intact male mixed breed dog, *Canis lupus familiaris*, canine

**History:** Shortly before death, the dog was apparently clinically normal. He was let outside for 15 minutes, and was subsequently found dead in the owner's back yard.

**Gross Pathology:** The gums were ashen blue with a line of redness along the periodontal margin. There were 30-50 white adult filarid nematodes consistent with *Dirofilaria immitus* in the right ventricle, right atrium, caudal vena cava, and main pulmonary artery. The right ventricle appeared mildly enlarged and dilated. The lungs were moist and diffusely dark red. On sectioning, the lungs effused copious amounts of blood. The margins of the liver were slightly rounded and it also effused blood on sectioning. No other pathologically relevant lesions were detected.

**Laboratory Results:** NA

**Histopathologic Description:** Heart: There were marked infiltrates of lymphocytes, plasma cells and occasional histiocytes throughout the myocardial endomysium in areas of myocardiocyte degeneration,

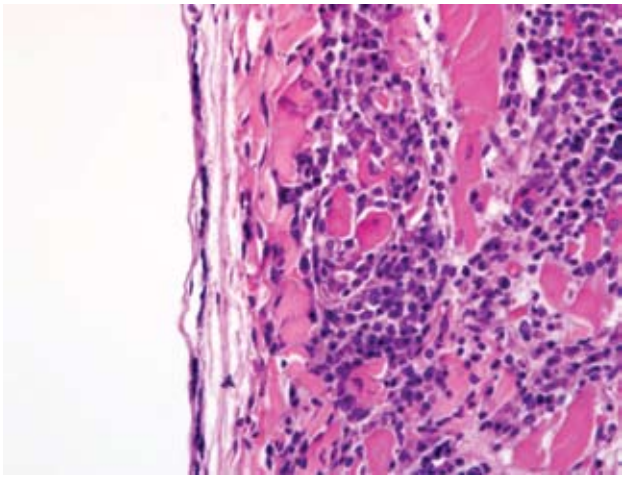

*4-1. Dog, heart. Multifocally, infiltrating and replacing the myocardium are moderate numbers of lymphocytes, plasma cell and fewer histiocytes which often separate and surround necrotic cardiac myocytes. Necrotic cardiac myocytes are shrunken, brightly eosinophilic, fragmented sarcoplasm that has lost cross striations and contains pyknotic nuclei. (HE 200X).*

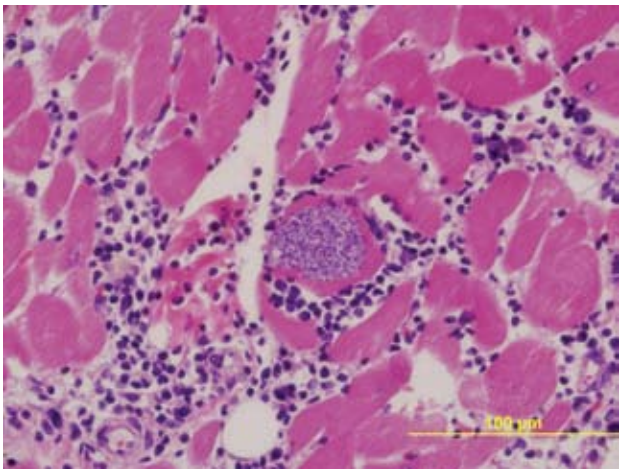

*4-2. Dog, heart. Cardiac myocyte containing amastigotes and adjacent necrotic cardiac myocyte.* *Photomicrograph courtesy of Department of Patho-biological Sciences, School of Veterinary Medicine, Louisiana State University, Baton Rouge, LA.*

fragmentation, necrosis, and loss **(Fig. 4-1)**. Occasional myocardiocytes have sarcoplasmic pseudocysts containing approximately 2-4 um diameter oblong amastigotes **(Fig. 4-2)** consistent with *Trypanosoma cruzi* (some slides may not have the organism). At 1000x magnification, amastigotes have both a basophilic round nucleus and smaller basophilic linear kinetoplast. Specific immunohistochemical stains confirm the organism's identity as *Trypanosoma cruzi* **(Fig. 4-3)**.

**Contributor's Morphologic Diagnosis:** Heart: Severe, multifocal to coalescing, lymphoplasmacytic and histiocytic myocarditis with intralesional myocardiocyte cytoplasmic amastigotes consistent with *Trypanosoma cruzi*

**Contributor's Comment:** Differential diagnoses for lymphoplasmacytic and histiocytic myocarditis in dogs include a long list of potential infectious and parasitic pathogens. Viral pathogens include canine parvovirus 2, canine morbillivirus, canine and porcine herpesviruses, and West Nile Virus.[11] Canine morbillivirus is more likely to cause degenerative changes than the mononuclear inflammation seen in this case.

Bacterial causes can include a multitude of organisms which may eventually cause chronic mononuclear cell infiltration and myocardial degeneration; however, in most cases there is a significant suppurative component. Some of the more commonly reported organisms include *Citrobacter* spp. and *Bartonella* spp. [4,6] *Borellia burdorferi* is the most commonly reported spirochete capable of causing myocarditis in dogs.

Fungal myocarditis has been reported in dogs associated with *Cryptococcus neoformans, Coccidioides immitis, Blastomyces dermatidis*, and *Aspergillus terreus*. Parasitic causes of myocarditis are also frequently reported and include *Angiostrogylus vasorum* (an eosinophilic component would be expected), and numerous protozoa. With the lymphoplasmacytic and histiocytic inflammation seen in this case, protozoal myocarditis was considered the top differential. Reported causes of protozoal myocarditis include T*oxoplasma gondii, Hepatozoan canis, Neospora canis, Trypanosoma cruzi*, and *Trypanosoma brucei*.

Immunohistochemical stains are available for the aforementioned protozoa. The morphology of protozoal amastigotes (with prominent kinetoplasts), intracardiomyocyte pseudocyst formation, and positive immunohistochemical staining for *T. cruzi* led to diagnosis of trypanosomiasis in this case.

Chagas disease is endemic to the southeastern United States and is considered an important differential for dogs with sudden death.[10] Widespread myocarditis can result in potentially fatal arrhythmias and/or cardiac contractile failure which can lead to peracute heart failure. One of

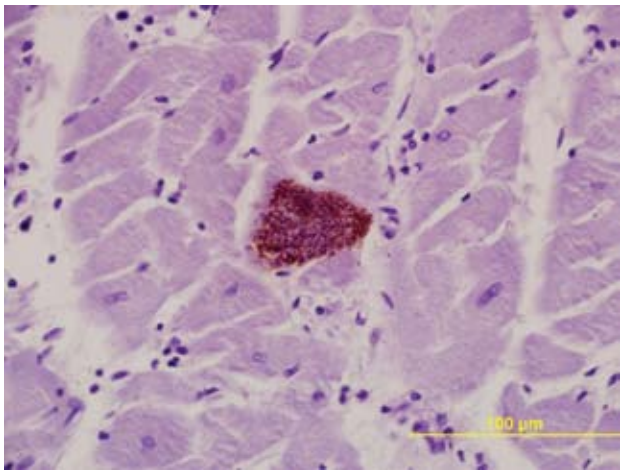


*4-3. Dog, heart. Immunohistochemical stain for* Trypanosoma cruzi *demonstrating diffuse immunopositivity. Photomicrograph courtesy of Department of Pathobiological Sciences, School of Veterinary Medicine, Louisiana State University, Baton Rouge, LA.*

the interesting features of the myocarditis and myocardial degeneration/necrosis seen in Chagas disease is that the most intense areas of inflammation and cardiomyocyte change are often unassociated with the parasite. Several studies have looked at the immunopathogenesis of Chagas disease and conclude that myocarditis may be a result of cell-mediated immune and/or autoimmune responses along with a microangiopathy.[1,2,5,9]

**AFIP Diagnosis:** Heart: Myocarditis, lymphoplasmacytic, multifocal, moderate with rare sarcoplasmic pseudocysts containing numerous amastigotes, etiology consistent with *Trypanosoma cruzi*

**Conference Comment:** There was substantial slide variation in this case, and some slides did not contain the parasite. This fact was duly noted during the selection process, but this case was used because it is an excellent representation of the inflammatory lesion and contained excellent contributor comments. The goal for the attendees was to provide a comprehensive histologic description leading to an acceptable and defensible differential diagnosis, which this case provided.

*T. cruzi*, the cause of Chagas disease, is an extremely important disease in not only the southern United States, but also throughout Central and South America. It has been estimated that up to 10 million people in Central and South America have Chagas, a majority of which are unaware they are infected. Chagas disease is spread by insects from the *Triatomidae* family. These insects are also known as "assassin bugs" or "kissing bugs." These bugs like to hide in the walls of mud huts to emerge at night for a blood meal. They feed near the oral or ocular mucous membranes, ingest a blood meal, and simultaneously defecate on their unfortunate victim. The person or animal bitten will scratch this area and introduce the trypomastigote form of *T. cruzi* into a mucous membrane or wound, and the organism enters the host. The trypomastigotes follow the blood stream to the heart, where they enter a cell and become amastigotes. This form multiplies by binary fission. Pseudocysts can be seen in cardiac myocytes at this stage. These cysts eventually rupture, releasing trypomastigotes. Trypomastigotes are taken up in the blood by the kissing bug, and in the intestinal tract the organism transforms into the epimastigote form. Once the organism travels to the rectal mucosa of the kissing bug, transformation back to the trypomastigote form occurs and the cycle continues.[3,7,8,9,12]

There is an acute phase of Chagas disease, characterized by nonspecific signs including fever, fatigue, diarrhea, and vomiting. Romana's sign, a characteristic swelling around the eye near the bite wound, is well recognized manifestation of this disease. The vast majority of people recover in 4-8 weeks. Several years later, a chronic phase develops in around 30% of those infected and manifests most commonly as a cardiomyopathy, or problems with the gastrointestinal system to include megaesophagus and megacolon. Less commonly it causes neurologic disease.[3,12]

*Trypanosoma cruzi* is a kinetoplastid, intracellular protozoan parasite. Ultrastructurally, the kineto-plast, which is a DNA-containing cytoplasmic organelle, can be used to identify protozoans. In *Trypanosoma* infections, the amastigotes have a kinetoplast that is parallel to the nucleus, whereas in *Leishmania*, the kinetoplast is smaller and is perpendicular to the nucleus. Other protozoans found in the heart, such as *Toxoplasma* and *Neospora*, do not have kinetoplasts.[7]

**Contributing Institution:** Louisiana State University School of Veterinary Medicine, Department of Pathobiological Sciences, www.vetmed.lsu.edu

**References:**

1. Andrade SG, Pimentel AR, de Souza MM, Andrade ZA: Interstitial dendritic cells of the heart harbor *Trypanosoma cruzi* antigens in experimentally infected dogs: importance for the pathogenesis of chagasic myocarditis. Am J Trop Med Hyg, **63**:64-70, 2000
2. Andrade ZA, Andrade SG, Correa R, Sadigursky M, Ferrans VJ: Myocardial changes in acute *Trypanosoma*

*cruzi* infection – ultrastructural evidence of immune damage and the role of microangiopathy. Am J Pathol, **144(6)**:1403-1411, 1994
3. Bowman DD, Lynn RC, Eberhard ML, Alcaraz A: Protozoans. *In:* Georgi's Parasitology for Veterinarians, 8th ed., pp. 83-87. Saunders Elsevier, St. Louis, MO, 2003
4. Breitschwerdt EB, Atkins CE, Brown TT, Kordick DL, Snyder PS. *Bartonella vinsonii* subsp. *Berkhoffii* and related members of the alpha subdivision of the *Protobacteria* in dogs with cardiac arrhythmias, endocarditis, or myocarditis. J of Clin Microbiol, **37(11)**:3618-3626, 1999
5. Caliari MV, de Lana M, Caja RAF, Carniero CM, Bahia MT, Santos CAB, Magalhaes GA, Sampaio IBM, Tafuri WL: Immunohistochemical studies in acute and chronic canine chagasic cardiomyopathy. Virchows Arch, **441**:69-76, 2002
6. Cassidy JP, Callahan JJ, McCarthy G, O'Mahony MC: Myocarditis in sibling boxer puppies associated with *Citrobacter koseri* infection. Vet Pathol, **39:**393-395, 2002
7. Cheville NF: Ultrastructural Pathology, pp. 716-721. Iowa State University Press, Ames, Iowa, 1994
8. Gardiner CH, Fayer R, Dubey JP: An Atlas of Protozoan Parasites in Animal Tissues, 2nd ed., pp. 3-5. Armed Forces Institute of Pathology, Washington, DC, 1998
9. Golgher D, Gazzinelli RT: Innate and acquired immunity in the pathogenesis of chagas disease. Autoimmunity, **37(5)**:399-409, 2004
10. Kjos SA, Snowden KF, Craig TM, Lewis B, Ronald N, Olson JK: Distribution and characterization of canine Chagas disease in Texas. Vet Parasitol, **152**:249-256, 2008
11. Lichtensteiger CA, Heinz-Taheny K, Osborne TS, Novak RJ, Lewis BA, Firth ML: West Nile Virus encephalitis and myocarditis in Wolf and Dog. Emerg Infect Dis, **9(10)**:1303-1306, 2003
12. McAdam AJ, Sharpe AH: Infectious disease. *In:* Robbins and Cotran Pathologic Basis of Disease, ed. Kumar V, Abbas AK, and Fausto N, 7th ed., pp. 405-406. Saunders Elsevier, Philadelphia, PA, 2005

**NOTES:**

The Armed Forces Institute of Pathology
Department of Veterinary Pathology

*Conference Coordinator:*
Todd M. Bell, DVM

WEDNESDAY SLIDE CONFERENCE 2008-2009

# Conference 9

12 November 2008

*Conference Moderator:*

Dr. Michelle Fleetwood, DVM, Diplomate ACVP

## CASE I – SDSU-1 (AFIP 3105831)

**Signalment:** 7 to 8-week-old pig (*Sus scrofa*)

**History:** Skin rash

**Gross Pathology:** Multifocal to coalescing skin lesions with mild to severe crusting were present over the entire body surface. Lesions were slightly raised. Periocular crusting was so severe the eyes appeared permanently closed. Generalized moderate lymphadenopathy was also present. This pig also had a large, reducible umbilical hernia.

**Histopathologic Description:** Within sections of skin, there is multifocal subcorneal pustular dermatitis with mild to moderate epidermal acanthosis and hyperkeratosis **(Fig. 1-1)**. Many cocci bacteria are present **(Fig. 1-2)**. Multifocal epidermal ulceration and suppurative folliculitis are evident in some areas (not present in every slide). Within the superficial dermis there is congestion, edema and multifocal hemorrhage. There is also mild perivascular to interstitial infiltration of the superficial dermis by lymphocytes. The dermal inflammation is more pronounced in areas of epidermal ulceration.

**Contributor's Morphologic Diagnosis:** Haired skin: Dermatitis, subcorneal, pustular and proliferative, acute to subacute, multifocal, mild to severe, with multifocal ulceration, and multifocal folliculitis due to *Staphlococcus hyicus*

**Contributor's Comment:** Exudative epidermitis (greasy pig disease) is caused by *Staphlococcus hyicus* and is most common in pigs 5–35 days of age.[1,2] Although *S. hyicus* is a member of the normal skin flora of healthy pigs, trauma resulting in a breach of the skin barrier may predispose pigs to developing skin lesions.[1,2] *S. hyicus* produces exotoxins which cause intra-epidermal cleavage, resulting in separation of epidermal cells and lesions typical of exudative epidermitis.[1]

The presence of cocci bacteria in the epidermal pustules of pigs affected by exudative epidermitis makes this condition similar to human bullous impetigo. Human bullous impetigo is an infection caused by staphylococcal exotoxins and characterized by epidermal pustules which contain many cocci bacteria.[1]

**AFIP Diagnosis:** Skin: Epidermitis, exudative and proliferative, multifocal, moderate with ulceration and mild superficial dermatitis and intracorneal cocci

***Sponsored by the American Veterinary Medical Association, the American College of Veterinary Pathologists, and the C. L. Davis Foundation.**

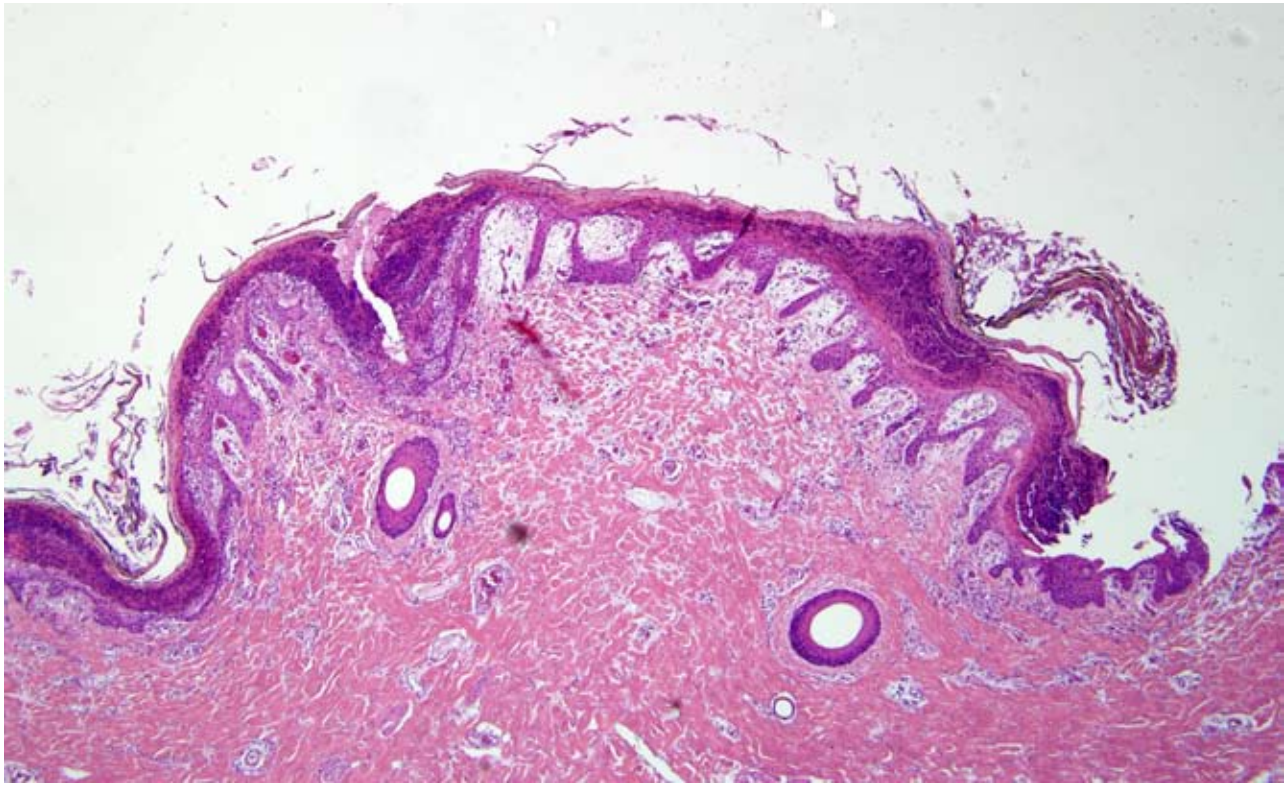

*1-1. Pig, haired skin. Multifocal to coalescing intracorneal pustules, epidermal hyperplasia, and mild perivascular lymphoplasmacytic infiltrate. (HE 40 X)*

**Conference Comment:** *Staphylococcus hyicus* causes a fatal generalized exudative epidermitis in neonatal pigs. The exotoxins produced by *S. hyicus* are metalloproteases that target the stratum granulosum, causing cleavage between the stratum corneum and stratum granulosum. In addition to the cutaneous lesions, piglets can have conjunctivitis, oral lesions and renal lesions. Renal lesions range from epithelial vacuolation, degeneration and exfoliatin of the cells lining the renal pelvis and collecting ducts that can lead to uretheral occlusion to suppurative pyelonephritis. Older pigs may develop subcutaneous abscesses, polyarthritis, necrosis of the ears and tail, abortion and mastitis. *S. hyicus* is the proposed cause of flank-biting and necrotic ear syndrome of pigs, which results in large ulcerated and crusty lesions in early weaned pigs. [2]

Exudative epidermitis of pigs is similar to two human conditions: staphylococcal scalded skin disease and bullous impetigo. Both of these conditions have exfoliotoxins that cause separation between the stratum spinosum and stratum granulosum. However, in bullous impetigo the cocci are present within the intact pustules like in exudative epidermitis, whereas in scalded skin syndrome the cocci are located at a distant often extracutaneous site.[2] *Staphylococcus intermedius* exfoliotoxins cause impetigo, bullous impetigo and superficial spreading pyoderma in dogs.[3]

Review of this slide led to a discussion of various cutaneous lesions in swine. *Sarcoptes scabiei* causes erythematous allergic dermatitis with secondary self trauma and crusting. Lesions are primarily located on the rump, flank and abdomen.[2] Zinc-responsive dermatosis in swine occurs in 2-4 month old growing pigs, and causes thick, dry scales and crusts that can produce deep fissures. Roughly symmetrical lesions are often found on the lower limbs, around the eyes, ears, snout, scrotum and tail. The microscopic lesion is marked hyperplastic dermatitis with parakeratotic hyperkeratosis.[2] Dermatosis vegetans is an inherited disorder in Landrace pigs that results in vegetating skin lesions, hoof malformations and giant cell pneumonia. Skin lesions range from brown-black plaques with a raised border and depressed center to dry-horny papillomatous lesions. The head is typically spared.[2] *Erysipelothrix rhusiopathiae* causes septicemia with cutaneous vasculitis and rhomboidal dermal infarcts, and is also known as "diamond back skin

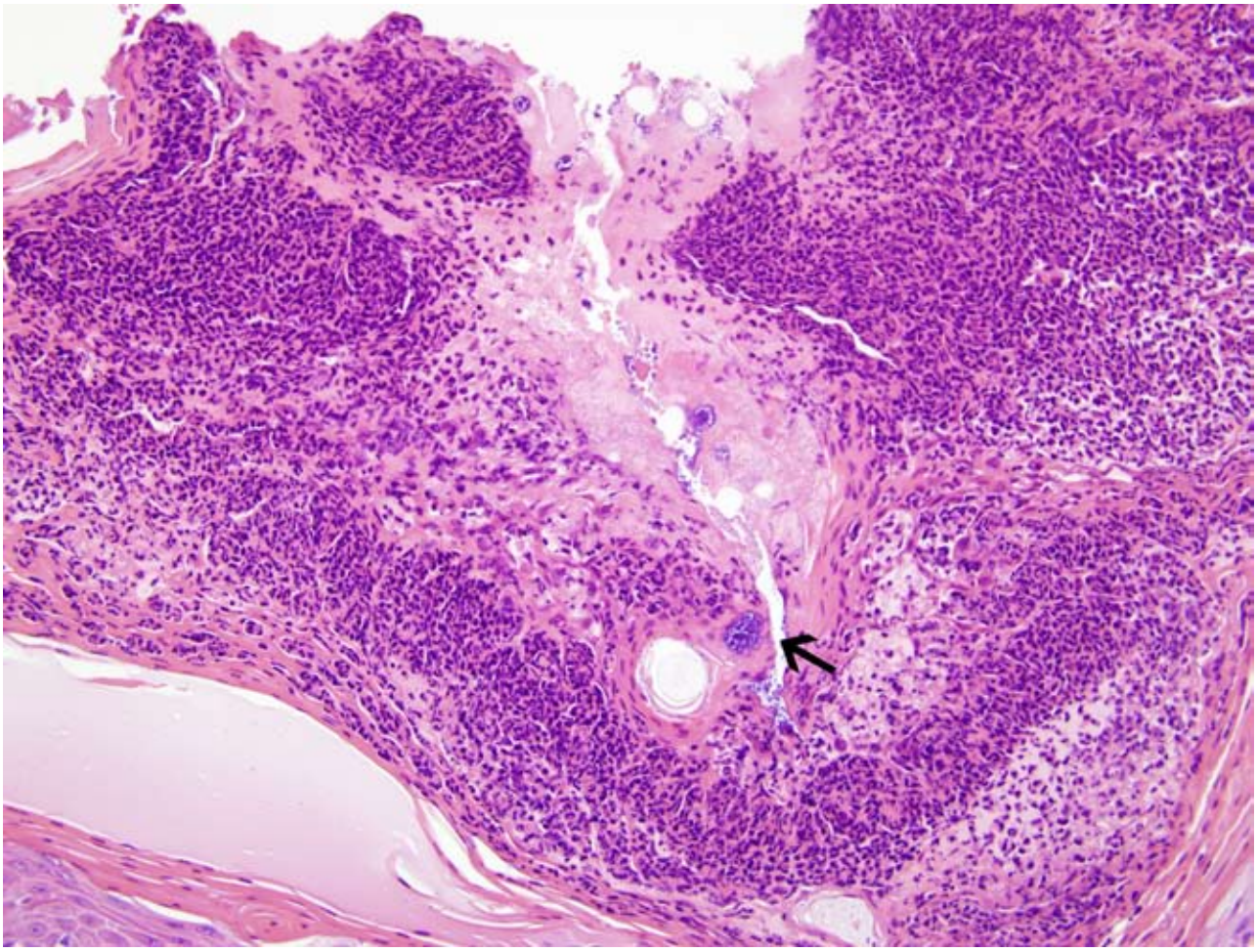

*1-2. Pig, haired skin. Colonies of cocci within the intracorneal pustules (arrows), admixed with numerous degenerate neutrophils. (HE 200X)*

disease." Additional lesions in acute cases include fibrinoid glomerular necrosis, renal intracapsular hemorrhage and fibrinous polyarthritis. The most common lesions in chronic cases include vegetative valvular endocarditis, chronic proliferative arthritis and diskospondylitis.[6] Blue discoloration of the ears, tail and snout are due to venous thrombosis most commonly caused by *Salmonella cholerasuis*, but also other septicemic and viral infections such as *Erysipelothrix rhusiopathiae*, porcine pestivirus (Classical swine fever) and porcine asfarvirus (African swine fever).[1] Porcine dermatitis and nephropathy syndrome causes a systemic necrotizing vasculitis with hemorrhagic dermal infarcts, exudative glomerulonephritis and interstitial nephritis in feeder pigs. Skin lesions typically occur on the perineal area of the hindquarters, limbs, dependent areas of the abdomen and thorax, and ear margins. The condition has been associated with Porcine circovirus-2 and Porcine reproductive and respiratory syndrome virus (PRRS).5 Porcine juvenile pustular psoriasiform dermatitis is most common in weaned Landrace pigs, and causes erythematous serpigenous plaques on the ventral abdomen and inner thighs. Histological lesions include eosinophilic perivascular inflammation, spongiform pustules and psoriasiform hyperplasia.[2] Swinepox is caused by suipoxvirus. Typical poxviral lesions include proliferative and necrotizing skin lesions with large eosinophilic intracytoplasmic inclusions. Lesions primarily occur on the ventral and lateral abdomen, lateral thorax and medial legs of young, growing pigs. Mucosal surfaces are rarely affected. *Hematopinus suis*, the sucking louse, acts as a mechanical vector.[2] Melanomas are often congenital in the Duroc, Sinclair minipig and in Hormel crosses.[2]

**Contributing Institution:** Animal Disease Research and Diagnostic Laboratory, South Dakota State University, Brookings, SD 57007, http://vetsci.sdstate.edu/

**References:**
1. Brown CC, Baker DC, Barker IK: Alimentary system. *In:* Jubb, Kennedy, and Palmer's Pathology of Domestic Animals, ed. Maxie MG, 5th ed., vol. 2, pp.196-197. Saunders, Edinburgh, Scotland, 2007
2. Ginn PE, Mansell JEKL and Rakich PM: Skin and appendages. *In:* Jubb, Kennedy, and Palmer's Pathology of Domestic Animals, ed. Maxie MG, 5th ed. Vol. 1, pp. 591-744. Saunders, Edinburgh, Scotland, 2007
3. Gross TL, Ihrke PJ, Walder EJ, Affolter VK: Skin Diseases of the Dog and Cat, 2nd ed., pp. 4-9. Blackwell Publishing, Ames, Iowa, 2005
4. Taylor DF: Exudative epidermitis. *In:* Diseases of Swine, eds. Leman AD, Straw BE, Mengeling WL, et al., 7th ed., pp. 522 – 525. Iowa State Press, Ames, Iowa, 1992
5. Thibault S, Drolet R, Germain M-C, D'Allaire S, Larochelle, and Magar R: Cutaneous and systemic necrotizing vasculitis in swine. Vet Pathol **35**:108-116, 1998
6. Thompson K: Bones and Joints. *In:* Jubb, Kennedy, and Palmer's Pathology of Domestic Animals, ed. Maxie MG, 5th ed., vol. 1, pp.163-164. Saunders, Edinburgh, Scotland, 2007

## CASE II – 3777-3 (AFIP 3107686)

**Signalment:** Juvenile, weaned harbor seal (*Phoca vitulina*)

**History:** Over the course of the last 10 years, 20 apparently healthy neonatal and juvenile harbor seals presented to local rehabilitation facilities having either died peracutely with no overt premonitory signs, or had an acute onset of lethargy, depression and dehydration, that rapidly progressed to death.

In this case, the animal had presented to rehabilitation as a neonate in late August, 2007, had been apparently normal for 4 weeks, and fed a herring-based formula. The animal presented acutely moribund, inappetant, unresponsive, and died.

**Gross Pathology:** On necropsy, this animal featured segmental to diffuse hemorrhagic enterocolitis characterized by dark red to pink mucoid intestinal contents that were frequently admixed with variable amounts of fibrin. In more severely affected segments of bowel, the mucosa was diffusely dark red, friable, and frequently featured miliary punctuate foci of acute hemorrhage. Mesenteric lymph nodes were enlarged, grey black, and glistening on sectioned surfaces.

**Laboratory Results:** NA

**Histopathologic Description:** Along varying levels of bowel revealed superficial to near full thickness necrosis of the mucosa with segmental to diffuse fibrin pseudomembrane formation. The lamina propria had variable congestion with multifocal hemorrhage and occasional scattered neutrophils.

**Contributor's Morphologic Diagnosis:** Intestine: Enteritis, fibrinous and erosive, marked, multifocal to segmental, presumptively due to *Clostridium difficile*

**Contributor's Comment:** In this case, aerobic and anaerobic culture of multiple levels of bowel yielded mixed growth of *Escherichia coli, Enterococcus* spp, and *Pseudomonas* spp. Culture with selective media isolated *Clostridium difficile*, and ingesta was positive for *Clostridium difficile* toxin A and B (ELISA, Premier TM Meridian Bioscience, Inc., Cincinnati, OH). Microscopically, these enteric lesions are consistent with a variety of bacterial pathogens, including *Salmonella* spp, *Clostridium perfringens, Clostridium difficile*, and strains of *Escherichia coli*, possibly exacerbated by agonal shock (peracute ischemia may present with similar mucosal changes). In human and veterinary medicine, many clostridial infections are polymicrobial and it is difficult to resolve their contribution to the pathogenesis of the lesions. Further microscopic characterization and possible in vitro studies or use of ligated bowel may assist in resolving the role of this pathogen in clinical disease.

Members of the genus *Clostridium* are considered ubiquitous within the environment, often associated with detritus, soil, ocean sediment, and as a component of the gastrointestinal tract flora of humans and other vertebrates. Many infections are considered endogenous. In humans, foals and piglets, this pathogen is associated with antibiotic associated diarrhea and pseudomembranous colitis and infection may be mild and self limiting or fatal due to enterocolitis. It is important to note that toxin positive animals may not exhibit signs or lesions and lab results should be correlated clinically and pathologically.

Even if this is not considered a significant pathogen from the host perspective, harbor seals in rehabilitation facilities may function as multiplying species for a potential zoonotic pathogen and staff should be appropriately educated about hygienic practices. The culture from this animal, and isolates from 4 other post mortem cases were forwarded

to the CDC, Atlanta, Georgia and the more virulent form of this bacteria, strain 027, was not detected by molecular screening.

**AFIP Diagnosis:** Small intestine, villi: Necrosis, acute, diffuse, with myriad bacilli

**Conference Comment:** *Clostridium difficile* causes pseudomembranous colitis in primates, and enteritis and/or colitis in many other species. Disease is usually associated with an imbalance in the intestinal flora and clostridial overgrowth secondary to antibiotics, stress or a change in feed.[1] In horses, *C. difficile* causes proximal enteritis and hemorrhagic enteritis in foals, and colitis in horses of all ages. Colitis X is an acute colitis in horses that is often attributed to *Clostridium perfringens* type A, or less commonly *C. difficile*.[1] In neonatal pigs, *C. difficile* causes fibrinous typhlocolitis with volcanic ulcers, and scrotal edema, hydrothorax and edema of the mesocolon similar to seen with Edema disease.[1] *C. difficile* causes disease in a variety of laboratory animals, but is most significant in the guinea pig where it results in antibiotic-associated dysbacteriosis. Although *C. difficile* can cause diarrhea in rabbits, the most common clostridial pathogen associated with the enteritis complex in juvenile rabbits is *Clostridium spiroforme*.[3]

*C. difficile* produces two major toxins: toxin A and toxin B. Toxin A is an enterotoxin that stimulates chemokine production, which attracts leukocytes. Toxin B is a cytotoxin that modulates cellular signaling pathways, induces cytokine production and causes apoptosis.[4,6]

**Contributing Institution:** Animal Health Center, 1767 Angus Campbell Road, Abbotsford, BC, V3G 2M3

**References:**

1. Brown CC, Baker DC, Barker IK: Alimentary system. *In:* Jubb, Kennedy, and Palmer's Pathology of Domestic Animals, ed. Maxie MG, 5th ed., vol. 2, pp. 221. Saunders, Edinburgh, Scotland, 2007
2. Hammitt MC, Bueschel DM, Keel MK, GLock RD, Cuneo P, DeYoung DW, Reggiardo C, Songer JG: A possible role for Clostridium difficile in the etiology of calf enteritis. Vet Microbiol. **127**:343-352, 2007
3. Percy DH, Barthold SW: Pathology of Laboratory Rodents and Rabbits, 3rd ed., pp. 225, 268. Blackwell Publishing, Ames, Iowa, 2007
4. McAdam AJ, Sharpe AH: Infectious Diseases. *In:* Pathological Basis of Disease, eds. Kumar V, Abbas AK, Fausto N, 7th ed., p. 394. Elsevier Saunders, Philadelphia, PA, 2005
5. Merck Veterinary Manual, 9th ed. Aiello S, Ed, Stoskopf M, Contributor Exotic and Laboratory Animals: Marine Mammals. Merck & Co, Inc., 2006
6. Liu C, Crawford JM: The gastrointestinal tract. *In:* Pathological Basis of Disease, eds. Kumar V, Abbas AK, Fausto N, 7th ed., pp. 836-838. Elsevier Saunders, Philadelphia, PA, 2005
7. Rodriques-Palacios A, Stampfli HR, Duffield T, Peregrine AS, Trotz-Williams KA, Arroyo LG, Brazier JS, Wese JS. Clostridium difficile PCR ribotypes in calves. Canada Emerg. Infect. Dis. **12**:1730-1736, 2006

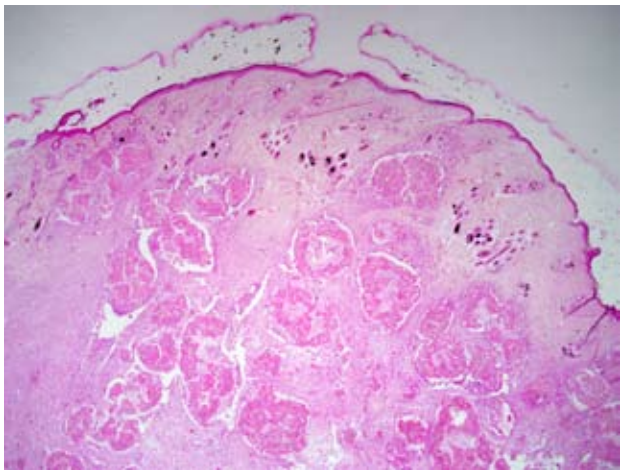

*3-1. Cat, skin. Expanding the panniculus and deep dermis are numerous multifocal to coalescing variably sized nodules composed of a deeply eosinophilic material bounded by a cellular infiltrate and fibrosis. (HE 40X)*

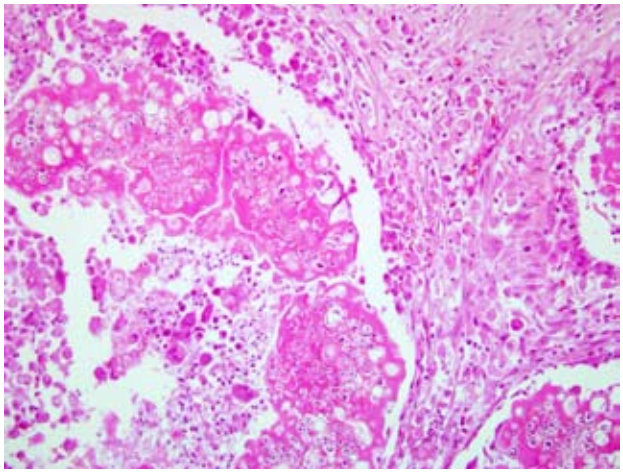

*3-2. Cat, skin. Pyogranulomtous inflammation, homogenous eosinophilic material and numerous fungal hyphae and which often exhibit bulbous swelling. (HE 400X)*

## CASE III – 5512 (AFIP 3106280)

**Signalment:** 5-year-old, female, persa, (*Felis catus*) feline

**History:** At the first examination the cat had numerous variably ulcerated dermal nodules at dorsal and mammary region, which drained purulent exudates with cement-like substances containing yellowish granules. The cat was treated with griseofulvin at 10 mg kg, orally twice a day. However, the size of the nodules increase after the fifth month of treatment and the cat showed progressive weight loss. Combination treatment of surgical excision with systemic antifungal therapy excision would be initiated, but the animal died during the surgical procedure.

**Gross Pathology:** External examination revealed numerous subcutaneous irregular shaped coalescing nodules (2.5–5.0 cm in size) at the back, mammary and inguinal regions. Fistulisation of the nodules was common. From the opened nodules drained an orange honey-like and finely granulous content. Skin on the nodules was alopecic, darkened with a blue or violaceous color and without erythema.

**Laboratory Results:** Microbiology of dermal lesions: Culture performed from nodules yielded dark yellow colonies consistent with *Microsporum canis*. No pathogenic bacteria were isolated.

**Histopathologic Description:** Histological lesions were characterized by a pyogranulomatous

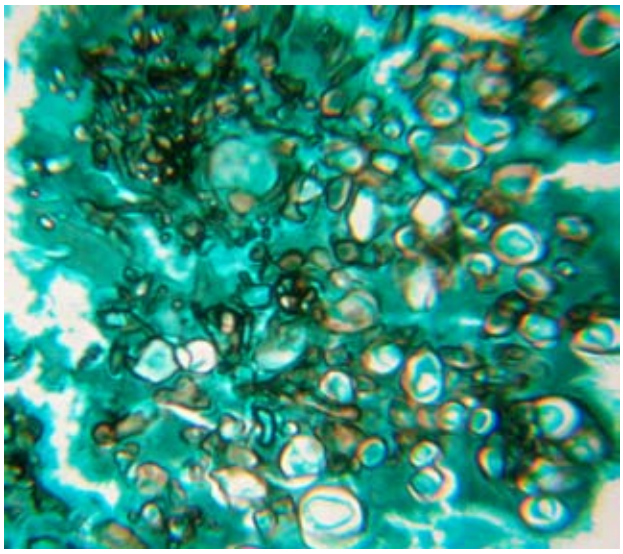

*3-3. Cat, skin. Subcutaneous tissue contains myriad fungal hyphae with bulbous swellings. (GMS). Photomicrograph courtesy of Departamento de Patologia Animal Faculdade de Veterinária UFPel – Campus Universitário s/nº 96010-900 Pelotas-RS Brazil.*

inflammation with giant cells, macrophages, neutrophils and lymphocytes surrounding oval to polyhedral, variable sized granule-like structures **(Fig. 3-1)**. Each of these granules was composed of fungal aggregates with markedly dilated bulbous spores and few vesicular septate hyphae **(Fig. 3-2)**. These fungal structures are embedded in abundant amorphous eosinophilic deposits characteristic of the Splendore-Hoeppli reaction. The periphery of the nodules was characterized by infiltration

of macrophages, lymphocytes and plasma cells, an intense fibroblastic reaction and angiogenesis. Overlying epidermis was ulcerated, or showed discrete acanthosis.

Organisms were strongly positive using periodic acid-Schiff stain. Mycelia was also evidenced with the Gomori's methenamine-silver stain **(Fig. 3-3)**. Both are used to demonstrate the fungal nature of the granules.

**Contributor's Morphologic Diagnosis:** Skin: Pseudomycetoma and granulomatous dermatitis focally extensive severe with fungal structures, *Felis catus*, feline

**Contributor's Comment:** Dermatophytic pseudomycetoma is a rare manifestation of *Microsporum canis* infection [11] and causes deep dermal/ subcutaneous infection of man and animals, with granulomatous/ pyogranulomatous reaction surrounding dermatophytic hyphal elements. The infection has been reported mostly in cats, in humans, rarely in dogs and horses.[7] Persian cats have a high incidence of pseudomycetoma formation, suggesting a heritable predisposition. Those cats may also show a concomitant typical dermatophytosis, but others were detected previously as asymptomatic carriers or can have no known history of previous ringworm.[2]

This type of dermatophytic infection differs from dermatophytosis, in which lesions are restricted to epidermal structures.[2] Pseudomycetomas must be distinguished from fungal mycetomas, or eumycotic mycetomas. True mycetoma is a nodular inflammation with fibrosis, fistulae draining from deep tissue, the presence of grain, and an indolent infection of certain fungi or higher bacteria inoculated into subcutaneous tissues.[4] In pseudomycetomas there are 1) multiple lesions, 2) lack of skin trauma history, 3) association with dermatophytes, most commonly *Microsporum canis* [1, 2, 7] histologically, lack of true cement material and a more abundant Splendore-Hoeppli reaction.[1,2,4] Additionally, in pseudogranules, there are fewer hyphal filaments than in true eumycotic granules. Pseudomycetoma granules have a sequential development, characterized by the presence of small to large clusters of mycelia elements.[4]

It is unclear why the cat developed a pseudo-mycetoma.[9] Several hypotheses on the pathogenesis of the disease have been proposed. In contrast to the supposed traumatic origin of a mycetoma, in pseudomycetoma some authors propose that mycelial elements escape from the hair follicle into the surrounding tissues [1, 7] where they aggregate and induce an immune response. The exact immunological mechanism responsible for the formation of the granules is much debated, as well as the predisposition of Persian cats to the disease.[1] There is a recent report of an intraabdominal pseudomycetoma in a Persian cat who had no suspicion of immunosuppression, no history of cutaneous ringworm infection, and no prior abdominal surgery. Possible sources of this infection include: ingestion of infected foreign material, secondary to prior castration, inoculation from rectal thermometer, or other penetrating wound.[9] A chronic evolution is the rule, and the prognosis is fair even with systemic antifungal therapy of long duration.[2]

A definitive diagnosis of pseudomycetoma involves a combination of histopathology and either identification of the causal organism by fresh tissue culture or by identification of the organism by immunohistochemical stains.[1,9]

The pathognomonic histologic lesion is the presence, deep in the dermis and subcutis, of aggregates of compact mycelia within a granulomatous tissue reaction. The fungi may be surrounded by amorphous eosinophilic material representing the Splendore-Hoeppli reaction. The overlying skin may show parasitized shafts in the absence of inflammation or the more typical folliculitis. Fungi in the superficial lesions have normal morphology. Invasion of hyphae through the external root sheath has been described.[11] Cytology is useful for making diagnosis of mycetomas in humans, but it can be difficult to perform.[9] A cytological diagnosis of pseudomycetoma should be suspected and is warranted if arthrospores and refractile septate hyphae are present in cytologic specimens from Persian cats with single or multiple dermal nodules, especially if pyogranulomatous inflammation is also present.[2]

Fungal culture represents by far the most reliable diagnostic evidence to ascertain the aetiological agent of these infections.[7] Microsporum canis is isolated in most cases, but colonies do not always have a typical appearance on primary cultures, and macroconidia are often lacking. Molecular tools have been used on histological sections for identification of dermatophytic mycetomas.[2] PCR seems to be a reliable and useful complementary method to identify the aetiological fungus from paraffin-embedded sections obtained from cases of dermatophytic pseudomycetoma in different animal species. Molecular biology could be a valid alternative identification method when 1) culture is unsuccessful; 2) in retrospective analysis, when only a stored histological section is available; 3) and in further studies on the aetiologic agents of Dermatophytic pseudomycetoma from biopsy confirmed pathological specimens.[7]

Differential diagnosis with nodulous tumoral diseases

is necessary, and a dermatophytic origin would be suspected for all pseudo-tumoral masses observed on feline skin [2] and, especially in Persian cats, when poorly marginated intraabdominal mass were detected on imaging examinations.[9]

**AFIP Diagnosis:** Skin: Panniculitis and dermatitis, pyogranulomatous, nodular, focally extensive, severe with multiple aggregates of fungal hyphae

**Conference Comment:** The contributor provided an excellent overview of the entity. Pseudomycetomas are most common in Persian and Himalayan cats. Other conditions that are more common in Persian cats include polycystic kidney disease, alpha-mannosidosis, facial dermatitis (Himalayan cats included), and Chediak-Higashi Syndrome. Polycystic kidney disease (PKD) is inherited as an autosomal dominant trait, like the adult form of PKD in humans. Fibrosis and cysts also occur within the liver of many affected cats.[8] Alpha-mannosidosis is most common in cattle (Angus, Murray Grey and Galloway) and cats (Persian and domestic). There is deficient lysosomal alpha-mannosidase activity in almost every cell but hepatocytes, resulting in cytoplasmic vacuolation most evident in neurons and secretory epithelium.[6] Facial dermatitis of Persian and Himalayan cats is an uncommon, idiopathic facial dermatitis that causes a matting of the facial hair by dark, greasy sebaceous material in young cats.[3] Chediak-Higashi syndrome is an autosomal recessive condition that is reported most commonly in humans, cattle, Persian cats, beige mice, rats and Aleutian mink.[10] Affected animals have a defective LYST/CHS1 gene that regulates intracellular protein trafficking and vesicle fusion.[5] This defect causes enlarged granules in melanosomes, granulocytes and platelets which results in color dilution, bleeding tendencies and recurrent infections.[10]

**Contributing Institution:** Animal Pathology Department /Veterinary Diagnostic Laboratory, Veterinary Faculty – Federal University of Pelotas. 96010-900 Pelotas, RS, Brazil.
http://www.ufpel.edu.br/fvet/oncovet/
http://www.ufpel.edu.br/fvet/lrd/

**References:**

1. Abramo F, Vercelli A, Mancianti F: Two cases of dermatophytic pseudomycetoma in the dog: an immunohistochemical study. Vet Dermatol **12**:203-207, 2001
2. Chermette R, Ferreiro L, Guillot J: Dermatophytoses in Animals. *Mycopathologia doi*:10.1007/s11046-008-9102-7, 2008.
3. Gross TL, Ihrke PJ, Walder EJ, Affolter VK: Skin Diseases of the Dog and Cat, 2nd ed., pp. 112-115. Blackwell Publishing, Ames, Iowa, 2005
4. Kano R, Edamura K, Yumikura H, Maruyama H, Asano K, Tanaka S, Hasegawa A: Confirmed case of feline mycetoma due to *Microsporum canis*. Mycoses, doi:10.1111/j.1439-0507.2008.01518.x, Apr 26, 2008
5. Kaplen J, De Domenico I, Ward DM: Chediak-Higashi syndrome. Curr Opin Hematol **15**:22-29, 2008
6. Maxie MG, Youssef S: Nervous system. *In:* Pathology of Domestic Animals, ed. Maxie MG, 5th ed., vol. 1, pp. 326-327. Elsevier, Edinburgh, UK, 2007
7. Nardoni S, Franceschi A, Mancianti F: Identification of *Microsporum canis* from dermatophytic pseudomycetoma in paraffin-embedded veterinary specimens using a common PCR protocol. Mycoses **50**:215–217, 2007
8. Stalker MJ, Hayes MA: Liver and biliary system. *In:* Pathology of Domestic Animals, ed. Maxie MG, 5th ed., vol. 2, p. 302. Elsevier, Edinburgh, UK, 2007
9. Stanley SW, Fischetti AJ, Jensen HE: Imaging diagnosis-sublumbar pseudomycetoma in a Persian cat. Veterinary Radiology & Ultrasound **49**:176–178, 2008
10. Valli VEO: Hematopoietic system. *In:* athology of Domestic Animals, ed. Maxie MG, 5th ed., vol. 3, p. 115. Elsevier, Edinburgh, UK, 2007
11. Yager JA, Scott DW: The skin and appendages. *In:* Pathology of Domestic Animals, eds. Jubb K.V.F., Kennedy P.C & Palmer N., 4th ed., vol. 1, pp. 707-718. Academic Press, San Diego, CA, 1993.

## CASE IV – 0707051 (AFIP 3075498)

**Signalment:** Canine, 2-year-old, female, Husky-cross, *Canis lupus familiaris*

**History:** A biopsy from the ear was submitted.

**Gross Pathology:** NA

**Laboratory Results:** NA

**Histopathologic Description:** A section of haired skin from the ear was submitted in which there is diffuse (and in other regions not included, multinodular foci of dense yeast-like organisms that extended from the superficial dermis to the deep dermis underlying a multifocally ulcerated epidermis with multifocal acanthosis and intraepidermal separation (just above the basal layer). There was associated neutrophilic inflammation and scattered foamy macrophages. Organisms were round

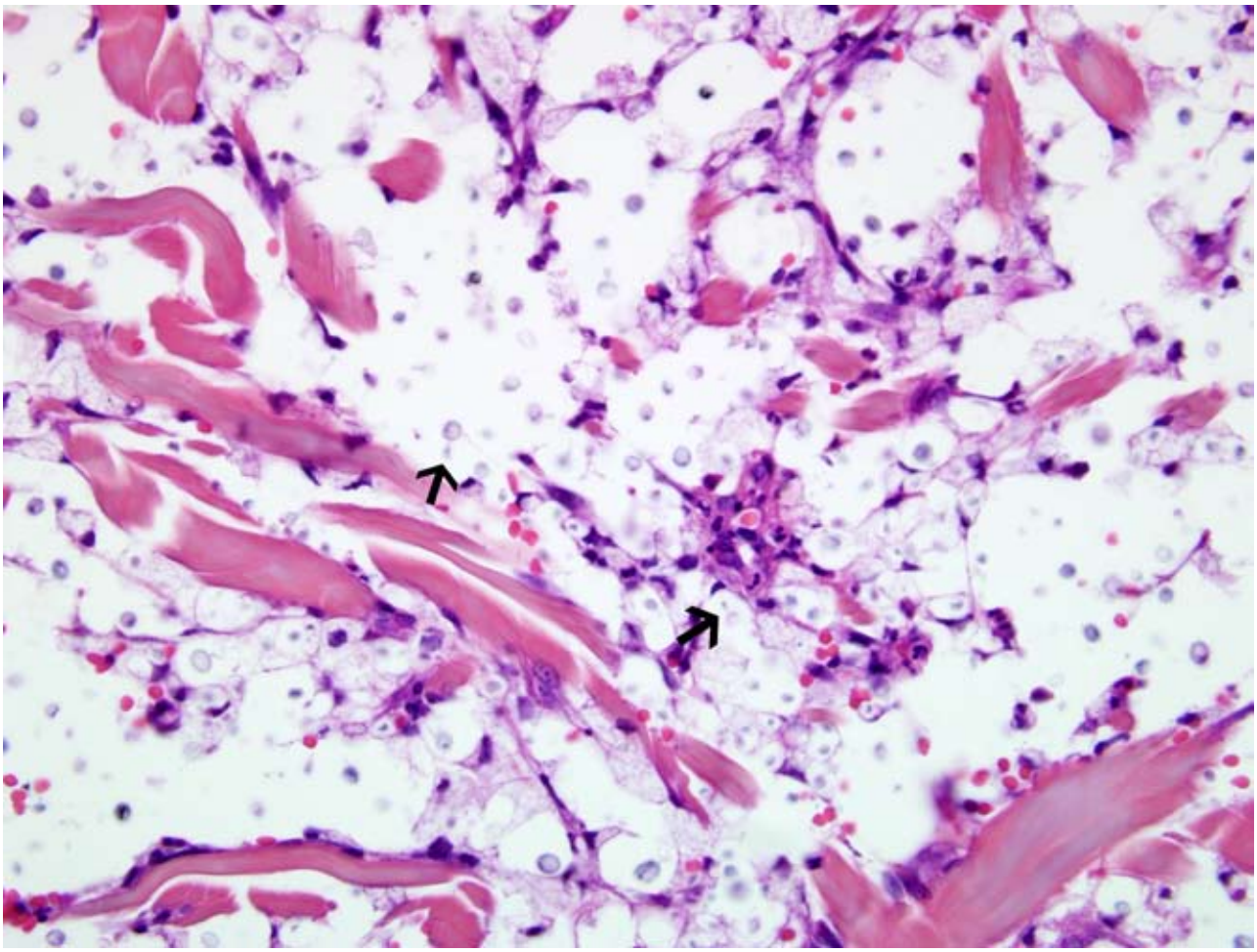

*4-1. Dog, skin. Diffusely with the dermis there are myriad yeast characterized by an approximately 15-20 micron nucleus surrounded by thick up to 40 micron clear capsule; occasional yeast exhibit narrow-based budding (arrows). (HE 400X).*

to oval (3-20 microns) and refractile surrounded by a clear capsule (up to 40 microns). Some structures exhibit narrow-based budding **(Fig. 4-1)**.

**Contributor's Morphologic Diagnosis:** Dermatitis, multifocal ulcerative with intradermal yeast-like fungi (*Cryptococcus neoformans*); cutaneous cryptococcosis

**Contributor's Comment:** Cutaneous crypto-coccosis is apparently rare in dogs and more common in cats.[2] The organism is a ubiquitous saprophyte that is common in nitrogen-rich, alkaline soil and particularly associated with pigeon excrement. The disease is seen most frequently in humid climates and is unusual in climates such as Wyoming. Inhalation of airborne organisms is frequently followed by local upper respiratory tract infection and cutaneous infection is thought to be local extension. Concurrent immunosuppressive conditions such as diabetes and neoplasia may predispose to infection but this association is still inconclusive.[3] Rare reports of cryptococcosis in dogs include infection of the central nervous system and rare cutaneous infection results from disseminated systemic disease.

**AFIP Diagnosis:** Dermatitis and panniculitis, pyogranulomatous, diffuse, severe with numerous yeast, etiology consistent with *Cryptococcus neoformans*

**Conference Comment:** *Cryptococcus neoformans* (*C. neoformans* ssp. *neoformans*) is the most common systemic fungal infection in cats. The respiratory system is primarily infected; with hematogenous spread to other organs, most commonly the central nervous systems, skin and eyes. Cryptococcal mastitis in cows is an ascending, rather than hematogenous, infection. *Cryptococcus* sp. is the only pathogenic fungus with a capsule. The capsule

causes the gross lesions to appear gelatinous and the histological lesions to have a "soap bubble" appearance.[1] Mucicarmine stains the capsule.

The major virulence factors of *Cryptococcus* are the capsule and the production of antioxidants such as melanin. The capsule impairs phagocytosis, activates complement, and possibly suppresses T lymphocytes. The rare acapsular strains of *Cryptococcus* sp. incite abundant granulomatous inflammation and are readily phagocytized, making them much less pathogenic than the capsular strains. The acapsular strains of *Cryptococcus neoformans* resemble *Blastomyces dermatitidis* but can be distinguished by the presence of narrow-based budding in the former and broad-based budding in Blastomyces dermatitidis. Some strains are able to produce antioxidants such as melanin and phenoloxidase (laccase), which protect the organism from oxidative damage by leukocytes.[1]

*Cryptococcus gattii* (previously *C. neoformans* ssp. *gattii*) is primarily found in tropical and subtropical climates. It is associated with eucalyptus trees and infections in koalas. However, it has recently been reported in the temperate Pacific Northwest, primarily in British Columbia, where it has infected humans, dogs, cats, porpoises and ferrets. Unlike *Cryptococcus neoformans*, it often infects immunocompetent hosts.[4]

**Contributing Institution:** Wyoming State Veterinary Laboratory, University of Wyoming, 1174 Snowy Range Rd. Laramie, Wyoming 82070, http://wyovet.uwyo.edu/

**References:**

1. Caswell JL, Williams KJ: Respiratory system. *In:* Pathology of Domestic Animals, ed. Maxie MG, 5th ed., vol. 2, pp. 642-644. Elsevier, Edinburgh, UK, 2007
2. Gross TL, Ihrke PJ, Walder EJ, Affolter VK: Skin Diseases of the Dog and Cat, pp. 295-297. Blackwell Science Ltd, Oxford, UK, 2005.
3. Jacobs GJ, Medleau L, Calvert C, Brown J: Cryptococcal infection in cats: factors influencing treatment outcome, and results of sequential serum antigen titers in 35 cats. J Vet Intern Med **11**:1-4, 1997
4. Stephen C, Lester S, Black W, Fyfe M, Raverty S: Multispecies outbreak of cryptococcosis on southern Vancouver Island, British Coulmbia. Can Vet J **43**:792-294, 2002

The Armed Forces Institute of Pathology
Department of Veterinary Pathology

*Conference Coordinator:*
Todd M. Bell, DVM

WEDNESDAY SLIDE CONFERENCE 2008-2009

# Conference 10

3 December 2008

*Conference Moderator:*

Dr. Richard Montali, DVM, Diplomate ACVP

## CASE I – 08-956-1 (AFIP 3106956)

**Signalment:** Approximately 2 to 3-year-old adult, male, Northern leopard frog (Rana pipiens)

History: The frog was euthanized and submitted for necropsy after presenting with a history of lethargy, distended abdomen and possible abdominal mass on palpation.

**Gross Pathology:** On external examination, the abdomen was severely distended and mild hyperemia and erythema were noted on the distal extremities. On incision, the ventral abdomen contained a large, approximately 4cm, space-occupying multilobulated, cauliflower-shaped pale pink soft tissue mass. The testes were positioned ventral to and in contact with the mass. The mass was not adhering to any viscera and caused displacement of the abdominal organs.

**Laboratory Results:** NA

**Histopathologic Description:** Abdominal mass: The examined section is composed of part of the abdominal mass, small segment of renal parenchyma and testes. The partially encapsulated, multilobulated and moderately cellular neoplastic mass is well-differentiated and composed of a proliferation of closely packed cells arranged in irregularly-shaped tubules or papillary projections that are supported by a fine fibro-vascular stroma (Fig. 1-1). Neoplastic cells are variably sized, mostly large, cuboidal to columnar with distinct cell borders and contain moderate amounts of eosinophilic, granular cytoplasm that often contains eosinophilic to mucinous globular droplets. The cells frequently form piles of 4-12 cell-layers deep. The nuclei of the cells are round to oval, central to basally positioned, with coarsely stippled chromatin, and contain one or more prominent basophilic nucleoli. Rarely, the nucleus contains 2-4 µm diameter eosinophilic inclusion-like material with a clear halo and marginated chromatin. Mitotic figures are 22 per 10 high-powered fields. There is mild anisocytosis and anisokaryosis. In multiple foci, individual cells to aggregates of necrotic/ghost cells are present. Many tubules contain ectatic lumen filled with necrotic cells, few lymphocytes and eosinophilic proteinaceous material.

Kidney: Within the submitted small remnant renal tissue, islands of dysplastic convoluted tubules mostly in the renal pelvis are also lined by epithelium with morphological features similar to those observed in the adjacent neoplasm.

*Sponsored by the American Veterinary Medical Association, the American College of Veterinary Pathologists, and the C. L. Davis Foundation.

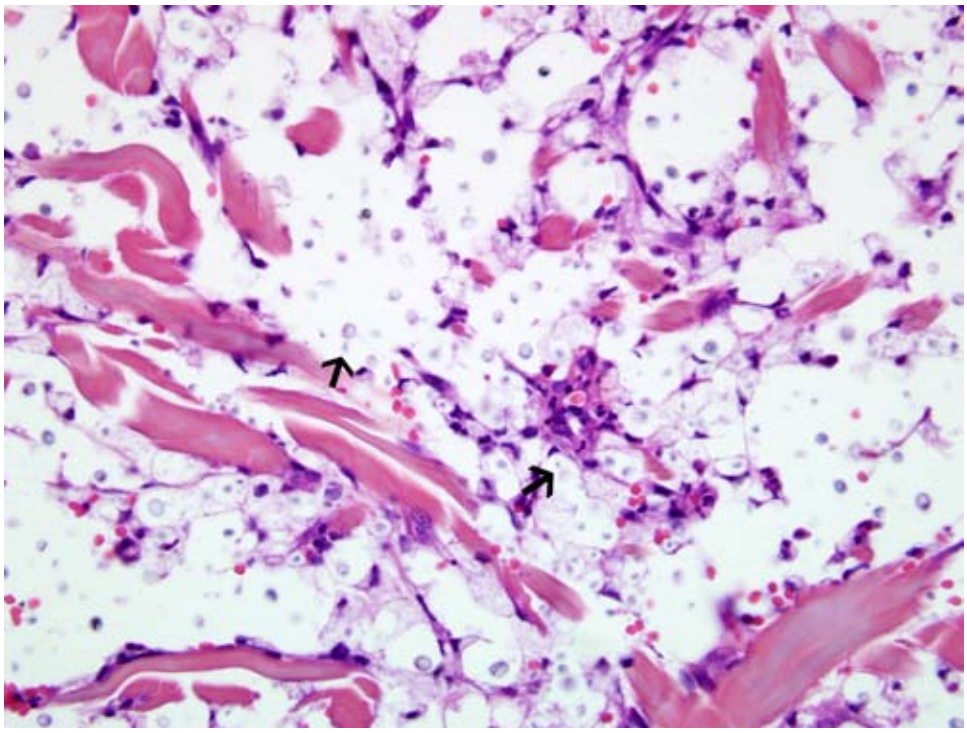

*1-1. Kidney, frog. Effacing normal renal tissue architecture and compressing adjacent parenchyma, is an unencapsulated, multilobular, moderately cellular neoplasm composed of cuboidal to columnar epithelial cells that form variably sized tubules and micropapillary structures and are supported by a fibrovascular stroma. HE 200X.*

The neoplastic cells variably contain faintly visible microvilli.

**Contributor's Morphologic Diagnosis:** Renal mass (presumed): Adenocarcinoma, well-differentiated, tubulo-papillary with rare eosinophilic intranuclear inclusion-like material

Contributor's Comment: This fairly large abdominal mass is suspected to be of renal origin, though no remnants of renal parenchyma were present within the actual mass. However, the presence of islands of tubules with features similar to those observed in the mass is highly indicative of renal origin along with the massive growth of the tumor effacing the normal renal parenchyma. Rarely, indistinct eosinophilic inclusion-like material was observed within the nucleus and rarely in the cytoplasm. The inclusions, though not of typical size, are considered to be herpes viral inclusions. Additional electron microscopic evaluation may be needed for confirmation. The morphological features are most consistent with that of Ranid herpesvirus 1 (RaHV-1) induced adenocarcinoma of leopard frogs.

RaHV-1 is the etiologic agent of Lucké renal adenocarcinoma and occurs spontaneously in Rana pipiens typically in frogs aged 2 years or older.[1] Tumor incidence can be as high as 50% in laboratory populations living at 25°C.[2] The viral replication and growth kinetics of the tumor are dependent on temperature and season. High environmental temperature during summer is permissive for viral invasion and rapid growth of tumor with very few inclusion bodies. During cooler, winter temperatures invasion is restricted but viral replication occurs in the convoluted tubules of the kidney with dormant phase of tumor growth.[1] When frogs are hibernating or maintained at low temperature, tumor cells contain intranuclear inclusions whereas frogs in summer months or maintained at 25°C do not contain virus or inclusions in tumor cells.[2] Frogs may not show clinical signs of lethargy, emaciation and ascites until the disease is well advanced.[1] Whitish tumors can be seen at necropsy on the kidneys, though tumors can grow very large and metastasize.[1] There is no treatment and affected animals should be euthanized.[1] The other well-known spontaneous amphibian tumor is lymphosarcoma, occurring in Xenopus laevis.[3]

**AFIP Diagnosis:** Kidney: Adenocarcinoma, tubulopapillary

**Conference Comment:** Lucke's tumor, or renal adenocarcinoma of frogs, is commonly found in the northern and northeastern United States. It can be found in up to 10% of frogs captured in the wild.[2] The Lucke tumor herpesvirus, (LTHV), is the causative agent of the tumor, and ultrastructurally the virions are icosahedral and 95-100nm.

Frogs shed this virus in the colder months of the year, and it travels via water to infect frog eggs during spawning season. Mortality due to renal adenocarcinoma usually occurs after spawning when temperatures are warmer and the tumor has grown considerably within the coelomic cavity. Frogs often seem clinically normal until just prior to death. Neoplastic cells can often be isolated from ascitic fluid to aid in an ante-mortem diagnosis.[1]

**Contributing Institution:** Division of Comparative Medicine, Building 16-849, Massachusetts Institute of Technology, 77 Massachusetts Avenue, Cambridge, Massachusetts 02139-4307
http://web.mit.edu/comp-med/

**References:**

1. Fox JG, Anderson LC, Loew FM, Quimby FW: Laboratory Animal Medicine, 2nd ed., pp. 817-818. Academic Press, London, England, 2002
2. Granoff A: Herpesvirus and the Lucké tumor. Cancer Res **33**:1431-1433, 1973
3. Ruben LN, Clothier RH, Balls M: Cancer resistance in amphibians. Altern Lab Anim **35**:463-470, 2007

## CASE II – 04/3025 D (AFIP 3102369)

**Signalment:** 3-year-old male Tasmanian Devil (*Sarcophilus harrisii*)

**History:** Wild male Tasmanian Devil, condition score 1.5 out of 5, trapped from the wild.

**Gross Pathology:** There were multi-centric tumors on the face, 6 in total, labeled T1 to T6. The mass labeled T4 was submitted to the Wednesday Slide Conference. T1 was a mass on the lower right lip measuring 6.2 x 4.4 x 2.8 cm. T2 was a mass at the right commissure of the lips measuring 1.5 x 0.7 cm. T3 was on the upper right lip measuring 0.5 x 0.2cm. T4 was a mass on the left side of the forehead measuring 5 x 4 x 1.7 cm. T5 was near the lateral canthus of the left eye measuring 1.2 x 0.7cm. T6 was a mass on the left cheek measuring 0.5 x 0.4 cm. There were no other significant internal findings at post mortem. There were fly larvae and eggs around the rump area (cutaneous myaisis).

**Laboratory Results:**

Significant clinical chemistry abnormalities included:

| | | |
|---|---|---|
| AST (IU) | 436 | (39.0-206.0) |
| Creatinine (umol/L) | 28 | (44.0-106.0) |
| Protein (g/L) | 75.6 | (52.0-69.0) |
| Albumin (g/L) | 24.3 | (28.0-37.0) |
| Globulin (g/L) | 51.4 | (18.0-37.0) |

Hematological abnormalities included:

| | | |
|---|---|---|
| WBC (x $10^9$/L) | 59.5 | (3.4-13.2) |
| Neutrophils (x $10^9$/L) | 55.93 | (0.82-9.33) |
| Monocytes ((x $10^9$/L) | 1.78 | (0.04-0.26) |
| Fibrinogen (g/L) | 12.0 | (0.0-3.0) |

Urinalysis

| | |
|---|---|
| Volume (ml) | 10 |
| Color | yellow |
| Turbidity | clear |
| Specific Gravity | 1.058 |
| pH | 7.0 |
| Protein | 3+ |
| Glucose | nil |
| Ketones | nil |
| Bilirubin | nil |
| Blood (heme) | 2+ |
| Urobilinogen | nil |
| Cells (per hpf) | 0 |
| Debris | 1+ |

**Comment:** The serum biochemistry changes indicate a moderate increase in AST, moderate decrease in Creatinine, mild hyperproteinemia characterized by a mild hypoalbuminemia and a moderate hyperglobulinemia. The leukon changes demonstrate a marked leukocytosis characterized by a marked neutrophilia and a moderate monocytosis. There is a marked hyperfibrinogenemia, moderate hemoglobinuria, and marked proteinuria. The increase in AST in this case could be attributed to a myopathy related to exertion or capture, since the hepatic function was normal. Although CK was within the normal reference range, AST can remain elevated for up to 5-6 days once released from the muscle, whereas CK can diminish rapidly (within 2 days). Moreover, a delay in sample collection may result in there being no apparent change in activity of CK. The decrease in serum creatinine can occur with severe cachexia and subsequent significant loss of muscle. Low albumin could be due to decreased intake (starvation) or reduced synthesis to maintain oncotic pressure (since globulins are increased). The hypoproteinemia and hyperglobulinemia are consistent with neoplasia and chronic inflammatory disease. The leukon changes (marked neutrophilia, moderate monocytosis and hyperfibrinogenemia) are consistent with severe inflammatory disease.

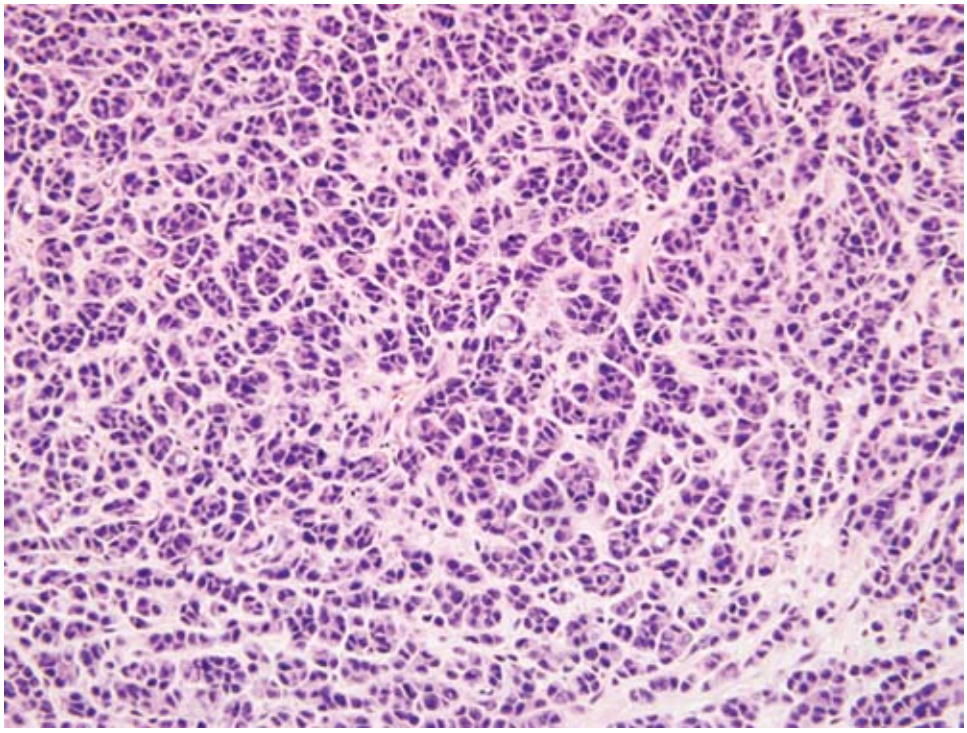

*2-1. Skin, Tasmanian Devil. Malignant neuroendocrine neoplasm. Round to polygonal cells with variably distinct cell borders and moderate finely granular eosinophilic cytoplasm that are often arranged in small nests and packets and separated by a fibrovascular stroma. HE 400X.*

**Histopathologic Description:** The dermis and hypodermis are expanded by a partially circumscribed, nodular, neoplastic proliferation of epithelial cells. The neoplastic cells are divided into lobules by fibrous connective tissue. Within the lobules the neoplastic cells are arranged in streams and nests, supported by delicate fibrovascular stroma **(Fig. 2-1)**. Scattered amongst the intact neoplastic cells are occasional, individual apoptotic and necrotic neoplastic cells. Within the center of many of the lobules are extensive areas of necrosis. Most of the neoplastic cells have a round to polyhedral or cuboidal shape with a moderate amount of eosinophilic cytoplasm. Nuclei are round to ovoid, with a stippled, basophilic chromatin pattern. Nucleoli are often multiple and mitoses range from 0-12 per field of 400x magnification. The epidermis overlying the neoplasm is extensively ulcerated. The exposed dermis is superficially necrotic and expanded and covered by a proteinaceous and neutrophilic exudate containing multifocal colonies of bacteria.

**Contributor's Morphologic Diagnosis:** Haired skin: Carcinoma "Devil Facial Tumor Disease"

**Contributor's Comment:** The history, gross and histopathological findings are consistent with Devil Facial Tumor Disease, a debilitating transmissible neoplastic condition affecting significant numbers of the wild population of Tasmanian Devils.

Out of all of Australia's unique wildlife, Tasmanian Devils are the largest living dasyurids, or carnivorous marsupials. They are iconic natives of Tasmania, where they inhabit the coastal forests, scavenging on dead or dying animals. A debilitating disease with proliferating facial masses was detected in wild populations of Tasmanian Devils in the mid 1990's.[1,5] Dubbed the Devil Facial Tumour Disease, this emerging new disease was quickly increasing in prevalence, with population declines of up to 80% in some areas.[1,2] Affected animals develop large, multicentric, flat soft tissue masses, often with ulcerative and exudative centers.[2] The tumors first develop around the face, mouth, and neck, but may spread to elsewhere in the body. As they enlarge, the tumors interfere with feeding, and the devils quickly lose condition, and usually succumb to the disease within 6 months.

A multi-disciplinary approach was taken to investigate and characterize this disfiguring, fatal disease. The main goal of this research was to maintain an ecologically sustainable population of Tasmanian Devils in the wild.[5] Standard cytology, histopathology, and electron microscopy were used to characterize these facial tumors. Loh et al (2006a) discovered that the neoplasm originated within the dermis, and was composed of dense, multinodular proliferations of pleomorphic round to polyhedral cells, with a high nuclear to cytoplasmic ratio.[2] These cells had a fibrillar, eosinophilic cytoplasm, indistinct cytoplasmic margins,

and single, basophilic nuclei with no obvious nucleoli.[2] The mitotic rate ranged from 0-12 per 400x magnification, and necrosis was observed in most samples.[2] Metastasis was also reported in 65% of the cases, with frequent involvement of the regional lymph nodes, and distant metastases mainly to the lungs, but also the spleen, heart, ovary, serosal surface of ribs, kidney, mammary, pituitary and adrenal glands.[2]

The pleomorphic neoplastic cells were difficult to characterize, and immunohistochemistry was utilized for final confirmation. The cells stained negative for cytokeratin, epithelial membrane antigen, von Willebrand factor, smooth muscle actin, desmin, glial fibrillary acid protein, CD 16, CD 57, CD3, and LSP1, but stained positive for vimentin, S-100, melan A, neuron specific enolase, chromogranin A, and synaptophysin 3. With this information, together with the morphological and ultrastructural features of the cells, it was concluded the neoplasm was consistent with a malignant neuroendocrine tumor.

In parallel with this work, cytogenetic studies were performed, and a unique, aneuploid karyotype was identified, which was shared by tumors from animals in many geographical locations within the state. These genetic rearrangements were identical in male and female animals from a range of ages, indicating that cytogenetically, DFTD is relatively stable.[4] Such findings, combined with the frequent habit of the devils engaging in "jaw wrestling" and the propensity for the tumors to arise in the lips, oral mucosa, or the face, is consistent with disease being spread as allografts. The most significant confirmative indicator that DFTD is a transmissible neoplasm has been the successful experimental transfer of DFTD cells derived from cell cultures and natural tumors to healthy devils with the subsequent variable development of DFTD. This work has fulfilled elements of Koch's postulates, confirming the transmissible neoplasm hypothesis.[5]

A collaborative effort to save the Tasmanian Devils has been established with the goal to investigate disease control mechanisms and identify management options to prevent further population decline.

**AFIP Diagnosis:** Haired skin: Malignant neuroendocrine neoplasm (Tasmanian Devil Facial Tumor Disease)

**Conference Comment:** There was considerable discussion at the post-conference meeting about the proper classification of this tumor. Based upon positive immunohistochemical staining for vimentin, S-100, melan A, neuron specific enolase, chromogranin A, and synaptophysin 3, we favor the diagnosis of malignant neuroendocrine tumor.

The contributor did an outstanding job of reviewing DFTD including transmission, gross and histologic findings and tumor karyotype.

Additionally, some attendees noted the incidental finding of intrafollicular mites consistent with Demodex in their sections.

**Contributing Institution:** Health Sciences, School of Veterinary and Biomedical Sciences, Murdoch University, South Street, Murdoch, 6150 WA Australia Murdoch University wwwvet.murdoch.edu.au

**References:**

1. Hawkins C, Baars C, Hesterman H, Hocking GJ, Jones ME, Lazenby B, Mann D, Mooney N, Pemberton D, Pyecroft S, Restani M, Wiersma J: Emerging disease and population decline of an island endemic, the Tasmanian Devil *Sarcophilus harrisii*. Conservation Biology **131**:307-324, 2006
2. Loh R, Bergfeld J, Hayes D, O'Hara A, Pyecroft S, Raidal S, Sharpe R: The pathology of Devil Facial Tumor Disease (DFTD) in Tasmanian Devils (*Sarcophilus harrisii*) Vet Pathol **43**:890-895, 2006
3. Loh R, Hayes D, Mahjoor A, O'Hara A, Pyecroft S, Raidal S: The immunohistochemical characterization of Devil Facial Tumor Disease (DFTD) in the Tasmanian Devil (*Sarcophilus harrisii*) Vet Pathol **43**:896-903, 2006
4. Pearse AM, Swift K: Transmission of Devil Facial Tumour Disease. Nature. **439**:549, 2006
5. Pyecroft SB, Pearse AM, Loh R, Swift, K, Belov K, Fox N, Noonan E, Hayes D, Hyatt A, Wang L, Boyle D, Church J, Middleton D, Moore R: Towards a case definition for Devil Facial Tumour: what is it? Ecohealth Journal Consortium, 2007

## CASE III – 60136 (AFIP 3102636)

**Signalment:** Adult, male American horseshoe crab (*Limulus polyphemus*)

**History:** This horseshoe crab was part of an aquarium touch-tank exhibit for two years and developed mild gill and shell lesions. The gill and shell lesions progressively worsened; the crab became moribund and was euthanized.

*3-1. Carapace, American Horseshoe Crab. Multifocal variably sized chitinolytic lesions on the surface of the carapace.* *Photograph courtesy of Johns Hopkins University Department of Molecular and Comparative Pathobiology, Baltimore, Maryland.*

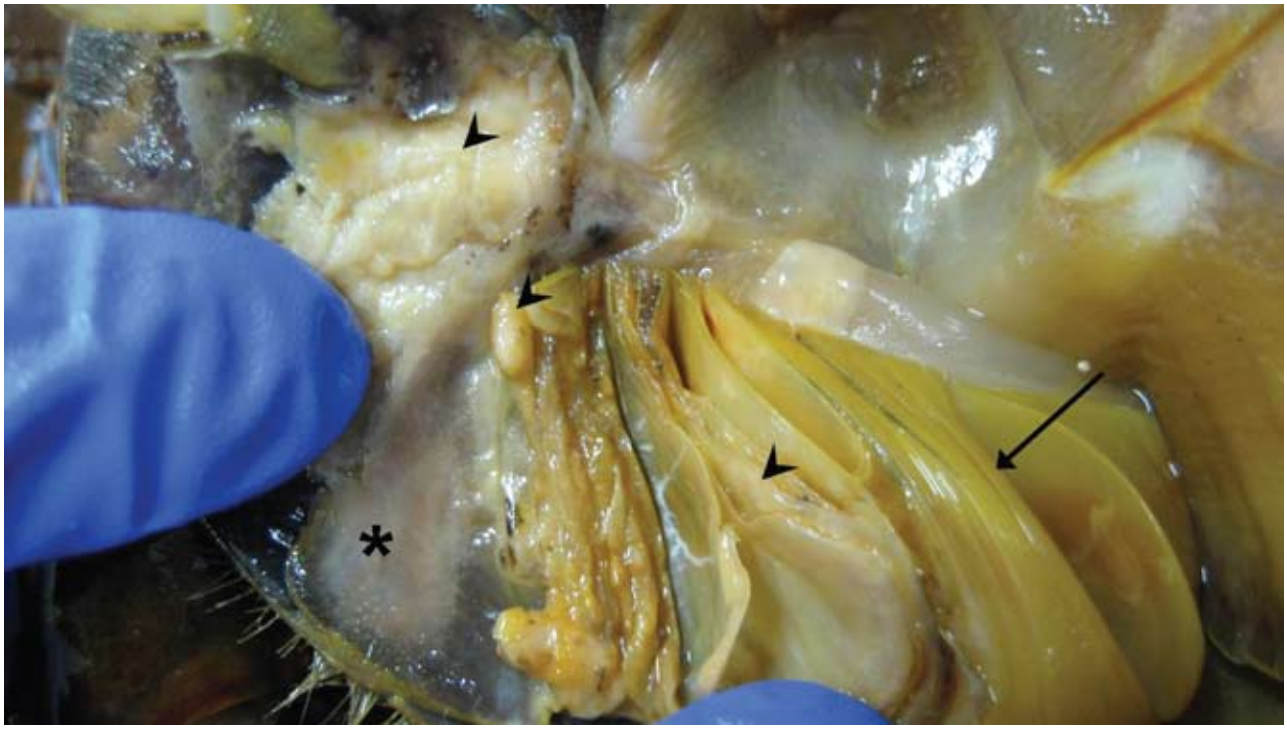

*3-2. Book gill (*) and book gill leaflets (arrow), American Horseshoe Crab. Multifocally there are opaque pale tan proliferative lesions, and leaflets are friable (arrowheads).* *Photograph courtesy of Johns Hopkins University Department of Molecular and Comparative Pathobiology, Baltimore, Maryland.*

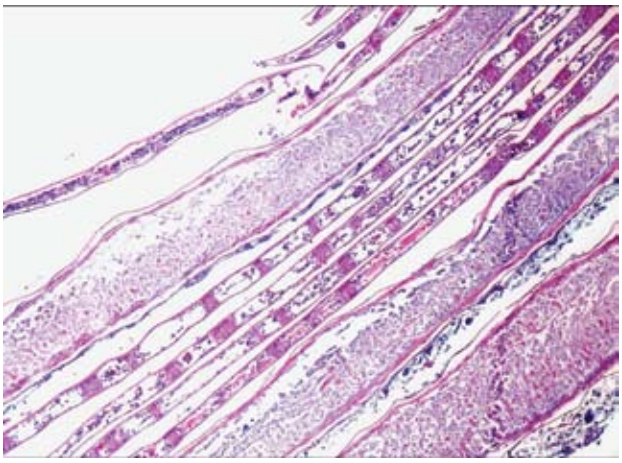

*3-3. Book gills, American Horseshoe Crab. Central vascular channels are disrupted and often expanded with necrotic debris and increased cellularity. HE 400X. Photograph courtesy of Johns Hopkins University Department of Molecular and Comparative Pathobiology, Baltimore, Maryland.*

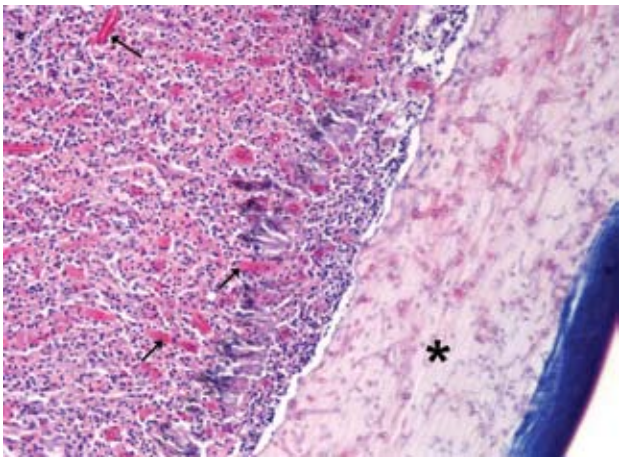

*3-4. Cuticle, American Horseshoe Crab. The cuticle (*) is thickened and penetrated by fungal hyphae. Some hyphae have invaded into the underlying parenchyma (arrows). HE 400X. Photograph courtesy of Johns Hopkins University Department of Molecular and Comparative Pathobiology, Baltimore, Maryland.*

**Gross Pathology:** The dorsal carapace (prosoma) had multifocal partial thickness pitting lesions with black and pale tan discoloration (**Fig. 3-1**). Book gill coverings had multifocal areas of black discoloration and several pale tan proliferative lesions along the caudal edges (**Fig. 3-2**). Individual book gill leaflets were very friable, tearing easily, and were opaque and pale tan (**Fig. 3-2**).

**Laboratory Results:** *Fusarium* sp. was isolated from the gill lesions, and it was speciated to *F. solani* using polymerase chain reaction (PCR).

**Histopathologic Description:** The cuticle of both the carapace and the book gill cover is multifocally thickened and the chitinous layers of the carapace are multifocally infiltrated and disrupted by fungal hyphae seen in longitudinal and cross section (**Fig. 3-4**). Fungal hyphae occasionally penetrate through the carapace into the underlying tissues (striated muscle and spongy parenchyma with prominent hemolymph channels). The affected tissues are hypereosinophilic (necrotic) with associated viable and degenerate amebocytes (hemolymph cells with eosinophilic cytoplasmic granules) (**Fig. 3-4**). Fungal hyphae are septate with mostly parallel appearing walls, and range from 4 to 7 um in diameter with occasional acute and right angle branching (**Fig. 3-5**). Some of the hyphae are poorly stained and appear swollen and non viable. The more viable forms stain with PAS and GMS fungal stains. Individual hyphae are sometimes seen on the outer surface of the cuticle and are pigmented brown (dematiaceous). Areas of disrupted cuticle have variably sized accumulations of basophilic granular material (bacteria, confirmed by Gram stain).

The cuticle of individual gill leaflets is multifocally thickened and penetrated by fungal hyphae. The central vascular channel of individual leaflets is expanded with hypereosinophilic and necrotic material, viable and degenerate amebocytes and bacteria (**Fig. 3-3**). There is necrotic debris mixed with bacteria between leaflets and sometimes pigmented fungal hyphae. Occasionally, there are some fungal hyphae on the surface of affected gill leaflets that are smaller (2-3 um diameter) than the invasive fungi.

Slides occasionally have metazoan parasites within the parenchyma and degenerate parasites associated with the surface of the carapace and/or gill leaflets.

**Contributor's Morphologic Diagnosis:** Carapace: Shell disease, acute and chronic, necrotizing, multifocal, severe, with intralesional fungal hyphae and bacteria
Gills: Branchitis, acute and chronic, necrotizing, multifocal, severe, with intralesional fungal hyphae and bacteria

**Contributor's Comment:** The American horseshoe crab is of extreme importance to the medical field because of the lysate extracted from amebocytes (hemolymph blood cell), which is used to test pharmaceuticals for bacterial endotoxin contamination (limulus amebocyte lysate assay). Despite the importance of the horseshoe crab,

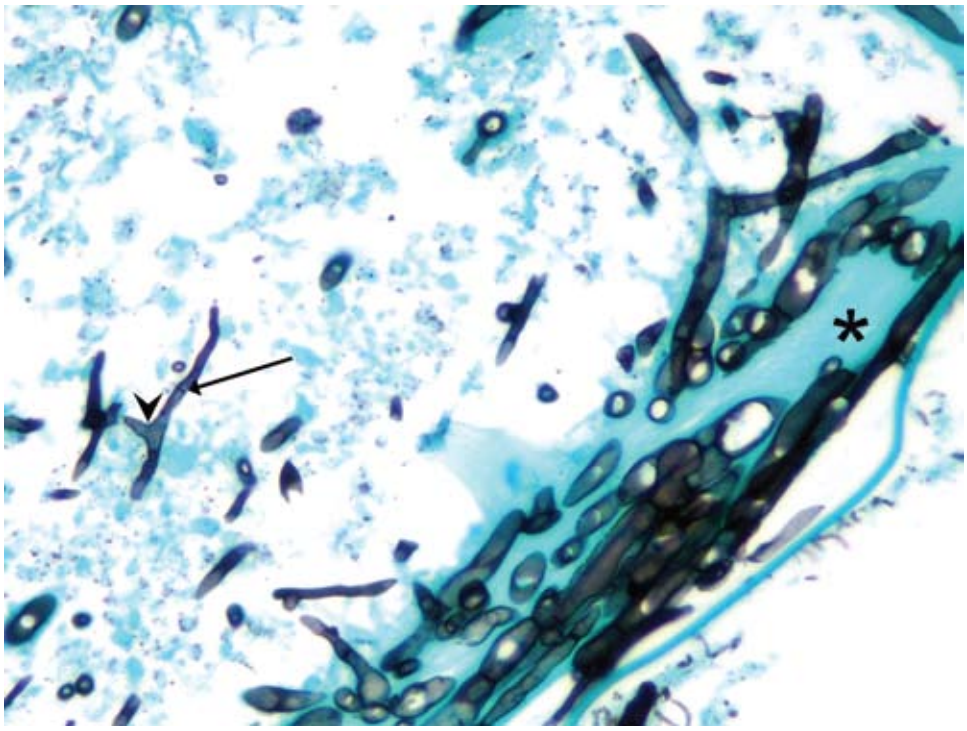

*3-5. Cuticle (*), American Horsehoe Crab. Fungal hyphae have septae (long arrow) and acute and right angle branching (arrow head). GMS 400X. Photograph courtesy of Johns Hopkins University Department of Molecular and Comparative Pathobiology, Baltimore, Maryland.*

there is a paucity of published information regarding its diseases. Infectious disease agents of horseshoe crabs include algae, fungi, cyanobacteria, Gram negative bacteria and many different parasites, with diseases of the shell being the most common manifestation.[8,9]

Mycotic shell disease has been reported only in captive horseshoe crabs. Specifically, mycotic infections of the carapace are reported in juvenile horseshoe crabs and most often in those housed without a sand substrate.[8,9] Gill and shell lesions similar to the ones seen in this crab are reported in a group of horseshoe crabs in a touch-tank at Ripley's Aquarium of the Smokies.[1] Single dose itraconazole therapy is well tolerated by horseshoe crabs, [1] but the efficacy of this treatment for the fungal lesions has not been investigated.

*Fusarium* species are saprophytes found ubiquitously within the environment and are the cause of diseases of both plants and animals including humans. *Fusarium* can cause disease in animals both by ingestion of mycotoxins and by fungal invasion of body tissues. Several examples of diseases caused by *Fusarium* infection in humans include keratitis, onychomycosis, dermatitis and disseminated disease.[3] Two recent reports of disease caused by *Fusarium* species reported in veterinary species include keratitis in a Holstein cow and intracranial fusariosis in a German shepherd dog.[4,5]

Invertebrate animals lack an adaptive immune system and respond to microbial antigens with a variety of innate immune responses including hemolymph coagulation, toll-like receptor mediated antimicrobial peptide production, melanin formation and lectin-mediated complement fixation. In horseshoe crabs, the hemolymph contains soluble antimicrobial proteins including C-reactive protein, alpha-2 microglobulins, lectins and hemocyanins. The granular amebocytes (also called hemocytes), which make up more than 99% of the circulating cells in the hemolymph, also contain antimicrobial proteins and coagulation proteins. Exposure to microbes causes degranulation of amebocytes and formation of a hemolymph clot. [6]

**AFIP Diagnosis:** 1. Carapace: Shell disease, necrotizing, acute and chronic, multifocal, severe, with fungal hyphae and bacteria
2. Gills: Branchitis, necrotizing, acute and chronic, multi-focal, severe, with fungal hyphae and bacteria

**Conference Comment:** Another Fusarium species of importance in veterinary medicine is *Fusarium moniliforme* because certain strains of this mold release the toxin fumonisin B1. Fumonisin B1 is a potent mycotoxin that induces hepatocellular carcinoma in rats and leukocencephalomalacia in horses. Pigs get pulmonary edema and hydrothorax from fumonisin B1 ingestion. This mycotoxin has also been shown to be hepatotoxic to pigs.[10]

Horses and pigs are exposed to this toxin when they eat corn infected with the mold *Fusarium moniliforme. Fusarium proliferatum* and *Fusarium verticilliodes* are also listed as producers of the mold fumonisin B1 in the newest edition of Jubb, Kennedy, and Palmer.[7]

Morphologically, the *Fusarium* sp. are identified by hyaline, septate hyphae measuring 4 to 7um in width with frequent, usually right angle branching. This is important in helping to distinguish these from *Aspergillus* sp*,* which tend to have dichotomous branching and are 3-5um in width.[2]

**Contributing Institution:** Department of Molecular and Comparative Pathobiology, Johns Hopkins University, School of Medicine, 733 N. Broadway, Baltimore, MD, 21205, *www.hopkinsmedicine.org/mcp*

**References:**

1. Allender MC, Schumacher J, Milam J, George R, Cox S, Martin-Jimenez T: Pharmacokinetics of intravascular itraconazole in the American horseshoe crab (*Limulus polyphemus*). J Vet Pharmacol Ther **31**:83-86, 2008
2. Chandler FW, Kaplan W, Ajello L: Color Atlas and Text of the Histopathology of Mycotic Diseases, pp. 76,79,101-102. Year Book Medical Publishers, Chicago, IL, 1980
3. Dignani MC, Anaissie E: Human fusariosis. Clin Microbiol Infect **10** (Suppl 1):67-75, 2004
4. Elligott CR, Wilkie DA, Kuonen VJ, Bras ID, Neihaus A: Primary Aspergillus and Fusarium keratitis in a Holstein cow. Vet Ophthalmol **9**:175-178, 2006
5. Evans J, Levesque D, de Lahunta A, Jensen HE: Intracranial fusariosis: a novel cause of fungal meningoencephalitis in a dog. Vet Pathol **41**:510-514, 2004
6. Iwanaga S, Lee BL: Recent advances in the innate immunity of invertebrate animals. J Biochem Mol Biol **38**:128-150, 2005
7. Maxie MG, Youssef S: *In:* Jubb, Kennedy and Palmer's Pathology of Domestic Animals, ed. Maxie MG, 5th ed., pp. 358-359. Elsevier Limited, Philadelphia, PA, 2007
8. Smith SA: Horseshoe Crabs. *In:* Invertebrate Medicine, ed. Lewbart GA, 1st ed., pp. 133-142. Blackwell Publishing, Ames, IA, 2006
9. Smith SA, Berkson J: Laboratory culture and maintenance of the horseshoe crab (*Limulus polyphemus*). Lab Animal **34**:27-34, 2005
10. Stalker MJ, Hayes MA: Liver and biliary system. *In:* Jubb, Kennedy and Palmer's Pathology of Domestic Animals, ed. Maxie MG, 5th ed., pp. 371-372. Elsevier Limited, Philadelphia, PA, 2007

## CASE IV – GF-D90-3 (AFIP 3102368)

**Signalment:** 6-month-old, female, *Cavia porcellus*, Hartley guinea pig

**History:** Experimental animal, infected via aerozolization with *Mycobacterium tuberculosis*. This animal was euthanized after being infected for 90 days.

**Gross Pathology:** The left mammary gland is markedly enlarged and exudes necrosuppurative material upon mild palpation. This affected region may incorporate and efface normal inguinal lymphoid architecture as this node is neither palpable nor observed. Approximately 30-40% of pulmonary parenchyma is replaced by primary tuberculoid lesions with the remaining lung parenchyma affected by secondary lesions. The primary lesions are depressed centrally and are surrounded by a dense fibrotic parenchyma. The mediastinal lymph nodes are diffusely enlarged with loss of lymphoid architecture and are further expanded by fibrinous adhesions which connect with the ventral aspect of the thoracic pleura. Multifocally, the spleen and the liver contain multifocal to coalescing granulomas and are markedly enlarged. The spleen is approximately 10x larger than normal.

**Laboratory Results:** Lung, viable cell count; approximately 9.8 X $10^6$

**Histopathologic Description:** Haired skin, subcutis, and mammary glandular tissue. The deep subcutaneous tissue is effaced by large coalescing nodules of epithelioid macrophages, admixed with heterophils, rare lymphocytes and multinucleated giant cells **(Fig. 4-1)**. Multifocally, these nodules contain central areas of necrosis characterized by degenerate heterophils, hypereosinophilic debris (necrosis), and karyorrhectic debris. In some sections, large areas of cavitation of these necrotic regions are observed. Admixed within this extensive inflammatory response are rare entrapped adipocytes and remnant mammary glands. There are no remaining ductules. Within the superficial subcutis, subjacent to the deep dermis, there are small granulomas comprised of macrophages and lymphocytes. There is superficial expansion of the epidermis by a moderate amount of orthokeratotic hyperkeratosis. An acid-fast stain revealed few positive bacilli within the necrotic centers.

**Contributor's Morphologic Diagnosis:** Mammary gland: Mastitis, necrosuppurative, granulomatous, regionally extensive, with intralesional acid- fast bacilli

**Contributor's Comment:** The guinea pig is used

extensively as an animal model of human tuberculosis.[5] The primary lesion complex in both humans and guinea pigs are similar and comprises multifocal granulomatous inflammatory lesions within the lung and draining lymph nodes. Similar to humans, guinea pigs develop small foci of mixed inflammation which subsequently develops into the characteristic granuloma which is comprised predominantly of macrophages and occasionally granulocytes.[8] As seen in this case, these large granulomas develop a central zone of necrosis, which is where the highest concentrations of bacterium can be observed in both humans and in guinea pigs.[1]

The guinea pig in this case was experimentally infected via aerosolization with *Mycobacterium tuberculosis* to evaluate pulmonary tuberculosis. Diagnosis of tuberculosis in the mammary gland was an incidental finding. To the contributor's knowledge, tuberculosis mastitis has never been reported in an experimentally infected guinea pig. In human patients, involvement of the mammary gland is a rare manifestation of the disease.[2] Clinically, tuberculoid granulomas of the mammary gland are unilateral and may mimic breast cancer and/or breast abscesses which are all managed differently making accurate diagnosis crucial.[3,9] The reliable diagnostic tests include bacteriologic culture, histopathology, and guinea pig inoculation.[6]

Tuberculosis mastitis (TM) in humans can occur as primary or secondary disease. Secondary involvement of the mammary gland is more common than primary infection of the mammary gland.[6] Common routes of infection include the lymphatic route, hematogenous route or from direct spread from local organs. The direct form of spread in humans may occur from an infected rib, cartilage, or joint.[6]

In humans, there are three forms of mammary tuberculosis: nodular, diffuse, and sclerosing. The nodular form is the most common presentation in women and is typically slow growing and often develops a caseating center.[7] The sclerosing form develops excess fibrous connective tissue and is often the most difficult to differentiate from mammary gland carcinoma.[7]

**AFIP Diagnosis:** Mammary gland: Mastitis, pyogranulomatous, focally extensive, severe with acid-fast bacilli

**Conference Comment:** Mycobacteria are non-motile, non-spore forming organisms with a lipid-rich cell wall that stains poorly with gram-stain. Acid-fast stains are commonly used to identify mycobacteria in tissue sections. The term "tuberculosis" is now conventionally used to describe only infections caused by *Mycobacterium bovis* and *Mycobacterium tuberculosis*, whereas diseases caused by other mycobacterial species are referred to as mycobacteriosis or atypical mycobacteriosis.[4]

Susceptibility to tuberculosis and organ system affected varies greatly among domesticated animal species. The hallmark lesion of tuberculosis is the granuloma. These granulomas may be in different organs with slightly different histologic appearances based on the route of entry and species affected. Below is a brief list of animal species, susceptibility, and organ systems affected by tuberculosis.

| Species | Susceptibility | Organ System Affected |
|---|---|---|
| Cat | More susceptible to *M. bovis* | Gastrointestinal disease – ingestion of contaminated wildlife or milk |
| Dog | Susceptible to *M. bovis* and *M. tuberculosis* | Respiratory form |
| Cattle | More susceptible to *M. bovis* | Respiratory and gastrointestinal forms – calcification can also occur |
| Pigs | Susceptible to both *M. bovis* and *M. tuberculosis* | Systemic infection |
| Small ruminants | Rare cases | Similar to cattle when infected |
| Horses | Rare; usually *M. bovis* | Gastrointestinal; also see lesions in retropharyngeal and mesenteric lymph nodes |
| Non-Human Primates | Very susceptible to *M. tuberculosis* | Infected humans transmit respiratory form to NHP's |
| Birds (Psittacines) | Only birds to get tuberculosis; get both *M. tuberculosis* and *M. bovis* | Respiratory form - transmitted from humans |

(4)

**Contributing Institution:** 1619 Campus Delivery, Colorado State University, Microbiology, Immunology, and Pathology, Fort Collins, CO 80523-1619; http://www.cvmbs.colostate.edu/

**References:**

1. Basaraba RJ, Bielefeldt-Ohmann H, Eschelback EK, Reisenauer C, Tolnay AE, Taraba LC, Shanley CA, Smith EA, Bedwell CL, Chlipala EA, Orme IM: Increased expression of host iron-binding proteins precedes iron accumulation and calcification of primary lung lesions in experimental tuberculosis in the guinea pig. Tuberculosis **88**:69-79, 2008

2. Bani- Hani KE, Yaghan RJ, Matalka II, Mazahreh TS: Tuberculous mastitis: a disease not to be forgotten.

International Journal of Tuberculosis Lung Disease **9**(8):920-925, 2005
3. Bedi US, Bedi RS: Bilateral breast tuberculosis. The Indian Journal of Tuberculosis 215-217, 2001
4. Caswell JK, Williams KJ: Respiratory system. *In:* Jubb, Kennedy and Palmer's Pathology of Domestic Animals, ed. Maxie MG, 5th ed., pp. 606-610. Elsevier Limited, Philadelphia, PA, 2007
5. Gupta UD, Katoch VM: Animal models of tuberculosis. Tuberculosis **85**:277-293, 2005
6. Hale JA, Peters GN, Cheek JH: Tuberculosis of the breast: rare but still extant. The American Journal of Surgery 150:620-624
7. Hamit HF, Ragsdale TH: Mammary tuberculosis. Journal of the Royal Society of Medicine **75**:764-765, 1982
8. McMurray DN: Guinea pig model of tuberculosis. *In:* Tuberculosis: Pathogenesis, Prevention, and Control, ed. Broom BR, pp. 135-147. ASM Press. Washington, DC, 1994
9. Mufide AN, Saglam L, Polat P, Erdogan F, Albayrak Y, Povoski SP: Mammary tuberculosis—importance of recognition and differentiation from that of a breast malignancy: report of three cases and review of the literature. World Journal of Surgical Oncology [5]:67-73, 2007

**NOTES:**

The Armed Forces Institute of Pathology
Department of Veterinary Pathology

*Conference Coordinator:*
Todd M. Bell, DVM

WEDNESDAY SLIDE CONFERENCE 2008-2009

# Conference 11

10 December 2008

*Conference Moderator:*

Tom Steinbach, DVM, Diplomate ACVP

## CASE I – Cat 3 (AFIP 3106179)

**Signalment:** 18-year-old, spayed female domestic short hair cat (*Felis catus*)

**History:** This cat initially presented for abnormal gait, difficulty climbing stairs, and inappropriate urination for at least a month. The owner also reported an increase in water intake. Physical examination revealed a thin cat with unkempt hair coat, plantar stance, and a gallop heart rhythm. Additionally, abdominal masses were palpated. Fasting clinical chemistry, hematology and urinalysis samples were obtained and analyzed. The erythron was within normal limits, lymphocyte count was mildly low, and there was a mild azotemia. Electrolyte abnormalities included mildly low potassium and minimally increased calcium. Serum glucose was 360 mg/dl (Normal 64-170). Serum T4 and cortisol concentrations were within normal limits. Urinalysis showed trace protein, moderate glucosuria and bacteria, and large numbers of amorphous crystals with a specific gravity of 1.019. Insulin therapy and treatment for the urinary tract infection were initiated.

**Ultrasound findings:** Several days after initial presentation, abdominal ultrasonographic evaluation was performed to investigate the abdominal masses. A mass in the location of the left adrenal measured 4.3 by 3.6 cm and a renal cortical mass measuring 3.2 by 2.6 cm were identified within and extending laterally from the right kidney. Due to poor prognosis and response to insulin therapy the animal was euthanized.

**Gross Pathology:** Abundant adipose tissue was present within the abdominal cavity. The right adrenal was not located; however, the left adrenal was markedly enlarged, multilobulated and pale yellow. The mass expanding from the right renal cortex measured approximately 3 x 3 x 2 cm and was multilobulated, pale pink and firm with several large vessels coursing over the surface. On cut section this discrete mass extended from the cortex and had numerous 1-2 mm diameter cysts containing clear fluid.

**Histopathologic Description:** Expanding from and within the cortex, adjacent to the corticomedullary junction of the right kidney, was a moderately cellular, multilobulated mass. Lobules were often defined by bands of mature collagen. Numerous tubular structures lined by a single layer of cuboidal cells were supported by moderate amounts of loose collagenous stroma within the lobules **(Fig. 1-1)**. The tubular lumena often contained a homogeneous eosinophilic material (proteinaceous

*Sponsored by the American Veterinary Medical Association, the American College of Veterinary Pathologists, and the C. L. Davis Foundation.

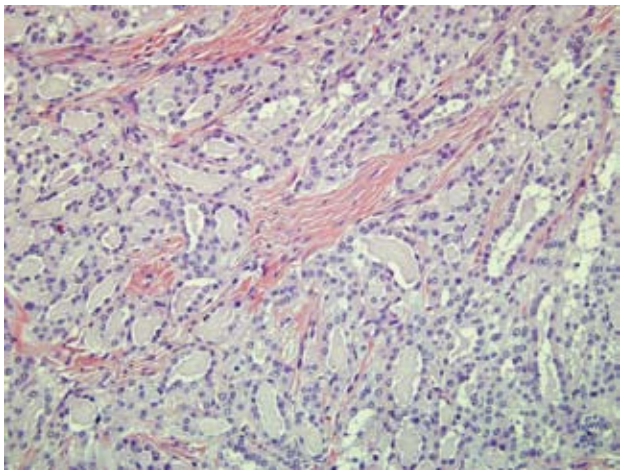

*1-1. Kidney, cat. Renal adenocarcinoma. Neoplastic cells form well defined tubules, have distinct cell borders, moderate amounts of lightly eosinophilic cytoplasm with oval nuclei, finely stippled chromatin. HE 400X.*

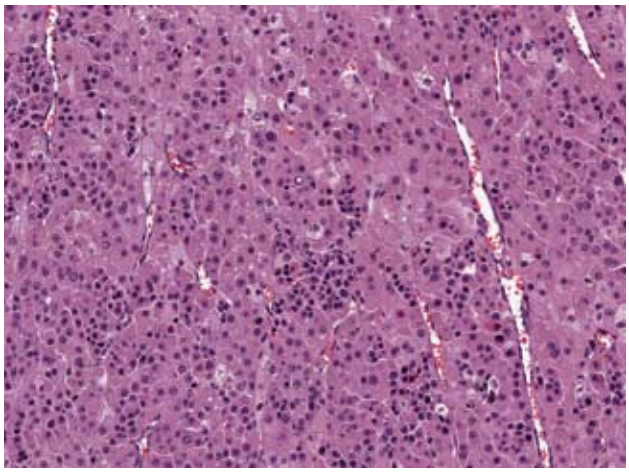

*1-2. Adrenal gland, cat. Adrenal cortical adenoma composed of nests and packets of polygonal cells with distinct cell borders, abundant eosinophilic granular cytoplasm, oval nuclei with finely stippled chromatin and variably distinct nucleoli. Photomicrograph courtesy of Eli Lilly and Company Lilly Research Laboratories P.O. Box 70 Greenfield, IN 46140*

fluid), and were dilated in several regions within the mass to several millimeters in diameter. The cuboidal cells lining the tubules were small to medium sized with slight anisocytosis and anisokaryosis with occasional crowding. Nuclei were round with finely stippled chromatin and a single medium-sized nucleolus. Mitotic figures rarely occurred and multinucleation was not noted. In several areas small extensions of neoplastic tubules pushed through the expansion capsule partially surrounding the mass. Rare, small foci of neutrophils were present within the supporting stroma and/or tubules. In the surrounding renal tissue, glomeruli had one or more of the following changes: moderately thickened basement membranes, senechia, thickened Bowman's capsule, and/or diffuse or nodular glomerulosclerosis characterized by hyaline thickening of capillary basement membranes and sclerosis of lobules within tufts and diffuse thickening of mesangium. Tubules also had thickened basement membranes and occasionally were dilated containing proteinaceous fluid. Multifocally the interstitium was expanded by accumulations of lymphocytes and plasma cells that were usually perivascularly oriented around medium-sized vessels. The interstitium throughout the section from papilla to capsule was diffusely expanded by increased amounts of mature collagenous stroma.

**Contributor's Morphologic Diagnosis:**

1. Severe, chronic, diffuse, membranous glomerulonephritis with glomerular sclerosis
2. Moderate, chronic, multifocal lymphoplasmacytic interstitial nephritis and pyelitis
3. Renal tubular carcinoma
4. Adrenocortical carcinoma (tissue not included)
5. Pancreatic islet amyloidosis (tissue not included)

**Contributor's Comment:** The submitted renal mass was an incidental finding and unrelated to the clinical condition. Renal carcinomas are uncommon in domestic species with an incidence of up to 0.5 percent in cats although there are reports of lower incidences. Most commonly, renal carcinomas are unilateral, and there does not appear to be a sex or breed predilection. Although the morphology of the cells in the renal mass was relatively benign, the size of the mass and presence of lobules of neoplastic cells invading into vessels warrants a diagnosis of carcinoma rather than adenoma.[6,8]

Clinical diagnosis of diabetes mellitus in this animal was complicated by the presence of a well differentiated adrenal tumor **(Fig. 1-2)**. This multilobulated adrenal tumor was densely cellular and composed of large polyhedral cells with abundant finely granular or vacuolated eosinophilic cytoplasm. Nuclei had finely granular chromatin and a single prominent nucleolus. These cells formed irregular trabeculae and nests supported by fine fibrovascular stroma. Mitotic figures were rare and the cells showed moderate anisocytosis and anisokaryosis. Binucleation was common. Multifocally there were areas of necrosis, and single necrotic cells were scattered throughout the mass. The size and histological features of this mass is

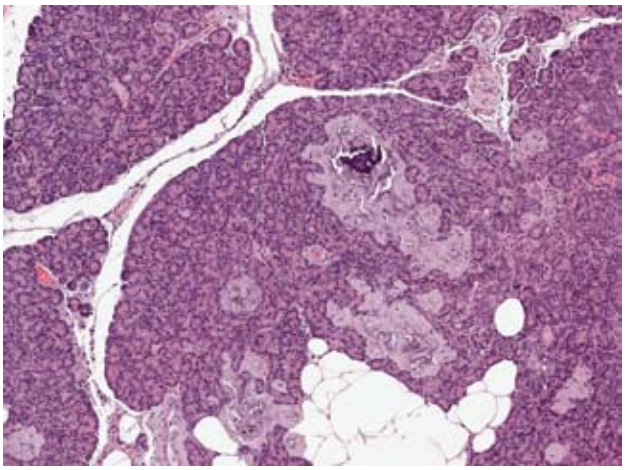

*1-3. Pancreas, cat. Ppancreatic islets are expanded by eosinophilic, homogenous, acellular, waxy material (amyloid). Photomicrograph courtesy of Eli Lilly and Company Lilly Research Laboratories P.O. Box 70 Greenfield, IN 46140*

consistent with a diagnosis of carcinoma.[3] Functional adrenocortical tumors in cats may produce cortisol, progesterone, aldosterone, or estradiol/testosterone. Most cats with hyperadrenocorticism, hyperaldosteronism or hyperprogesteronism are also hyperglycemic.[1,5,10] Unfortunately, many clinical signs for these endocrinopathies are vague and not useful in distinguishing between them. In this case, however, hyperaldosteronism is unlikely due to the mild hypokalemia which is more consistent with hypokalemia associated with an untreated diabetic state. The absence of cutaneous changes (alopecia, dermal fragility) [7] commonly reported in cats with cortisol and progesterone secreting tumors suggests that the mass was also not producing either of these hormones. Additionally, basal cortisol concentrations were within normal limits. Although not associated with hyperglycemia, a report of excessive production of sex steroids in cats increased aggression, thickened skin and vulval hyperplasia, [2] none of which were noted in this animal. Unfortunately due to the euthanasia of this animal prior to complete clinical evaluation, the contribution of the adrenal mass to the clinical condition is unknown.

In the submitted case, pancreatic islet amyloidosis, a characteristic lesion of feline diabetes and Type 2 diabetes in humans [4,9] and in combination with hyperglycemia, strongly supported diabetes mellitus. This finding was characterized by replacement of islet cells throughout the pancreas by an amorphous, pale eosinophilic material consistent with amyloid **(Fig. 1-3)**. The changes described above in the renal tissue surrounding the mass and urinalysis are also findings commonly identified in cases of chronic diabetes mellitus, including an ascending bacterial pyelitis.[4]

**AFIP Diagnosis:**

1. Kidney: Renal adenocarcinoma
2. Kidney: Nephritis, interstitial, lymphoplasmacytic, chronic, multifocal, moderate with fibrosis and pyelitis
3. Kidney, glomeruli: Glomerulonephritis, membranous, global, multifocal, moderate with tubular proteinosis

**Conference Comment:** There was extensive discussion in the post-conference session regarding the diagnosis of benign versus malignant renal tumor and acknowledgement that diagnosis may be difficult in some cases. As the contributor mentioned, renal tumors are fairly uncommon in cats, and they have not been extensively studied with a subsequent paucity of published literature. This case was reviewed by the AFIP Department of Genitourinary Pathology, and they agreed with the diagnosis of renal cell carcinoma.

Renal adenomas are rare tumors in domestic animals and are usually an incidental finding at necropsy. Grossly, adenomas are well circumscribed, individual tumors normally located in the cortex of the kidney.[8] Multiple adenomas can occur in dogs and cows. In German shepherds with dermatofibrosis, multiple renal adenomas may be found as well as renal adenocarcinoma.[8] There are three distinct histologic patterns of renal adenomas: papillary, tubular, or solid.[8]

Renal carcinomas are an uncommon tumor encountered in veterinary medicine, and by the time these tumors manifest clinically in dogs, cats, and horses, they have usually metastasized. Most renal carcinomas are unilateral and often times are located at the pole of the kidney.[8] These tumors historically have been reported to be larger than 2 cm in diameter.[8] Carcinomas have been classified in the histologic subtypes mentioned previously, but the histologic subtype appears to have no bearing on tumor behavior.[8]

**Contributing Institution:** Eli Lilly and Company, Greenfield, IN

**References:**

1. Ash RA, Harvey AM, Tasker S: Primary hyperaldosteronism in the cat: a series of 13 cases. J Fel Med Surg **7**:173-182, 2005

2. Boag AK, Nieger R, Curch DB: Trilostane treatment of bilateral adrenal enlargement and excess sex steroid

hormone production in a cat. J Small Anim Pract **45**:263-266, 2004
3. Capen CC: Tumors of the endocrine glands. *In:* Tumors in Domestic Animals, ed. Meuten DJ, 4th ed., pp. 607-696. Iowa State Press, Ames, Iowa, 2002
4. Charles JA: Pancreas. *In:* Jubb, Kennedy and Palmer's Pathology of Domestic Animals, ed. Maxie MR, 5th ed. vol. 2, pp. 389-424. Elsevier Saunders, Philadelphia, Pennsylvania, 2007
5. Gunn-Moore D: Feline endocrinopathies. Vet Clin Small Anim **35**:171-210, 2005
6. Henry CJ, et al: Primary renal tumors in cats: 19 cases (1992-1998). J Fel Med Surg **1**:165-170, 1999
7. Hoenig M: Feline hyperadrenocorticism – where are we now? J Fel Med Surg **4**:171-174, 2002
8. Meuten DJ: Tumors of the urinary system. *In:* Tumors in Domestic Animals, ed Meuten DJ, 4th ed., pp. 509-546 Iowa State Press, Ames, Iowa
9. O'Brien TD: Pathogenesis of feline diabetes mellitus. Mol and Cell Endoc **197**:213-219, 2002
10. Rossmeisl JH, Scott-Moncrieff JKR, Siems J, Snyder PW, Wells A, Anothayanontha L, Oliver JW: Hyperadrenocorticism and hyperprogesteronemia in a cat with an adrenocortical adenocarcinoma. J Am Anim Hosp Assoc **36**:512-517, 2000

## CASE II – YN06-328 (AFIP 3109441)

**Signalment:** 3-year-old, female, rhesus macaque, (*Macaca mulatta*)

**History:** This animal was born at the Yerkes National Primate Research Center in June 2003. The animal had two incidents of trauma to the hands and feet that resulted in amputation of digits between December 2003 and March 2004. The digit wounds from both episodes healed after routine surgery and treatment with antibiotics and anti-inflammatory drugs, and the animal was returned to her social group. Swelling of both hands, due to subcutaneous deposition of a white material, was reported in March 2006, and the animal was suspected to have calcinosis. The calcified material was debulked surgically and the animal replaced in her group. In October 2006, the white chalky material had returned and the swelling had progressed. Serum ionized calcium level was within normal limits at 1.35 in October 2006. Due to the severity of the condition affecting both hands the animal was humanely sacrificed.

**Gross Pathology:** The animal weighed 5.3 kilograms at necropsy. Digits from both the hands and feet had been previously amputated and were replaced by multiple, blunt, subcutaneous nodules. On sectioning, these foci contained subcutaneous deposition of a white gritty material. Occasionally, liquefied white material exuded from these nodules.

**Laboratory Results:** Normal phosphate, calcium and serum ionized calcium levels. No significant pathogen isolated from the skin lesions.

**Histopathologic Description:** The deep dermis and subcutis are expanded by extensive multifocal deposition of a basophilic granular material (mineral) which often disrupts and replaces the normal dermal architecture (**Fig. 2-1**). The mineral is surrounded by dense aggregates of multinucleate giant cells and macrophages which are occasionally further surrounded by mature fibrous connective tissue. Rare aggregates of degenerate and viable neutrophils are also observed in the dermis. Von Kossa stain revealed localized deposits of calcium salts in the skin and subcutis. Special stains for bacteria and fungi were negative for any infectious agent in these lesions.

**Contributor's Morphologic Diagnosis:** Skin, Calcinosis cutis circumscripta

**Contributor's Comment:** Calcinosis cutis is a rare disorder characterized by deposition of hydroxyapatite crystals or amorphous calcium phosphate in the skin. Depending on the pathophysiologic mechanism, calcinosis can be classified as dystrophic, metastatic or idiopathic.[6] Dystrophic calcinosis is characterized by normal calcium and phosphate serum levels in the presence of tissue damage. The internal organs are not affected. Metastatic calcification occurs in undamaged tissues and is associated with elevated serum phosphate or calcium levels or both.[1] Renal failure, paraneoplastic hypercalcemia, hypervitaminosis D and hyperparathyroidism may develop metastatic deposits of calcium in organs like lung, stomach, kidney, and vasculature.[4] Idiopathic calcification occurs in the absence of evident tissue or metabolic abnormalities.[6]

Dystrophic calcification occurs because of local tissue injuries or abnormalities like alterations in collagen, elastin, or subcutaneous fat, which may precipitate calcification even with normal serum levels of calcium and phosphate.[3] Dystrophic calcification has been divided into calcinosis cutis universalis, which has widespread deposits of calcium, and calcinosis cutis circumscripta, which has only a few localized deposits.[6] Apocrine gland

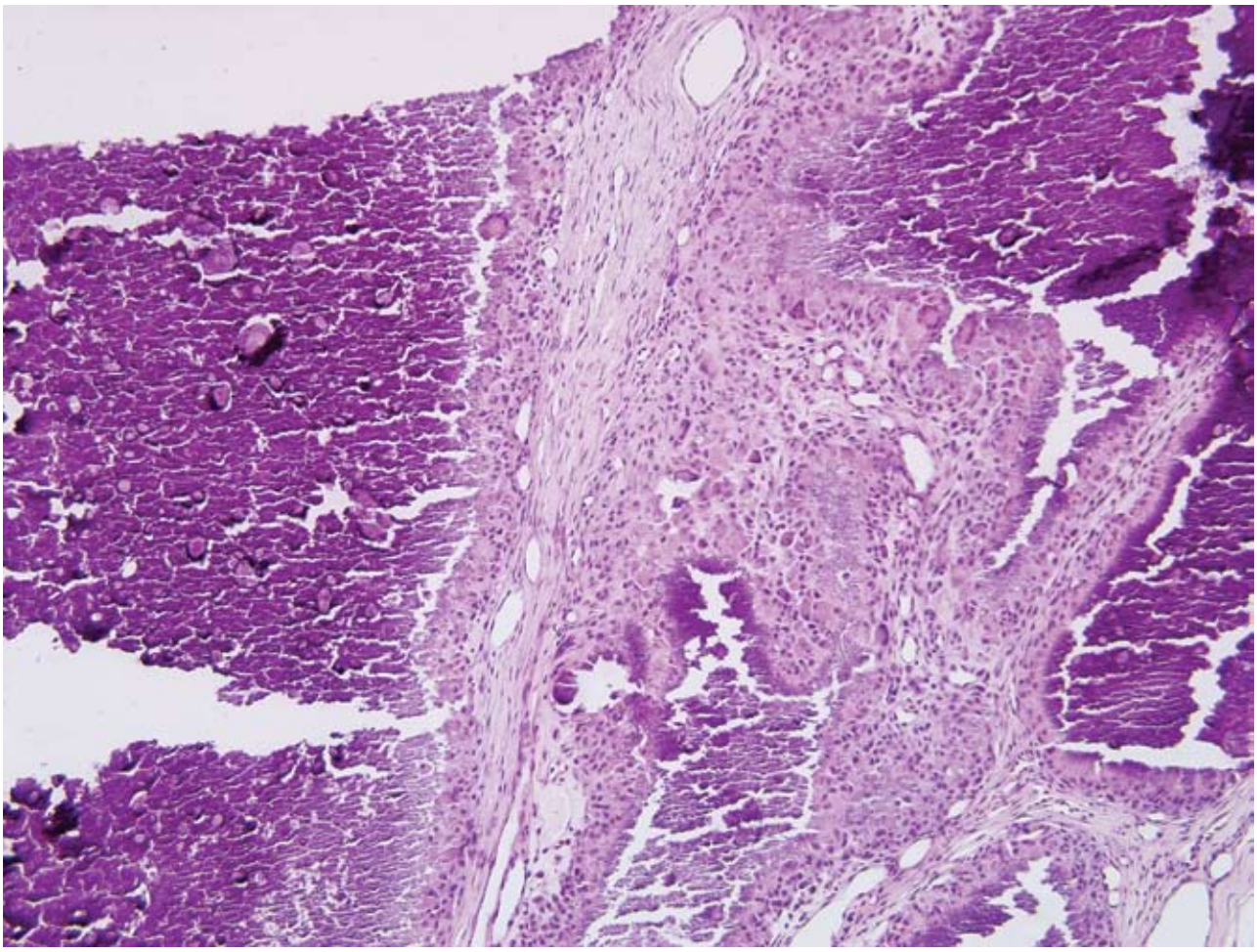

*2-1. Dermis, macaque. Calcinosis circumscripta. Multiple variably sized nodules composed of a central core of basophilic granular material surrounded by epithelioid macrophages, fewer multinucleated giant cells, and fibrosis. HE 200X.*

cysts, follicular cysts and skin tumors have been associated with calcinosis cutis circumscripta. Hyperadrenocorticism and diabetes mellitus have been associated with calcinosis cutis universalis.[7]

The gross and histological appearance of the calcified masses in the hands and feet in this case were compatible with a diagnosis of dystrophic mineralization, specifically calcinosis cutis circumscripta. Events potentially leading to these lesions in this macaque included the trauma to digits in hands and feet. Metastatic calcinosis was excluded from the diagnosis due to the presence of normal phosphate, calcium and serum ionized calcium levels. No evidence of mineralization in multiple organs was found on radiographs, grossly at necropsy or histologically. A retrospective analysis done at the Yerkes Primate Center showed 11 cases of calcinosis cutis. Previous trauma was reported at the calcinosis site in digits, tails and in the inguinal area of these animals. In literature, calcinosis cutis circumscripta has been reported in four rhesus macaques without any history of trauma and in a marmoset with a history of trauma.[5]

**AFIP Diagnosis:** Haired skin: Granulomas, calcareous, multifocal to coalescing (calcinosis circumscripta)

**Conference Comment:** The different types of calcification and the pathogenesis of these lesions were discussed. Pathologic calcification occurs when calcium salts and small amounts of other trace mineral salts form within tissues. In dystrophic mineralization, such as in this monkey, the end result is the formation of crystal phosphate mineral apatite. There are two phases to the mineralization process dubbed initiation and propagation, and both can occur inside and outside the cell. Dystrophic mineralization can either be a signpost for an area of previous disease or it may cause significant organ dysfunction as seen in valvular disease secondary to

calcification.[2]

Hypercalcemia can worsen a nidus of dystrophic calcification. In domestic species there are numerous causes of hypercalcemia. The mnemonic "HARD IONS" may be useful to remember some common causes of hypercalcemia in domestic animals. This is by no means an all inclusive list.

| | |
|---|---|
| H | Hyperparathyroidism |
| A | Addison's (Hypoadrenocorticism), Acidosis |
| R | Renal failure (horses and familial renal disease in Lhasa Apso's) |
| D | Vitamin D toxicity (rodenticides, hypervitaminosis D, and vitamin D glycoside-containing plants) |
| I | Immobilization |
| O | Osteolytic lesions |
| N | Neoplasia (Apocrine gland tumors, carcinomas in bone, lymphoma, multiple myeloma) |
| S | Spurious (granulomatous disease, hyperproteinemia, and hemoconcentration) |

[1]

**Contributing Institution:** http://www.yerkes.emory.edu/

**References:**

1. Ferguson DC, Hoenig M: Endocrine system. *In:* Duncan & Prasse's Veterinary Laboratory Medicine, Clinical Pathology, 4th ed., pp. 270-303. Blackwell Publishing, Ames, IA, 2003
2. Kumar V, Abbas AK, Fausto N: Robbins and Cotran Pathologic Basis of Disease, 7th ed., pp 40-42. Elsevier Saunders, Philadelphia, PA 2005
3. Larralde M, Giachetti A, Cáceres MR, Rodríguez M, Casas J: Calcinosis cutis following trauma. Pediatric Dermatology **22**:227–229, 2005
4. Poesen N, Heidbüchel M, Van der Oord JJ, Morren M: Chronic renal failure and skin calcifications. Dermatology **190**:321–323, 1995
5. Wachtman LM, Pistorio AL, Eliades S, Mankowski JL: Calcinosis circumscripta in a common marmoset (*Callithrix jacchus jacchus*). JAALAS **45**:54-57, 2006
6. Walsh JS, Fairely JA: Cutaneous mineralization and ossification. *In:* Dermatology in General Medicine, eds. Eisen AZ, Wolf K, Freedberg IM, Austen KF, 6th ed., pp. 1490–1496. McGraw-Hill, New York, 2003
7. Wilkinson AC, Harris LD, Saviolakis GA, Martin DG: Cushing's syndrome with concurrent diabetes mellitus in a rhesus monkey. Contemporary Topics in Laboratory Animal Science **38**:62-66, 1999

## CASE III – S0709546 (AFIP 3109545

**Signalment:** 3-month-old, female Saanen goat

**History:** A 3-month-old, unvaccinated Saanen goat was anaesthetized for the purpose of performing a laparotomy to inject 100 mls of a 20% solution of cornstarch into the abomasum, followed by inoculation of the duodenum with a 200 ml culture of Clostridium perfringens type D (approximately 1 x $10^8$ CFU per ml). The animal recovered completely from anaesthesia within 30 minutes after surgery, developed hemorrhagic diarrhea 8 hours post-inoculation, and was euthanized 12 hours later. Necropsy was performed immediately.

**Gross Pathology:** The wall of the colon was thickened with mild serosal and mesocolonic edema. The colon contained red fluid and the diffusely red colonic mucosa was lined by strands of tan fibrinous exudates **(Figs. 3-1, 3-2)**. Other findings included dilatation and mucosal congestion of the small intestine, and cerebellar coning (herniation of posterior cerebellum into foramen magnum).

**Laboratory Results:** None

**Histopathologic Description:** Multifocal to diffuse necrosis of superficial to mid-mucosa is accompanied by formation of a diphtheritic membrane composed of fibrin, mucus, exfoliated epithelial debris, neutrophils, erythrocytes and abundant bacteria (predominantly large bacilli) on the luminal surface of the necrotic mucosa. Clumps of similar fibrinocellular exudate and bacteria also lie free within the lumen. Crypts underlying the necrotic, eroded surface epithelium are distended with catarrhal exudate and lined by necrotic to attenuated epithelium; and associated lamina propria is markedly congested, hemorrhagic and infiltrated by numerous neutrophils. Deep crypts are frequently mildly distended with mucus or catarrhal exudate, and the deep lamina propria and muscularis mucosae are populated by occasional clusters of neutrophils. Scattered lymphatic vessels within the submucosa, tunica muscularis and serosa/mesocolon are distended with proteinaceous fluid. The submucosa is irregularly, mildly/moderately expanded by proteinaceous effusion, infiltrated by small numbers of neutrophils, and populated by scattered clusters of lymphoid cells, and the serosa is mildly, irregularly edematous.

**Contributor's Morphologic Diagnosis:** Multifocal to diffuse, moderate/severe, pseudomembranous (fibrino-necrotic) colitis, etiology subacute, caprine *Clostridium perfringens* type D enterotoxemia

*3-1. Colon, goat. Diffusely, there is thickening of the mucosa, hemorrhage, edema, necrosis and adherent to and overlying the mucosa a tan-yellow fibrinonecrotic membrane.* *Photograph courtesy of California Animal Health and Food Safety Laboratory, University of California, Davis.*

**Contributor's Comment:** Enterotoxemia caused by *Clostridium perfringens* type D occurs in several animal species but has been studied most thoroughly in sheep. The pathogenesis of *C. perfringens* type D enterotoxemia in sheep and goats is mostly mediated by epsilon toxin. (2,3)

In sheep, type D enterotoxemia mostly occurs following a sudden change of diet, particularly to feeds rich in fermentable carbohydrates (resulting in large amounts of undigested carbohydrates entering the small intestine). Ovine type D enterotoxemia produces acute to chronic neurologic disease (ranging from sudden death to blindness, opisthotonus, bleating, convulsions and recumbency with paddling) frequently accompanied by respiratory signs and uncommonly accompanied by diarrhea.[3] The

*3-2. Colon, goat. Diffusely there is marked mesocolonic edema and there is thickening of the mucosa, hemorrhage, edema, necrosis and adherent to and overlying the mucosa a tan-yellow fibrinonecrotic membrane.* *Photograph courtesy of California Animal Health and Food Safety Laboratory, University of California, Davis.*

neurologic signs are caused by cerebral perivascular proteinaceous edema (observed in 90% of cases), and in chronic cases multifocal, bilaterally symmetrical necrosis of white matter. The respiratory signs are caused by pulmonary edema. There are usually no significant gross or microscopic changes in the intestinal tract of sheep dying from enterotoxemia.[2,3]

Less is known about predisposing factors of caprine type D enterotoxemia. Cases of type D enterotoxemia have occurred in goats on a regular hay diet.[3] In goats with type D enterotoxemia, the most consistent clinical signs are diarrhea, respiratory distress and central nervous system (CNS) signs including recumbency, paddling, bleating and convulsions. Pseudomembranous colitis, similar to that observed in this goat, is the most characteristic postmortem change in caprine enterotoxemia. Histological changes in the brain are not a consistent feature of caprine type D enterotoxemia; however, cerebral vasogenic edema can be observed in some cases of subacute type D enterotoxemia such as this. Accompanying small intestinal lesions are uncommon in goats and were not observed in this case. Cerebellar coning in this goat was considered to be a consequence of cerebral vasogenic edema.[2,3]

In summary, the major difference between type D enterotoxemia in sheep and goats is the response of the intestinal tract to the disease. The reason for the caprine-specific, selective damage to the large intestine has not been determined. It is possible the caprine small intestine is simply more resistant than the large bowel to the effects of the epsilon toxin (or possibly other *C. perfringens* type D toxins). Antibiotic-associated pseudomembranous colitis in humans, caused by *Clostridium difficile*, has a similar disease pattern; however, the reason for the lesion distribution has not been identified.[2] It is also possible that the small intestinal mucosa of sheep is more susceptible to damage by epsilon toxin through facilitating absorption of the toxin into the bloodstream with more pronounced systemic effects (CNS lesions). It has also been suggested that the selective damage of the large bowel in goats is a consequence of toxin modification by enzymes in the goat colon. However *C. perfringens* epsilon toxin, produced as an inactive prototoxin, is activated following cleavage by trypsin. Because trypsin is secreted in the small intestine, epsilon toxin should be activated in the small intestine of both sheep and goats.[2] Transit speed of the intestinal content should not be a factor with regard to the different disease pattern of type D enterotoxemia in sheep and goats because of the similar transit time in both ruminants (normally approximately three hours for small intestine, and 18 hours for large bowel).[2]

**AFIP Diagnosis:** Colon: Colitis, fibrinonecrotic, multifocal to coalescing, marked, with hemorrhage and superficial cocci and bacilli **(Fig. 3-3)**

**Conference Comment:** *Clostridium perfringens* type D, also known in the veterinary literature as "overeating disease", or "pulpy kidney disease", is an agriculturally important disease of ruminants. Unfortunately, this disease often affects the hardiest animals on the farm and is caused by excessive intake of starch. The two major types of toxins produced by *C. perfringens* type D include alpha and epsilon, with epsilon being the major contributor to disease.[1] In sheep, epsilon toxin binds to endothelial cells (especially in the brain) leading to focal symmetrical encephalomalacia (FSE). Grossly, lesions often appear in the basal ganglia, thalamus, or substantia nigra. Within

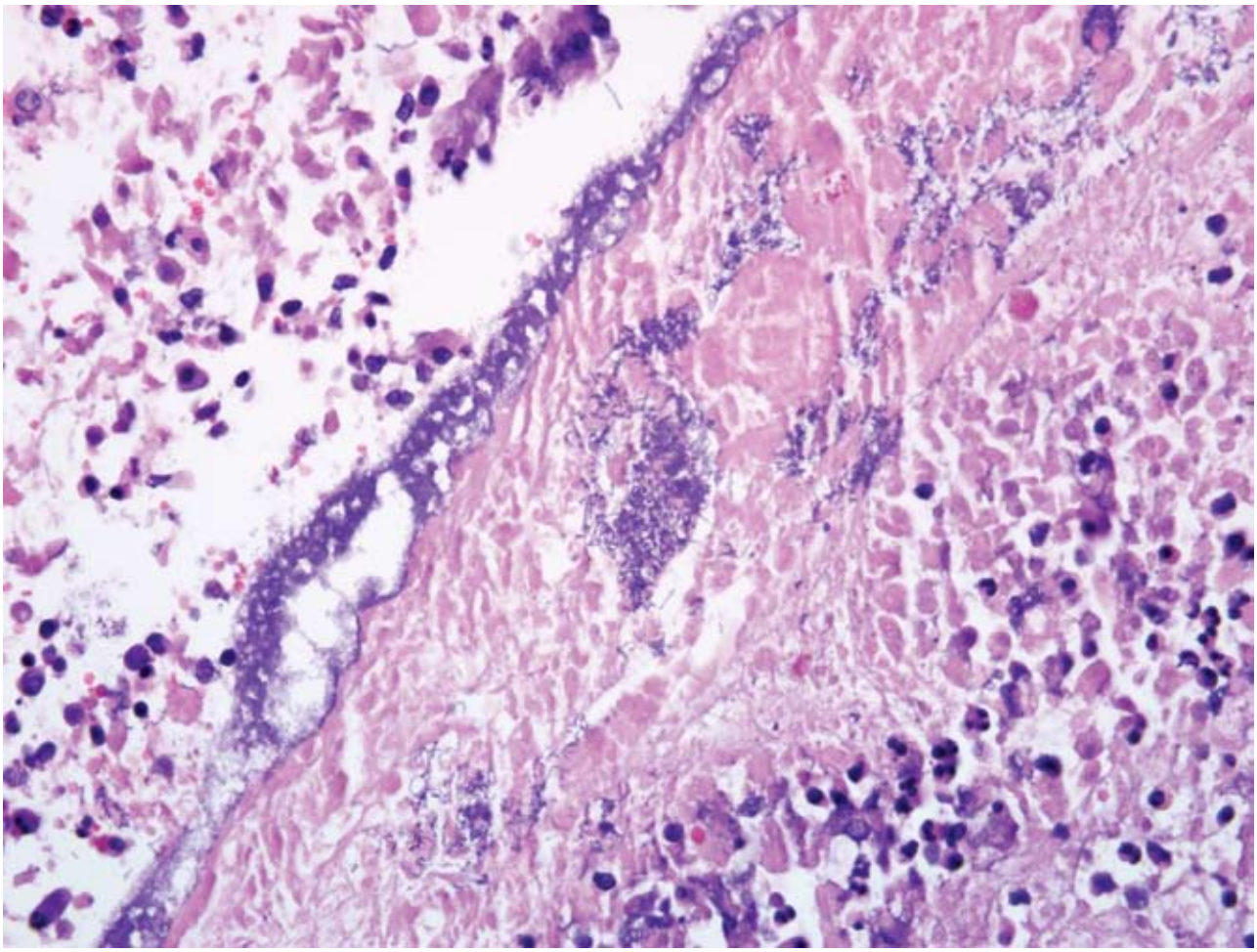

*3-3. Colon, goat. Multifocally, within the fibrinosuppurative exudate there are colonies of 2-3 micron bacilli. HE 400X.*

the kidney, once bound to distal renal tubular epithelium, the tubules degenerate and the result is a "pulpy kidney". Rapid autolysis of the sheep carcass is also thought to contribute to the "pulpy" appearance of the kidney.

There are four clinical forms of *Clostridium perfringens* type D enterotoxemia in goats: peracute, acute, chronic and subclinical. The peracute form manifests as sudden death with little to no warning. The acute form is characterized by diarrhea and colic of a few days duration, and this turns into the chronic form if the animal does not either fully recover or die within a few days of clinical onset. Mentioned by the contributor, the distal small intestine, cecum, and large intestine are most severely affected in goats. Histologically, affected areas are hyperemic and may be covered by a layer of fibrin with a moderate number of inflammatory cells present in the lamina propria.[1]

**Contributing Institution:** California Animal Health and Food Safety Laboratory, UC Davis http:/cahfs.ucdavis.edu

**References:**

1. Brown CC, Baker DC, Barker I: Alimentary system. *In:* Jubb, Kennedy and Palmer's Pathology of Domestic Animals, ed. Maxie MG, 5th ed., vol 1, pp. 212-220. Elsevier Limited, Philadelphia, PA, 2007
2. Uzal FA, Kelly WR: Experimental *Clostridium perfringens* type D enterotoxemia in goats. Vet Pathol. **35**:132-140, 1998
3. Uzal FA, Songer JG: Diagnosis of *Clostridium perfringens* intestinal infections in sheep and goats. J Vet Diagn Invest **20**:253-265, 2008

## CASE IV – Case 1 (AFIP 3102509)

**Signalment:** 11-year-old, male, entire, Cavalier King Charles Spaniel, *Canis familaris*, dog

**History:** This dog presented with a two month history of dyspnoea, lethargy, inappetance, and hemoptysis. Following hospitalization, anthelmintic treatment and concurrent supportive medical therapy (diuretics and corticosteroids), the dog's condition deteriorated acutely with marked respiratory distress. The dog died following respiratory and then cardiac arrest. The dog was submitted for a complete post mortem examination.

**Gross Pathology:** On post mortem examination, the dog was in good body condition with adequate muscle mass and body fat stores. The lung parenchyma contained multifocal areas of dark red discoloration and consolidation **(Fig. 4-1)**. The tracheo-bronchial lymph nodes were enlarged. The heart was markedly enlarged with a heart to body weight ratio of 1.48% (normal range 0.43-0.99%). The right atrium was dilated. The right ventricular wall was thickened (right atrial dilation and right ventricular hypertrophy). The right ventricle contained a thrombus, which was partially adhered to the endocardium, and numerous slender nematode worms measuring up to 15mm in length.

**Laboratory Results:** Microscopic examination of a direct faecal smear revealed the presence of nematode larvae consistent with *Angiostrongylus vasorum* larvae. On routine blood count, a moderately regenerative anemia with a hematocrit of 25.5% (reference value: 37-55%) was present. There was an inflammatory leukogram with leukocytosis (27.8 x109/L; reference value: 6.0 -17.1 x109/L), neutrophilia with mild toxic change (16.4 x109/L; reference value: 3.0 -11.5 x109/L) and monocytosis (3.06 x 109/L; reference value: 0.15 - 1.50 109/L). Biochemistry indicated increased total bilirubin (4.8µmol/L; reference value: 0.0-2.4µmol/L).

**Histopathologic Description:** Lungs: The lung parenchyma was markedly effaced by multifocal to coalescing areas of granulomatous inflammation interspersed with areas of hemorrhage and edema.

The granulomatous inflammation was characterized by the presence of histiocytes, multinucleated giant cells of the foreign body type, fibroblasts, lymphocytes and plasma cells, which were arranged concentrically around myriad parasitic larvae and eggs. Very few eosinophils were noted. Larvae were elongate with a thin eosinophilic cuticle and a primitive enteron measuring 10-20 µm in diameter (**Fig. 4-2**). The thin-walled eggs were ovoid, measured 50-60 µm in diameter and contained either a morula or larva. Larvae and some histiocytes and multinucleated giant cells were also observed within bronchiolar and bronchial lumens surrounded by multinucleate giant cells. Lumens of numerous alveolar spaces and scattered bronchioli and bronchi contained proteinaceous material (edema) and red blood cells (acute hemorrhage). Lumens of some pulmonary arteries contained nematodes measuring about 300 x 150 µm (**Fig. 4-3**). The nematodes were characterized by an outer smooth cuticle, a hypodermis with accessory hypodermal cords, a coelomyarian musculature, and a body cavity with an oligocytous syncytous intestine and reproductive organs (consistent with adult Metastrongyles, **Fig. 4-4**). Intravascular nematodes were often surrounded by thrombi, which were partially adhered to the vessel wall. These thrombi were composed of fibrillary eosinophilic material (fibrin) or fibrous connective tissue containing multiple small blood filled channels (organized and recanalized thrombi).

*4-1. Lung, canine. Multifocally, predominately within the cranial lung lobes, there are areas of consolidation and hemorrhage.*
*The Royal Veterinary College Department of Pathology and Infectious Diseases, Hawkshead Lane, North Mymms, Hatfield, Herts AL97TA, UK*

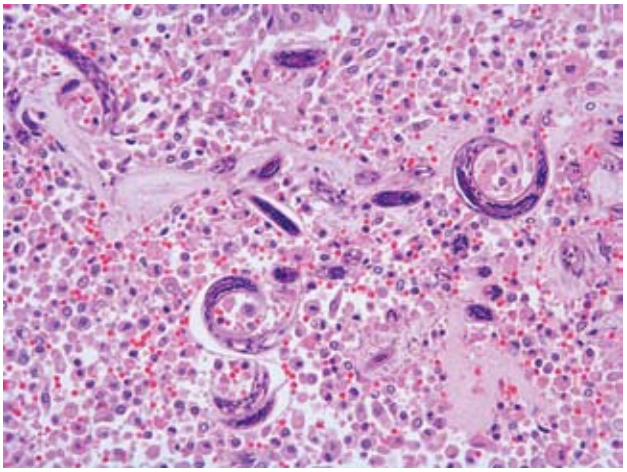

*4-2. Lung, canine. Diffusely, filling alveoli and disrupting normal lung parenchyma are numerous nematode larvae that are surrounded by high numbers of alveolar macrophages, occasional multinucleated giant cells, few eosinophils and admixed with fibrin, hemorrhage, edema and cellular debris. HE 400X.* *Photomicrograph courtesy of The Royal Veterinary College Department of Pathology and Infectious Diseases, Hawkshead Lane, North Mymms, Hatfield, Herts AL97TA, UK*

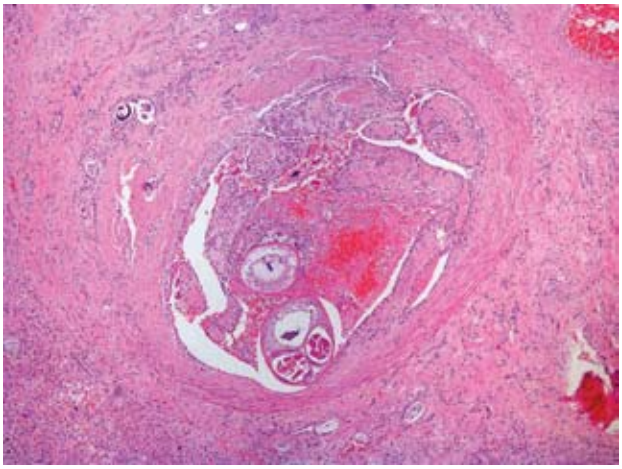

*4-3. Lung, canine. Adult nematodes surrounded by variably organized and recanalized thrombi that often occlude the lumen. The tunica media of numerous vessels is markedly thickened (smooth muscle hypertrophy). HE 200X.* *The Royal Veterinary College Department of Pathology and Infectious Diseases, Hawkshead Lane, North Mymms, Hatfield, Herts AL97TA, UK*

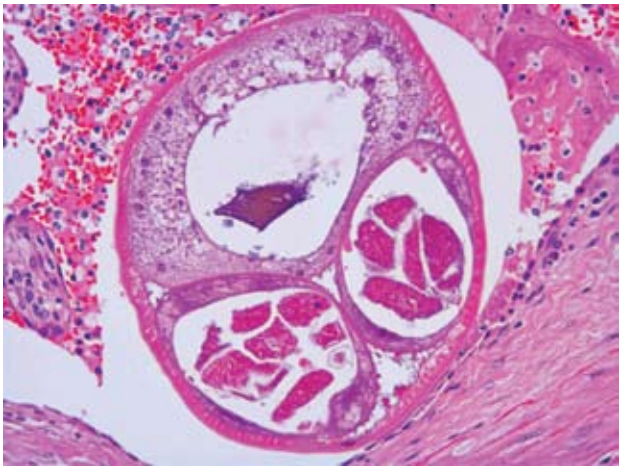

*4-4. Lung, canine. Nematodes are characterized by a smooth cuticle, coelomyarian musculature, and a body cavity with an oligocytous syncytous intestine and reproductive organs (consistent with adult Metastrongyles). HE 400X.* *The Royal Veterinary College Department of Pathology and Infectious Diseases, Hawkshead Lane, North Mymms, Hatfield, Herts AL97TA, UK*

The tunica media of numerous pulmonary arteries was markedly thickened (smooth muscle hypertrophy). The pleura was segmentally thickened by fibrous connective tissue (pleural fibrosis) and contained scattered eggs and larvae, which were surrounded by some histiocytes.

Microscopic examination of additional organs: The parenchyma of tracheo-bronchial lymph nodes, kidneys and brain contained scattered nematode larvae surrounded by granulomatous inflammation.

**Contributor's Morphologic Diagnosis:** Lungs: Pneumonia, granulomatous with myriad intralesional nematode eggs and larvae and acute hemorrhage and edema
Lungs, pulmonary arteries: Intralesional adult metastrongyle nematodes, thrombosis and media hypertrophy

**Contributor's Comment:** Microscopic examination together with parasitology showed the presence of verminous pneumonia due to *Angiostrongylus vasorum* (*A. vasorum*) infestation.

*A. vasorum* is a nematode parasite (superfamily Metastrongyloidae, family Angiostrongyloidae) of which domestic dogs and wild canids are the definitive hosts. Wild foxes serve as an important reservoir for infection in domestic dogs, and natural infection has also been reported in coyotes (*Canis latrans*), wolves (*Canis lupus*) and badgers (*Meles meles*).[3,9] Discrete endemic foci of *A. vasorum* infection in domestic and wild canids are recognized in Europe (France, Ireland, Denmark, Germany, Italy, Spain, Switzerland, Wales, England and Scandinavia), Africa (Uganda), South America (Columbia, Brazil), and more recently in Canada.[4,6]

*A. vasorum* has an indirect lifecycle. Adult worms live in the pulmonary arteries of the definitive host, and eggs are deposited in the lung parenchyma where they develop and hatch producing larvae (L1). L1 penetrate capillary and alveolar walls moving into alveoli, and the large airways are coughed up and secreted in saliva, or swallowed and then excreted in the feces. Aquatic and terrestrial gastropods ingest larvae and serve as the intermediate host in which larvae mature through L2 to L3 stages. Frogs may serve as paratenic and intermediate hosts.[2] When intermediate or paratenic hosts are ingested by the definitive host, *A. vasorum* larvae migrate via lymphatics or hepatic portal vessels to the right side of the heart where they develop to sexual maturity.

*A. vasorum* infection is a cause of chronic heart failure and pyogranulomatous interstitial pneumonia in dogs.[5] Aberrant migration of larvae, which was also observed in the present case, can be a cause of complications. Granulomatous foci, with or without association with larvae and eggs, have been reported in the brain, kidney, tracheo-bronchial lymph nodes, adrenal gland, skin, liver, pancreas, peripheral blood, cerebrospinal fluid, pericardial sac, urinary bladder, femoral artery, intestinal tract, thyroid gland, pituitary gland, skeletal muscle, heart, and eye.[4,7,10,11] Hemorrhage into tissues may also be observed. This is thought to occur secondarily to inappropriate activation of the clotting cascade by immune complex formation and compliment fixation directed against the parasites, leading to a consumptive coagulopathy.[12,13]

Interestingly, a low number of eosinophils were observed within the tissue of this case. This may have occurred secondarily to the use of glucocorticoids in the medical therapy for this case. Via their modulatory effects on cytokine production, glucocorticoids are thought to reduce numbers of eosinophils present in the airways by inducing apoptosis (via inhibition of granulocyte macrophage – colony stimulating factor (GM-CSF) and IL-5) and perhaps through decreasing production in the bone marrow.[1]

Strongyle parasites of the respiratory tract in domestic and wild animals include Metastrongyloidean and Trichostrongyloidean parasites. Common Strongyle parasites of verminous pneumonia in domestic species are listed in Table 1.

Nematode parasites can be identified by the presence of a cuticle, hypodermis and underlying musculature (platymyarian or coelomyarian) surrounding the pseudocoelom containing digestive and reproductive tracts.[8] The cuticle of the strongyle-type parasite is usually smooth and the intestine large and composed of a few multi-nucleated cells (syncytous, oligocytous intestine). Metastrongyloidean parasites are characterized by the presence of coelomyarian musculature, which is in contrast to the platymyarian musculature of the true strongyles and trichostrongyles. Adult females may produce either eggs or fully developed embryos. Metastrongyle L1 larvae are indentified by their distinctive kinked tail morphology and small dorsal spine.

Table 1 Strongyle parasites of the respiratory system of domestic animals [5]

| Superfamily | Definitive host | Family | Species | Intermediate host | Paratenic host | Location of adult worms | Notes |
|---|---|---|---|---|---|---|---|
| **Metastrongylidae** | **Domestic and wild canids** | **Filaroididae** | *Oslerus oselri*<br><br>*Filaroides (F.) hirthi* | **Direct lifecycle, L1 infective**<br>**Direct lifecycle, L1 infective** | | **Tracheal nodules**<br><br>**Alveoli and respiratory bronchioles** | **Differentiate from** *A. milksi* |
| | | **Crensomatidae** | *Crensoma vulpis* | **Gastropod** | | **Bronchioles and small bronchi** | |
| | | **Angiostrongyloidae** | *Angiostrongylus vasorum*<br><br>*Andersonstrongylus (A.) milksi* **(prev.** *Angiostrongylus milksi, Filaroides milksi)* | **Gastropod, frog**<br><br>**Gastropod host proposed, life cycle unknown** | **Frog** | **Pulmonary arteries and right ventricle**<br><br>**Alveoli and respiratory bronchioles** | **Differentiate morphologically from Dirofilaria spp.**<br>**Differentiate from** *F. hirthi* |
| | **Domestic cats** | **Angiostrongyloidae** | *Aelurostrongylus abtrusus* | **Gastropod** | **Birds, rodents, frogs, lizards** | **Terminal and respiratory bronchioles** | |
| | **Pig** | **Protostrongylidae** | *Metastrongylus apri*<br><br>*M. pudendotectus*<br><br>*M. salmi* | **Earthworm** | | **Bronchi and bronchioles** | |
| | **Sheep, goats** | **Protostrongylidae** | *Muellerius capillaris*<br><br>*Protostrongylus rufescens*<br><br>*Neostrongylus linearis* | **Gastropod**<br><br>**Gastropod**<br><br>**Gastropod** | | **Alveoli, rarely bronchioles**<br>**Terminal**<br><br>**bronchioles** | |
| **Trichostrongyloidea** | **Cattle** | Dictyocaulidae | *Dictyocaulus viviparus* | **Direct lifecycle, L1 > L3 in environment** | | **Large bronchi** | |
| | **Sheep, goats** | Dictyocaulidae | *Dictyocaulus filaria* | **Direct lifecycle, L1 > L3 in environment** | | **Small bronchi** | |

**AFIP Diagnosis:** Lung, arteries: Endarteritis, chronic, multifocal, severe with thrombi and intravascular adult nematodes consistent with *Angiostrongylus vasorum*
Lung: Pneumonia, granulomatous, multifocal to coalescing, severe with hemorrhage and nematode larvae and eggs

**Conference Comment:** The contributor did an outstanding job of not only describing this particular parasite but also giving an extensive list of other pulmonary parasites in domestic animals.

**Contributing Institution:** Royal Veterinary College, Department of Pathology and Infectious Diseases, Hawkshead Lane, Hatfield, Hertfordshire, United Kingdom AL97TA, www.rvc.ac.uk

**References:**

1. Barnes PJ, Pederson S, Busse WW: Efficacy and safety of inhaled corticosteroids. American Journal of Respiratory and Critical Care Medicine **157**:S1-S53, 1998
2. Bolt G, Monrad J, Frandsen F, Henriksen P, Dietz HH: The common frog (*Rana temporaria*) as a potential paratenic and intermediate host for *Angiostrongylus vasorum*. Parasitology Research **79**:428-430, 1993
3. Bolt G, Monrad J, Koch J, Jensen JL: Canine angiostrongylosis: a review. The Veterinary Record **135**:447-452, 1994
4. Bourque AC, Conboy G, Miller LM, Whitney H: Pathological findings in dogs naturally infected with *Angiostrongylus vasorum* in Newfoundland and Labrador, Canada. Journal of Veterinary Diagnostic Investigation **20**:11-20, 2008
5. Caswell JL, Williams KJ: Respiratory System. *In:* Jubb, Kennedy, and Palmer's Pathology of Domestic Animals, ed. Maxie MG, pp. 523 - 653. Elsevier Limited, Philadelphia, PA, 2007
6. Conboy GA: Canine angiostrongylosis (French heartworm). *In:* Companion and Exotic Animal Parasitology, ed. Bowman DD, www.ivis.org, accessed May 8 2008
7. Cury MC, Lima WS: Rupture of femoral artery in a dog infected with *Angiostrongylus vasorum*. Veterinary Parasitology **65**:313-315, 1996
8. Gardiner CH, Poynton SL: An atlas of metazoan parasites in animal tissues. Armed Forces Institute of Pathology, Washington DC, 1999
9. Koch J, Willesen JL: Canine pulmonary angiostrongylosis: an update. The Veterinary Journal: doi:10.1016/j.tvjl.2007.11.014, 2007
10. Oliveira-Júnior SD, Barçante JMP, Barçante TA, Ribeiro VM, Lima WS: Ectopic location of adult worms and first-stage larvae of *Angiostrongylus vasorum* in an infected dog. Veterinary Parasitology **121**:293-296, 2004
11. Perry AW, Hertling R, Kennedy MJ: Angiostrongylosis with disseminated larval infection associated with signs of ocular and nervous disease in an imported dog. The Canadian Veterinary Journal **32**:430-431, 1991
12. Ramsey IK, Littlewood JD, Dunn JK, Herrtage ME: Role of chronic disseminated intravascular coagulation in a case of canine angiostrongylosis. The Veterinary Record **138**:360-363, 1996
13. Schelling CG, Greene CE, Prestwood AK, Tsang VC: Coagulation abnormalities associated with acute *Angiostrongylus vasorum* infection in dogs. American Journal of Veterinary Research **47**:2669-2673, 1986

The Armed Forces Institute of Pathology
Department of Veterinary Pathology

*Conference Coordinator:*
Todd M. Bell, DVM

WEDNESDAY SLIDE CONFERENCE 2008-2009

# Conference 12

17 December 2008

*Conference Moderator:*

Tony Alves, DVM, Diplomate ACVP

## CASE I – 08-22155 (AFIP 3107719)

**Signalment:** 3-7-year-old Texas Longhorn Bull (*Bos texanus*)

**History:** This bull is from an Amish dairy farm with approximately 15 Texas Longhorns. The bulls were bred in Ohio and moved to New York. Currently, they are kept on a separate but nearby pasture from where the diary cattle are kept. The owner feeds "good quality" hay but not ad lib and it is unknown if grain is fed. The owner does not vaccinate the dairy cattle. The bull's vaccination history is unknown. The owner reported that five bulls had died in the previous month. In February of 2008, the referring veterinarian performed a field necropsy on the most recently deceased animals and submitted tissues to Cornell University for histopathological evaluation. Because of ambient conditions, the tissues were partially frozen at the time of necropsy and fixation.

**Gross Pathology:** The referring veterinarian could not perform a complete field necropsy since the carcasses were partially frozen. Both bulls were in poor body condition with a lack of perirenal and cardiac adipose tissue. Ruminal content consisted of a normal quantity of fiber and some stones. The feces were solid, and a small to moderate number of non-specified parasites were seen on fecal examination. Buccal and lingual ulcers were present in one animal, and the other animal had reddened Peyer's patches.

**Laboratory Results:** Virus FA results for Bovine Viral Diarrhea virus was negative

**Histopathologic Description:** Tongue: Skeletal muscle fibers are disrupted by multiple variably sized coalescing nodules composed of central aggregates of hyperesoinophilic, radiating, club-shaped hylanized material (Splendore-Hoeppli material) that often contain moderate numbers of cocco-bacilli and a thin peripheral rim of densely basophilic granular material (mineral) **(Fig. 1-1)**. These nodules are surrounded by concentric layers of degenerate neutrophils admixed with a moderate amount of pale eosinophilic fibrillar material (fibrin) and macrophages with occasional Langerhan's type multinucleated giant cells. Dissecting between the remaining myofibers and the inflammatory foci are dense bundles of collagen and regularly arranged fibroblasts admixed with moderate numbers of lymphocytes and plasma cells. The remaining myofibers are often hyperesoinophilic with floccular

*Sponsored by the American Veterinary Medical Association, the American College of Veterinary Pathologists, and the C. L. Davis Foundation.

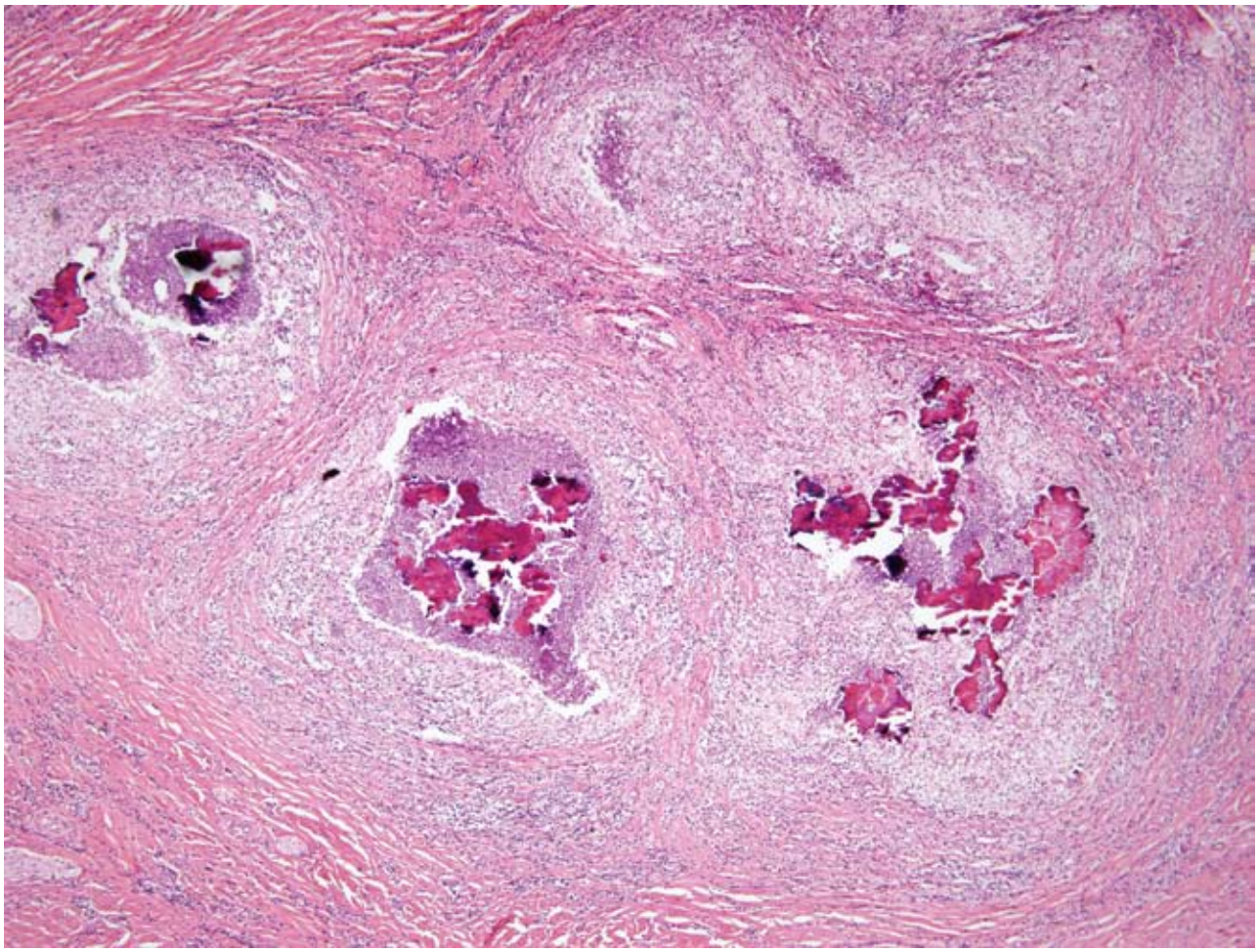

*1-1. Tongue, ox. Multiple coalescing pyogranulomatous nodules composed of a central core of eosinophilic, globular material (Splendore-Hoeppli) admixed with cellular and necrotic debris and bounded by fibrous connective tissue. (HE 40X)*

cytoplasm and lack cross striations (degeneration). There are multiple ulcers of the lingual epithelium and there are several dense intraepithelial aggregates of degenerate neutrophils, acantholytic keratinocytes, and nuclear debris (microabcesses).

Gram's stain of the tongue: There are moderate numbers of Gram negative cocco-bacilli within the Splendore-Hoeppli material.

**Contributor's Morphologic Diagnosis:** Tongue: Severe, multifocal to coalescing, chronic, pyogranulomatous glossitis with Splendore-Hoeppli material, mineralization, intralesional bacteria, fibrosis, ulceration and myonecrosis ('Wooden Tongue')

**Contributor's Comment:** Wooden tongue, or actinobacillosis, is caused by the bacteria *Actinobacillus lignieresii*. This bacterium has been isolated in a variety of species. The organism is ubiquitous and causes sporadic disease of primarily of cattle, sheep, and goats. Since the organism is a commensal of the oral cavity in ruminants, development of disease is most frequently associated with damage to the oral mucosa. In cattle, the tongue is the most common site of infection and thought to be associated with their use of the tongue to prehend food. Comparatively, sheep, which use their lips to prehend food, most frequently have lesions associated with their lips and cheeks. The bacterium has also been isolated from the rumen.[6]

Clinically, affected animals present with weight loss and hypersalivation. This is due to the extensive destruction of the tongue and oral tissues. Gross lesions commonly manifest as variably sized, hard, circumscribed nodules that measure up to several millimeters in diameter. These

nodules are most commonly found in the tissues and skin of the face, and can progress to form soft abscesses which can fistulate and discharge through the mouth or skin. The discharged purulent material is odorless and contains abundant granules.[6] This infection induces in the tongue a severe fibroblastic response causing it to become large and immobile making chewing and swallowing difficult. This hardening of the tongue is the genesis of the common name of the disease "wooden tongue." The formation of granulation tissue within the fibrous connective tissue gives the nodular appearance to these lesions. Additionally, small yellow foci (sulfur granules) can often be seen within the dense granulation tissue. These represent the bacterial colonies within the lesion.

Oral infection with *A. lignieresii* will commonly spread via lymphatics to local lymph nodes. Infections are less commonly found in the forestomachs, lungs, skin and uterus.[4] Grossly, infected lymph nodes contain yellow-orange granulomatous nodules which frequently project above the normal nodal capsular contour and are surrounded by sclerosing inflammation.[2] Affected lymphatics are diffusely thickened with similar nodules.[2] The most commonly affected lymph nodes are the retropharyngeal and submaxillary nodes.

Histologically, these nodular lesions consist of multiple pyogranulomas surrounding aggregates of Gram negative cocco-bacilli embedded in homogenous eosinophilic material. The hypereosinophilic material along with the bacteria forms the club-shaped microcolonies which is characteristic of this disease.[6] These formations are thought to be associated with immune complex deposition.[2] Surrounding the central area of bacteria is a band of inflammatory cells composed predominantly of neutrophils with macrophages and occasional giant cells. The external layer of the pyogranuloma consists of a dense layer of fibrous connective tissue containing variable numbers of lymphocytes and plasma cells. These lesions are often concurrently infected with *Actinomyces pyogenes*, *Streptococcus* spp., and *Pseudomonas aeruginosa*.[4]

*A. lignieresii* has been isolated from laboratory rodents associated with middle ear infections and conjunctivitis [5] and from healthy and diseased horses.[3] There is one report of the bacteria being isolated from a horse with an enlarged tongue.[1] In swine it is seen as granulomas or abscesses of the teats associated with wounds from the sharp teeth of suckling piglets. In horses this bacteria infrequently causes lower airway disease and abscess.[4]

The most important differential diagnoses for actinobacillosis include *Actinomyces bovis, Staphylococcus aureus* (botryomycosis) and *Mycobacterium bovis*. *A. bovis* also contains sulfur granules within discharge. However, infections with this agent tend to be associated with infection of bone, in particular the mandible.[4] In addition, *A. bovis* is a Gram positive filamentous organism, and this infection does not consistently spread to local lymph nodes. Botryomycosis classically has chronic granulomas with centers of numerous Gram positive cocci embedded in a homogenous matrix and the purulent material associated with this infection has botryomycotic granules.[4]

**AFIP Diagnosis:** Tongue: Glossitis, pyogranulomatous, multifocal to coalescing, severe with Splendore-Hoeppli material, fibrosis, myocyte degeneration, necrosis, and loss

**Conference Comment:** The contributor provided an excellent review of this entity.

Splendore-Hoeppli material is intensely eosinophilic, club-shaped material that radiates around certain fungi, bacteria, parasites and biologically inert substances such as suture. The material is generally composed of antigen-antibody complexes, debris and fibrin.[7] The most common infections and conditions that result in the Splendore-Hoeppli phenomenon include botryomycosis, *Nocardia* sp., *Actinomyces* sp., and feline dermatophytic pseudomycetomas.[7] It has also been reported with *Pythium insidiosum, Sporothrix schenckii, Candida albicans, Aspergillus* sp., and zygomycetes such as *Conidiobolus* sp. and *Basidiobolus* sp., *Coccidioides immitis*, nematodes, schistosomiasis, and hypereosinophilic syndrome.[7]

The presence of the Splendore-Hoeppli material led to a discussion of antigen-antibody complexes. Deposition of immune complexes causes tissue damage primarily by activation of the complement cascade and activation of neutrophils and macrophages through their Fc receptors.[8] Immune complexes also cause platelet aggregation and activation of Hageman factor which lead to microthombi formation and kinin activation. Activated complement produces chemotactic factors such as C5a which recruits macrophages and neutrophils, and anaphylatoxins such as C3a and C5a which increase vascular permeability.[8] The leukocytes are activated by binding of their C3b and Fc receptors by the immune complexes. Activated leukocytes release prostaglandins, chemotactic substances, oxygen free radicals, and lysosomal enzymes that include proteases capable of digesting collagen.[8]

**Contributing Institution:** Cornell University, College of Veterinary Medicine, Department of Biomedical Sciences, S2-121 Schurman Hall, Ithaca, NY 14850, http://www.vet.cornell.edu/

**References:**
1. Baum KH, Shin SJ, Rebhun WC, Patten VH: Isolation of *Actinobacillus lignieresii* from a horse with an enlarged tongue. Journal of the American Veterinary Association, **185**:792-793, 1984
2. Brown CC, Baker DC, Barker IK: Alimentary system. *In:* Pathology of Domestic Animals, ed. Maxie MG, 5th ed., vol. 2, pp. 20-21. Elsevier Saunders, Philadelphia, PA, 2007
3. Christensen H, Bisgaard M, Angen, O, Olsen JE: Final classification of Bisgaard taxon 9 as *Actinobacillus arthritidis* sp. nov. and recognition of a novel genomospecies for equine strains of *Actinobacillus lignieresii*. International Journal of Systematic and Evolutionary Microbiology **52**:1239-1246, 2002
4. Henton MM, Van Der Lugt JJ: Actinobacillus Infections in Infectious Diseases of Livestock, eds. Coetzer JAW, Tustin, RC, 2nd ed., vol. 3, pp. 1648-1651 Oxford University Press, Cape Town South Africa, 2004
5. Lentsch RH, Wagner JE: Isolation of *Actinobacillus lignieresii* and *Actinobacillus equuli* from Laboratory Rodents. Journal of Clinical Microbiology **2**:351-354, 1980
6. Rycroft AN, Garside LH: Actinobacillus species and their role in disease. The Veterinary Journal 159:18-36, 2000
7. Hussein MR: Mucocutaneous Splendore-Hoeppli phenomenon. Journal of Cutaneous Pathology **35**:979-988, 2008
8. Abbas AK: Diseases of immunity. *In:* Pathological Basis of Disease, eds. Kumar V, Abbas AK, Fausto N, 7th ed., pp. 213-214. Elsevier Saunders, Philadelphia, PA, 2005

## CASE II – NIAH-2 (AFIP 3106267)

**Signalment:** A 66-day-old, male, mixed, swine (*Sus scrofy*)

**History:** Seven of 41 piglets in a herd of 70 sows became affected at approximately 40 to 50 days of age. The affected piglets suddenly developed paralysis of the hind limbs and became recumbent. In spite of the severe flaccid paralysis of the hind limbs, they could move by using their forelimbs. In all cases, their body temperatures were within the normal range, their appetites remained normal, and none died spontaneously.

**Gross Pathology:** No gross abnormalities were seen in any of the piglets

**Laboratory Results:** Portions of the cerebrum, brainstem, cerebellum, spinal cord (cervical and lumber enlargement) and tonsils of 4 piglets were taken for virus isolation purposes. Each tissue was routinely homogenized in Earle's medium and inoculated onto porcine kidney cell line (CPK) cultures that were then observed microscopically for seven days. Three further passages were made of each sample. CPK cells were harvested when the cells displayed characteristic cytopathic effects. Viral RNA was extracted from the CPK cells with ISOGEN-LS (Nippon Gene, Toyama, Japan) according to the manufacturer's instructions. The RT-PCR was performed with a RNA PCR kit (Takara) according to the manufacturer's instructions. The amplified product was visualized by standard gel electrophoresis of 10µl of the final reaction mixture on a 2% agarose gel. Amplified DNA fragments of specific sizes were located by ultraviolet fluorescence after staining with ethidium bromide. Fragment lengths were verified by comparison with a digested lambda standard on the same gel. PCR products were purified using a High Pure PCR Product Purification kit (Roche). The nucleotide sequences of the purified PCR products were determined by use of BigDye chemistry (Applied Biosystems, Foster City, CA) with the ABI 310 Sequencer (Applied Biosystems). The sequences of which were compared with each other and the PTV (Porcine Teschovirus) sequences available in the GenBank/EMBL/DDBJ using GENETYX-WIN version 4.0 (Software Development Co., Ltd, Tokyo, Japan). The cytopathogenic agents were recovered from the homogenate of cerebellum and tonsils of 3 piglets including this present piglet, and from the brainstem of this presented piglet. All cytopathogenic agents isolated from piglets were amplified in CPK cells, and the resulting extracted RNA was reacted with primers specific for PTV by RT-PCR. PCR products isolated from cerebellum and brainstem of this presented piglet were sequenced. These sequences were identical and the homology between this sequence and other PTV's were 91.2-95.6%. Based on this observation, the pathogenic agent isolated from this pig was identified as PTV. Virus was not isolated from the cerebrum and spinal cord.

**Histopathologic Description:** Histologically, lesions were limited to the central nervous system (CNS) and peripheral nerve fibers. All clinically affected piglets had similar histological changes. The changes observed were those of nonsuppurative encephalomyelitis, characterized

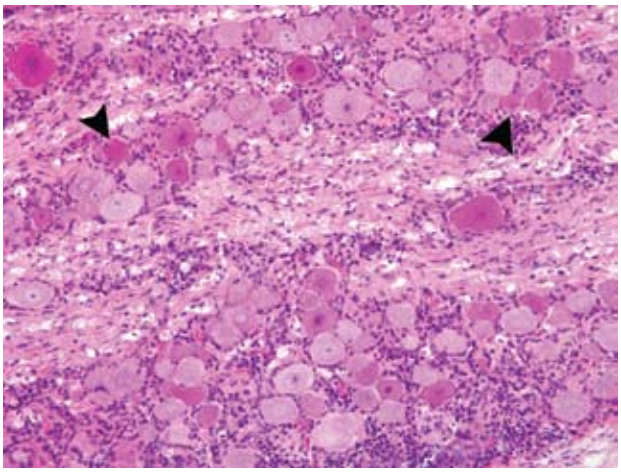

*2-1. Spinal nerve root ganglion, pig. Separating, surrounding and moderately expanding the endoneurium and perineurium are moderate numbers of lymphocytes and plasma cells. Multifocally there are low numbers of degenerate neurons characterized by shrunken, hypereosinophilic cytoplasm and faded or pyknotic nuclei (arrowheads). (HE 400X)*

by perivascular cuffing of the mononuclear cells, focal gliosis, neuronal necrosis and neuronophagia. The spinal cord was severely affected and the lesion was seen along the full length of the spinal cord. In the ventral horns, nerve cells were degenerated to varying degrees up to, and including, necrosis accompanied by neuronophagia, inflammatory or glial nodules, occasional hemorrhage, and a rather diffuse infiltration of mononuclear cells. In the white matter of the spinal cord, perivascular cuffing and infiltration of mononuclear cells and focal gliosis were also observed. In addition to the infiltrative changes, severe vacuolar changes and axonal swelling were observed in the white matter of the spinal cord. Infiltration of mononuclear cells was observed in the dorsal root ganglia, spinal nerves, and sciatic nerves. In some dorsal root ganglia, degenerated ganglion cells and neuronophagia were observed **(Fig. 2-1)**. Swollen myelin sheaths and axonal spheroids were seen in the spinal roots, and in peripheral nerves, including the brachial plexus and sciatic nerves. The cerebellar nuclei and the gray matter of the brainstem were also severely affected. In the cerebral hemisphere, only slight perivascular cuffing was present.

Immunohistochemically, PTV antigens were detected in the cytoplasm of large nerve cells and glial cells in the cerebellar nuclei, the gray matter of the brain stem, and the ventral horn of the spinal cord of all examined pigs. In the spinal ganglia, PTV antigen was strongly detected in the cytoplasm of ganglion cells. In the nervous system, the distribution of PTV antigen was consistent with the lesion distribution. In the lesion, no antigens were seen in the central severe area. Antigens were mainly seen in the periphery of the severe lesions and, especially, in minimal to mild lesions around areas of perivascular cuffing.

**Contributor's Morphologic Diagnosis:** Spinal cord: nonsuppurative, necrotizing, myelitis, with vacuolar changes in the white matter, mixed pig, swine
Dorsal root ganglia: nonsuppurative, ganglionitis

**Contributor's Comment:** Enterovirus encephalomyelitis (previously known as Teschen/Talfan disease) caused by at least 9 serotypes of porcine teschovirus (PTV 1, and 2-6, 8, 12, 13 which are responsible for the milder form of the disease) of the picornaviridae family is considered to be of socioeconomic importance.[5] Infection appears to be selective for specific neuronal populations, resulting in a characteristic clinical syndrome of lower motor neuron paralysis. A diagnosis of enterovirus encephalomyelitis is made by virus isolation from the central nervous system of pigs showing neural signs[5] The disease was first described as Teschen disease.[5] Less virulent forms of the disease were later recognized in the United Kingdom (Talfan disease) and in Denmark (poliomyelitis suum).[5] These later diseases were described as resulting in lower morbidity and mortality, the clinical syndrome expressed as paresis and ataxia (which seldom progresses to complete paralysis).[1,2] The histological changes were those of nonsuppurative polioencephalomyelitis.[2,3,5] The lesions in the spinal cord in each syndrome were largely confined to the gray matter, particularly the ventral horns, but may selectively involve the dorsal horns in very young pigs.[3] Infections from PTV are most often asymptomatic, and PTV is still frequently isolated from the faces, tonsils and other non-neural organs of apparently unaffected pigs.[4]

In the present cases, the morbidity and mortality were low and the characteristic clinical signs were flaccid paralysis of the hind limbs. The nonsuppurative lesions were distributed mainly in the gray matter of the brainstem and the spinal cord. These clinical and histological features of the present disease are similar to those of the disease produced by less virulent PTV strains, especially those of Talfan disease.[3,4] In previous reports of experimental Talfan disease, axonal degeneration was seen in the ventral root and sciatic nerves.[1] In the white matter of the spinal cord, slight degenerative changes were seen only in the dorsal funiculus.[1] In contrast, demyelination and axonal degeneration in the present cases, which resulted from a natural outbreak in Japan, appeared in the whole white matter, and in either the ventral or dorsal root.

Immunohistochemically, anti-PTV monoclonal antibody (no.9, IgM) (National Institute of Animal Health, Japan) 6 was used as the primary antibody. PTV antigens were detected in cytoplasm of nerve cells, glial cells and endothelial cells in the cerebellar nuclei, the gray matter of the midbrain, pons, and medulla oblongata and the ventral horn of the spinal cord and of ganglion cells in the spinal ganglion corresponding to those lesions characterized as nonsuppurative encephalomyelitis and ganglionitis in the pigs. The results suggest that nerve cells of the brainstem and spinal cord, and ganglion cells of the spinal ganglion permit PTV replication and represent the main target cell population of PTV.

The isolation of PTV from CNS is important for diagnosing enterovirus encephalomyelitis.[1] However, it has been reported that isolation of virus from CNS is quite difficult, and virus isolation is not always possible using routine techniques in the cases of enterovirus encephalomyelitis of pigs.[4] The optimum conditions for virus isolation from CNS, including the relationship of clinical signs to the presence of infectious virus and anatomic site where the virus is present in high density, have not been clarified in this disease. In the present cases, PTV was isolated from cerebellum and/or brainstem in the pigs slaughtered about three weeks after the onset of neural signs, but not from the cerebrum. These results suggest that sampling for virus isolation should be from the cerebellum or brainstem for the successful diagnoses enterovirus encephalomyelitis.

**AFIP Diagnosis:** Spinal cord: Poliomyelitis and ganglioneuritis, nonsuppurative, multifocal, marked with neuronal degeneration and necrosis, neuronophagia, gliosis, astrocytosis, satellitosis, and spheroids

**Conference Comment:** The contributor provided an excellent review of porcine teschovirus (PTV) which targets selective neuronal populations in the ventral horn of the spinal cord, brain stem, and ganglion cells of the spinal ganglion resulting in neuronal necrosis, nonsuppurative polioencephalomyelitis and lower motor neuron paralysis. In naturally infected cases, the PTV antigens (but no lesions) were also present in bronchial epithelium, tonsillar epithelium, hepatocytes and the myenteric nerve plexus, but not in the cerebral hemispheres.[9] In addition to the typical neurological disease, some strains of the virus have been associated with female reproductive disorders, enteric disease, pneumonia, pericarditis and myocarditis. Lesions have been described in the kidney, liver, spleen, adrenal gland and thyroid gland.[9] PTV is frequently isolated from the feces, tonsils and non-neural organs of clinically normal pigs.[9] The proposed pathogenesis includes virus replication within the gut, mucosal lymphoid tissue and local lymph nodes; followed by viremia; and subsequent central nervous system invasion.[9]

Conference participants discussed other viruses affecting the nervous system of pigs. Pseudorabies (suid herpesvirus 1) causes nonsuppurative encephalitis primarily affecting the gray matter, neuronal necrosis and ganglioneuritis in the paravertebral ganglia.[7] Eosinophilic intranuclear inclusion bodies are present in the neurons and astroglia. Lesions are most severe in the cerebral cortex (differentiating it from porcine teschovirus), brain stem, spinal ganglia and basal ganglia[7] Very young and aborted pigs typically have small areas of necrosis with eosinophilic intranuclear inclusions in the liver, tonsils, lung, spleen, placenta and adrenal glands.[7] Porcine hemagglutinating encephalitis virus (HEV) is a coronavirus that causes two clinical syndromes in young pigs: neurological signs occur in 4-7-day-old piglets and "vomiting and wasting disease" occurs in 4-14-day-old piglets.[7] Neurological lesions include nonsuppurative encephalomyelitis affecting the gray matter of the medulla and brain stem, and inflammation within the trigeminal, paravertebral and autonomic ganglia, and the gastric myenteric plexus.[7] Classical swine fever (porcine pestivirus) causes vascular lesions that result in hemorrhage, infarction, necrosis and disseminated intravascular coagulation.[6] Common lesions include hemorrhages in various organs (especially the lymph nodes), renal petechiae and splenic infarction.[6] Neural lesions occur in the gray and white matter, and primarily affect the medulla oblongata, pons, colliculi and thalamus.[10] There is endothelial swelling, proliferation and necrosis; perivascular lymphocytic cuffing; hemorrhage and thrombosis; gliosis; and neuronal degeneration.[10] In utero infections result in cerebellar hypoplasia and spinal cord hypomyelinoogenesis.[7] Two paramyxoviral diseases of pigs include porcine rubulavirus encephalomyelitis (Blue eye disease) and Nipah virus. Porcine rubulavirus causes encephalomyelitis, reproductive failure and corneal opacity primarily in Mexico. There is nonsuppurative polioencephalomyelitis affecting the thalamus, midbrain and cortex. Additional lesions include anterior uveitis, corneal edema, epididymitis, orchitis and interstitial pneumonia.[7] Nipah encephalitis is an emerging disease causing severe and rapidly progressive encephalitis and pneumonia in pigs, other animals and humans.[7] Fruit bats are the natural reservoir. There is necrotizing vasculitis and fibrinoid necrosis of arterioles, venules and capillaries with endothelial syncytial cells resulting in large areas of hemorrhage and infarction. Eosinophilic intracytoplasmic and intranuclear inclusions are occasionally found in neurons and endothelial syncytia. Blood vessels in the lung, brain, glomeruli and lymphoid organs are most commonly affected. [7] Additional lesions include bronchointerstitial pneumonia with necrotizing bronchiolitis, lymphocytic and neutrophilic meningitis, nonsuppurative encephalitis and gliosis.[7]

**Contributing Institution:** National Institute of Animal Health (http://niah.naro.affrc.go.jp/index.html), 3-1-5 Kannondai, Tsukuba, Ibaraki, 305-0856 Japan.

**References:**

1. Edington N, Christofinis GJ, Betts AO: Pathogenicity of Talfan and Konratice strains of Teschen virus in gnotobiotic pigs. J Comp Pathol **82**:393-399, 1972
2. Harding JDJ, Done JT, Kershaw GF: A transmissible polio-encephalomyelitis of pigs (Talfan disease). Vet Rec **69**:824-832, 1957
3. Jubb KVF, Huxtable CR: The nervous system. *In*: Pathology of Domestic Animals, eds. Jubb KVF, Kennedy PC and Palmer N, 4th ed., vol. 1, pp. 267-439. Academic Press, San Diego, CA, 1993
4. La Rosa G, Muscillo M, Di Grazia A, Fontana S, Iaconelli M, Tollis M: Validation of RT-PCR assays for molecular characterization of porcine teschoviruses and enteroviruses. J Vet Med B **53**:257-265, 2007
5. Mádr V: Enterovirus encephalomyelitis (previously Teschen/Talfan disease). *In*: Manual of standards for diagnostic tests and vaccines, 4th ed., pp. 630-637. Office International des Epizooties, Paris, 2000
6. Maxie MG, Robinson WF: Cardiovascular system. *In*: Jubb, Kennedy, and Palmer's Pathology of Domestic Animals, ed. Maxie MG, 5th ed., vol. 3, pp. 78-82. Saunders Elsevier, London, UK, 2007
7. Maxie MG, Youssef S: Nervous system. *In*: Jubb, Kennedy, and Palmer's Pathology of Domestic Animals, ed. Maxie MG, 5th ed., vol. 1, pp. 321-433. Saunders Elsevier, London, UK, 2007
8. Yamada M, Kaku Y, Nakamura K, Yoshii M, Yamamoto Y, Miyazaki A, Tsunemitsu H, Narita M: Immunohistochemical detection of porcine teschovirus antigen in the formalin-fixed paraffin-embedded specimens from pigs experimentally infected with porcine teschovirus. J Vet Med A **54**:571-574, 2007
9. Yamada M, et al. Al.: Immunohistochemical distribution of viral antigens in pigs naturally infected with porcine teschovirus. J Vet Med Sci **70**:305-308, 2008
10. Zachary JF: Nervous system. *In*: Pathological Basis of Veterinary Disease, eds. McGavin MD, Zachary JF, 4th ed., p. 967. Mosby Elsevier, St. Louis, MO, 2007

## CASE III – 0806396 (AFIP 3105581)

**Signalment:** 6-month-old, spayed female, Siamese cross cat, *Felus catus or domesticus*

**History:** Chronic vomiting and weight loss. Exploratory laparotomy revealed an abnormal ileocecal region that was resected and submitted for histologic examination. The cat did poorly following the exploratory laparotomy and was euthanized. Although the owner declined a complete postmortem examination, they consented to collection and submission of some tissues for identifying the fungal agent.

**Gross Pathology:** A 5.1 x 5.0 cm section of cecum with attached short segments of ileum and colon was submitted.

**Laboratory Results:** Fresh liver, small intestine, and a swab from the colon were submitted for definitive fungal identification. *Candida albicans* was cultured from all three sites.

**Histopathologic Description:** At the diverticulum of the cecum there was a focally extensive area of severe necrosis with coalescing bands and large aggegrates of inflammatory cells (neutrophils, histiocytes [includes epithelioid and vacuolated forms], small lymphocytes and plasma cells) admixed with irregular streams of spindled cells with a plump nucleus. Multiple aggregates of nonpigmented, branching, pseudohyphae and septate hyphae (4 to 8 um thick) were present within the inflammatory infiltrate and on the mucosal surface **(Fig. 3-1)**. Sections from the ileum and colon were unremarkable.

**Contributor's Morphologic Diagnosis:** Severe, focally extensive, necrotizing, pyogranulomatous typhlitis due to *Candida albicans*

**Contributor's Comment:** Members of the genus Candida are saprophytic, dimorphic fungi in the family *Cryptococcaceae*.[3] In the yeast phase, *Candida* species normally inhabit the alimentary, upper respiratory and genital mucosae of mammals.[3,1] *Candida* species are first acquired by neonates as they pass through the birth canal, colonize the oral, gastrointestinal, upper respiratory and genital mucosae for the life of the animals.[3] Their presence normally evokes no reaction. Under certain circumstances, *Candida* species can invade deeper host tissues and proliferate as blastoconidia, pseudohyphae and

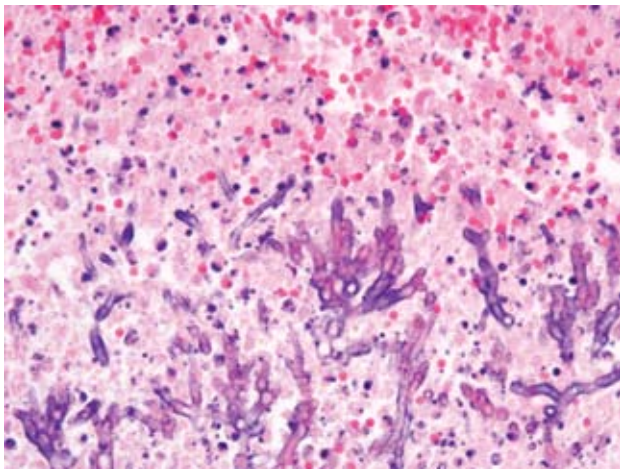

*3-1. Cecum, cat. Within areas of lytic necrosis there are numerous fugal hyphae that are characterized by thin, septate, parallel walls and dichotomous branching. (HE 400X)*

branched, septate hyphae.[3] In other instances, they can disseminate via the bloodstream to many tissues. [3]

Pathogenic factors of *Candida* species are important in determining their relative virulence in the host.[3] *Candida albicans* can invade the columnar epithelium of the intestines.[3] The yeast form of *C. albicans* colonizes epithelia, while hyphae are the more invasive form and are found within deeper tissue invasion.[3]

Local proliferation of *Candida* species on mucosal surfaces is the first step in the spread of infection. Overgrowth of *Candida* species within the gastrointestinal tract is inhibited by mucosal microflora.[1] Factors that upset the balance of normal endogenous microflora may cause *Candida* organisms to proliferate. Intestinal candidiasis may be sequelae to parvoviral infections or alterations in microflora caused by systemic antibiotic therapy.[3,1,5] Mycotic ileitis and colitis in cats have been reported as a secondary complication of infection with feline panleukopenia virus.[5,7] Localized candidiasis has been reported to occur in chronically immunosuppressed cats and in those with nonhealing ulcers of the gastrointestinal tract.[3] However, in one study retroviral status (feline leukemia virus, FeLV and feline immunodeficiency virus, FIV) did not influence the ability to isolate *C. albicans* from feline cutaneous and mucosal samples.[6] The FeLV and FIV status of this patient was not established and routine bloodwork, that may have demonstrated panleukopenia, was not performed.

Histologic examination of lesions reveals multifocal abscesses or areas of necrosis that contain abundant blastoconidia, pseudohyphae and true hyphae surrounded by mixed inflammatory cells.[3] Infiltrates tend to be minimal in profoundly immunosuppressed or leukopenic animals.[3] The proprial infiltrate in the cecum from this cat would suggest it was not immunosuppressed or leukopenic.

*Candida* species grow well on blood agar and are often isolated from specimens submitted for bacterial culture. Organisms may sometimes be cultured from many tissues at surgery or necropsy, but such results should be interpreted cautiously.[3] Culture of *Candida* species from cutaneous, mucosal or exudates alone are not an indicator of infection.[3] Histologic confirmation of invasion and host reaction are essential.[3] Mucosal and cutaneous biopsies should be submitted for histologic and culture examination simultaneously. A definitive histologic diagnosis can sometimes be made in the presence of negative culture results.

**AFIP Diagnosis:** 1. Cecum (per contributor): Typhlitis, necrotizing and pyogranulomatous, diffuse, severe, with vasculitis, fibrin, hemorrhage, edema, intralesional hyphae and pseudohyphae, and rare eosinophilic intranuclear inclusion bodies
2. Lymph node: Lymphoid depletion, diffuse, severe, with draining hemorrhage, edema, and rare eosinophilic intranuclear inclusion bodies

| | PV | FAE | CoV | EUE |
|---|---|---|---|---|
| Necrosis | crypts | crypts (less severe) | villar | crypts |
| Inflammation | ↑ (T cells) | ↑↑ (T cells) | ↑ ↑ (lymphocytes) | ↑↑ (macrophages) |
| Lymphoid tissue | depleted | Normal to hyper-plastic | | depleted |
| Bone marrow | ⇓ | Slight ↑ | Slight ↑ | Slight ↑ |

**Conference Comment:** The contributor provides an excellent review of *Candida* sp. In addition, several eosinophilic intranuclear inclusion bodies were observed within lymphocytes in the lymph node in the intestinal epithelium. Immunosuppression is suspected to have predisposed this 6-month-old cat to concurrent viral and *Candida* infections. The inclusion bodies, along with the necrotizing lesion and lymphoid depletion, are suggestive of feline parvovirus (PV) infection. Inclusion bodies are generally found only early in infection.[2] Intestinal lesions of PV are similar to those seen with feline leukemia virus associated enteritis (FAE), feline enteric coronavirus (CoV), and enteritis of unknown etiology (EUE). Crypt necrosis is the primary lesion observed with PV, FAE and EUE, while necrosis of the villar tip is the primary lesion with CoV. The inflammation is marked in FAE, EUE and CoV, unlike in PV. Many macrophages are present in EUE. The inflammation is composed primarily of T lymphocytes in PV and FAE. There is lymphoid depletion with PV and EUE. Lymphoid tissue is normal to hyperplastic with FAE. There is decreased bone marrow activity in PV. Bone marrow activity is slightly increased with FAE, CoV and EUE.[4] Intrauterine infection results in congenital cerebellar hypoplasia in kittens.[2]

**Contributing Institution:** Prairie Diagnostic Services, 52 Campus Drive, Saskatoon, Saskatchewan, Canada, S7N 5B4, www.usask.ca/pds

**References:**

1. Brown CC, Baker DC, Barker IK: Alimentary system. *In:* Pathology of Domestic Animals, ed. Maxie MG, 5th ed., vol. 2, p. 230. Saunders Elsevier, London, UK, 2007
2. Gelberg HB: Alimentary system. *In:* Pathological Basis of Veterinary Disease, eds. McGavin MD, Zachary JF, 4th ed., pp. 378-380. Mosby, St. Louis, MO, 2007
3. Greene CE and Chandler FW. Candidiasis and Rhodotorulosis. *In:* Infectious Diseases of the Dog and Cat, ed. Greene CE, 3rd ed., pp. 627- 632. Saunders Elsevier, London, UK, 2006
4. Kipar A, Kremendahl J, Jackson ML, Reinacher M: Comparative examination of cats with feline leukemia virus-associated enteritis and other relevant forms of enteritis. Vet Pathol **38**:359-371, 2001
5. Lorenzini R and De Bernardis F: Antemortem diagnosis of an apparent case of feline candidiasis. Mycopathologia **93**:13-14, 1986
6. Ochiai K, Valentine B and Altschul M: Intestinal candidiasis in a dog. Vet Rec **146**:228-229, 2000
7. Sierra P, Guillot J, Jacob H, Bussieras S, Chermette R: Fungal flora on cutaneous and mucosa surfaces of cats infected with feline immunodeficiency virus or feline leukemia virus. American Journal of Veterinary Research **61**:158-161, 2000

## CASE IV – V08-03243 (AFIP 3106654)

**Signalment:** Two-year-old female bovine (*Bos taurus*), breed unknown

**History:** This producer had lost 10 head of young cattle (6-18 months of age) over a period of approximately 10 days. Most cattle were simply found dead; this one was seen "staggering, depressed", and died before attending veterinarian could get to the premises.

**Gross Pathology:** The animal was in good nutritional and post-mortem condition. Age was estimated at approximately 1 year. There were multifocal variably sized and irregular shaped purplish-black areas of discoloration of skeletal muscle occurring with random distribution in the caudal neck, brisket, and quadriceps muscles; these were bilateral distribution on both sides of the animal. Lesions were present both on the surfaces of the muscles, and deeper into musculature. These lesions were quite "dry" and there was crepitus on palpation.

**Laboratory Results:** Bacteriology – *Clostridium chauvoei* was detected via both fluorescent antibody and anaerobic culture methods.

**Histopathologic Description:** Skeletal muscle fibers were in varying stages of necrosis, varying from early coagulation necrosis to complete fragmentation and collapse. There were large zones of hemorrhage with some aggregates of neutrophils and macrophages were found between muscle fibers, as well as edema fluid. Multifocal pockets of emphysema were also seen, primarily in fascial planes. Occasional rectangular bacterial organisms were seen, again primarily in fascial planes.

**Contributor's Morphologic Diagnosis:** Myositis, necrotizing, due to *Clostridium chauvoei* (blackleg)

**Contributor's Comment:** The lesions are virtually pathognomonic grossly, and bacterial FA techniques can verify a diagnosis quite rapidly. Differential diagnoses would include other clostridial disease (i.e., *C. septicum* or pseudo-blackleg)[3]; however, *C. chauvoe* is the only disease that consistently produces gas pockets in the muscles in freshly dead animals, coupled with the prominent areas of discoloration (due to hemolyzed erythrocytes). Microscopic lesions are typical, but relatively moderate in severity. Death is caused by the production and absorption of a potent exotoxin by the organism, thus causing a toxemia with subsequent muscular hemorrhages

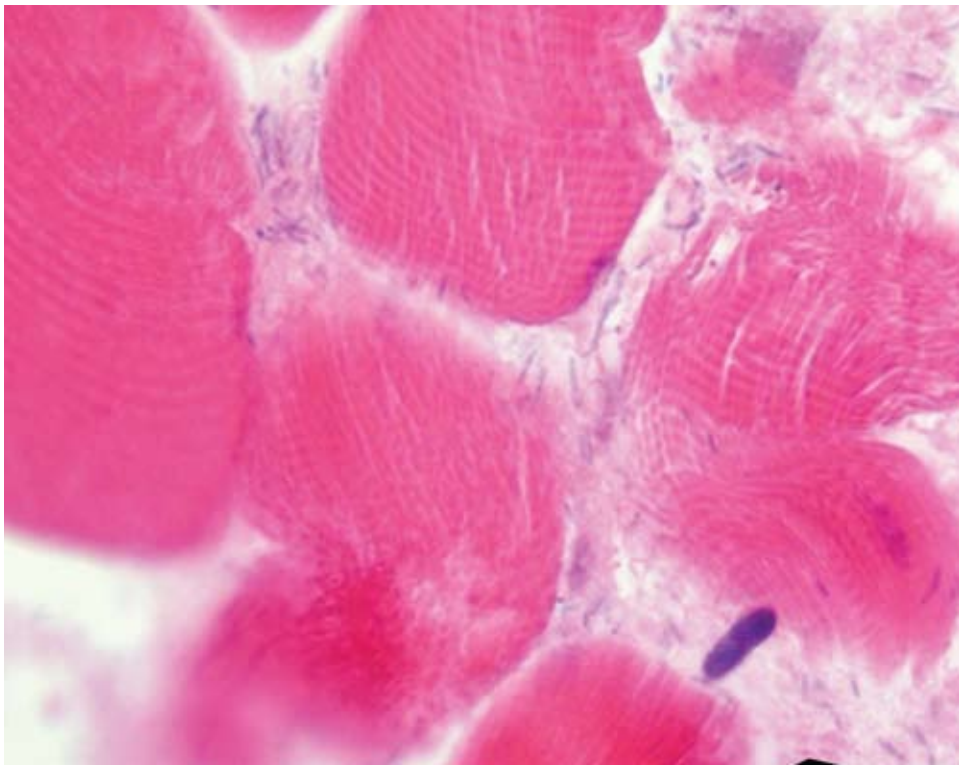

*4-1. Skeletal muscle, ox. Multifocally and rarely within the endomysium there are aggregates of low numbers of bacilli (arrow). (HE 400X)*

and edema.[2,3] The progress of the disease is extremely rapid, thus in some cases it may produce only moderate histologic lesions associated with the toxemia, or they may be widespread and severe, as with this one.

This case was submitted because this condition is not commonly seen anymore due to better herd management practices and good vaccines being available and in use in most cattle operations.

However, in the Southwestern United States, we do see blackleg occasionally due to some management issues that are unique to our geography and climate. In a desert environment, large acreages are required to range (i.e., pasture) cattle; yearling cattle such as these would require a minimum of 40-60 acres per animal, depending upon availability of forage, drought, etc. Requirements for cow/calf pairs commonly range from 60-100 acres per animal; hence, a 200 cow herd would require 12,000-20,000 acres (20-30 sections). Many operations leave the bulls out with the cows all year, thus having year round calving and calves of many different sizes and weights. Thus, these large ranges (often in very rugged and inaccessible country, except by horseback) make doing a "gather" for any reason difficult, very labor intensive, time consuming, and requires experienced and savvy cowboys. As a result, cattle are often only gathered up once a year, usually to select and market heavier calves. Obviously, with these types of management problems, installation of a comprehensive herd health (including vaccinations) program is often a hit-and-miss proposition, as was the case with these animals. This particular animal had not been vaccinated (nor had any of the others).

**AFIP Diagnosis:** Skeletal muscle: Myocyte degeneration and necrosis, multifocal, moderate, with hemorrhage, emphysema, and few intralesional bacteria **(Fig. 4-1)**

**Conference Comment:** The pathogenesis of blackleg involves ingestion and passage of spores across the intestinal mucosa, and distribution to tissues where they are stored for long periods in the phagocytic cells. The latent spores germinate when there is muscle damage or low oxygen tension.[3] The large muscles of the pelvic and pectoral girdles are most often affected, but any striated muscle is susceptible including the tongue, heart and diaphragm.[3] Grossly, the peripheral tissue is dark red and edematous, while the center is red-black, dry, friable and emphysematous. Additional findings include a rancid-butter odor, rapid autolysis of tissues, and fibrinohemorrhagic pleuritis (without corresponding severe pneumonia). Histologically, leukocytes are sparse since they are destroyed by the exotoxins.[3]

Differentiating blackleg from pseudo-blackleg, gas gangrene and malignant edema has important management implications. Pseudo-blackleg is caused by the activation of latent spores of *C. septicum* in the muscle. *C. septicum* proliferates rapidly after death, unlike *C. chauvoei*, so the carcass must be examined immediately after death. Pseudo-blackleg lesions are often multiple and are much less emphysematous. *C. septicum* also causes hemorrhagic abomasitis (Braxy) in ruminants.[3] Blackleg results from activation of latent spores in muscle, whereas gas gangrene and malignant edema results from contamination of an open wound.[3] Gas gangrene and malignant edema can be caused by a single or mixed infection of *C. chauvoei, C. septicum, C. perfringens* and *C. novyi*. The most common cause of malignant edema is *C. septicum*. Ruminants, horses and swine are most susceptible.[3] Malignant edema causes primarily a cellulitis, rather than a myositis as in gas gangrene. Also, the gas characteristic of gas gangrene is not a feature of malignant edema. [3] *C. novyi* also causes "swelled head" in rams, resulting from the infected head wounds received during fighting.[3] *C. novyi* is also the cause of necrotic hepatitis (Black disease) in sheep, and *C. haemolyticum* causes bacillary hemoglobinuria in cattle and sheep. In both diseases, clostridial spores are ingested, cross the intestinal mucosam, and remain latent within Kupffer cells. Migrating larvae of the common liver fluke, *Fasciola hepatica*, cause necrosis which leads to activation of the latent clostridial spores. The spores release beta toxin, a necrotizing and hemolytic lecithinase (phospholipase C), that causes necrosis of the surrounding tissue and hemolysis in bacillary hemoglobinuria. Grossly, there are large pale areas of necrosis surrounded by broad zones of hyperemia. The necrotic area in bacillary hemoglobinuria is usually focal and larger than in Black disease. Bacillary hemoglobinuria causes intravascular hemolysis with anemia and hemoglobinuria.[2]

**Contributing Institution:** NMDA/Veterinary Diagnostic Services, 700 Camino de Salud NE Albuquerque, NM 87106, http://nmdaweb.nmsu.edu/animal-and-plant-protection/veterinary-diagnostic-services

**References:**

1. Jones TC, Hunt RD: Veterinary Pathology, 5th ed., pp. 579-580. Lea Febiger, Philadeplphia, PA, 1983
2. Stalker MJ, Hayes MA: Liver and biliary system. *In:* Pathology of Domestic Animals, ed. Maxie MG, 5th ed., vol. 2, pp. 355-356. Saunders Elsevier, London, UK, 2007
3. Van Vleet JF, Valentine BA: Muscle and tendon. *In:* Pathology of Domestic Animals, ed. Maxie MG, 5th ed., vol. 1, pp. 259-264. Saunders Elsevier, London, UK, 2007

**NOTES:**

The Armed Forces Institute of Pathology
Department of Veterinary Pathology

*Conference Coordinator:*
Todd M. Bell, DVM

WEDNESDAY SLIDE CONFERENCE 2008-2009

# Conference 13

7 January 2009

***Conference Moderator:***

Dr. Don Schlafer, DVM, DACVP, DCVM, DACT, PhD

## CASE I – 42029 (AFIP 3107596)

**Signalment:** Day of birth, gender undetermined, Friesian, *Bos Taurus*, Bovine.

**History:** The mass (figure 1) was attached to the placenta accompanying the assisted delivery of a normal full-term male fetus.

**Gross Pathology:** Attached to the placenta by a 15cm pedicle resembling umbilical cord was a soft, roughly circular (greatest diameter = 15cm) discoid mass with 'aerofoil' shaped cross-section (greatest thickness = 4cm), and weight of 0.316kg. The mass consisted of multiple lobules (0.5-2.5cm diameter) of fragile pink to grey tissue with a slightly granular appearance and without obvious differentiation into fetal tissues or variation in appearance from one lobule to another. Each lobule was surrounded by a thin, translucent external capsule that merged externally with the pedicle **(Fig. 1-1)**.

**Laboratory Results:** NA

**Histopathologic Description:** The discoid mass is formed from multiple lobules whose tissue elements are essentially similar to those of normal cotyledon. However, the villi are more compact, often convoluted and anastomotic, and are separated from adjacent lobules by a discrete but thin fibrous capsule. Although the epithelium is hyperplastic, individual trophoblastic cells are cytologically normal, including many syncytial forms, with bi- and multinucleated forms present. They are attached to a basal lamina overlying the delicate fibrovascular stroma of the villus projections. In some areas, the interstitial region of the lobules is expanded by more extensive loose stroma, which is oedematous. Blood vessels appear normal. Small numbers of lymphocytes and plasma cells are present in the interstitial tissue throughout the mass.

**Contributor's Morphologic Diagnosis:** Placenta: Cotyledonary dysplasia with irregular villus hypertrophy and trophoblastic hyperplasia (trophoblastic non-hydatidiform mole), Friesian, bovine

**Contributor's Comment:** The pedicle consisted of vascular, mesenchymal and epithelial (typical of the urachal extension) elements present in normal umbilical cord, while the similarity of the lobular tissue to chorionic villi of cotyledonary tissue was striking. No maternal elements were identified in any areas of the lesion.

*Sponsored by the American Veterinary Medical Association, the American College of Veterinary Pathologists, and the C. L. Davis Foundation.

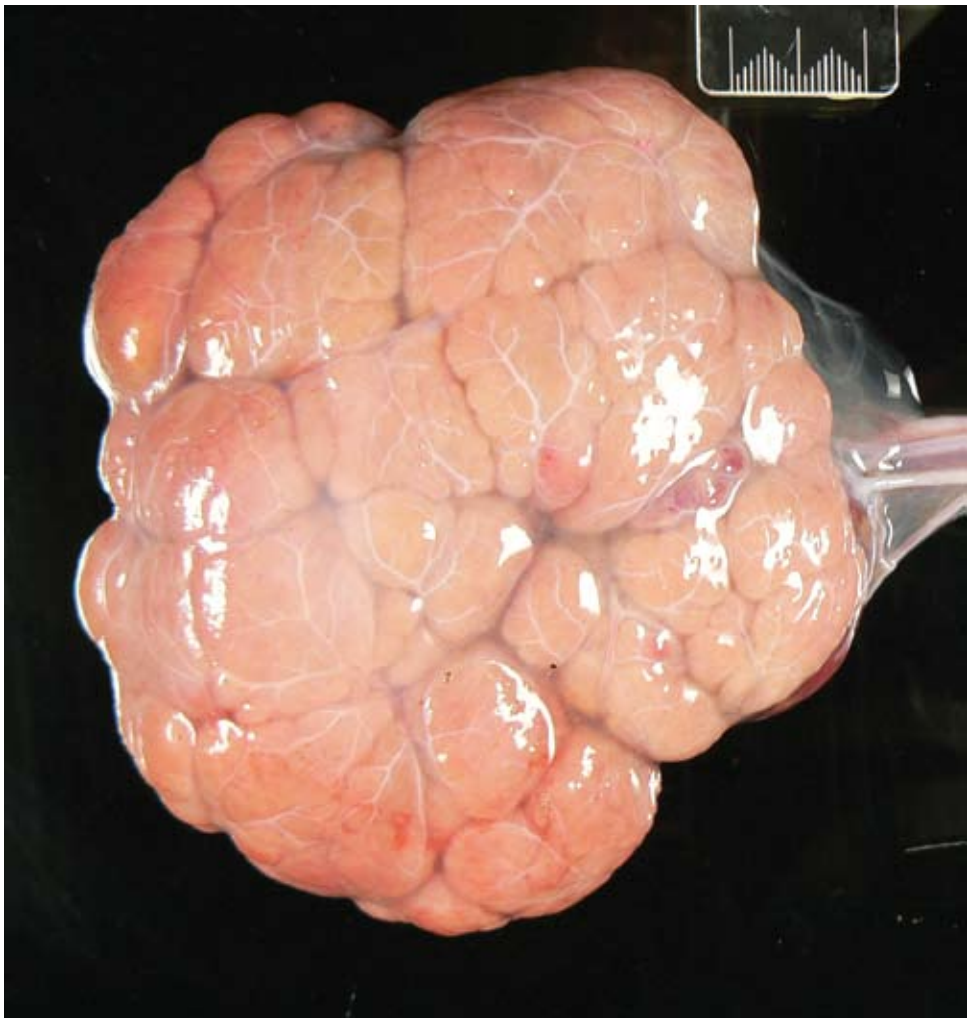

*1-1. Placenta, ox. Discoid mass attached to the placenta by a 15cm pedicle resembling umbical cord.* *Photograph courtesy of Pathobiology Group, Institute of Veterinary, Animal and Biomedical Sciences, Massey University, Palmerston North, New Zealand.*

Mole is a term 'pirated' from the human literature which refers to the gestational trophoblastic diseases that are characterised by formation of an irregular mass of chorionic villi and varying degrees of trophoblastic proliferation, often with disruption of lymphatic drainage and subsequent cystic transformation of the mass.[6] The latter form is referred to as hydatidiform. In bovid species, all forms of moles are rare, with fewer than 10 published reports. All of these reports have been associated with a co-twin and its own placenta.[4,5] The absence of any detectable fetal structures such as skin distinguishes them from the more common amorphous globosus, which is often referred to as a fetal mole.[3]

Two forms of hydatidiform mole have been identified in humans: the complete mole and the partial mole. The former results from fertilisation of an unviable oocyst by one or more sperm. Thus, the genome of a complete hydatidiform mole comes entirely from the paternal side. Greater than 90% of such moles have a 46 XX diploid karyotype.[6] Partial moles, on the other hand, are nearly always triploid and usually result from fertilisation of an haploid ovum either by two sperm, or one sperm which duplicates its genome.[1] The rarity of the bovid condition has prevented similar detailed cytogenetic investigation in cows. In complete trophoblastic moles of humans, because of the absence of a viable maternally derived genome, no viable embryo is produced and no fetal tissues develop. Instead, the paternally derived genome is able to dominate, resulting in excess development of the extra-embryonic tissues, particularly the placenta and its trophoblast. Thus, the mole becomes an hyperplastic mass of trophoblastic tissue.[1]

In humans, 20% of patients with hydatidiform moles can be expected to develop malignant sequelae but such sequelae have not been reported in cattle.

**AFIP Diagnosis:** Placenta: Cotyledonary hyperplasia with irregular villus hypertrophy and trophoblastic hyperplasia (placental hamartoma)

**Conference Comment:** During the extensive conference discussion Dr. Schlafer was hesitant to call this particular lesion a hydatiform mole. Dr. Schlafer and the contributor mentioned the paucity of moles reported in bovids, which added to the speculation that this entity is a true hydatiform mole. A differential list for discrete

placental masses in bovids discussed during the conference included: amorphous globosus, adventitial placentation, and a co-twin that has died.[7]

In the human literature, a hydatiform mole is defined as a cystic swelling of chorionic villi accompanied by trophoblastic proliferation.[2] This description does not quite fit the histologic features of this lesion. The human literature further subdivides these moles into complete and partial moles. Complete moles are characterized histologically by diffusely edematous villi with diffuse trophoblastic hyperplasia, whereas partial moles have a mix of edematous and non-edematous villi with focal trophoblastic proliferation. The contributor mentioned the different karyotypes of these two moles. Because of the lack of female chromosomes, complete moles have no development of fetal parts. In contrast, partial moles can have development of some fetal parts because they have a karyotype with X and Y chromosomes allowing at least partial fetal development.[2]

In human medicine, it is extremely important to classify moles as either complete or partial because complete moles may precede choriocarcinoma.[2]

**Contributing Institution:** Institute of Veterinary, Animal and Biomedical Sciences, Massey University, Palmerston North, New Zealand. Web site:www.massey.ac.nz

**References:**

1. Jauniaux E: Partial moles: from postnatal to prenatal diagnosis. Placenta **20**:379–88, 1999
2. Kumar V, Abbas AK, Fausto N: Robbins and Cotran Pathologic Basis of Disease, 7th ed., pp. 1110. Elsevier Saunders, Philadelphia, PA 2005
3. Long S: Abnormal development of the conceptus and its consequences. *In:* Veterinary Reproduction and Obstetrics, eds. Arthur GH, Noakes DE, Pearson H, Parkinson TJ, 8th ed., pp 129–30. WB Saunders, London, UK, 2001
4. Meinecke B, Kuiper H, Drögemüller C, Leeb T, Meinecke-Tillmann S: A mola hydatidosa coexistent with a foetus in a bovine freemartin pregnancy. Placenta **24**:107–12, 2002
5. Morris FJ, Kerr SM, Laven RA and Collett MG: Large hydatidiform mole: An unusual finding in a calving cow. New Zealand Veterinary Journal (in press).
6. Robboy SJ, Duggan MA, Kurman RJ: The female reproductive system. *In:* Pathology, eds. Rubin E, Farber JL, 2nd ed., pp 967–70. JB Lippincott Company, Philadelphia, USA, 1994
7. Schlafer DH, Miller RB: Female genital system. In: Jubb, Kennedy, and Palmer's Pathology of Domestic Animals, ed. Maxie MG, vol 3., pp. 474-480. Elsevier Limited, Philadelphia, PA, 2007

## CASE II – 08/14596 (AFIP 3106183)

**Signalment:** Male sheep (*Ovis aries*), Dorset poll breed; age not specified

**History:** Accreditation serology for *B. ovis* was inconclusive in this potential breeding animal.

**Gross Pathology:** The animal was euthanized, and its entire genital tract was submitted for evaluation. The tail of the right testicle was noted to be firm and increased in size.

**Laboratory Results:** Cultures for *Histophilus somni, Brucella ovis* were negative. Modified ZN and Gram stains of impression smears made from the gonads indicated large numbers of Gram negative rods in the seminal vesicles. *Actinobacillus seminis* was cultured from both seminal vesicles and ampullae.

**Histopathologic Description:** There is a focal (in some sections multifocal) accumulation of histiocytes and multinucleated giant cells within the epididymal interstitium, surrounded by a collar of lymphocytes and plasma cells admixed with variable neutrophils **(Fig. 2-1)**. In numerous sections, there is distinct mineralization and Splendore-Hoeppli like reaction at the center of the focus (foci). There are myriad fragments of spermatids noted at the center of the foci, often within histiocytes. There is compression of adjacent ducts, which occasionally have hyperplastic epithelium, and there is fibrosis of the interstitial connective tissue. Large numbers of sarcocyts are noted in the cremaster muscle.

**Contributor's Morphologic Diagnosis:** Multifocal or focal (depending on slide) granulomatous epididymitis with necrosis, interstitial fibrosis and epididymal epithelial hyperplasia (sperm granuloma)

**Contributor's Comment:** Spermatic granulomas are relatively common findings in rams [1] and are often associated with other conditions which induce leakage of spermatids into the interstitium. The testicle is an immunologically privileged site, and sperm are highly antigenic, containing cell walls rich in lipids and phospholipids. Epididymitis due to bacterial agents such as *Brucella ovis, Histophilus somni,* and *Actinobacillus*

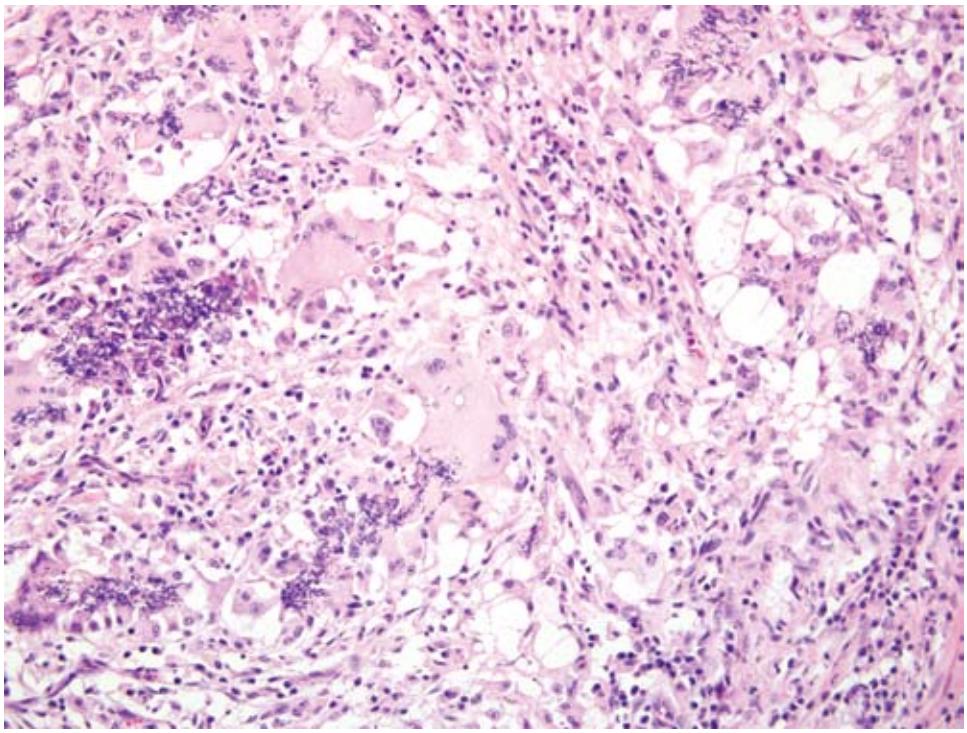

*2-1. Epididymis, sheep. Granulomatous inflammation characterized by numerous epithelioid macrophages, plasma cells, lymphocytes and few multinucleate giant cells. (HE 200X)*

*seminis* often leads to spermatic granulomas as well as agent specific epididymitis and orchitis.

In this particular case, additional sections of epididymis, prostate gland and seminal vesicle displayed mild multifocal accumulations of neutrophils, which were presumed incited by ascending infection of *Actinobacillus seminis*.

**AFIP Diagnosis:** 1. Epididymis: Epididymitis, granulomatous, focally extensive, moderate with a sperm granuloma
2. Epididymis: Epithelial hyperplasia, multifocal, moderate

**Conference Comment:** Dr. Schlafer discussed the anatomy of the epididymis and the importance of grasping the basic anatomic features to help in identifying and understanding the pathogenesis of various entities that affect the male reproductive system.

Sperm are produced within the testes and inside the seminiferous tubules. Sperm travel through a plexus of channels called the rete testes. From the rete testes, numerous small efferent ductules transport sperm to the head of the epididymis. Within the head and body of the epididymis sperm undergo changes that transform them into fertile cells. Sperm traverse the head and body over a period of several days, and eventually reach the tail of the epididymis for storage prior to ejaculation via the ductus deferens.[2] The contributor mentioned the highly antigenic nature of sperm; any release of sperm into the extratubular compartment leads to a foreign body type reaction. This is followed by a strong immune response resulting in an accumulation of large numbers of plasma cells, CD4 and CD8 positive lymphocytes, and an up-regulation of MHC I in epithelial cells. As in the case of a foreign body, a chronic immune response leads to fibrosis and walling off of the lesion. This often leads to spermiostasis, a spermatocele, or a sperm granuloma.[1]

The known causes of sperm granulomas were discussed; they include congenital duct anomalies, adenomyosis, trauma, and infections. Bacteria are implicated most frequently, as mentioned by the contributor, and the route of infection is via ascension from the urethra and accessory sex glands. The immunologically privileged site allows for the organism to proliferate unabated. This often leads to formation of a sperm granuloma and loss of fertility.[1]

There was extensive slide variation with this particular case. The contributor mentioned "distinct mineralization and Splendore-Hoeppli like reaction at the center of the foci" which was not present on all of the submitted slides.

**Contributing Institution:** NSW Department of Primary lndustries, EMAI Regional Veterinary Laboratory Woodbridge Rd, Menangle, 2568 Australia.

**References:**

1. Foster RA, Ladds PW: Male genital system. *In:* Jubb, Kennedy, and Palmer's Pathology of Domestic Animals,

vol 3 ed. Maxie MG, pp. 565-621. Elsevier Limited, Philadelphia, PA, 2007
2. Senger PL: Pathways to Pregnancy and Parturition, 1st ed., pp. 32-57. The Mack Printing Group-Science Press, Ephrata, PA, 1997

## CASE III – Case 1 (AFIP 3103339)

**Signalment:** Tissues are from a 4-year-old, intact male Poodle dog (*Canis familiaris*)

**History: Kennel History:**
The kennel has a 10-11 month history of infertility.
Three stud dogs and 11 bitches.
No litters from March until Jan 27, 2008. (One puppy born to a previously negative bitch was bred to a positive male in Nov. Her most recent *B. canis* test at Cornell for AGID month #2 in kennel eradication.) Tested 14 dogs, Jan 4, 2008, 8 of 14 positive at Cornell by AGID.
Euthanized 5 dogs Jan 30, 2008
Spayed and neutered 2 dogs on Feb 1, 2008 and started on Doxycycline (28 days) and Gentamicin (7 days) unless culture and sensitivity reveal better options.

**Patient History:** Infertility. Small soft testicles with firm epididymis bilateral. Left testicle had a fluid filled lesion on ultrasound. Prostate enlarged, fluctuant and painful, straining to defecate and blood in stool. Mild conjunctivitis.

**Gross Pathology:** Significant findings were restricted to the genital system. The prostate gland is mildly enlarged, but symmetrical. The testicles are atrophied and soft. They are slightly yellow-tan colored and lack normal lobular appearance. The right testicle contains a central, 0.5cm area of cavitation containing exudates or sequestered necrotic tissue. The epididymis (bilateral) is slightly firm, but no gross lesions are noted when incised.

**Laboratory Results:** Bacteriology Results; Aerobic Culture; Tissue: Testicle; Organism ID: *Brucella canis*

**Histopathologic Description:** *Testicles:* There is diffuse, severe atrophy of the seminiferous tubules. In several areas, there are small clusters of remaining tubules that are small, hypocellular and have thickened hyalinized basement membranes. There is no evidence of spermatogenesis. Conspicuous clusters of interstitial cells are present within the testicle. There is diffuse lymphohistiocytic infiltration throughout the parenchyma.

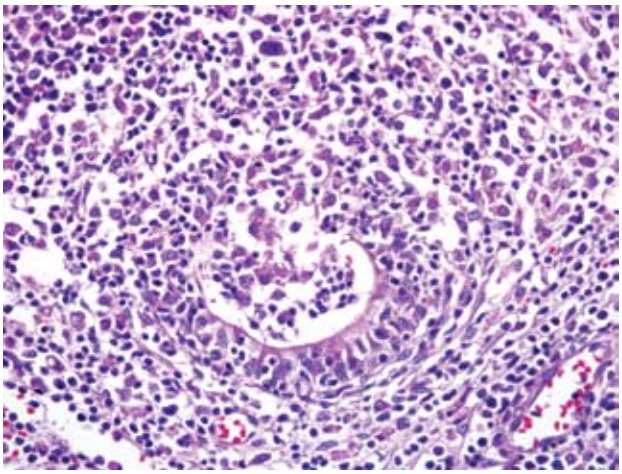

*3-1. Epididymis, dog. Cellular infiltrate composed of numerous lymphocytes, plasma cells, and fewer histiocytes that often transmigrate and segmentally replace ductular epithelium. (HE 400X)*

In addition, there is one cavity containing ischemic necrotic tissue sequestrum surrounded by dense lymphohistiocytic infiltrates.

*Epididymis:* The lesions are similar to those in the testicle with diffuse, dense sheets of lymphohistiocytic cells, atrophic tubules, inflammatory cell infiltrates in tubular walls, plus intense lymphohistiocytic clusters within tubules **(Fig. 3-1)**. There are no spermatids in epididymal tubules.

*Prostate gland:* The majority of the prostate gland examined is composed of hyperplastic acini lined with a single layer of tall, plump columnar epithelium with abundant eosinophilic cytoplasm. An occasional small lymphoid nodule is present within the interstitium of these areas. Within one lobe, there is marked acinar atrophy with reduction in the number of acini and diffuse, dense sheets of lymphocytes, plasma cells and macrophages. The remaining acinar walls are moderately infiltrated with primarily lymphocytes.
*** Sections submitted will contain either testicle, testicle and epididymis, or prostate gland.

**Contributor's Morphologic Diagnosis:** Testicles: Orchitis, lymphohistiocytic, chronic, severe, diffuse with marked seminiferous tubular atrophy and focal necrosis **(Fig. 3-2)**
Epididymis: Epididymitis, lymphohistiocytic, chronic, severe

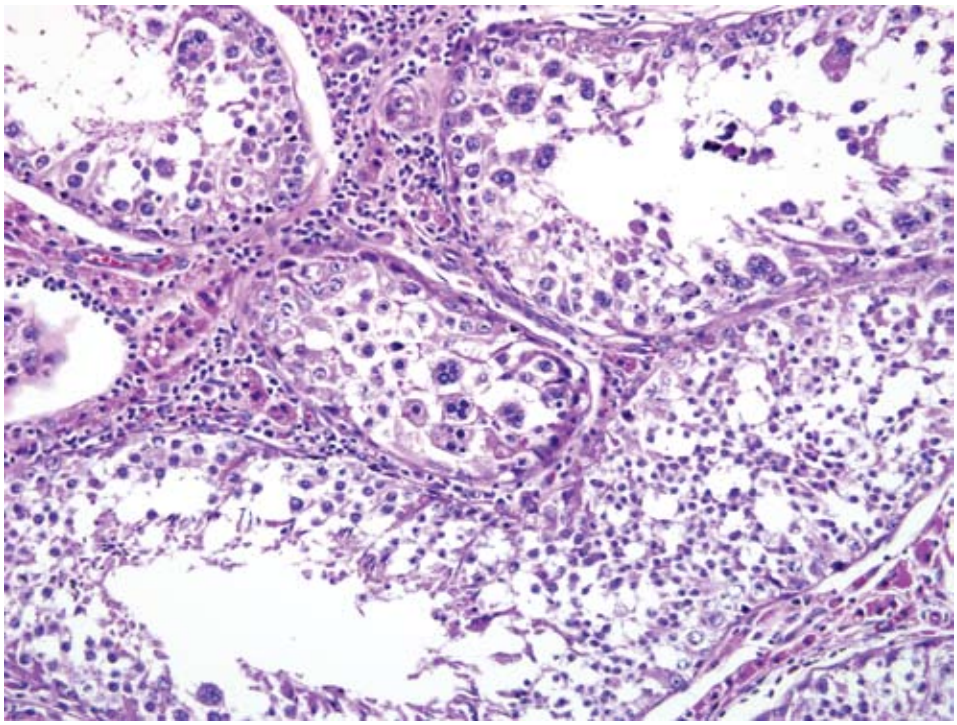

*3-2. Testicle, dog. Seminiferous tubules are degenerative characterized by thickened and undulating basement membranes, paucity of germinal cells, vacuolation and loss of Sertoli cells, and numerous intraluminal multinucleate cells. Lymphoplasmacytic inflammation expands the interstitium and surrounds tubules (HE 200X)*

**Contributor's Comment:** This case represents one of several dogs seen from the same kennel with a history of infertility. Most of the patients either tested positive for *Brucella canis* by agar gel immunodiffusion or yielded positive bacterial cultures from either epididymis/testes, lymph nodes or prostate glands. In the male reproductive system, the classic appearance of canine brucellosis is a severe epididymitis that is accompanied by varying degrees of testicular atrophy. Inflammation of the testicles (orchitis) is infrequently seen. Therefore, the unique feature of this case is the level of inflammation/destruction in the testicle. When orchitis occurs secondary to *B. canis*, it can be severe and characterized by primarily lymphoplasmacytic infiltrates with destruction of seminiferous tubules and occasional foci of necrosis.[1,3] Inflammation can extend into the vaginal tunic with draining ulcers from the scrotum.[3]

Brucellosis in dogs has been described with *B. melitensis*, *B. suis, B. abortus* and *B. canis*; however, only *B. canis* is considered epidemiologically significant.[4] *B. canis* has been reportedly recovered from just about every bodily fluid and/or surface: vaginal secretions, semen, abortuses, milk, urine, saliva, ocular secretions and feces.[4] The organism is transmitted through venereal and/or oral routes. Following entry, the organism is taken up by the mononuclear-phagocytic system and distributed to the lymphoid and genital compartment where the organisms multiply.[4] Bacteremia develops and proliferation of the organism in the target organs results in the lesions typical of the disease: uterine infection and abortion in females, epididymitis and prostatitis in males, lymphadenitis, discospondylitis, anterior uveitis, dermatitis, meningoencephalitis (refer to nice flow chart, pg. 197 of Ref. #4). Diagnosis is achieved through serology, agglutination tests, agar gel immunodiffusion, ELISA, and immunofluorescence; however, definitive diagnosis can only be made through retrieval of the organism from bacterial culture.[4] Treatment is difficult, in part because of the intracellular nature of the organism. Many different drugs and drug combinations have been tried, but no combination has been found to be 100% effective.[4] Combination drug treatments have shown better efficacy than single antibiotic therapies.[4] Lastly, *B. canis* has zoonotic potential. The incidence of human infections is not known.[4] People contract the disease through contact with the organism shed during abortions or in research laboratories where people work directly with the organism.[4]

**AFIP Diagnosis:** 1. Testicle: Orchitis, lymphohistiocytic, chronic, diffuse, severe, with marked seminiferous tubular atrophy and loss, and interstitial cell hyperplasia
2. Epididymis: Epididymitis, lymphohistiocytic, chronic, diffuse, severe
3. Epididymis: Epithelial hyperplasia, diffuse, marked

**Conference Comment:** Considerable time was spent discussing the changes within the interstitial cell

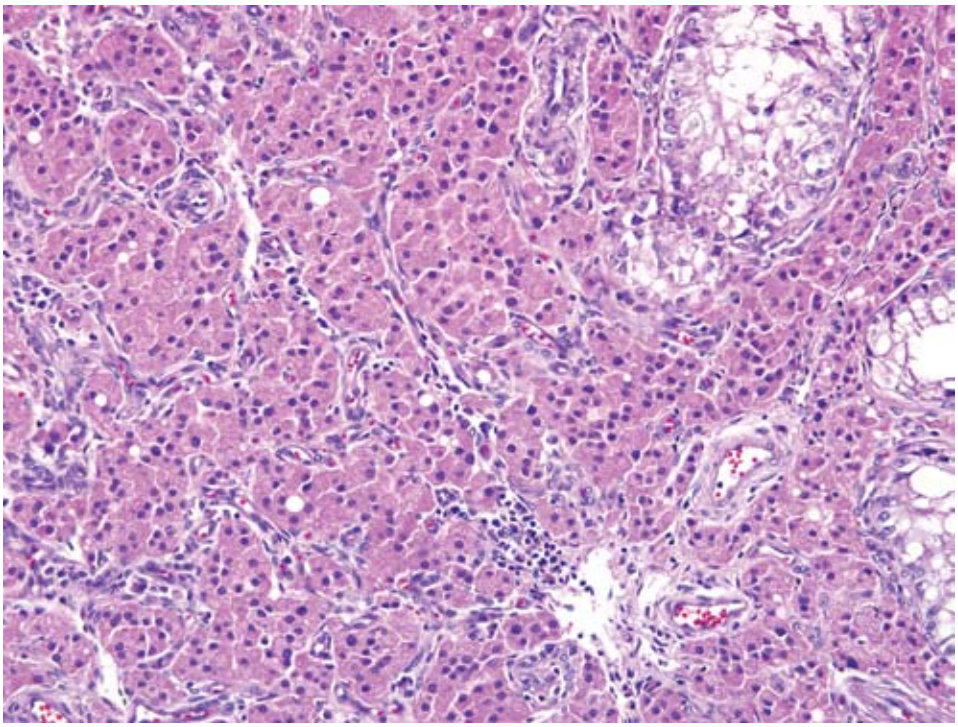

*3-3. Testicle, dog. Iinterstitial hyperplasia markedly expands the interstitium and separates and surrounds degenerate seminiferous tubules. (HE 200X)*

population **(Fig. 3-3)**. Dr. Schlafer and the attendees discussed the proliferation of interstitial cells and debated hyperplasia versus neoplasia. The contributor mentioned a "conspicuous cluster of interstitial cells" when describing the proliferation, and at the end of the conference considerable disagreement still existed as to whether this change represented interstitial cell hyperplasia or an interstitial cell tumor.

Abortions caused by *B. canis* are normally late gestational abortions that occur after 50 days. As seen in this case, the usual sequelae to *B. canis* infection in male dogs is epididymitis and testicular degeneration. This often causes severe scrotal irritation and affected dogs often focus on this discomfort and lick the area until it is ulcerated. Lymphadenopathy of the mandibular and retropharyngeal lymph nodes is common. Placental lesions consist of necrosis of chorionic villi with a plethora of bacteria within infected trophoblastic cells. Infected females often discharge copious amounts of foul vaginal secretions after abortion, which is an excellent means of disease transmission. Fetal lesions are fatal and include pneumonia, endocarditis, and hepatitis.[2]

*Brucella canis* is caused by a mucoid strain of *Brucella* that is similar to *Brucella suis*. Because of its mucoid nature, *B. canis* lacks surface antigens that *B. abortus* and *B. melitensis* have, thus rendering conventional test methods ineffective.[2]

**Contributing Institution:** Oklahoma Animal Disease Diagnostic Laboratory and Center for Veterinary Health Sciences, Oklahoma State University, Stillwater, OK. www.okstate.edu

**References:**

1. Gleiser CA, Sheldon WG, VanHoosier GL, Hill WA. Pathologic changes in dogs infected with a *Brucella* organism. Lab Anim Sci. **21**:540-545, 1971
2. Schlafer DH, Miller RB: Female genital system. *In:* Jubb, Kennedy, and Palmer's Pathology of Domestic Animals, ed. Maxie MG, vol. 3, pp. 484-489. Elsevier Limited, Philadelphia, PA, 2007
3. Schoeb TR, Morton B: Scrotal and testicular changes in canine brucellosis: a case report. J Am Vet Med Assoc. **172**:598-600, 1978
4. Wanke, MM: Canine brucellosis. Anim Reprod Sci. **82-83**:195-207, 2004

## CASE IV – 04-26927 (AFIP 2937766)

**Signalment:** Four-year-old, female, Labrador retriever, canine (*Canis familiaris*)

**History:** The patient was presented for a routine ovariohysterectomy.

**Gross Pathology:** The ovary was gray and shriveled.

**Laboratory Results:** None

**Histopathologic Description:** None

**Contributor's Morphologic Diagnosis:** Ovarian ganglioneuroma

**Contributor's Comment:** Neoplasms and hyperplasias of ganglionated plexuses outside the central nervous system are called ganglioneuromas and ganglioneuromatosis, respectively.[1-4] These lesions are rare and have been reported in a steer [2], a horse [1], a cat, and dogs.[3,4] They are composed of variably sized neurons, nerve fibers, and connective tissue stroma. Ganglioneuromas tend be solitary, unencapsulated but well demarcated masses. Mitotic figures are rare or absent. There are no reports of metastasis.[4] Ganglioneuromatoses tend to segmental, infiltrative and involve all layers of the intestine.[2] In human beings, ganglioneuromatosis has been associated with multiple endocrine neoplasia.

Diagnosis can be confirmed by a variety of methods to include transmission electronmicroscopy (TEM), histochemistry, and immunohistohemistry. TEM reveals dense core vesicles in ganglion cells and neuronal processes. Umyelinated axons are encased by Schwann cells. Histochemical stains for axons and myelin reveal that nerve fibers are nonmyelinated. Immunohistochemical stains revel that ganglion cells are positive for NSE and Schwann cells are positive for S-100 and vimentin. Nerve fibers are positive for neurofilament protein.[4]

Neurogenic tumors of the canine ovary have not been described. The nerve supply to the ovary is via a sympathetic plexus that accompanies the ovarian vessels. This relationship may explain the numerous small vessels enmeshed in the tumor.

**AFIP Diagnosis:** Ovary: Teratoma, favor monodermal variant

**Conference Comment:** Our differential diagnosis for this neoplasm included ganglioneuroma and central nervous tissue component of teratoma. Ganglioneuromas consist of large ganglion cells separated by fusiform

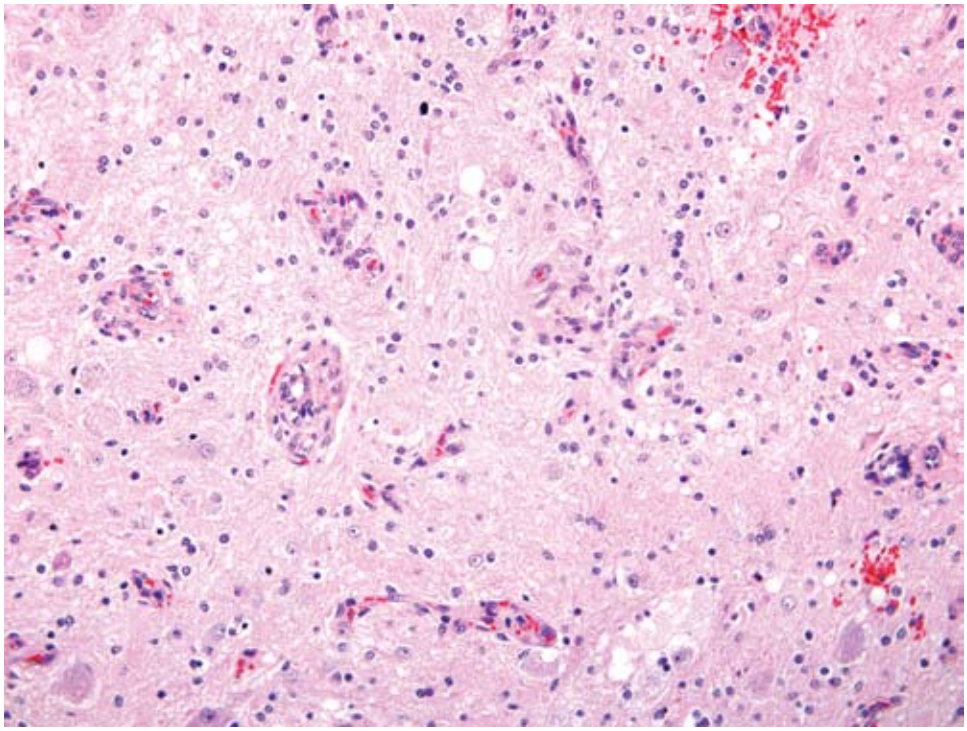

*4-1. Ovary, dog. The neoplasm is composed of neuroectodermal tissue which recapitulates neural tissue characterized by neuropil, neurons and glial cells. (HE 400X)*

Schwann cells and collagen. The neurons in the present case were separated by a felt-like background of cellular processes resembling neuropil; this neuropil also contained cells resembling oligodendrocytes and astrocytes. We interpret this as central nervous tissue differentiation rather than peripheral nervous tissue differentiation, and therefore the neoplasm is consistent with the central nervous tissue component of teratoma. Differentiation along other embryonic cell layers is not evident in the sections examined during conference. Examination of other regions of the tumor is needed to confirm that differentiation along other embryonic layers is not present. Pathologists from the AFIP Departments of Gynecologic and Breast Pathology, Neuropathology, and Soft Tissue Pathology concurred with the diagnosis.

Although teratomas are usually defined as neoplasms composed of tissue derived from at least two germinal layers [6], occasional ovarian tumors may be composed of cells from only one layer. In humans, these tumors are derived predominately or exclusively of endodermal or ectodermal tissue and are referred to as monodermal teratomas.[7] Rarely these neoplasms are composed almost exclusively of neuroectodermal tissue, including astrocytes, oligodendroglial cells, and ganglion cells.[7] Arguably such tumors may be hamartomas rather than true neoplasms.

**Contributing Institution:** liggett@tifton.uga.edu

**References:**

1. Allen D, Swayne D, Belknap JK: Ganglioneuroma as a cause of small intestinal obstruction in the horse: A case report. Cornell Vet **79**:133-141, 1989
2. Cole DE, Migaki,G, Leipold HW: Colonic ganglioneuromatosis in a steer. Vet Pathol **27**:461-462, 1990
3. Fairley, McEntee MF: Colorectal ganglioneuromatosis in a young female dog (Lhasa Apso). Vet Pathol **27**:206-207, 1990
4. RibasJL,KwapienRP,PopeER:Immunohistochemistry and ultrastructure of intestinal ganglioneuroma in a dog. Vet Pathol **27**:376-379, 1990
5. Schlafer DH, Miller RB: Female genital system. *In:* Jubb, Kennedy, and Palmer's Pathology of Domestic Animals, vol 3 ed. Maxie MG, pp. 450-456. Elsevier Limited, Philadelphia, PA, 2007
6. MacLachlan NJ, Kennedy PC: Tumors of the genital systems. *In:* Tumors in Domestic Animals, ed. DJ Meuten, 4th ed., p. 554. Blackwell, Ames, IA, 2002
7. Scully RE, Young RH, Clement PB: Monodermal Teratomas. *In:* Atlas of Tumor Pathology, Tumors of the Ovary, Maldeveloped Gonads, Fallopian Tube, and Broad Ligament, ed. J Rosai, Third series, Fascicle 23, pp. 285-306, Armed Forces Institute of Pathology, Washington, DC, 1996

**NOTES:**

The Armed Forces Institute of Pathology
Department of Veterinary Pathology

*Conference Coordinator:*
Todd M. Bell, DVM

WEDNESDAY SLIDE CONFERENCE 2008-2009

# Conference 14

14 January 2009

*Conference Moderator:*

Dr. Bruce Williams, DVM, Diplomate ACVP

## CASE I – Case 05-2373 (AFIP 3026964)

**Signalment:** Twelve-week-old female Chihuahua dog (*Canis familiaris*)

**History:** This puppy presented for evaluation of non-responsive hypoglycemia of several weeks duration. She subsequently developed diarrhea. On presentation blood glucose was 38 mg/dL (73-116), total protein was 2.6 g/dL (5.5-7.2), albumin was <1.0 g/dL (2.8-4) and PCV was 18%. Coccidial oocysts were found on fecal flotation and therapy was initiated. The puppy deteriorated over the next two days and eventually died.

**Gross Pathology:** The examined puppy was in decreased nutritional condition (BCS 1.5/5) with moderately to markedly reduced subcutaneous and intra-abdominal adipose tissue. There was scant adipose tissue present in the peri-renal mesentery and within the coronary groove of the heart. The stomach contained a small amount of tan mucoid ingesta, the small intestines segmentally contained scant beige pasty ingesta and there was no fecal material present in the colon. No other remarkable gross lesions were present.

**Laboratory Results:** None

**Histopathologic Description:** Jejunum: Diffusely there is marked blunting and fusion of villi **(Fig. 1-1).** The lamina propria is expanded by a cellular infiltrate composed of numerous neutrophils, lymphocytes, plasma cells, and macrophages that multifocally extend into the submucosa. Multifocally crypts are distended and filled with similar inflammatory cells admixed with pyknotic and karyorrhectic debris (crypt abscesses). Segmentally along villi there are small aggregates of 1x2 um bacilli that are intimately attached to the apical tips of enterocytes **(Fig. 1-2)**. Multifocally crypts are filled with aggregates of spirochete bacteria. Free in the lumen of the jejunum and attached to the apical surface of remaining villous epithelium are scattered 3-6um diameter round, amphophilic protozoal organisms (cryptosporidium) **(Fig. 1-3).**

**Contributor's Morphologic Diagnosis:** Diffuse, severe neutrophilic and lymphoplasmacytic enteritis with intralesional bacilli, cryptosporidia and spirochetes

**Contributor's Comment:** This puppy suffered from a severe, malabsorptive protein-losing enteropathy secondary to multiple pathogens. The most pathogenic organism in this case is likely enteroadherent (attaching-effacing) *Escherichia coli*. These bacteria are categorized as enteropathogenic *E. coli* (EPEC) and colonize the

*Sponsored by the American Veterinary Medical Association, the American College of Veterinary Pathologists, and the C. L. Davis Foundation.

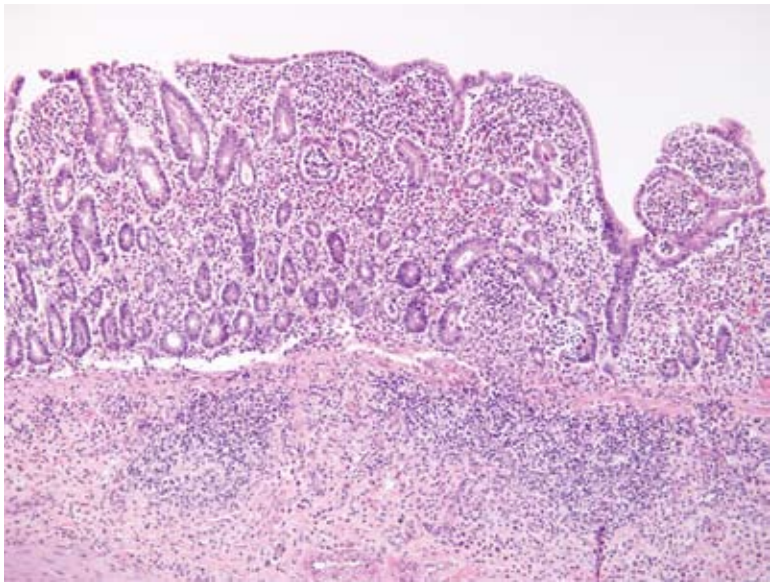

*1-1. Small intestine, dog. Diffuse atrophy, blunting, and fusion of the villi with severe crypt loss. (HE 100X)*

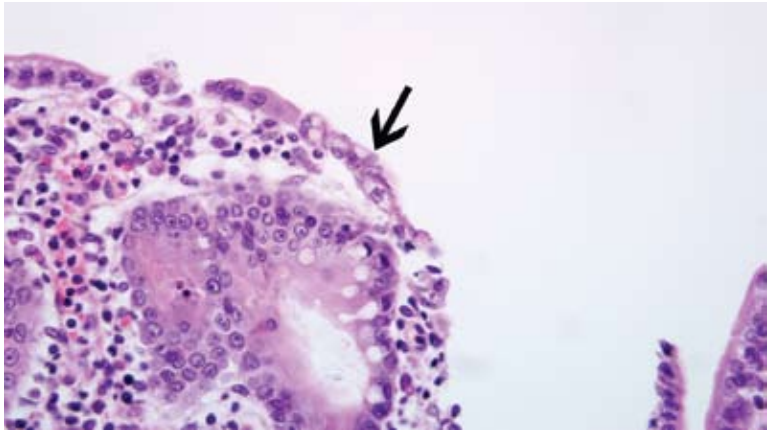

*1-2. Small intestine, dog. Multifocally adherent to the enteric mucosa are small numbers of 2-6 micron round apicomplexan schizonts and gamonts (arrow). Crypts contain numerous helical bacteria which measure approximately 1x8 microns (arrowhead). (HE 400X)*

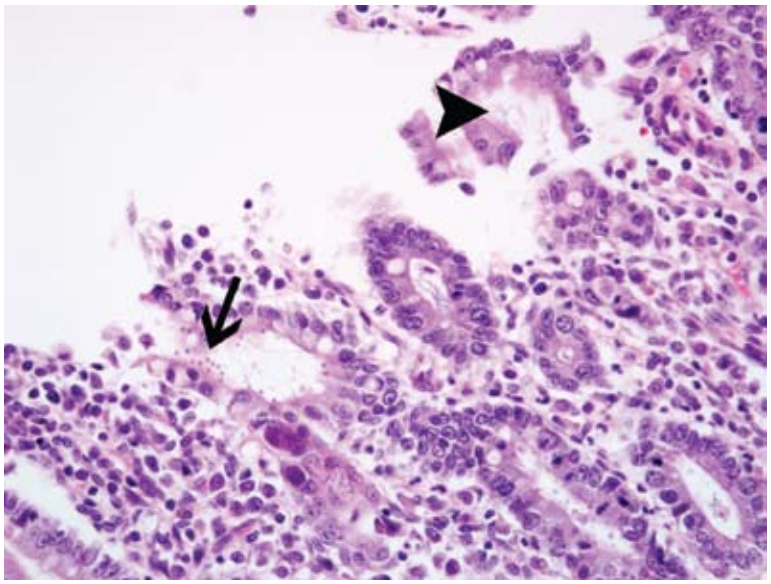

*1-3. Small intestine, dog. Randomly attached to the villar epithelium are small aggregates of robust bacilli which measure up to 2x3 microns (arrow). (HE 400X)*

mucosa by a nonpilus adhesion termed EPEC adhesive factor.[1] Concurrent infection with cryptosporidium and coccidia has been reported in an immunosuppressed puppy and they were considered opportunistic pathogens.[6] Cryptosporidium in dogs is seldom reported in the United States and typically occurs in immunosuppressed puppies. *Cryptosporidium parvum* and *C. canis* have been isolated from naturally infected dogs.[4] There was prominent lymphoid depletion present in the spleen and mesenteric lymph nodes, indicating this puppy was likely immunosuppressed secondary to viral infection or a primary underlying immunosuppression. There were no lesions of parvovirus or distemper.

No coccidial organisms were seen in multiple sections of intestine; however, there may have been low numbers of organisms due to the previous treatment. The numbers of spirochete bacteria are impressive in this case, but they are not a primary pathogen and this likely represents secondary opportunistic overgrowth. Weakly beta-haemolytic intestinal spirochaetes identified as *Brachyspira pilosicoli* have been isolated from puppies and dogs with diarrhea.[3,5] *Brachyspira canis* has been isolated from clinically healthy dogs, suggesting it is a commensal organism. [5]

**AFIP Diagnosis:** Small intestine (jejunum): Enteritis, subacute, diffuse, severe, with marked villus atrophy, fusion, and blunting, crypt necrosis and loss, and attaching bacilli, apicomplexans and intracrypt helical bacteria

**Conference Comment:** There are several different types of *E. coli* that affect domestic species and each type has virulence characteristics that manifest as varying disease entities. "Enteropathogenic" *E. coli* (EPEC) attaches to the mucosa and causes a malabsorptive diarrhea. Some strains of EPEC do not produce toxins, but they do cause blunting and fusion of villi with subsequent diarrhea. The nomenclature for *E. coli* can be extremely confusing, and this type of *E. coli* is also known as "enteroadherent" *E. coli* (EAEC), and "attaching and effacing" *E. coli.*[2]

EPEC attaches to a host enterocyte via long fimbria and subsequently releases proteins known as adhesins to form a secure attachment to the surface epithelium. Translocated intimin receptor, another protein produced by EPEC, is transported from the bacteria into the host cell. This causes a conformational change in the host cell's cytoskeleton. The affected enterocyte forms a "pedestal-like structure" beneath the bacteria and this unfortunate cell also loses its surface microvilli. The pathogenicity of EPEC is largely determined by the density of organisms on the surface of enterocytes. As the contributor mentioned, co-infections are common and lead to a much worse clinical picture. Bacterial attachment is most prolific in the distal small intestine and large intestine. Profuse diarrhea with EPEC results from a combination of maldigestion and malabsorption.[2]

**Contributing Institution:** Department of Population Health and Pathobiology, North Carolina State University College of Veterinary Medicine, 4700 Hillsborough St. Raleigh, NC 27606 www.cvm.ncsu.edu

**References:**

1. Barker IK, Van Dreumel AA, Palmer N: The alimentary system. *In:* Pathology of Domestic Animals, eds. Jubb KVF, Kennedy PC, Palmer N, vol. 2, 4th ed., pp. 200-213. Academic Press, Philadelphia, PA, 1993
2. Brown CC, Baker DC, Barker IK: Alimentary system. *In:* Jubb, Kennedy, and Palmer's Pathology of Domestic Animals, ed. Maxie MG, vol 2 ed., pp. 183-193. Elsevier Limited, Philadelphia, PA, 2007
3. Manabe M, Suenaga I, Ogawa Y, Adachi Y: *Brachyspira pilosicoli* isolated from two beagles and one mongrel in Japan. J Vet Med Sci. **66**(5):589-92, 2004
4. Miller DL, Liggett A, Radi ZA, Branch LO: Gastrointestinal cryptosporidiosis in a puppy. Vet Parasitol. **115**(3):199-204, 2003
5. Oxberry SL, Hampson DJ: Colonisation of pet shop puppies with *Brachyspira pilosicoli*. Vet Microbiol. **93**(2):167-74, 2003
6. Willard MD, Bouley D: Cryptosporidiosis, coccidiosis, and total colonic mucosal collapse in an immunosuppressed puppy. J Am Anim Hosp Assoc. **35**(5):405-9, 1999

## CASE II – G07-120059 (AFIP 3106379)

**Signalment:** Juvenile, female, Mahogany, (*Mustela vison*), mink

**History:** Farmed mink from a ranch with 9700 kits are experiencing reduced feed intake, increased mortality in this season's juveniles (averaging 10 deaths per week, recently up to 10 deaths per day). This ranch was cleaned and restocked 1.5 years ago. Kits are vaccinated with a four-way vaccine (against botulism, distemper, mink enteritis virus, *Pseudomonas aeruginosa*) at 10 weeks of age; no Aleutian disease testing has been done since restocking.

**Gross Pathology:** This female mink exhibited pulmonary congestion and edema, splenic enlargement

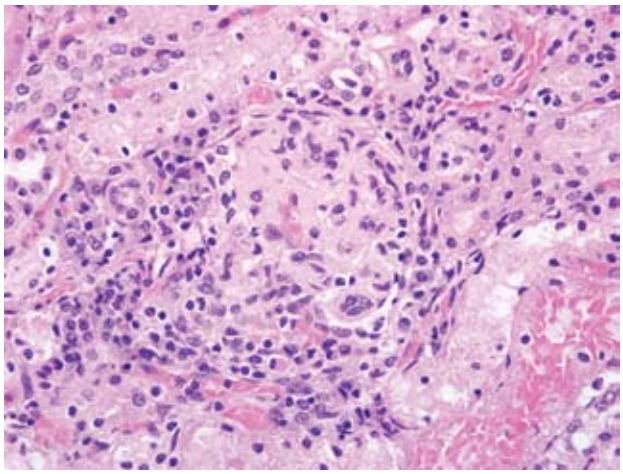

*2-1. Kidney, mink. Multifocally, the cortical perivascular interstitium is expanded by a cellular infiltrate which occasionally surrounds, separates, or replaces tubules and glomeruli. (HE 40X)*

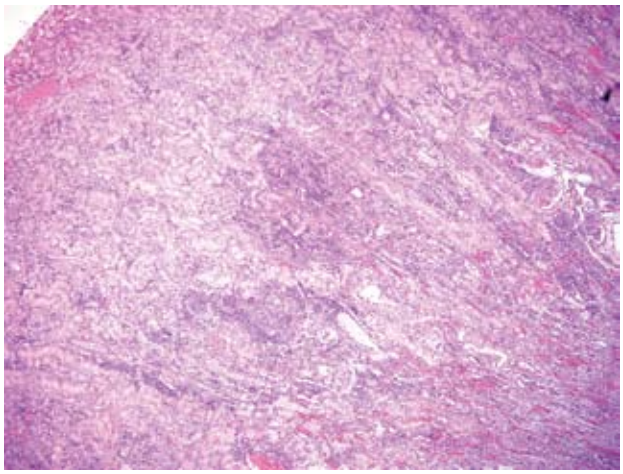

*2-2. Kidney, mink. There is increased cellularity of the glomerular tufts with glomerular and periglomerular infiltrate of low numbers of neutrophils, macrophages, and lymphocytes; the mesangial matrix is expanded by a homogenous eosinophilic material. (HE 400X)*

and an empty gastrointestinal tract on gross postmortem.

**Laboratory Results:** Seven of eight serum samples submitted tested POSITIVE for Aleutian disease parvovirus antibodies by counterimmunoelectrophoresis (CIE). Spleen tissue from this mink tested positive for Aleutian disease parvovirus by PCR.

**Histopathologic Description:** Kidney: Glomeruli throughout the section exhibit a variety of lesions, including increased cellularity of the glomerular tuft with segmental to diffuse mesangial hyperplasia and hyalinization, and thickened glomerular basement membranes and Bowman's capsules **(Fig. 2-1)**. Some glomeruli are obsolescent. There are prominent interstitial infiltrates of plasma cells and lymphocytes, with associated tubular degeneration **(Fig. 2-2, 2-3)**. Many tubules contain protein or cellular casts. Occasional small to medium-sized arterioles display fibrinoid necrosis of vessel walls, with infiltrating inflammatory cells and cuffs of mixed inflammatory cells **(Fig. 2-4)**.

Urinary bladder: Arteries within the muscular wall and adjacent mesentery are surrounded by thick concentric cuffs of mixed inflammatory cells, including macrophages, plasma cells, neutrophils and eosinophils. There is fibrinoid necrosis of the vessel walls, some with infiltrating inflammatory cells.

**Contributor's Morphologic Diagnosis:**
Generalized, segmental to diffuse glomerulonephritis
Interstitial nephritis
Necrotizing arteritis, kidney, urinary bladder

**Contributor's Comment:** The histologic lesions in this case are compatible with Aleutian disease. This diagnosis is supported by the positive serology testing and confirmed by PCR. Aleutian disease, a chronic progressive disease of mink caused by the Aleutian disease parvovirus, is considered the most important disease affecting mink production worldwide, causing increased early kit mortality and chronic disease with high mortality in juveniles and adults.[3] Disease severity and development of lesions is dependent on the age and genetics of the mink, and the virulence of the strain of infecting virus.[2] While kits succumb to interstitial pneumonia and respiratory failure, the chronic form of the disease is result of immune complex glomerulonephritis and vasculitis, and death is usually a result of renal failure. The humoral immune response plays a direct role in the pathogenesis of Aleutian disease.[1] Antiviral antibody can be detected as early as five days post-infection, with development of a marked, progressive polyclonal hypergammaglobulinemia. While antibody can have a partially protective role via viral neutralization and incomplete restriction of virus replication in ACV-infected mink kits, it does not prevent infection. In older animals, antiviral antibody is thought to exacerbate disease through a variety of mechanisms, including antibody-dependent enhancement of infection (where antibody bound to virus facilitates viral entry into macrophages via Fc receptors; Fc receptor binding stimulates IL-10 production, which inhibits interferon signaling, promotes antibody production

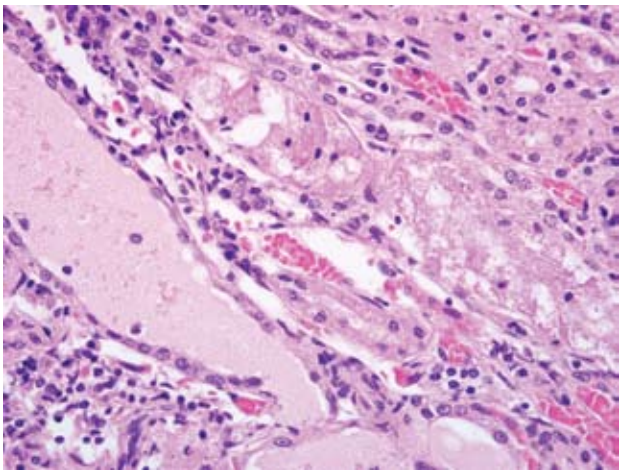

*2-3. Kidney, mink. The walls of small vessels contain abundant brightly eosinophilic proteinaceous material, cellular debris, and low numbers of neutrophils and lymphocytes which occasionally occludes vessel lumens (fibrinoid necrosis). Perivascular interstitium is expanded by moderate numbers of neutrophils, lymphocytes, plasma cells, and histiocytes. (HE 400X)*

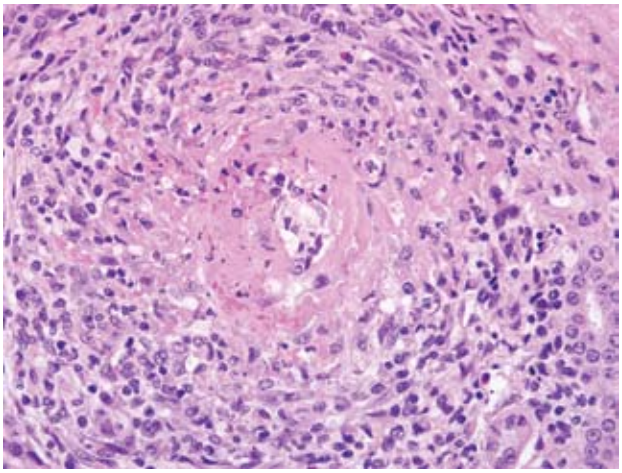

*2-4. Kidney, mink. Multifocally, renal tubule epithelia are attenuated, degenerative, or necrotic, and tubules are often ectatic and contain a brightly eosinophilic proteinaceous material. (HE 400X)*

and suppresses cytotoxic T-cell-mediated killing of virus-infected cells), and formation and tissue deposition of immune complexes, with subsequent development of immune-complex vasculitis and glomerulonephritis.

**AFIP Diagnosis:** Kidney: Glomerulonephritis, membranoproliferative and necrotizing, diffuse, moderate with multifocal necrotizing arteriolitis, subacute interstitial nephritis, and rare protein casts

**Conference Comment:** Aleutian disease was first reported in 1956 in Aleutian mink homozygous for the gene that is responsible for their steel- blue color. Mink and ferrets are susceptible to Aleutian mink disease (ADV). Genetic susceptibility plays a major role in ADV infections. Mink homozygous for the autosomal recessive Aleutian gene are more severely affected by ADV often resulting in death. ADV can cause disease in other types of mink ranging from death to subclinical infection.[2]

During the conference discussion Dr. Williams stated that the lesions in this case were quite striking and more severe than most cases of ADV he has seen. As the contributor mentioned, kits get an interstitial pneumonia, and type II pneumocytes are the primary site of replication leading to death of infected cells and a fulminant pneumonia with death. Rarely intranuclear inclusions are found in pneumocytes, and severe cases of pneumonia can lead to alveolar hyaline membrane formation.[1] Infection of adults leads to an insidious chronic form with splenomegaly, lymphadenopathy, hypergammaglobulinemia, and acute interstitial nephritis.[1] Chronic disease causes death via uremia and kidney failure.[3]

Gross lesions in the chronic form include ulceration of the mouth, tongue, footpad, and stomach secondary to uremia.[3] Histologic lesions in the chronic form are impressive and consist of lymphoplasmacytic interstitial nephritis, marked glomerulonephritis, and a necrotizing vasculitis of the small and medium sized arteries.[3]

**Contributing Institution:** Animal Health Laboratory, University of Guelph, Guelph, Ontario, Canada
http://ahl.uoguelph.ca

**References:**

1. Best, SM, Bloom, ME: Pathogenesis of Aleutian mink disease parvovirus and similarities to B19 infection. J Vet Med B **52**:331-334, 2005
2. Hadlow WJ, Race RE, Kennedy RC: Comparative pathogenicity of four strains of Aleutian disease virus for pastel and sapphire mink. Infect Immun **41**:1016-1023, 1983
3. Hunter DV: Aleutian Disease. *In:* Mink biology, health and disease, eds. Hunter DB, Lemieux N, pp. 8-21 – 8-26. University of Guelph, ON, 1996

## CASE III – 06-34302 (AFIP 3027307)

**Signalment:** 3-week-old female miniature donkey, (*Equus asinus*)

**History:** Found in recumbency, treated with IV fluids and antibiotics. Brown urine was discharged shortly before death.

**Gross Pathology:** The lungs were edematous. Several ulcers up to 5mm length were present in the squamous mucosa of the stomach. The urinary bladder contained brown urine.

**Laboratory Results:** Liver selenium concentration was 0.7 ug/g (reference range 0.7-2.0 ug/g); liver Vitamin E concentration was < 2.5 ug/g (reference range 15.0-25.0 ug/g).

**Histopathologic Description:** There is diffuse to segmental degeneration and necrosis of skeletal muscle fibers, characterized by fragmentation of fibers and condensation of the sarcoplasm into hypereosinophilic coagulum with loss of cross striations **(Fig. 3-1)**. There is eosinophilic, granular to fibrillary debris within the fibers and extending into the interstitium around the affected fibers. Rarely, macrophages or satellite cells surround affected fibers.

**Contributor's Morphologic Diagnosis:** Skeletal muscle myofiber degeneration

**Contributor's Comment:** Nutritional myopathy was diagnosed in this donkey foal based on the muscle lesions and extremely low concentration of vitamin E in the liver. Selenium concentration in the liver was in the low normal range. Nutritional myopathy usually occurs in young animals on diets deficient in selenium and/or vitamin E, with or without the conditioning factors such as an excessive quantitiy of polyunsaturated fatty acids in the diet.[5] Vitamin E is an antioxidant that prevents oxidative damage to sensitive membrane lipids by decreasing hydroperoxide formation.[3] Selenium is an essential component of the enzyme glutathione peroxidase (GSH-PX). GSH-PX catalyzes the breakdown of hydrogen peroxide and other organic hydroperoxides produced by glutathione during the process of redox cycling.

Microscopic lesions similar to those in skeletal muscle were also present in the heart of this donkey, but were more mild. Granular eosinophilic material compatible with hemoglobin or myoglobin was present in tubular lumens of the kidney. This material is most likely myoglobin released from the affected skeletal muscle fibers. Although gross lesions were not detected in the heart or skeletal muscle of this foal, pale areas in the heart and skeletal muscle can be observed in cases of nutritional myopathy of foals, however is not always observed.[7] Degenerate muscle may be very difficult

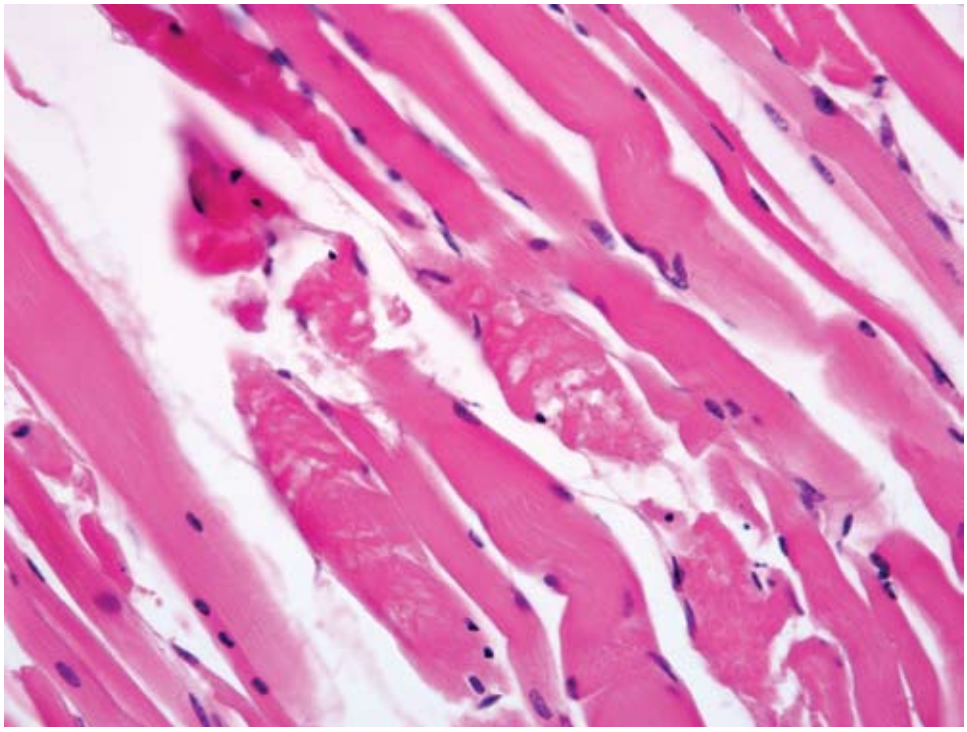

*3-1. Skeletal muscle, donkey. Multifocally, there is random individual myocyte degeneration characterized by sarcoplasmic swelling, pallor, and vacuolization, or myocyte necrosis characterized by sarcoplasmic hypereosinophilia, loss of cross-striations, fragmentation, pyknosis, and karyorrhexis. (HE 400X)*

to detect grossly when it is uncalcified, and is likely to escape detection.[3] Mineralization of muscle fibers is not always present in cases of nutritional myodegeneration in foals.[7]

There were approximately 50 female donkeys in this herd, with this being the only donkey diagnosed with nutritional myopathy, although foals had died in previous years with similar signs. The female donkeys were fed brome grass hay year-round, never being pastured on green grass, or supplemented with vitamins or minerals. Green, growing forages should provide adequate vitamin E as α-tocopherol, but the vitamin E content is greatly reduced in grass that is dried for hay. Mature plants contain less α-tocopherol than younger plants, and mature grass cut for hay can have loss of up to 80% of the tocopherols when dried in the sun for 4 days.[1] Plasma vitamin E status of horses is highest from May to August when fresh grass is being grazed and lowest when horses are fed harvested or stored feed during the same period.[2]

**AFIP Diagnosis:** Skeletal muscle: Degeneration and necrosis, multifocal, moderate

**Conference Comment:** Differentials for this lesion in horses were discussed during the conference and included white muscle disease, capture myopathy, exertional rhabdomyolysis, and toxic myopathy due to toxic plants and ionophores. Nutritional myopathy causes a polyphasic, multifocal lesion in affected muscle while ionophore toxicity causes monophasic, multifocal lesion thus allowing for microscopic differentiation of these two conditions.[6]

Nutritional myopathy is common in calves, lambs, swine, and foals.[6] It can be caused by a lack of dietary intake of vitamin E or selenium or from competitive binding of selenium by copper, zinc, silver, or tellurium. Foods high in polyunsaturated fats such as fish require intake of more vitamin E to minimize oxidative damage from the metabolic processing of these foods.[6]

Vitamin E and selenium are important in preventing damage from free radicals from both within and from outside the cell. Free radicals are molecules with an odd number of electrons produced during normal cell functions or from tissue radiation, drug reactions, or inflammation. Free radicals are highly reactive molecules that can cause damage to mitochondria, endoplasmic reticulum, or the cytosol via damage to important cellular proteins or peroxidation and damage of cellular lipid membranes. When cellular membranes are damaged, ion gradients can not be properly maintained. Extracellular calcium moves into the cytosol and the cell responds by attempting to protect calcium-sensitive myofilaments by pushing calcium into mitochondria. Mitochondria quickly accumulate excess calcium and lose their ability to produce energy for the cell. Myofibrils exposed to leaking calcium hypercontract leading to degeneration and necrosis of myofibers.[6]

The attached table provides a non-comprehensive list of diseases considered to be associated with an imbalance or deficiency in either selenium or vitamin E.

| | |
|---|---|
| Cattle | Nutritional myopathy<br>Retention of fetal membranes |
| Horse | Nutritional myopathy |
| Swine | Mulberry heart disease<br>Hepatosis dietetica<br>Exudative diathesis<br>Iron hypersensitivity<br>Nutritional myopathy<br>Anemia |
| Sheep | Nutritional myopathy<br>Infertility<br>Poor growth potential |
| Dogs | Intestinal liposfuscinosis |
| Cats; mink; birds; pigs; rabbits; reptiles | Steatitis (yellow fat disease) |
| Chickens and Turkeys | Encephalomalacia (superficial cerebellar hemorrhage – crazy chick disease) |

[4,5]

**Contributing Institution:** Kansas State University, http://www.vet.k-state.edu/depts/dmp/

**References:**

1. Ballet N, Robert JC, Williams PEV: Vitamins in forages. *In:* Forage Evaluation in Ruminant Nutrition, eds., Givens DI, Owen E, Axford RFE, Omed HM, pp. 399-43. CABI Publishing, New York, NY, 2000
2. Blakley BR, Bell RJ: The vitamin A and vitamin E status of horses raised in Alberta and Saskatchewan. Can Vet J **35**:297-300, 1994
3. Hulland TJ: *In:* Pathology of Domestic Animals, eds., Jubb JVF, Kennedy PC, Palmer N, pp. 228-234. Academic Press, Inc. San Diego, CA, 1993

4. Jones TC, Hunt RD, King NW: Nutritional deficiencies. *In:* Veterinary Pathology, 6th ed, pp. 789-794, Williams and Wilkins, Baltimore, MD, 1997
5. Radostits OM, Gay CC, Blood DC, Hinchcliff KW: Veterinary Medicine. *In:* A Textbook of the Diseases of Cattle, Sheep, Pigs, Goats and Horses, pp. 1515-1533. WB Saunders Company, London, 2000.
6. Van Vleet JF, Valentine BA: Muscle and tendon. *In:* Jubb, Kennedy, and Palmer's Pathology of Domestic Animals, vol 1 ed. Maxie MG, pp. 236-243. Elsevier Limited, Philadelphia, PA, 2007
7. Wilson TM, Morrison HA, Palmer NC, Finley GG, van Dreumel AA: Myodegeneration and suspected selenium/vitamin E deficiency in horses. J Am Vet Med Assoc **169**:213-217, 1976

## CASE IV – 07-52047 (AFIP 3096747)

**Signalment:** 21-month-old spayed female border collie, (*Canis familiaris*) dog

History: The dog lived near Tampa, Florida and was maintained in a fenced yard containing a small area of marshy terrain. The presenting history included progressive lameness, pain, and subcutaneous edema of the right forelimb. Over an eight-week period, the dog developed worsening fever, dyspnea, mature neutrophilia, and hypoproteinemia that did not respond to symptomatic treatment or antibiotic therapy. The skin of the right axilla and forelimb contained several well defined areas of deep red discoloration overlying 1-3 cm diameter, fluctuant subcutaneous nodules that extended into subjacent soft tissues. Radiographs revealed linear areas of radiolucency in the soft tissue of the right shoulder region. Surgical pathology of a nodule revealed fibroplasia and chronic panniculitis. Later, a surgical incision into a nodule of the right axilla revealed a 2-cm diameter cystic cavity containing coiled aggregates of many (>10) intact and fragmented white worms ranging from 10-30 mm in length and 2-4 mm in width. The dog was treated with praziquantel (generic, Phoenix Scientific, Vedco, 20mg/kg PO SID x 5 days) and fenbendazole (Panacur®, DPT Laboratories, Intervet, 50 mg/kg PO SID x 3 days), in addition to antibiotics. Upon identification of the worms as plerocercoids (spargana) of a pseudophyllidian tapeworm, anthelmentic therapy was changed to cefpodoxime proxetil (Simplicef®, Pfizer, 2.5 mg/kg PO SID x 10 days), metronidazole (generic, PLIVA, Inc, 24 mg/kg PO BID x 7 days), and fenbendazole (100 mg/kg, PO, BID). Praziquantel (Praziject, IVX Animal Health, Inc., 50 mg/kg SQ divided among six sites) was given once a week for 3 weeks. After two weeks of clinical improvement, new nodules developed over the ventral chest, neck, right axillary region, and these encompassed cystic spaces containing many spargana. A right pleural cavity effusion developed, and approximately 500 ml of cloudy serosanguinous fluid were removed by thoracocentesis. Complete blood count and serum biochemical profile revealed mild anemia, normal WBC with mild monocytosis, and moderate hypoalbuminemia. Bacterial culture and sensitivity of the fluid identified *Pseudomonas aeruginosa*, and enrofloxacin therapy (Baytril®, Bayer, 3.5 mg/kg PO BID) was initiated. Praziquantel (Biltricide®, Bayer) was administered at 30 mg/kg PO SID for 8 days. Within two weeks, the dog developed a peritoneal exudate. The dog's overall condition continued to deteriorate and the owners authorized euthanasia and necropsy.

**Gross Pathology:** The subcutis and intermuscular fascia of the right forelimb, right axilla, ventral thoracic midline, and ventral cervical region contained many inflammatory tissue cysts filled with nodules of entangled intact and fragmented ribbon-shaped white larval cestodes (spargana) surrounded by red, cloudy, thick fluid **(Fig. 4-1)**. There was severe atelectasis of the right lung, and the right pleural cavity contained about 150 ml of thick, cloudy, tan fluid with two larval cestodes and scattered white, friable fragments. There was partial atelectasis of the left lung, and the left pleural cavity contained about

*4-1. Skeletal muscle, dog. Forming a cyst within subcuticular skeletal muscle are multiple cestode larvae. Photograph courtesy of the Department of Pathobiology, College of Veterinary Medicine, Auburn University, Auburn, Alabama.*

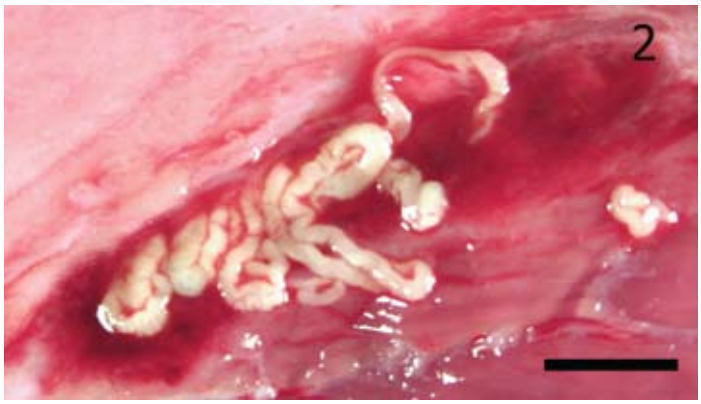

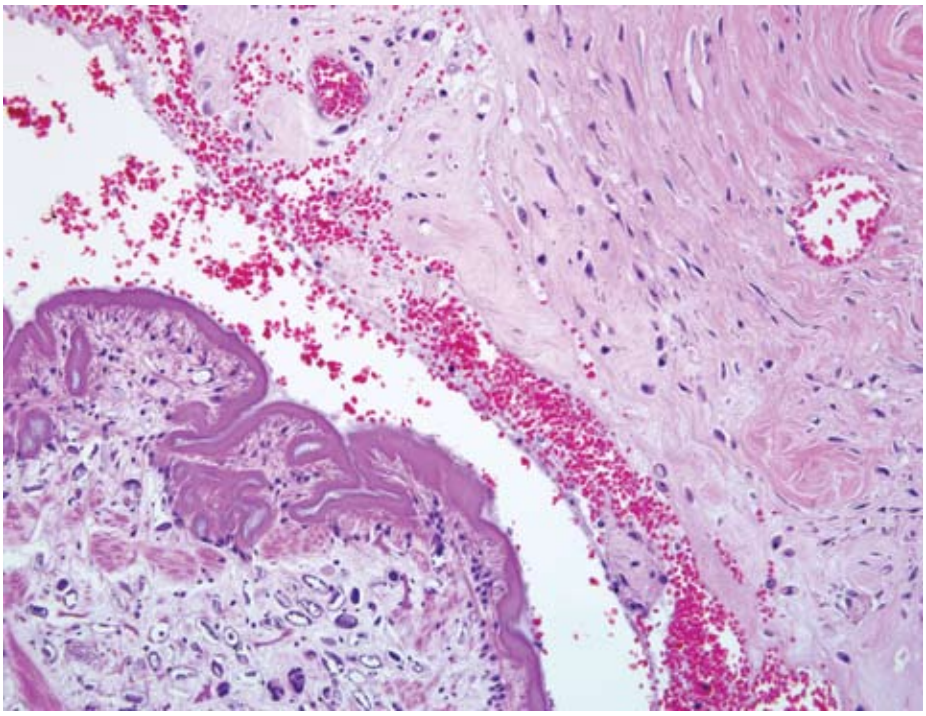

*4-2. Skeletal muscle and subcutis, dog. The cestode larva is characterized by a 7-10 micron thick tegument with small fibrilated projections (microtriches), a spongy parenchymous body cavity without a pseudocoelom, a row of somatic cell nuclei immediately subjacent to the tegument, numerous calcareous corpuscles, and numerous tortuous branching invaginations of the tegument (excretory ducts). The cyst wall is composed of fibrous connective tissue admixed with moderate amounts of hemorrhage and fibrin, and low numbers of neutrophils, eosinophils, macrophages, and lymphocytes bounded by large amounts of granulation tissue. (HE 200X)*

100 ml of cloudy tan fluid with several free-floating larval cestodes. Microscopic examination of the pleural fluid after Wright-Giemsa staining revealed many bacteria both extracellularly and within neutrophils. The peritoneal cavity contained about 250 ml of red cloudy fluid in the caudoventral region containing many bacteria and segmented neutrophils. There were many fibrous adhesions between the omentum and serosal surfaces of the small intestine, spleen, and stomach. At least two larval cestodes were present in the peritoneal fluid.

**Laboratory Results:** Samples of the parasites were submitted to the Diagnostic Parasitology Service, Department of Pathobiology, College of Veterinary Medicine, Auburn University for identification. The worms were identified as larval cestodes (plerocercoids or spargana) of a pseudophyllidian tapeworm, most likely, *Spirometra* sp. Nucleic acids were extracted from intact, frozen spargana with a robotic extractor (Maxwell® 16, Promega Corporation) and used as template in PCR of an 18S rDNA fragment employing eucestode primers 84 and 90 as previously described.[7] Amplicons were sequenced (courtesy of Dr. Susan E. Little and M.D. West, Oklahoma State University) using an ABI3730 capillary sequencer and the sequence compared to those previously reported from *Spirometra erinacei* (D64072), *Diphyllobothrium latum* (AM778553), *Mesocestoides corti* (AF286984), and *Taenia solium* (DQ157224). Sequence of the spargana from this dog (EU392209) most closely resembled (99.4% identical) that previously reported from *Spirometra erinacei*, a pseudophyllidian cestode.

**Histopathologic Description:** Tissues from the skin and soft tissues of the right axilla are submitted. The deep dermis and subcutis of haired skin contain a parasitic cyst with a wall comprised of fibrous connective tissue and a lumen partially filled with larval cestodes, blood, fibrin, and proteinaceous fluid **(Fig. 4-2)**. Macrophages and neutrophils are rare in the region of the cyst, and there is congestion of surrounding vasculature. The larval cestodes lack discernible scolices or suckers and have shallow invaginations of the deeply eosinophilic tegument, resulting in segmentation and formation of tortuous parenchymal cavities (excretory ducts) filled with intensely eosinophilic granular substance. Microtriches occasionally project from the surface of the tegument. Columnar cells (subtegumentary cells) are often located in a parallel row beneath the tegument. The larval body is comprised of a fine fibrillar stroma with many calcareous corpuscles and a few striated muscle fibers, sometimes arranged as loose bundles beneath the tegument. The overlying skin is characterized by hyperkeratosis, epidermal atrophy, follicular keratosis, dermal edema, and venous congestion.

**Contributor's Morphologic Diagnosis:** Tissue from right axilla: Subcutaneous parasitic cyst, with intralesional larval cestodes and mild focal granulomatous panniculitis

**Contributor's Comment:** The progressive disease in this young adult dog was attributed to proliferative sparganosis, caused by proliferating larval cestodes (spargana) of the organism *Sparganum proliferum*.[9,12] The spargana were widely distributed throughout the subcutis and intermuscular fascia of the cranial half of the body, the pleural cavities, and the peritoneal cavity. Morbidity resulted from widespread parasitism and septic pleuritis and peritonitis due to *Pseudomonas aeruginosa* infection. Bacteria were presumably introduced through tracts established by the encysted parasites.

Sparganosis is a disease characterized by the presence of larval pseudophyllidian cestodes in the host's tissues.[13] Tapeworms may be characterized in tissue sections by the absence of a digestive tract, the presence of a thick layered cuticle with a basement membrane, the presence of calcareous corpuscles, and evidence of a segmented body. [4] Plerocercoid larvae are usually solid, club-shaped forms in which scolices and suckers are absent.

Spargana were located in tissue cysts. In histologic sections, there is abundant space around individual spargana (arrows) and the discernible capsule (C) is comprised of eosinophilic amorphous material and relatively few inflammatory cells. Spargana are characterized by invaginations of the tegument resulting in segmentation. Columnar subtegumentary cells form a row beneath the densely eosinophilic tegumentary syncytium, which is covered by a row of dense microtriches. The body is comprised of evenly distributed loose parenchyma with calcareous corpuscles (arrowheads), muscle fibers (M), and excretory ducts (E). Muscle fibers are loosely arranged in a discontinuous row that is oriented parallel to the tegument. Scolices or suckers are not evident.

There are two forms of sparganosis: non-proliferative and proliferative.[7,10] Most infections are of the non-proliferative type associated with the presence of a single larva of either *Spirometra erinaceieuropaei* or *Spirometra mansonoides*. Proliferative sparganosis is caused by the asexual replication of larvae of *Sparganum proliferum* in host tissues and the migration of these larvae to new tissues where they grow and repeat the process, ultimately resulting in the death of the host.[3] In 2001, *Sparganum proliferum* was identified phylogenetically as a new species in the order Pseudophyllidea.[9] The first human infection by *S. proliferum* in the United States was reported in 1908.[14] Infection by *S. proliferum* has been reported in cats, dogs, and feral hogs, but this appears to be the first case of canine proliferative sparganosis in North America.[1-3,6]

The life cycle of *S. proliferum* has not yet been confirmed [12] but probably resembles that of other members of a related pseudophyllidian tapeworm, *Spirometra* spp. Adult tapeworms reside in the intestinal tract of a carnivorous definitive host, where they shed operculated eggs in the feces following discharge from the uterine pore of adult tapeworms. The operculated eggs then hatch in water, releasing a ciliated intermediate form (coracidium). The coracidium is ingested by the first intermediate host, a copepod crustacean (*Cyclops* sp.), where it develops into the procercoid stage. After the infected copepod is ingested by any one of a broad array of possible second intermediate hosts (any vertebrate other than a fish), the procercoids develop into plerocercoids (spargana) and migrate throughout the soft tissues of the body. If the second intermediate host is eaten by another non-fish vertebrate serving as a transport host, the plerocercoids migrate through the tissues but may remain as plerocercoids. The larval *Spirometra* can infect and survive in a series of transport hosts until finally consumed by a carnivore definitive host.[7] The ova are released from the uterine pore and are evident in the host's feces 10-30 days after infection.[1,6,7,11] Infection of the dog can occur through three different ways: ingestion of contaminated water, direct infection of open wounds with plerocercoids, or ingestion of plerocercoids in intermediate vertebrate hosts [11,12] Due to its requirement for an aquatic primary intermediate host, clinical disease is usually associated with exposure to aquatic environments. Sparganosis is zoonotic; thus, precautions should be made to block human infection by preventing consumption of infected water and insufficiently cooked fish or game, or the application of infected medicinal poultices to wounds. It is interesting to note that the first human case of proliferative sparganosis in North America was reported in 1908 in a Florida resident living in the same geographic region as the current canine case.[14]

Currently, there are no products labeled for treatment of *Spirometra* spp infections.[7] The lack of treatment options for proliferative sparganosis warrants a poor prognosis for survival. Infection of dogs is best controlled by preventing the consumption of infected water or the ingestion of vertebrates that could serve as secondary intermediate hosts.

**AFIP Diagnosis:** Skeletal muscle: Rhabdomyositis and panniculitis, pyogranulomatous and eosinophilic, focally extensive, mild with encysted larval cestodes

**Conference Comment:** The contributor did an outstanding job of describing this parasite in depth and in full, so this comment will focus on distinguishing trematodes from cestodes and some common larval forms of cestodes found in domestic animals.

Adult cestodes are normally present in the intestine of

the final host with larval forms present in tissue or body cavities of unfortunate intermediate hosts. Cestodes are split into segmented sections called proglottids that contain both female and male reproductive organs. Both larval and adult cestodes have suckers on their anterior end that may also have hooks depending on the species of cestode.[5]

Several types of cystic larval cestodes are often seen in tissue sections, and these include cysticercoids, cysticercus, coenurus, and the hydatid cyst. Cysticercoids are tiny larvae with a very small bladder and scolex that is encircled by parenchymous tissue. Cysticercus can be identified by a bladder with an inverted neck and scolex that always has four suckers. Coenurus is very similar in appearance to cysticercus but has more than one scolex. Hydatid cysts have a bladder with large numbers of very small scolices. [5]

In tissue section trematodes and cestodes look very similar, but to the trained eye they can be differentiated by a few key features. Both cestodes and trematodes are described as having a spongy parenchyma with no body cavity. Cestodes lack a digestive tract in contrast to trematodes which are endowed with one. Cestodes have calcareous corpuscles which are basophilic clear corpuscles of unknown function. Trematodes are devoid of calcareous corpuscles.[5] These features can help to delineate these two similar appearing parasites.

**Contributing Institution:** Department of Pathobiology, College of Veterinary Medicine, Auburn University, Auburn, AL. (http://www.vetmed.auburn.edu/index.pl/patho)

**References:**

1. Bengtson SD, Rogers F: Prevalence of sparganosis by county of origin in Florida feral swine. Vet Parasitol **97**:239-242, 2001
2. Beveridge I, Friend SC, Jeganathan N, Charles J: Proliferative sparganosis in Australian dogs. Aust Vet J **76**:757-759, 1998
3. Buergelt CD, Greiner EC, Senior DF: Proliferative sparganosis in a cat. J Parasitol **70**:121-125, 1984
4. Chitwood M, Lichtenfels J: Parasitological Review: Identification of Parasitic Metazoa in Tissue Sections. Experimental Parasitology **32**:407-519, 1972
5. Gardiner CH, Poynton SL: An Atlas of Metazoan Parasites in Animal Tissues. Armed Forces Institute of Pathology, Washington DC, 1999
6. Gray ML, Rogers F, Little S, Puette M, Ambrose D, Hoberg EP: Sparganosis in feral hogs (*Sus scrofa*) from Florida. J Am Vet Med Assoc **215**:204-208, 1999
7. Little S, D A: Spirometra Infection in Cats and Dogs. Compendium on continuing education for the practicing veterinarian *22*:299-306, 2000
8. Mariaux J: A molecular phylogeny of the eucestoda. J Parasitol *84*:114-124, 1998
9. Miyadera H, Kokaze A, Kuramochi T, Kita K, Machinami R, Noya O, Alarcon de Noya B, Okamoto M, Kojima S: Phylogenetic identification of *sparganum proliferum* as a pseudophyllidean cestode by the sequence analyses on mitcochondrial COI and nuclear sdhB genes. Parasitology International **50**:93-104, 2001
10. Moulinier R, Martinez E, Torres J, Noya O, de NBA, Reyes O: Human proliferative sparganosis in Venezuela: report of a case. Am J Trop Med Hyg **31**:358-363, 1982
11. Mueller JF: The biology of Spirometra. J Parasitol **60**:3-14, 1974
12. Nakamura T, Hara M, Matsuoka M, Kawabata M, Tsuji M: Human proliferative sparganosis. A new Japanese case. Am J Clin Pathol **94**:224-228, 1990
13. Noya O, Alarcon de Noya B, Arrechedera H, Torres J, Arguello C: *Sparganum proliferum*: an overview of its structure and ultrastructure. Int J Parasitol **22**:631-640, 1992
14. Stiles W: The occurance of a proliferating cestode larva (*sparganum proliferum*) in a man in Florida. Bulletin of the Hygienic Laboratory **40**:7-18, 1908

**NOTES:**

The Armed Forces Institute of Pathology
Department of Veterinary Pathology

*Conference Coordinator:*
Todd M. Bell, DVM

WEDNESDAY SLIDE CONFERENCE 2008-2009

# Conference 15

28 January 2009

*Conference Moderator:*

Michael H. Goldschmidt, BVMS, MRCVS, DACVP

## CASE I – T8944-07 (AFIP 3102252)

Signalment: 2-year-old female neutered Siamese cat, feline, (*Felis catus*)

**History:** The cat was presented to the clinician with a 9 month history of prednisolone treatment due to a diagnosis of food hypersensitivity. The skin of the dorsum resembled wet tissue paper and was sensitive to touch. From the left and right thigh, blood vessels were directed towards the lesion. The practitioner excised a 13 x 4 x 0.3 cm skin sample, which showed several tears and detachment of the dermis from the panniculus **(Fig. 1-1)**. The sample was fixed in formalin and routinely processed for histopathological evaluation.

**Gross Pathology:** None

**Laboratory Results:** None

**Histopathologic Description:** Haired skin: The main lesion is a complete lack of subcutaneous adipose tissue which is replaced by a large clear cleft, extending throughout the whole tissue sample and leading to dermo-hypodermal separation. Collagen fibres in this area have a torn and stretched appearance. The epidermis consists of only one or two layers of partly flattened keratinocytes, interpreted as severe epidermal atrophy **(Fig. 1-2)**, and is covered by a layer of lamellar eosinophilic material (lamellar orthokeratotic hyperkeratosis). Superficial and periadnexal dermis show a perivascular to interstitial infiltrate composed of moderate numbers of lymphocytes, less macrophages, neutrophils and mast cells, and a few eosinophils and plasma cells. Around vessels of the superficial vascular plexus there are moderate numbers of extravasated erythrocytes (haemorrhage). Dermal collagen is extremely attenuated and shows a pale staining in H&E stained sections. Adnexal structures demonstrate a complete lack of anagen hair follicles, and the perifollicular fibrous sheaths of many telogen follicles are thickened. Sebaceous glands are decreased in size and number, interpreted as atrophy. Follicular infundibula are extended and filled with large amounts of an eosinophilic lamellar material (infundibular hyperkeratosis).

**Contributor's Morphologic Diagnosis:** 1. Skin and subcutis: Severe atrophy of epidermis and the subcutaneous panniculus with cleft formation, consistent with feline acquired skin fragility syndrome, Siamese cat, feline
2. Skin: Subacute suppurative dermatitis, superficial and perivascular, mild

*Sponsored by the American Veterinary Medical Association, the American College of Veterinary Pathologists, and the C. L. Davis Foundation.

*1-1 Haired skin, cat. There are multifocal tears which extend through the diffusely thin epidermis and dermis to the level of the panniculus with minimal associated hemorrhage.* *Photograph courtesy of Institut fuer Veterinaer-Pathologie, Universitaet Giessen, Giessen, Germany.*

**Contributor's Comment:** Different disease entities are described in man and animal species with an obvious fragility of the skin. Ehlers-Danlos syndrome (syn. collagen dysplasia, dermatosparaxia, cutaneous asthenia, cutis hyperelastica) as a congenital disease with abnormal collagen synthesis has been described in man, cattle, sheep, dogs, cats, mink and rabbits.[4] In man, six main types of the disease are defined due to biochemical, clinical and molecular studies.[7] In addition to skin lesions abnormal collagen synthesis leads to alterations in ligaments, joints, blood vessels and cardiac valves. In cats with Ehlers-Danlos syndrome skin lesions occur predominantly as cutaneous asthenia or dermatosparaxia. In contrast to other species a remarkable joint laxity is not typical in cats.[4]

Recently in man the usage of the term "dermatoporosis" has been presumed for skin lesions in aged people. In this syndrome an increased fragility of the skin is attributed to age-related alterations of the extracellular matrix metabolism.[6] A primary form due to aging or unprotected sun exposure and an iatrogenic form (after corticosteroid administration) are distinguished.

An ectodermal dysplasia with a congenital skin fragility syndrome due to a mutation in the desmosomal protein plakophilin 1 has been reported in man.[2]

Feline acquired skin fragility syndrome is a rare disease with marked skin lesions of multiple etiologies but without a genetic background. The syndrome has been reported only in cats. It has been noted in combination with several other diseases, such as diabetes mellitus, cholangiocarcinoma or hepatic lipidosis, and administration of different drugs.[4,5,8] Most commonly the syndrome is associated with iatrogenic or naturally occurring hyperglucocorticism.[5] There is one report of acquired skin fragility syndrome associated with phenytoin treatment. Since phenytoin inhibits collagen synthesis in vitro the authors assume that cats could acquire collagen disorders during treatment with phenytoin.[1]

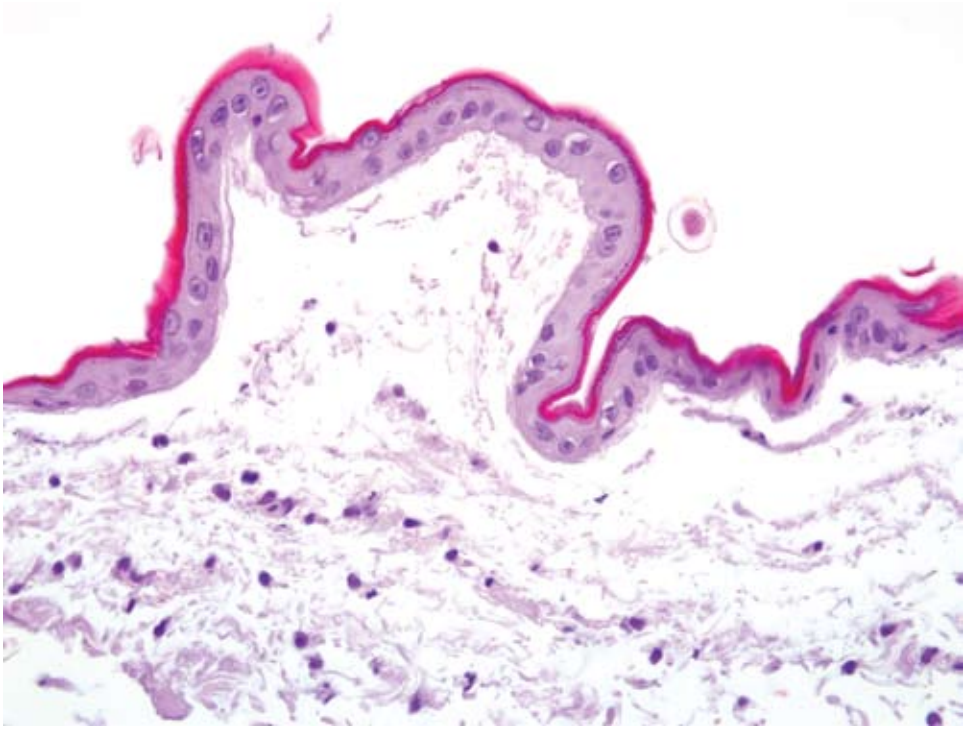

*1-2 Haired skin, cat. The markedly thin epidermis in some areas is only one cell layer thick. There is a paucity of dermal adnexa and collagen, and existing collagen fibers vary greatly in thickness. (HE 400X)*

Clinical features of acquired skin fragility syndrome are striking. Affected cats show markedly thin skin which tears with minor trauma and commonly leaves great flaps of loose skin. The lesions are most commonly seen at the back. Partial alopecia occurs in most affected regions.[5]

Differential diagnosis is not problematic since the lesions are typical. The patients normally are middle-aged or older and compared to Ehlers-Danlos syndrome the skin is abnormally thin but without evidence of hyperextensibility.[5] Histologically the lesions in Ehlers-Danlos syndrome and feline acquired skin fragility syndrome are similar or indistinguishable.[4]

To confirm the histopathologic diagnosis, Masson's trichrome stain was performed due to described staining abnormalities (abnormal collagen fibers, presence of segmental red staining defects, birefringence of polarized light).[3] Unfortunately fiber abnormalities are not limited to acquired skin fragility syndrome. Similar alterations can also be seen in cutaneous asthenia.[3] In our case no staining abnormalities were detectable.

**AFIP Diagnosis:** Skin: Epidermal and dermal atrophy, diffuse, marked with follicular atrophy and loss, dermal clefting, and mild subacute dermatitis

**Conference Comment:** Dr. Goldschmidt concentrated on the gross and histologic features of this disease during the discussion and described ways to differentiate feline acquired skin fragility syndrome from Ehlers-Danlos syndrome (EDS) both grossly and via histologic evaluation.

Cats with feline acquired skin fragility syndrome have extremely thin skin resembling tissue paper that tears very easily and is not hyperextensible. In contrast to feline acquired skin fragility syndrome, EDS is characterized clinically by the ability to stretch the skin to great lengths without tearing. The skin does not appear to be attached to the underlying subcutis. EDS is also a heritable disease, whereas feline acquired skin fragility syndrome is normally secondary to endocrine disorders, neoplasia, or improper drug administration.[5]

As the contributor stated these two entities are histologically similar. However, Dr. Goldschmidt pointed out features that allow them to be differentiated histologically in most cases. In feline acquired skin fragility syndrome, the epidermis is thin and there is also severe dermal atrophy with marked thinning of collagen fibers. Adnexal structures may also be atrophic. In contrast, the epidermis in EDS is generally unaffected, and the dermis may be of normal thickness or partially reduced in total thickness. The dermal collagen is abnormally arranged with affected fibers having red cores when stained with Masson's trichrome stain.[5]

**Contributing Institution:** Institut fuer Veterinaer-Pathologie, Universitaet Giessen
Frankfurter Str. 96, 35392 Giessen, Germany, http://www.vetmed.uni-giessen.de/vet-pathologie

**References:**

1. Barthold SW, Kaplan BJ, Schwartz A: Reversible dermal atrophy in a cat treated with phenytoin. Vet Pathol 17:469-476, 1980
2. Ersoy-Evans S, Erkin G, Fassihi H, Chan I, Paller AS, Sürücü S, McGrath JA: Ectodermal dysplasia-skin fragility syndrome resulting from a new homozygous mutation, 888delC, in the desmosomal protein plakophilin 1. J Am Acad Dermatol **55**:157-161, 2006
3. Fernandez CJ, Scott DW, Erb HN, Minor RR: Staining abnormalities of dermal collagen in cats with cutaneous asthenia or acquired skin fragility as demonstrated with Masson's trichrome stain. Vet Dermatol **9**:49-54, 1998
4. Ginn PE, Mansell JEKL, Rakich PM: Skin and appendages. *In:* Jubb, Kennedy and Palmer's Pathology of Domestic Animals, ed. Maxie GM, 5th ed., vol 1, pp 389-391, Saunders, Edinburgh, 2007
5. Gross TL, Ihrke PJ, Walder EJ, Affolter VK: Skin diseases of the dog and cat, 2nd ed., pp 386-391. Blackwell, Oxford, UK, 2005
6. Kaya G, Saurat JH: Dermatoporosis: a chronic cutaneous insufficiency/fragility syndrome. Clinico-pathological features, mechanisms, prevention and potential treatments. Dermatol **215**:284-294, 2007
7. Parapia LA, Jackson C: Ehlers-Danlos syndrome-a historical review. Br J Haematol **141**:32-35, 2008
8. Trotman TK, Mauldin E, Hoffmann V, Del Piero F, Hess RS: Skin fragility syndrome in a cat with feline infectious peritonitis and hepatic lipidosis. Vet Dermatol **18**:365-369, 2007

## CASE II – 05-3388 (AFIP 3103426)

**Signalment:** 6-year-old male Basset hound

**History:** There was a 3.5 x 3.5 x 1cm raised, red, ulcerated subcutaneous nodule on the right dorsal elbow. The lesion had been present for months, and was removed because it limited the range of motion of the elbow.

**Gross Pathology:** None

**Laboratory Results:** None

**Histopathologic Description:** The superficial and deep dermis contains multiple cystic structures that occasionally compress or displace adnexal structures. The cysts are lined by a stratified squamous epithelium. The basal layer of the epithelium frequently forms short rete pegs that extend into the surrounding dermal collagen **(Fig. 2-1).** There is extensive luminal acantholysis of the stratum spinosum, with frequent cleft formation. There are dyskeratotic/apoptotic keratinocytes within the stratum spinosum and acantholytic cells within the clefts or within the cyst lumen, which also contains abundant keratin **(Fig. 2-2)**. Some cysts contain large numbers of neutrophils and there are multiple foci of mineralization of the luminal debris. Cysts are surrounded by varying degrees of dermal fibrosis. Moderate numbers of lymphocytes, plasma cells and histiocytes surround some of the cysts, as well as surround blood vessels in the deep dermis.

In some sections there is rupture of the cyst wall with release of acantholytic cells and keratin debris into the dermis. A mild infiltrate of neutrophils and epitheloid macrophages surround these areas.

**Contributor's Morphologic Diagnosis:** Skin: Warty dyskeratoma

**Contributor's Comment:** Warty dyskeratomas were first described and named in humans. The first and only report in the veterinary literature is of warty dyskeratomas arising in 2 dogs.[1] There are not enough reports to comment on age, breed or location predispositions. In our database from 2004 to present, there are three warty dyskeratomas (including the present case). Two of these tumors were in Bassett hounds and one was in a Yorkshire terrier. Dogs ranged in age from 8 months to 14 years. The case described here was on the right elbow, while the other two cases arose on the right hip or thigh. Lesions ranged in size from 3 to 13cm.

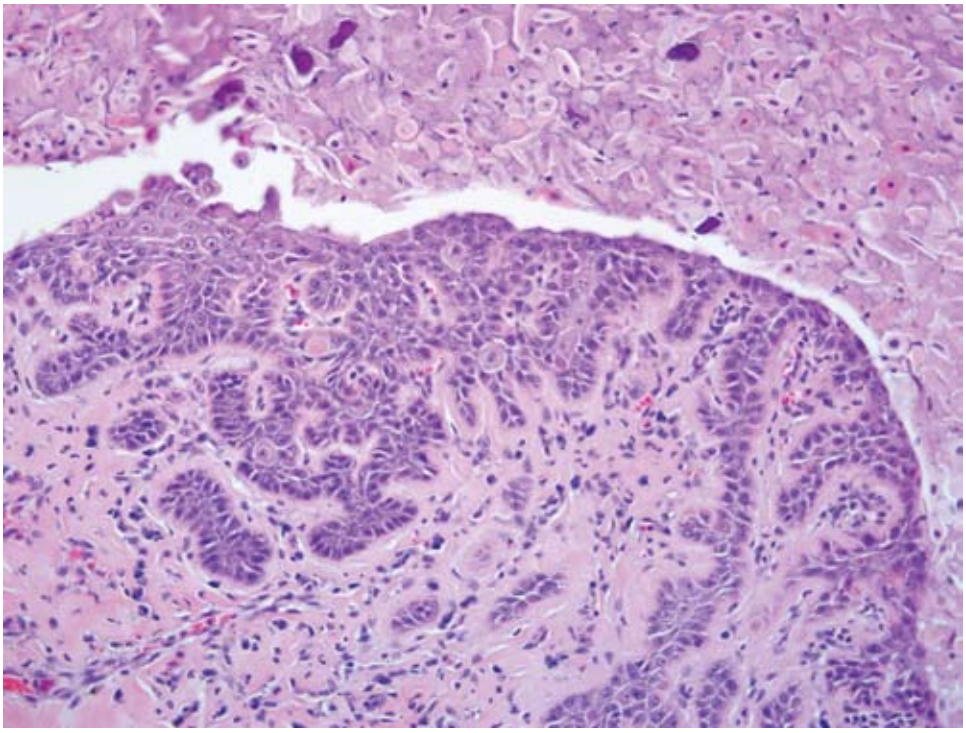

*2-1. Haired skin, dog. Warty dyskeratoma. Basal cells thrown into convoluted folds and projections. There is multifocal dyskeratosis within the suprabasilar strata, with occasional suprabasilar clefting. Scattered acantholytic keratinocytes are mineralized. (HE 400X)*

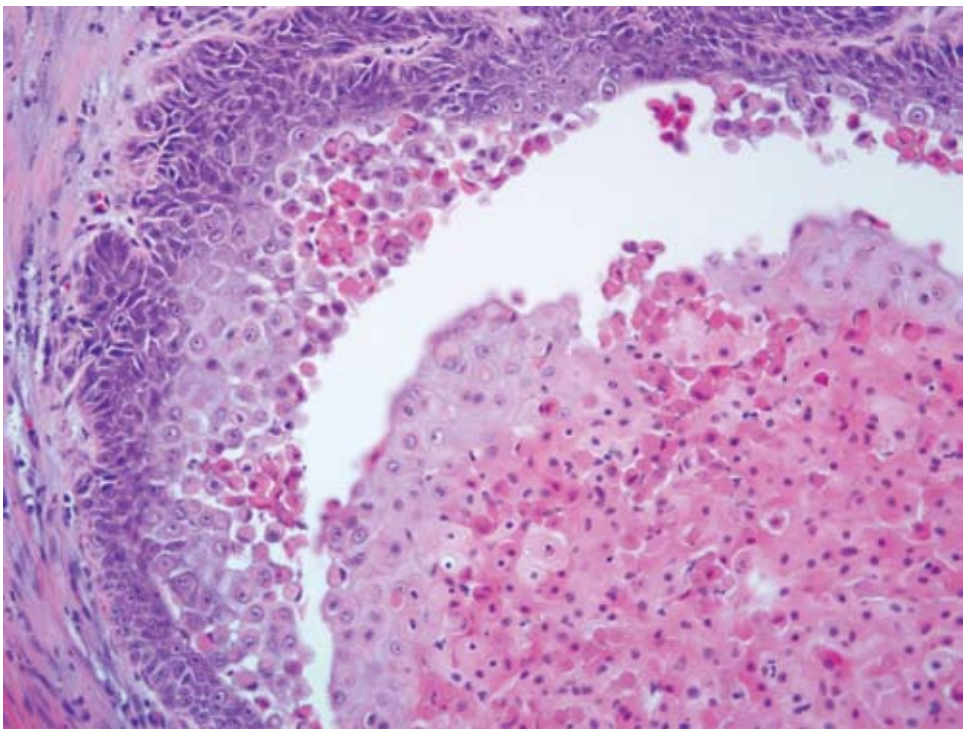

*2-2. Haired skin, dog. Warty dyskeratoma. The cyst lumina are filled with parakeratotic debris, acantholytic keratinocytes, and sloughed apoptotic cells with condensed cytoplasm and nuclei. (HE 400X)*

Warty dyskeratomas are rare benign tumors that are believed to arise from hair follicles. Histologically there are single to multiple cystic structures in the dermis that are lined by a stratified squamous epithelium that is hyperplastic and forms rete pegs that extend into the surrounding dermis. There is acantholysis of the stratum spinosum which can result in separation of the superficial layers of epithelium from the basal layers. There is frequent keratinocyte apoptosis or dyskeratosis. The cyst lumen is usually filled with keratin debris and acantholytic cells. Secondary inflammation from release of cyst contents into the surrounding dermis is common.[2]

**AFIP Diagnosis:** Haired skin: Warty dyskeratoma

**Conference Comment:** Dr. Goldschmidt stated he has seen just a few of these over the last twenty years at the University of Pennsylvania, and this entity seems to be very rare in domestic animals.

Warty dyskeratomas in animals can be confused with an acantholytic variant of squamous cell carcinoma originating from the hair follicle. Squamous cell carcinomas often have extensive apoptosis as a distinguishing feature. Warty dyskeratomas are benign tumors and do not infiltrate through the basement membrane.[1]

In humans, warty dykeratomas are solitary verrucous epidermal neoplasms with marked acantholysis and dyskeratosis of proliferating neoplastic cells.[3] In humans, these tumors generally are found on sun-exposed body parts, and these lesions usually involve hair follicles with some reported cases of oral involvement. Tumors appear as single, raised nodules with umbilicated centers and are usually benign tumors. Histologically, these masses are endophytic with densely packed keratin and suprabasilar clefts with marked acantholysis. Acantholytic cells are described as either "corps ronds," which are suprabasilarly located, large, eosinophilic, rounded cells with perinuclear halos, or "corps grains," which are small intensely eosinophilic, ovoid cells with pyknotic flattened nuclei. These two types of cells are often adjacent to an acantholytic stratum granulosum and parakeratotic stratum corneum.[3]

**Contributing Institution:**
University of Tennessee, College of Veterinary Medicine, Department of Pathobiology, http://www.vet.utk.edu/

**References:**
1. Gross TL, Ihrke PJ, Walder EJ, Affolter VK: Skin Disease of the Dog and Cat: Clinical and Histopathologic Diagnosis. 2nd ed., pp 612-614. Blackwell Science, Denmark, 2005

2. Hill, JR: Warty dyskeratoma in two dogs. *In:* Proceedings of the 3rd AAVD/ACVD Meeting, Phoenix, (1987) p.40.

3. Murphy GR, Elder DE: Atlas of Tumor Pathology, Non-Melanocytic Tumors of the Skin, 3rd Series, vol 1, pp. 27-28. Armed Forces Institute of Pathology, Washington DC, 1991

## CASE III – E28794 2 (AFIP 3103391)

**Signalment:** 17-year-old, spayed female, domestic-mixed, cat, (*Felis silvestris catus*)

**History:** The cat was presented for a solitary cutaneous mass in the right thoracic area **(Fig. 3-1)**. At clinical examination, a solitary disc-shaped, well-circumscribed nodule was observed. No other nodular lesion was seen. Cutaneous mass and superficial cervical lymph node were resected surgically. Five months later, the cat died, but necropsy was not performed.

**Gross Pathology:** The disc-shaped nodule was 30 x 30 x 5 mm in size. A part of overlying skin was ulcered. The cut surface was solid and white in color.

**Laboratory Results:** None

**Histopathologic Description:** The mass consisted mainly of round tumor cells infiltrated throughout dermis and deep subcutaneous tissue near the cutaneous muscle layer **(Fig. 3-2)**. The tumor cells proliferated in superficial layer to deep dermis, but did not invaded into epidermal layer of the skin and hair follicles. The proliferating pattern of tumor cells was solid but also trabecular or cord-like in some area **(Fig. 3-3)**. The size of the tumor cells varied considerably from small cells resembling mature lymphocyte to large cells with polygonal nucleus up to 3 times of small one. The cytoplasm of many tumor cells is scanty but small amount of cytoplasmic rims were also visible in many cells. Many nuclei contained fine granular chromatin and multiple small nucleoli. Mitotic figures and apoptotic cells were frequent. Necrotic area was frequent in the tumor mass and a large necrotic area extended from just beneath the epidermis to deep dermis in some. Occasionally, tumor cells are arranged in cords- or gland-like structures with rare intracytoplasmic cysts. Metastasis to lymph node was also seen.

Grimelius reaction for argyrophilic granules was positive in tumor cells, because they often showed small dark granules

*3-1. Haired skin, cat. Merkel cell carcinoma. Solitary well-circumscribed disc-shaped, ulcerated neoplasm.* *Photograph courtesy of the Faculty of Pharmaceutical Science, Setsunan University, Osaka, Japan.*

in cytoplasm. Immunohistochemically, almost all tumor cells were positive for cytokeratin 20 and synaptophysin. The positivity for cytokeratin 20 has a perinuclear dot-like structure **(Fig. 3-4)**. Tumor cells have shown focal reactivity for chromogranin A and PGP9.5. However, no positive reaction was observed for cytokeratin 8/18, AE1/AE3, S100, CD3, CD20, and vimentin.

**Contributor's Morphologic Diagnosis:** Skin: Merkel cell carcinoma

**Contributor's Comment:** The light and immunohistochemical findings in this tumor supported the diagnosis of Merkel cell carcinoma. The differential diagnosis included lymphoma, trichoblastoma, sweat gland tumor and metastatic neuroendocrine tumor. Contrary to the round nuclei with dense chromatin and distinct large nucleoli, and scanty cytoplasm of the tumor cells in malignant lymphoma, the tumor cells in the present case was characterized by scanty but constantly visible cytoplasm, and round nuclei with small multiple nucleoli and fine granular chromatin taking a dusty appearance. Tumor cells often formed trabecular or cord-like structure, suggesting the epithelial origin in some area. Immunohistochemically negative staining for CD3 and CD20 is most definitive evidence to distinguish from malignant lymphoma.

Trichoblastoma and sweat gland tumor was most difficult to differentiate from Merkel cell carcinoma. In our case, gland-like structure and intracytoplasmic cyst suggested sweat gland origin of tumor cells. However, morphologic pattern of immunohistochemical positivity for cytokeratin 20 was very characteristic and suggestive of Merkel cell tumor. Recently, it was reported that immunohistochemical examination using cytokeratin 20 is extremely useful in distinguishing Merkel cell tumor from trichoblastoma and sweat gland tumor.[3] According to this report, Merkel cell tumor was characterized by perinuclear dot-like structure (keratin button) for cytokeratin 20 like those in the present

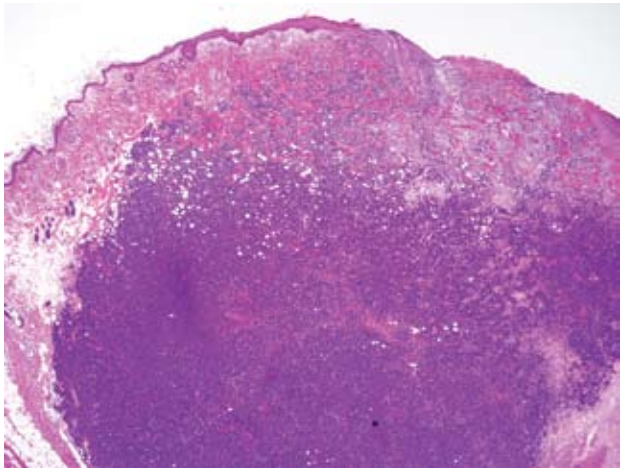

*3-2. Haired skin, cat. Expanding the dermis, elevated the overlying ulcerated epidermis, infiltrating subcutaneous adipose tissue, and effacing adnexa, is an unencapsulated, poorly circumscribed, densely cellular neoplasm. There are multifocal areas of necrosis within and surrounding the neoplasm. (HE 20X)*

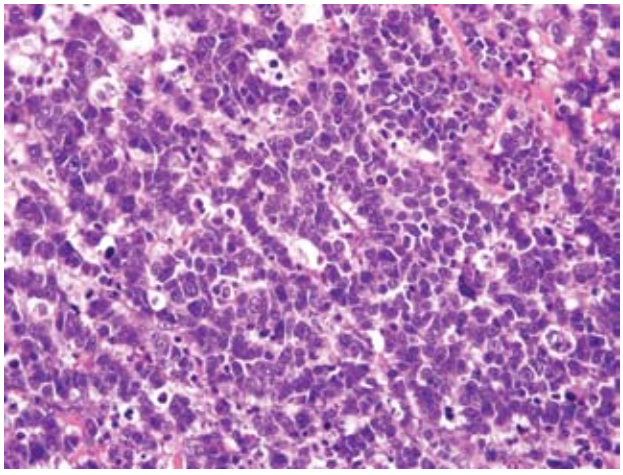

*3-3. Haired skin, cat. The neoplasm consists of sheets, solid nests, and vague cords of round cells surrounded by a fine fibrovascular stroma. (HE 400X)*

case. In addition, negative staining for cytokeratin 8/18 was able to deny sweat gland differentiation. Trichoblastoma often included focal positivity for synaptophysin and chromogranin A, indicating neuroendocrine differentiation. However, in our case, many tumor cells were positive for synaptophysin and focal positivity for PGP9.5 was seen. Therefore, our case was derived from neuroendocrine cells.

In humans, small cell carcinoma of lung often metastasizes to the skin. The growth pattern of that tumor resembles Merkel cell tumor. Cytokeratin 20 was usually negative in small cell carcinoma, but there was no report in animals.[3] In our case, as necropsy was not performed, metastatic tumor could not be completely denied. However, positivity for cytokeratin 20 strongly suggested Merkel cell origin.

Only two cases of Merkel cell carcinoma of cats have been reported.[1,4] One case was a relapse and pulmonary metastasis, but another case showed no relapse and metastasis. In our case, lymph node metastasis and multiple mitotic figures indicated malignant behavior of this tumor. In dogs, Merkel cell tumor was benign, but in humans it was malignant.[2] Therefore, clinical behavior of cats was similar to that of humans.

**AFIP Diagnosis:** Haired skin: Merkel cell carcinoma

**Conference Comment:** Merkel cells are located in the stratum basale of the epidermis and are mechanoreceptors responsible for tactile sensing. These cells are numerous in the rostal nasal planum of pigs, the nasal planum of carnivores, and the external root sheath of tactile hairs in most species. They are normally flat cells with intracytoplasmic, light staining, dense core granules. These cells also have numerous desmosomes.[2]

Debate over the origin of Merkel cells continues, and it is now commonly thought that these cells arise from the neural crest. Immunhistochemical staining helps support this theory because Merkel cells stain for neuron-specific enolase, chromogranin A, and synaptophysin. As the contributor mentioned, Merkel cells are also positive for CK 20, and they are negative for CD45 and CD18 ruling out a leukocyte origin. Rare cases of Merkel cell tumors have been reported in dogs, and this is only the third reported case in a cat. Merkel cell tumors are normally intradermal, unencapsulated tumors composed of solid, dense nests and packets separated and supported by a fine fibrovascular stroma. There is normally little cellular atypia, and mitotic figures are rare. Ultrastructurally, Merkel cells have characteristic membrane-bound dense core granules and rudimentary desmosomal structures.[3]

Dr. Goldschmidt pointed out an area adjacent to the neoplasm of abrupt transition from normal epidermis to an area of flat raised acanthotic epidermis (not evident in all sections) strongly suggestive of viral plaque. Pathologists in the AFIP Department of Soft Tissue Pathology reviewed this case and concurred with the diagnosis of Merkel cell carcinoma.

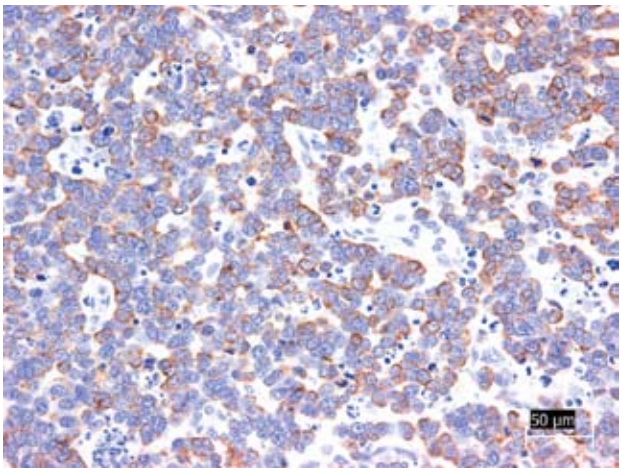


*3-4. Haired skin, cat. Diffusely, neoplastic cells show cytoplasmic immunopositivity for cytokeratin 20. Photomicrograph courtesy of the Faculty of Pharmaceutical Science, Setsunan University, Osaka, Japan.*

**Contributing Institution:** Department of Pathology, Faculty of Pharmaceutical Science, Setsunan University, 45-1 Nagaotohge-cho, Hirakata, Osaka 573-0101, JAPA, narama@pharm.setsunan. ac.jp

**References:**

1. Bagnasco G, Properzi R, Porto R, Nardini V, Poli A, Abramo F: Feline cutaneous neuroendocrine carcinoma (Merkel cell tumour): clinical and pathological findings. Vet Dermatol **14**:111-115, 2003
2. Konno A, Nagata M, Nanko H: Immunohistochemical diagnosis of a Merkel cell tumor in a dog. Vet Pathol **35**:538-540, 1998
3. Moll R, Lowe A, Laufer J, Franke WW: Cytokeratin 20 in human carcinomas. A new histodiagnostic marker detected by monoclonal antibodies. Am J Pathol **140**:427-447, 1992
4. Patnaik AK, Post GS, Erlandson RA: Clinicopathologic and electron microscopic study of cutaneous neuro-endocrine (Merkel cell) carcinoma in a cat with comparisons to human and canine tumors. Vet Pathol **38**:553-556, 2001

## CASE IV – H07-0778 (AFIP 3102248)

**Signalment:** Adult male southern brown bandicoot (*Isoodon obesulus*)

**History:** A southern brown bandicoot (*Isoodon obesulus*) was found at Lesmurdie, Western Australia (32° 00'S, 116° 02'E) showing lethargy, weight loss, and abnormal diurnal behaviour during April 2007. It was taken to Kanyana Wildlife Rehabilitation Centre and then Wattle Grove Veterinary Hospital for veterinary attention. During initial examination, multifocal to coalescing irregular, raised, alopecic and erythematous plaques were observed over the skin of the flanks, face and limbs. Routine skin scraping was performed, but no ectoparasites or fungal pathogens were identified. The prescribed treatments included weekly ivermectin 200 µg/kg PO and weekly Malaseb baths. During this treatment, the bandicoot's weight and level of activity increased and behaviour normalized. General improvement of the skin condition was noted at a follow-up veterinary examination, but the raised plaques persisted. The southern brown bandicoot was referred to the Murdoch University School of Veterinary and Biomedical Sciences for further diagnostic investigation.

**Gross Pathology:** Clinical examination revealed numerous multifocal to coalescing flat and slightly raised, red-black, alopecic skin plaques involving approximately 10-15% of the total skin surface area. These lesions were evident on the fore- and hindpaws, fore- and hindlegs, thorax, flanks, lips, chin and face. The claw of the left lateral digit was overgrown and deformed medially across the palmar aspect of the left forepaw.

**Laboratory Results:**

*Blood smear:* Rare extracellular *Hepatozoon* sp. gamonts were observed.
*Microbiology:* Negative for fungal growth
*PCR:* Total DNA extracted from the papillomas was positive using FAP59/64 degenerate primers for amplifying sequences within the L1 ORF of papillomaviruses.(1)
*In situ hybridizations:* All DNA in situ hybridization (ISH) probes designed to anneal with BPCV1 DNA sequences failed to stain papillomas from the southern brown bandicoot.(2) All DNA ISH probes designed to anneal with BPCV2 DNA sequences (within the L1, L2 and small t antigen ORFs as well as a BPCV2 genomic DNA probe) stained the nuclei of many keratinocytes within the affected epidermis and root sheath.[3]

**Histopathologic Description:** Histopathology demonstrated moderate to marked, multifocal, irregular

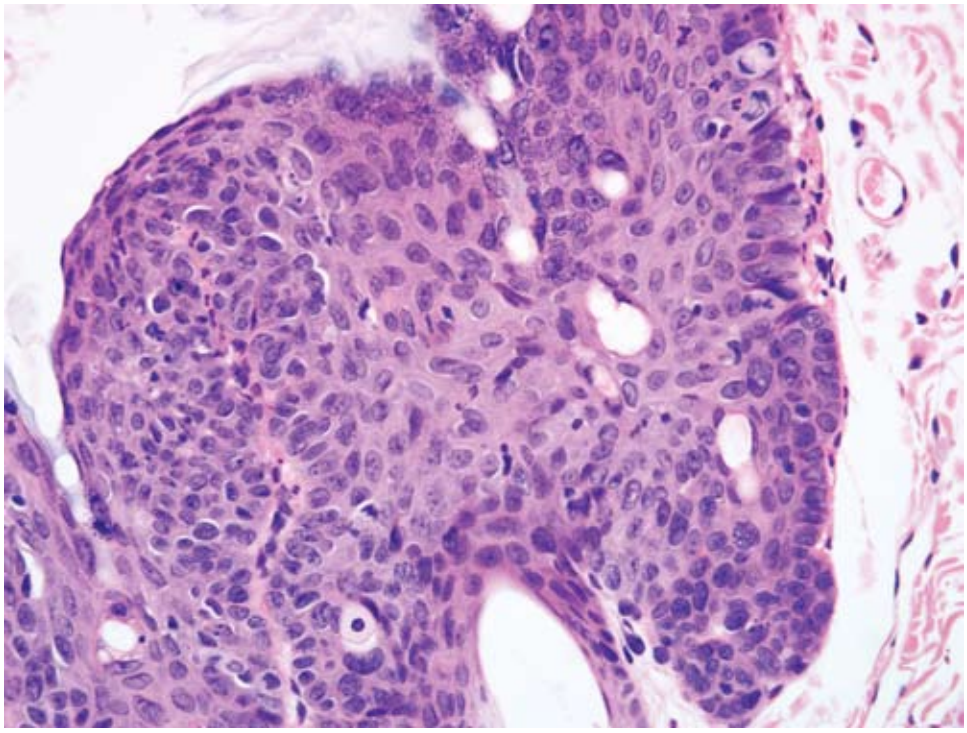

*4-1. Haired skin, bandicoot. Irregular hyperplasia and dysplasia of follicular and surface epithelium with altered polarity of keratinocyte differentiation, dyskeratosis, and suprabasilar mitoses. (HE 400X)*

hyperplasia and hyperkeratosis of the outer root sheath of hair follicles and to a lesser extent the overlying epidermis. The hyperplastic changes involved mainly the stratum spinosum and granulosum. Keratinocyte proliferation and differentiation was often disorderly **(Fig. 4-1)**. There were scattered suprabasilar mitotic figures and basilar and suprabasilar apoptotic keratinocytes. Keratinocytes in both the hyperplastic outer root sheath and epidermis demonstrated mild to moderate anisocytosis and anisokaryosis. The cytoplasm of occasional spinous layer keratinocytes appeared vacuolated (koilocytosis). There were mild multifocal infiltrates of mixed inflammatory cells (predominantly neutrophils, but also some lymphocytes and plasma cells) in the superficial dermis, epidermis and surrounding some hair follicles in some sections, with concurrent mild dermal oedema. Some sections also contained serocellular crusts on the skin surface, which consisted of cellular debris and degenerate neutrophils, set in an amorphous eosinophilic (proteinaceous) background.

**Contributor's Morphologic Diagnosis:** Haired Skin: 1. Moderate, multifocal to coalescing, chronic, irregular, follicular and epidermal hyperplasia, hyperkeratosis and dysplasia with occasional koilocytosis 2. Mild, multifocal, subacute, neutrophilic and lymphoplasmacytic superficial and exudative dermatitis

**Contributor's Comment:** No parasitic, bacterial or fungal organisms were demonstrable using haematoxylin and eosin, Gram Twort or periodic acid Schiff's (PAS) staining techinques. No papillomavirus capsid proteins were detected with indirect immunohistochemistry (using a rabbit polyclonal anti-bovine papillomavirus type 1 antibody [Dako-Cytomation]), though the positive control tissue section from a canine oral papillomavirus-infected tissue sample stained strongly positive. No virions were visualized in the skin fragments processed for transmission electron microscopy, though intranuclear inclusions were not identified by light microscopy of histology sections either.

Multiply primed rolling circle amplification [4] successfully amplified a circular double-stranded DNA genome, which upon restriction enzyme digestion (*Eco*RI, *Bam*HI, *Sal*I, *Bgl*II, *Hin*dIII, *Kpn*I) was ~7.3 kilobase pairs (kb). PCR results indicated the presence of papillomavirus-like L1 and L2 ORFs and polyomavirus-like T antigen ORFs1,3,5. DNA sequencing of the amplicons generated through PCR confirmed these findings.[2] The PCR and restriction enzyme digestion results indicated that the current isolate was similar but not identical to bandicoot papillomatosis carcinomatosis virus type 1 (BPCV1).[7,10] This was later confirmed by complete genomic sequencing of the current virus isolate (GenBank# EU277647), which was consequently named bandicoot papillomatosis carcinomatosis virus type 2 (BPCV2).[2]

In situ hybridization results demonstrated that both the papillomavirus-like and polyomavirus-like parts of the BPCV2 genome could be found within the nuclei of keratinocytes of cutaneous papillomatous lesions of the affected southern brown bandicoot.[7]

Bandicoot papillomatosis carcinomatosis virus type 1 was recently discovered in western barred bandicoots (*Perameles bougainville*) in association with papillomatous and carcinomatous epithelial lesions grossly similar to the lesions evident on the southern brown bandicoot.[1,2,10,11] The BPCVs have certain genomic characteristics typical of *Papillomaviridae* and other genomic features classically associated with *Polyomaviridae*5. Their ~7.3 kb double-stranded, circular DNA genomes are similar in size to known papillomaviruses, and they encode structural proteins similar to the L1 and L2 capsid proteins of established papillomavirus types.[2,10] The transforming protein-encoding ORFs, most similar to large T antigen and small t antigen, occur on the opposite DNA strand to the structural protein-encoding ORFs: features characteristic of viruses classified within the *Polyomaviridae*.[2,10]

Mitochondrial DNA evidence suggests the two extant genera, within the family Peramelidae, *Isoodon* and *Perameles*, diverged from a common bandicoot ancestor approximately 10 million years ago.[2,5] The divergence of the host genera from a common ancestor appears to approximately coincide with the divergence of the BPCVs affecting them.[2] This observation is supportive of the concept of virus-host co-speciation in which both modern day hosts and viruses arose from common ancestors.[6,8]

As it stands, the current virus taxonomic paradigm does not comfortably accommodate the BPCVs whose genomic features are intermediate between *Papillomaviridae* and *Polyomaviridae*.[2,10] It is clear the BPCVs are demonstrably and distinctly different to both polyomaviruses and papillomaviruses and as such, their taxonomic position is presently undefined.

The presence of *Hepatozoon* sp. gamonts in blood smears was considered an incidental finding. The prevalence of *Hepatozoon* sp. infection in *I. obesulus* from Perth, Western Australia was 48% by examination of stained blood smears and 58% by PCR of DNA extracted from blood in a recent survey.[9]

**AFIP Diagnosis:** Skin: Follicular and epidermal hyperplasia and dysplasia, focally extensive, marked with hypergranulosis

**Conference Comment:** The contributor provided an excellent summary of this condition in bandicoots. Koilocytes were not seen in the sections reviewed in conference.

Papilloma viruses, of the *Papoviridae* family, are double stranded DNA viruses that form paracrystalline arrays. Cutaneous papillomas of viral origin are quite common in domestic animals. Papillomas can either be viral induced or an idiopathic proliferation of the epidermis. With the exception of bovine papilloma viruses, papilloma viruses are normally site and species specific. Bovine papilloma viruses have been linked to feline cutaneous fibropapillomas and equine sarcoids. There are two general categories of viral induced papillomas, the squamous papilloma and the fibropapilloma.[4]

Squamous papillomas are filiform, exophytic, wart-like masses with marked epidermal hyperplasia and either orthokeratotic or parakeratotic hyperkeratosis with support provided by a thin dermal stalk. The stratum spinosum is markedly acanthotic, and the cytoplasm of virally infected cells may exhibit ballooning degeneration with eccentrically placed nuclei. These cells are known as koilocytes and are a helpful histologic feature. There is also hypergranularity of the stratum granulosum characterized by large, abnormally shaped eosinophilic granules within the cytoplasm. Eosinophilic, intracytoplasmic inclusions represent aggregates of keratin in dying keratinocytes and should not be confused with pox inclusions. Small, rare, basophilic intranuclear inclusions can also occur.[4]

Fibropapillomas, represented by equine sarcoids and feline fibropapillomas, are nodular lesions covered by a hyperkeratotic and hyperplastic epidermis with rete ridge formation. The predominant feature of these lesions is the marked expansion of the dermis by proliferating fibroblasts arranged in haphazard whorls.[4]

**Contributing Institution:** School of Veterinary and Biomedical Sciences, Murdoch University, Murdoch, Western Australia, 6150, http://wwwvet.murdoch.edu.au/

**References:**

1. Bennett MD, Woolford L, O'Hara AJ, Warren KS, Nicholls PK: In situ hybridization to detect bandicoot papillomatosis carcinomatosis virus type 1 in biopsies from endangered western barred bandicoots (*Perameles bougainville*). J Gen Virol **89**:419-423, 2008

2. Bennett MD, Woolford L, Stevens H, Van Ranst M, Oldfield T, Slaven M, O'Hara A J, Warren KS, Nicholls PK: Genomic characterization of a novel virus found in papillomatous lesions from a southern brown bandicoot (*Isoodon obesulus*) in Western Australia. Virology **376**:173-182, 2008

3. Forslund O, Antonsson A, Nordin P, Stenquist B,

Hansson BG: A broad range of human papillomavirus types detected with a general PCR method suitable for analysis of cutaneous tumours and normal skin. J Gen Virol **80**:2437-2443, 1999
4. Ginn PE, Mansell JEKL, Rakich PM: Skin and appendages. *In:* Jubb, Kennedy and Palmer's Pathology of Domestic Animals, ed. Maxie MG, 5th ed., pp. 748-751. Elsevier Saunders, Philadelphia, PA, 2007
5. Nilsson MA, Arnason U, Spencer PBS, Janke A: Marsupial relationships and a timeline for marsupial radiation in South Gondwana. Gene **340**:189-196, 2004
6. Rector A, Lemey P, Tachezy R, Mostmans S, Ghim S-J, Van Doorslaer K, Roelke M, Bush M, Montali RJ, Joslin J, Burk RD, Jenson AB, Sundberg JP, Shapiro B, Van Ranst M: Ancient papillomavirus-host co-speciation in Felidae. Genome Biol **8**:R57, 2007
7. Rector A, Tachezy R, Van Ranst M: A sequence-independent strategy for detection and cloning of circular DNA virus genomes by using multiply primed rolling-circle amplification. J Virol **78**:4993-4998, 2004
8. Shadan FF, Villarreal LP: Coevolution of persistently infecting small DNA viruses and their hosts linked to host-interactive regulatory domains. Proc Natl Acad Sci USA **90**:4117-4121, 1993
9. Wicks RM, Spencer PBS, Moolhuijzen P, Clark P: Morphological and molecular characteristics of a species of *Hepatozoon* Miller, 1908 (Apicomplexa: Adeleorina) from the blood of *Isoodon obesulus* (Marsupialia: Peramelidae) in Western Australia. System Parasitol **65**:19-25, 2006
10. Woolford L, Rector A, Van Ranst M, Ducki A, Bennett MD, Nicholls PK, Warren KS, Swan RA, Wilcox GE, O'Hara AJ: A novel virus detected in papillomas and carcinomas of the endangered western barred bandicoot (*Perameles bougainville*) exhibits genomic features of both the *Papillomaviridae* and *Polyomaviridae*. J Virol **81**:13280-13290, 2007
11. Woolford L, O'Hara AJ, Bennett MD, Slaven M, Swan R, Friend JA, Ducki A, Sims C, Hill S, Nicholls PK, Warren KS: Cutaneous papillomatosis and carcinomatosis in the western barred bandicoot (*Perameles bougainville*). Vet Pathol **45**:95-103, 2008

The Armed Forces Institute of Pathology
Department of Veterinary Pathology

*Conference Coordinator:*
Todd M. Bell, DVM

WEDNESDAY SLIDE CONFERENCE 2008-2009

# Conference 16

4 February 2009

*Conference Moderator:*

Dr. Tabitha Viner, DVM, DACVP

## CASE I – 08-0165-WSC-2 (AFIP 3115836)

**Signalment:** 10-year-old, male white faced ibis (*Plegadis chihi*)

**History:** Animal presented to the Department of Animal Health for digital abnormalities. During amputation of P2 and P3 of right D2, bird arrested under anesthesia. Resuscitative efforts (IM and IV epinephrine, atropine, dopram, and fluids; cardiac massage; positive pressure ventilation with 100% oxygen) were unsuccessful.

**Gross Pathology:** The white-faced ibis is in excellent postmortem condition. There is sufficient musculature overlying the keel and moderate stores of coelomic and subcutaneous adipose tissue. The small intestine contains minimal amounts of tan, mucoid digesta, and the colon contains small amounts of urates. There is marked curvature of the spine between T4 and T7. There is a healed fracture at P2 of digit 3 on the left. Digit 2 on the right is absent distal to P1.

**Laboratory Results:** Hypophosphatemia (phosphorus 0.7 mg/dl) was observed in a blood sample collected near the time of death.

**Histopathologic Description:** Small Intestine: There are a few heterophils scattered throughout the lamina propria. Multifocally throughout the sections there are many, 5 x 10 micron, crescent-shaped to oval trophozoites overlying the mucosa (*Giardia*) **(Fig. 1-1)**.

**Contributor's Morphologic Diagnosis:** Intestine, small: Giardiasis, moderate, with mild, heterophilic enteritis

**Contributor's Comment:** *Giardia* sp. are flagellated protozoa that can be found in the upper intestine of many species of mammals, birds, reptiles, and amphibians. Though the taxonomy is poorly understood and subject to debate, it is generally accepted that *Giardia duodenalis* (a.k.a. *Giardia lamblia*) is classified into approximately eight separate assemblages.[5] Giardia appear to be host specific [5] with assemblages A and B being most common in humans; dogs are associated with assemblage C; and organisms from assemblage E have been isolated from livestock. *G. psittaci* has been isolated from budgerigars [6], *G. ardeae* from herons, and a genetically similar strain from straw-necked ibis.[2] Many animals harbor the organism in their intestinal tracts without evidence of clinical illness, indicating that there is a natural carrier state.[1]

Giardia colonize the upper small intestine, usually the duodenum, in the trophozoite form.[1] The trophozoites

*Sponsored by the American Veterinary Medical Association, the American College of Veterinary Pathologists, and the C. L. Davis Foundation.

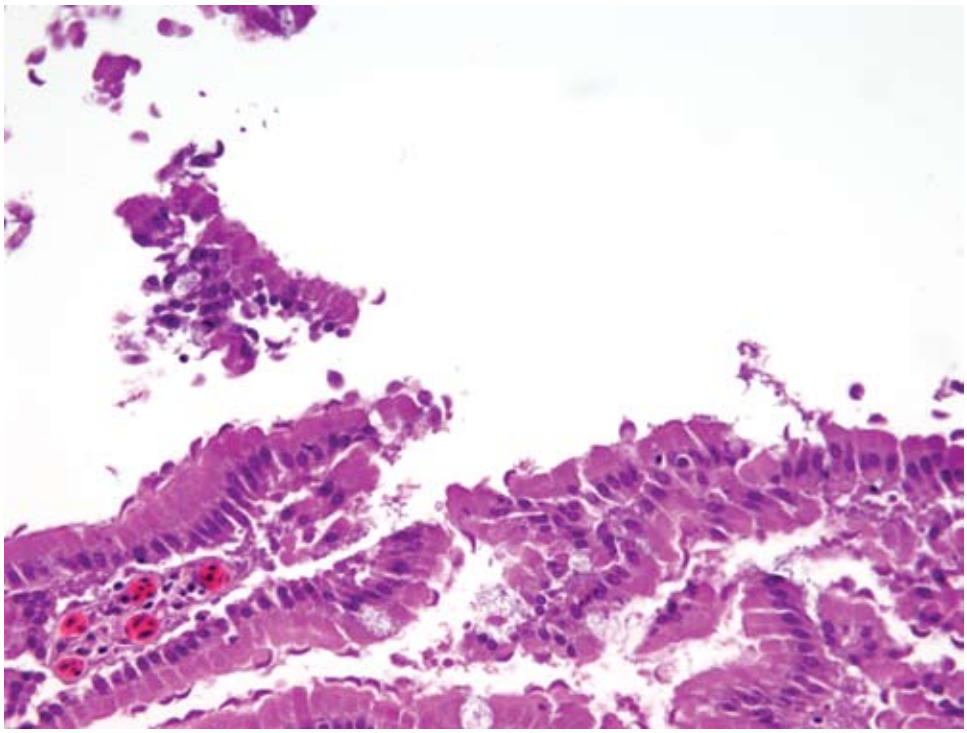

*1-1. Small intestine, ibis. Within the intestinal lumen, and adherent to crypt and villar enterocytes are numerous, 10 x 6 micron, flagellated, binucleate protozoal trophozoites. (HE 400X)*

are piriform, with four paired flagella, paired nuclei and a ventral disk on the concave surface which attaches to the host enterocyte. Reproduction by binary fission occurs in the gut lumen. This form may be passed in the feces, but more commonly, oval cysts are seen in direct smears. Transmission of the environmentally-stable cyst is by the fecal-oral route.[1] Diagnosis is best made by seeing the organism in a direct fecal preparation from a clinically ill animal, but ELISA and PCR tests have been developed.

Though giardiaisis is generally an asymptomatic condition, the presence of the organism has been associated with vitamin E/selenium deficiencies in cockatiels.[6] The proposed mechanism involves malabsorption of these nutrients due to the presence of the organisms on the intestinal mucosal surface. Though speculative, hypophosphatemia in this white-faced ibis may also have resulted from a focally extensive and heavy parasite load. Phosphorus is absorbed from the diet in the proximal small intestine where the heaviest load of parasitism was found in this bird. The bird of this report had adequate fat and muscling, but antemortem bloodwork revealed a PO4 of 0.7mg/dl (ref. 3.1-6.6mg/dl). Additionally, marked thoracolumbar scoliosis was present in addition to the fractured and dislocated digits. Thus, while the protist in this particular animal did not appear to cause a direct effect on intestinal health, it may have acted indirectly on bone health by blocking absorption of some nutrients needed for maintenance of healthy, structural bone.

**AFIP Diagnosis:** Small intestine: Enteritis, heterophilic, diffuse, mild with numerous surface-associated trophozoites, etiology consistent with *Giardia* sp.

**Conference Comment:** Dr. Viner, the conference moderater, submitted this case and did an excellent job elucidating the importance of this organism in domestic species. The preservation of morphologic detail of the organism in the sections was excellent. This particular slide did not have extensive associated tissue reaction, thus driving home the point that Giardia species often cause minimal gross and histologic lesions and also often cause subclinical infections.

Giardia is an ubiquitous organism with worldwide distribution and is the most common flagellate of mammals and birds.[3] Giardiasis is also a zoonotic disease. The life cycle of Giardia species is direct. Trophozoites and cysts are present in feces and passed from infected hosts into the environment. Once outside the host the trophozoites die, but the cysts are resistant. They are protected from the environment by a membranous layer with an inner and outer cyst membrane and filamentous layer forming a dense mat of interlacing branches.[2] Cysts are ingested via fecal-oral transmission. Enzymes within the stomach and small intestine cause excystation releasing two trophozoites. The organisms attach and feed in the upper small intestine and multiply by binary fission. Once the organisms reach the colon, they encyst in preparation for

the external environment.

**Contributing Institution:** http://nationalzoo.si.edu/

**References:**
1. Brown CC, DC Baker, IK Barker: Alimentary system. *In:* Pathology of Domestic Animals, ed. MG Maxie, 5th ed., pp. 277-279. Elsevier, Philadelphia, PA, 2007
2. Cheville NF: Ultrastructural Pathology, pp. 722-723. Iowa State University Press, Ames, Iowa, 1994
3. Gardiner CH, Poynton SL: An Atlas of Metazoan Parasites in Animal Tissues, 2nd ed., pp. 6-7. Armed Forces Institute of Pathology, Washington, DC 1984
4. McRoberts KM, BP Meloni, UM Morgan, R Marano, N Binz, SL Erlandsen, SA Halse, RCA Thompson: Morphological and molecular characterization of *Giardia* isolated from the straw-necked ibis. J Parasitol **82**(5):711-718, 1996
5. Monis PT, RCA Thompson: *Cryptosporidium* and *Giardia*-zoonoses: fact or fiction? Infection, Genetics and Evolution **3**:233-244, 2003
6. Ritchie B, GJ Harrison, LR Harrison: Avian Medicine: Principles and Application. pp. 732, 1014-5. Wingers Publishing, Lake Worth, FL, 1994

## CASE II – 07-18567 (AFIP 3103629)

**Signalment:** Adult, intact female, great blue heron (*Ardea herodias*)

**History:** The heron was presented to the wildlife clinic with a poor body condition score (1.5/5), as well as being dehydrated and weak. The heron was initially treated with metacam, claforan, and lactated Ringer's solution. Over the next 24 hours the heron developed subcutaneous edema ventral to the bill and was started on colloid therapy (Hetastarch). The heron failed to improve and was found dead 36 hours after presentation.

**Gross Pathology:** The pectoral muscles were moderately atrophied and the keel was prominent on palpation. The subcutaneous tissues ventral to the bill down to the thoracic inlet were moderately edematous. The ventral serosal surface of the proventriculus and adjacent ventriculus was focally overlain by a mass of multiple, tortuous intertwining tubules and a few ovoid cysts. Tubule diameters were up to 2 mm and cysts measured up to 1 cm long X 0.5 cm in diameter. The tubules and cysts were filled with dark red to brown, crumbly, soft debris and multiple pale nematodes 0.5 mm in diameter and up to 3 cm long. The ventriculus contained scant digested blood.

**Laboratory Results:**
Initial laboratory results:
Blood glucose = 297
PCV = 45
Total protein = 3.8
Fecal floatation detected ascarids

**Histopathologic Description:** The wall of the proventriculus, including the mucosa, muscularis, and serosa and the adjacent mesentery contain multiple variably sized granulomas. The core of each granuloma consists of a layer of eosinophilic, granular and necrotic debris mixed with degenerate eosinophils and heterophils surrounding longitudinal and cross sections of well to poorly preserved nematodes. The layer of eosinophilic debris is, in turn, surrounded by a prominent layer of macrophages and multinucleated giant cells. The outermost layer is a thick but sparsely collagenous, reticular capsule composed of both immature and mature fibrocytes. Scattered throughout the capsule are eosinophils and macrophages, fewer lymphocytes, plasma cells, and heterophils, and small foci of hemorrhage. The capsule is multifocally intersected by variably sized vessels lined by plump endothelial cells. Structural characteristics of the nematodes include one or more of the following: a thick, eosinophilic, smooth cuticle; polymyarian-coelomyarian musculature; a pseudocoelom; a ventral nerve cord; a glandular esophagus with associated pseudomembranes; many thick shelled, operculated, oval eggs 70 microns X 40 microns; an intestinal tract lined by tall columnar cells; and male or female reproductive tracts **(Figs. 2-1, 2-2)**. Occasionally, the profile of nematodes is obscured and replaced by eosinophilic necrotic debris, degenerate granulocytes, and/or colonies of bacilli along with free floating nematode eggs. The proventriculus contains multiple aggregates of eosinophils, macrophages, and lymphocytes and is mildly edematous. Glands of the proventriculus often contain sloughed epithelial cells, granular eosinophilic debris, and few leukocytes. The mesentery is mildly edematous and adipose tissue is atrophied.

**Contributor's Morphologic Diagnosis:** Proventriculus: Proventriculitis, chronic-active, granulomatous **(Fig. 2-3)**, eosinophilic, and heterophilic, multifocal, moderate, with multifocal mesenteric granulomas, serous atrophy of fat and intralesional adult nematodes consistent with *Eustrongylides* sp.

**Contributor's Comment:** *Eustrongylides* sp. infections have been reported from birds throughout the

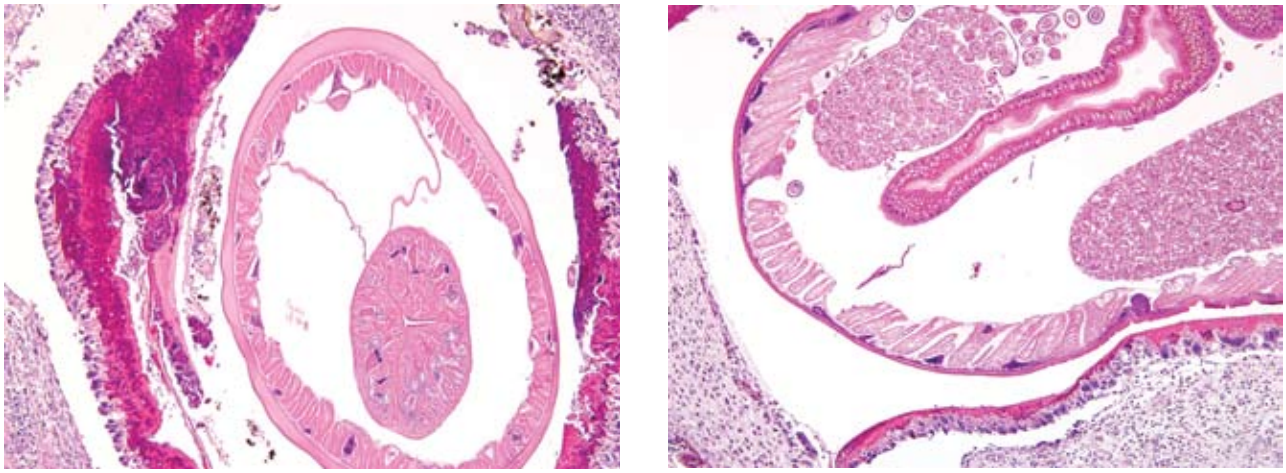

*2-1, 2-2. Proventriculus, heron. Nematodes are characterized by a 7 – 10 micron thick cuticle, a pseudocoelom, coelomyarian-polymyarian musculature, bacillary bands, a glandular esophagus attached to the body wall with pseudomembranes, an intestine lined by uninucleate cells with a prominent brush border, male and female gonads, and a ventral nerve chord. (HE 100X)*

world and have been implicated as a significant cause of morbidity and mortality in wading birds.[1,4,5,7,9,11] *Eustrongylides* undergo four developmental stages and require two intermediate hosts. Ciconiiformes (wading birds) are a definitive host for *Eustrongylides* [11] and shed eggs in the feces into the environment. The first larval stage then develops within the eggs and is consumed by freshwater oligochaetes (worms). The eggs then hatch and develop into second and third stage larvae. Small fish feed on the oligochaetes and the third stage larvae become encysted within the fish and develop into the infective fourth stage larvae. Wading birds then consume the fish and become infected. Alternatively, transport hosts, including amphibians, reptiles, and other fish, consume the smaller fish with the fourth stage larvae and then are consumed by wading birds. Larvae penetrate the wall of the proventriculus and ventriculus within 3 to 5 hours following ingestion of infected fish [7] and become adults in 2 to 8 days.[7] The shedding of eggs has been reported 10-17 days [1] and 14-23 days [7] post infection. *Eustrongylides* have no oral structures to allow attachment to the mucosal surface of the gastrointestinal tract, which may explain the rapid penetration of the proventriculus and ventriculus as well as clinical signs of regurgitation and vomiting as a way to remove the parasite.[7] Additional clinical signs reported include lethargy, depression, and emaciation.[11]

Significant lesions are frequently observed in birds infected with *Eustrongylides*.[4] Gross lesions reported following acute infections include minimal inflammation and hemorrhage, perforations of the proventriculus, ventriculus, and other organs, hematoma formations, severe fibrinous coelomitis involving multiple visceral organs, necrosis, and/or the presence of nematodes in the coelom.[2,4,5,7,8,11] Histologic evaluation of tissues show a severe granulomatous response including heterophils, macrophages, and multinucleated giant cells surrounding the organisms, hemorrhage or hematomas, fibrinous coelomitis with or without bacteria, and necrosis.[1,4,7,11] Lesions associated with more chronic infections include firm granulomas, air sacculitis, large, intertwining, firm, pale tan tubules crossing over the serosal surfaces of multiple organs often containing intact or decomposing organisms and/or necrotic debris.[1,4,7,11] Tubules are usually patent and open into the ventriculus.[7] Histologic lesions include the presence of intact and degenerate nematodes surrounded by a zone of cellular debris, bacteria, fragments of cuticle, and eggs which, in turn, is surrounded by eosinophilic debris, multinucleated giant cells, and fibrous connective tissue.[7] Active inflammation may also be present on the surface of the tubules.[6]

Eustrongylidosis in ciconiiformes is caused by three species of *Eustrongylides*: *E. tubifex, E. ignotus*, and *E. excisus*, and the prevalence of *Eustrongylides* sp. varies worldwide. A survey of ciconiiformes in Brazil revealed a 31% infection rate.[4] In the United States, eustrongylidosis has been implicated as a cause or contributor to losses of colonies of wading birds in Indiana [9], Delaware [8, 11], Louisiana [5], Florida [6], Texas [1], and Virginia.[1] In one survey from Florida, 13% of nestling wading birds and 24% of adult wading birds were infected.[6] The most commonly infected birds in that survey were adult Great blue herons (51%) followed by adult and nestling Great egrets (34% and 21%, respectively). 35% of nestlings in Texas, 6% in California, and 4% in Rhode Island were infected in a separate survey.[2] High mortality due to *Eustrongylides ignotus* has been observed in Delaware,

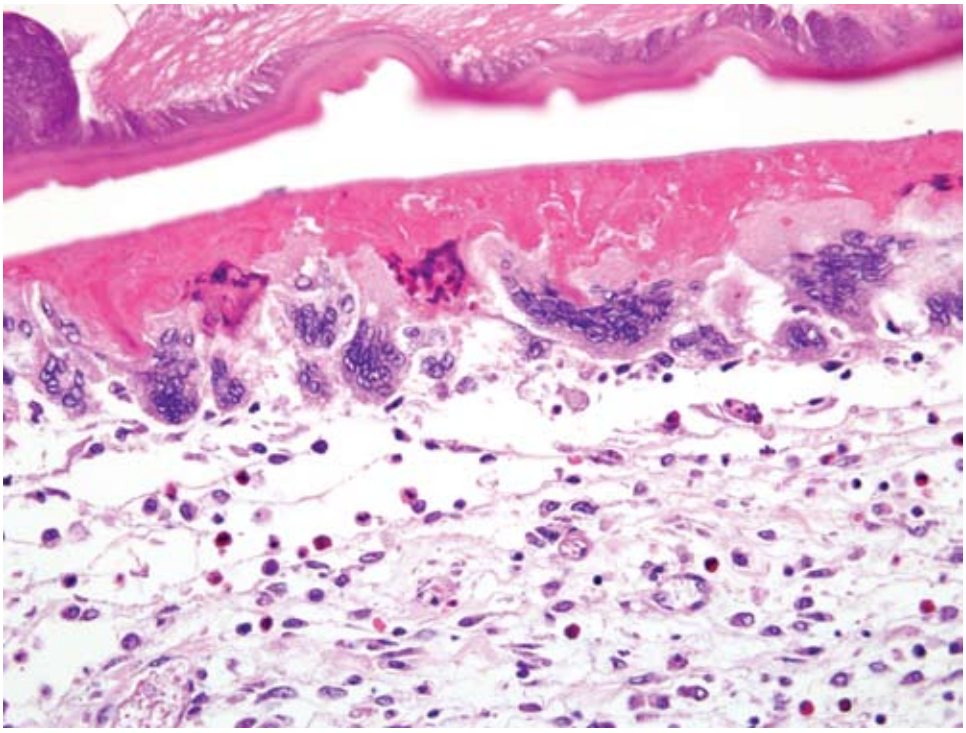

*2-3. Proventriculus, heron. Nematodes (top) are surrounded by granulomas that consist of eosinophilic cellular and proteinaceous debris bounded by numerous multinucleated and epithelioid macrophages, further bounded by granulocytic and mononuclear inflammatory cells and fibroblasts. (HE 400X)*

where the mortality rate reached 84% in snowy egret nestlings.[8] Multiple surveys have shown that nestlings and hatchlings are particularly sensitive and have high rates of mortality.[1,6,8,11] Infected adult birds, on the other hand, have lower rate of mortality, which serves as a source of continued shedding of eggs into the environment.[6] This can result in the reinfection of ciconiiformes, significantly impacting the overall health and reproductive success of wading bird colonies. Furthermore, the report of a human infection by *Eustrongylides* sp. resulting from the consumption of sushi [10] highlights the zoonotic potential of this parasitic nematode.

**AFIP Diagnosis:** Proventriculus: Proventriculitis, granulomatous, multifocal, moderate with nematodes consistent with *Eustrongylides* sp.

**Conference Comment:** *Eustrongylides* species are nematodes belonging to the subclass Aphasmidia, which have very characteristic morphologic features. These parasites have stichosomes, which are basophilic structures that surround the esophagus. The stichosome is formed from a row of cells called stichocytes, which are esophageal gland cells.[3] Aphasmids also have a bacillary band, which is a boomerang shaped, densely basophilic band of nuclei present in the hypodermis. Adult female aphasmids have only one genital tract in contrast to two tracts in phasmid nematodes. Eggs in most aphasmid species have bipolar plugs. Commonly encountered aphasmid parasites include *Trichuris* sp., *Eustrongylides* sp., *Dioctyophyma* sp., and *Capillaria* sp.

**Contributing Institution:** Department of Veterinary Pathobiology, College of Veterinary Medicine, University of Illinois at Urbana-Champaign (http://www.cvm.uiuc.edu/path/)

**References:**

1. Cole RA: Eustrongylidosis. *In:* Field Manual of Wildlife Diseases: General Field Procedures and Diseases of Birds, Biological Resources Division, ed. Ciganovich EA, pp. 223-228: United States Geological Survey, United States Department of the Interior, Washington, DC, 1999
2. Franson JC, Custer TW: Prevalence of eustrongylidosis in wading birds from colonies in California, Texas, and Rhode Island, USA. Colonial Waterbirds **17**:168-172, 1994
3. Gardiner CH, Poynton SL: *In:* An Atlas of Metazoan Parasites in Animal Tissues, 2nd ed., pp. 40. Armed Forces Institute of Pathology, Washington, DC, 1998
4. Pinto RM, Barros LA, Tortelly L, Teixeira RF, Gomes DC: Prevalence and pathology of helminths of ciconiiform birds from the Brazilian swamplands. Journal of Helminthology **78**:259-64, 2004
5. Roffe TJ: *Eustrongylides* sp. epizootic in young common egrets (*Casmerodius albus*). Avian Diseases **32**:143-7, 1988
6. Spalding MG, Bancroft GT, Forrester DJ: The

epizootiology of eustrongylidosis in wading birds (ciconiiformes) in Florida. Journal of Wildlife Diseases **29**:237-49, 1993
7. Spalding MG, Forrester DJ. Pathogenesis of *eustrongylides ignotus* (nematoda: Dioctophymatoidea) in ciconiiformes. Journal of Wildlife Diseases **29**:250-60, 1993
8. Wiese JH, Davidson WR, Nettles VF: Large scale mortality of nestling ardeids caused by nematode infection. Journal of Wildlife Diseases **13**:376-382, 1977
9. Winterfield RW, Kazacos KR: Morbidity and mortality of great blue herons in Indiana caused by *eustrongylides ignotus*. Avian Diseases **2**:448-51, 1977
10. Wittner M, Turner JW, Jacquette G, Ash LR, Salgo MP, Tanowitz HB: Eustrongylidiasis-a parasitic infection acquired by eating sushi. The New England Journal of Medicine **320**:1124-1126, 1989
11. Ziegler AF, Welte SC, Miller EA, Nolan TJ: Eustrongylidiasis in eastern great blue herons (*Ardea herodias*). Avian Diseases **44**:443-8, 2000

## CASE III – 08N0017 (AFIP 3102498)

**Signalment:** 7-year-old male Fulvous whistling duck (*Dendrocygna bicolor*)

**History:** Marked caudal coelomic distension with a very firm mass was noted. Otherwise, the duck showed no clinical signs. A CBC revealed a heterophilic (13,710/ul) leukocytosis (21,240/ul), and on serum chemistry analysis there was marked hypoalbuminemia (0.2 g/dl) and mildly increased uric acid (10.4 mg/dl). Radiographs confirmed a large soft tissue density extending from the mid- to caudal coelomic cavity and displacing the intestines caudally. The duck was euthanized.

**Gross Pathology:** A 7-year-old male fulvous whistling duck was presented in fair nutritional condition with marked firm distension of the caudal coelomic cavity due to a massively and diffusely enlarged liver (21% of body weight). The capsular surface of the liver was rough, slightly irregular, and tan with several indistinct irregular white foci, predominantly on the right lobe **(Fig. 3-1)**. On cut section, these foci corresponded to firm, coalescing 0.2 to 1 cm diameter nodules with thick white capsules around brown caseous centers which replaced approximately 95% of the parenchyma of the right lobe and were scattered in small numbers throughout the left lobe **(Fig. 3-2)**. The remaining hepatic parenchyma was pale tan, firm and waxy. Additional very firm, multinodular, pink and tan mottled masses composed of encapsulated caseous material were present in the fascia of cervical area, dorsal to the syrinx, and attached to the serosa of several loops of intestine. The spleen and kidneys were also markedly enlarged.

**Laboratory Results:** With Congo red staining, the suspected amyloid was diffusely dull brick red and had a variable apple green birefringence under polarized light. This staining was lost when tissues were pretreated with potassium permanganate ($KMnO_4$). Electron microscopy confirmed that the deposits were extracellular and composed of long, haphazardly-arranged, non-branching fibrils that were on average 10 nm in diameter.

Both Ziehl-Neelsen and Fite's stains showed very large numbers of thin, variable length, acid-fast rods admixed with the debris at the center of the granulomas and occasionally within the surrounding multinucleated giant cells. These bacteria were gram positive with a Brown & Brenn stain. Immunohistochemical staining for Bacillus Calmette-Guerin (BCG) showed abundant amorphous immunoreactive material within the granulomas. The organism was identified as *Mycobacterium avium* complex by HPLC at the National Jewish Medical Center.

**Histopathologic Description:** In two sections of liver examined, the parenchyma is moderately to severely disrupted and replaced by abundant amorphous pale eosinophilic extracellular hyaline material (consistent with amyloid) and multifocal to coalescing granulomas **(Fig. 3-3)**. Deposition of the hyaline material variably expands the space of Disse and vessel walls, separating and disrupting cords of shrunken (atrophic) hepatocytes and occluding sinusoids. In other areas, coalescing sheets of hyaline material replace large areas of the parenchyma, with only small islands of hepatocytes and hyperplastic bile ducts remaining **(Figs. 3-4, 3-5)**. Hyaline material is also frequently present within Kupffer cells and the numerous multinucleated giant cells. The granulomas consist of a dense core of amorphous and cellular hypereosinophilic debris mixed with large numbers of wispy, amphophilic bacterial colonies surrounded by a thick rim of multinucleated giant cells and numerous fibroblasts, lymphocytes and plasma cells with fewer heterophils.

**Contributor's Morphologic Diagnosis:** Liver: Severe multifocal to coalescing granulomatous hepatitis with intralesional acid-fast rod bacteria **(Fig. 3-6)** (*Mycobacterium avium* complex)
Liver: Severe amyloidosis

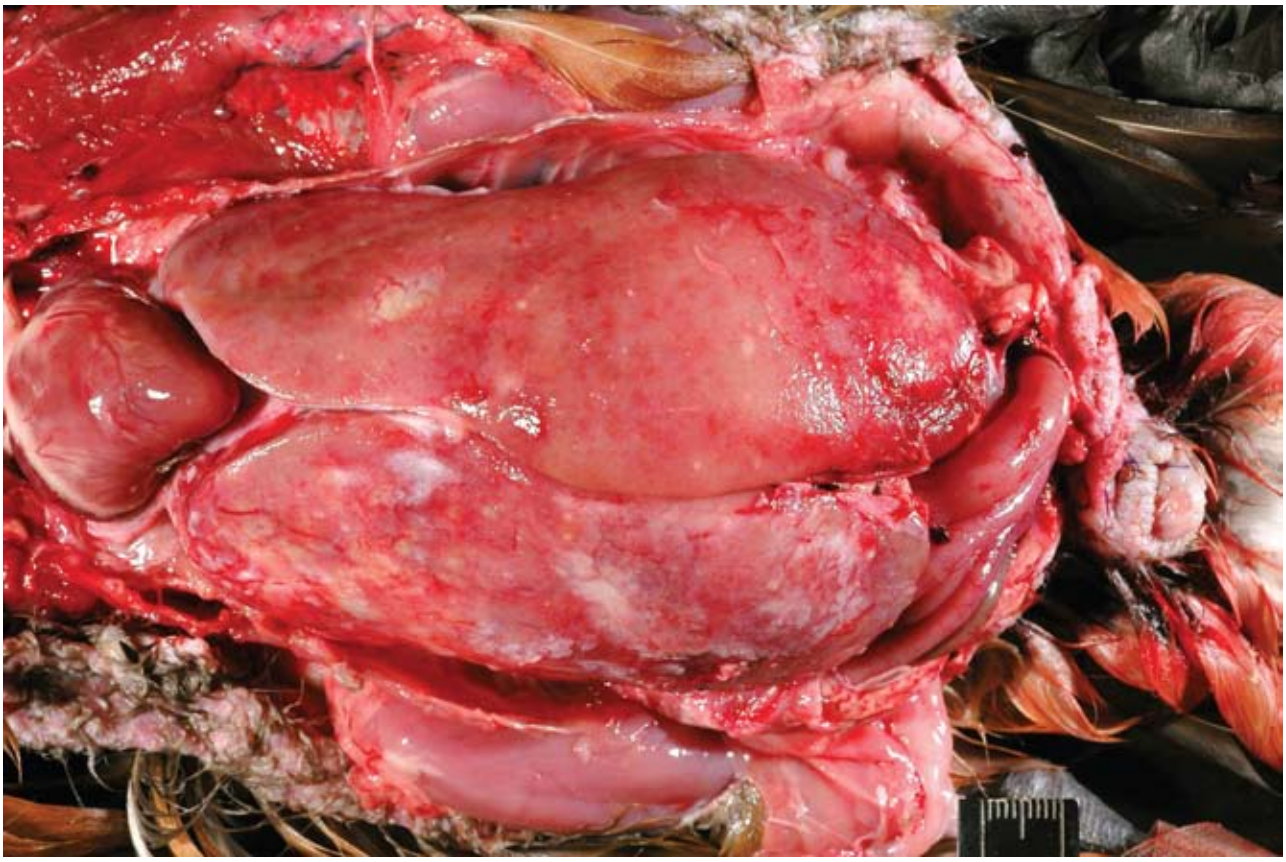

*3-1. Liver, duck. Diffuse hepatomegaly, with tan, waxy discoloration and irregular capsular surface.* *Photograph courtesy of Rebecca M. Gruffey, Anatomic Pathology Service Manager, University of California – Davis, Veterinary Teaching Hospital, Anatomic Pathology, Davis California.*

**Contributor's Comment:** This duck had systemic amyloidosis secondary to a chronic disseminated mycobacterial infection. In both birds and mammals with this type of amyloidosis, the liver, spleen, and kidney are most consistently involved, with variable involvement of other organs.[1,5] In addition to the liver in this case, the spleen, kidneys (interstitium and glomeruli), and adrenal glands were severely affected, but amyloid was also present in the vessel walls/interstitium of the thyroid glands, parathyroid glands, testes, bone marrow, lungs, and heart. As was demonstrated in this case, the deposits begin in the space of Disse (liver), within vessel walls, and along basement membranes, eventually leading to disease through compression of adjacent tissue and/or restriction of blood flow.[1,5]

The term amyloid encompasses a group of biochemically distinct proteins with a similar beta-pleated sheet conformation arranged in variable length, 7.5-10 nm wide, nonbranching filaments (visible by electron microscopy) which give amyloid its characteristic Congo red staining and green birefringence, as well as its fluorescence with thioflavin-T or S.[1,4,5] At least 17 amyloid proteins have been characterized in humans and animals, with AA (derived from serum amyloid A), AL (derived from immunoglobulin light chains), and Aβ (β-amyloid protein found in cerebral Alzheimer disease lesions) being the most common in humans.[1] Of these, except for a single report of β-amyloid in cerebral vessels of an aged woodpecker, [7] only AA-amyloidosis has been reported in birds.[5] The precursor protein for AA, serum amyloid A (SAA), is a soluble acute phase response protein synthesized in the liver in response to inflammation via cytokines Il-1, Il-6, and TNF.[1,4,5] The mechanisms by which insoluble derivatives of SAA are deposited and accumulate are poorly understood, but because of its association with persistently elevated SAA concentrations, as occurs in chronic inflammatory conditions, this type of amyloidosis is known as secondary, or reactive, amyloidosis.

Among birds, amyloidosis has been reported in most orders, but is particularly common in captive Anseriformes where

*3-2. Liver, cross section, duck. Multifocal to coalescing 0.2 – 1 cm diameter granulomas with necrotic centers.* *Photograph courtesy of Rebecca M. Gruffey, Anatomic Pathology Service Manager, University of California – Davis, Veterinary Teaching Hospital, Anatomic Pathology, Davis California.*

incidences may be almost 80% in ducks and 50% in geese and swans examined at necropsy.[5] In approximately 60-70% of amyloidosis cases in Anseriformes, an associated chronic inflammatory or infectious disease, such as mycobacteriosis, fungal disease, or enteric parasites, can be identified.[2,5,10] It has also been associated with bumblefoot in Pekin ducks and can be induced experimentally in ducks and chickens with injections of a variety of bacterial and adjuvant components.[5] The cases in which systemic amyloidosis is present without inflammation may be considered idiopathic or a result of nonspecific stresses associated with environmental conditions. For example, a study in white Pekin ducks free of chronic disease and parasites showed that increased crowding corresponded to increased rate and incidence of development of amyloidosis.[3] Amyloidosis has been seen in approximately 20% of avian mycobacteriosis cases overall, [6] and in up to 50-60% of the cases in Anseriformes.[2,8]

Mycobacteriosis in birds is predominantly caused by *Mycobacterium avium-intracellulare* (MAI) complex organisms or *Mycobacterium genavense* and is spread by fecal-oral transmission (rarely aerogenous) from environmental contamination.[9] They have low zoonotic potential, except to immunocompromised individuals, who are nevertheless more likely to acquire the infection from a common environmental source.[9] Some studies have found disproportionate susceptibility of waterfowl, especially perching ducks, to *Mycobacterium* sp. in zoologic collections.[9] The infection in this duck was systemic with severe involvement of the liver and scattered granulomas present in the spleen, on the serosal surface of the intestinal tract, and in the fascia of the cervical and syringeal regions. It was identified as a *Mycobacterium avium* complex species.

**AFIP Diagnosis:** 1. Liver: Granulomas, multiple, with acid fast bacilli, etiology consistent with *Mycobacterium* sp.
2. Liver: Amyloidosis, diffuse, severe, with moderate hepatocellular atrophy, loss, degeneration, and necrosis and multifocal, moderate granulomatous hepatitis

**Conference Comment:** The conference discussion centered predominately on the different types of amyloid and the cytokines involved in inflammation and amyloidosis. Scattered granulomatous inflammation in some areas did not appear to be associated with the acid-fast bacteria. The contributor did an outstanding job of describing this entity.

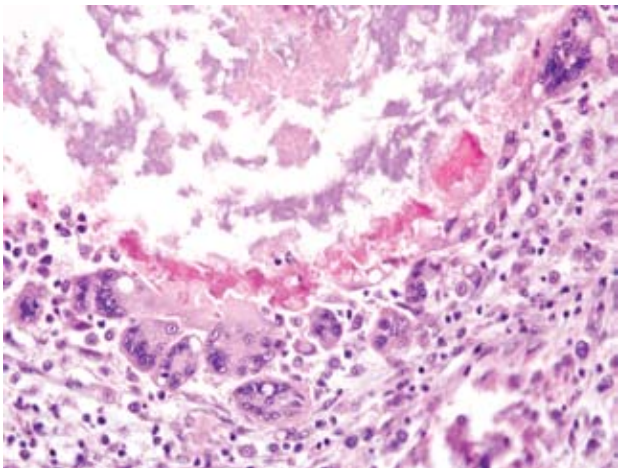

*3-3. Liver, duck. Granulomas are composed of a central area of dropout and necrosis admixed with poorly staining 0.5 x 2 micron bacilli. This is bounded by numerous multinucleated giant cells, epithelioid macrophage, mononuclear inflammatory cells, and fibroblasts. (HE 400X)*

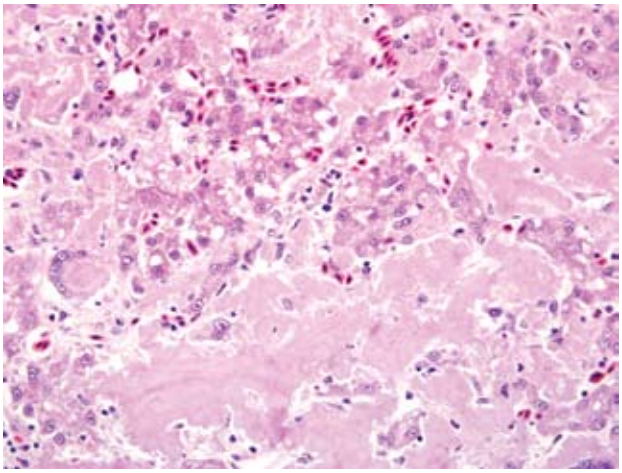

*3-4. Liver, duck. Hepatic cords and sinusoids are effaced by large amounts of waxy homogenous eosinophilic material (amyloid), which is occasionally found within multinucleated giant cells. Remaining hepatocytes are degenerative, characterized by cytoplasmic vacuoles and faded, swollen nuclei. (HE 400X)*

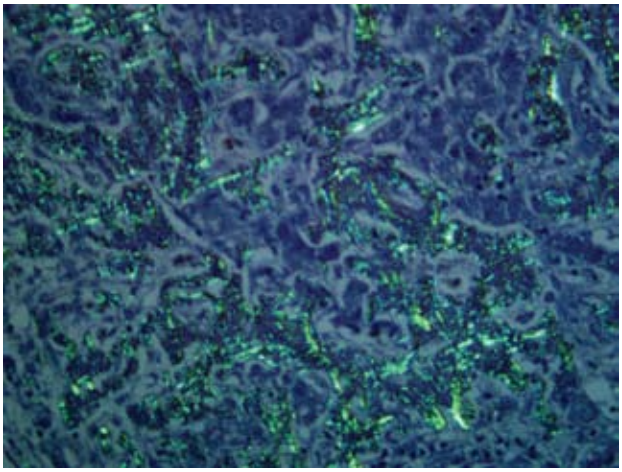

*3-5. Liver, duck. Congophilic amyloid material effacing hepatic cords and sinusoids displays apple green birefringence under polarized light. (CongoRed 400X) Photomicrograph courtesy of Rebecca M. Gruffey, Anatomic Pathology Service Manager, University of California – Davis, Veterinary Teaching Hospital, Anatomic Pathology, Davis California.*

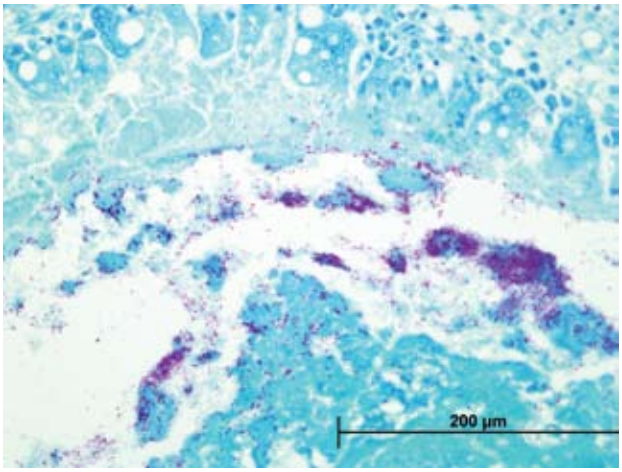


*3-6. Liver, duck. There are numerous acid fast bacilli within granulomas. (Fite-Foraco 400 X) Photomicrograph courtesy of Rebecca M. Gruffey, Anatomic Pathology Service Manager, University of California – Davis, Veterinary Teaching Hospital, Anatomic Pathology, Davis California.*

**Contributing Institution:** University of California Veterinary Medical Teaching Hospital, VM3-A, Anatomic Pathology, One Shields Avenue, Davis, CA 95616

**References:**

1. Abbas AK: Diseases of immunity: amyloidosis. *In*: Robbins and Cotran Pathologic Basis of Disease, eds. Kumar V, Abbas AK, Fausto N, 7th ed., pp. 258-264. Elsiever, Inc., Philadelphia, PA, 2005

2. Brassard A: Amyloidosis in captive Anseriformes. Can J Comp Med Vet Sci **29**:253-258, 1965

3. Cowan DF, Johnson WC: Amyloidosis in the white Pekin duck. Lab Invest **23**:551-555, 1970

4. King NW, Alroy J: Intarcellular and extracellular depositions, degenerations: Amyloidosis. *In:* Veterinary Pathology eds., Jones TC, Hunt RD, King NW, 6th ed., pp. 50-54. Lippincott Williams & Wilkins, Baltimore, 1997

5. Landman WJM, Gruys E, Gielkens ALJ: Avian

amyloidosis. Avian Pathol **27**:437-449, 1998
6. Montali RJ, Bush M, Thoen CO, Smith E: Tuberculosis in captive exotic birds. JAVMA **169**:920-927, 1976
7. Nakayama H, Katayama KI, Ikawa A, Miyawaki K, Shinozuka J, Uetsuka K, Nakamura SI, Kimura N, Yoshikawa Y, Doi K: Cerebral amyloid angiopathy in an aged great spotted woodpecker (*Picoides major*). Neurobiol Aging **20**:53-56, 1999
8. Saggese MD, Riggs G, Tizard I, Bratton G, Taylor R, Phalen DN: Gross and microscopic findings and investigation of the aetiopathogenesis of mycobacteriosis in a captive population of white-winged ducks (*Cairina scutulata*). Avian Pathol **36**:415-422, 2007
9. Tell LA, Woods L, Cromie RL: Mycobacteriosis in birds. Rev Sci Tech Off Int Epiz **20**:180-203, 2001
10. Zschiesche W, Linke RP: Immunohistochemical characterization of spontaneous amyloidosis in captive birds as AA-type, using monoclonal and polyclonal anti-AA antibodies against mammalian amyloid. Acta Histochem **86**:45-50, 1989

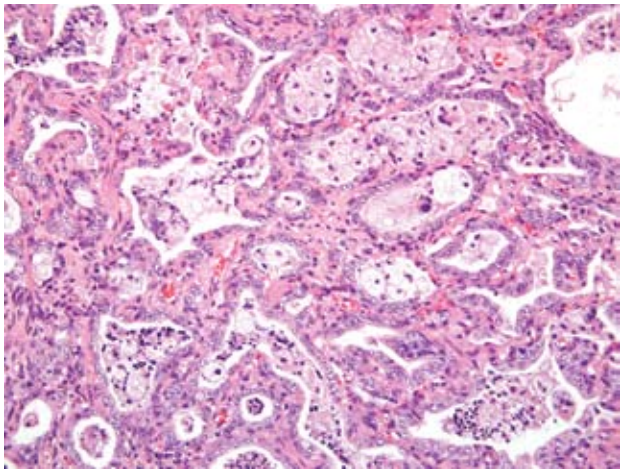

*4-1. Lung, cat. Alveolar septa are markedly expanded by large amounts of fibrosis, smooth muscle proliferation, and an inflammatory infiltrate composed of histiocytes and lymphocytes. Alveolar are flooded by either a cellular exudates composed of viable and degenerate neutrophils and fewer macrophages, or by numerous large foamy alveolar macrophages which contain many small indistinct vacuoles. Diffusely, alveoli are lined by type II pneumocyte hyperplasia. (HE 200X)*

## CASE IV – BA 652/07 (AFIP 3102244)

**Signalment:** 9-year-old, female neutered, Persian cross-bred, feline (*Felis domesticus*)

**History:** The cat was referred to the Royal (Dick) School of Veterinary Studies with a 4 month history of intermittent coughing and retching, which was unresponsive to furosemide (diuretic) and Synulox (antibiotic). Broncho-alveolar lavage fluid prior to referral contained very large numbers of monomorphic epithelial cells but was otherwise non-diagnostic. The cat presented with a severe tachypnoea (100-160 bpm). Thoracic radiographs were performed and revealed a mixed alveolar, interstitial, nodular and bronchial pattern with bullous change in the caudo-dorsal lung lobes. PCR for *Mycoplasma* sp. was negative. A clinical diagnosis of Idiopathic Pulmonary Fibrosis was made. The cat was prescribed steroids, Sildenafil (Viagra), Colchicine and Salbutamol (Ventolin). Some response to the steroid treatment was observed but this was limited. Over the following 9 months the cat deteriorated with several episodes of hospitalization.

**Gross Pathology:** The cat was in obese body condition (4.2kg). The lungs were diffusely mottled dark and light pink with numerous multifocal to coalescing firm, yellow-brown to yellow-green, depressed areas over the surface. These ranged from 2-12 mm diameter and extended into the parenchyma. This was more pronounced in the caudal right lung lobe. The airways were clear. Mild, multifocal bilateral chronic renal cortical infarcts were also noted, characterized by firm, depressed, tan foci.

**Laboratory Results:** None

**Histopathologic Description:** Lung – Right caudal lung lobe – 1 section

Approximately 70-80% of the lung parenchyma is remodeled by multifocal to coalescing areas of increased cellularity, predominantly located subpleurally, but also extending into the central parenchyma. In these areas, the pulmonary interstitium is markedly expanded by fusiform and plump mesenchymal cells (fibrocytes and fibroblasts), and thick bundles of plump spindloid cells with moderate amounts of eosinophilic cytoplasm, and a medium sized oval to elongated nucleus with a reticular chromatin pattern (myofibroblasts) **(Fig. 4-1)**. Where present, alveolar spaces are lined by a single to occasionally multiple layers of low columnar to cuboidal epithelial cells with indistinct cell borders, a moderate amount of pale eosinophilic, finely granular cytoplasm and a basally located, round to oval nucleus with a finely stippled chromatin pattern, and

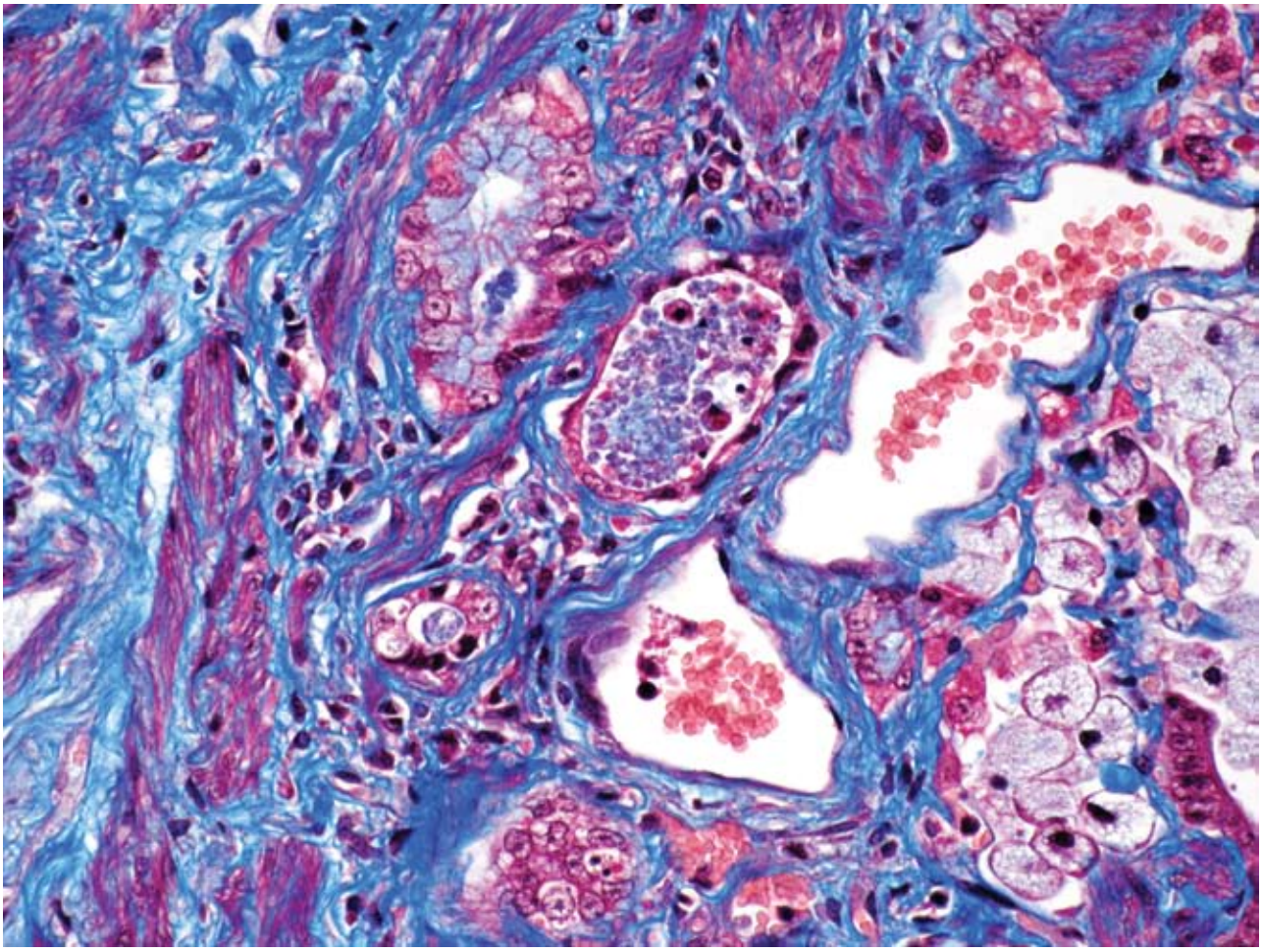

*4-2. Lung, cat. Masson's trichrome stain demonstrates alveolar interstitial fibrosis and smooth muscle proliferation.* *Photomicrograph courtesy of Veterinary Pathology Unit, University of Edinburgh, Royal (Dick) School of Veterinary Studies, Easter Bush Veterinary Centre, Easter Bush, Midlothian, Scotland. (MAS 400X)*

one to two medium sized nucleoli consistent with type II pneumocytes ("honeycomb lung").

Within the alveolar lumen are numerous, plump, polyhedral to round cells with abundant, highly vacuolated, pale eosinophilic cytoplasm and a medium sized oval nucleus with a finely stippled chromatin pattern and a single, medium sized nucleolus (alveolar macrophages). These cells are occasionally binucleated and multinucleated. Small aggregates of lymphocytes and plasma cells are scattered throughout the remaining pulmonary parenchyma.

Small to medium sized bronchi contain numerous alveolar macrophages interspersed with abundant pale amphophilic to basophilic, lightly fibrillar, acellular material (mucus), small areas of deeply basophilic, cracked acellular material (mineral) and acicular (cholesterol) clefts. At the periphery of the large bronchi are numerous, small peribronchiolar glands. In less severely affected areas, the alveolar lumens are multifocally enlarged by non-staining spaces (emphysema).

**Special stains/Immunohistochemistry:** The cuboidal cells lining the alveolae are strongly positive for cytokeratin, confirming their epithelial nature. The interstitial mesenchymal proliferation stained variably blue and pink (collagen and smooth muscle, respectively) **(Fig. 4-2)** and large areas stained strongly with smooth muscle actin confirming the presence of smooth muscle **(Fig. 4-3).**

**Contributor's Morphologic Diagnosis:** Lung – Right cranial lung lobe - Severe, multifocal to coalescing interstitial fibrosis with fibroblast and myofibroblast foci, type II pneumocyte hyperplasia (honeycomb lung) and

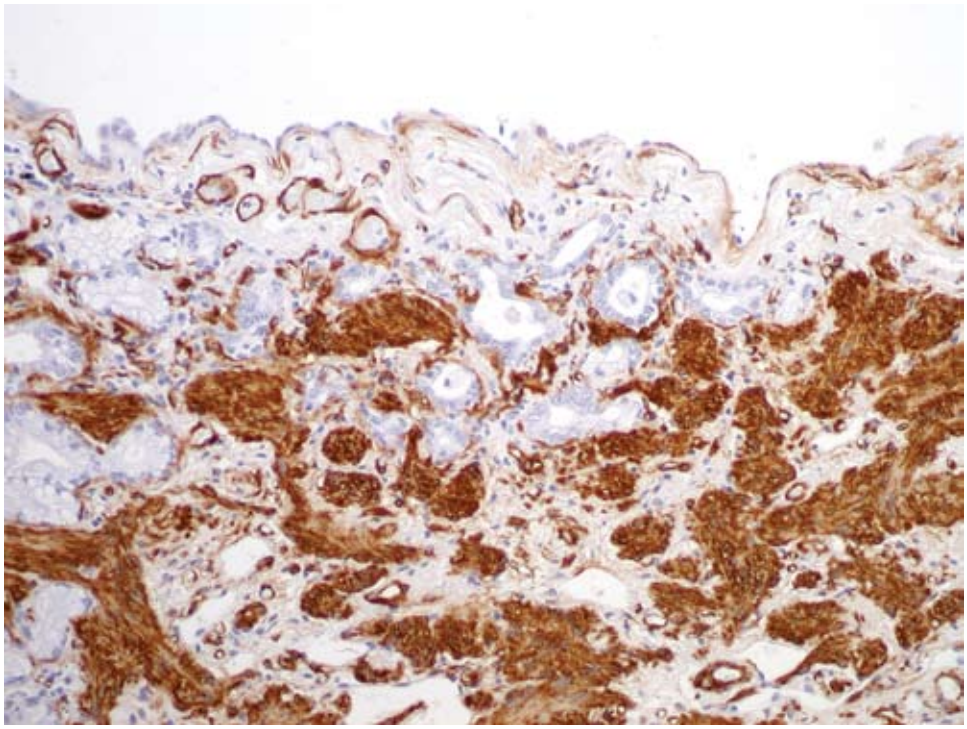

*4-3. Lung, cat. Smooth muscle actin immunohistochemical stain demonstrating positive cytoplasmic immunoreactivity within areas of alveolar interstitial smooth muscle proliferation. Photomicrograph courtesy of Veterinary Pathology Unit, University of Edinburgh, Royal (Dick) School of Veterinary Studies, Easter Bush Veterinary Centre, Easter Bush, Midlothian, Scotland. (SMA 200X)*

alveolar interstitial smooth muscle proliferation

**Contributor's Comment:** The severe, multifocal to coalescing interstitial fibrosis, interstitial smooth muscle proliferation, alveolar macrophages and excess mucus production are consistent with the clinical diagnosis of feline idiopathic pulmonary fibrosis (FIPF). The lesions were similar in nature throughout the lung but were more severe in the right caudal lung lobe than the left cranial lung lobe. There was also squamous metaplasia in sections of the cranial lung lobe, which is also a feature of this condition.

FIPF is an uncommon condition, first described in 2000 by Rhind and Gunn-Moore. [2] The average age of onset is approximately 8.7 years and the average time between onset clinical signs to death is 5.5 months.[1] This case has many features characteristic of this condition: sub-plural and caudo-dorsal distribution, persistent progressive fibrosis with temporal heterogeneity of lesions, alveolar type II pneumocyte hyperplasia and small foci of alveolar epithelial squamous metaplasia in some sections. This condition has been associated with the development of bronchoalveolar carcinoma, which was not a feature of this case. The aetiology is not currently known. Toxic, hypersensitivity, inflammatory and genetic origins have been investigated.

Parallels have been drawn between FIPF and Usual Interstitial Pneumonia (UIP) in man.[3] Salient features of UIP in man include interstitial fibrosis with fibroblast/myofibroblast proliferation, temporal heterogeneity of lung remodeling, subpleural orientation, "honeycomb" change, interstitial smooth muscle proliferation and scant inflammation.

A type II pneumocyte defect has been described in a familial form of human interstitial pulmonary fibrosis (IPF), with abnormal cytoplasmic lamellar body-like inclusions seen on electron microscopy.[3] Similar ultrastructural changes were observed in type II pneumocytes of affected cats by Williams et al. The authors suggested that FIPF may be due to a defect in the type II pneumocyte and that cats potentially represent a spontaneous model of IPF in humans.

A**FIP Diagnosis:** Lung: Interstitial fibrosis, multifocally extensive, severe with fibroblast and smooth muscle proliferation, type II pneumocyte hyperplasia, and alveolar histiocytosis

**Conference Comment:** Idiopathic pulmonary fibrosis is a respiratory disease of humans that affects 11 male and 8 female patients per 100,000 individuals per year. Consequently, a representative animal model to study this malady is highly coveted and bleomycin-treated rodents have not proved to be adequate subjects to date.[3] The contributor did an excellent job of outlining what is

currently known about this disease in cats.

**Contributing Institution:** Veterinary Pathology Unit, University of Edinburgh, Royal (Dick) School of Veterinary Studies, Easter Bush Veterinary Centre, Easter Bush, Midlothian, EH25 9RG, Scotland, UK.
www.vet.ed.ac.uk

**References:**

1. Cohn L, Norris E, Hawkins E, Dye J, Johnson C and Williams K: Identification and characterization of an Idiopathic Pulmonary Fibrosis-like condition in cats. J Vet Intern Med **18**:623-641, 2004
2. Rhind S and Gunn-Moore D: Desquamative form of cryptogenic fibrosing alveolitis in a cat. J Comp Path **123**:226-229, 2000
3. Williams K, Malarkey D, Cohn L, Patrick D, Dye J and Toews G: Identification of spontaneous feline idiopathic pulmonary fibrosis. Chest **125**:2278-2288, 2004

**NOTES:**

The Armed Forces Institute of Pathology
Department of Veterinary Pathology

*Conference Coordinator:*
Todd M. Bell, DVM

WEDNESDAY SLIDE CONFERENCE 2008-2009

# Conference 17

11 February 2009

*Conference Moderator:*

**Dr. Fabio Del Piero, DVM, DACVP**

## CASE I – S0 10582 (AFIP 3113965)

**Signalment:** 20-year-old, gelding, Arabian horse (*Equus caballus*)

**History:** A cecal mass was submitted for histopathology.

**Gross Pathology:** The submitted tissue was an approximately 4x5x4 cm round, firm, nodular, dark gray, well encapsulated mass with intact surface mucosa. On cut section the mass was distinct from the mucosa, white-tan and multilobulated.

**Laboratory Results:** None

**Histopathologic Description:** The mass is a well demarcated, encapsulated, multilobulated, expansile mass located from deep tunica muscularis to the serosa compressing the adjacent tissues and muscle layers. The mass is composed of multiple large lobules separated by a thick dense fibrous connective tissue. The mass is made of a large number of spindle shaped cells arranged in interconnected and branching trabeculae separated by sinuses filled with large amount of basophilic mucinous material as well as clusters of erythrocytes **(Fig. 1-1)**. The neoplastic cells have indistinct cell borders, large amount of eosinophilic cytoplasm, one oval to elongated nucleus with rounded poles and finely granular heterochromatin and 1-2 small basophilic nucleoli. The cells have moderate anisokaryosis with rare mitotic figures per HPF (40X). There are scattered hemosiderin laden macrophages within the mass. There are multifocal areas of chronic hemorrhages with aggregations of siderophages present in the capsule.

Immunohistochemistry was performed. The submitted mass was strongly positive for vimentin and c-kit and slightly positive for NSE. It did not stain with desmin, smooth muscle actin and S100. Unfortunately, no history was submitted with this mass to know the reason for removal.

**Contributor's Morphologic Diagnosis:** Cecum: Gastrointestinal stromal tumor with peripheral hemorrhage and siderophages

**Contributor's Comment:** Equine gastrointestinal stromal tumors are unique, benign mesenchymal tumors often found in the cecum of horses. They are detected at surgery, meat inspection or necropsy and may occur in stomach, small intestine and most commonly in the

*Sponsored by the American Veterinary Medical Association, the American College of Veterinary Pathologists, and the C. L. Davis Foundation.

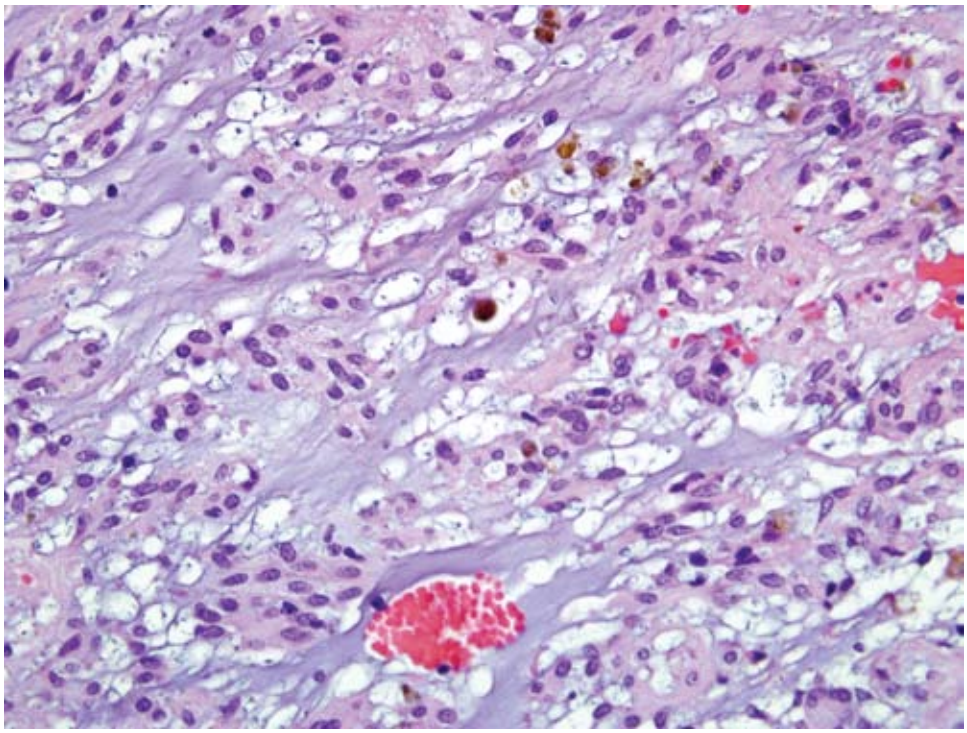

*1-1. Large intestine, horse. Gastrointestinal stromal tumor. Neoplastic cells are separated by myxomatous matrix with scattered hemorrhage and few hemosiderin-laden macrophages. (HE 400X)*

cecum (as in this case) and colon.[1] These tumors are different from leiomyomas although they have common features. Grossly, these tumors are distinct and form exophytic multinodular masses on the serosal surface or transmurally. Histologically, they are usually composed of interlacing fascicles with multiple sinuses filled with mucinous materials stained by alcian blue. There are often hemorrhagic and may have myxomatous islands within their parenchyma.[3] Immunohistochemically, they are positive for c-kit protein (CD117), vimentin and neuron specific enolase and mildly for smooth muscle actin.[4]

**AFIP Diagnosis:** Cecum: Gastrointestinal stromal tumor, myxoid

**Conference Comment:** Gastrointestinal stromal tumors (GISTs) have been reported in numerous domestic species and are thought to arise from the interstitial cells of Cajal, the precursors to the pacemaker cells in the intestinal wall.[2] Histologically, these tumors closely resemble leiomyosarcomas, and immunohistochemistry is needed to differentiate them. GISTs are normally composed of spindle cells arranged in interlacing fascicles or in a whirling pattern. Another less common pattern is the myxoid pattern characterized by epithelioid cells arranged in trabeculae or sheets within a myxoid matrix.[1]

These tumors are a recently recognized entity in veterinary medicine, and thus criteria for malignancy have not yet been solidified. In humans, larger size and greater mitotic activity point to malignancy and a poor prognosis, but future studies will be needed to determine their behavior in domestic animals.[1]

**Contributing Institution:** CAHFS – UC Davis; www.cahfs.ucdavis.edu

**References**:

1. Brown C., Baker D.C, Barker I: Alimentary system. *In:* Jubb, Kennedy and Palmer's Pathology of Domestic Animals. 5th ed., pp. 127-128. Mosby Saunders, Philadelphia, PA, 2007
2. Cooper BJ, Valentine BA: Tumors of muscle. *In:* Tumors in Domestic Animals. ed Meuten DJ, 4th ed, pp. 328-333, Iowa State Press, Ames, Iowa, 2002
3. Del Piero F, Summers BA, Credille KM, Cummings JF, Mandelli G: Gastrointestinal stromal tumors in Equidae. Vet Pathol **33**:611, 1996
4. Hafner S. Harman G. King T: Gastrointestinal stromal tumors of equine cecum. Vet Pathol **38**:242-246, 2001

## CASE II – 23279-08 (AFIP 3103695)

**Signalment:** 10-year-old female equine Thoroughbred (*Equus caballus*)

**History:** The mare had signs of equine protozoal myeloencephalitis (EPM) then developed pneumonia. The mare responded to EPM therapy but had continuing weight loss and cachexia despite a variety of treatments for pneumonia. The mare was euthanized due to continued loss of body condition.

**Gross Pathology:** Significant changes were restricted to the lungs. Bilaterally, lung lobes were diffusely firm and failed to collapse when the thoracic cavity was opened. Throughout the pulmonary parenchyma were multifocal to coalescing firm, light pink, irregularly round nodules that varied in size from 1cm to large confluent masses. The nodules were separated by normal appearing tissue. When sectioned, the masses had a firm fibrous texture and bulged slightly on cut surface.

**Laboratory Results:** None

**Histopathologic Description:** Sections of lung are characterized by multifocal areas of pulmonary fibrosis and inflammation bordered by more normal appearing lung tissue. Alveolar septa are moderately to severely expanded by well organized mature collagen **(Fig. 2-1)**. Alveoli are often lined by plump cuboidal cells (Type 2 pneumocyte hyperplasia), and alveolar lumens contain a mixture of sloughed epithelial cells, intact and degenerate neutrophils, large foamy macrophages, and few multinucleated giant cells. Rare macrophages contain large, brightly eosinophilic, round, intranuclear inclusion bodies that peripheralize nuclear chromatin and are occasionally surrounded by a clear halo **(Fig. 2-2)**.

**Contributor's Morphologic Diagnosis:** Severe multifocal nodular fibrosing interstitial pneumonia with intranuclear inclusion bodies, *Equus caballus*; Equine multinodular pulmonary fibrosis

**Etiology:** Equine Herpesvirus-5 (EHV-5)

**Contributor's Comment:** Equine multinodular pulmonary fibrosis (EMPF) is a distinct entity in the category of equine chronic pulmonary disease. It is differentiated from other fibrosing inflammatory diseases, such as recurrent airway obstruction (RAO) or chronic pneumonia, by the nodular pattern of fibrosis. This disease may have been previously reported under the names "idiopathic interstitial pneumonia with fibrosis" or "idiopathic pulmonary fibrosis."

EMPF is most common in middle-aged horses. Horses with this disease present with non-specific signs of respiratory disease including cough, fever, weight loss, tachypnea, increased respiratory effort, and nasal discharge. Treatment with antibiotics may result in short-term improvement, but symptoms recur after treatment is discontinued. Pulmonary nodules can be visualized

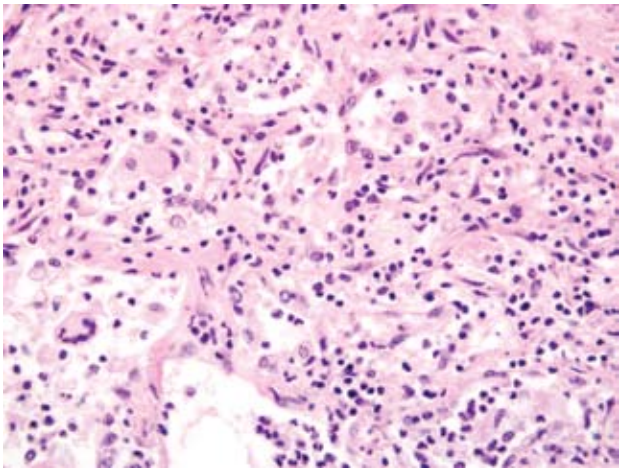

*2-1. Lung, horse. Equine multinodular pulmonary fibrosis. Abundant septal fibrosis, moderate type II pneumocyte hyperplasia, numerous lymphocytes, histiocytes, and neutrophils, with scattered multinucleated giant cells. (HE 400X)*

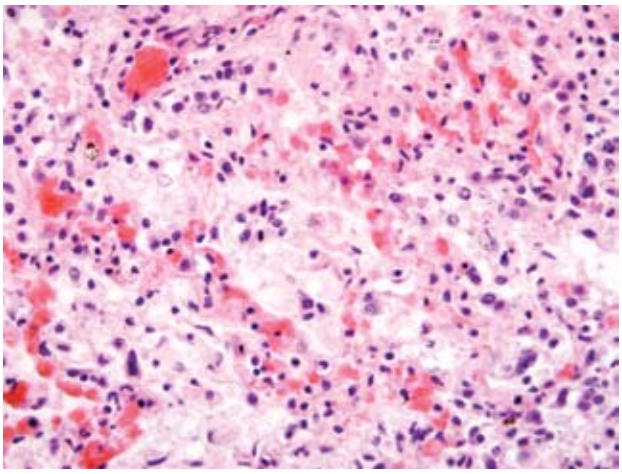

*2-1. Lung, horse. Equine multinodular pulmonary fibrosis. Abundant septal fibrosis, moderate type II pneumocyte hyperplasia, numerous lymphocytes, histiocytes, and neutrophils, with scattered multinucleated giant cells. (HE 400X)*

with ultrasonography and/or radiography. Rule outs include neoplasia, fungal pneumonia, and granulomatous pneumonia, which may also result in a nodular pattern. Treatment of choice includes long-term (at least 6 weeks) administration of corticosteroids. Prognosis for the disease is considered fair to poor. Many horses are euthanized due to continued respiratory complications and poor athletic performance.

Lung tissue from this horse was positive via polymerase chain reaction (PCR) for EHV-5. EHV-5 is a DNA gammaherpes virus that has only recently been associated with this disease entity. The pathogenesis of EHV-5 in this disease has not been fully elucidated but may contribute to a "pro-fibrotic" lung environment via a Th-2 lymphocyte inflammatory response. PCR can be performed on bronchoalveolar lavage samples or lung tissue. Unlike EHV-2, another common viral cause of equine respiratory disease, EHV-5 is not isolated from healthy horses or horses with respiratory disease due to other etiologies. A study by Bell identified EHV-5 in 64% of young racehorse nasal swabs, while a study performed by Wang identified the virus in 48% of 5-9 month old Thoroughbred foals.

Intranuclear inclusion bodies are not a common feature in gammaherpes infections but may be observed in California sea lions infected with genital carcinoma caused by gammaherpes virus. Murine herpesvirus-68 is a gamma herpesvirus associated with experimental fibrotic lung disease in mice.

**AFIP Diagnosis:** Lung: Fibrosis, interstitial, nodular, multifocal, severe with neutrophilic and histiocytic alveolitis, type II pneumocyte hyperplasia and rare intrahistiocytic eosinophilic intranuclear inclusions

**Conference Comment:** There are several alpha herpesviruses that are of significance in domestic animals. Listed below are some of the major alpha herpesviruses of significant importance in veterinary medicine.

| Alpha herpesvirus | Disease |
|---|---|
| Equine herpesvirus 1 | Abortion, foal mortality, neurologic and respiratory disease |
| Equine herpesvirus 3 | Coital exanthema |
| Equine herpesvirus 4 | Rhinopneumonitis |
| Bovine herpesvirus 1 | Infectious bovine rhinotracheitis, infectious pustular vulvovaginitis |
| Bovine herpesvirus 2 | Bovine mammilitis, pseudo-lumpyskin disease |
| Porcine herpesvirus 1 (pseudorabies; Aujeszky's Disease) | Abortion in adults and generalized disease in younger animals; death in other species |
| Canine herpesvirus 1 | Pneumonia, hepatitis, nephritis – hemorrhagic disease |
| Feline herpesvirus 1 | Feline viral rhinotracheitis |
| Gallid herpesvirus 1 (chickens) | Infectious laryngotracheitis |
| Gallid herpesvirus 2 (chickens) | Marek's disease |
| Anatid herpesvirus 1 | Duck plague |
| Cercopithecine herpesvirus 1 (B virus) | Herpes simplex-like disease in macaques; encephalitis and death in humans |

1

**Contributing Institution:** University of Kentucky, Livestock Disease Diagnostic Center, Lexington, Kentucky; www.lddc.uky.edu

**References:**
1. Murphy FA, Gibbs EPJ, Horzinek MC, Studdert MJ: Herpesviridae: *In:* Veterinary Virology, eds. Murphy FA, Gibbs EPJ, Horzinek MC, Studdert MJ, 3rd ed., pp. 301-325. Academic Press, San Diego, California, 1999
2. Williams KJ, Maes R, Del Piero F, Lim A, Wise A, Bolin DC, Caswell J, Jackson C, Robinson NE, Derksen F, Scott MA, Uhal BD, Li X, Youssef SA, Bolin SR: Equine multinodular pulmonary fibrosis: a newly recognized herpesvirus-associated fibrotic lung disease. Vet Pathol **44**(6):849-62, 2007
3. Wong DM, Belgrave RL, Williams KJ, Del Piero F, Alcott CJ, Bolin SR, Marr CM, Nolen-Walston R, Myers RK, Wilkins PA: Multinodular pulmonary fibrosis in five horses. J Am Vet Med Assoc **15**:898-905, 2008

## CASE III – 63383-02 (3103693)

**Signalment:** 10-month gestation placenta, Thoroughbred, (*Equus caballus*), equine

**History:** The mare was due to foal on January 20, 2003, but the mare foaled on December 28, 2002.

**Gross Pathology:** A complete placenta is submitted for examination. Along the chorionic surface of the body and non-pregnant horn are multifocal regions of denuded villi covered with a thick mucoid exudate. Adjacent villi are thickened and edematous. No other significant gross lesions are observed.

**Laboratory Results:**
Bacteriology
—Placenta: *Cellulosimicrobium cellulans* formerly known as *Oerskovia xanthineolytica* (numerous)
—FA testing for the detection of *Leptospira interrogans* on the placenta was negative.

**Histopathologic Description:** Allantochorion: Amorphous eosinophilic material with scattered aggregates of bacteria, intact and degenerate neutrophils, and cellular debris multifocally overlies the chorionic surface. The chorionic villi, lined by hypertrophic trophoblasts with mild to moderate cytoplasmic vacuoles, are multifocally blunted. Aggregates of moderate to large numbers of lymphocytes, plasma cells, and neutrophils occupy the superficial stroma adjacent to the villi and villous projections. The supporting stroma is characterized by diffuse, moderate edema, an infiltrate of low to moderate numbers of lymphocytes, neo-vascularization and moderate fibroplasia.

**Contributor's Morphologic Diagnosis:** Severe multifocal necrotizing exudative placentitis; *Equus caballus*

**Contributor's Comment:** *Cellulosimicrobium cellulans* is a gram positive, branching, motile, oxidase negative, catalase positive, non-acid fast-bacillus. When grown on agar, the colonies have a characteristic yellow color.[3] The bacteria are found in soil and have been associated with middle and late term abortions, as well as premature births in horses.[1] Lesions are typically but not always seen in the both the fetus and placenta. Fetal lesions include firm, expanded lungs, and mildly enlarged friable livers with occasional pale foci along the capsular surface that extend into the parenchyma.[1] Lesions observed in the allantochorion include a brown mucoid exudate overlying well demarcated areas of denuded villi along the chorion. In previous reports, portions of the chorion affected include areas adjacent to the cervical star, along the body, or encompassing the horns. Microscopically, the chorionic surface is covered by an eosinophilic exudate and had blunted villi and marked inflammation of both the villi and supporting stroma. Often seen with the placentitis is a pyogranulomatous pneumonia characterized by multinucleated giant cells, macrophages, and neutrophils occupying the lumens of alveoli, bronchi, and bronchioles.[1]

Given the presence of an exudative placentitis, the distribution of the placental lesions, and the characteristics of *Cellulosimicrobium cellulans*, there are similarities between the bacteria described here and placentitis resultant of a *Crossiella equi* infection. Pyogranulomatous pneumonia, as seen with *Cellulosimicrobium cellulans*, does not accompany nocardioform placentitis.

Common bacterial agents resulting in placentitis and abortion in the horse include *Leptospira* spp, nocardioform, *Escherichia coli*, *Streptococcus zooepidemicus*, *Pseudomonas aeruginosa*, *Streptococcus equisimilis*, *Enterobacter agglomerans*, *Klebsiella pneumoniae*, and alpha- hemolytic *Streptococcus*.[2]

**AFIP Diagnosis:** Placenta, allantochorion: Placentitis, necrotizing, subacute, diffuse, moderate, with squamous metaplasia **(Fig. 3-1)**, fibrin, edema, and large colonies of coccobacilli **(Fig. 3-2)**

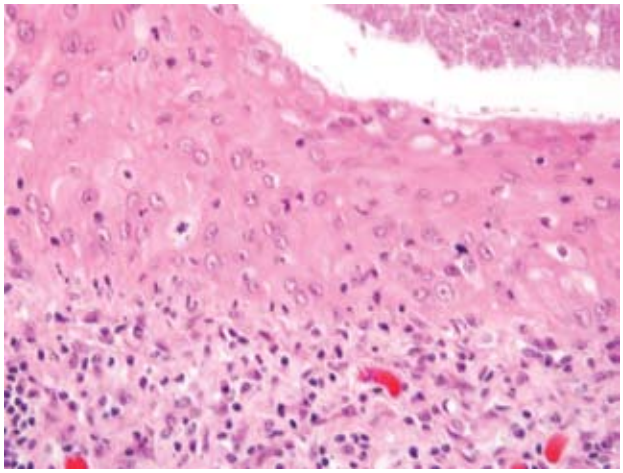

*3-1. Chorioallantois, horse. Necrosuppurative bacterial chorionitis. Squamous metaplasia of the allantoic epithelium. (HE 400X)*

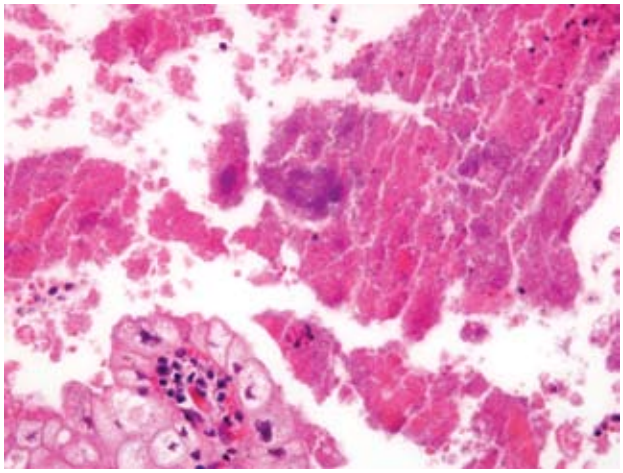

*3-2. Chorioallantois, horse. Necrosuppurative bacterial corionitis. Multifocally within necrotic chorionic villi, there are large colonies of 0.5 x 1 micron basophilic coccobacilli. (HE 400X)*

**Conference Comment:** *Cellulosimircobium cellulans*, formerly named *Oerskovia xanthineolytica*, is rarely found in humans and is generally an opportunistic pathogen in immunocompromised hosts.[1] This organism is being recognized more frequently as a cause of equine abortion.

The bulk of the conference discussion centered on the outbreak of abortions in Kentucky in the spring of 2001 and 2002 dubbed Mare Reproductive Loss Syndrome (MRLS). MRLS caused large numbers of abortions reaching epidemic proportions in Kentucky.[4] The economic loss alone has been estimated at almost $500 million.

Mares with MRLS abort late in gestation or at term and the fetuses are still enclosed within the placenta and in good condition. Mares show no overt clinical illness prior to abortion. In the fetus, gross lesions include hemorrhages in the chorion, amnion, and amniotic segment of the umbilical cord, pleura, and heart, hypema, and uninflated lungs. Additionally, the amniotic cord is often dull gray and thickened. Histologically, macrophages and neutrophils are seen in ulcerated areas on the surface of the amniotic cord in association with bacteria. The allantochorion also has similar lesions. Funisitis, amnionitis, pneumonia, fetal bacteremia, and chorionitis are also evident microscopically.

The most commonly implicated cause for MRLS is the eastern tent caterpillar (ETC). Feeding of the eastern tent caterpillar to pigs has resulted in abortions in one study. Similar studies in horses have demonstrated that the feeding of the exoskeleton of the eastern tent caterpillar causes abortion in mares. One of the most current hypotheses is that a portion of the caterpillar cuticle is responsible for its abortifacient effects.[4]

**Contributing Institution:** University of Kentucky; Livestock Disease Diagnostic Center; Lexington, Kentucky; 40512; www.lddc.uky.edu

**References**:

1. Bolin DC, Donahue JM, Vickers ML, Giles RC, Harrison L, Jackson C, Poonacha KB, Roberts JF, Sebastian MM, Sells SF, Tramontin R, Williams NM: Equine abortion and premature birth associated with *Cellulosimicrobium cellulans* infection. J Vet Diagn Invest **16**:333-336, 2004

2. Hong CB, Donahue JB, Giles RC, Petrites-Murphy MB, Poonacha KB, Roberts AW, Smith BJ, Tramontin RR, Tuttle PA, Swerczek TW: Etiology and pathology of equine placentitis. J Vet Diagn Invest **5**:56-63, 1993

3. Rihs JD, McNeil MM, Brown JM, Yu VL: *Oerskovia xanthineolytica* implicated in peritonitis associated with peritoneal dialysis: case report and review of *Oerskovia* infections in humans. J Clin Microbiol **28**:1934-1937, 1990

4. Schlafer DH, Miller RB: Female genital system. *In:* Jubb, Kennedy, and Palmer's Pathology of Domestic Animals, ed. Maxie MG, vol 3, pp. 506-507. Elsevier Limited, Philadelphia, PA, 2007

## CASE IV – S07-514.1 (AFIP 3103232)

**Signalment:** Suckling pig, about 4 weeks of age, female, porcine, breed unspecified (*Sus domestica*)

**History:** Reduced weight gain within the herd. Suckling pigs show heavy breathing and die unexpectedly.

**Gross Pathology:** Multiple tongue erosions, yellowish secretion from the nose, yellowish plaques on nasal turbinates.

**Laboratory Results:** *Corynebacterium* spp. were isolated from the nasal turbinate.

**Histopathologic Description:** Nasal turbinate: Diffusely, the subepithelial connective tissue is expanded and infiltrated by numerous lymphocytes, plasma cells, and fewer macrophages. Epithelial cells of the nasal mucous glands and the respiratory epithelium are multifocally slightly enlarged (cytomegaly) with abundant, foamy, eosinophilic cytoplasm and a single 20-30 mm, basophilic, irregular, smudgy and granular, intranuclear inclusion body **(Fig. 4-1)** that fills and distends the karyomegalic nucleus. Multifocally the mucous glands are ectactic, lined by attenuated epithelium, and contain variable amounts of eosinophilic cellular and karyorrhectic debris (necrosis) with rare neutrophils. The respiratory epithelium is multifocally lost and replaced by a moderate amount of karyorrhectic and pyknotic cell debris (necrosis). In the nasal passage, there is an exudate composed of erythrocytes, sloughed epithelial cells, and some slightly eosinophilic material (mucous).

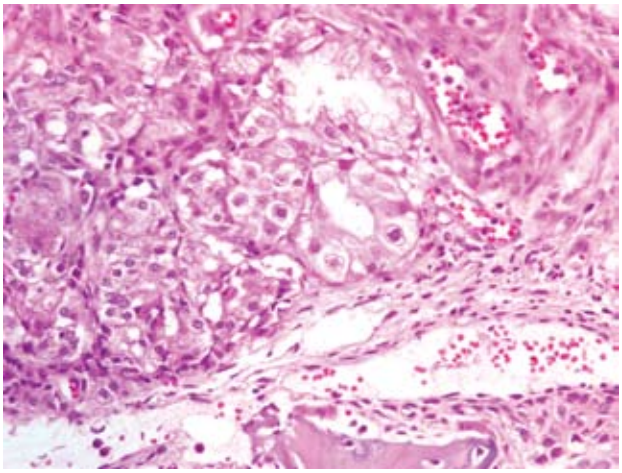

4-1. Nasal turbinates, pig. Inclusion body rhinitis. Amphophilic to eosinophilic intranuclear inclusion bodies within mucosal epithelium and glandular epithelium of the nasal turbinates. (HE 400X)

There is a large focally extensive necrotic area (not included in every slide), characterized by a large amount of eosinophilic karyorrhectic and pyknotic cell debris, and bordered by an abundant amount of small and medium caliber vessels surrounded by reactive fibroblasts and collagen (granulation tissue).

**Contributor's Morphologic Diagnosis:** Nasal turbinate: Rhinitis, lymphoplasmacytic and necrotizing, subacute, diffuse, marked, with glandular epithelial karymegaly due to intranuclear inclusion bodies

**Contributor's Comment:** Inclusion body rhinitis – porcine cytomegalovirus (PCMV)
PCMV infections are ubiquitous and occur throughout the world, but clinical disease is much less frequent. Inclusion body rhinitis is typically an acute to subacute disease of 3-5-week-old suckling piglets. Piglets exhibit fever, sneezing, catarrhal nasal exudate, shivering, and occasional dyspnoe. Morbidity is high and mortalitiy is low unless secondary bacterial infections develop. Systemic cytomegalovirus infections usually infect piglets less than 3 weeks of age. These piglets may be found dead without premonitory signs, or exhibit sneezing, lethargy, anorexia, subcutaneous edema of the jaw and tarsal joints, and dyspnea. Infection of naïve pregnant sows induces mild lethargy, anorexia, and delivery of stillborn or weak piglets. Inclusion body rhinitis is caused by PCMV, a beta-herpesvirus. Piglets commonly shed the virus soon after weaning at 3 weeks of age, suggesting that infection is usually acquired by contact with nasal secretions of infected cohorts. Other pigs, particularly those that develop generalized disease, are probably infected from the sow in the neonatal period. The virus replicates in nasal submucosal and lacrimal glands. Viremia develops at 5-14 days after infection depending on the age of the pig and leads to infection of epithelial cells in renal tubules, liver, duodenum, and elsewhere. Pulmonary alveolar and splenic macrophages may be additional sites of viral replication. Virus is shed in nasal and ocular secretions, in the urine, and in vaginal secretions of sows.[3]

Infection can be diagnosed by the presence of characteristic large, basophilic, intranuclear inclusion bodies in cytomegalic cells of the nasal glandular epithelium. Such inclusion bodies and mononuclear cellular infiltrations can also be detected in the tubular epithelia of the kidneys, as well as the epithelia of the salivary and tear glands. Other, less frequent, lesions include interstitial pneumonia and lymphocytic perivasculitis in the brain. Predisposing factors of the infection are not fully known. A low level of immunity within the herd, e.g., in newly established

| **Herpesviridae** | | |
|---|---|---|
| **Alphaherpesvirinae:** focal lesions in skin and mucosa of resp. and genital tract; abortion; neonates: necrosis in multiple organs, latency in nerves | Equine herpesvirus 1: Equine herpesviral abortion, rhinopneumonitis, neurologic disease | horse |
| | Equine herpesvirus 3: Equine coital exanthema | horse |
| | Equine herpesvirus 4: Equine rhinopneumonitis | horse |
| | BHV-1: infectious bovine rhinotrcheitis/infectious pustular vulvovaginitis/infectious balanoposthitis | cattle |
| | BHV-2: bovine mammilitis virus (bovine herpes mammilitis) | cattle |
| | BHV-5: bovine herpesvirus encephalitis | cattle |
| | SHV-1: Aujezky´s disease, Pseudorabies | pig>others |
| | Canine herpesvirus 1: | dog |
| | Feline herpesvirus 1: upper respiratory tract disease (rhinotracheitis) and conjunctivitis (ulcers) | cats |
| | Feline herpesvirus 1: feline herpesvirus ulcerative dermatitis | cats |
| | Gallid herpesvirus-1: Infectious laryngotracheitis (ILT) | chicken |
| | Gallid herpesvirus-2: Marek´s disease | chicken |
| | Psittacine herpesvirus: Pacheco's disease | psittacines |
| | Anatid herpesvirus-1: Duck plaque/Duck virus enteritis | ducks, geese, swan |
| | Simplexvirus: HSV-1, HSV-2, HBV, BHV-2 | |
| | Herpesvirus simplex, type 1/type 2 | human & nonhuman primates |
| | Herpesvirus simiae/Herpes B/Cercopithecine HV | rhesus macaques |
| | Simian varicella virus | macaques, AGM, Patas monkeys |
| **Betaherpesvirinae:** no cell lysis, karyomegaly, latency in secretory glands, lymphoreticular organs, kidney | HHV-5, HHV-6, MCMV-1 | humans |

| | | |
|---|---|---|
| | Porcine herpesvirus 2: porcine cytomegalovirus disease/Inclusion body rhinitis | porcine |
| | Cytomegalovirus | humans + nonhuman primates |
| **Gammaherpesvirinae**: primates: lymphoproliferative disease, latency in lymphoid tissue | EHV-2 | |
| | EHV-5 | |
| | BHV-4: bovine herpes mammary pustular dermatitis | cattle |
| | OHV-2/AHV-1: malignant catarrhal fever | various ruminants |
| | Epstein-Barr virus (lymphocryptovirus-gamma 1) | primates |
| | Kaposi-sarcoma-associated herpesvirus/human herpesvirus-8 (KSHV/HHV8) (Rhadinovirus-gamma 2) | primates |
| **Deltaherpesvirinae** | Anatid herpesvirus-1: duck plague | |
| | SHV-2: Eischlusskörperchenkrankheit | pig |
| | Karpfenpocken | fish |
| **Uncharacterized viruses** | Koi-herpesvirus (KHV, carp nephritis and gill necrosis virus, CNGV, Cyprinid-Herpesvirus-3, CyHv-3) | fish |

herds, and immunosuppressive effects may play a role. Seroconversion due to PCMV is probably much more frequent than clinical disease.[1] In our case, sows in the herd had problems with insufficient lactation.

**AFIP Diagnosis:** 1. Nasal turbinates: Rhinitis, necro-ulcerative, subacute, diffuse, moderate, with glandular epithelial eosinophilic intranuclear inclusions
2. Haired skin and bone: Necrosis, focally extensive, with granulation tissue, fibrosis, osteonecrosis and osteolysis

**Conference Comment:** The contributor provides a comprehensive summary of this condition. One additional rule-out considered by attendees was atrophic rhinitis; however, changes in the nasal turbinate cartilage and bone would be an expected finding, as well the absence of inclusion bodies. For comparison purposes, a brief discussion of atrophic rhinitis is included here. Atrophic rhinitis is also a common disease in pigs worldwide. Atrophic rhinitis can be split into nonprogressive atrophic rhinitis (NPAR), caused by *Bordetella bronchiseptica*, or progressive atrophic rhinitis (PAR), caused by toxigenic *Pasteurella multocida* as a single agent or in combination with *Bordetella bronchiseptica*. Both of these disease cause hypoplasia of the nasal turbinates that clinically manifest as frequent sneezing by affected swine. Progression of either of these diseases can lead to distortion of the snout. Nasal hemorrhage is commonly seen in PAR; NPAR nasal hemorrhage is uncommon.[2]

Both *Bordetella bronchiseptica* and *Pasteurella multocida* produce their own toxins, and the severity of disease is dependent on the amount of toxin absorbed. One major difference between these two organisms is the age of affected pigs. PAR can affect pigs older than 3 months of age, whereas NPAR normally only affects pigs up to 6 weeks of age.[2]

Gross lesions in PAR are restricted to the nasal cavity and adjacent bone with the ventral scrolls of the nasal turbinates

most often suffering the worst lesions. Histologically, the pathognomonic lesion of PAR is replacement of the bony plates of the ventral conchae with fibrous tissue. Metaplasia of adjacent respiratory epithelium is also common.[2]

**Contributing Institution:** Institute of Veterinary Pathology of the University of Zurich, CH-8057 Zurich, Switzerland, www.vetpathology.unizh.ch

**References:**

1. Deim Z, Glavits R, Biksi I, Dencso L, Raczne AM: Inclusion body rhinitis in pigs in Hungary. Vet Rec. **158**(24):832-4, 2006

2. De Jong MF:Progressive and nonprogressive atrophic rhinitis. *In:* Diseases of Swine, ed. Straw BE, Zimmerman JJ, D'Allaire S, Taylor DJ, 9th ed., pp.577-602. Blackwell Publishing, 2006

The Armed Forces Institute of Pathology
Department of Veterinary Pathology

*Conference Coordinator:*
Todd M. Bell, DVM

WEDNESDAY SLIDE CONFERENCE 2008-2009

# Conference 18

25 February 2009

*Conference Moderator:*

Dr. James Raymond, DVM, MS, DACVP

## CASE I – S0704434(AFIP 3071894)

**Signalment:** Female adult Muscovy duck (*Cairina moschata*)

**History:** The duck was one of 2 birds to die from a total of 75 ducks. Submitted for necropsy. No clinical history was given.

**Gross Pathology:** The bird was in good flesh and tissues were in a good state of postmortem preservation. The liver was uniformly pale and there was generalized congestion of other visceral organs. Matured ovules of the ovary were markedly hemorrhagic. No other lesions were noted grossly.

**Laboratory Results:** Mixed flora was isolated from the lung, liver, ovule and intestines; duck enteritis virus (DVE) was detected by PCR.

**Histopathologic Description:** Liver: At the subgross level there is multifocal pallor or clear areas interpreted as loss of hepatic architecture. On close examination there is edema around most blood vessels and multifocal necrosis. There is dissociation of hepatocytes and some hepatocytes are swollen, disrupted or ruptured. There is abundance of eosinophilic intranuclear inclusion bodies with thinly marginated chromatin **(Fig. 1-1)**. There are no appreciable inflammatory cell infiltrates.

**Contributor's Morphologic Diagnosis:** Liver: Multifocal necrosis and degeneration, multifocal, acute, with perivascular edema and abundant eosinophilic intranuclear inclusion bodies

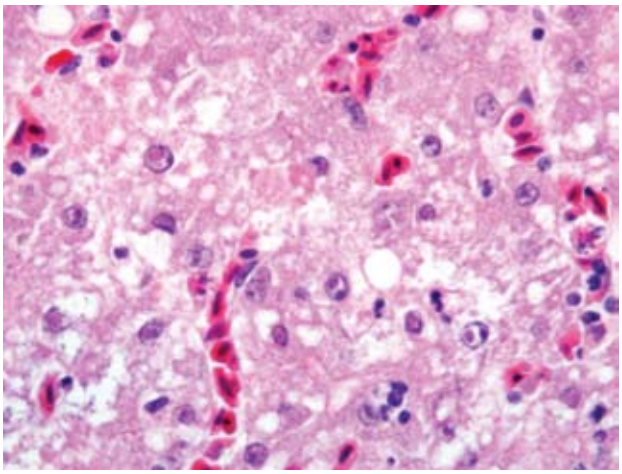

*1-1. Liver, duck. Multifocally within hepatocytes are brightly eosinophilic 5-8 micron in diameter intranuclear inclusions which frequently marginate nuclear chromatin. (HE 1000X)*

***Sponsored by the American Veterinary Medical Association, the American College of Veterinary Pathologists, and the C. L. Davis Foundation.**

**Contributor's Comment:** DVE is an acute, contagious herpesvirus infection of ducks, geese, and swans, characterized by vascular damage, tissue hemorrhages, digestive mucosal eruptions, lesions of lymphoid organs, and degenerative changes in parenchymatous organs.[6] Although there is no mention of clinical signs in this bird, the disease has an incubation period of 3 to 7 days. Once overt signs appear, death usually follows within 1 to 5 days. Naturally occurring infection has been observed in ages ranging from 7-day-old ducklings to mature breeder ducks.[6] DVE was first diagnosed in the United States in 1967 in a commercial Pekin duck-producing area of Long Island, NY, where it caused serious economic losses.[2,4] Mature ducks die in good flesh. Typically clinical signs consisted of prolapse of the penis in male matured breeders, and a marked drop in egg production in laying flocks. As DVE progresses within a flock more signs are observed: Photophobia, inappetence, thirst, nasal discharges, diarrhea, weakness, tremors of the head and neck. Mortality may range from 5 to 100%.[6] Based on the histopathologic findings the disease is considered non inflammatory and retrograde in nature; and the distribution of the inclusion bodies suggests that the virus is reticulo-endotheliotropic.[6]

In this bird, in addition to the liver lesions, mucosal lesions were noted in the digestive tract (esophagus, proventriculus), characterized by erosions and ulcerations with rare eosinophilic intranuclear inclusion bodies in few remaining epithelial cells.

Typically, lesions of DVE are those of vascular damage, eruptions of specific locations on mucosal surface of the gastrointestinal tract, lesions of lymphoid organs, and degenerative sequelae in parenchymatous organs. When these lesions are collectively present, are diagnostic of DVE.[6] In the present case the diagnosis was confirmed by PCR on tissue pools.

Differential diagnosis requires consideration of other diseases producing hemorrhagic and necrotic lesions in anseriforms. Such diseases include duck virus hepatitis, pateurellosis, necrotic enteritis, coccidiosis, and specific intoxications.[6]

To prevent this disease from spreading, strict decontamination and depopulation should be carried out whenever possible.[3] A vaccine is also available for prevention of DVE but approval by animal health authorities is required before it can be used.[7]

**AFIP Diagnosis:** Liver: Hepatitis, necrotizing, acute, random, moderate with eosinophilic intranuclear inclusion bodies, etiology consistent with herpesvirus

**Conference Comment:** Duck viral enteritis, also known as duck plague, is in the family *Herpesviridae*, and subfamily *Alphaherpesvirinae*. Two other extremely important herpes viruses in this subfamily are gallid herpesvirus 1 also known as infectious laryngotracheitis virus, and gallid herpesvirus 2 also known as Marek's disease.[5]

The pathogenicity of this virus depends on the particular species of duck infected. The blue-winged teal (*Anas discors*) is most susceptible to DVE, while the pintail duck (*Anser acuta*) is the least susceptible.[2] Muscovy ducks, as seen in this case, are highly susceptible to this particular virus. This virus is a major concern because migratory birds can spread this virus to naïve populations leading to massive outbreaks with high mortality.[4]

Dr. Raymond briefly integrated some general pathology topics as they relate to this particular case, and he focused on mechanisms by which free radicals cause damage to cells.

Free radicals are molecules with an unpaired electron making them highly reactive. These molecules are generated as by-products of normal cell function via oxidative metabolism or are a by-product of exposure to radiation, toxins, drugs, or other chemicals. Free radicals are also produced by neutrophils and macrophages in inflammation. Free radicals can damage cells by 1) peroxidation of cellular phospholipid membranes; 2) DNA injury; 3) oxidative modification of proteins.[1]

Free radical damage is minimized by several different antioxidants within the body. These antioxidants include enzymatic and nonenzymatic antioxidants. Enzymatic antioxidants include superoxide dismutase, catalase, and glutathione peroxidase. Nonenzymatic antioxidants include transport proteins transferrin, ferritin, lactoferrin, and ceruloplasmin. Vitamins A, C and E, and other dietary compounds such as lycopenes, flavonoids, genistein, and reserpines help to minimize the damage done by free radicals.[1]

**Contributing Institution:** California Animal Health and Food Safety Laboratory, UC Davis
http:/cahfs.ucdavis.edu

**References:**

1. Abbas, AK: Cellular adaptations, cell injury, cell death. *In:* Robbins and Cotran Pathologic Basis of Disease, 7th edition, pp. 16-18V. Kumar, A. K. Abbas, N. Fausto (eds). Elsiever, Inc., Philadelphia, PA, 2000
2. Burges, EC, Ossa CJ, Yuill TM: Duck Plague: a carrier

state in waterfowl. Avian Dis **23**:940-949. 1979
3. Davidson S, Converse KA, Hamir NA, Eckroade RJ: Duck viral enteritis in domestic muscovy ducks in Pennsylvania. Avian Dis **37**:1142-1146, 1993
4. Leibovitz L, Hwang J: Duck plague on the American continent. Avian Dis **12**:361-378, 1967
5. Murphy FA, Gibbs EPJ, Horzinek MC, Studdert MJ: Herpesviridae. *In:* Veterinary Virology, eds. Murphy FA, Gibbs EPJ, Horzinek MC, Studdert MJ, 3rd ed., pp. 301-325. Academic Press, San Diego, California, 1999
6. Sandhu, TS, and Leibovitz L: Duck virus enteritis (duck plague). *In:* Disease of Poultry, eds., Calneck BW, Barnes HJ, Beard CW, McDougald LR, Saif YM, 10th ed., pp. 675-682. Iowa State University Press, Ames, IA, 1997
7. Whiteman CE, Bickford AA: Avian disease manual. 3rd ed. American Association of Avian Pathologists, Kennett Square, PA, 1988
8. Kumar V, Abbas AK, Fausto N: Robbins and Cotran, Pathologic Basis of Disease, 7th ed., pp. 16-18. Elsevier Saunders, Philadelphia, PA, 2005

## CASE II – N2008-0451 (AFIP 3103941)

**Signalment:** Adult, female Northern bobwhite (*Colinus virginianus* [no subsp.])

**History:** Found dead with no premonitory signs

**Gross Pathology:** At gross necropsy the animal was extremely thin with no visible fat stores and severe pectoral muscle atrophy. The proventriculus was markedly distended and filled with a large amount of thick, off-white, mucoid material. The proventricular walls were severely thickened, particularly the mucosa, which was 3 mm thick, yellow white and gelatinous. Numerous short, white, coiled nematode parasites were present within and adhered to the mucosal lining of the proventriculus and the proximal ventriculus. There was a 0.7 cm diameter region of the proventricular mucosa that was thinner than the adjacent mucosa, and dark red.

**Laboratory Results:** Multiple nematodes were collected and examined microscopically. The nematodes were white, between 4 and 7 mm long, less than 1 mm in diameter and typically coiled. On microscopy 4 characteristic wavy cuticular ornaments (cordons) extended from the base of the lips posteriorly. (Figure 1) Myriad 20 x 40 micron embryonated eggs were scattered throughout the background. (Figure 2) The parasite was identified as Dispharynx nasuta at the time of necropsy and later confirmed by the Cornell University, College of Veterinary Medicine, Animal Health Diagnostic Center.

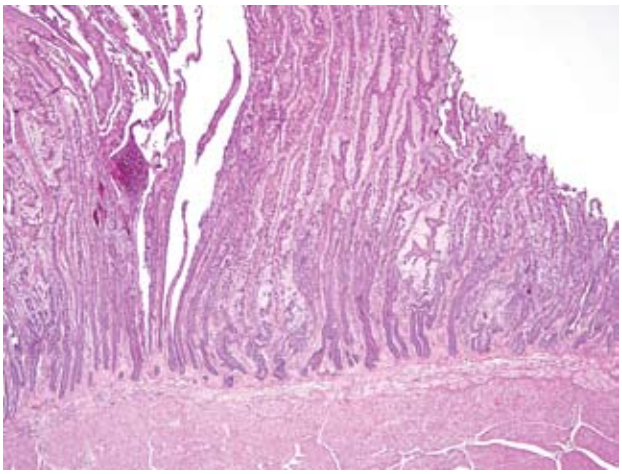

*2-1. Proventriculus, quail. Marked proliferation of the mucosa. (HE 200X )*

**Histopathologic Description:** The section submitted is from the proventriculus near the junction with the esophagus. The superficial mucosa varies from thickened and hyperplastic **(Fig. 2-1)** in some sections to severely eroded in other sections. In areas of erosion there is severe necrosis of the superficial portion of the glands with fibrin deposition and hemorrhage. Both the superficial and deep portions of the proventricular glands are distended by a mixture of mucus and numerous Spirurid nematode parasites. In cross section, the nematodes vary from 200 to 600 um in diameter. All have an approximately 5 to 15 um thick cuticle, which varies from smooth to ridged, a thick layer of coelomyarian musculature, a predominantly glandular esophagus, and a prominent intestinal tract composed of cuboidal to columnar cells with a brush border. The coelom contains a small amount of eosinophilic fluid **(Fig. 2-2)**. Female nematodes typically demonstrate a distended uterus containing numerous small (20 by 40 um), thick shelled, embryonated eggs **(Fig. 2-3)**. Within the lamina propria there is a diffuse infiltrate of eosinophils with smaller numbers of lymphocytes and plasma cells. Dilated glands have an attenuated epithelial lining and when free of nematodes contain a large amount of mucus and sloughed necrotic epithelial cells. A thick layer of mucus admixed with similar quantities of epithelial cells and eosinophils covers the mucosal surface. Scattered colonies of mixed bacteria are present within the mucus.

**Contributor's Morphologic Diagnosis:** Proventriculus: Proventriculitis, erosive to proliferative, eosinophilic, lymphocytic, plasmacytic, diffuse,

*2-2. Proventriculus, quail. Cross section of a spirurid nematode with characteristic polymyarian-coelomyarian musculature, abundant eosinophilic material within the pseudocoelom, and numerous external cuticular cordons. (HE 400X)*

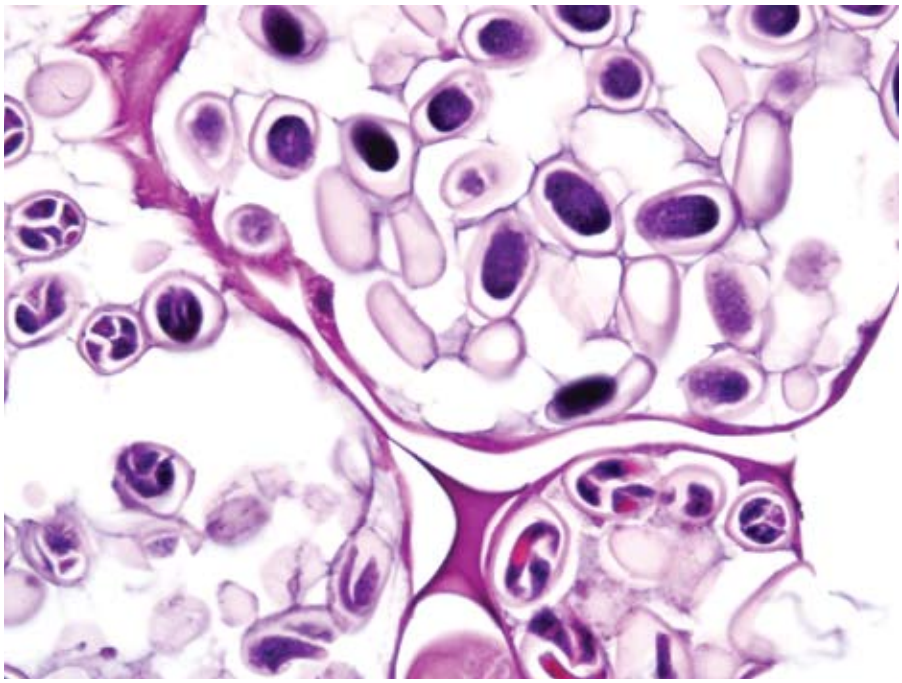

*2-3. Proventriculus, quail. Adult female nematodes contain prominent paired gonads which contain numerous small, oval, thick-shelled embyonated eggs. (HE 400X)*

moderate to severe with intralesional Spirurid nematodes (*Dispharynx nasuta*)

**Contributor's Comment:** *Dispharynx nasuta* (syn. *Dispharynx (Acuaria) spiralis*), also known as the 'proventricular worm', is a spirurid nematode parasite of the proventriculus of many passerine, columbiform and free ranging gallinaceous birds.[5,11] It has been identified in a variety of game birds (ruffed grouse, blue grouse, American woodcock) including the bobwhite quail.[5,7,8] There is a single case report of infection in a captive princess parrot.[11] The highest prevalence and levels of infection are seen in juvenile birds, with infection occurring by 3 to 4 days of age in regions of high incidence.[5,7]

The life cycle of *Dispharynx* is indirect utilizing an

intermediate terrestrial isopod host. Adult female *D. nasuta* pass embryonated eggs into the lumen of the proventriculus, which are later shed in the feces.[11] The eggs are consumed by the intermediate host, wood lice (*Armadillidium vulgare*) or sow bugs (*Porcellio scaber*), in which the larvae subsequently hatch and penetrate the host tissues. First stage larvae (L1) develop into the infective third stage (L3) within 26 days. The third stage larvae (L3) can survive in the infected intermediate host for up to 6 months. Once the intermediate host is consumed by a susceptible bird the third stage larvae (L3) further develop, reaching sexual maturity in 27 days.[7]

Sexually mature adults primarily infect the proventriculus, though in severe cases they can also infect the adjacent esophagus and ventriculus. The nematodes attach by their anterior end to the mucosal epithelial cells initially causing ulceration at the site of attachment. In most avian species these worms cause only a mild nodular reaction in the mucosa and a small amount of inflammation. However in some species (American wood cock, ruffed grouse, blue grouse) *D. nasuta* acts as a primary pathogen.[5,7] When present in large numbers (10 or more), the infection causes severe hyperplasia of the proventricular glands. Associated with the glandular proliferation is an increase in mucus production, as well as excessive sloughing of mucosal epithelial cells. As a result, the lumen of the proventriculus becomes distended by a thick, white, coagulum of mucus and sloughed cells which creates a functional obstruction of the proventriculus and secondary starvation.[5,7]

Diagnosis in this case was made based on the characteristic proventricular lesion, egg and adult worm identification. As stated previously, the significance of this parasite is variable. In most birds this nematode is an incidental finding. However in some species, particularly the ruffed grouse and blue grouse, these organisms are believed to be a significant cause of mortality and decline in wild populations. While not typically considered a primary pathogen of free ranging bobwhites, significant mortality has been seen in cage-reared animals.[5,7,8]

**AFIP Diagnosis:** 1. Proventriculus: Proventriculitis, proliferative and heterophilic, diffuse, marked with glandular ectasia and adult spirurids
2. Serosa, adipose tissue: Atrophy, diffuse, moderate

**Conference Comment:** Spirurid nematodes often have several distinguishing characteristics in histologic section. Several types of spirurids have cuticular ornamentations around the buccal cavity varying from spines to cords to collars. Eosinophilic fluid is found in the body cavity and is a distinguishing characteristic of this group of nematodes. Lateral cords can be extremely large in size and are often vacuolated. Most adult females in this group also produce thick shelled, embryonated eggs. Other examples of spirurids in domestic animals include: *Physaloptera* sp., *Gonnglyonema* sp., *Draschia* sp., *Spirocerca* sp., *Thelazia* sp.[4]

In a retrospective study done by Drs. Raymond, Miller, and Garner it was found that in two cases infection with *D. nasuta*, also known as adenomatous proliferative proventriculitis (APP), the lesions progressed to proventricular adenocarcinoma.[9] In humans and domestic animals, several parasites have been associated with subsequent neoplasia. A brief, non-comprehensive list is included.

| **Parasite** | **Associated Neoplasm** |
|---|---|
| *Spirocerca lupi* | Esophageal sarcoma in dogs |
| *Opisthorchid flukes* | Cholangiocarcinoma in cats and man |
| *Cysticercus fasciolaris* | Hepatic sarcoma in rats |
| *Clonorchis sinensis* | Cholangiocarcinoma in cats and man |
| *Schistosoma haematobium* | Carcinoma in bladder of humans |
| *Trichosomoides crassicauda* | Papillomas in urothelium in rats |

[2,3,6,10]

**Contributing Institution:** Wildlife Conservation Society (http: //www.wcs.org)

**References:**
1. Bolette DP: Dispharynxiasis in a captive princess parrot. Journal of Wildlife Diseases **34**:390-391, 1998
2. Brown CC, Baker DC, Barker IK: The alimentary system. *In:* Jubb, Kennedy and Palmer's Pathology of Domestic Animals, ed. Maxie MG, 5th ed., vol. 2, p. 40-41, 256. Saunders Elsevier, Philadelphia, PA, 2007
3. Epstein JI: The lower urinary tract and male genital system. *In:* Robbins and Cotran Pathologic Basis of Disease, eds. V. Kumar, A. K. Abbas, N. Fausto, 7th ed., pp. 1032, Elsiever, Inc., Philadelphia, PA, 2005
4. Gardiner CH, Poynton SL: *In:* An Atlas of Metazoan Parasites in Animal Tissues, 2nd ed., pp. 30-34. Armed Forces Institute of Pathology, Washington, DC 1998
5. Goble FC, Kutz HL: The genus dispharynx (*Nematoda: Acuariidae*) in galliform and passeriform birds. Journal of Parasitology **31**:323-331, 1945
6. Percy DH, Barthold SW: Pathology of Laboratory Rodents and Rabbits, 3rd ed., pp.160. Blackwell Publishing, Ames, Iowa, 2007
7. Proventricular or Stomach Worm. http://www.michigan.gov/dnr/0,1607,7-153-10370_12150_12220-27255--,00.html
8. Purvis JR, Peterson MJ, Lichtenfels JR, Silvy NJ: Northern bobwhites as disease indicators for the endangered Attwater's prairie chicken. Journal of Wildlife Diseases **34**:348-354
9. Raymond JT, Miller C, Garner MM: Adenomatous proliferative proventriculitis (APP) in birds. Journal Proceedings, AAZV Conference, Milwaukee, WI, 2002
10. Stalker MJ, Hayes MA: Liver and biliary system. *In:* Jubb, Kennedy and Palmer's Pathology of Domestic Animals, ed. Maxie MG, 5th ed., vol. 2, pp.363. Saunders Elsevier, Philadelphia, PA, 2007
11. Urquhart GM, Armour J, Duncan JL, Dunn AM, Jennings FW: Veterinary Parasitology, pp.82 – 83, Churchill Livingstone Inc., 1994

## CASE III – 122103-07 (AFIP 3107607)

**Signalment:** Adult house sparrow (*Passer domesticus*)

**History:** Examined is a house sparrow from a wild caught research colony that was submitted for necropsy after the colony began to experience high mortalities. An adjacent colony of American goldfinches (*Carduelis tristis*) experienced high mortalities with the same clinical signs prior to the sparrows. Clinical signs within both colonies consisted of muscle wasting and diarrhea.

**Gross Pathology:** Within the sampled population of sparrows and goldfinches (16 birds in total) the most severely affected birds exhibited marked wasting of the pectoral muscles, poor coelomic adipose stores, severe thickening of the proximal small intestine that gradually tapered toward the ileum and small, variably sized, irregular foci of pallor on the liver that extended into the parenchyma on section. Most birds had no significant findings and one bird was severely autolyzed.

**Laboratory Results:** Fecal floatation was run on one bird and *Isospora* spp. were identified but not speciated. CD3 immunohistochemistry was carried out on the intestines and liver to determine if the lymphoblasts were of B cell or T cell lineage. Diffusely the infiltrates exhibited intense membranous staining for CD3 indicating T-cell lineage. The intestinal staining varied between birds with strong immunoreactivity in the basal lamina propria and variable staining in the plical folds and villi. Electron microscopy was performed to rule out viral causes for the lymphocytic infiltrate; no viral particles were identified.

**Histopathologic Description:** Small intestine: Diffusely infiltrating and severely expanding the lamina propria is a marked mixed inflammatory infiltrate composed predominantly of lymphoblasts, with fewer histiocytes, plasma cells and eosinophils. Multifocally this inflammation extends transmurally with mild accumulations on the serosal surface. Within the luminal epithelial cells there are abundant approximately 20x15µm coccidian parasites at various stages of development **(Fig. 3-1)**. There are abundant macrogamonts characterized by a peripheral ring of large eosinophilic granules; fewer microgamonts that are smaller (approximately 15x10µm) and have more densely packed basophilic cytoplasmic granules; rare schizonts that contain abundant 1-2µm merozoites and occasional unsporulated oocysts that have a thin capsule and a homogenous finely granular amphophilic cytoplasm.

Liver: Infiltrating and partially effacing the peri-portal hepatocytes is a mild to moderate mononuclear inflammatory infiltrate composed predominantly of lymphoblasts with fewer histiocytes and plasma cells. The cytoplasm of scattered lymphoblasts contain 1-5, small, oval, 1-2µm diameter basophilic organisms within a thin, clear, well demarcated parasitophorous vacuole. Rarely these organisms peripheralize and indent the nucleus of the infected cells. Small numbers of the basophilic organisms are free amongst the inflammatory infiltrate. Small aggregates of the lymphoblasts are scattered within the sinusoids.

Spleen (not in every section): Diffusely the peri-

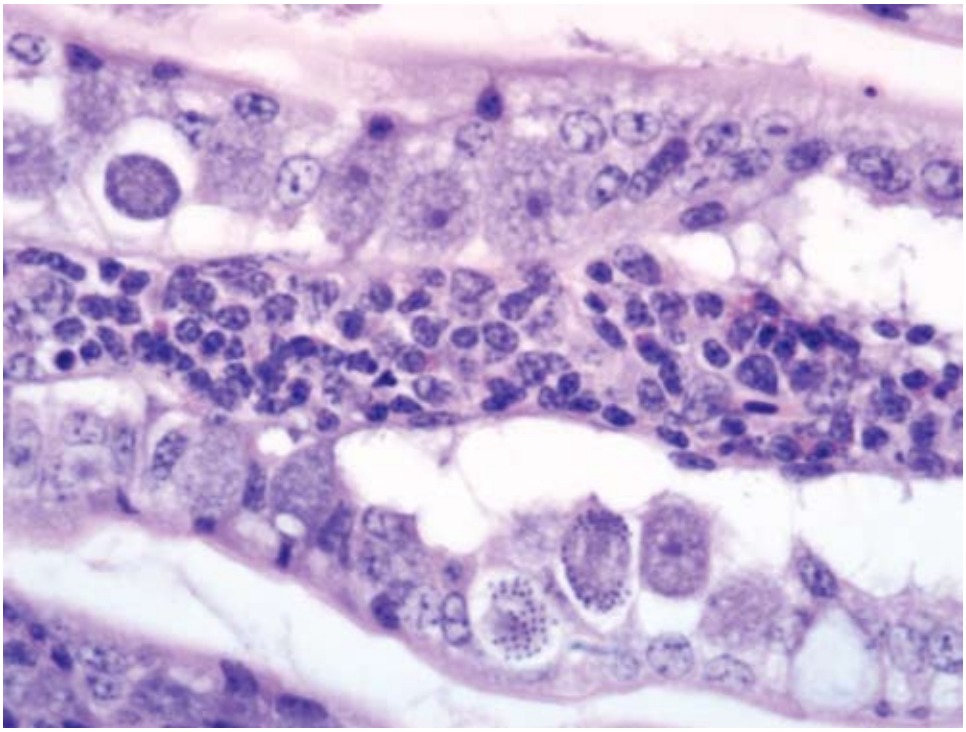

*3-1. Small intestine, house sparrow. Multifocally within intestinal epithelium are numerous protozoal schizonts, microgametocytes, macrogametocytes, and sporulated oocyts. (HE 400X, HE 1000X)*

arteriolar lymphoid sheaths are moderately expanded with variable numbers of small, oval, 1-2µm diameter basophilic organisms with a thin, clear, well demarcated parasitophorous vacuole within the cytoplasm of occasional lymphocytes **(Fig. 3-2)**. Rarely these organisms are present in the sinusoidal histiocytes.

**Contributor's Morphologic Diagnosis:** Small intestine: Diffuse, severe, chronic, lymphoplasmacytic, histiocytic and eosinophilic enteritis with intraepithelial coccidian parasites
Liver: Moderate, diffuse, lymphocytic peri-portal hepatitis with intralesional merozoites consistent with *Atoxoplasma* spp.
Spleen: Moderate lymphoid hyperplasia with intralesional merozoites consistent with *Atoxoplasma* spp.

**Contributor's Comment:** At low magnification the trans-mural intestinal infiltrate and the peri-portal hepatic infiltrate resemble lymphoma. At higher magnification and with the aid of immunohistochemistry it is apparent that the intestinal infiltrate is composed of a mixed cellular infiltrate, with T lymphocytes predominating. One case documents intestinal lymphoma with metastasis and an incidental intestinal coccidian infection that was attributed to immunosuppression from the tumor.[8] No connection between the coccidian parasites and the severe lymphoproliferative infiltrate was made in that case.
Other potential causes of lymphoproliferative disorders and lymphoma in avian species include Marek's disease virus, an alpha-herpesvirus, and Avian leucosis virus, a retrovirus, which can cause lymphoma-like lesions in multiple organs in chickens and many avian species respectively. As the immunohistochemistry results were overwhelmingly positive for CD3, a T cell antigen, a retroviral-induced lesion was determined to be less likely as these viruses typically induce B-cell proliferation. Transmission electron microscopy was performed on the inflammatory infiltrate to rule out viral induced lymphoma. No viral particles were identified in the examined tissues; Atoxoplasma merozoites were not evaluated.

*Atoxoplasma* spp are host specific apicomplexian parasites that are infective to birds within the family Passeriformes. This is a large family encompassing many different species of birds. Within this family it is the finches, sparrows, thrushes and other small songbirds that are most commonly reported to be affected by this parasite. In the wild these parasites are endemic in low levels [3, 14] however it is likely that the levels are underestimated due to the difficulty in identifying the circulating merozoites.[5,7,8] Atoxoplasma has become a major cause of mortality in zoos and research facilities that utilize wild caught colonies of passeriform birds.[5,6] The stress from being in captivity and poor sanitary conditions have been identified as contributing causes for the high morbidity in these facilities.[6,7,12] Interestingly Atoxoplasma has been reported in raptors.[10] However, as so few cases exist, the

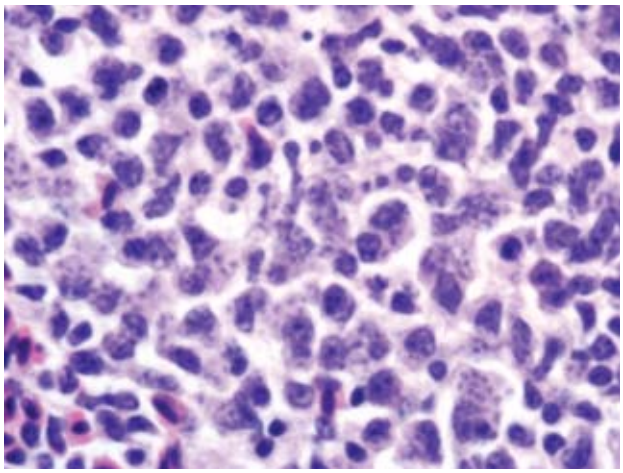

*3-2. Spleen, house sparrow. Multifocally within the red pulp are many leukocytes which contain numerous 1-2 micron intracytoplasmic protozoal merozoites. (HE 1000X)*

significance of the parasite outside of the passerine birds is unknown.

Affected birds will exhibit a loss of appetite with subsequent weight loss and reduction of the pectoral musculature, which is termed "going light". The animal can become depressed, have ruffled feathers, a distended abdomen, and develop diarrhea, dehydration and a loss of balance.[2,11] Subclinically infected birds will show no outward signs of infection but will shed infective oocysts into the environment. In infected colonies morbidity can approach 100% with a significant mortality rate. Grossly, there are varying degrees of pectoral musculature atrophy, coelomic adipose depletion and enteritis.

Since the discovery of this parasite there has been considerable debate as to how it should be classified. In 1950 Garnham proposed the name Atoxoplasma [12] as it was felt this name addressed the fact that the parasite resembled Toxoplasma but was not Toxoplasma. Since that time it was determined that these parasites belong to the family Eimeriidae and closely resemble *Isospora* spp. Both Atoxoplasma and Isospora oocysts contain two sporocysts each containing four sporozoites. Both parasites follow the basic coccidian life cycle where the sporozoites will excyst in the intestinal tract and invade the enterocytes, undergo merogony, develop into microgamonts or macrogamonts within the enterocytes and undergo sexual reproduction to form unsporulated oocysts. The oocysts are passed in the feces and sporulate in the environment where they will be ingested by the next host.

*Atoxoplasma* spp differ from *Isospora* spp during merogony. After ingestion of the Atoxoplasma oocysts the sporozoites and merozoites can directly infect mononuclear cells that have been recruited into the intestine in response to the coccidian parasites.[1,7,9,11,12] The merozoites enter into the circulation where they continue to undergo merogony within the mononuclear inflammatory cells. Through a currently unknown mechanism this parasite initiates a marked lymphoproliferative response. Perivascular accumulations of mononuclear inflammatory cells develop systemically and often contain intracytoplasmic merozoites. Depending on the severity of the infection the inflammatory infiltrates can resemble mild lymphohistiocytic inflammatory response to widespread lymphoma.

As previously mentioned the Atoxoplasma merozoites were not evaluated under the electron microscope. The reported ultrastructural characteristics of this parasite include a pellicle consisting of an outer plasma membrane and an inner complex of two membranes, subpellicular microtubules, a conoid, rhoptries, micronemes, mitochondria, and a micropore all within a parasitophorous vacuole.[2,9,11]

In summary, when evaluating tissue from a passerine bird and a coccidial infection with severe lymphoproliferative lesions, Atoxoplasma should be high on the differential list. Close evaluation of the lymphocytic infiltrates for intracellular merozoites is warranted in these cases.

**AFIP Diagnosis:** 1. Small intestine: Enteritis, lymphoblastic, transmural, diffuse, severe, with crypt loss, intraleukocytic apicomplexan merozoites, and intraepithelial gamonts and schizonts
2. Liver: Hepatitis, portal, lymphoblastic, diffuse, marked, with intracytoplasmic apicomplexan merozoites

**Conference Comment:** The contributor does an outstanding job of covering all aspects of atoxoplasmosis in their case submission report. The moderator mentioned two other very important diseases in birds that result in lymphoproliferative disorders. Marek's disease (gallid herpesvirus 2) is common in chickens and manifests as mononuclear cellular infiltrates in the skin, peripheral nerves, and the iris.[15] Viruses within the avian leukosis/sarcoma group (family Retroviridae) cause many benign and malignant neoplasms.[4]

**Contributing Institution:** http://www.vet.cornell.edu/biosci/pathology/

**References:**

1. Adkesson MJ, Zdziarski JM, Little SE: Atoxoplasmosis in Tanagers. J Zoo Wildlife Med **36**:265-272, 2005

2. Ball SJ, Brown MA, Daszak P, Pittilo RM: Atoxoplasma (Apicomplexa: Eimeriorina: Atoxoplasmatidae) in the Greenfinch (*Carduelis chloris*). J Parasitol **84**:813-817, 1998
3. Bennett GF, Garvin M, Bates M.: Avian hematozoa from west-central Bolivia. J Parasitol *77*:207-211, 1991
4. Fadly AM, Payne LN: Leukosis/sarcoma group. *In:* Disease of Poultry, ed. Saif YM, Barnes HJ, Glisson JR, Fadly AM, McDouglad LR, Swayne DE, 11th ed., pp. 465-516. Iowa State University Press, Ames, Iowa, 2003
5. Giacoma R, Stefania P, Ennio T, Giorgina VC, Giovanni B, Giacomo R: Mortality in Black Siskins (*Carduelis atrata*). J Wildlife Dis **33**:152-157, 1997
6. McAloose D, Keener L, Schrenzel M, Rideout B: Atoxoplasmosis: Beyond Bali Mynahs. Proc. Am. Assoc. Zoo Vet pp. 64-67, 2001
7. McNamee P, Pennycott T, McConnell S: Clinical and pathological changes associated with atoxoplasma in a captive bullfinch (*Pyrrhula pyrrhula*). Vet Rec **136**:221-222, 1995
8. Middleton AL: Lymphoproliferative disease in the American Goldfinch, *Carduelis tristis*. J Wildlife Dis **19**:280-285, 1983
9. Quiroga MI, Aleman N, Vazquez S, Nieto JM: Diagnosis of Atoxoplasmosis in a Canary (*Serinus canaries*) by histopathologic and ultrastructural examination. Avian Dis **44**:465-469, 2000
10. Remple JD: Intracellular hematozoa of raptors: A review and update. J Avian Med Surg **18**:75-88, 2004
11. Sanchez-Cordon PJ, Gomez-Villamandos JC, Guierrez J, Sierra MA, Pedrera M, Bautista MJ: Atoxoplasma spp. infection in captive canaries (*Serinus canaria*). J Vet Med A **54**:23-26, 2007
12. Schrenzel MD, Maalouf GA, Gaffney PM, Tokarz D, Keener LL, McClure D, Griffey S, McAloose D, Rideout BA: Molecular characterization of Isosporoid coccidia (*Isospora* and *Atoxoplasma* spp.) in passerine birds. J Parasitol **91**:635-647, 2005
13. Swayne DE, Getzy D, Siemons RD, Bocetti C, Kramer L: Coccidiosis as a cause of transmural lymphocytic enteritis and mortality in captive Nashville Warblers (*Vermivora ruficapilla*). Journal of Wildlife Diseases **27**:615-620, 1991
14. van Riper III C, van Riper S: Discovery of Atoxoplasma in Hawaii. J Parasitol [73]:1071-1073, 1987
15. Witter RL, Schat KA: Marek's disease. *In:* Disease of Poultry, eds. Saif YM, Barnes HJ, Glisson JR, Fadly AM, McDouglad LR, Swayne DE, 11th ed., pp. 407-449. Iowa State University Press, Ames, Iowa, 2003

## CASE IV – UNL/VDC 2301-06 (AFIP 3075580)

**Signalment:** Fifteen-week-old mixed breed pig (*Sus scrofa domesticus*)

**History:** Diarrhea was reported in which there were flecks of undigested blood in a group of pigs. Approximately 10% of the pigs had diarrhea and 5% were markedly emaciated.

**Gross Pathology:** The carcass of the euthanized pig was gaunt and the hair coat roughened. Stomach and small intestine contained scant amounts of ingesta. There was a moderate amount of semi-liquid feces in the spiral colon. Fresh blood and fibrin was mixed with the colon contents. Colonic mucosa was glistening and rough in appearance.

**Laboratory Results:** Polymerase chain reaction testing for *Brachyspira hyodysenteriae* on bacterial colonies from anaerobic cultures were positive.

**Histopathologic Description:** These sections of large intestine are characterized by multiple large mucosal erosions. Luminal surface is covered by a thick layer of neutrophilic debris mixed with mucus and occasionally extravasated erythrocytes. Rare large protozoa with a morphology consistent with *Balantidium coli* are seen associated with the eroded areas. Mixed bacteria (including myriad long slender spirochetes) are seen in the luminal debris, eroded areas, and in superficial areas of mucosal crypts. Superficial mucosal crypts are mildly dilated with mucous "plugs". Crypt epithelium is mildly hyperplastic and there are reduced numbers of goblet cells.

**Contributor's Morphologic Diagnosis:** Mild to moderate acute focally extensive erosive and catarrhal colitis

**Contributor's Comment:** This is a classic case of swine dysentery (SD) caused by *Brachyspira hyodysenteriae.*[3] Along with diarrhea, other signs seen with SD include fever, anorexia and dehydration. Diarrhea is the result of malabsorption of fluids and electrolytes in the large intestine.[1] Death is usually the result of dehydration, acidosis, and hyperkalemia.[3] Pathogenesis of SD is poorly understood, but in gnotobiotic pigs, there is a synergistic effect with other anaerobic bacteria.[5] *B. hyodysenteriae* colonizes the mucus on the surface of the mucosa and in crypts and invades surface epithelial cells.[1] The main virulence factor shown to be associated with severity of disease is a hemolysin.[4]

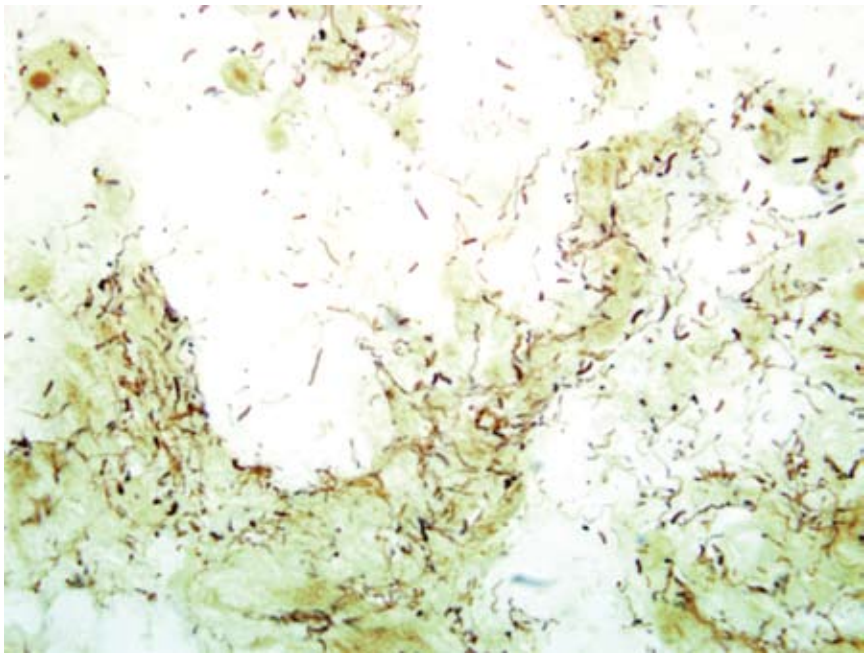

*4-1. Colon, pig. Diffusely adherent to epithelium and free within the lumen are many 0.5 x 4.0 micron argyrophilic spirochete bacteria. (Warthin-Starry 1000X)*

**AFIP Diagnosis:** Colon: Colitis, erosive, multifocal, moderate, with necrosis, luminal mucin accumulation and argyrophilic spiral bacteria **(Fig. 4-1)**

**Conference Comment:** Swine dysentery (SD) generally affects pigs during the grow-finish phase of production. It causes a mucohemorrhagic diarrhea of the colon, and it can cause serious economic setbacks in a herd of pigs. SD is caused by *Brachyspira hyodysenteriae*, a gram-negative, beta-hemolytic anaerobic spirochete. This organism was also formerly known as *Treponema hyodysenteriae*, and then was reclassified as *Serpulina hyodysenteriae*, and it is now known as *Brachyspira hyodysenteriae*.[2] At least 4 other intestinal spirochetes have been identified in swine with *Brachyspira pilosicoli* being the only other one to cause clinical disease. *B. pilosicoli* can cause a mild colitis in pigs.[2]

Gross lesions for SD are normally present only in the large intestine. The ileocecal junction is normally the boundary for lesions caused by SD. Lesions often begin as hyperemic and edematous mucosal lesions and progress to a mucosa covered by copious amounts of mucus and fibrin admixed with blood. These lesions often form a pseudomembrane. There also may be multifocal erosions of the surface mucosa, and ulcerative lesions are not generally seen.[2]

Microscopically acute lesions consist of mucosal congestion, edema, and neutrophilic infiltrates in superficial lamina propria near blood vessels. Spirochetes may be seen in colonic crypts, and hyperplasia of goblet cells is common. These lesions progress with the development of superficial mucosal erosions and a characteristic mat of fibrin, mucous, hemorrhage, and cellular debris forms on the mucosal surface. Silver stains can be used to identify these spirochetes in tissue section.[2]

**Contributing Institution:** Veterinary Diagnostic Center, Lincoln, NE

**References:**

1. Duhamel GE: The alimentary system. *In:* Jubb, Kennedy, and Palmer's Pathology of Domestic Animals, 5th edition; Maxie MG ed., Academic Press, Inc., Vol 2, pp. 210-213, 2007

2. Hampson DJ, Fellstrom C, Thomson JR: Swine dysentery. *In:* Disease of Swine, eds. Straw BE, Zimmerman JJ, D'Allaire S, Taylor DJ, 9th ed, pp. 785-805. Blackwell Publishing, Ames, Iowa, 2006

3. Harris DL, Hampson DJ, Glock RD: Swine Dysentery. *In:* Disease of swine, eds. Straw BE, D'Allaire S, Mengeling WL, Taylor DJ, 89th ed., pp.579-600. Iowa State University Press, Ames, Iowa, 1999

4. Muir S, Koopman MB, Libby SJ, Joens LA, Heffron F, Kusters JG: Cloning and expression of a *Serpula* (*Treponema*) *hyodysenteriae* hemolysin gene. Infect Immun 60:529-35, 1992

5. Whipp SC, Robinson IM, Harris DL, Glock RD, Matthews PJ, Alexander TJ: Pathogenic synergism between *Treponema hyodysenteriae* and other selected anaerobes in gnotobiotic pigs. Infect Immun **26**:1042-7, 1979

The Armed Forces Institute of Pathology
Department of Veterinary Pathology

*Conference Coordinator:*
Todd M. Bell, DVM

WEDNESDAY SLIDE CONFERENCE 2008-2009

# Conference 19

4 March 2009

*Conference Moderator:*

Amanda Fales-Williams, DVM, PhD, Diplomate ACVP

## CASE I – UFSM-2 (AFIP 3105599)

**Signalment:** 2-year-old, male, mixed breed, bovine (*Bos taurus*)

**History:** This bovine belonged to a herd of 2-year-old cattle that were placed in a pasture highly infested with bracken fern (*Pteridium aquilinum*). Five cattle (including the one of this report) died after presenting clinical signs that included high fever, hemorrhages through the nose, petechiae in mucous membrane and hematuria. The 12 cattle had been placed in the bracken fern-infested pasture in mid-October (spring) and the deaths occurred from late December to early January (summer). When examined for the first time, the bovine of this report was depressed and had a rough hair coat, few petechiae in the ocular mucosae, slightly red discolored urine, soft stools with small blood clots and rectal temperature of 40.2°C. In the following days the rectal temperature peaked to 42.2°C and the clinical signs got worse with frank hematuria, hemorrhages through the nose, depression, and foul smelling black soft stools with blood clots. This bovine died after a 6-day clinical course (the other 4 affected cattle died after clinical courses that varied from 25 days). In the terminal phase of the disease the rectal temperature dropped to 39°C.

**Gross Pathology:** Large hemorrhages were seen in the subcutaneous tissue of the trunk and abdominal cavity, mainly in the areas of attrition. Multiple 0.5 cm diameter subepicardial hemorrhagic foci were observed in both ventricles. The natural and cut surfaces of lymph nodes and spleen were hemorrhagic. Petechiae, ecchymosis and hematomas were observed in the omentum and mesentery **(Fig. 1-1)**, in the intestine at its junction with the mesentery and in the serosa of the fore stomachs. Several small ulcers were observed in the abomasal mucosa and a large (17x4 cm) cylindrical blood clot was observed in the lumen of the abomasum, near the pylorus. There were ulcers covered with blood in the intestinal mucosa mainly over the Peyer's patches. Partial blood was admixed with the contents of the large intestine and a large cylindrical clot (15x3 cm) was observed in the lumen of the cecum. The mucosa of the ureters were markedly edematous and hemorrhagic. The bladder contained approximately 200 ml of urine and blood, and the bladder mucosa was swollen and hemorrhagic. There was partially clotted blood in the joint cavities of the pelvic limbs.

**Laboratory Results:** Severe thrombocytopenia and neutropenia were seen. Below are results of blood tests performed on the day before the bovine of this report died.

*Sponsored by the American Veterinary Medical Association, the American College of Veterinary Pathologists, and the C. L. Davis Foundation.

**Blood coagulation tests**

| Parameter | Unity | Reference values | Affected bovine |
|---|---|---|---|
| Partial time of activated thromboplastin | seg | 25-45 | 49.3 |
| Prothrombin time | seg | | 20.2 |

**Complete blood cell count**

| Parameter | Unity | Reference values | Affected bovine |
|---|---|---|---|
| Red blood cells | ($x10^6/mm^3$) | (5.0-10.0) | 5.1 |
| Hemoglobin | (g/dl) | (8.0-15.0) | 7,9 |
| Packed cell volume | (%) | (24-46) | 23 |
| Mean corpuscular volume | (fl) | (40.0-60.0) | 45.1 |
| Mean corpuscular hemoglobin concentration | (%) | (30.-36.0) | 34.3 |
| Leucocytes | ($/mm^3$) | (4,000-12,000) | 5,100 |
| Neutrophils | (%) | (15%-45%) | 0 |
| | ($/mm^3$) | (600-4,000) | 0 |
| Lymphocytes | (%) | (45%-75%) | 100 |
| | ($/mm^3$) | (2,500-7,500) | 5,100 |
| Monocytes | (%) | (2%-7%) | 0 |
| | ($/mm^3$) | (25-840) | 0 |
| Eosinophils | (%) | (0%-20%) | 0 |
| | ($/mm^3$) | (0-2,400) | 0 |
| Basophils | (%) | (0%-2%) | 0 |
| | ($/mm^3$) | (0-200) | 0 |
| Platlets | ($x10^3/mm^3$) | (100-800) | 3 |

*1–1 Omentum, mesentery, and small intestine, ox. Multifocal to coalescing petechial and ecchymotic hemorrhage.* *Photograph courtesy of Departamento de Patologia, Universidade Federal de Santa Maria, 97105-900 Santa Maria, RS, Brazil. http://www.ufsm.br/lpv*

**Histopathologic Description:** The hemorrhages observed grossly were confirmed on histopathological examination. Sections of the bone marrow of the sternum were prepared from the affected bovine **(Fig. 1-2)** and from a normal age matched control **(Fig. 1-3)**. Both sections are arranged in the same glass histoslide submitted. There was severe aplasia of the bone marrow of the affected bovine as compared to the control. The sinusoids of the marrow are distended due to the lack of pressure usually posed by the large numbers of hematopetic cells. There is paucity or absence of nucleated cells, including megacariocytes, which can be observed in normal regular numbers in the control section.

**Contributor's Morphologic Diagnosis:** Bovine, bone marrow, sternum, aplasia, severe,
Etiologic diagnosis: toxic bone marrow aplasia
Etiology: toxic substance(s) in *Pteridium aquilinum*
Condition: acute poisoning by *Pteridium aquilinum*

**Contributor's Comment:** Bracken fern (*Pteridium aquilinum*) is the second most important plant poisoning in southern Brazil and responsible for 12% of all cattle deaths caused by poisonous plants in this region.[11] The ingestion of bracken fern results in three forms of clinical disease in cattle (two of those are chronic and characterized by development of neoplasms): 1) squamous cell carcinomas in the upper digestive tract (base of tongue, esophagous and entrance of the rumen) [13]; 2) several types of the neoplasms in the urinary bladder.[14] This latter condition is associated with bleeding from the urinary bladder and universally known as enzootic hematuria. The cocarcinogenesis of bracken fern with bovine papillomavirus-4 (BPV-4) and BPV-2 is implicated respectively in the pathogenesis of upper digestive tract squamous cell carcinomas and bladder tumors. [11, 12] 3) A third condition caused by the ingestion of the plant is characterized by bone marrow aplasia and generalized bleeding tendency [17] and is the one affecting the bovine of this report. This condition

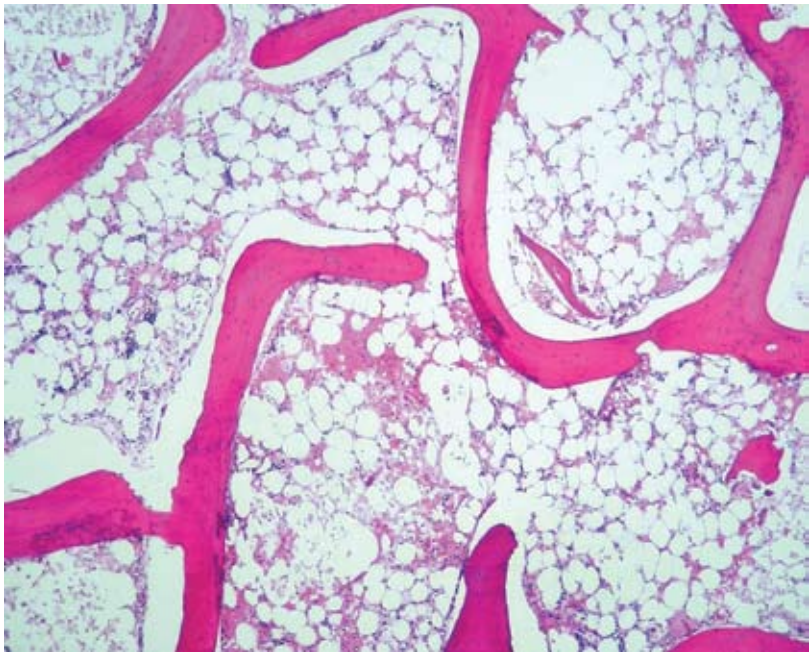

*1–2 Bone marrow, ox. Severe bone marrow aplasia.* *Photomicrograph courtesy of Departamento de Patologia, Universidade Federal de Santa Maria, 97105-900 Santa Maria, RS, Brazil. http://www.ufsm.br/lpv*

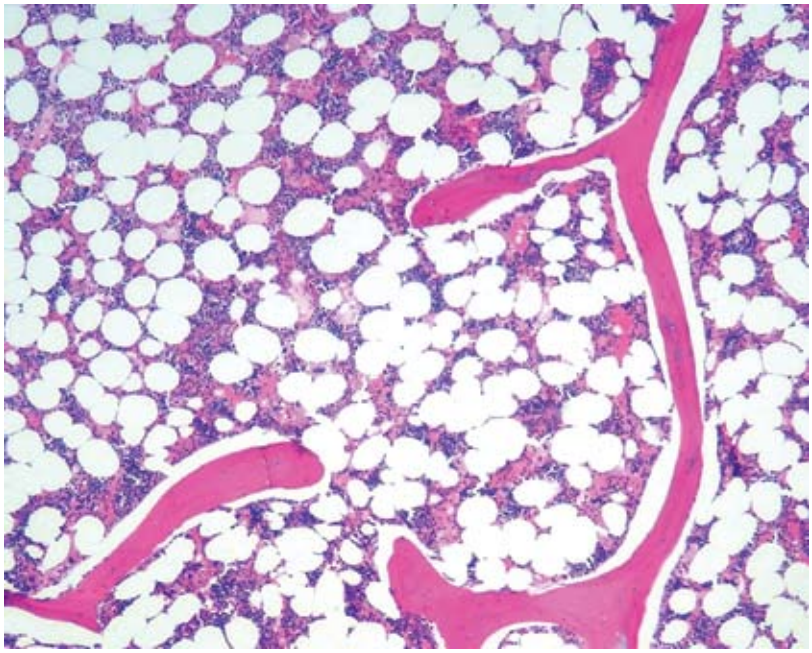

*1–3 Bone marrow, ox. Bone marrow from a normal age-matched control.* *Photomicrograph courtesy of Departamento de Patologia, Universidade Federal de Santa Maria, 97105-900 Santa Maria, RS, Brazil. http://www.ufsm.br/lpv*

is generally referred to as the acute form of bracken fern poisoning. It is mostly a disease of cattle but has been occasionally reported in sheep. Acute bracken fern poisoning in cattle was originally reported in England at the end of 19th century as an acute disease characterized by high fever, hemorrhages and high lethality rates.[16] During this time the etiology was only suspected but it was confirmed in the following year [1] and in later years by successive experiments in cattle being fed with large amounts of the plant for prolonged periods.[4,5,9,15] The same disease was observed during the autumn of 1917-1920 in cattle from the state of New York [2] but only confirmed later as being caused by the ingestion of bracken fern.[5] Since then the disease has been reported from several other countries.[17,18]

Clinical signs associated with acute form of bracken fern poisoning in cattle include high fever (up to 42.5°C), severe

hemorrhages in various tissues and organs, neutropenia and thrombocytopenia.[4,8,10,15,16] High fever appears to be the first clinical sign of the disease, and some believe [14] the intensity of fever that occurs in acute bracken fern poisoning is not duplicated by any other diseases in cattle. Fever is followed by hemorrhage through nasal cavity and depression. In the advanced stages of the disease the fever may subside.[4,9,10,12]

Acute bracken fern poisoning in cattle has been subdivided by some [10, 12] into two types: 1) *enteric*, which is the most common and characterized mainly by depression, anorexia, high fever, and weak pulse, blood clots in the feces and foul smelling feces, pale mucous membranes and bleeding from mucous membranes of the nose, eyes, vagina, and anus; and 2) *laryngeal*—with clinical signs including high fever, roaring, laborious breathing and edema of the larynx. In our experience, however, it is not uncommon to observe signs of both types overlapping in the same animal, as is the case of the bovine of this report. Hemorrhages from venipunctures, from insect bites and in the milk are commonly observed. Death ensues usually 2-3 days after the first clinical signs; however peracute cases of 4-10 hours and cases of recovery are also reported.[4,17] In our region (unpublished data) acute bracken fern poisoning generally occurs in spring and summer months, in hill camps where the ecology is conducive of fern growth, with morbidity rates of 12.5%-21.5% and high lethality rates.

The primary lesion in the acute bracken fern poisoning in cattle is a severe suppression (aplasia) of the bone marrow (as observed in the bovine of this report) which results in thrombocytopenia and neutropenia. No changes are observed in red blood cell [9] and any deficit in RBCs numbers are due more to the hemorrhaging than to the bone marrow suppression since the RBC half-life in cattle is considerably greater (157-162 days) than that of platelets (5-10 days) and neutrophils (12 hours). Usually death due to bleeding related to thrombocytopenia occurs when the numbers of platelets are lower than 10,000/mm$^3$ of blood. In these cases fatal bleeding within body cavities occurs. In the case of this report platelets were 3,000/mm$^3$ one day before death.

There is usually bacteremia related to the almost complete lack of neutrophils in the peripheral blood.[4,9] If after the onset of the bacteremia the bovine survives for several days, infarcts may occur in the liver, lung, kidney and spleen. Death occurs because of internal hemorrhage or septicemia.[10,12]

The most remarkable necropsy findings are hemorrhages of almost any size in almost any organ.[10,12,15] Petechiae and ecchymosis occur in the subcutaneous tissue and there is edema and hemorrhages in lymph nodes; petechiae and paint-brush hemorrhages are observed on serosal surfaces of several organs from abdominal and thoracic cavities. Abundant collections of partially clotted blood can be found in the peritoneal cavity. Mucosal ulcerations and blood clots in the lumen of fore stomachs, abomasum, small and gross intestine are observed. Pale necrotic areas of necrosis can usually be observed in the liver but also in the heart, kidney and spleen. These areas are usually referred to as infarcts but probably are caused by toxins of bacteria and not really by ischemia due to compromise of the vasculature. Pharyngeal and laryngeal edema can be marked.[10,12,16]

The hemorrhages observed grossly can be confirmed histologically. Additionally, foci of coagulative necrosis associated with clusters of bacteria can be found in the liver, heart, kidney and spleen. The most striking histological change is the severe aplasia of the bone marrow.[4,9]

The norsesquiterpene glucoside ptaquiloside is the toxin in *P. aquilinum* responsible for the bone marrow suppression in acute disease [6]; this toxin has cumulative properties and the time elapsed from the beginning of the ingestion of the plant and the development of the clinical signs will depend of the amount of ingested plant.[4,12] Usually the ingestion of daily amounts equal to or above than 10 g/kg/bw during 2-11 weeks are necessary to produce the disease.[4,9]

The list of differential diagnosis for acute bracken fern poisoning in cattle should include anaplasmosis, pneumonic mannheimiosis (differential for the laryngeal form), septicemia pasteurellosis, leptospirosis, sweet clover poisoning, bacillary hemoglobinuria.[12] A similar disease caused by bone marrow suppression is reported in cattle from Australia and is caused by the ingestion of an yet different poisonous plant (*Cheilanthes sieberi*).[3]

**AFIP Diagnosis:** Bone marrow: Hypoplasia, trilineage, diffuse, severe

**Conference Comment:** Bracken fern toxicosis occurs in several domestic species including pigs, horses, sheep and cattle. Susceptibility depends on the species affected, with cattle and horses being highly susceptible. Sheep rarely eat this plant and are thus affected less often, and pigs are rarely affected.[7,8,19] The plant is most toxic when it is green and actively growing. This plant is not very palatable, so it is often only eaten in large quantities during drought conditions. In monogastrics, bracken fern poisoning leads to a thiamine deficiency. This results in neurologic and cardiac disease most commonly reported in pigs and horses.[7,8,19]

There are numerous toxins within bracken fern including quercetin, ptaquiloside, shikimic acid, aquilide A, and prunasin.[7,8,19] The two major syndromes commonly seen in cattle are aplastic anemia and enzootic hematuria. The severity of disease depends upon how much of the plant is ingested. There is a cumulative affect with this poison. Morbidity is low and mortality is high with this disease. If enough of the toxin is ingested over weeks to months, death via thrombocytopenic hemorrhage or septicemia secondary to neutropenia is often the result.[7,8,19]

In cattle and sheep, bracken fern poisoning results in an irreversible trilineage marrow hypoplasia and resultant aplastic pancytopenia. The chronic form is usually from long term, low level ingestion of bracken fern resulting in persistent hematuria and alimentary tract neoplasia.[7,8,19] Bracken fern toxicity also commonly causes neoplasia within the urinary bladder.[7,8,19] Papillomas, fibromas, and hemagiomas are most common in the urinary bladder.

Hemorrhages can be found in almost any tissue with bracken fern poisoning, but they are usually most numerous in the stomach and small intestine. Multiple neoplasms of the bladder wall or esophagus and forestomachs may also been seen at necropsy. Marrow cellularity is often markedly diminished and the marrow appears pink and soft.[7,8,19]

**Contributing Institution:** Departamento de Patologia, Universidade Federal de Santa Maria, 97105-900 Santa Maria, RS, Brazil. http://www.ufsm.br/lpv

**References:**

1. Anonymous: Fern Poisoning. J. Comp Path Therap **7**:165-167,1984
2. Bosshart JK, Hagan WA: A fatal unidentified disease of cattle in New York State. Cornell Vet **10**:102-13,1920
3. Clark IA, Dimmock CK: The toxicity of Cheilanthes sieberi to cattle and sheep. Aust Vet J **47**:149-152, 1971
4. Evans WC, Evans ET, Hughes LE: Studies on bracken poisoning. Part III. Field outbreaks of bovine bracken poisoning. Brit Vet J **110**:426-442, 1954
5. Hagan WA, Zeissig A: Experimental bracken poisoning of cattle. Cornell Vet **17**:194-208, 1927
6. Hirono I, Kono Y, Takahashi K, Yamada K, Niwa H, Ojika M, Kigoshi H, Hiiyama K, Uosaki Y: Reproduction of acute bracken poisoning in a calf with ptaquiloside, a bracken constituent. Vet. Rec. **115**:375-378, 1984
7. Maxie MG, Youssef S: Nervous system. *In:* Jubb, Kennedy, and Palmer's Pathology of Domestic Animals, ed. Maxie MG, 5th ed., vol 1, pp. 354-357. Saunders Elsevier, Philadelphia, PA, 2007
8. Maxie MG, Newman SJ: Urinary system: *In:* Jubb, Kennedy, and Palmer's Pathology of Domestic Animals, ed. Maxie MG, 5th ed., vol 2, pp. 518-520. Saunders Elsevier, Philadelphia, PA, 2007
9. Naftalin JM, Cushnie GH: Pathology of bracken fern poisoning in cattle. J. Comp. Path Therap **64**:54-74, 1954
10. Osebold JW: An approach to the pathogenesis of fern poisoning in the bovine species. J Am Vet Med Assoc **121**:440-441, 1951
11. Rissi DR, Rech RR, Pierezan F, Gabriel AL, Trost ME, Brum JS, Kommers GD, Barros CSL: Plant and plant-associated mycotoxins poisoning in cattle in Rio Grande do Sul, Brazil: 461 cases. [Intoxicação por plantas e micotoxinas associadas a plantas em bovinos no Rio Grande do Sul]. Pesq Vet Bras **27**:261-268, 2007. (In Portuguese, Abstract in English)
12. Sippel WL: Bracken fern poisoning. J Am Vet Med Assoc **121**:9-13, 1952
13. Souto MAM, Kommers GD, Barros CSL, Piazer JVM, Rech RR, Riet-Correa F & Schild AL: Neoplasms of the upper digestive tract of cattle associated with spontaneous ingestion of bracken fern (*Pteridium aquilinum*). [Neoplasias do trato alimentar superior de bovinos associadas ao consumo espontâneo de samambaia (*Pteridium aquilinum*)]. Pesq Vet Bras **26**:112-122, 2006. (In Portuguese, Abstract in English)
14. Souto MAM, Kommers GD, Barros CSL, Rech RR, Piazer JVM: Urinary bladder neoplasms associated with bovine enzootic. [Neoplasmas da bexiga associados à hematúria enzoótica bovina]. Ciência Rural **36**:1647-1650, 2006. (In Portuguese, Abstract in English)
15. Stamp JT: A review of bracken poisoning in cattle. J Brit Grasslands Soc. **2**:191-194, 1947
16. Storrar DM: ses of vegetable poisoning in cattle. J Comp Path Therap **6**:276-279, 1893
17. Tokarnia CH, Döbereiner J, Canella CFC: Ocorrência da intoxicação aguda por samambaia (Pteridium aquilinum (L.) Kuhn) em bovinos no Brasil. Pesq Agropec Bras **2**:329-336, 1967
18. Tustin RC, Adelaar TT, Medal-Johnsen CM: Bracken fern poisoning in cattle in Natal Midlands. J S Afr Vet Med Assoc **39**:91-999, 1968
19. Valli VEO: Hematopoietic system: *In:* Jubb, Kennedy, and Palmer's Pathology of Domestic Animals, ed. Maxie MG, 5th ed., vol 3, pp. 216-221. Saunders Elsevier, Philadelphia, PA, 2007

## CASE II – 1008-1080 (AFIP 3111136)

**Signalment:** 2-year-old spayed female Boxer dog (*Canis familiaris*)

**History:** A 2-year-old female spayed Boxer presented to MSU CVM for chronic anemia. The referring veterinarian administered multiple blood transfusions, and initiated treatment with doxycyline, prednisone and vitamin K. On presentation, the dog was bright and alert. The mucus membranes were pale, and a grade 4/6 systolic heart murmur was auscultated. A complete blood count revealed severe anemia and mild thrombocytopenia. Serum chemistries, PT, PTT, radiographs and abdominal ultrasound were within normal limits. A direct Coombs test was positive. An echocardiogram revealed mild tricuspid regurgitation.

A blood smear was submitted for review.

**Gross Pathology:** None

**Laboratory Results:**
CBC -

| DAY | 1 | 2 | 3 (post transfusion) |
|---|---|---|---|
| Hematocrit (34-60%) | 18.5% | 15.8% | 30.2% |
| Platelet estimate | 128 K/µL | 48 K/µL | 128 K/µL |
| Segmented neutrophils (3,000-11,500/ µL) | 12,638/µL | NA | 2,686/ µL |

**Chemistry – no significant abnormalities**
**Prothrombin time – 7.4 sec (5-12)**
**Partial Thromboplastin Time 7.8 sec (10-20)**
**Canine Direct Coombs test – positive**
**Serology -**
*Babesia canis* – positive 1:320
*Babesia gibsoni* – positive 1:640
*Borrelia burgdorferi* – positive 1:640
**PCR -**
*Babesia gibsoni* – positive for Asian genotype

**Histopathologic Description:** A blood smear from a 2-year-old spayed female Boxer dog is submitted for review. The red cell density is markedly decreased indicating a severe anemia. There is moderate polychromasia and anisocytosis suggestive of a regenerative erythroid response. Scattered Howell-Jolly bodies and metarubricytes are also observed. Small (1-2µm) signet ring-shaped organisms and larger (2-3µm) piriform-shaped organisms are seen individually within erythrocytes **(Fig. 2-1)**. The platelets appear mildly decreased. However, moderate platelet clumping is noted. Many megaplatelets are observed suggestive of a regenerative response to platelet consumption or destruction. The leukocytes appear normal in morphology and a mild left shift is present and is suggestive of an inflammatory process.

**Contributor's Morphologic Diagnosis:** Severe regenerative anemia; mild thrombocytopenia; intraerythrocytic organisms consistent with *Babesia* species

**Contributor's Comment:** Canine Babesiosis is a hemoprotozoan infection which is typically caused by *Babesia gibsoni* or *Babesia canis*. *Babesia gibsoni* is small (1 x 3.2µm), pleomorphic, signet ring-shaped, and is usually observed as a single organism within the erythrocyte. *Babesia canis* is larger (2.4 x 5µm), and is generally observed as a paired, pyriform structure within the erythrocyte. Both species have Ixodid tick vectors and are found throughout Africa, Asia, Europe, the Middle East, and North America. *B. canis* is typically more prevalent. However, there has been an increase in the frequency of *B. gibsoni* infections, particularly in North America.[1] The specific vector for *B. gibsoni* in the United States has not been established. *Rhipicephalus sanguineus* and *Dermacentor variabilis* are suspected as possible vectors, but transmission studies have been unsuccessful or inconclusive.

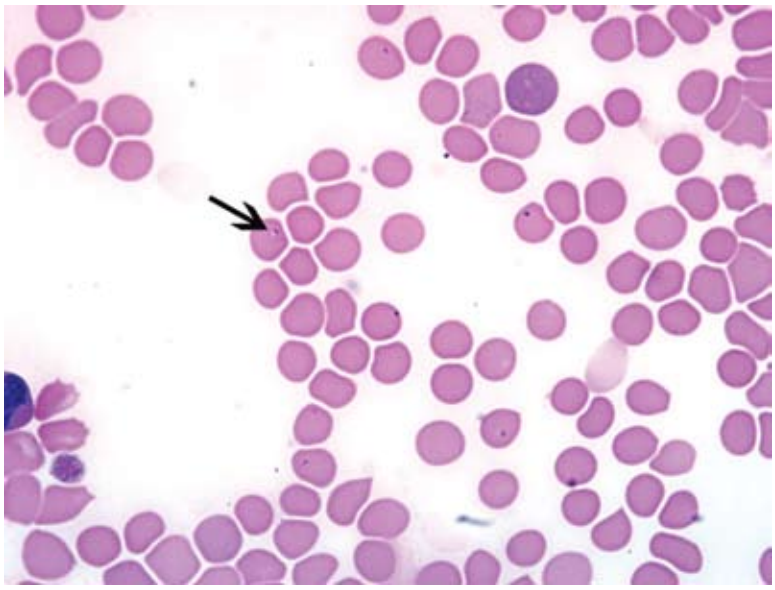

*2-1. Peripheral blood smear, dog. Among the erythrocytes, there is mild to moderate anisocytosis and polychromasia. Occasionally, there are 1-2 micron, round to crescent shaped intraerythrocytic merozoites (arrow). (HE 1000X)*

The organisms are transmitted through the bite of an infected tick. Once inside the host, the organisms attach to the erythrocyte membrane and are endocytosed. While in the cytoplasm, the organisms undergo binary fission resulting in the formation of merozoites. Ticks become infected during feeding by ingesting merozoites. Transtadial and transovarial (*B. gibsoni*) transmission result in the formation of sporozoites within the tick's salivary glands. While feeding, saliva and sporozoites from the infected tick are passed into the host's circulation. For transmission to occur, the tick must remain attached for 2-3 days.[2]

Infected dogs may present with a variety of clinical signs, ranging from hemolytic anemia to multiple-organ dysfunction syndrome (MODS). Subclinical infection is common in American pit bull terriers, which have a strong breed predilection for *B. gibsoni*. The predominant feature of babesiosis is hemolytic anemia. Thrombocytopenia is also quite common. The anemia is a result of both extra- and intravascular hemolysis. Parasitemia results in increased osmotic fragility, shortened erythrocyte life span, and erythrophagocytosis. The infected erythrocytes have parasite antigens on their surface, which induce opsonization by host antibodies and removal by the mononuclear-phagocyte system. The induction of serum hemolytic factors and production of antierythrocyte membrane antibodies with resulting damage from the secondary immune system also contribute to the pathogenesis of this disease. Other factors thought to be involved include oxidative damage, impaired hemoglobin function, as well as sludging and sequestration of infected erythrocytes.

Diagnosis may be made by identifying the parasite on a blood smear, serology (IFA and ELISA), or PCR which can detect low levels of parasitemia. Coinfection with other tick borne pathogens occurs relatively often as a single vector can harbor several infectious organisms.[1]

**AFIP Diagnosis:** Cytological specimen, peripheral blood smear: Moderate polychromasia and anisocytosis (regenerative anemia) with intraerythrocytic organisms consistent with Babesia species

**Conference Comment:** The proposed pathogenesis of babesiosis is as follows: tick transmission →parasitized erythrocytes→hemolysis (intravascular and extravascular) → anemia (hemoglobinemia, bilirubinuria, icterus) →decreased available oxygen for cellular machinery →anaerobic metabolism → acidosis → hypoxic cell damage → shock → death. DIC is often a sequelae of terminal babesiosis.[3]

Differential diagnoses for babesiosis include parasitic, immune-mediated, oxidative, and traumatic causes of hemolytic anemia.[3] Normally, infected animals present with anemia and thrombocytopenia. The anemia starts out as a normocytic, normochromic anemia and progresses to a macrocytic, hypochromic, regenerative anemia. Serum chemistries are generally within normal limits, with hypokalemia sometimes occurring in severely affected animals.[3]

Other intra-erythrocytic parasites of veterinary importance include:

| Species affected | Parasite |
|---|---|
| Dogs | *Babesia canis, Babesia gibsoni* |
| Cats | *Babesia cati, Babesia felis* |
| Cattle | *Anaplasma marginale, Anaplasma centrale*<br>*Babesia bovis, Babesia bigemina*<br>*Theileria mutans, Theileria annulata* |
| Sheep | *Babesia ovis, Babesia motasi* |
| Horses | *Babesia equi, Babesia caballi* |
| Deer, Elk | *Theileria cervi* |
| Birds | *Hemoproteus* spp., *Leukocytozoon* spp., *Plasmodium* spp. |

2

**Contributing Institution:** Mississippi State University College of Veterinary Medicine, www.cvm.msstate.edu

**References:**

1. Boozer L, Macintire D. *Babesia gibsoni*: An emerging pathogen in dogs. Compendium **27**(1): 33-41, 2005
2. Brockus CW, Andreasen CB: Erythrocytes. *In:* Duncan & Prasse's Veterinary Laboratory Medicine, Clinical Pathology, eds. Latimer KS, Mahaffey EA, Prasse KW, 4th ed., pp. 19-21. Blackwell Publishing, Ames, IA, 2003
3. Taboada J, Lobetti R: Babesiosis. *In:* Infectious Diseases of the Dog and Cat, ed. Green CE, 3rd ed., pp 722-736. WB Saunders, St. Louis, MO. 2006

## CASE III – 07H7837A (AFIP 3103707)

**Signalment:** 7-month-old Aberdeen Angus bovine steer (*Bos taurus*)

**History**: The animal presented for a short history of anorexia that progressed to ataxia, head pressing, and ultimately recumbency. Upon presentation, the calf was severely depressed, lethargic, unresponsive and severely ataxic in all four limbs. There was absence of menace reflex bilaterally, and the animal appeared to be blind. The owner stated that the calf was in a group of animals consuming a ration containing corn gluten.

**Gross Pathology:** Gross lesions were limited to the brain. There were multiple locally extensive areas within the cerebrum where the gray matter was markedly thinned. In these areas, remaining gray matter was characterized by fragmentation, softening and slight yellow to tan discoloration. Multifocally there was cleft formation at the gray matter-white matter junction where gray matter was separated from the underlying white matter **(Figs. 1-1 and 1-2)**. When ultraviolet light was applied to the fresh brain, distinct autofluorescence of these areas was observed **(Fig. 1-3)**.

**Laboratory Results:** Cerebral spinal fluid: Protein = 578.1 mg/dL; CK = 505 IU/L (normal range 0-5 IU/L); CSF cytology revealed mononuclear pleocytosis; blood lead was negative.

**Histopathologic Description:** Multifocally the deep cortical gray matter adjacent to underlying white matter is disrupted, fragmented and rarefied in a laminar pattern. There is disruption, vacuolation and/or loss of the neuropil in these areas (malacia). There is loss of cortical neurons, and remaining neurons are often shrunken, angular, hypereosinophilic and contain pyknotic nuclei (neuronal necrosis) **(Fig. 3-4)**. Multifocal remaining neurons are

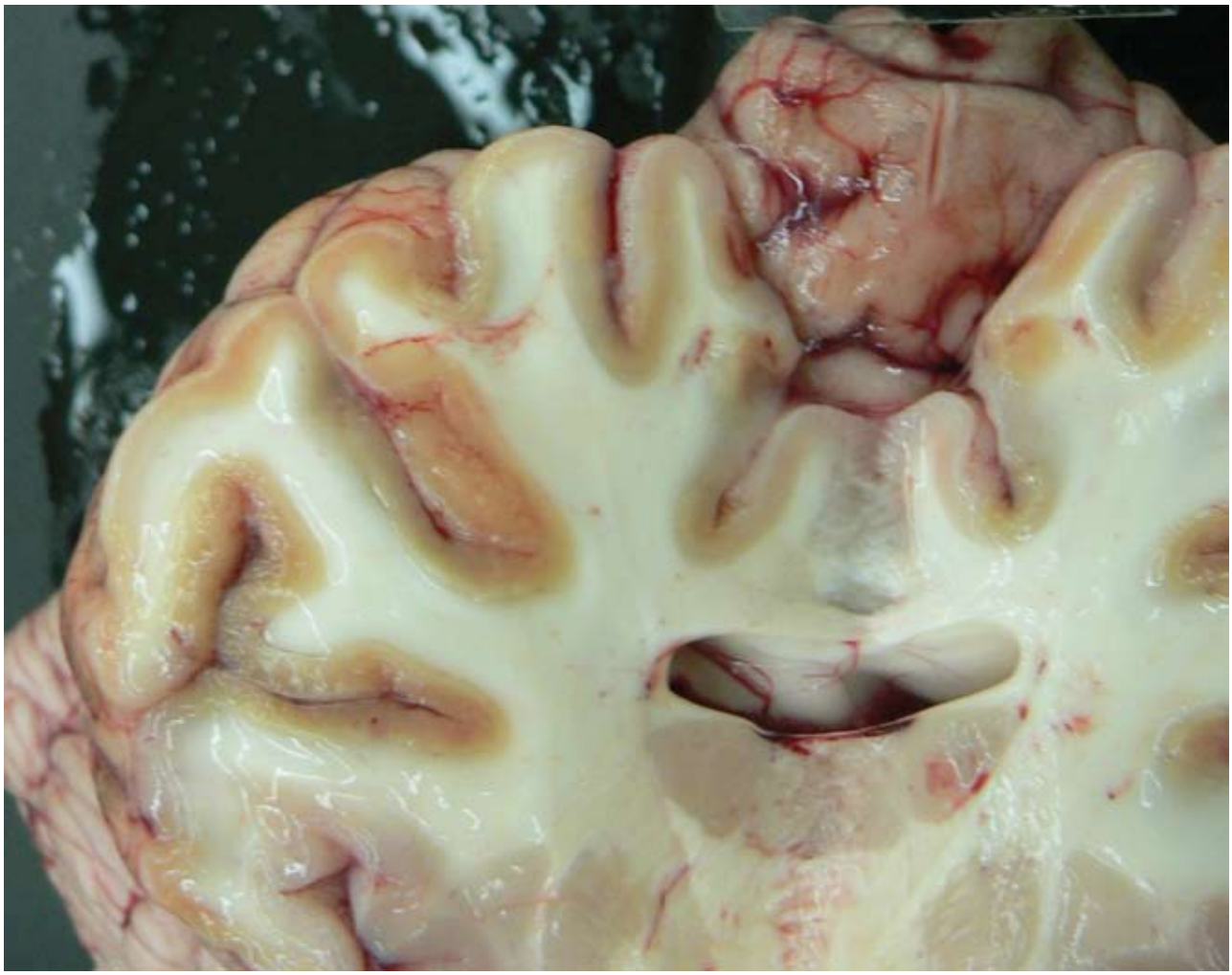

*3-1. Cerebrum, ox. Cortical laminar necrosis.* *Photograph courtesy of Iowa State University College of Veterinary Medicine, Department of Veterinary Pathology; http://www.vetmed.iastate.edu/departments/vetpath*

surrounded by glial cells (satellitosis and neuronophagia). Diffusely throughout the sections are increased numbers of glial cells (gliosis) including reactive astrocytes. In addition, there are multifocal random accumulations of erythrocytes (hemorrhage) and moderate numbers of gitter cells with fewer lymphocytes, neutrophils and in some sections karyorrhectic cellular debris. Axonal fibers are occasionally separated and surrounded by clear space (edema) and swollen axonal sheaths contain swollen hypereosinophilic bodies (spheroids) or gitter cells. Vessels are lined by plump endothelial cells (hypertrophy) and are frequently surrounded by clear space (edema) or moderate numbers of macrophages or lymphocytes. In some sections, the meninges are moderately expanded by clear space and low numbers of macrophages.

**Contributor's Morphologic Diagnosis:** Brain (cerebrum): Necrosis and neuronal loss, cortical, laminar, multifocal, moderate to severe with moderate multifocal histiocytic and lymphocytic meningoencephalitis

**Contributor's Comment:** The gross and histologic lesions in the cerebrum of this calf are characteristic of nutritional polioencephalomalacia (PEM) that is commonly seen in growing ruminants. The pathogenesis of nutritional PEM associated with thiamine deficiency is well established in carnivores (progressive encephalopathy); a thiamine-PEM association in ruminants is less clear. PEM in ruminants was thought at one time to be exclusively caused by thiamine deficiency, but it is now known that the laminar cortical necrosis can be caused by sulfur toxicity, lead toxicity, and hypoxia in addition to thiamine deficiency.[2] Confusion regarding the cause of PEM in cattle is partly due to the lack of a method to accurately

*3-2. Cerebrum, ox. Cortical laminar necrosis. Multifocally there is clefting and separation of malacic gray matter from the underlying white matter tracts.* *Photograph courtesy of Iowa State University College of Veterinary Medicine, Department of Veterinary Pathology; http://www.vetmed.iastate.edu/departments/vetpath*

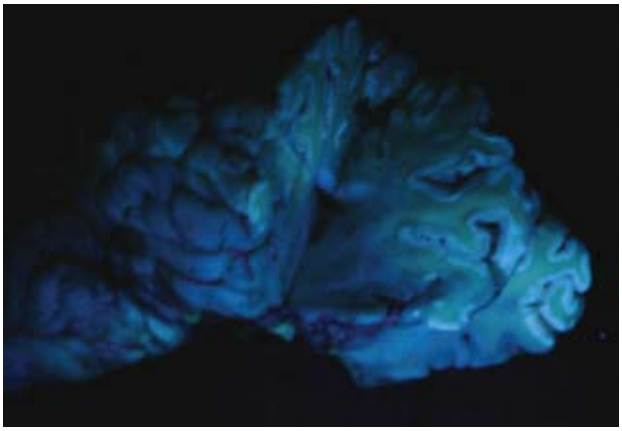

*3-3. Cerebrum, ox. Cortical laminar necrosis. When ultraviolet light was applied to the fresh brain, distinct autofluorescence of these areas was observed.* *Photograph courtesy of Iowa State University College of Veterinary Medicine, Department of Veterinary Pathology; http://www.vetmed.iastate.edu/departments/vetpath*

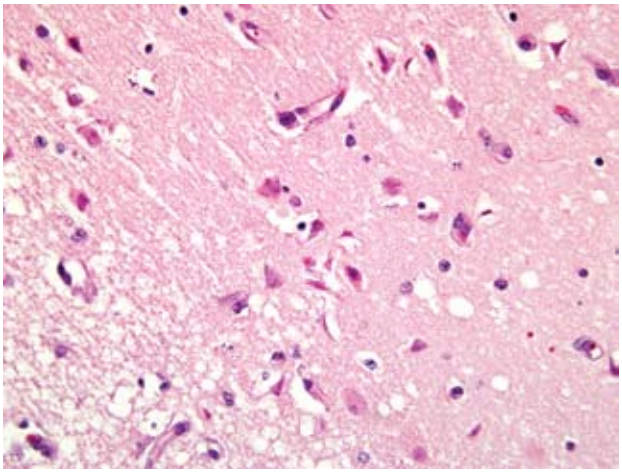

*3-4. Cerebrum, ox. Within the gray matter, primarily at the interface of white and gray matter, there is rarefaction of the neuropil, multifocal neuronal necrosis, and occasional gemistocytic astrocytes. (HE 400X)*

evaluate thiamine status in animals as well as thiamine-responsiveness that is frequently noted clinically.

The basis of sulfur-associated PEM in ruminants appears to be the excessive production of ruminal sulfide caused by the ruminal microbial reduction of ingested sulfur. Soluble hydrosulfide anion is in the rumen fluid phase, and hydrogen sulfide gas accumulates in the rumen gas cap. Non-reduced forms of sulfur (sulfate and elemental sulfur) are relatively nontoxic, while hydrogen sulfide and its ionic forms are highly toxic substances that interfere with cellular energy metabolism.[1] Sulfide inhibits cellular respiration by blocking cytochrome C oxidase in the electron transport chain. It is likely that sulfide produced in the rumen is absorbed into the blood and is capable of inhibiting energy metabolism of neurons and that this either directly causes neuronal necrosis or leads to necrosis by interfering with local cerebral blood flow and creating regional ischemia.[3] The most important route of sulfide absorption is unknown, but potentially occurs via the gastrointestinal mucosa or pulmonary mucosa after inhalation of eructated ruminal gas. The role of thiamine in these cases is not completely clear; however most current evidence indicates that sulfur-associated PEM does not involve reduced concentrations of thiamine in blood/tissues or reduced activity of transketolase, a thiamine-dependent enzyme.[3] A significant portion of PEM cases in ruminants may in fact be sulfur-associated rather than thiamine-associated, as was once thought.

Exposure to large amounts of sulfur can occur from a variety of sources including both feed and water. The

occurrence of PEM in ruminants associated with high dietary sulfur intake has been recognized with increasing frequency, particularly in Midwestern United States. This appears to be associated with the recent expansion of the fuel ethanol industry, as byproducts of corn (maize)-to-fuel ethanol production are being used with increasing frequency in ruminant diets. Ethanol byproducts are attractive feed ingredients due to their nutritional (especially protein) value and they are readily available at reduced cost (compared to corn) in Midwestern states. Sulfuric acid is utilized in ethanol byproduct production, and byproducts thus often contain significantly elevated levels of sulfur which represent a major source of dietary sulfur for these animals. In addition, there is much variation in the sulfur content of ethanol byproducts both within and between plants, and for this reason periodic monitoring is recommended for producers utilizing these products in rations.[2] In this case, the history of corn gluten meal feeding (a commonly fed ethanol byproduct) is considered to be the likely source of elevated sulfur, though feed samples were not evaluated for confirmation. This case represents a classic case of ruminant PEM both clinically and pathologically. Sulfur-related PEM manifests clinically as acute blindness, recumbency, seizures and death or a more subacute form characterized by visual impairment and ataxia. Lesions are classic and are characterized by extensive necrosis of cerebrocortical neurons. Grossly, there is fragmentation, malacia and loss of cortical gray matter that in some cases autofluoresces brightly when exposed to 366-nm UV light. At later stages, affected tissue becomes cavitated as macrophages infiltrate and necrotic tissue is removed.[1]

**AFIP Diagnosis:** Brain, cerebrum: Necrosis and neuronal loss, cortical, laminar, multifocal, moderate to severe, with edema and moderate multifocal histiocytic and lymphocytic meningoencephalitis

**Conference Comment:** The contributor does a magnificent job describing PEM in ruminants. Thiamine deficiency in carnivores (Chastek paralysis) is also mentioned and a brief review follows.

Thiamine, or vitamin B1, is an essential dietary need in carnivores. Ruminants are able to produce their own thiamine from the diet via microbial production in the rumen.[3] Thiamine deficiency in carnivores often results from eating a diet high in fish containing thiamine-splitting enzymes (thiaminases). Sulfur dioxide, often used to preserve that "fresh fish" appearance, can destroy thiamine after it is metabolized into sulfates.[3]

If the disease is recognized early in its progression, thiamine supplementation can reverse the course of the disease. If clinical signs are present for several days, and a point of no return is passed, death is the result. Microscopic lesions include vacuolation of the neuropil, vascular dilation, hemorrhage, and necrosis. The periventricular gray matter is highly susceptible and the lesion is almost always bilateral and symmetrical most often involving the inferior colliculi.[3]

**Contributing Institution:** Iowa State University College of Veterinary Medicine, Department of Veterinary Pathology; http://www.vetmed.iastate.edu/departments/vetpath/

**References:**

1. Department of Veterinary Diagnostic and Production Animal Medicine, Iowa State University, Ames, IA website. Polio in cattle can be caused by sulfur toxicity. Accessed July 05, 2008 http://www.vetmed.iastate.edu/departments/vdpam/vdl.aspx?id=2070
2. Gould, D: Update on sulfur-related polioencephalomalacia. *In:* The Veterinary Clinics of North America: Food Animal Practice: Toxicology, eds. Osweiler GD and Galey FD. pp 481-496. 16(3): November 2000
3. Maxie MG, Youssef S: Nervous system. *In:* Jubb, Kennedy and Palmer's Pathology of Domestic Animals, ed. Maxie MG, 5th ed., vol 1, pp.351-356. Elsevier Limited, Philadelphia, PA, 2007
4. McAllister, MM: Feed-Associated toxicants: sulfur. In: Clinical Veterinary Toxicology, ed. Plumlee K, pp 133-134. Mosby, St Louis, MO, USA, 2004

## CASE IV – Case 1 (AFIP 3093118)

**Signalment:** 8-week-old, intact female, English springer spaniel, (*Canis familiaris*), dog

**History:** This female English springer spaniel was purchased from a farm. Per clinical history, she showed vomiting and diarrhea followed by icterus and oliguria.

On clinical presentation, the dog had pale and icteric mucous membranes. Her femoral pulses were weak and intermittent with marked deficits. Electrocardiography suggested atrial fibrillation. The dog had tachypnea and increased respiratory effort, with harsh lung sounds on thoracic auscultation.

Acute oliguric renal failure was diagnosed based on clinical signs and laboratory data (see below). Despite

fluid therapy, diuretics and treatment for hyperkalemia, three days following the commencement of clinical signs the dog developed ventricular fibrillation, which progressed to cardiopulmonary arrest that was refractory to resuscitation including defibrillation.

**Gross Pathology:** The oral mucosa was pale with yellowish discoloration. The subcutaneous adipose connective tissue had yellow discoloration (icterus). The lungs were reddened and firm. The kidneys were pale and bilaterally the cortices contained petechial hemorrhages.

**Laboratory Results:** A complete blood count revealed minimal neutrophilia 11.7x$10^9$/L (reference value: 3-11.5 x$10^9$/L), moderate monocytosis 2.98x$10^9$/L (reference value: 0.15-1.5 x$10^9$/L) and a borderline normochronic, normocytic anemia with an HCT of 27.2% (reference value: 31.4%).

Serum biochemistry revealed a moderate panhypoproteinemia 41g/L (reference value: 49-71g/L) due to hypoalbuminemia 21.2g/L (reference value: 28-39g/L) and minimal hypoglobulinemia 19.8g/L (reference value: 21-41 g/L). Further abnormalities included marked hyperkalemia 9.9mmol/L (reference value: 4.1-5.3 mmol/L), marked hypercalcemia 4.12mmol/L (reference value: 2.13-2.7 mmol/L) and marked hyperphosphatemia 6.89mmol/L (reference value: 0.8-2.0 mmol/L). A marked azotemia with elevated blood urea nitrogen (BUN) 64.1mmol/L (reference value: 3-9.1 mmol/l) and elevated creatinine 601µmol/L (reference value 98-163mmol/L) was also present. Other tested parameters included increased amylase 1874U/L (reference value: 176-1245U/L), increased lipase 4470U/L (reference value: 72-1115U/L), hyperbilirubinemia 92.1mmol/L (reference value: 0-2.4 mmol/L) and an increased alkaline phosphatase (ALP) 933 U/L (reference value: 19-285 U/L).

Urinalysis revealed isosthenuria (specific gravity 1.010), pH 7.0 and elevated glucose (3+). Urine culture revealed no bacterial isolates after 48 hours incubation.

Antibody titers to several *Leptospira* spp., which can be pathogenic to dogs, were tested. All Leptospira serovar pool titers were negative.

**Histopathologic Description:** Lungs. There is multifocal deposition of blue granular material within interalveolar septae (interpreted as mineralization, **Fig. 4-1**). Numerous alveolar spaces contain strands of eosinophilic fibrillar material. Multifocally, histiocytes are present in alveolar spaces and often surround mineralized septae. Extravasated erythrocytes and very rare neutrophils are also present in some alveolar spaces. Capillaries and blood vessels are congested and there is moderate to focally marked expansion of the perivascular interstitium by clear spaces (oedema). Bronchiolar lumens contain fibrin strands, small to moderate numbers of erythrocytes and sloughed cellular debris. Brown-black staining of alveolar septae using a von Kossa stain indicates the deposition of calcium salts and thus confirms tissue mineralization **(Fig. 4-2)**.

**Contributor's Morphologic Diagnosis:** Lungs, alveolar septae; Mineralization with histiocytosis, moderate, diffuse
Lungs, alveoli: Fibrin exudation, moderate with histiocytosis

**Contributor's Comment:** Pathologic mineralization is defined as the abnormal tissue deposition of principally calcium salts, with smaller amounts of other salts, and thus is synonymous with the term tissue calcification.[7] In general, calcification can be dystrophic, occurring locally at sites of tissue necrosis, metastatic, in which calcium deposition occurs in otherwise healthy tissue as a result of altered calcium metabolism or idiopathic if no obvious underlying cause can be detected.[7,11] Metastatic mineralization can be caused by several conditions, which are summarized below.

1) *Hyperparathyroidism*: Hyperparathyroidism is associated with elevated parathyroid hormone/parathormone (PTH) causing bone resorption and thus hypercalcemia.
*Primary hyperparathyroidism* is characterized by the autonomous secretion of PTH due to parathyroid gland neoplasia.[2,8]
*Pseudohyperparathyroidism* is caused by the secretion of PTH-like proteins by malignant tumors (hypercalcemia of malignancy) e.g. lymphoma and anal sac apocrine gland adenocarcinoma.[2,8] Non-parathyroid neoplasia has been reported as the most frequent cause of hypercalcemia in dogs and cats.[4]

2) *Bone destruction:* Hypercalcemia can be observed with osteolytic lesions caused by multiple myeloma and tumor metastasis to bone.[5]
3) Vitamin D intoxication: Ingestion of increased amounts of vitamin D analogues, e.g. calcinogenic plants, dietary supplements, rodenticide baits, or other calcinogenic products are other possible causes of hypercalcemia.[5,6]
4) Certain types of *granulomatous disease* can lead to hypercalcemia, for example blastomycosis in dogs. Activated macrophages have the ability to synthesize the active form of vitamin D3, calcitriol.[5]
5) *Renal failure* (please see below): Renal failure is associated with phosphate retention (hyperphosphatemia). The increased serum phosphorus (PO4) forms complexes

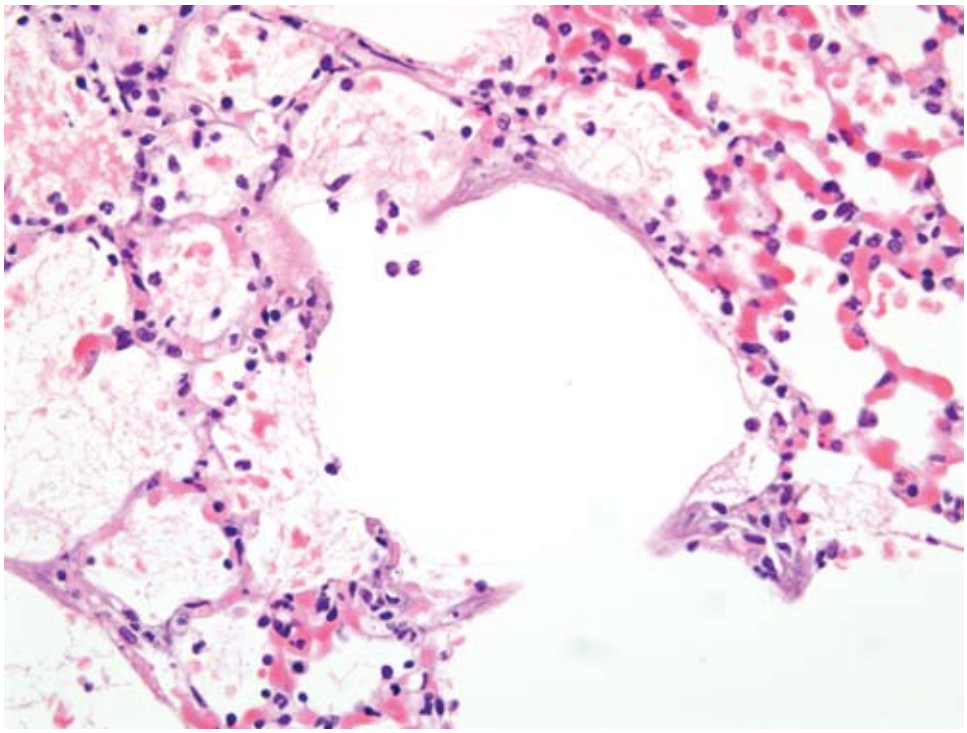

*4-1. Lung, dog. Diffusely, alveolar septa are necrotic and replaced by hyaline membranes, often admixed with scant amounts of granular mineral. Multifocally, alveoli are flooded with large amounts of fibrin, small amounts of hemorrhage, and few alveolar macrophages. (HE 400X)*

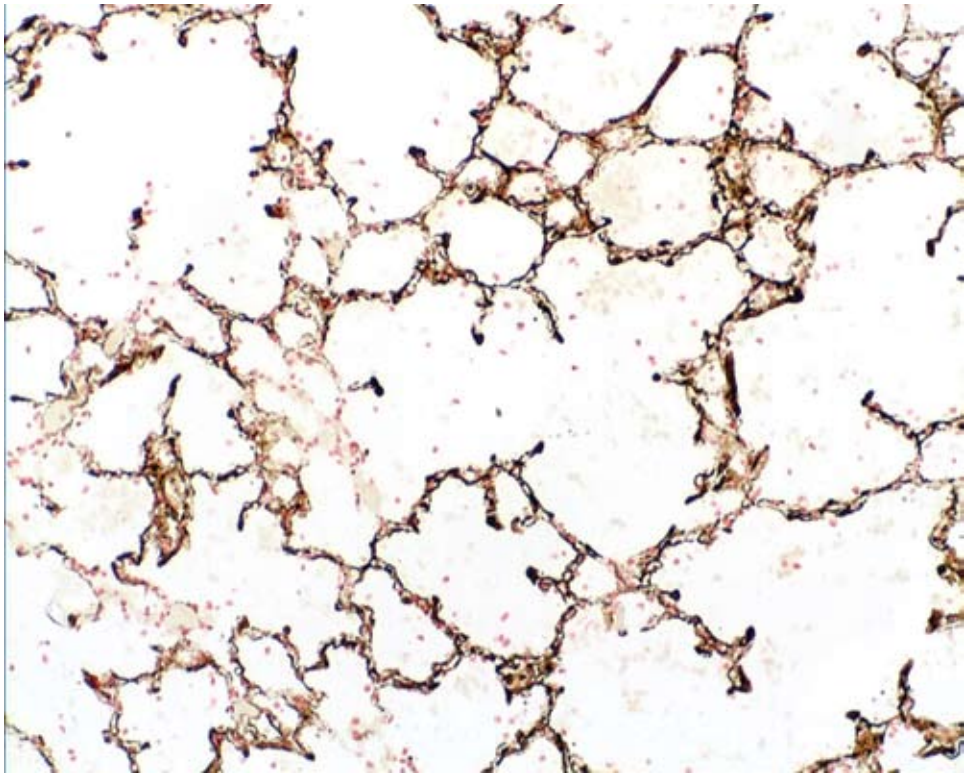

*4-2. Lung, dog. Diffusely within alveolar septa, there is mineral which stains positively with Von Kossa stain. (Von Kossa 400X)*
*Photomicrograph courtesy of Department of Pathology & Infectious Disease, The Royal Veterinary College, Hawkshead Lane, North Mymms, Hatfield, Hertfordshire, AL9 7TA, United Kingdom, www.rvc.ac.uk*

with serum calcium (Ca2+) and metastatic tissue mineralization develops if the product of Ca2+ x PO4 exceeds a certain threshold value.[13]

In the present case, metastatic calcification was observed. In addition to the pulmonary mineralization, mineral deposition was present in the gastric mucosa, renal tubular epithelial cells and renal vessel walls. On macroscopic and microscopic examination of the dog and multiple tissues, the parathyroid glands were unremarkable and no evidence of neoplasia was found. The laboratory data indicated renal failure due to the concurrent presence of hypoalbuminemia, hyperphosphatemia and hyperkalemia and increased BUN and creatinine. The hypoalbuminemia was likely caused by renal loss of protein. The cause of the mild hypoglobulinemia is uncertain. No intestinal lesions were observed at post mortem examination. Hyperphosphatemia, hyperkalemia and increased BUN and creatinine develop following decreased glomerular filtration. The increased levels of amylase and lipase were also likely related to the renal disease, since no lesions suggestive of pancreatitis were observed. Interestingly, the dog also had hypercalcemia. In dogs with renal failure, there are usually hyperphosphatemia and hypocalcemia. In some cases, however, hypercalcemia has been described.[13] The elevated ALP and hyperbilirubinemia suggest decreased hepatic function. The young age of the dog may have contributed to the elevated calcium, phosphorus and ALP levels. Renal failure is classified as *pre-renal, renal* or *post-renal* renal failure. The main features of the different types of renal failure are listed below.

*Pre-renal renal failure* is related to a reduced perfusion of the kidneys, which can be caused by low cardiac output, increased renal vasculature resistance, extra-cellular fluid volume depletion or low systemic vascular resistance.[10]
*Renal renal failure* is caused by impaired renal function, which could be related to tubular injury, glomerulonephritis, tubulointerstitial nephritis, acute vascular nephropathy or neoplasia.[10]
*Post-renal renal failure* is caused by urinary tract obstruction, e.g. tubular precipitation, urethral obstruction or bladder obstruction.[10]

In this case, the absence of obstruction in the urinary tract rules out post-renal failure. Because of the history of vomiting and diarrhea, reduced renal perfusion has to be considered as a possible cause of the renal failure. Microscopic examination of the kidneys revealed the presence of mineralization in some tubular epithelial cells and in the walls of occasional blood vessels. Furthermore, mild tubular degeneration and regeneration were observed. The degeneration affected approximately 20-30% of tubules in the cortex and medulla. In addition, the renal interstitium contained a mild multifocal infiltrate of lymphocytes and plasma cells. Thus, pre-renal and renal causes likely contributed to the renal failure. Reportedly, vomiting and diarrhea develop prior to the acute renal failure. Vomiting and diarrhea, however, can also be observed secondary to renal failure.[5,10]

In secondary renal hyperparathyroidism raised levels of ionized plasma phosphate cause hypocalcemia through the precipitation of calcium and phosphorus. The reduction in ionized serum calcium stimulates PTH secretion and the mobilization of calcium from bone stores. This results in bone resorption with the release of phosphorus and calcium. The stimulation of PTH secretion is compounded by the damaged kidneys, which have a reduced capacity to hydroxylate the inactive form of vitamin D 25-hydroxycholecalciferol to the active form of vitamin D, i.e. 1,25-dihydroxycholecalciferol (calcitriol). Thus, the intestinal absorption of calcium is reduced. Calcitriol, which is also suppressed by hyperphosphatemia, normally inhibits PTH secretion. By reducing calcitriol production a physiological control on PTH secretion is removed and eventually parathyroid chief cell hyperplasia occurs, a process termed renal secondary hyperparathyroidism.[12]

PTH enhances calcium release from bone by activating osteoclast resorption through their indirect stimulation. Osteoclasts do not have a receptor for PTH, thus PTH binds to osteoblasts which stimulate osteoblasts to increase their expression of receptor activator of NFκB ligand (RANK ligand). RANK ligand binds to osteoclast precursors containing receptor activator of NFκB (RANK). The binding of RANK ligand to RANK stimulates these precursors to fuse and to form osteoclasts which ultimately enhances the resorption of bone.[3]

The biochemical abnormality characterized by elevated BUN and creatinine is termed azotemia and when this is associated with clinical signs and other biochemical abnormalities it is termed uremia.[10] Non-renal lesions of uremia include pulmonary edema and soft tissue mineralization. In uremia, pulmonary edema most likely occurs via two mechanisms a) mineralization of alveolar septae leading to diffuse alveolar damage, and b) uremic toxins causing increased permeability of alveolar capillaries with leakage of protein-rich fluid containing fibrin.[10] Histiocytic cells, including alveolar macrophages have a role in preventing the accumulation of native proteins within alveoli and thus their increased infiltration would be expected in response to proteinaceous edema containing fibrin. In addition, the mineral deposits stimulate a foreign body response causing histiocytic infiltration.[10]

The pathogenesis of soft tissue mineralization in the uremic animal is not fully understood, however, deposition of calcium phosphate mineral favors tissues with an internal alkaline compartment, principally gastric mucosa, kidneys, lungs, systemic arteries and pulmonary veins but other local factors such as tissue glycosaminoglycans may play a role.[7] Renal mineralization compounds the problem by causing further damage and thus a further reduction in glomerular filtration.

In the present case, the pulmonary lesions might be caused by uremia. Due to the concurrent presence of hyperphosphatemia and hypercalcemia, however, hypervitaminosis D cannot be ruled out.[5]

Leptospirosis has also been considered as one possible cause of concurrent elevated renal and hepatic parameters in dogs.[1,10] Canine infection is caused by *Leptospira (L.) interrogans* or *L. kirschneri* and many pathogenic serovars have been identified with *Leptospira canicola, icterohaemorrhagiae, grippotyphosa, pomona* and *bratislava* being the most commonly identified in dogs.[9,14] Following cutaneous or mucosal penetration, leptospires are disseminated via the blood to target tissues such as the kidneys, liver, spleen and central nervous system. The extent of damage to internal organs varies with the virulence of the organism and host susceptibility. In addition, some serovars show a predilection for the liver or kidney. The mechanisms by which leptospires cause disease are not well understood, and leptospiral lipopolysaccharide may play a role in inflammatory and coagulatory abnormalities that occur. Renal damage occurs following colonization and replication of the organisms in renal tubular epithelial cells, whereas histochemical studies have shown that the fundamental hepatic lesion is due to subcellular effects on enzyme systems.[9] In this case the standard serologic test, microscopic agglutination test (MAT), was performed however titers to all tested serovars were negative. It has been reported that in acute or peracute disease antibody responses have not yet developed and as such serological tests are not useful until 7 to 10 days after infection.[1,9]

**AFIP Diagnosis:** Lung: Pneumonia, interstitial, fibrinonecrotizing, acute, multifocal to coalescing **(Fig. 4-1)**, marked with edema, hemorrhage, hyaline membranes and alveolar septal mineralization **(Fig. 4-2)**

**Conference Comment:** Animals that die due to complications of acute renal failure and subsequent uremia often develop terminal pulmonary edema. The pathogenesis is not clear, but increased permeability of the alveolar capillaries is the most likely cause. Mineralization of alveolar and bronchiolar walls can also occur secondary to fatal renal disease. This is often referred to as uremic pneumonitis or uremic lung.[10]

In reviewing the clinical chemistry data from this case, the moderator emphasized to attendees that an increase in ALP may occur for a variety of reasons, e.g. cholestasis, steroid induction. Furthermore, there may have been increased activity of the bone isoenzyme of ALP due to the young age of the puppy in the case, or perhaps increased osteoclastic activity due to the suspected renal hyperparathyroidism. Most importantly, ALP is independent and non-predictive of hepatic function. Analysis of pre- and post-prandial bile acid concentration is the only direct method to assess hepatic function; albumin and BUN concentrations (if low) may provide indirect clues to the status of liver function.

The moderator and conference participants also prefer the use of the term "azotemia" versus "renal failure" in the otherwise well-crafted contributor section on pre-, renal and post-renal azotemia. Renal failure, defined as an increase in BUN/Creatinine and decreased urine specific gravity, is present in this case.

**Contributing Institution:** Department of Pathology & Infectious Disease, The Royal Veterinary College, Hawkshead Lane, North Mymms, Hatfield, Hertfordshire, AL9 7TA, United Kingdom
www.rvc.ac.uk

**References:**

1. Andre-Fontaine G: Canine leptospirosis--do we have a problem? Vet Microbiol **117**:19-24, 2006
2. Capen CC: Endocrine glands. *In:* Jubb, Kennedy, and Palmer's Pathology of Domestic Animals, ed. Maxie GM, 5th ed., pp. 363-375. Elsevier Limited, St Louis, MO, 2007
3. Capen CC: Endocrine glands. *In:* Jubb, Kennedy, and Palmer's Pathology of Domestic Animals, ed. Maxie GM, 5th ed., pp. 355-356. Elsevier Limited, St Louis, MO, 2007
4. Elliott J, Dobson JM, Dunn JK, Herrtage ME, Jackson KF: Hypercalcaemia in the dog: a study of 40 cases. J Small Anim Pract **32**:564-571, 1991
5. Ferguson DC, Hoenig M: Endocrine system. *In:* Duncan & Prasse's Veterinary Laboratory Medicine Clinical Pathology, eds. Latimer KS, Mahaffey EA and Prasse KW, 4th ed., pp. 270-278. Blackwell, Ames, Iowa, 2003
6. Hilbe M, Sydler T, Fischer L, Naegeli H: Metastatic calcification in a dog attributable to ingestion of a tacalcitol ointment. Vet Pathol **37**:490-492, 2000
7. Kumar V, Abbas AK, Fausto N: General Pathology - Cellular adaptations, Cell injury, and Cell death. *In:* Robbins and Cotran Pathologic Basis of Disease, eds. Kumar V, Abbas AK and Fausto N, pp. 41-42. Elsevier

Saunders, Philadelphia, PA, 2005
8. La Perle KMD, Capen CC: Endocrine system. *In:* Pathologic Basis of Veterinary Disease, eds. McGavin DM and Zachary JF, 4th ed., pp. 731-734. Mosby, St Louis, MO, 2007
9. Langston CE, Heuter KJ: Leptospirosis. A re-emerging zoonotic disease. Vet Clin North Am Small Anim Pract **33**:791-807, 2003
10. Maxie GM, Newman SJ: Urinary system. *In:* Jubb, Kennedy, and Palmer's Pathology of Domestic Animals, ed. Maxie GM, 5th ed., pp. 432-436. Elsevier Limited, St Louis, MO, 2007
11. Maxie GM, Robinson WF: Cardiovascular system. *In:* Jubb, Kennedy, and Palmer's Pathology of Domestic Animals, ed. Maxie GM, 5th ed., pp. 61-62. Elsevier Limited, St Louis, MO, 2007
12. Newman SJ, Confer AW, Panciera RJ: Urinary system. *In:* Pathologic Basis of Veterinary Disease, eds. McGavin DM and Zachary JF, 4th ed., pp. 641-644. Elsevier Limited, St Louis, MO, 2007
13. Stockham SL, Scott MA: Calcium, phosphorus, magnesium, and their regulatory hormones. *In:* Fundamentals of Veterinary Clinical Pathology, eds. Stockham SL and Scott MA, 1st ed., pp. 401-417. Blackwell, Ames, Iowa, 2002
14. Stokes JE, Forrester SD: New and unusual causes of acute renal failure in dogs and cats. Vet Clin North Am Small Anim Pract **34**:909-922, vi, 2004

**NOTES:**

The Armed Forces Institute of Pathology
Department of Veterinary Pathology

*Conference Coordinator:*
Todd M. Bell, DVM

WEDNESDAY SLIDE CONFERENCE 2008-2009

# Conference 20

11 March 2009

***Conference Moderator:***

Dr. F. Yvonne Schulman, DVM, Diplomate ACVP

## CASE I – 07-1158 (AFIP 3102611)

**Signalment:** 6-year-old, spayed female, mixed breed dog (*Canis familiaris*)

**History:** 6-week history of progressive neurologic deficits that began as posterior paresis and progressed to cerebellar ataxia. Neurologic exam revealed cranial nerve V involvement and central vestibular signs.

**Gross Pathology:** No gross lesions in brain

**Laboratory Results:** MRI and CSF analysis are both normal. Immunohistochemistry for GFAP was negative.

**Histopathologic Description:** The pons and medulla have a diffuse infiltration of neoplastic elongate cells within gray and white matter. The cells have indistinct cytoplasm, elongate nuclei with dense, hyperchromatic chromatin, mild anisokaryosis and no mitotic figures. They resemble fibrillary astrocytes. The neoplasm does not form a distinct mass and has no borders, but infiltrates the neuropil diffusely without damaging the normal tissue. The cells tend to stream along the axis of white matter fiber tracts and often wrap around neurons, but no neuronal lesions are seen **(Fig. 1-1)**. Tumor cells form a thin subpial layer in the cerebellum and extend into the cerebellar folia with regional loss of Pukinje cells. An occasional perivascular cuff of lymphocytes is observed.

**Contributor's Morphologic Diagnosis:** Gliomatosis cerebri

**Contributor's Comment:** Gliomatosis cerebri is a neoplasm of unknown cell origin but is classified as a glial cell tumor in the WHO classification of tumors of the nervous system. The tumor cells resemble fibrillary astrocytes but GFAP immunostaining is variable; some tumors stain negative and others have few positive staining cells. Gliomatosis in man is divided into two subtypes. Type I is the most common and presents as a diffuse infiltration of the brain with no mass lesion. Type II gliomatosis presents as a mass lesion.

Gliomatosis cerebri was established in dogs in a report of 6 cases [5] and based upon lesions that are very similar to those in man. Four of the cases in dogs were type I, and two cases were type II. The case presented here represents type I gliomatosis. The neoplasm in dogs has many similarities to the disease in man, but GFAP staining has been consistently negative in dogs, as it was in this case.

**AFIP Diagnosis:** Brainstem: Gliomatosis cerebri

*Sponsored by the American Veterinary Medical Association, the American College of Veterinary Pathologists, and the C. L. Davis Foundation.

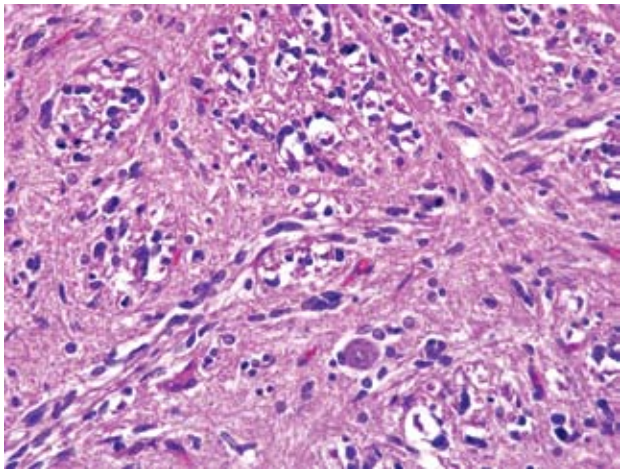

*1-1. Brainstem, dog. Gliomatosis cerebri. Diffusely infiltrating grey and white matter, often surrounding axons, are high numbers of neoplastic glial cells. (HE 400X)*

**Conference Comment:** The differential diagnosis including gliosis, diffuse astrocytoma, lymphoma, primitive neuroectodermal tumors (PNETs) and microgliomatosis was discussed at the conference. Widespread infiltration of the central nervous system, atypia and mitotic activity are typical for gliomatosis cerebri and help to differentiate it from gliosis. Gliomatosis cerebri is also more widespread than diffuse astrocytoma and, in dogs, is usually negative for GFAP.[5,6] In lymphoma, neoplastic cells are round with round to irregularly round nuclei and scant to small amounts of cytoplasm, and lymphomas tend to efface tissue. CD3 or CD79 positivity helps to identify lymphoma and prevent an incorrect diagnosis of gliomatosis cerebri. PNETs also tend to efface tissue and are usually seen in young animals. Microgliomatosis is a neoplasm of microglial origin, the resident macrophage of the central nervous system, and should be positive for CD18.

**Contributing Institution:** College of Veterinary Medicine, Virginia Tech, Blacksburg, VA 24061
www.vetmed.vt.edu

**References:**

1. Burger PC, Scheithauer BW: Tumors of neuroglia and choroid plexus. *In:* AFIP Atlas of Tumor Pathology, Tumors of the Central Nervous System, ed. Silverberg SG, Sobin LH, Series 4, pp. 83-86. ARP Press, Washington, DC, 2008
2. Koestner A, Bilzer T, Fatzer R, Schulman FY, Summers BA, Van Winkle TJ: Histological classification of tumors of the nervous system of domestic animals. *In:* World Health Organization Histological Classification of Tumors of Domestic Animals, ed. Schulman FY, Second Series, vol. 5, pp. 21. Armed Forces Institute of Pathology, Washington, DC, 1999
3. Koestner A, Bilzer T, Fatzer R, Schulman FY, Summers BA, Van Winkle TJ: Lymphomas and hematopoietic tumors. *In:* World Health Organization Histological Classification of Tumors of the Nervous Sytstem of Domestic Animals, ed. Schulman FY, Second Series, vol. 5, pp. 32. Armed Forces Institute of Pathology, Washington, DC, 1999
4. Maxie MG, Youssef S: Nervous system. *In:* Jubb, Kennedy, and Palmer's Pathology of Domestic Animals, ed. Maxie MG, 5th ed., vol. 1, pp. 294-295, 448. Saunders Elsevier, Philadelphia, PA, 2007
5. Porter B, de Lahunta A, Summers B: Gliomatosis cerebri in six dogs. Vet Pathol **40**:97-102, 2003
6. Vandevelde M, Fankhauser R, Luginbuhl H: Immunocytochemical studies in canine neuroectodermal brain tumors. Acta Neuropathol **66**:111-116, 1985
7. Louis DN, Ohgaki H, Wiestler OD, Cavenee WK, Burger PC, Jouvet A, Scheithauer BW, Kleihues P: The 2007 WHO classification of tumours of the central nervous system. Acta Neuropath **114**(2):164-172, 2007

## CASE II – UNAM Case 1 (AFIP 3102490)

**Signalment:** 10-year-old, male, Boxer dog, canine (*Canis familiaris*)

History: This dog presented with a one-week history of ataxia, general weakness and occasional temporary loss of consciousness. Neurological examination showed cranial nerve reflexes within normal limits. Two to three hours later, the animal had lost the sense of smell, palpebral and swallowing reflexes, perception of painful stimuli, and was blind. Two hours later the patient was in a coma. The owner elected euthanasia due to poor prognosis. The carcass was submitted for necropsy examination.

**Gross Pathology:** The left cerebral hemisphere showed moderate edematous swelling with flattening of the cortical gyri and narrowing of the sulci. In transverse section there was a mass primarily located in the subcortical white matter of the frontal lobe, which extended cranially to the olfactory bulb and caudally to the pellucid septum. The growth was infiltrative, poorly circumscribed, soft, gelatinous and grayish white, with extensive areas of hemorrhage. The mass compressed surrounding tissues and distorted the cerebral hemispheres **(Fig. 2-1)**.

**Laboratory Results:** None

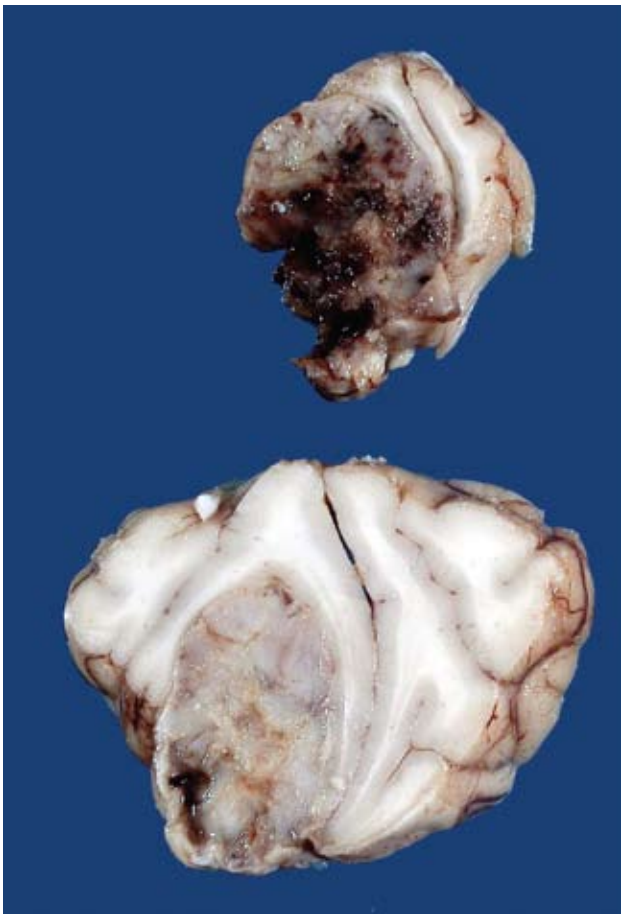

*2-1. Cerebrum, dog. Anaplastic oligodendroglioma within the left cerebral hemisphere with multifocal hemorrhage. Photograph courtesy of Departamento de Patologia, Facultad de Veterinaria, Universidad Nacional Autonoma de Mexico, Mexico City, Mexico.*

**Histopathologic Description:** Sections of the brain show a poorly circumscribed, hypercellular mass compressing the surrounding tissue. The tumor is primarily located in the white matter and is composed of dense sheets of small round cells. These cells have moderate amount of clear eosinophilic and vacuolated cytoplasm, with poorly defined cell boundaries**(Fig. 2-2)**. Nuclei are round to oval, hyperchromatic, with clumped chromatin, inconspicuous nucleoli, and show moderate anisokaryosis. Mitotic figures are present (0-3 per random 40x field). Rarely, atypical astrocytes are scattered among the neoplastic cells. Occasionally, in some areas, tumor cells show poorly stained cytoplasm (perinuclear halo) with distinct cell membrane. In other areas, cellularity is low to moderate, and tumor cells have euchromatic nuclei with a vesicular chromatin pattern, single small basophilic nucleoli, fibrillary processes, and microcystic degeneration.

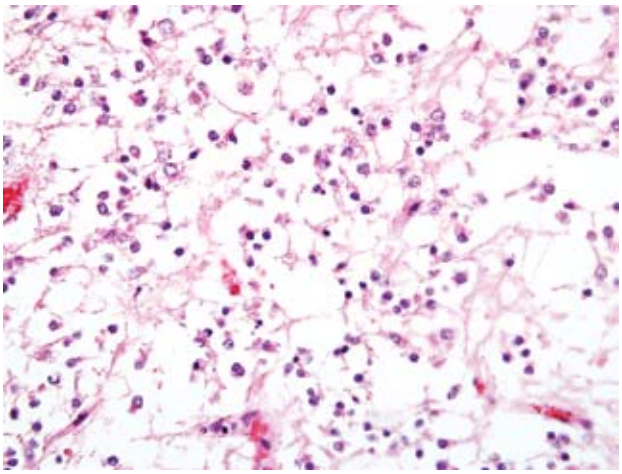

*2-2. Cerebrum, dog. Anaplastic oligodendroglioma. Neoplastic cells have a dense nuclear chromatin pattern, poorly staining cytoplasm, and indistinct cell borders, giving the appearance of a perinuclear halo. (HE 400X)*

The neoplasm exhibits pronounced branching vascular proliferation **(Fig. 2-3)** with abundant glomeruloid vessels **(Fig. 2-4)**. Multifocal extensive areas of necrosis, with hemorrhages and small numbers of foamy macrophages (gitter cells) are also seen. In addition, small spaces filled with pale, gray-blue mucinous material (mucinous cystic degeneration) are also present in some sections (slides not submitted).

**Contributor's Morphologic Diagnosis:** Cerebrum: Oligodendroglioma, anaplastic

**Contributor's Comment:** Oligodendrogliomas appear to be the most common primary brain tumors in mature dogs (older than 5 years). Their overall incidence in dogs ranges from 5 to 12 %.[1] A predilection for brachycephalic dog breeds, such as the present case, has been recognized in glial tumors.[2,3] Oligodendroglioma is usually located in the subcortical white matter of the cerebral hemispheres, particularly the frontal lobe. In brachycephalic dog breeds, these tumors appear to arise within remnants of the germinal matrix adjacent to the lateral ventricles. Clinically, the dogs show depression, blindness, ataxia, and change in temperament from nerve damage.[3] Microscopically, the tumor cells have small, round, hyperchromatic nuclei with poorly stained cytoplasm. A perinuclear halo effect is common with delayed fixation which results in the artifactual but characteristically described "honeycomb" cell pattern.[1] Other important characteristics include pronounced branching capillary proliferation forming a delicate vascular "chicken-wire" pattern [2] and the formation of vascular loops or glomerular-like tufts often arranged in

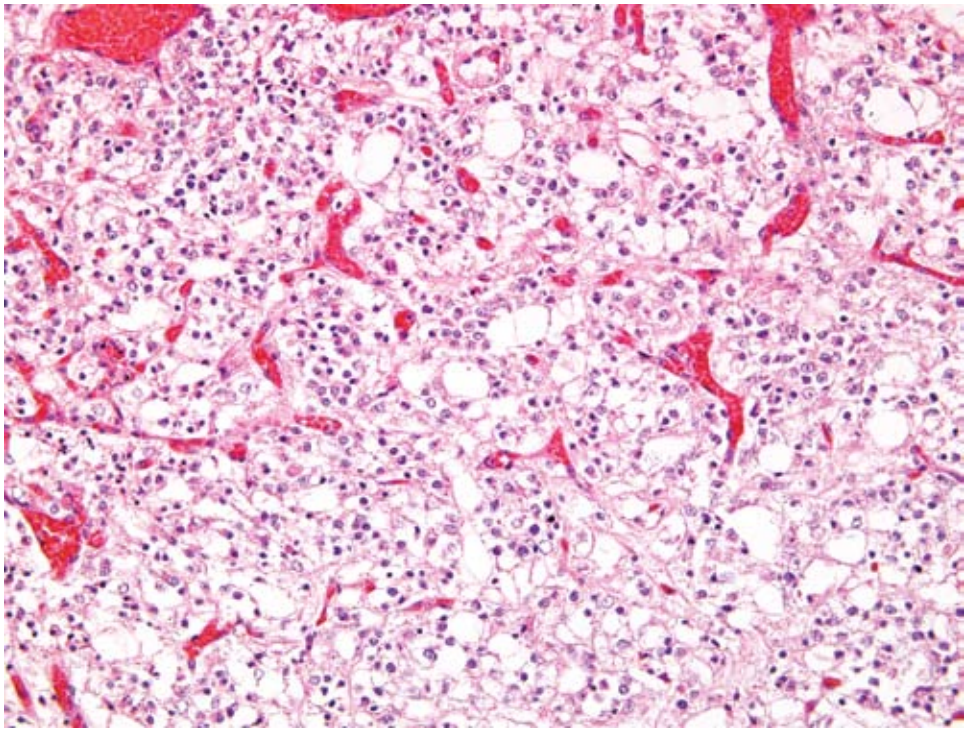

*2-3. Cerebrum, dog. Anaplastic oligodendroglioma. Multifocally, there is pronounced branching vascular proliferation. (HE 200X)*

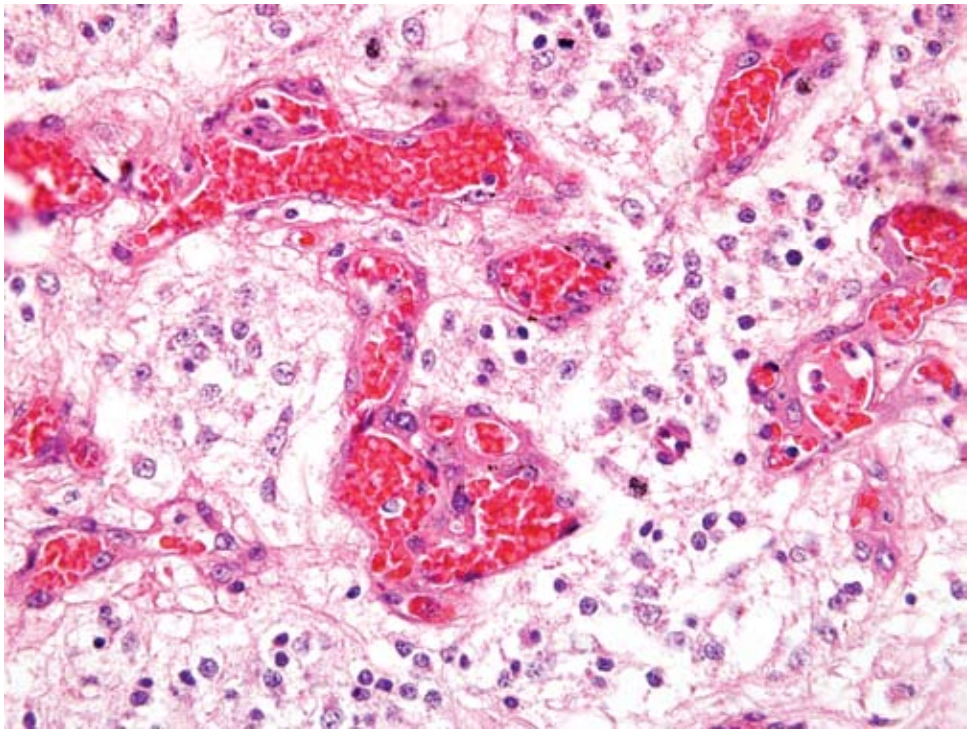

*2-4. Cerebrum, dog. Anaplastic oligodendroglioma. Occasionally, vascular proliferation have 'glomeruloid' morphology. (HE 400X)*

long lines or clusters, at the margins of or throughout the tumor.[1] Mucinous cystic degeneration and multifocal mineralization sometimes occur.[1,3] Other glial cells such as astrocytes and transitional forms between astrocytes and oligodendrocytes may be present in varying numbers.[2]

There are no antibodies for specific markers for oligodendrogliomas that have been formalin fixed and paraffin embedded.[1] The results of immunohistochemical staining of canine oligodendroglioma with antibody against myelin basic protein are generally negative. Many oligodendrogliomas show a mixture with GFAP-positive astroglial cells. The interpretation of the finding is controversial whether the astrocytes indicate a capacity for immature oligodendrocytes to express astrocytic differentiation or reactive astrocytes.[3]

In our case, the neoplasm was considered to be anaplastic due to the findings of high cellularity in some areas, frequent mitotic figures, nuclear pleomorphism, prominent proliferation of glomeruloid vascular tufts, and extensive necrosis. Anaplastic (malignant) oligodendroglioma and astrocytoma share several histomorphological features, including high cellularity, necrosis, high mitotic rate, and prominent proliferation of glomeruloid vessels; thus, distinguishing between these two glial neoplasms may be difficult.[2] In addition, the presence of intermingled astrocytic cells is common in anaplastic oligodendrogliomas and may further complicate the histologic picture. However, the presence of several distinguishing features in the tumor cells such as round, hyperchromatic nuclei surrounded by small amounts of clear to lightly stained cytoplasm, and distinct cell borders, as well as the branching capillary proliferation, support the diagnosis of oligodendroglioma in this case.

**AFIP Diagnosis:** Cerebrum: Oligodendroglioma, anaplastic

**Conference Comment:** Oligodendrogliomas have been reported in several animal species including dogs, cats, horses, and cattle. Grossly, these tumors are generally well demarcated, gray, grey-pink or pink -red, soft, gelatinous and may have cystic foci.[3,5] Necrosis and hemorrhage are uncommonly present.

The differential diagnosis discussed during the conference included oligoastrocytoma and neurocytoma.

Oligoastrocytomas (mixed gliomas) are glial neoplasms with astrocytes and oligodendroglial cells either intermingled or separated into distinct groups of cells.[4] When the cell populations are distinct, the diagnosis is uncomplicated. When the two cell populations are intermixed, at least 25% of the cells must be astrocytes to be classified as an oligoastrocytoma.[4] Tumors with less than this threshold of astrocytes are considered anaplastic oligodendrogliomas with reactive astrocytes.[4] Interpretation of the histogenesis of intratumoral cells can be complicated by the presence of minigemistocytes (gliofibrillary oligodendrocytes) which are neoplastic cells with round, oligodendroglial-type nuclei and GFAP-positive, eccentric eosinophilic cytoplasm.

The first reported case of a neurocytoma in domestic animals involved the spinal cord of a dog and was published in 2008.[2] Neurocytomas stain strongly positive for synaptophysin allowing differentiation from oligodendrogliomas.[3]

**Contributing Institution:** Departamento de Patología, Facultad de Medicina Veterinaria y Zootecnia, Universidad Nacional Autónoma de México, Circuito Exterior, Ciudad Universitaria, Delegación Coyoacán, MEXICO, D.F. 04510. http://www.fmvz.unam.mx

**References:**

1. Burger PC, Scheithauer BW: Tumors of neuroglia and choroid plexus. *In:* AFIP Atlas of Tumor Pathology, Series 4, Tumors of the Central Nervous System, ed. Silverberg SG, Sobin LH, Series 4, Fascicle 7, pp. 225-233, ARP Press, Washington, DC, 2007
2. Huisinga M, Henrich M, Frese K, Burkhardt, Kuchelmeister K, Schmidt M, Reinacher M: Extraventricular neurocytoma of the spinal cord in a dog. Vet Pathol 45:63-66, 2008
3. Koestner A, Higgins RJ: Tumors of the nervous system. *In:* Tumors in Domestic Animals, ed. Meuten DJ, 4th ed., pp. 703-706. Iowa State Press, Ames, Iowa, 2002
4. Koestner A, Bilzer T, Fatzer R, Schulman FY, Summers, BA, Van Winkle TJ: Histological classification of tumors of the nervous system of domestic animals. *In:* World Health Organization Histological Classification of Tumors of Domestic Animals, ed. Schulman FY, 2nd series, vol. 5, pp. 18-21, Armed Forces Institute of Pathology, Washington DC, 1999
5. Maxie MG, Youssef S: Nervous system. *In:* Jubb, Kennedy and Palmer's Pathology of Domestic Animals, ed. Maxie MG, 5th ed., vol 1, pp. 446-448. Elsevier Limited, Philadelphia, PA, 2007
6. Summers BA, Cummings JF, de Lahunta A: Tumors of the central nervous system. In: Veterinary Neuropathology, Summers BA, Cummings JF, de Lahunta A, eds., pp. 370-373, Mosby, St. Louis, MO, 1995

## CASE III – AFIP 08 CASE 1 (AFIP 3115317)

**Signalment:** Domestic feline, less than 1 yr. of age (*Felis domesticus*)

**History:** Euthanized because of non-responsive weight loss, generalized poor condition.

**Gross Pathology:** Not available.

**Laboratory Results:** Not performed

**Histopathologic Description:** Two sections of kidney are on the slide. Evident at the low magnification are an irregular cortex and multiple basophilic areas that comprise approximately 20 – 30% of each of the sections with some sections having up to 50% involvement. The irregular serosa has multifocal areas of predominantly plasma cell infiltrates with scattered areas of mixed inflammatory cells and fibrosis. The basophilic areas localized to the cortical regions consist of inflammatory cells infiltrates, which vary in composition. Some areas consist of primarily plasma cells, some areas are mixtures of plasma cells with neutrophils and macrophages, and there are areas of granulomatous inflammation with confluent infiltrates of macrophages **(Fig. 3-1)**. The infiltrates separate relatively normal tubules in some areas, while in other areas there is tubular degeneration and necrosis **(Fig. 3-2)**, and the inflammation has replaced the renal parenchyma with fibrosis. There is one focus of necrosis approximately 1- 2 mm in diameter that is occupied with hemorrhage and fibrin. Multiple glomeruli in the affected areas have hypertrophied parietal epithelium, but glomeruli in the non-involved regions are normal in appearance.

Other changes consist of occasional scattered minor proteinaceous tubular casts and diffuse moderate vacuolation of the tubular epithelium consistent with lipid accumulation that was considered excessive for the feline species and suggestive of perhaps a metabolic abnormality in addition to the obvious inflammatory disease process.

**Contributor's Morphologic Diagnosis:** Moderate bilateral multifocal mixed cell to granulomatous inflammation, kidney

**Contributor's Comment:** Signalment (age) and morphologic changes were consistent with feline infectious peritonitis.[2,6]

**AFIP Diagnosis:** Kidney: Nephritis and phlebitis, granulomatous, necrotizing, chronic, multifocal, severe, with multifocal mild tubular degeneration, necrosis, and regeneration

**Conference Comment:** Feline infectious peritonitis (FIP) is caused by feline coronavirus (FCoV), an enveloped, positive-stranded, RNA virus.[1] Cats that develop FIP are usually less than two years of age and come from a multi-cat environment.[2]

FCoV is spread via fecal-oral transmission, and the

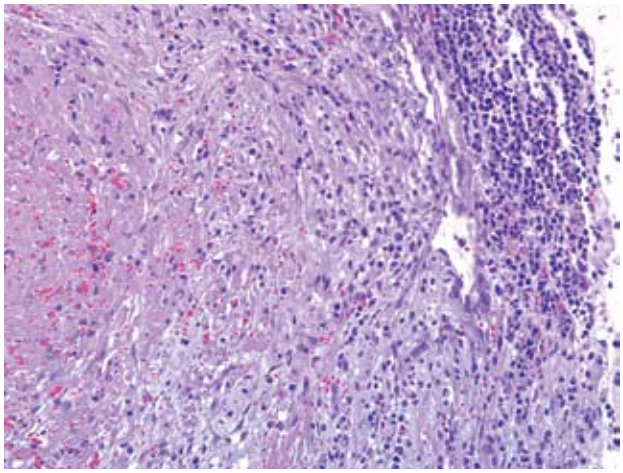

*3-1. Kidney, cat. Multifocally within the cortex and medulla, there is phlebitis, characterized by loss of endothelium and vascular tunics and replacement by necrotic debris, macrophages, fibroblasts, and variable numbers of plasma cells. Vessel lumens often contain fibrin thrombi. (HE 200X)*

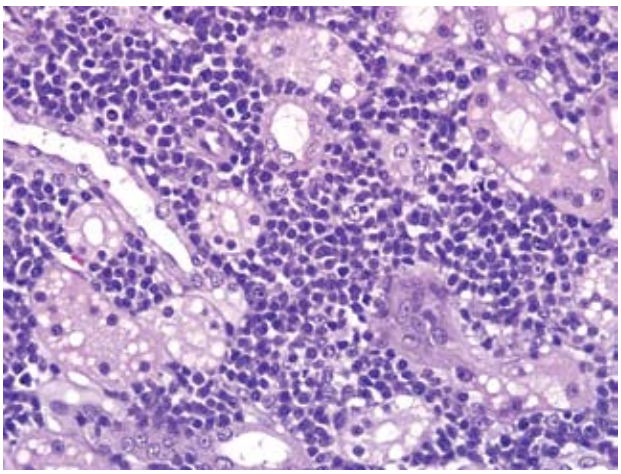

*3-2. Kidney, cat. Multifocally, the interstitium is expanded by large numbers of plasma cells and fewer lymphocytes and macrophages. Multifocally, tubular epithelium is attenuated or regenerative. (HE 400X)*

prevalence of coronavirus infection is high but the number of clinical cases of FIP is low.[1,7] The most commonly accepted theory for this peculiar finding is that FCoV undergoes a mutation and acquires virulence factors by deletions in open reading frames 3 and 7 to cause FIP.[7] Recent studies also strongly suggest that monocytes not only disseminate the virus, but also mediate the development of phlebitis associated with FIP.[7]

A strong cell mediated immune response is essential for protection against developing FIP.[1,2] Two forms of FIP, wet and dry, are generally referred to when describing FIP. If a weak cell-mediated immunity is mounted, the virus can persist in macrophages for months causing release of a variety of inflammatory mediators leading to perivascular pyogranulomatous inflammation in affected organs. This is the dry form. The wet or effusive form occurs when no cell mediated immunity is present and continued viral replication leads to the production of large quantities of non-neutralizing antibodies and immune complex deposition.[1,2]

Peritonitis is common in both the dry and wet forms. In the effusive form, copious amounts of flocculent yellow exudate may be found in the abdominal cavity, and serosal surfaces are often covered with fibrin.[1,2] Pyogranulomas are commonly found in the kidney, uvea, and peritoneum. Cervical and thoracic lymph nodes are often enlarged, and hydrocephalus is often found in cats with neurologic symptoms.[2] The classic histologic lesion of FIP is phlebitis with circumferential rings of pyogranulomatous inflammation.[2] Immunohiostochemical detection of coronavirus antigen in macrophages can be used to confirm a diagnosis of FIP.

A recent report associated FIP with papular cutaneous lesions [4] and fatal systemic coronavirus infections have recently been reported in ferrets [5] and dogs.[3]

**Contributing Institution:** Wyeth Research, 641 Ridge Rd, Chazy, NY

**References:**

1. Addie DD, Oswald J: Feline coronavirus infections. *In:* Infectious Diseases of the Dog and Cat, ed. Greene CE, 3rd ed., pp. 88-104. W.B. Saunders Elsevier, St. Louis, MO, 2006
2. Brown C, Baker D, Barker I: Alimentary System. *In:* Jubb Kennedy and Palmer's Pathology of Domestic Animals, Vol. 2, ed. Maxie M. 5th ed., pp. 1-296. Saunders Elsevier, New York, NY, 2007
3. Buonavoglia C, Decaro N, Martella V, Elia G, Campolo M, Desario C, Castagnaro M, Tempesta M: Canine coronavirus highly pathogenic for dogs. Emerg Infect Dis **12**(3):492-494, 2006
4. Declercq J, De Bosschere H, Schwarzkopk I, Declercq L: Papular cutaneous lesion in a cat associated with feline infectious peritonitis. Vet Dermatol **19**(5):255-8, 2008
5. Garner MM, Ramsell K, Morera N, Juan-Salles C, Jimenez J, Ardiaca M, Montesinos A, Tefke JP, Lohr CV, Evermann JF, Baszler TV, Nordhausen RW, Wise AG, Maes RK, Kiupel M: Clinicopathologic features of a systemic coronavirus-associated disease resembling feline infectious peritonitis in the domestic ferret (Mustela putorius). Vet Pathol **45**:236-246, 2008
6. Maxie M and Newman S: Urinary system. *In:* Jubb, Kennedy, and Palmer's Pathology of Domestic Animals. ed. Maxie M, vol. 2, 5th ed., pp. 425-522. Saunders Elsevier, New York, NY, 2007
7. Kipar A, May H, Menger S, Weber M, Leukert W, Reinacher M: Morphologic features and development of granulomatous vasculitis in feline infectious peritonitis. Vet Pathol **42**(3)21-330, 2005

## CASE IV – 08N0486 (AFIP 3102517)

**Signalment:** 10-year-old, female, mixed Labrador retriever, (Canis familiaris)

**History:** The dog was presented for evaluation of decreased mobility of 3 weeks duration culminating in intermittent tetraparesis. On neurological examination the dog had severe ataxia, was able to stand with support, but would knuckle in all limbs and was most weak on the right thoracic limb, which had noticeable biceps and triceps muscle atrophy. Decreased withdrawal was observed in the right thoracic limb. Conscious proprioceptive deficits were present in all four limbs. There was severe pain on cervical palpation or manipulation. With magnetic resonance neuroimaging, axial slices from cervical cord segments C1 to C3 detected a well defined dural-based mass in the right dorsal lateral aspect of the spinal canal cranial to C2, causing severe compression and displacement of the spinal cord ventrally and to the left. The mass caused focal dilatation of the subarachnoid space at C2. The mass was isointense and hyperintense on T1 and T2 weighted images respectively. There was homogeneous intense contrast enhancement of the mass. From a surgical biopsy of the mass a diagnosis of chordoid meningioma was made and the dog was euthanized at the owners' request seven days later due to a poor prognosis.

**Gross Pathology:** On the right dorsolateral aspect of C2, a grayish, smooth, gelatinous, partly translucent, poorly demarcated intradural mass measuring 1.5 cm x 1 cm x 0.5

cm was firmly attached to the dura mater. On transverse section the mass had indistinct borders and compressed the spinal cord to the left and ventrally **(Fig. 4-1)**.

**Laboratory Results:** None

**Histopathologic Description:** On histological exam of transverse sections of the spinal mass an intradural, extraparenchymal, well-demarcated tumor was on the right dorsal aspect of the spinal cord, causing severe displacement of the cord ventrally and to the left. The tumor was organized in a pattern of trabeculae, clusters, or columns of cells in a basophilic mucinous matrix**(Fig. 4-2)**. The cells were uniformly polygonal with an abundant eosinophilic cytoplasm, with a round to oval nucleus and sometimes with a prominent nucleolus and had a well-defined cytoplasmic border. Mitotic figures were rare. At the periphery of the mass were prominent blood vessels while intratumorally there were multifocal inflammatory cell infiltrates of predominant lymphocytes. One dorsal nerve root fascicle was invaded by neoplastic cells. On the lateral aspect of the cord, there was also extensive hemorrhage and fibrin deposition in addition to an amorphous basophilic foreign material consistent with surgical gelfoam associated with the previous biopsy site. The white matter of the spinal cord, compressed by and adjacent to the tumor, had multifocal sites of axon spheroids, axonal necrosis, demyelination and macrophages. The neoplastic cells were uniformly strongly immunoreactive for vimentin and focal subpopulations of cells (about 15% total) were immunoreactive for cytokeratins using a low and high molecular weight antibody cocktail (Lu5, Biocare Medical). The proliferative index, assessed by MIB1 immunoreactivity, was approximately 1%.

**Contributor's Morphologic Diagnosis:** Spinal Cord (Segments C2-3): Chordoid Meningioma

**Contributor's Comment:** This tumor was classified histologically as a chordoid meningioma based on location, morphology and immunohistochemistry and using criteria from the latest update of the human WHO classification of tumors of the central nervous system.[5] Although this tumor was relatively benign cytologically, in humans chordoid meningiomas are graded as atypical (WHO Grade II) based on the high incidence of post surgical recurrence.[2,5] Certainly the invasive nature of this tumor within nerve roots fascicles would support this grade. Classification of canine meningiomas using the human WHO classification into one of three histological grades (benign, atypical, anaplastic) using carefully defined and clinically tested criteria in humans may also be useful for predicting clinical behavior and outcome in dogs.[6,8]

In dogs spinal cord chordoid meningiomas have been reported with a predilection site in the cervical region as in this case; [6,8] however, in another series of canine meningiomas this type occurred in the forebrain.[1] Confusingly, these tumors have been classified for unknown reasons as myxoid meningiomas in the veterinary literature. The chordoid type is a histological variant of meningioma, defined histologically by cords or trabeculae of polygonal cells with an eosinophilic cytoplasm in an abundant basophilic mucinous matrix. Chronic inflammatory cell infiltrates may be prominent as in this case.[2,5] In humans this chordoid pattern is not an uncommon focal pattern in atypical or aggressive meningiomas, however it is rare in pure form.[2] Meningiomas in people and dogs are uniform and strongly immunoreactive for vimentin and

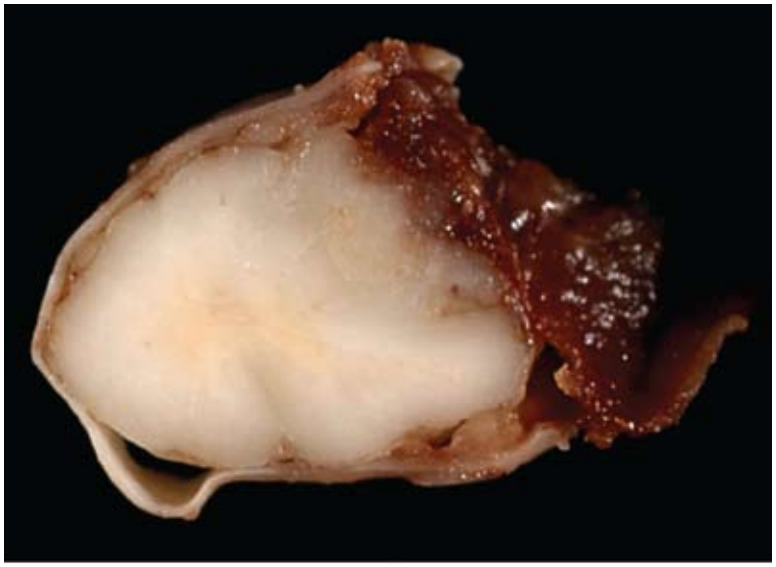

*4-1. Spinal cord, dog. Chordoid meningioma. The gray, gelatinous neoplasm compresses and distorts the contour of the spinal cord. There is an adjacent area of hemorrhage possibly associated with a previous biopsy procedure.* *Photograph courtesy of University of California, Davis, Veterinary Medical Teaching Hospital VM3A, Anatomic Pathology, 1 Garrod Drive, Davis, CA 95616 http://www.vetmed.ucdavis.edu/pmi/*

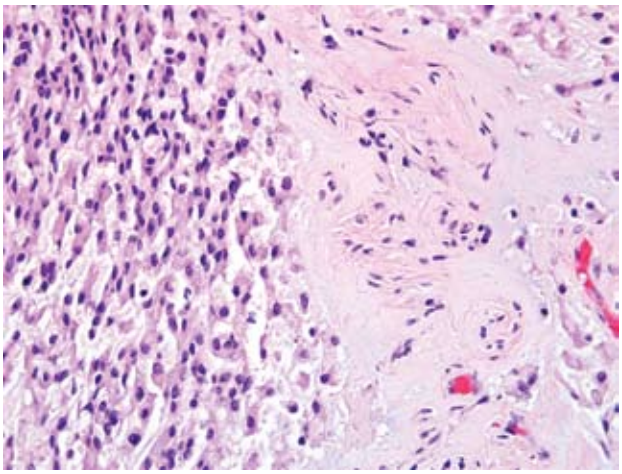

*4-2. Spinal cord, dog. Chordoid meningioma. Trabeculae of neoplastic cells are often surrounded by an amphophilic to lightly basophilic mucinous matrix. (HE 400X)*

subpopulations of cells are variably immunoreactive for pancytokeratins.[1,2,5,9] Many human meningiomas are immunoreactive for epithelial membrane antigen and this is therefore a useful diagnostic feature, but unfortunately this epitope is not expressed in the dog.

The differential diagnoses for chordoid meningiomas include: chordoma, myxoid chondrosarcoma, and metastatic carcinoma. Chordomas arise from the axial skeleton, have characteristic fibrous lobularity, the hallmark physaliphorous cells and are strongly uniformly immunoreactive for low-molecular-weight cytokeratin. Myxoid chondrosarcomas do not exhibit immunoreactivity for keratin. Chordoid meningiomas lack the anaplasia of metastatic carcinomas. [2]

**AFIP Diagnosis:** Cervical spinal cord, meninges: Meningioma, chordoid (myxoid) with focal hemorrhage and surgical gel

**Conference Comment:** Meningiomas are derived from meningothelial cells of the arachnoid membrane.[4] Meningiomas tend to be discrete, well-demarcated tumors with a broad attachment to the meninges.[4] They rarely metastasize.[7]

There are nine meningioma subtypes listed in the second series of the WHO International Histological Classification of Tumors of Domestic Animals: meningotheliomatous, fibrous, transitional, psammomatous, angiomatous, papillary, granular cell, myxoid, and anaplastic.[3] The myxoid variant is comparable to the chordoid variant as seen in humans. As one of the aims of the WHO International Histological Classification of Tumors in Domestic Animals was to follow the WHO histological classification for human tumors as closely as possible to facilitate communication between pathologists, diagnosticians and researchers, perhaps the chordoid terminology should have been used.

In a recent publication, canine meningiomas were divided into histologic grades according to the WHO classification used for human meningiomas. 56% of canine meningiomas were grade I, 43% were grade II and 1% were grade III, as compared to 80% grade I, 8% grade II and <3% grade III meningiomas reported in humans.[8] The biological significance of these differences is not known.

**Contributing Institution:** University of California, Davis, Veterinary Medical Teaching Hospital
VM3A, Anatomic Pathology, 1 Garrod Drive, Davis, CA 95616
http://www.vetmed.ucdavis.edu/pmi/

**References:**

1. Barnhart KF, Wojcieszyn J, Storts RW: Immunohistochemical staining patterns of canine meningiomas and correlation with published immunophenotypes. Vet Pathol **39**:311-312, 2002
2. Burger PC et al: Surgical Pathology of the Nervous System and its Coverings, 4th ed., pp. 59-61. Churchill Livingstone, New York, NY, 2002
3. Koestner A, Bilzer T, Fatzer R, Schulman FY, Summers BA, Van Winkle TJ: Histological classification of tumors of the nervous system of domestic animals. *In:* World Health Organization Histological Classification of Tumors of Domestic Animals, ed. Schulman FY, Second Series, vol 5, pp. 27-29. Armed Forces Institute of Pathology, Washington, DC, 1999
4. Koestner A, Higgins RJ: Tumors of the nervous system. *In:* Tumors in Domestic Animals, ed. Meuten DJ, 4th ed., pp. 703-706. Iowa State Press, Ames, Iowa, 2002
5. Louis DN, Ohgaki H, Wiestler OD, Cavenee WK, Burger PC, Jouvet A, Scheithauer BW, Kleihues P: The 2007 WHO classification of tumours of the central nervous system. Acta Neuropath **114**(2):164-172, 2007
6. Petersen SA et al: Canine intraspinal meningiomas: imaging features, histopathologic classification, and long-term outcome in 34 dogs. J Vet Intern Med **22**(4):946-53, 2008
7. Schulman FY, Ribas JL, Carpenter JL, Sisson AF, LeCouteur RA: Intracranial meningioma with pulmonary metastasis in three dogs. Vet Pathol **29**:196-202, 1992
8. Sturges BK et al. Magnetic resonance imaging and histological classification of intracranial meningiomas in 112 dogs. J Vet Intern Med **22**:586-595, 2008
9. Van Winkle TJ, et al: Myxoid meningiomas of the rostral cervical spinal cord and caudas fossa in four dogs. Vet Pathol **31**:468-471, 1994

**NOTES:**

The Armed Forces Institute of Pathology
Department of Veterinary Pathology

*Conference Coordinator:*
Todd M. Bell, DVM

WEDNESDAY SLIDE CONFERENCE 2008-2009

# Conference 21

1 April 2009

***Conference Moderator:***

**Dr. Steven Weisbrode, VMD, DACVP, PhD**

## CASE I – 07-1829 (AFIP 3106281)

**Signalment:** 6-week-old female mixed breed horse

**History:** Five day history of lameness of right rear leg. Radiographic findings were interpreted to represent septic arthritis of the right coxofemoral joint.

**Gross Pathology:** The foal was in good post mortem condition and had a body condition score of 3/5. Approximately 50% of the cartilage of the right femoral head was ulcerated. On cross section, the subchondral bone underlying the ulcerated articular cartilage was white for a distance of up to 2 mm from the surface. The dorsolateral aspect of the right femoral head had a large cartilage flap that was attached at the margins of the articular surface, and the ventrolateral aspect of the right femoral head had a 4 cm long fissure within articular cartilage that remained attached to subchondral bone. The dorsal region of the acetabular cartilage was irregular with exposure of subchondral bone (ulceration). The right medial trochlear ridge had 2 cm focus of articular cartilage that extended 1 cm into subchondral bone (found on cutting in a horizontal plane using a band saw). The contralateral coxofemoral joint, stifle joint, and both humeral joints were examined and found to be within normal limits.

**Laboratory Results:** None

**Histopathologic Description:** Medial trochlear ridge of the right femur: There is a rectangular area of epiphyseal growth cartilage (AE complex) which extends deeper into the epiphysis (retained cartilage) compared with the adjacent cartilage **(Fig. 1-1).** The deep edge of this retained cartilage has cartilage cores present indicating active cartilage mineralization and vascular invasion as seen in endochondral ossification. The chondrocytes in this retained cartilage and the chondrocytes contiguous within its overlying growth cartilage have eosinophilic chondrocytes interpreted as chondrocyte coagulation necrosis compared with chondrocytes not associated with the retained region. In the overlying epiphyseal cartilage, in addition to chondrocyte coagulation necrosis, is a focus of loss of basophilia of the cartilage matrix (loss of proteoglycan staining). The blood vessels in the cartilage canals within this region of proteoglycan loss appear normal, but the contents of some of the cartilage canals in the contiguous growth cartilage with dead chondrocytes appear necrotic compared with contents of cartilage canals in adjacent cartilage with viable chondrocytes

*Sponsored by the American Veterinary Medical Association, the American College of Veterinary Pathologists, and the C. L. Davis Foundation.

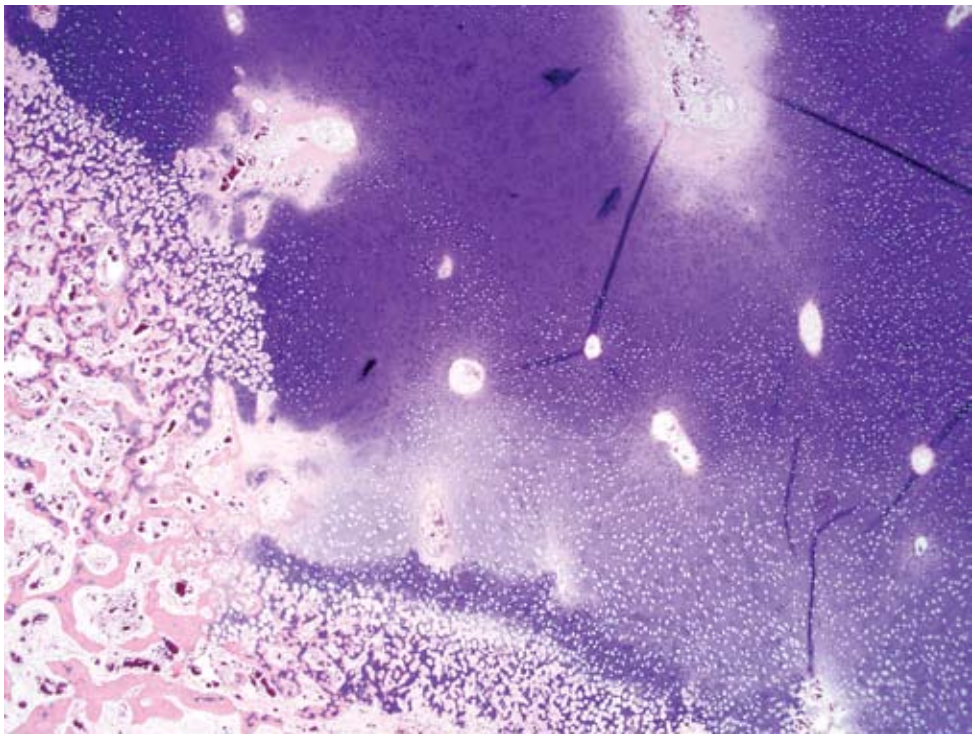

*1-1. Articular cartilage, horse. There is a focally extensive area of epiphyseal growth cartilage which is retained to a greater depth within the epiphysis compared to adjacent cartilage. Multifocally, particularly surrounding cartilage canals, there is a loss of basophilia within the cartilage matrix interpreted as loss of proteoglycan staining. (HE 20X)*

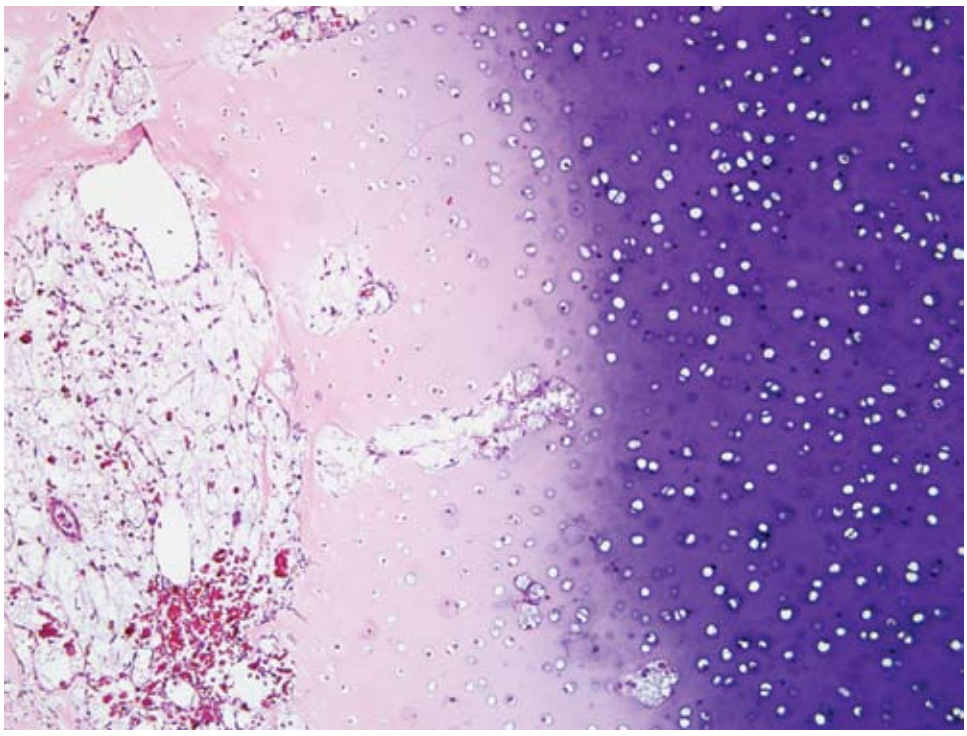

*1-2. Articular cartilage, horse. Multifocally, there is chondrocyte necrosis within retained cartilage and overlying growth cartilage. (HE 100X)*

**(Fig. 1-2)**. The primary trabeculae deep to the area of retained cartilage are course and occasionally fractured. In most of these trabeculae the bone is dead (karyolytic osteocytes) often with overlying viable woven bone. There is mild to moderate reactive fibrosis in the marrow in this region.

**Contributor's Morphologic Diagnosis:** Focal chondronecrosis and retention (delayed endochondral ossification) of growth cartilage of the articular epiphyseal complex with osteonecrosis and infraction of subjacent trabeculae and associated marrow fibrosis

**Contributor's Comment:** This lesion represents articular epiphyseal complex dysplasia of osteochondrosis. This lesion likely was not clinically significant. The clinical signs in this case were attributed to the lesions in the femoral head which, after microscopic examination, were interpreted to be sequelae to suppurative osteomyelitis. The lesions in the distal femur were found on gross examination of sawed sections to check for foci of osteochondrosis.

Using terminology suggested in recent literature, the lesion in the distal femur is a good example of chondrocyte coagulation necrosis in both a focus of osteochondrosis latens and osteochondrosis manifesta.[3] Often the chondrocyte coagulation necrosis is limited to the focus of osteochondrosis latens and it is hypothesized that this necrosis is secondary to ischemia and might be the initiating lesion of osteochondrosis. In the foal as in other species, it has been suggested that this cartilage necrosis is secondary to necrosis of blood vessels in the cartilage canals of growth cartilage.[1] Interesting in this lesion is the presence of cartilage cores at the deep margin of the retained cartilage. This indicates cartilage mineralization and vascular invasion are taking place. This is not usually found in lesions of osteochondrosis manifesta. Osteochondrosis manifesta lesions are known to be able to resolve [2]; therefore active endochondral ossification might represent attempts to resolve the lesion. The abnormal modeling, fractures and marrow fibrosis are presumed secondary to the altered endochondral ossification secondary to the osteochondrosis. The cause of the bone necrosis is uncertain but might be secondary to ischemia in this region due to fibrosis and fractures.

**AFIP Diagnosis:** Bone: Articular epiphyseal complex dysplasia, chronic, focally extensive, severe with osteonecrosis and infraction of subjacent trabeculae and marrow fibrosis

**Conference Comment:** Osteochondrosis is an extremely important joint disorder of multiple species including pigs, horses, large breed dogs, cattle, sheep, and deer.[2] By definition, osteochondrosis is a focal disturbance of endochondral ossification.[3] The exact pathogenesis of osteochondrosis is unclear, but the most likely explanation is focal ischemic necrosis of growth cartilage precipitated by necrosis of cartilage canal blood vessels.[3] Synonyms for osteochondrosis include osteochondrosis dissecans and osteochondritis dissecans.[2] In domestic animals osteochondrosis often leads to degenerative joint disease and lameness in affected animals.[2]

As mentioned by the contributor, a recent article has suggested new terminology adding modifiers to osteochondrosis. Osteochondrosis latens is defined as a lesion confined to the epiphyseal cartilage; osteochondrosis manifesta is a lesion resulting in delayed endochondral ossification that is visible on macroscopic and radiographic examination; osteochondrosis dissecans is the name of the lesion formed when a crack or fissure forms in an area of necrotic cartilage that extends up to the articular cartilage.[3]

**Contributing Institution:** Department of Veterinary Biosciences, The Ohio State University, Columbus, Ohio 43220, http://vet.osu.edu/biosciences.htm

**References:**

1. Olstad K, Ytrehus B, Ekman S, Carlson CS, Dolvik NI: Early lesions of osteochondrosis in the distal tibia of foals. J Orthop Res. **25**(8):1094-105, 2007
2. Thompson K. Diseases of Bones and Joints. *In:* Pathology of Domestic Animals, vol. 1, ed. Maxie G, 5th ed., pp. 136-145. WB Saunders, Edinburgh, Scotland, 2007
3. Ytrehus B, Carlson CS, Ekman S: Etiology and pathogenesis of osteochondrosis. Vet Pathol **44**:429-448, 2007

## CASE II – APO7-2888 (AFIP 3103608)

**Signalment:** Seven-month-old, intact female Pomeranian, canine (*Canis familiaris*)

**History:** The patient presented to the referring veterinarian at two months of age with generalized non-pruritic alopecia and tiring during play with littermates. Skin scrape was negative and the alopecia cleared with no treatment by five months of age. At that time a physical exam revealed bowing of the forelegs and thickened

distal radial growth plates. Serum biochemistry revealed hypocalcemia and vitamin D and calcium supplementation was initiated approximately one week later. Despite increasing Calcitriol and $CaCO_3$ treatment over the next few months (see table below), the patient became increasingly weaker and developed muscle tremors and seizure activity. The patient was transported to the NCSU College of Veterinary Medicine on November 29, 2007 with rigid extension of forelegs and neck and muscle tremors. Her total calcium on presentation was 5.6 mg/dL. Radiographs revealed generalized osteopenia, as well as flaring of the distal ulnar and radial physis and marginated zones of increased lucency with adjacent bands of bone sclerosis **(Fig. 2-1)**. A vertebral body fracture of T11 with cord compression was also detected. Deep pain sensation was absent in both rear limbs and the tail; euthanasia was elected. All other littermates were normal.

**Gross Pathology:** A retained upper right canine tooth is present and many other teeth appear immature (mixture of deciduous and permanent teeth). The gingiva is diffusely enlarged and swollen and all teeth are easily moveable. All costochondral junctions are enlarged approximately three times normal size, forming what is commonly referred to as a "rachitic rosary" **(Fig. 2-2)**. A small round hard nodule (0.5 cm) is present in the middle of the left eighth rib (fracture callus). All ribs bend and break easily on manipulation and are readily cut with a knife. T12 vertebra is displaced dorsally but no abnormal movement is noted between T11 and T12. Two bony nodules are present on either side of the dorsal spinous processes overlying the dorsally displaced T12 vertebral body (fracture calluses). The brain and parathyroid glands are grossly normal.

**Laboratory Results:**

Calcium and Parathyroid Hormone Levels with Initiation of Treatment

| Date | Treatment | | Calcium Blood Level (RR 8.6-11.8 mg/dL) | Parathyroid Hormone Level (RR 27-155 pg/mL) |
|---|---|---|---|---|
| | Calcitriol (ng/day) | CaCO3 (mg/day) | | |
| 8-17-07 | N/A | N/A | 5.6 | 782.1 |
| 8-25-07 | 150 | 100 | - | - |
| 9-15-07 | 200 | 250 | 6.0 | - |
| 9-20-07 | 250 | 250 | 5.1 | - |
| 10-1-07 | 350 | 250 | 4.9 | - |
| 10-20-07 | 400 | 300 | 5.7 | 863.8 |

**Histopathologic Description:** Bone, radius: Within the physis, disarray and disorganization (absence of orderly longitudinal columnar alignment) are present throughout the zone of proliferation while the zone of hypertrophy is markedly reduced to segmentally absent **(Fig. 2-3)**. Several infoldings of cartilage are present that extend below the physis into the metaphysis. Within the primary spongiosa increased numbers of osteoclasts **(Fig. 2-4)** surround trabeculae while osteoblasts lining trabeculae are rare. Many trabeculae are surrounded by a broad band of unmineralized osteoid (wide osteoid seams). Wispy fibrous connective tissue is present between trabeculae in the primary spongiosa (fibrosis). Bony trabeculae within the secondary spongiosa are sparse and thin and do not form anastomoses with other trabeculae.

**Contributor's Morphologic Diagnosis:** Radius: Failure of endochondral ossification (vitamin D-resistant rickets, Type II)

**Comment:** Rickets is a defect in mineralization of growing bones due to a lack of vitamin D activity. In

*2-1. Distal radius and ulna, dog. There is flaring of the distal ulnar and radial physes and zones of increased epiphyseal lucency with adjacent bands of sclerosis.* *Radiograph courtesy of NCSU College of Veterinary Medicine, 4700 Hillsborough Street, Raleigh, NC 27606.*

*2-2. Thorax, dog. Diffusely, costochondral junctions are enlarged up to three times normal.* *Photograph courtesy of NCSU College of Veterinary Medicine, 4700 Hillsborough Street, Raleigh, NC 27606.*

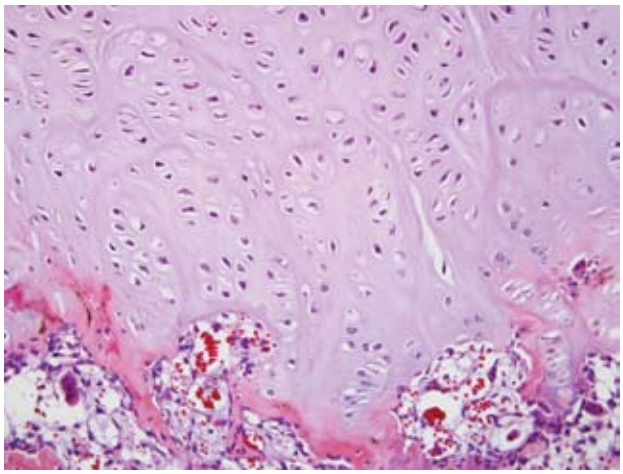

*2-3. Bone, dog. Multifocally within the physis, there is a lack of regimentation and organization of chrondrocytes within the zone of proliferation, and the zone of hypertrophy is either absent or reduced. (HE 200X)*

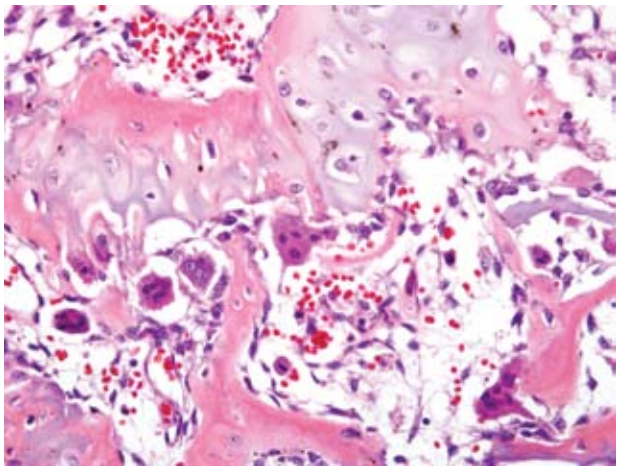

*2-4. Bone, dog. Multifocally within the primary spongiosa, there are moderately increased numbers of osteoclasts, and there is moderate fibrosis between the trabeculae. (HE 400X)*

most species vitamin D is obtained primarily through the diet and metabolized in the liver. It is converted into its active form in the kidney. Low vitamin D activity leads to hypocalcemia and secondary hyperparathyroidism. This hyperparathyroidism causes mineral loss, especially calcium from bone. Rickets occurs when these changes take place during growth.

Two main forms of vitamin D-resistant rickets are characterized in humans. Type I is an inborn error in conversion of 25-(OH)$D_3$ to 1,25$(OH)_2D_3$ due to a deficiency of the renal 1-hydroxylase enzyme. This condition responds to large doses of vitamin $D_2$ and $D_3$. Vitamin D-resistant rickets Type II (VDRR II) in humans is an end organ resistance to 1,25$(OH)_2D_3$ due to an autosomal recessive congenital defect in the vitamin D receptor (VDR) or a site distal to it. This type of rickets has been reported in a few cats, [4,5,6] but has never before been reported in a canine. In one of the feline cases the cat had signs of hypocalcemia, including muscle tremors, similar to the clinical signs in this canine patient.[5] Two other cats had similar radiologic changes of the radius and ulna, as in the present case, as well as similar costochondral junction changes.[4,6] Similarly these cases had no response to high levels of vitamin D or calcium supplementation; [4,6] however, in two of the cases, the cats became normal after physeal closure.[4,5]

Three main intracellular defects have been identified in human cases of VDRR II:

1. Hormone binding defects including decreased number of sites, decreased binding affinity, or complete absence of binding.
2. Deficient nuclear localization – in these cases there is normal binding affinity and capacity, but unmeasurable localization to the nucleus.
3. A post-receptor defect characterized by normal receptors but deficiency in the induction of the 25-(OH)D-24 hydroxylase enzyme in response to 1,25$(OH)_2D$.[3]

Defects can be detected using in vitro assessment of VDR binding or the subsequent cellular response to VDR binding by 1,25 dihydroxycholecalciferol (1,25-$(OH)_2D$) in cells, typically fibroblasts cultured from skin biopsies, derived from individuals affected by clinical signs of VDRR II and compared with normal controls.[4] A diagnosis of VDRR II was made in the present case based on clinical signs, radiographic findings, biochemistry, parathyroid levels, and the inability of fibroblasts from the skin of the dog to bind 1,25-$(OH)_2D$. A vitamin D receptor defect was verified through genetic testing on cultured fibroblasts from this dog at Stanford University, confirming the diagnosis of VDRR II in this patient.

This patient also presented with generalized alopecia, as is the case in approximately 50% of human cases of VDRR II.[3] Keratinocytes contain vitamin D receptors and can respond to the 1,25$(OH)_2D_3$ produced. The alopecia found in VDR deficient patients suggests a biologic role for the VDR in the epidermis, particularly in the hair follicle.[8] In VDR knock out mice models, the mice are fully haired and grossly normal after birth until approximately three

months of age, progressing to generalized alopecia by eight months of age.[8] These findings indicate that the prenatal hair growth and development of the epidermis and first hair growth cycle does not require VDR, but is important in the onset of the second hair growth cycle.[8] Examination of the skin in this canine patient revealed large cystic follicles filled with keratin which corresponds to dermal changes noted in human cases and in rodent models of the disease.[8]

Humans with VDRR II, as well as the patient in this case, are born with normal hair, but become alopecic by six months of age and have rachitic changes that are resistant to all forms of vitamin D therapy.[1] Alopecia generally does not improve in human patients,[1] but normal pelage returned in our canine patient after several months. It is not clear if the alopecia is a genetically linked abnormality or related to the effect of 1,25-$(OH)_2D_3$ on the hair follicle.[1] In humans, alopecia seems to be a marker of a more severe form of the disease as judged by the earlier age at presentation, marked clinical aberrations and poor response to therapy.[3]

Therapy in humans begins with very large doses of vitamin D and oral calcium supplements but has had limited success. Refractory cases need long term nocturnal intravenous calcium infusions and these have successfully "healed" rickets and promoted mineralization in these patients;[2] however, the therapy is cost prohibitive in veterinary cases.

**AFIP Diagnosis:** Bone: Physeal dysplasia characterized by disordered columns of chondrocytes with marrow fibrosis

**Conference Comment:** The contributor did a magnificent job of describing the physiology behind vitamin D-resistant rickets. A lack of dietary vitamin D, inadequate absorption of vitamin D from the gastrointestinal system, or a lack of adequate photobiosynthesis of vitamin D can also cause rickets.

Hypophosphatemia can lead to rickets, and is known as hypophosphatemic vitamin D-resistant rickets (renal hypophosphatemic rickets).[7] Hypophosphatemia, normocalcemia, and decreased renal tubular reabsorption of phosphate are characteristic of hypophosphatemic vitamin D-resistant rickets. Hypophosphatemia is the sequela of inadequate absorption of phosphorus from the gastrointestinal system or decreased/inadequate reabsorption of phosphorous from the renal system.[7]

Gross lesions of rickets are most striking at sites of rapid growth. The metaphyseal and epiphyseal regions of long bones and the costochondral junctions are commonly affected, producing the classic "rachitic rosary" in affected animals.[7]

The classic histologic appearance of rickets is the disorganization of columns of chondrocytes and persistence of hypertrophic chondrocytes at sites of endochondral ossification, both at the physes and beneath the articular cartilage.[7] The underlying trabecular bone is often disrupted, and irregular tongues of cartilage are often seen in the metaphyses due to disorganized and disrupted endochondral ossification.

**Contributing Institution:** North Carolina State University, College of Veterinary Medicine, 4700 Hillsborough Street, Raleigh, NC 27606
http://www.cvm.ncsu.edu

**References:**

1. Al-Khenaizan S, Vitale P: Vitamin D-dependent rickets type II with alopecia: two case reports and review of the literature. Int J Dermatol **42**:682-685, 2003
2. Avioli LV and Krane SM: Metabolic Bone Disease and Clinically Related Disorders, 3rd ed., pp. 221, 767-777, Academic Press, San Diego, CA, 1998
3. Favus, MJ: Primer on the Metabolic Bone Diseases and Disorders of Mineral Metabolism, 3rd ed., pp. 311-316, Lippincott-Raven, Philadelphia, PA, 1996
4. Godfrey DR, Anderson RM, Barber PJ, Hewison M: Vitamin D-dependent rickets type II in a cat. J Small Anim Pract **46**:440-444, 2005
5. Schreiner CA, Nagode LA: Vitamin D-dependent rickets type 2 in a four-month old cat. JAVMA **222**:337-339, 2003
6. Tanner E, Langley-Hobbs SJ: Vitamin D-dependent rickets type 2 with characteristic radiographic changes in a 4-month-old kitten. J Feline Med Surg **7**:307-311, 2005
7. Thompson K: Diseases of bones and joints. *In:* Jubb, Kennedy, and Palmer's Pathology of Domestic Animals, ed. Maxie MG, 5th ed., vol. 1, pp. 75-82. WB Saunders, Edinburgh, Scotland, 2007
8. Xie Z, Komuves L, Yu Q-C, Elalieh H, Ng DC, Leary C, Chang S, Crumrine D, Yoshizawa T, Kato S, Bikle DD: Lack of the vitamin D receptor is associated with reduced epidermal differentiation and hair follicle growth. J Invest Dermatol **118**:11-16, 2002

**CASE III – 07-5491 (AFIP 3067227)**

**Signalment:** Late term fetus, unknown gender, Red Angus, (*Bos taurus*), bovine

**History:** Four abortions have occurred in this herd. Some of the aborted calves have had a short lower jaw.

**Gross Pathology:** The mandible was between 2 and 3 cm shorter than the maxilla. Both the upper and lower molars were impacted. On cut surface, the marrow cavities of the bones at the base of the skull were filled with excessive bone. The marrow cavity of the tibia and femur was filled with bone, leaving no marrow cavity. The cortex of the tibia and femur is thin.

**Laboratory Results:** Immunohistochemistry negative for BVD virus

**Histopathologic Description:** There is lack of resorption of the primary spongiosa in the distal metaphysis, with retention of cartilage deep into the distal metaphysic **(Fig. 3-1)**. Surfaces of primary spongiosa lack osteoclasts.

**Contributor's Morphologic Diagnosis:** Metaphysis - persistence of primary spongiosa

**Contributor's Comment:** Osteopetrosis, also referred to as marble bone disease, occurs in multiple species of animals, and may have an inherited basis, or may have an acquired cause.[5] The osteopetroses are a heterogeneous group of bone remodeling disorders characterized by an increase in bone density due to a defect in osteoclastic bone resorption.[1] In cattle, osteopetrosis occurs in black and red Angus cattle in North America, and is assumed to be inherited as an autosomal recessive trait.[2] Affected calves are small, premature (251-276 days of gestation), and usually stillborn. Clinically, they show brachygnathia inferior, impacted molar teeth and protruding tongue. The long bones are shorter than normal, and easily fractured. Radiographically, the medullary cavities are dense, without clear differentiation between the cortex and medulla. Vertebrae are shortened, frontal and parietal bones are thick, and bones of the cranial base are thick and dense. On cut surface, the metaphyses and diaphyses of long bones are filled with dense, unresorbed cones of primary spongiosa extending from the metaphysis to the center of the diaphysis. The bones are more fragile than normal and may be fractured. As a result of the skull abnormalities, the cerebral hemispheres are rectangular with flattened dorsal surfaces, the cerebellum is partially herniated through the foramen magnum, and the optic

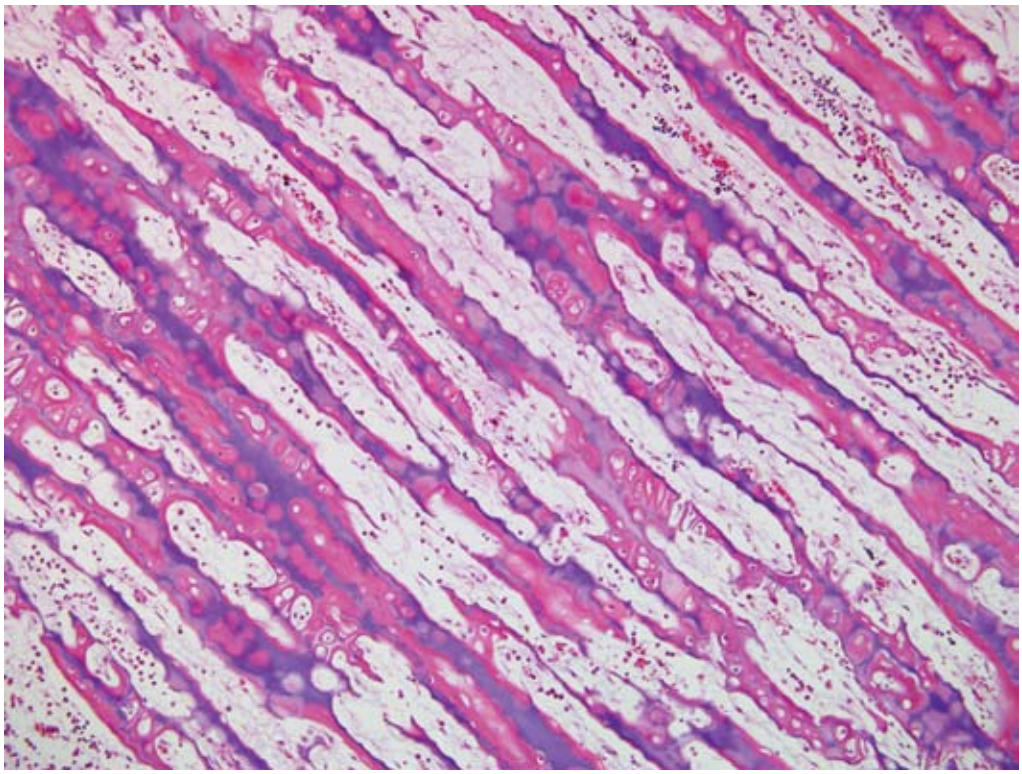

*3-1. Bone, ox. Diffusely, there is persistence of primary spongiosa to the level of the metaphysis with retention of cartilage cores and markedly reduced numbers of osteoclasts. (HE 100X)*

nerves are hypoplastic.

Osteopetrosis also occurs in Hereford and Simmental cattle, resembling that of Angus calves.[4,5] BVD virus infection can cause osteopetrosis in cattle.[4] The osteopetrotic lesions are believed to be caused by transitory virus-induced osteoclast depletion. The gross lesions of BVD virus-induced osteopetrosis are different from the inherited variety in cattle.

Osteopetrosis-like lesions with metaphyseal sclerosis may occur in association with canine distemper virus infection in pups and in lead poisoning.[5]

In humans two forms of osteopetrosis are recognized: a severe, recessively inherited, lethal (malignant) form, with lesions present at birth, and a dominant (benign) form which becomes manifest later in life. In animals, most descriptions of osteopetrosis appear analogous to the malignant form and autosomal recessive inheritance is suspected in most cases.[5]

Histologically, growth plates are essentially normal but metaphyses are relatively avascular.[5] Dense chondro-osseous tissue, consisting of cartilage matrix lined by a thick layer of woven bone, occupies the medulla. Osteoclasts are rare and when present they appear to be inactive. Failure to replace the primary spongiosa and its associated woven bone with thicker trabeculae of mature lamellar bone presumably accounts for the increased fragility of osteopetrotic bones.

The lack of osteoclastic resorption of bone can occur as a deficiency in numbers of osteoclasts, or dysfunction in osteoclasts that may be present in normal numbers. Osteoclasts are capable of breaking down both the inorganic and organic matrix of bone.[1]

**AFIP Diagnosis:** Bone: Osteosclerosis, diffuse, severe, with retention of cartilage cores

**Conference Comment:** Osteopetrosis has also been reported in four Peruvian Paso foals and one Appaloosa. The disease in horses has the same clinical and pathologic manifestations of the disease seen in the severe lethal form in Angus calves. Histologically, the only major difference is the presence of normal to increased numbers of osteoclasts. Ultrastructurally, osteoclasts in these foals do not have a ruffled border suggesting a functional defect in osteoclasts.[5]

Osteopetrosis has also been reported in white-tailed deer, Dachshund puppies, in an Australian Shepherd and a Pekingese dog, and in cats. In cats, osteopetrosis has been linked to vitamin D toxicosis and feline leukemia virus.[5]

**Contributing Institution:** Dept Diagnostic Medicine/Pathobiology, Mosier Hall, 1800 Denison Ave., Kansas State University, Manhattan, KS 66506; http://www.vet.k-state.edu/depts/dmp/

**References:**

1. Balemans W, VanWesenbeeck L, VanHul W: A clinical and molecular overview of the human osteopetroses. Calcif Tissue Int 77:263-274, 2005
2. Greene HJ, Leipold HW, Hibbs CM, Kirkbride CA: Congenital osteopetrosis in Angus calves. J Am Vet Med Assoc **164**:389-395, 1974
3. Ojo SA, Leipold HJ, Cho DY, Guffy MM: Osteopetrosis in two Hereford calves. J Am Vet Med Assoc **166**:781-783, 1975
4. Scruggs DW, Fleming SA, Waslin WR, Grace AW: Osteopetrosis, anemia, thrombocytopenia, and marrow necrosis in beef calves naturally infected with bovine virus diarrhea virus. J Vet Diagn Invest **7**:555-559, 1995
5. Thompson K: Diseases of bones and joints. *In:* Pathology of Domestic Animals, ed. Maxie G, 5th ed., vol. 1, pp 38-40. WB Saunders, Edinburgh, Scotland, 2007

## CASE IV – 0120-08 (AFIP 3103199)

**Signalment:** 9-year-old, gelding, Swedish Warmblood riding horse (SWH), equine

**History:** The horse had been lame in different limbs for more than one year. The clinical examination this day showed mild right front limb lameness. Some problems with the left hind limb were also noticed, with pain from the superficial digital flexor tendon. Images including plain radiographs and scintigraphic examination showed intense focal activity of the distal right humerus **(Fig. 4-1)**. Radiographic examination revealed suspected radiodensity in the mid distal right humerus in close proximity to a vascular channel. The lesions were considered as enostosis-like. The horse had previous problems with gait asymmetries for more than a year and also showed evidence of tendonitis of the superficial digital flexor tendon of the left hind limb, hence the owner elected euthanasia.

**Gross Pathology:** A chronic tendonitis of the superficial digital flexor tendon of the right hind leg was found. Lesions were also seen in right distal humerus

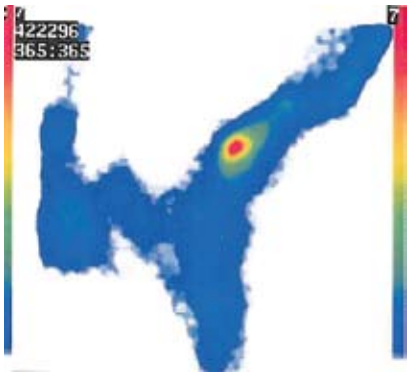


*4-1. Bone, horse. There is a focal area of intense scintigraphic activity within the medullary cavity.* *Scintograph courtesy of SLU, department of BVF, division of Pathology, Pharmacology & Toxicology, Box 7028, SE-750 07 Uppsala, Sweden.*

*4-2, 4-3. Bone, horse. Within the medullary cavity and effacing bony trabeculae, there is a focally extensive proliferation of dense bony tissue.* *Photographs courtesy of SLU, department of BVF, division of Pathology, Pharmacology & Toxicology, Box 7028, SE-750 07 Uppsala, Sweden.*

macroscopically after the bone had been sawed **(Figs. 4-2, 4-3)**. Bone tissue in trabecular and dense structures could be seen in the medullary cavity of the distal third (metadiaphyseal) humerus

**Laboratory Results:** None

**Histopathologic Description:** Sections from the distal area of humerus show a normal compacta with lamellar bone. In the medullary cavity intermingeled with adipose tissue, bone growth of trabecular bone tissue is found **(Fig. 4-4)**. The bone trabeculae are lined by several osteoblasts and are composed of woven bone but often lined by lamellar bone structure. The larger trabecular are predominately of a lamellar pattern. A few osteoclasts can be seen adjacent to bone trabeculae. This type of idiopathic nonneoplastic bone growth in the medullary cavity would suggest enostosis-like lesions. The numerous osteoblasts explain the increased radiopharmaceutical uptake seen on scintigraphic examination.

**Contributor's Morphologic Diagnosis:** Intramedullary trabecular bone growth with osteoblastic activity compatible with enostosis-like lesions, right distal humerus, equine

**Contributor's Comment:** In man[2], enostosis is described as a relatively common lesion (14% in

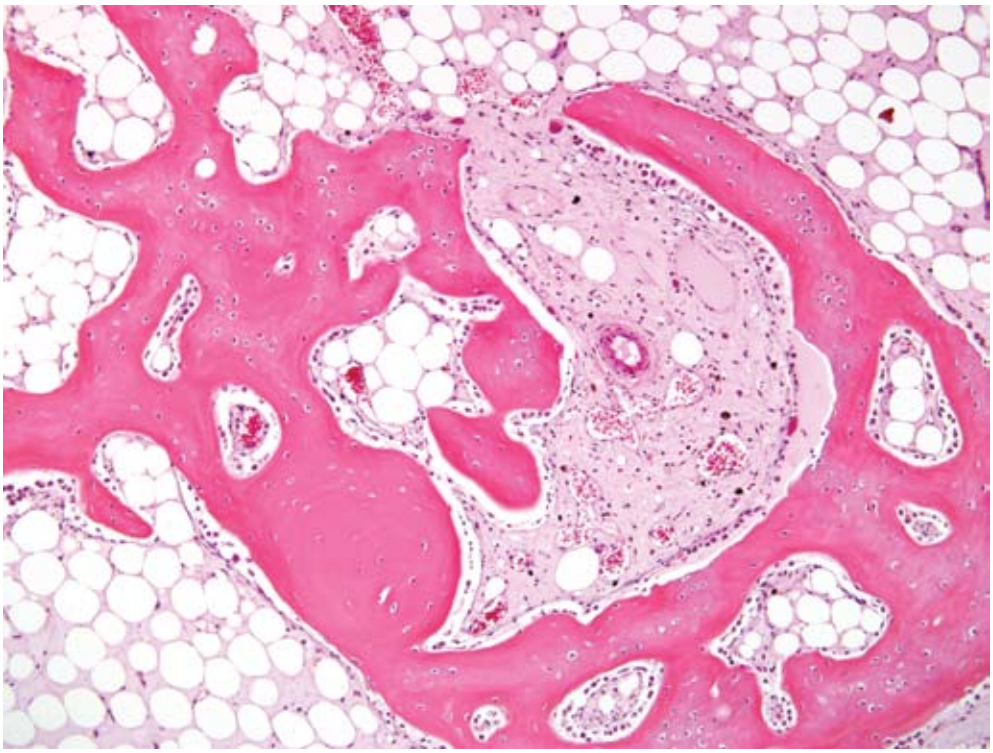

*4-4. Bone, horse. Within the medullary cavity, often contiguous with normal bony trabeculae, there is a focally extensive proliferation of woven bone. (HE 200X)*

cadaveric material). Enostosis has been defined as "a mass of proliferating bone within a bone." The lesions are often referred to "bone islands, calcified medullary defects, cortical defects, enosteomas." Enostoses of man are mostly found in the pelvis, spine, ribs and metaphyseal and epiphyseal parts of femur. Scintigraphy often shows absence of radiopharmaceutical uptake, indicating chronic lesions without osteoblast activity.

Canine panosteitis is described as an idiopathic disease, characterized by bone sclerosis of the diaphyses and metaphyses of long bones of large breeds. The dogs may be showing signs of illness with fever. Lameness is often presented as intermittent involving more than one limb. Multifocal areas of radio densities, often in association with nutrient foramen can be seen on radiographs. The bone changes will disappear and the dog recover completely.

In equine, enostosis-like lesions were first described as multifocal sclerotic areas within the medullary cavity of long bones and were reported in six Thoroughbreds, three Standardbreds and one Appoloosa.[1] Most of the horses had a history of chronic lameness. The bone sclerotic areas seen on radiographs and as abnormal increased radioisotope uptake at scintigraphic examination were localized to the diaphyseal areas of the long bones. The lesions were endosteal and/or medullary. These lesions were named "enostosis-like" in order to differentiate them from enostosis (bone islands seen in man) and panosteitis seen in dog. Later, Ramzan [4] also described enostosis-like lesions in 12 Thoroughbreds. Some of these lesions appeared related to lameness, but in many horses no association could be made. The author concluded that enostosis-like lesions are transient phenomena, with scintigraphic and radiographic resolution occurring over months. Multiple enostosis-like lesions has been reported in a racing Thoroughbred.[3] As treatment of the disease, box rest and controlled exercise during 1-6 months have been suggested. Most of the horses recover and return to working or racing.

The etiology and pathogenesis of theses lesions are not known. Often the bone lesions have been found in the diaphyseal area close to the nutrient foramen, hence bone infarcts has been discussed as a cause. Stress fractures are also mentioned, but never proven to be associated with the radiodense areas. Microscopic examinations of the enostosis-like lesions in horses are not presented in the literature, hence a comparison of the present case and the reported enostosis-like lesions can not be made; however, the radiographic and scintigraphic findings are similar.

The present microscopic picture is that of a non-neoplastic non-specific bone growth with osteoblast activity, within the medullary cavities, very similar to changes seen microscopically in canine panosteitis.

This horse had had a long history of gait asymmetries also involving tendonitis and the owner elected euthanasia. The enostosis-like lesions probably would have resolved and was not the reason for euthanasia.

**AFIP Diagnosis:** Bone: Intramedullary woven bone formation (enostosis), focal, moderate

**Conference Comment:** The contributor briefly mentioned canine panosteitis, a disease of unknown cause often seen in young large and giant breed dogs. Clinically, shifting leg lameness is often seen in affected animals. Thickening of the bone can occur on the periosteal and endosteal surfaces.[5]

Clinically, an increase in radiodensity in the marrow is initially seen and is caused by rapidly expanding areas of fibrovascular tissue that is quickly remodeled and converted to woven bone. Because of this rapid cyclical process of formation and resorption of bone, both osteoblasts and osteoclasts are often observed in the same microscopic field. Resting and reversal lines can also be present in relatively close proximity within medullary trabecular bone.[5]

Inflammation is usually not a feature of this disease, and the lesions resolve spontaneously over time. The cause is currently unknown, but canine distemper virus has been suggested as a potential suspect.[5]

**Contributing Institution:** SLU, department of BVF, division of Pathology, Pharmacology & Toxicology, Box 7028, SE-750 07 Uppsala, Sweden, www.slu.se

**References:**

1. Bassage LH, Ross MW: Enostosis-like lesions in the long bones of 10 horses: scintigraphic and radiographic features. Equine Vet J **30**:35-42, 1998
2. Gould CF, Ly JQ, Lattin Jr GE, Beall DP, Sutcliffe JB: Bone tumor mimics: avoiding misdiagnosis. Curr Probl Diagn Radiol **36**:124-141, 2007
3. Jones E, McDiarmid A: Case report. Multiple enostosis-like lesions in a racing Thoroughbred. Equine Vet Education. **17**:92-95, 2005
4. Ramzan PHL: Equine enostosis-like lesions: 12 cases. Equine Vet J. **14**:143-148, 2002
5. Thompson K: Diseases of bones and joints. *In:* Pathology of Domestic Animals, ed. Maxie G, 5th ed., pp.104-105, vol 1. WB Saunders, Edinburgh, Scotland, 2007

The Armed Forces Institute of Pathology
Department of Veterinary Pathology

*Conference Coordinator:*
Todd M. Bell, DVM

WEDNESDAY SLIDE CONFERENCE 2008-2009

# Conference 22

15 April 2009

***Conference Moderator:***

**Dr. Thomas Van Winkle, DVM, PhD, Diplomate ACVP**

## CASE I – 07-V6182 (AFIP 3110669)

**Signalment**: 9-week-old, female, large white pig, porcine (*Sus*)

**History:** At a hog grower operation two sheds had been cleaned out and the water turned off from each shed prior to the introduction of a new batch of pigs. On a Thursday, 400 9-week-old grower pigs were introduced into each shed. It was not realized until the following Saturday that drinking water to each shed had not been turned on. The pigs engorged with water on Saturday and Sunday, and by Monday many of the pigs were paddling and had muscle fasciculation, others were blind, and many were having seizures or were down and non-responsive. To confirm the field diagnosis, the attending veterinarian collected and submitted to the laboratory three entire brains fixed in 10% neutral buffered formalin and three meningeal swabs for bacteriology.

**Gross Pathology:** No significant gross pathological lesions were evident in the brain.

**Laboratory Results:** On meningeal swabs from three pigs, no bacteria grew on horse blood agar, and haemolysed blood agar plates incubated aerobically for 72 hours.

**Histopathologic Description:** Lesions varied in severity in each of the three brains. The most consistent findings were as follows: brain, forebrain, in which the leptomeninges, particularly in the sulci are multi-focally and segmentally thickened by increased numbers of well differentiated eosinophils. In the cerebral cortical laminar blood vessels, particularly veins and venules, show thick perivascular cuffs of eosinophils **(Fig. 1-1)**, 1 to 3 cells deep, rarely there are macrophages. Multi-focally blood vessels in the cerebral cortical laminae have prominent and swollen endothelial cells. Segmentally along the cerebral cortical laminae, particularly in the sulci, there is a well delineated multi-focal astrogliosis and microgliosis.

**Contributor's Morphologic Diagnosis:** Chronic severe multifocal eosinophilic meningoencephalitis

**Contributor's Comment:** This was a case of indirect salt poisoning also known as water deprivation or water intoxication. Of the 800 at risk pigs, 600 died or were euthanized. Only pigs with the mildest of clinical signs survived. It was two weeks before clinical signs ceased in the surviving pigs. Interestingly, the farmer said that one or two pigs started to have seizures before the water supply

*Sponsored by the American Veterinary Medical Association, the American College of Veterinary Pathologists, and the C. L. Davis Foundation.

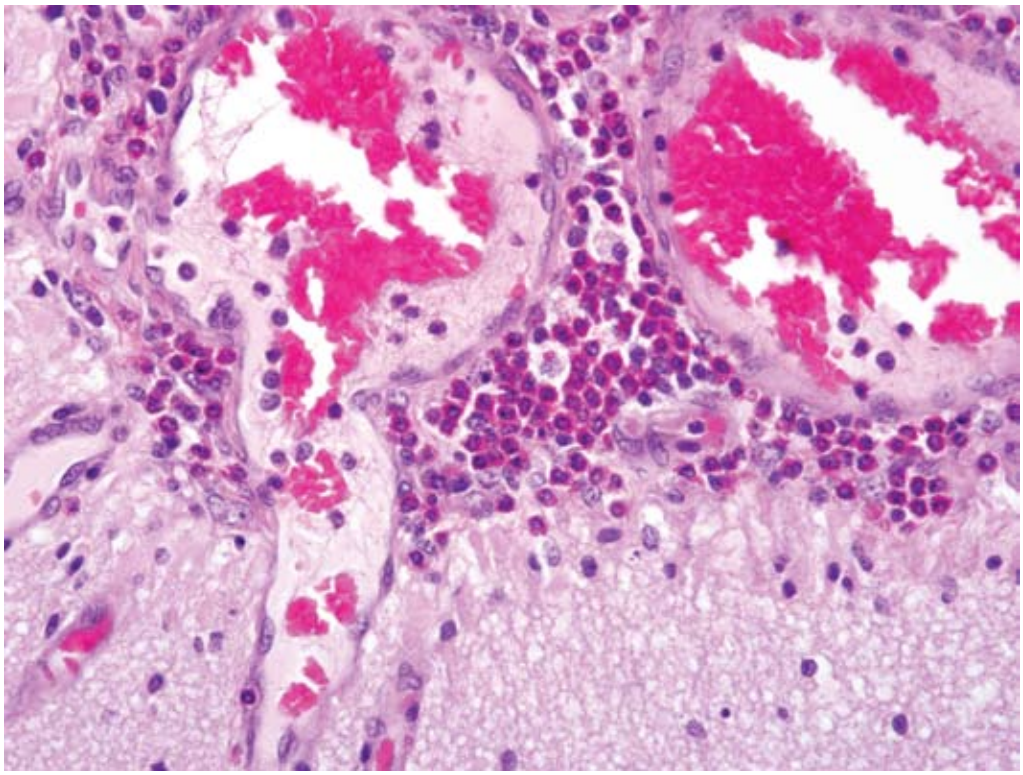

*1-1. Cerebrum, pig. The endothelium of vessels within the gray matter and meninges is often hypertrophied, and Virchow-Robin spaces are moderately expanded by eosinophils. (HE 400X)*

was turned on. The attending veterinarian immediately recognized this as a case of indirect salt poisoning (water deprivation) and collected brains for histology to confirm and provide evidence of the clinical diagnosis. Bacterial swabs were collect to exclude the possibility of bacterial meningitis. The farmer was a contract grower for a parent company. The parent company was furious and treated this as a serious breach of animal welfare and a situation that should not have occurred. Furthermore the company protocol for pigs that have been deprived of water is to turn the overhead sprinklers on and gradually re-introduce water allowing pigs to lick water off the floor. The contributor has only seen one previous case of indirect salt poisoning and that was in pigs delayed in road transport that when they finally arrived engorged on water.

In domestic animals direct salt poisoning occurs in cattle, horses, sheep and pigs with the ingestion of excessive amounts of sodium chloride. Direct salt poisoning can occur in pigs where bore water is used for livestock drinking or diets with excessive salt including salted fish waste, salt whey from cheese factories and excessive salt in baker's bread dough.[2] Indirect salt poisoning involves a normal intake of sodium chloride, but with limited water intake.[4] The latter is also termed water deprivation or water intoxication. Indirect salt poisoning has only been proven to occur in pigs, with circumstantial evidence in cattle and sheep.[1] Pigs are particularly susceptible to indirect salt poisoning because of the relatively high salt diets. Restriction of water intake to pigs, 4 to 12 weeks of age, fed prepared diets containing 2% salt can result in clinical disease.[2] Poisoning occurs when the animals again have access to unlimited water.

Indirect salt poisoning with decreased water intake, but normal sodium chloride intake results in an accumulation of sodium ions in the brain and other tissues over several days. High sodium accumulation inhibits anaerobic glycolysis, preventing active transport of sodium out of the cerebrospinal fluid. When there is access to water again, water migrates to the tissues to re-establish the salt-water balance. Acute cerebral edema develops and increased intracranial pressure results. Specific to pigs and of diagnostic significance, is that there is an influx of eosinophils into the meninges. [2,4]

In cases of salt poisoning there are two characteristic changes.[4] The first is eosinophilia of the leptomeninges and Virchow-Robin spaces in the cerebral cortex. The second, develops with increased duration of the lesion, is cerebral cortical necrosis and with advanced lesions cavitating areas of malacia.[1] A mixture of both reactions is most common, but either alone may be encountered.[4]

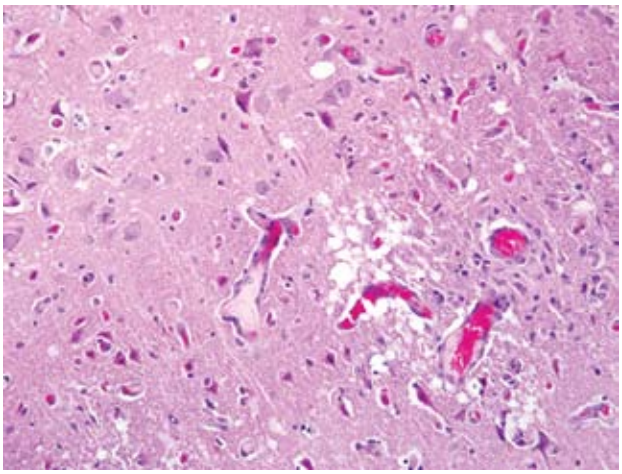

*1-2. Cerebrum, pig. Within the gray matter there is neuronal necrosis and spongiosis within the neuropil. (HE 400X)*

The differential diagnosis for CNS signs in young pigs includes viral encephalomyelitis, Aujeszky's disease, edema disease, Streptococcal meningitis, Glasser's disease, toxicosis, nutritional deficiencies and Mulberry heart disease.[3] Meningeal and perivascular infiltrates can occur in the brains of pigs with leukomalacia of Mulberry heart disease and other causes of encephalitis.[1] However, the combination of laminar cortical cerebral necrosis and cerebral eosinophilia is pathognomonic for direct or indirect salt poisoning.[1] Histologically, eosinophilic meningoencephalitis can also occur with parasitic infections. In Australia, parasitic encephalitis is rare. In dogs, *Angiostrongylus cantonensis* occurs infrequently, but has not been observed in pigs.

The importance of this report is that direct or indirect salt poisoning cases often affect many animals and mortalities can be high. In cases of indirect salt poisoning veterinary pathologists should recognize that a restricted water intake is often the cause and this may be due to an underlying animal welfare issue. Veterinary pathologists should recognize that they play an important role in recognizing or confirming animal welfare associated diseases.

**AFIP Diagnosis:** Brain, cerebrum: Meningoencephalitis, eosinophilic, acute, multifocal, moderate with neuronal necrosis **(Fig. 1-2)**

**Conference Comment:** The lesion in this brain had a striking eosinophilic component. Other causes of eosinophilic meningoencephalitis in domestic species include parasitic nematodes and protozoans.[1]

Idiopathic eosinophilic meningoencephalitis has also been reported in dogs and one cat. Severe neurologic signs including recumbency and loss of consciousness have been reported with this syndrome. Eosinophilia and CSF pleocytosis with a predominance of eosinophils are common clinical pathologic findings. Grossly, the meninges often have a green tinge because of the eosinophilic inflammatory infiltrate. Histologic changes include eosinophilic and granulomatous meningitis of cerebrum and cerebellum with eosinophilic perivascular cuffing. In dogs, Golden Retrievers and Rottweilers are the most commonly affected breeds.[1]

In pigs, salt toxicity can cause laminar cortical necrosis. Several of the submitted slides did have very good examples of neuronal necrosis, while other slides had a dearth of necrotic neurons. Slides submitted for this case were from three different pigs, so that may be the reason for slide variation. In ruminants, differentials for laminar cortical necrosis include lead poisoning, salt toxicity, sulfur toxicity, hypoxia, and thiamine deficiency.[1]

**Contributing Institution:** Gribbles Veterinary Pathology, 1868 Dandenong Rd Clayton, Melbourne, Victoria, Australia, 3168.

**References:**

1. Maxie MG, Youssef S: Nervous system. *In:* Jubb, Kennedy and Palmer's Pathology of Domestic Animals, ed. Maxie MG, 5th ed., vol 1, pp.351-358 445. Elsevier Limited, Philadelphia, PA, 2007
2. Radostits OM, Gay CC, Hinchcliff KW, Constable PD: Diseases associated with inorganic and farm chemicals. *In:* Veterinary Medicine. A textbook of the diseases of cattle, horses, sheep, pigs and goats. 10th ed. pp 1824 - 1826, Saunders Elsevier, Edinburgh, Scotland, 2007
3. Straw BE, Dewey CE, Wilson MR: Differiential diagnosis of swine disease. *In:* Diseases of Swine 8th ed. Straw BE D'Allaire S, Mengeling WL, Taylor DJ. pp. 62-65, Blackwell Science, London, UK, 1999
4. Summers BA, Cummings JF, de Lahunta A: Degenerative Diseases of the Central Nervous System. *In:* Veterinary Neuropathology. pp254-255. Mosby, St Louis, MO, 1995

## CASE II – NP 392/07 (AFIP 3110887)

**Signalment:** Bavarian Warmblood, 11 yrs, female, equine

**History:** Two week history of fever, depression, gait abnormalities and anorexia. The animal was euthanized after unsuccessful symptomatic treatment.

**Gross Pathology:** At macroscopic inspection, the brain appeared normal.

**Laboratory Results:** Brain was positive for Borna disease virus (BDV) antigen by immunohistochemistry and negative for Rabies virus antigen by immunoflourescence test.

**Histopathologic Description:** Slices of the brain reveal moderate, multifocal, perivascular and parenchyma infiltrating mononuclear immune cells **(Fig. 2-1)** affecting slightly more gray than white matter with a severe generalized astrogliosis and microglia activation throughout the whole brain. Lesions are most severe in the lateroventral parts of the cerebral cortex, mesencephalon and hippocampal gyrus. Inflammation cells are also infiltrating plexus epithelia and leptomeninges. Moderate neuronal and axonal degeneration (spheroids) can be found and some neurons undergo neuronophagia **(Fig. 2-2)**. No neuronal intranuclear acidophilic inclusion bodies, Cowdry type B, (Joest Degen bodies) are detectable in these slices.

**Contributor's Morphologic Diagnosis:** Polioencephalitis, meningitis, plexitis, nonpurulent, multifocal, subacute, moderate

**Contributor's Comment:** Borna disease occurs naturally in horses, sheep[1], rarely in cats[2, 3], and other warm-blooded animals.[1,4] Borna disease virus has been classified as the prototype of a new virus family, Bornaviridae (mononegavirales)[1, 5], though the disease has been recognized in Central Europe for more than 250 years and apparently in Asia.[6,8] Because experimental infection of rodents, sheep and horses is achievable by intranasal application of virus, some researches already assume that the natural infection with BDV might occur by the olfactory nerve [1, 8, 9] and several studies indicate wild rodents being a common virus reservoir.[1,10]

The highly neurotropic but noncytolytic virus [9], similar to rabies virus, is transported by retrograde axonal transport from the periphery to the CNS. After infection, BDV causes a persistent infection of the central nervous system and induces an immune-mediated encephalomyelitis. The

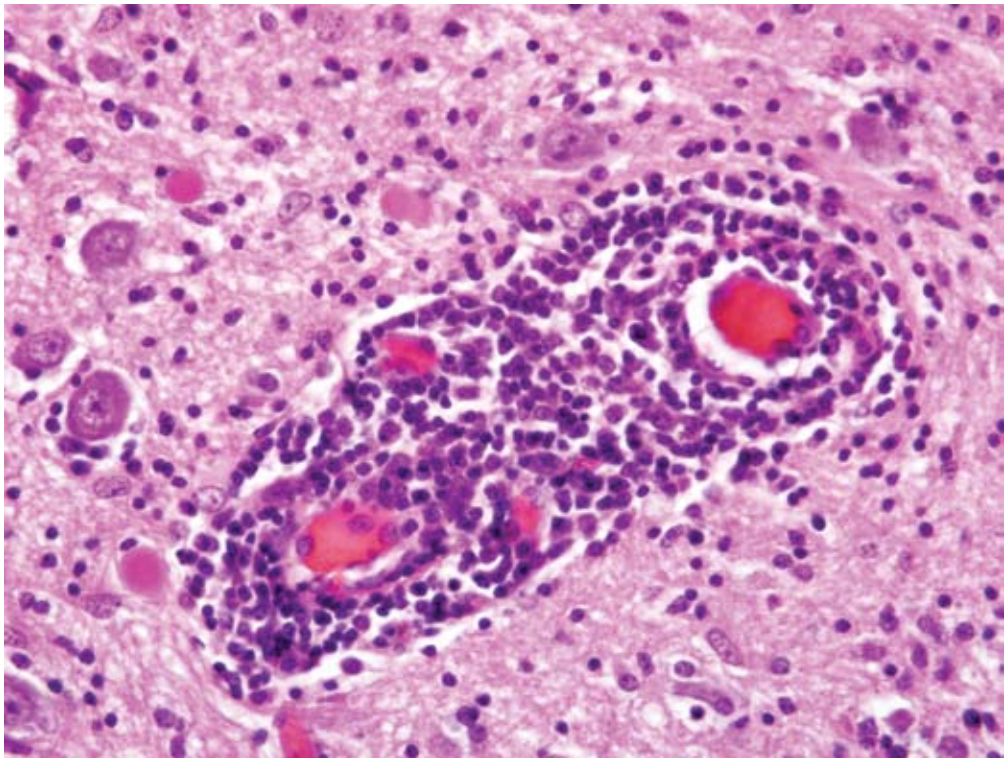

*2-1. Cerebrum, horse. Expanding Virchow-Robin spaces of the cerebral vasculature are high numbers of lymphocytes, plasma cells, and few histiocytes. (400X)*

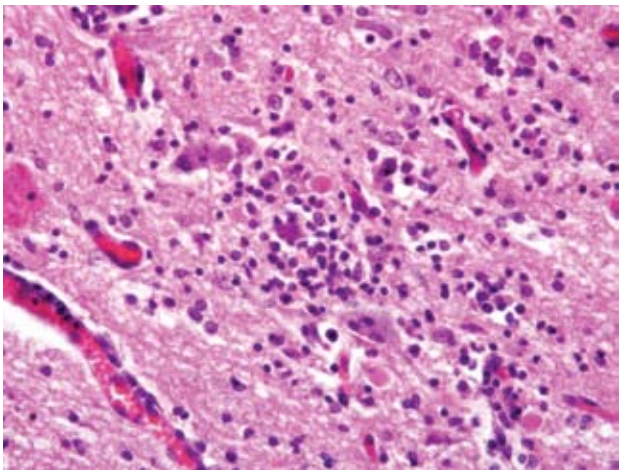

*2-2. Cerebrum, horse. Diffusely within the gray matter, there is generalized gliosis, with multifocal glial nodules surrounding necrotic neurons and necrotic debris. Multifocally within gray matter, there are few spheroids. (HE 400X)*

infiltrating immune cells have been characterized as CD4-positive T-cells, CD8-positive T-cells, macrophages and B cells.[11] The virus can then also spread centrifugally via the peripheral nervous system, resulting in infection of nonneural tissue.[9] A proposed mechanism for the behavioral changes involves protein interference with neurotransmitter function of infected neurons, especially those located in the limbic lobe.[12]

The first evidence that some human psychiatric patients might be infected with BDV, or a BDV-related virus, came from serological studies using immunofluorescence assays.[13] However, several key experiments could not be reproduced by independent laboratories and started a still ongoing, highly controversial, worldwide debate about whether BDV infects humans and causes psychiatric problems.[1,14,15] In this case, the detection of viral antigen in fresh brain tissue by immunohistochemistry, the clinical manifestations and the characteristic histopathological changes within the brain all contribute to the diagnosis of Borna disease.

**AFIP Diagnosis:** Brain, thalamus: Meningoencephalitis, lymphocytic, multifocal, moderate

**Conference Comment:** Borna disease virus (BDV) is a single-stranded RNA virus and is the sole member of the family *Bornaviridae* in the order *Mononegavirales*.[4] It is named after the village Borna in Germany where the first major outbreak of this disease was recognized in the late 1800's.[15] BDV has a very wide host range, but sheep and horses are the most susceptible species to disease. Borna disease is most prevalent in Europe, but positive titers have been found in the United States.[10] Recently, Borna disease virus has been suggested as a potential cause of proventricular dilatation disease in birds. Research is currently ongoing to prove this link.

Gross lesions are not seen in infections with BDV. Histologic lesions are generally present in the grey matter of the olfactory bulbs, hippocampus, limbic system, basal ganglia, and brain stem. The cerebellum and dorsal aspect of the cerebrum are usually unaffected.[10] Common histologic lesions are a nonsuppurative encephalitis with perivascular cuffing composed of mononuclear cells, gliosis, and neuronophagia. Perivascular cuffing is often pronounced with cells layering upon one another up to seven cells deep.[10] Inclusion bodies (Joest-Degen bodies) are nearly pathognomonic for BDV infection, and, if present, are normally in nuclei and rarely in the cytoplasm. The hippocampus is reported as the best area to find inclusions.[10] This virus is also unique because it replicates in the nucleolus of the host cell.[10]

Dr. Van Winkle discussed the importance of narrowing this particular case down to a list of differentials, and then using the tools available at your particular institution to make a diagnosis. In horses, differentials for this lesion include: West Nile virus, Japanese encephalitis virus, Murray Valley encephalitis, St. Louis encephalitis, Western equine encephalitis, Eastern equine encephalitis, and Venezuelan equine encephalitis.[1] Other potential differentials discussed during the conference included equine protozoal myelitis and equine herpesvirus type 1. Dr. Van Winkle commented that geographic location in many cases of equine encephalitis is a good indicator of what differential should be at the top of the list.

**Contributing Institution:** Institute of Veterinary Pathology, Veterinärstr. 13, D-80539 Munich, Germany www.patho.vetmed.uni-muenchen.de

**References:**

1. Bode L, Ludwig H: Borna disease virus infection, a human mental-health risk. Clin Microbiol Rev **16**:534-545, 2003
2. Carbone KM: Borna disease virus and human disease. Clin Microbiol Rev **14**:513-527, 2001
3. Carbone KM, Duchala CS, Griffin JW, Kincaid AL, Narayan O: Pathogenesis of Borna disease in rats: evidence that intra-axonal spread is the major route for virus dissemination and the determinant for disease incubation. J Virol **61**:3431-3440, 1987
4. Carbone KM, Rubin SA, Nishino Y, Pletnikov MV: Borna disease: virus-induced neurobehavioral disease pathogenesis. Curr Opin Microbiol **4**:467-475, 2001
5. de la Torre JC, Carbone KM, Lipkin WI: Molecular

characterization of the Borna disease agent. Virology **179**:853-856, 1990
6. Hagiwara K, Okamoto M, Kamitani W, Takamura S, Taniyama H, Tsunoda N, Tanaka H, Iwai H, Ikuta K: Nosological study of Borna disease virus infection in race horses. Vet Microbiol **84**:367-374, 2002
7. Honkavuori KS, Shivaprasad HL, Williams BL, Quan PL, Hornig M, Street C, Palacios G, Hutchison SK, Franca M, Egholm M, Briese T, Lipkin WI: Novel borna virus in psittacine birds with proventricular dilatation disease. Emerg Inf Dis Vol 14, Num 12, Dec 2008
8. Inoue Y, Yamaguchi K, Sawada T, Rivero JC, Horii Y: Demonstration of continuously seropositive population against Borna disease virus in Misaki feral horses, a Japanese strain: a four-year follow-up study from 1998 to 2001. J Vet Med Sci **64**:445-448, 2002
9. Kamhieh S, Flower RL: Borna disease virus (BDV) infection in cats. A concise review based on current knowledge. Vet Q **28**:66-73, 2006
10. Maxie MG, Youssef S: Nervous system. *In:* Jubb, Kennedy and Palmer's Pathology of Domestic Animals, ed. Maxie MG, 5th ed., vol 1, pp.421-426. Elsevier Limited, Philadelphia, PA, 2007
11. Morales JA, Herzog S, Kompter C, Frese K, Rott R: Axonal transport of Borna disease virus along olfactory pathways in spontaneously and experimentally infected rats. Med Microbiol Immunol **177**:51-68, 1988
12. Planz O, Bilzer T, Stitz L: Immunopathogenic role of T-cell subsets in Borna disease virus-induced progressive encephalitis. J Virol **69**:896-903, 1995
13. Reeves NA, Helps CR, Gunn-Moore DA, Blundell C, Finnemore PL, Pearson GR, Harbour DA: Natural Borna disease virus infection in cats in the United Kingdom. Vet Rec **143**:523-526, 1998
14. Rott R, Herzog S, Fleischer B, Winokur A, Amsterdam J, Dyson W, Koprowski H: Detection of serum antibodies to Borna disease virus in patients with psychiatric disorders. Science **228**:755-756, 1985
15. Staeheli P, Sauder C, Hausmann J, Ehrensperger F, Schwemmle M: Epidemiology of Borna disease virus. J Gen Virol **81**:2123-2135, 2000
16. Weissenbock H, Nowotny N, Caplazi P, Kolodziejek J, Ehrensperger F: Borna disease in a dog with lethal meningoencephalitis. J Clin Microbiol **36**:2127-2130,1998

## CASE III – N07-649 (AFIP 3109554)

**Signalment:** 4-year-old spayed female mixed breed dog (*Canis familiaris*)

**History:** 3-week history of seizures, nystagmus, strabismus, lateral recumbency at about weekly intervals. On each occasion, supportive care with intravenous fluid, administrated at the referring veterinarian was sufficient to bring about temporary recovery from symptoms. The dog was admitted to the University of Florida Veterinary Medical Center (UF VMC) obtunded with lateral nystagmus, anisocoria, and strabismus. She had patellar hyperreflexia, good palpebral reflexes, miosis of the right pupil, and mydriasis of the left pupil with no pupillary light responses, and good reflexes in all four limbs. Cystic lesions in the brain were diagnosed at the referring veterinarian. The dog began to decline and the owner opted to euthanize.

**Gross Pathology:** The lateral ventricles in the brain were moderately enlarged. There was a 2cm diameter, poorly-demarcated red focus in the meninges over the right lateral occipital area. One gyrus in this region was expanded and contained an 8x5 mm grey focus.

The kidneys contained numerous irregular depressions on the subcapsular surface that extend into the cortex. The capsule did not peel off easily.

**Laboratory Results:** Sodium mEq/L = 137 (145-154), potassium = 5.6 mEq/L (4.1-5.3), BUN = 102 mg/dL (8-31), Creatinine = 4.6 mg/dL (0.8-1.6).

**Histopathologic Description:** Vessels in the meninges are frequently markedly distended with a neoplastic population of round cells (lymphocytes) **(Fig. 3-1)** which are predominantly confined to the lumina of capillaries, arteries, and veins, but also extend into the perivascular tissue. The lymphocytes are large, have large round to oval nuclei, one to several nucleoli, coarsely clumped chromatin, and small amounts of amphophilic cytoplasm. There is marked anisocytosis and anisokaryosis, and an average of 1-2 mitotic figures per 400X field. There is frequent individual cell necrosis. Frequently, there are scant erythrocytes in the vessels along with the neoplastic lymphocytes. There are thrombi present in a low number of affected vessels. Throughout the parenchyma, in both the gray and white matter, there are a low number of vessels which contain neoplastic lymphocytes. There are several areas in the cerebral cortex which contain increased numbers of small vessels

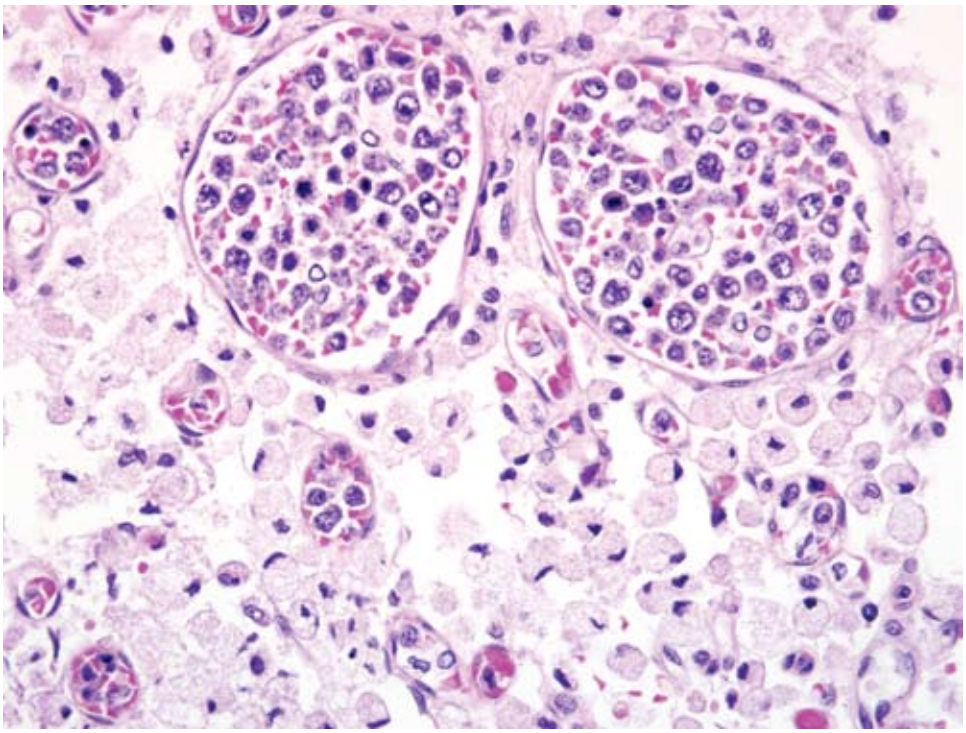

*3-1. Cerebrum, dog. Vessels within the cerebrum and meninges are variably dilated or occluded by neoplastic lymphocytes. The surrounding gray matter is often effaced by large numbers of macrophages with abundant foamy cytoplasm. (HE 400X)*

with prominent endothelial cells and neoplastic cells often present within the vessels. In these foci, there is rarefaction of the neuropil, necrotic neurons and/or loss of neurons, swollen axons, and accumulation of gitter cells (infarcts). Neoplastic lymphocytes rarely extend into the neuropil in these foci.

**Contributor's Morphologic Diagnosis:**
1. Intravascular lymphoma, with thrombosis and subacute to chronic infarction, brain
2. Moderate hydrocephalus

**Contributor's Comment:** Canine intravascular lymphoma is a rare large cell lymphoma in which lymphocytes proliferate within blood vessels in the absence of a primary extravascular mass or leukemia.[1] Blood vessels in nearly all tissues examined contained luminal neoplastic lymphocytes, which often largely filled the vessel lumen. Thrombosis was also identified in numerous tissues, and thrombosis resulted in infarction in the brain, spleen and heart. Infarcts were variably prominent in submitted sections. Multifocal cerebral cortical infarctions were the cause of neurologic clinical signs. The hydrocephalus diagnosed on gross examination was most likely congenital and an incidental finding.

Canine intravascular lymphoma is also known as malignant angioendotheliomatosis. Although most human cases are of B cell origin, [3] canine cases are typically classified as T cell or non-B, non-T cell.[1] Most human cases present with CNS or cutaneous signs.[3] CNS signs are most common in affected dogs.[1]

In a retrospective study of 17 cases of canine intravascular lymphoma, neoplastic lymphocytes rarely extended outside of vessels into the surrounding parenchyma and were not present in lymph nodes or the bone marrow in the 4 cases where these organs were examined.[1] Bone marrow and lymph node involvement were described in an additional canine case report [2] and bone marrow involvement was reported in 4/5 human patients in which neoplastic lymphocytes were also identified in peripheral blood smears.[4] While neoplastic lymphocytes were observed outside of vessels in multiple locations in this case (brain, kidney, pancreas, lung, lymph node, and bone marrow), the overwhelming distribution of neoplastic lymphocytes was within vessels, with comparatively little involvement of the organ parenchyma, suggesting the diagnosis of intravascular lymphoma. Additionally, leukemia was not identified previously while this animal was having neurologic signs, which presumably were due to intravascular lymphoma, thrombosis and infarction. It was uncertain if this animal was leukemic at the time of death, as no bloodwork was done at the UF VMC. The absence of neoplastic lymphocytes in peripheral blood smears in these dogs makes antemortem diagnosis extremely difficult and the diagnosis was made antemortem in a single dog in this study.[1]

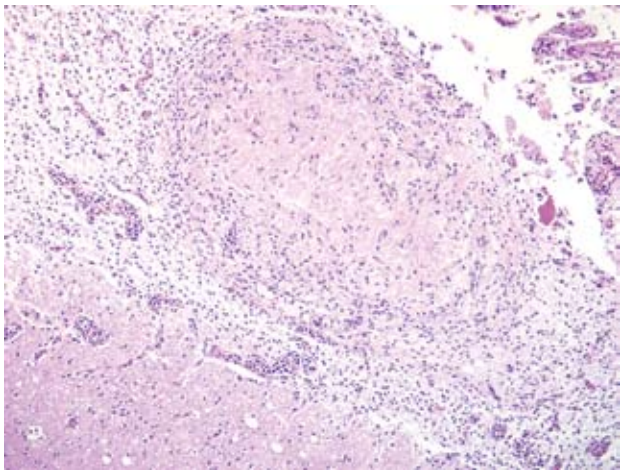

*3-2. Cerebrum, dog. In some sections there is an unusual well demarcated focus composed of a central core of coagulative necrosis bounded by numerous fibroblasts and glial cells, interpreted as a sequestrum. (HE 100X)*

**AFIP Diagnosis:** Brain, cerebrum: Intravascular lymphoma, with fibrin thrombi and multifocal infarcts

**Conference Comment:** In addition to the diagnosis listed above, some but not all sections contain an interesting well-demarcated focus within an area of rarefaction. This nodular focus is composed of a central core of coagulative necrosis bounded by numerous fibroblasts and glial cells, interpreted as a sequestrum **(Fig. 3-2)**.

The majority of cases of intravascular lymphoma in humans can be placed into four distinct presentations: 1) central nervous system form, 2) cutaneous form, 3) fever of unknown origin, and 4) hemophagocytic form.[4] Most human patients present with neurologic signs, while about 1/3 of human patients present with cutaneous lesions. Cutaneous lesions are not as common in animals with IVL as they are in their human counterparts.[1]

As mentioned by the contributor, most human cases are of B cell origin, while IVL in animals has been shown to be derived primarily from T cells or non-B, non-T lymphocytes with rare cases of B cell tumors.[1] The source of neoplastic cells in IVL is still uncertain, but there is speculation that they may originate from the red pulp of the spleen.[1] The behavior of these neoplasms suggest that initial movement into the bloodstream is possible with subsequent problems related to adhesion and emigration resulting in intravascular accumulations of neoplastic cells as opposed to deposition within organs.[1]

**Contributing Institution:** University of Florida, College of Veterinary Medicine, Department of Infectious Diseases and Pathology, http://www.vetmed.ufl.edu/college/departments/patho/

**References:**

1. McDonough SP, Van Winkle TJ, Valentine BA, van Gessel YA, Summers BA: Clinicopathological and Immunophenotypical features of canine intravascular lymphoma (Malignant Angioendotheliomatosis). J Comp Pathol **126**:277-288, 2002
2. Steinberg, H: Multisystem angiotropic lymphoma (malignant angioendotheliomatosis) involving the humerus in a dog. J Vet Diag Invest **8**:502-505, 1996
3. Xanthopoulos V, Galanopoulos, AG, Paterakis G, Apessou D, Argyrakos T, Goumakou E, Papadhimitriou SI, Savvidou I, Georgiakaki M, Anagnostopoulos NI: Intravascular B-cell lymphoma with leukemic presentation: case report and review of the literature. Eur Jour Haematol, 2007
4. Zuckerman D, Seliem R, Hochberg E: Intravascular Lymphoma: The Oncologist's "Great Imitator." The Oncologist **11**:496-502, 2006

## CASE IV – 07-2223-6 (AFIP 3106259)

**Signalment:** 4-year-old, castrated male, Border Collie, (*Canis familiaris*), canine

**History:** The dog presented to OSU Small Animal Services for evaluation of progressive neurologic disease of two weeks duration. Initially, the left pupil was dilated and the dog was diagnosed with and treated for anterior uveitis. One and a half weeks later, the dog's condition rapidly deteriorated with the onset of weakness, lethargy, anorexia, and disorientation.

**Gross Pathology:** The dog was in good body condition. There were no significant gross lesions of the thoracic, abdominal viscera, or eyes. There was a 3 x 2.5 cm soft, grayish-tan, fixed mass ventral to the thalamus which surrounded the optic chiasm and extended from the ventral temporal lobe rostral to the chiasm to the level of cranial nerve V caudally. Following formalin fixation and sectioning, the mass extended 3-4 cm into the overlying brain parenchyma, involving approximately the ventral third of the brain. The majority of the mass was positioned to the left of midline, causing deviation of normal structures to the right.

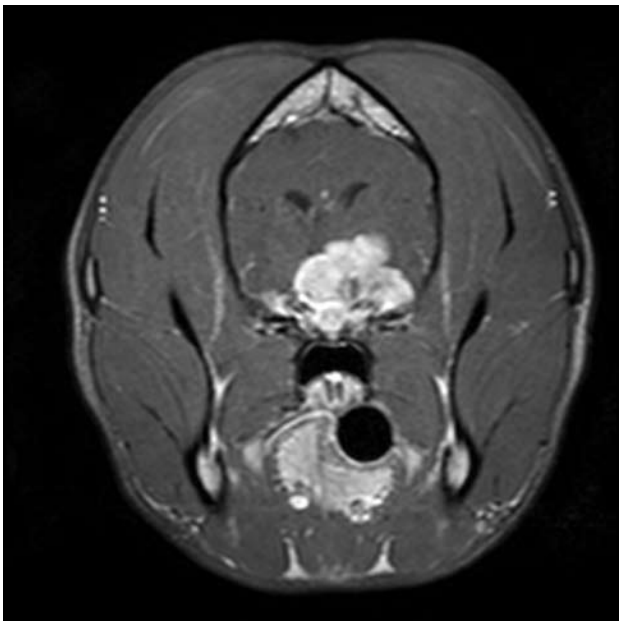

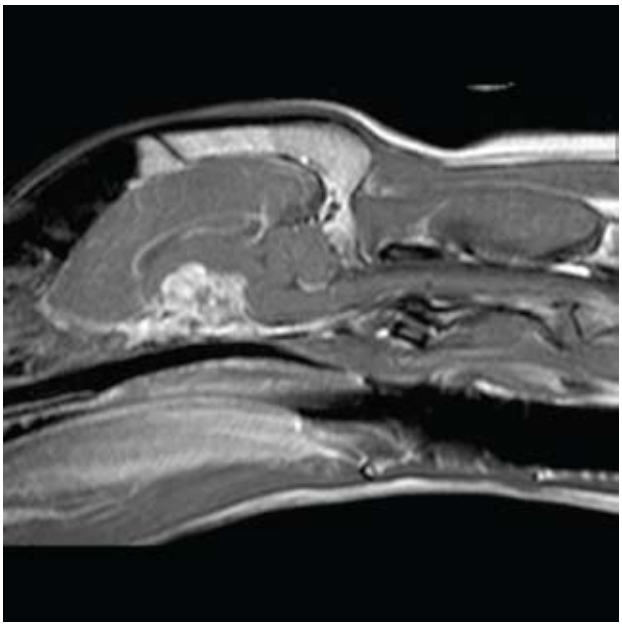

*4-1., 4-2. Computed tomography, skull, dog. There is a contrast-enhancing extra-axial mass ventral to the thalamus which displaces the thalamic parenchyma and third ventricle dorsally and to the right.* *Images courtesy of Department of Veterinary Biosciences, The Ohio State University, 1925 Coffey Road, Columbus Ohio 43210.*

**Laboratory Results:**

- **CBC/Profile:** No abnormalities noted (performed by the referring veterinarian).
- ***Borrelia burgdorferi* titer:** Positive (performed by an emergency clinic, thought to be due to previous vaccination).
- **Cranial MRI:** Contrast-enhancing extra-axial mass ventral to the thalamus with dorsal displacement of adjacent structures. Meningioma suspected (performed by OSU) **(Figs. 4-1, 4-2)**.
- **Cerebrospinal fluid analysis:** Mildly elevated protein levels and red blood cell count (performed by OSU).

**Histopathologic Description:** Diencephalon at optic chiasm. There is focally extensive infiltration of the ventral thalamus by a sharply demarcated but unencapsulated, multinodular, hypercellular mass. The mass is an admixture of cells exhibiting three distinct morphologies: 1) small round to polyhedral ("germinal") cells with scant amphophilic cytoplasm which form dense packets separated by a thin fibrous stroma reminiscent of seminoma **(Fig. 4-3)**, 2) large polygonal ("hepatoid") cells with abundant brightly eosinophilic cytoplasm which form broad sheets of anastomosing chords and which contain one or more large discrete clear cytoplasmic vacuoles that marginate the ovoid vesicular nuclei of the cells **(Fig. 4-4)**, and 3) large, closely-adherent polygonal ("epithelial") cells with abundant eosinophilic cytoplasm and central round to ovoid vesicular nuclei which form irregular smaller sheets and chords **(Fig. 4-5)**, and exhibit occasional squamoid differentiation **(Fig. 4-6)**. Neoplastic cells of all three types exhibit a wide range of anisocytosis, anisokaryosis, and nucleoli of variable number and size. The epithelial cells occasionally keratinize and form small concentric whorls of keratin (keratin pearls). There are multifocal areas of coagulation necrosis-characterized by loss of differential staining, pyknosis, and karyorrhexis with accumulation of amorphous cellular and nuclear debris- and hemorrhage within the mass. Neoplastic cells, mainly of the hepatoid type, also appear to produce small lakes of homogeneous eosinophilic material (colloid) multifocally (not present in all sections). Mitotic figures are rare (<1 per 40 x field) though they are more common within the germinal neoplastic cell population than elsewhere. Occasional abnormal mitotic figures are noted. Brain tissue immediately adjacent to the mass is markedly compressed and has mild multifocal hemorrhage. There is no evidence of vascular invasion or of ventricular involvement (ventricle not present in all sections).

Regions of the neoplasm comprised of the epithelial and hepatoid cell populations were cytokeratin positive by immunohistochemistry.

**Contributor's Morphologic Diagnosis:** Diencephalon at optic chiasm: Suprasellar (Perichiasmatic) germ cell tumor with necrosis, hemorrhage, and local tissue invasion and compression

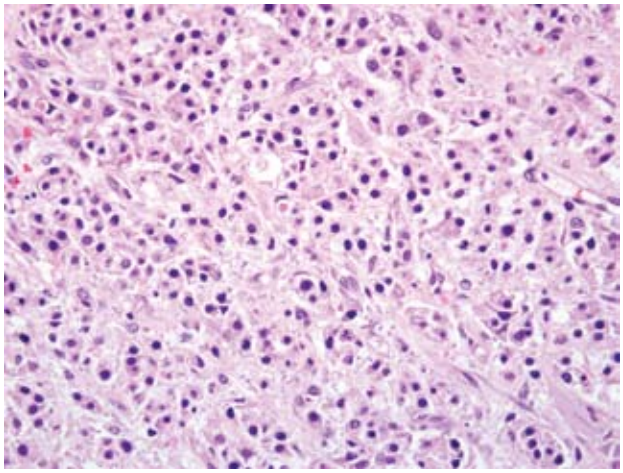

*4-3. Cerebellum, dog. Suprasellar germ cell tumor, one of three distinct cell populations within the neoplasm. Nests and packets of round to polygonal cells which have scant eosinophilic cytoplasm separated by a fine fibrovascular stroma. (HE 400X)*

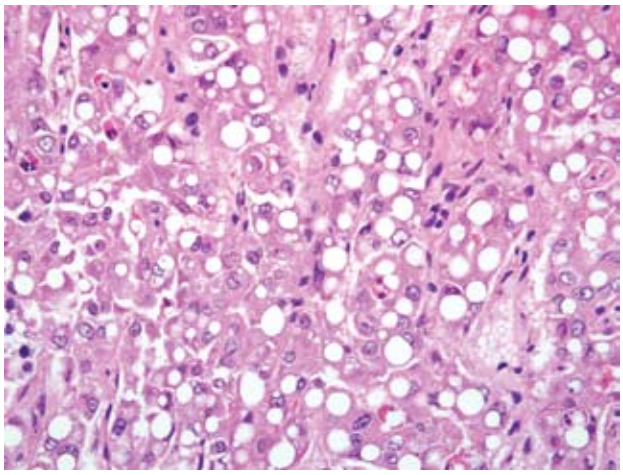

*4-4. Cerebellum, dog. Suprasellar germ cell tumor, one of three distinct cell populations within the neoplasm. Anastomosing cords of polygonal cells with abundant brightly eosinophilic cytoplasm which frequently contain one or more large discrete clear vacuoles that marginate the vesiculate nucleus. (HE 400X)*

**Contributor's Comment:** The diagnosis of suprasellar germ cell tumor was made based upon the location and upon the presence of three diverse neoplastic cell populations within the tumor. Intracranial germ cell tumors can also occur within the pineal gland.[4,5] Human variants are further classified as seminoma, choriocarcinoma, entodermal sinus tumor, or teratoma based upon additional microscopic features of the tumor.[3] The cell of origin is presumed to be ectopic embryonic germ cells that have failed to migrate from the yolk sac to the developing gonad.[4,5] The neoplastic germ cells develop three distinct populations based upon morphology and growth pattern which are characteristic for intracranial germ cell tumors: 1) pleomorphic cells which form nests and sheets reminiscent of seminomas (Germinomatous cells) 2) large polygonal cells with abundant cytoplasm which contain lipid vacuoles and form nests (Hepatoid cells), and 3) epithelial cells reminiscent of intestinal or respiratory epithelium which can exhibit acinar, tubular, or squamoid differentiation and frequent keratinization.[1,2,3,5] Epithelial elements are thought to represent teratomatous change within the tumor.[4] Colloid-containing follicles were a minor component in this case and mineralization which is common in intracranial germ cell tumors was not present.[1,4] The epithelial elements of the tumor in this case were positive for cytokeratin by immunohistochemistry. The neoplastic cells within suprasellar germ cell tumors are also reported to exhibit positive a-fetoprotein staining by immunocytochemistry.[4,5] Clinically, middle-aged dogs are most commonly affected by this rare tumor, with breed predisposition in Doberman Pinschers.[5] Neurologic signs are acute in nature and are most commonly those of cranial nerve involvement (CN III and IV most frequently exhibit deficits, though CNII – XI may be involved) and/or thalamic compression (lethargy and stupor), both of which were present in this case.[5]

**AFIP Diagnosis:** Brain, diencephalon at the level of the optic chiasm: Suprasellar germ cell tumor

**Conference Comment:** Extragonadal germ cell tumors are uncommon in both domestic animals and humans.[5] Due to their location and pattern, suprasellar germ cell tumors must be distinguished from pituitary adenomas and craniopharyngiomas.[3] Germ cell tumors generally arise in either the pineal gland or next to the sella turcica.[5] In man, most tumors occur in the pineal region, in contrast to the [predominately suprasellar location in dogs.[5] In humans, in addition to staining for alpha-fetoprotein, these tumors also often stain with human chorinonic gonadotropin, and placental alkaline phosphatase.[5]

Grossly, these tumors are usually very large, gray to white, extramedullary masses attached to the ventral aspect and often compressing the diencephalon.[5] Often admixed within the trivariant neoplastic cells are aggregates of lymphocytes that form small accumulations within the neoplasm.[5]

**Contributing Institution:** Department of Veterinary Biosciences, College of Veterinary Medicine, The Ohio State University, Columbus, OH, http://vet.osu.edu/

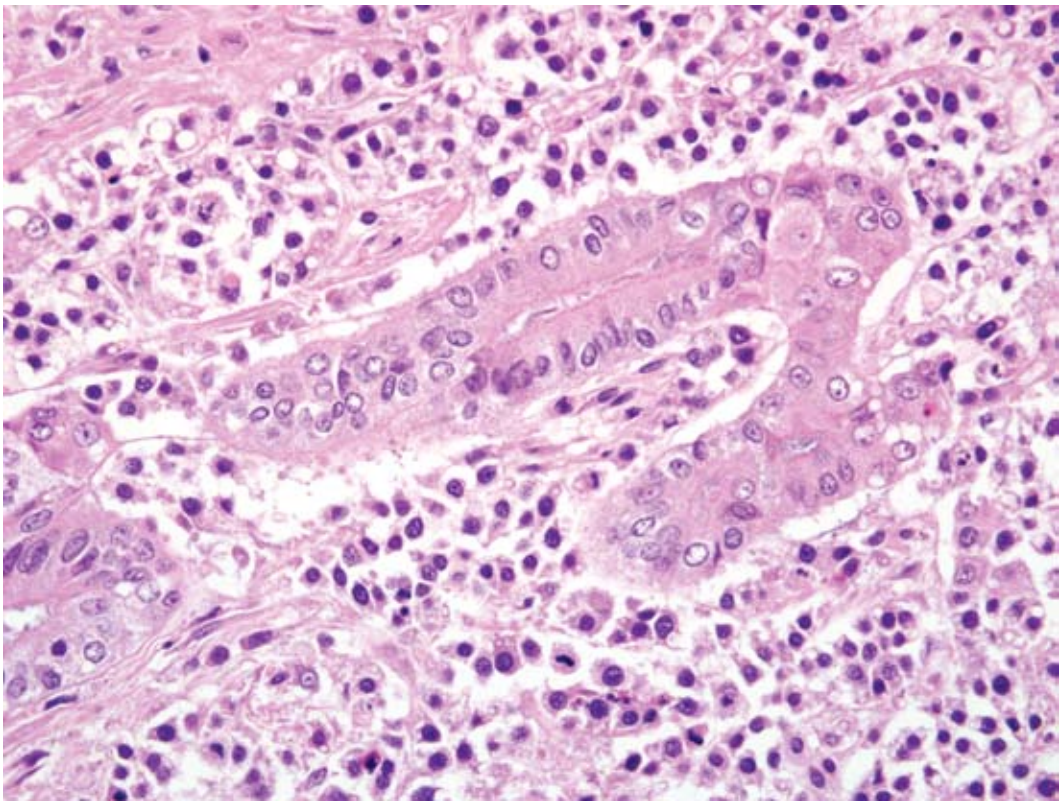

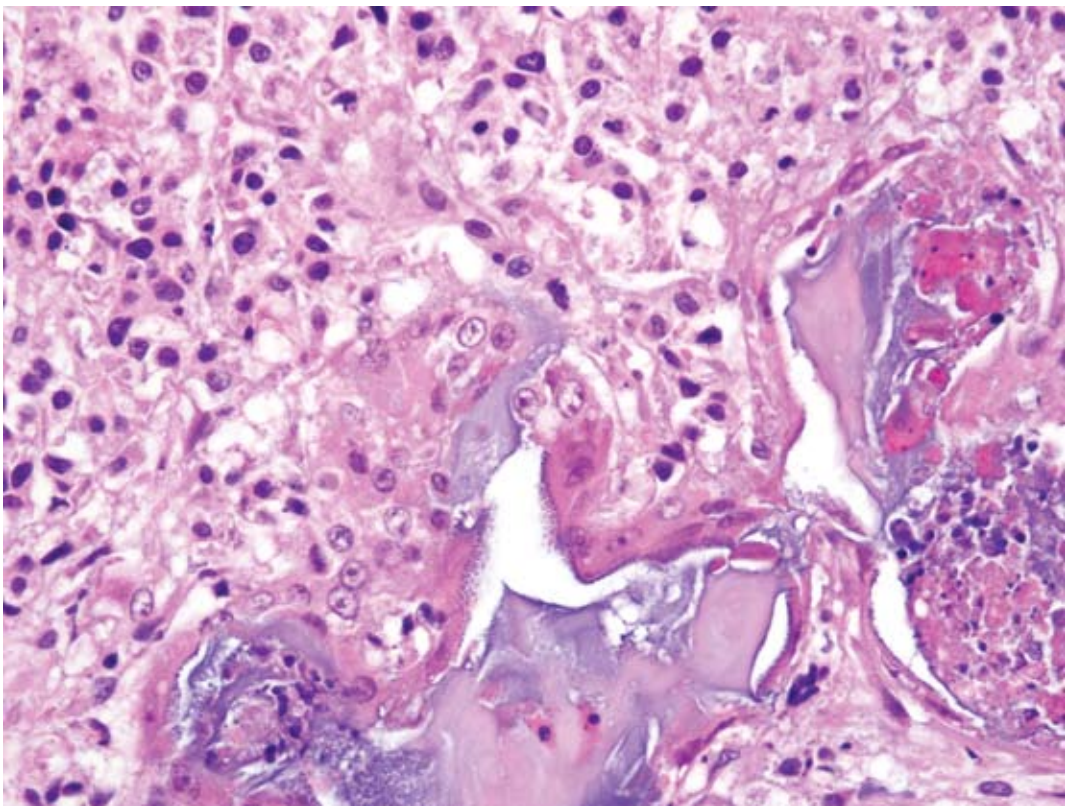

*4-5, 4-6. Cerebellum, dog. Suprasellar germ cell tumor, one of three distinct cell populations within the neoplasm. Cords and tubules of closely adherent polygonal (epithelial) cells which have abundant eosinophilic cytoplasm and occasionally undergo squamous differentiation (demonstrated in figure 4-6 below). (HE 400X)*

biosciences.htm

**References:**

1. Capen, CC: Endocrine glands. *In:* Pathology of Domestic Animals, Volume 3, eds. Jubb KVF, Kennedy PC, Palmer N, 4th ed., pp. 346-347, Academic Press, Inc., San Diego, CA, 1993
2. Koestner, A, Bilzer T, Fatzer A, Schulman FY, Summers BA, Van Winkle TJ: Histological classification of tumors of the nervous system of domestic animals. pp.32-34, Armed Forces Institute of Pathology, Washington, DC, 1999
3. Maxie, MG, Youssef S: Nervous system. *In:* Pathology of Domestic Animals, Volume 1, eds. Jubb KVF, Kennedy PC, Palmer N, 4th ed., pp. 454, Academic Press, Inc., San Diego, CA, 1993
4. Meuten, DJ: Tumors in domestic animals. 4th Ed, pp. 623-623, 728. Iowa State Press, Ames, Iowa, 2002
5. Summers, BA, Cummings JF, de Lahunta A: Veterinary Neuropathology. pp. 384-386. Mosby-Year Book, Inc., 1995

The Armed Forces Institute of Pathology
Department of Veterinary Pathology

*Conference Coordinator:*
Todd M. Bell, DVM

WEDNESDAY SLIDE CONFERENCE 2008-2009

# Conference 23

22 April 2009

***Conference Moderator:***

**Dr. Don Nichols, DVM, Diplomate ACVP**

## CASE I – 060536-20 (AFIP 3113832)

**Signalment:** Adult male African green monkey (*Chlorocebus aethiops*). All monkeys described in this report were maintained in a facility at the US Army Medical Research Institute of Infectious Diseases accredited by the American Association for Accreditation of Laboratory Animal Care. All research was conducted under approved animal protocols in adherence with the Guide for the Care and Use of Laboratory Animals (Committee on Care and Use of Laboratory Animals of the Institute of Laboratory Animal Resources, National Research Council, National Institutes of Health Publication No. 86–23, revised 1996).

**History:** The African green monkey (AGM) was received at our facility on 13 June, 2003 and in good condition. ITS telemetry surgery was performed on 1 March 2006 and the AGM recovered without incident. The next month, on 18 April 2006, prior to being placed into biocontainment, a routine physical examination was performed. An 8- to 10-cm-diameter mass was found on the right dorsal flank. No other abnormal findings were observed at the time. Within 24 hours of initial discovery, the fluid-filled mass ruptured and was draining a thick, mucoid discharge. The abscess was cultured, surgically debrided and lavaged, a Penrose drain was placed, and antibiotic treatment was initiated. An abdominal mass was palpated 24 hours following surgery and was described as a 3 cm by 1 cm irregularly shaped, firm mass in the cranial abdomen. The mass enlarged over several days, and exploratory laparotomy revealed mesenteric abscesses centered at the ileocecocolic junction and also involving the duodenum, ileum, cecum, colon, the right ureter, and the body wall inferior to the right kidney. Surgical removal was not possible, and the animal was euthanatized.

**Gross Pathology:** The most significant findings at necropsy were chronic pyogranulomatous peritonitis and polyserositis; chronic pyogranulomatous panniculitis of the right flank (surgical abscess site); and a defect in the abdominal wall subjacent to the panniculitis. There were multiple fibrous adhesions present in the cranial abdomen. Buried within these adhesions were multiple chronic abscesses that sometimes contained a viscous fluid. Serosal and mesenteric adhesions enveloped and intertwined loops of small and large bowel, adhered to the right ureter and kidney, and extended into the retroperitoneal space with fingerlike projections. The abdominal wall inferior to the subcutaneous lesion of the right flank was disrupted, or breached, and an abdominal fibrous band of tissue was present extending to the cecum.

*Sponsored by the American Veterinary Medical Association, the American College of Veterinary Pathologists, and the C. L. Davis Foundation.

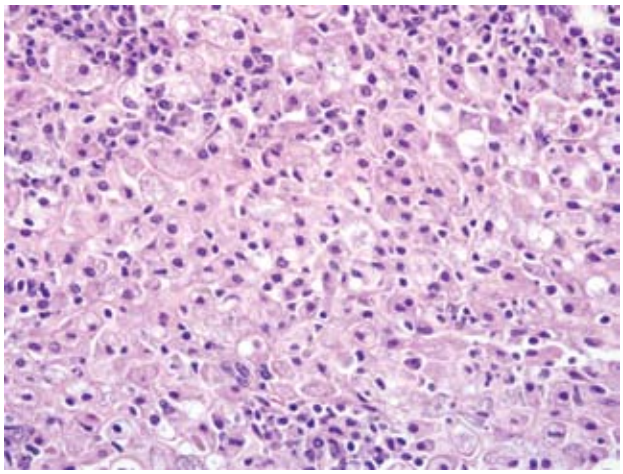

*1-1. Mesentery, African Green Monkey. Expanding the mesentery is a cellular infiltrate composed of numerous epithelioid macrophages with abundant foamy vacuolated cytoplasm admixed with fewer neutrophils, lymphocytes and plasma cells. (HE 400X)*

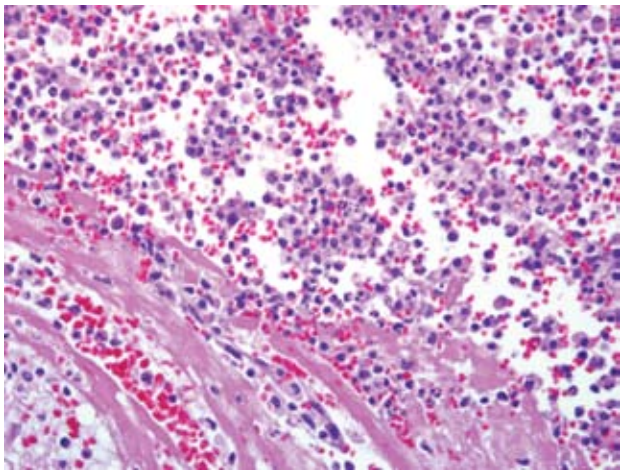

*1-2. Lymph node, African Green Monkey. Effacing normal nodal architecture are large swaths of fibrin, necrosis, pyogranulomatous cellular infiltrate, and abundant hemorrhage. (HE 400X)*

**Laboratory Results:** Bacteria in the abscess fluid were identified as *Klebsiella pneumoniae* by routine culture and biochemical methods and were further characterized as *K. pneumoniae* subsp. pneumoniae serotype K2 by capsular serotyping using a slide agglutination technique.[1] Furthermore, bacterial colonies plated on a blood agar plate exhibited a hypermucoviscosity phenotype, as demonstrated by a positive string test (formation of a 0.5 mm mucoviscous string when a loop is passed through a colony). Genetic analysis of the sequence of a 760-bp amplicon of the bacterial 16S rRNA from the isolate was submitted to a basic local alignment search tool search and found to be 99% identical to several *K. pneumoniae* entries. Additional analysis for 2 novel genes, magA (mucoviscosity-associated gene A) and rmpA gene (regulator of the mucoid phenotype) suggested as potential hypermucoviscosity-associated genes in human cases, was performed by PCR using previously described primers.[8] The bacterial isolate from this case was positive for the rmpA gene and was negative for the magA gene.[6]

**Histopathologic Description:** Diffusely, the serosa of the small intestine (ileum at ileocecocolic junction) and mesentery are greatly expanded by broad bands of fibrous tissue that strongly adhere mesentery and serosa into a mass. There are mesenteric lymph nodes surrounded and entrapped by fibrous tissue. Interspersed sporadically within the fibrous tissue are abscesses composed primarily of macrophages that contain abundant cytoplasm, fewer lymphocytes and plasma cells, rare neutrophils, cellular debris, and sometimes hemorrhage **(Fig. 1-1)**.

Select mesenteric lymph nodes are multifocally expanded and disrupted by large numbers of macrophages that contain abundant cytoplasm, cellular and karyorrhectic debris, edema, and hemorrhage **(Fig. 1-2)**.

The mucosa of the small intestine is multifocally eroded. Occasionally cellular debris may be found in the lumen and in the submucosa. Lymphocytes and plasma cells mildly expand the submucosa. There are moderate numbers of bacilli multifocally within the lumen, on the surface of erosive areas, and invading the mucosa and submucosa.

**Contributor's Morphologic Diagnosis:** 1. Mesentery and ileum: Peritonitis and serositis, histiocytic, chronic, multifocal, marked, with fibrosis, necrosis, and rare hemorrhage, African green monkey (*Chlorocebus aethiops*)

2. Lymph node, mesenteric: Lymphadenitis, histiocytic, subacute, multifocal, moderate, with necrosis and hemorrhage

3. Small Intestine: Enteritis, erosive, multifocal, mild to moderate, with bacilli

**Contributor's Comment:** Within a year and 5 months, six additional AGM with clinical and pathologic features similar to the AGM described here, were positively diagnosed with K. pneumoniae by bacterial culture and/or immunohistochemistry. Clinical signs in these additional monkeys varied from none to palpable abdominal masses

noted during routine clinical examination. One monkey was found dead in its cage with no premonitory clinical signs. All seven affected monkeys were either housed within, or were in contact with monkeys housed within, one animal room in our facility.

*Klebsiella pneumoniae* is a gram-negative, aerobic, nonmotile bacillus and is a common cause of a wide range of infections in humans and animals.[6] Our differential diagnosis for Gram-negative pathogens in nonhuman primates included, but were not limited to, *Yersinia enterocolitica* (forms large colonies in tissues, which were not present in our cases), *Shigella* sp. (*S. dysenteriae, S. Flexneri, S. boydii, S. sonnei*), *Campylobacter* sp. *(C. jejuni, C. coli), Salmonella* sp. *(S. typhimurium, S. Dublin, S. enteriditis, S. Stanley*). In Old and New World monkeys, infection with K. pneumoniae causes pneumonia, meningitis, peritonitis, cystitis, and septicemia.[9] *K. pneumoniae* also constitutes normal fecal and oral flora in many nonhuman primates. In the past two decades, a new type of invasive *K. pneumoniae* disease has emerged in humans in Taiwan and other Asian countries, and more recently from non-Asian countries, including the USA.[3,4,5,7] Fatal human infections with invasive strains of K. pneumoniae involve pulmonary emboli or abscess, meningitis, endophthalmitis, osteomyelitis, or brain abscess. Recently, a highly invasive *K. pneumoniae* causing primary liver abscesses in humans has also been reported.[3] These invasive, abscess-forming strains of *K. pneumoniae* are associated with the so-called hypermucoviscosity (HMV) phenotype, a bacterial colony trait identified by a positive string test.[4,5,6] The HMV phenotype is seen in *K. pneumoniae* expressing either the capsular serotypes K1 or K2. K1 serotypes of *K. pneumoniae* have two potentially important genes, rmpA, a transcriptional activator of colanic acid biosynthesis, [10] and magA, which encodes a 43-kD outer membrane protein. Five K2 serotypes of *K. pneumoniae* also have rmpA but do not have magA. Capsular serotypes K1 and K2 are reported to play an important role in the invasive ability of HMV *K. pneumoniae*.[3,10] The role of rmpA and magA in the pathogenesis of invasive *K. pneumoniae*, however, seems less certain. *K. pneumoniae* expressing the HMV phenotype has not been reported to cause natural disease in nonhuman primates, nor in other animal species.

The means by which the causative *K. pneumoniae* may have spread or caused disease in individual monkeys in our colony is unknown. The only significant epidemiologic factor we identified was that affected monkeys were maintained in the same room or had contact with a monkey housed in that room. African green monkeys may be quite susceptible to invasive *K. pneumoniae* infection. Therefore, veterinarians, laboratory workers, and research pathologists should be aware of this pathogen as a cause of abdominal masses and multisystemic abscessation in the AGM. In addition, the AGM may provide another useful animal model to understand the pathogenesis of this emerging human pathogen.

**AFIP Diagnosis:** 1. Ileocecocolic junction: Serositis and peritonitis, granulomatous, multifocal to coalescing, severe with marked fibrosis
2. Lymph node, mesenteric: Lymphadenitis, pyogranulomatous, diffuse, severe

**Conference Comment:** The abundant foamy material within macrophages was discussed during the conference. Dr. Nichols speculated that the foamy material within macrophages may be phagocytized mucus which the Klebseilla bacteria have produced. He also mentioned it is important to rule out mycobacterial causes when macrophages of this type are present in a lesion. In this case, an acid-fast stain was done and was negative.

In domestic animals, *Klesiella pneumonia* is the cause of numerous maladies. In foals, *K. pneumoniae* is a common cause of neonatal septicemia and pneumonia.[1,2] *K. pneumoniae* has also been commonly implicated in equine abortions.[8]

**Contributing Institution:** USAMRIID, Pathology Division, 1425 Porter Street, Ft. Detrick, MD

**References:**

1. Brown CC, Baker DC, Barker IK: Alimentary system. *In:* Jubb, Kennedy, and Palmer's Pathology of Domestic Animals, vol 3 ed. Maxie MG, pp. 507. Elsevier Limited, Philadelphia, PA, 2007
2. Caswell JL, Williams KJ: *In:* Jubb, Kennedy and Palmer's Pathology of Domestic Animals, ed. Maxie MG, 5th ed., pp. 632. Elsevier, Philadelphia, Pennsylvania, 2007
3. Chuang YP, Fang CT, Lai SY, Chang SC, Wang JT: Genetic determinants of capsular serotype K1 of *Klebsiella pneumoniae* causing primary pyogenic liver abscess. J Infect Dis **193**:645–654, 2006
4. Fang CT, Chuang YP, Shun CT, Chang SC, Wang JT: A novel virulence gene in *Klebsiella pneumoniae* strains causing primary liver abscess and septic metastatic complications. J Exp Med **199**:697–705, 2004
5. Fang FC, Sandler N, Libby SJ: Liver abscess caused by magA+ *Klebsiella pneumoniae* in North America. J Clin Microbiol **43**:991–992, 2005
6. Kawai T: Hypermucoviscosity: an extremely sticky phenotype of *Klebsiella pneumoniae* associated with emerging destructive tissue abscess syndrome. Clin Infect Dis **42**:1359–1361, 2006

7. Rahimian J and JT Wang: The Emerging Role of Klebsiellae in Liver Abscess. *In:* Emerging Infections, eds. Scheld WM, DC Hooper, and JM Hughes, pp. 199-211. ASM Press, Washington, DC, 2007
8. Schlafer DH, Miller RB: Female genital system. *In:* Jubb, Kennedy, and Palmer's Pathology of Domestic Animals, vol 3 ed. Maxie MG, pp. 507. Elsevier Limited, Philadelphia, PA, 2007
9. Twenhafel NA, Whitehouse CA, Stevens EL, Hottel HE, Foster CD, Gamble S, Abbott S, Janda JM, Kreiselmeier N, Steele KE: Multisystemic abscesses in African green monkeys (*Chlorocebus aethiops*) with invasive *Klebsiella pneumoniae*-identification of the hypermucoviscosity phenotype. Vet Pathol **45**:2, 2008
10. Yu WL, Ko WC, Cheng KC, Lee HC, Ke DS, Lee CC, Fung CP, Chuang YC: Association between rmpA and magA genes and clinical syndromes caused by *Klebsiella pneumoniae* in Taiwan. Clin Infect Dis :1351–1358, 2006

## CASE II – L08-2351 (AFIP 3103348)

**Signalment:** Adult, female, South African-clawed frogs (*Xenopus laevis*)

**History:** This frog belonged to a colony of female South African-clawed frogs, the ova of which were used for cell-cycle research purposes. The frogs were obtained from a commercial vendor and were originally laboratory-bred. The investigator had reported "red leg," lethargy, and sudden unexpected mortalities of a few of the frogs. This was one of 5 frogs submitted dead (and frozen) for pathologic investigation.

**Gross Pathology:** This 135 g female South African-clawed frog presented dead in lean body condition and good but frozen post mortem condition (mild autolysis). There was marked erythema of the entire ventral surface of the frog, and diffusely, the skin easily sloughed off. All other organs and tissues were within normal gross limits.

**Laboratory Results:** No growth was obtained from bacterial cultures of the skin and heart blood from all 5 frogs.

**Histopathologic Description:** Sections of skin are examined, revealing marked epidermal hyperplasia (characterized predominantly by acanthosis) associated with presence of cross-, tangential, and longitudinal sections of aphasmid adult nematodes that lie within tortuous intraepidermal tunnels **(Fig. 2-1)**. The aphasmid adult nematodes are approximately 25 to 50 microns in diameter, and possess a thin smooth external cuticle with hypodermal bacillary bands and unapparent musculature that surround a pseudocoelom that may contain an esophagus encased by a stichosome, and a single often gravid uterus. The eggs are roughly ovoid, approximately 25 to 35 microns in diameter, and may or may not be embryonated. Additionally within the tunnels (with or without associations with the adult nematodes), small numbers of embryonated eggs, small numbers of heterophils, small amounts of amorphous eosinophilic cellular debris, and small colonies of basophilic coccobacilli are seen. There is also separation of epidermis from underlying dermis with or without complete loss of overlying epidermis. There is a mild, multifocal, heterophilic and lymphocytic infiltrate in the underlying stratum spongiosum, and superficial vessels within the stratum spongiosum are distended with moderate numbers of heterophils.

**Contributor's Morphologic Diagnosis:** Skin: epidermal hyperplasia, diffuse, marked, chronic with mild heterophilic and lymphocytic chronic-active dermatitis, and intraepidermal adult aphasmid nematodes and embryonated eggs (consistent with *Capillaria xenopodis*/*Pseudocapillaria xenopi*)

**Contributor's Comment:** All 5 South African-clawed frogs examined from this investigation were infected with *Capillaria xenopodis*/*Pseudocapillaroides xenopi*, which is an aphasmid nematode.

In general, the key histologic characteristics of aphasmid nematodes include a thin smooth external cuticle with hypodermal bacillary bands, unapparent musculature, an esophagus encased by a stichosome, and presence of a single uterus in females.[1] Additional specific microscopic features of *Capillaria xenopodis*/*Pseudocapillaroides xenopi* include sexual dimorphism (females are 4 times longer and 2 times wider than males), and the presence of unembryonated and embryonated eggs within the uterus (as opposed to presence of only unembryonated eggs in other aphasmid nematodes).[4]

*Capillaria xenopodis*/*Pseudocapillaroides xenopi* is the only reported nematode parasite of the epidermis of South African-clawed frogs, and is potentially a significant cause of morbidity and mortality in populations of South African-clawed frogs in the laboratory setting. Clinically, a small proportion of infected frogs in a laboratory animal population will display signs of *Capillaria xenopodis*/*Pseudocapillaroides xenopi* infection, which is often characterized as a nonspecific "wasting syndrome" (often lasting 3 to 4 months) that may include one or more of the following signs: lethargy, anorexia, skin color change,

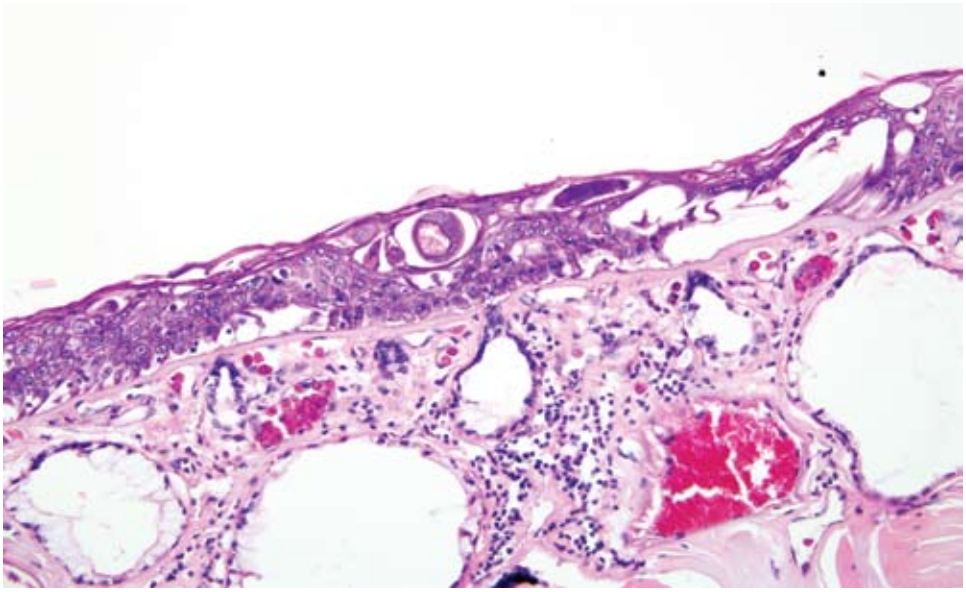

*2-1. Skin, Xenopus frog. Diffuse epidermal hyperplasia up to two times normal thickness and numerous cross and tangential sections of adult and larval nematodes. (HE 400X)*

rough "flaky" skin, decreased egg production in females, and unexpected death. Often the first sign of this syndrome is the presence of large fragments/"flakes" of desquamated epithelium in the tank water.[3]

Histologically, *Capillaria xenopodis*/*Pseudocapillaroides xenopi* infection is characterized by profound epidermal hyperplasia (and variable associated epidermal/dermal inflammation) along with the presence of the nematodes and eggs in tunnels within the epidermis. This epidermal hyperplasia is thought to cause significant impairment of normal epidermal functions that result in overall debilitation and/or death of the animal. Specifically, the normal respiratory and metabolic functions (including gas exchange, waste removal, and osmotic balance) of the skin are compromised. Additionally, the normal physical barrier of the skin is compromised, often allowing for localized secondary skin infections and septicemia (including infection by Gram-negative bacteria, such as *Aeromonas hydrophila*, the cause of "red leg").[3]

Diagnosis of infection can be made by direct examination of unstained skin sections (including the desquamated "flakes" in the tank water), and histopathology.

*Capillaria xenopodis*/*Pseudocapillaroides xenopi* has a direct lifecycle, with all stages of the lifecycle completed within the epidermis of the skin. Because of the direct lifecycle, autoinfection is also possible.[3] Levamisole has been described as an effective treatment for *Capillaria xenopodis*/*Pseudocapillaroides xenopi* infection in laboratory South African-clawed frogs.[2]

Other aphasmid parasites that primarily infect and cause hyperplasia of epidermal/epithelial surfaces include: *Capillaria* spp. (*C. annulata, C. contorta, C. obsignata*) in the crop and esophagus of birds; *Capillaria philippinensis* in the small intestines of humans; *Capillaria bohmi* in the nasal mucosa of canids; *Trichosomoides crassicauda* in the urinary bladder of rats; *Anatrichosoma* spp. of the skin and nasal mucosa of primates; and *Gongylonema* spp. in the nasal mucosa, oral mucosa, and esophagus of primates and cattle.

**AFIP Diagnosis:** Skin: Epidermal hyperplasia, diffuse, marked with multifocal degeneration and necrosis, orthokeratotic hyperkeratosis and intraepidermal aphasmid nematodes

**Conference Comment:** African clawed frogs are found in several areas of Africa south of the Sahara. They are aquatic frogs with several distinct anatomic features including a flattened head and body but no external ear or tongue.[3] Because these frogs have no tongue, they use their unwebbed fingers or front feet to push food into their mouths. Their hind feet are webbed and the inside three toes of each foot have claws from which their name is derived.[3] They can also change color to match that of their environment and they have a lateral line system similar to fish.[3] These frogs are commonly used in biomedical research, so a cursory understanding is important to be able to interpret potential lesions.

Dr. Nichols discussed several aspects of amphibian skin during the conference, and it was noted that the skin of this animal was markedly hyperkeratotic and hyperplastic. Dr. Nichols opined that frog skin should not be more

than a few cell layers thick with sparse to unnoticeable keratin. He also pointed out that frogs perform several physiologic processes with their skin to include respiration, thermoregulation, and electrolyte homeostasis. Due to this complex interaction with the external environment, it is easy to speculate that this type of skin lesion would be enough to cause mortality. Dr. Nichols also referenced the large serous glands containing eosinophilic secretory product in the dermis and the adjacent mucous glands containing clear to slightly amphophilic flocculent material. These glands combine to provide the slime cover of these aquatic amphibians.

Other aphasmids of note in domestic animals that the contributor did not mention include *Trichuris* sp., *Trichinella* sp., *Dioctophyma* sp., and *Eustrongylides* sp.[1]

**Contributing Institution:** Veterinary Services Center, Department of Comparative Medicine
Stanford School of Medicine, http://med.stanford.edu/compmed/

**References:**

1. Gardiner CH, et al: An Atlas of Metazoan Parasites in Animal Tissues, pp. 40-43. American Registry of Pathology, Washington, DC, USA, 1999
2. Iglauer F, et al: Anthelmintic treatment to eradicate cutaneous capillariasis in a colony of South African clawed frogs (Xenopus laevis). Lab Anim Sci 47:477-82, 1997
3. Reptiles & Amphibians, Fact Sheet, African Clawed Frog, National Zoo, http://nationalzoo.si.edu/Animals/ReptilesAmphibians/Facts/FactSheets/Africanclawedfrog.cfm
4. Stephen LC, et al: Epidermal capillariasis in South African clawed frogs (*Xenopus laevis*). Lab Anim Sci **37**:341-344, 1987

## CASE III – 080261-01 (AFIP 3113794)

**Signalment:** Juvenile, undetermined sex, bluegill fish (*Lepomis macrochirus*)

**History:** A group of juvenile bluegill was purchased from a commercial fish hatchery for use in respiratory physiology studies. The fish were then group-housed in a large indoor water tank. Approximately 2 weeks after their arrival in the laboratory, several fish were noted to have white cutaneous nodules on their fins and/or bodies. Three affected fish were removed from the tank, euthanized, and submitted for necropsy.

**Gross Pathology:** A 3 mm diameter, firm, white, multilobulated, exophytic, nodular, cutaneous mass protrudes from the dorsal midline of fish #1 at the cranial margin of the dorsal fin . Three smaller (<1mm) white nodules are present along the dorsocaudal aspect of this fish's dorsal fin. Similar nodules of varying sizes and lobulation are located on the caudal peduncle, anal fin, and ventral midline of fish #2 and the tail fin and ventral midline of fish #3.

**Laboratory Results:** NA

**Histopathologic Description:** A tranverse section of the whole body is present on the slide. The skin overlying the dorsal midline and, in some slides, including the base of the dorsal fin, contains an irregularly shaped nodular dermal mass measuring up to 2 mm in greatest diameter **(Fig. 3-2)**. This mass contains multiple large round to oval cells **(Fig. 3-3)**, measuring up to 350 µm in diameter, each of which has a 2-10 µm thick lightly basophilic hyaline capsule, abundant amounts of flocculent basophilic cytoplasm, and often a single irregularly shaped degenerate karyomegalic nucleus (up to 80 µm in diameter) containing condensed chromatin and a single large nucleolus. Within the cytoplasm of most of these cells, primarily in a subcapsular location, are irregularly shaped basophilic inclusions that often coalesce to form a fine lattice. Multifocally, there is rupture of the cell capsule and/or intracellular infiltration by macrophages and lymphocytes. The dermis between the large cells is diffusely infiltrated by low to moderate numbers of macrophages and lymphocytes. Multifocally, the overlying epidermis is mildly hyperplastic. However, there are also foci of epidermal erosion.

No significant changes are present in other organs of this fish.

**Contributor's Morphologic Diagnosis:** Skin; focal (nodular) dermal fibroblast hypertrophy, severe, with karyomegaly, hyaline capsule formation, basophilic intracytoplasmic inclusions, degeneration, lymphohistocytic inflammation, epidermal hyperplasia, and epidermal erosion

**Contributor's Comment:** All histology slides submitted for this case are from fish #1, and the lesion present is depicted grossly in Figure 3-1. The gross and histologic findings are consistent with the fish disease known as "lymphocystis".[5] The severely hypertrophied dermal fibroblasts with hyaline capsules and basophilic intracytoplasmic inclusions are pathognomonic for this disease and are known as "lymphocystis cells"; an individual cell, which may enlarge up to a million (106) times normal size, appears grossly as a cream-colored nodule or "lymphocyst" measuring up to 2 mm


*3-1. Bluegill. A firm, white, multilobulated exophytic cutaneous mass protrudes from the midline at the cranial aspect of the dorsal fin. Image courtesy of US Army Medical Research Institute of Infectious Diseases, ATTN: MCMR-UIP, 1425 Porter Street, Fort Detrick, MD 21702, donald.k.nichols@amedd.army.mil.*

in diameter.(1) Nodules may occur singly or grouped together in raspberry-like clusters (as in this lesion). These nodules are most commonly seen on the fins and body. Occasionally, the gills, peritoneum, and/or internal organs may be affected.[1,5]

Lymphocystis is a common and widespread disease of teleost fish that has been reported in more than 140 species of freshwater and marine fish.[1] Species in the order Perciformes (which includes bluegill) and order Pleuronectiformes ("flatfish" such as flounder, sole, plaice, and dab) constitute approximately 75% and 10%, respectively, of the species affected.[1]

This disease is caused by infection with lymphocystis disease virus (LDV), which is a DNA virus in the genus Lymphocystivirus of the family Iridoviridae.[3] Currently, there are two recognized species of LDV: LDV-1 and LDV-2.[3] However, there appear to be different strains of the viruses that vary in size and host specificity.[1,5] Viral particles are non-enveloped and display icosahedral symmetry; by transmission electron microscopy (TEM), they usually appear hexagonal and may form paracrystalline arrays within the cytoplasm of infected cells – as seen in one of the lesions removed from fish #3 **(Fig. 3-4)**.

Viral infection may occur through the gills, digestive tract, or skin wounds.[1] Infected fibroblasts soon begin to enlarge; increases in cytoplasm are accompanied by nuclear and nucleolar enlargement.[5] As the cell enlarges, irregularly shaped basophilic cytoplasmic inclusions develop; TEM reveals that these are sites of viral assembly.[1] The characteristic hyaline capsule of a lymphocystis cell appears at approximately the mid-stage of maturation.[5] Cellular degeneration begins with nuclear condensation followed by breakdown of the capsule; infiltrates of macrophages and lymphocytes surround and eventually invade degenerate cells.[5] Rupture of the degenerate cells releases the viral particles which may then infect adjacent fibroblasts or, if released into the environment, infect other fish.[1,5]

Lymphocystis is a benign disease with very low mortality; lesions usually heal completely. However, secondary bacterial or fungal infection of the lesions may result in debilitation and/or death.[1]

Interestingly, the first isolation and in vitro cultivation of LDV was done with samples collected from infected bluegill and the first experimental pathogenesis studies were performed with this fish species.[2] In these studies it was found that for fish kept at 25°C the time from experimental infection to lesion regression was approximately 28 days.[2] In a later study with experimentally infected plaice kept at 10°C, it took 3 months for the lesions to regress.[5]

After the diagnosis of lymphocystis in the three bluegill described above, the following measures were taken to

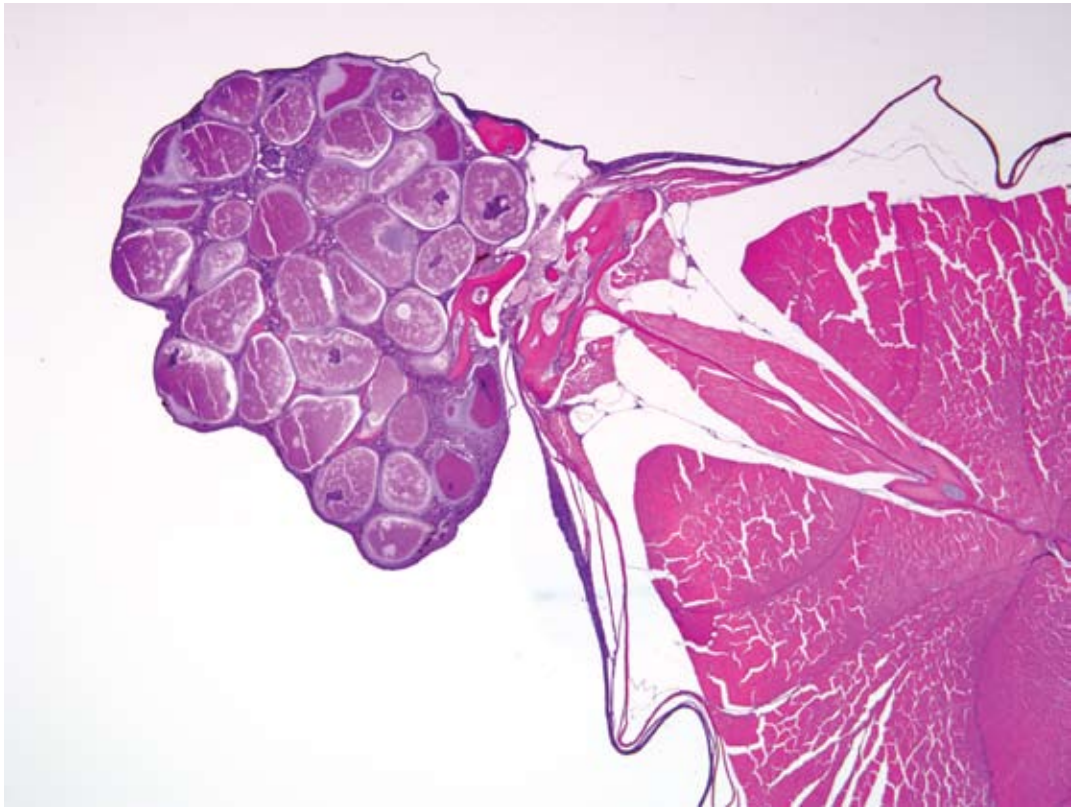

*3-2. Skin, bluegill. The skin overlying the dorsal midline is markedly expanded by a nodular dermal mass measuring 3 mm in diameter which is composed of multiple large round to oval cells. (HE 20X)*

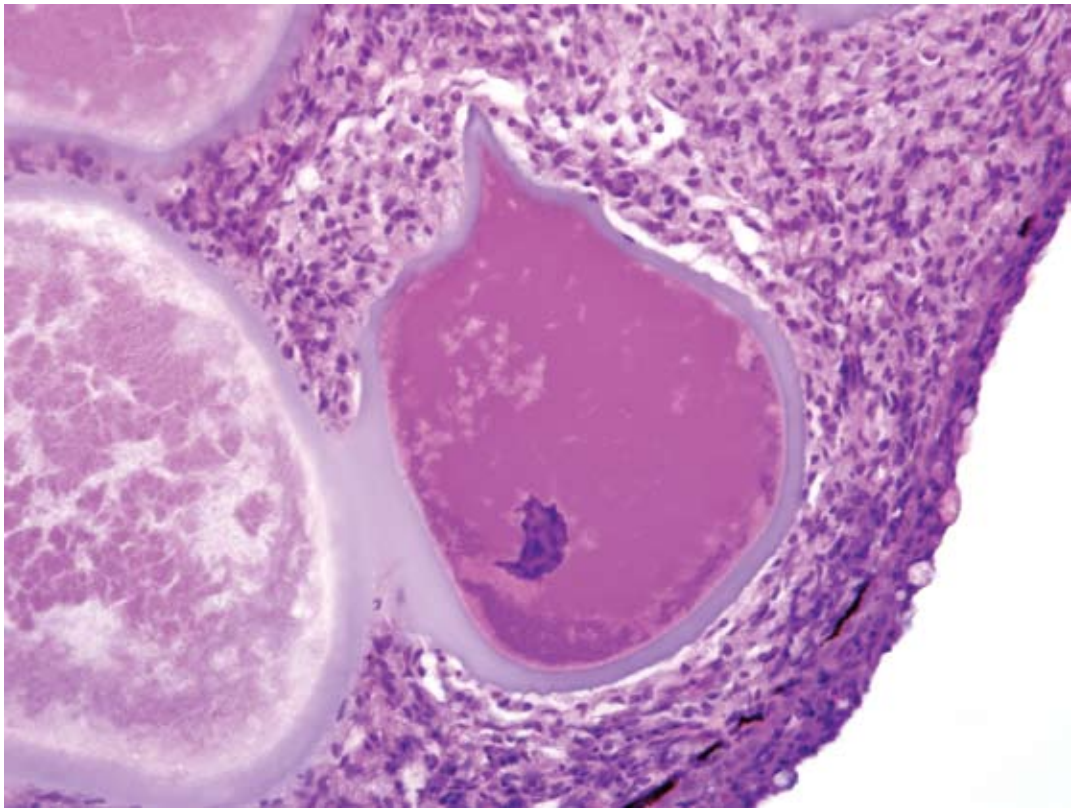

*3-3. Skin, bluegill. Dermal mass is composed of multiple hypertrophied fibroblasts measuring up to 350 um in diameter which have a 2-3 um hyaline capsule, abundant amounts of flocculent amphophilic cytoplasm, irregular basophilic cytoplasmic viral inclusion material, and an irregularly shaped karyomegalic nucleus. The remaining dermis between the hypertrophied cells contains moderate numbers of macrophages and lymphocytes. (HE 400X)*

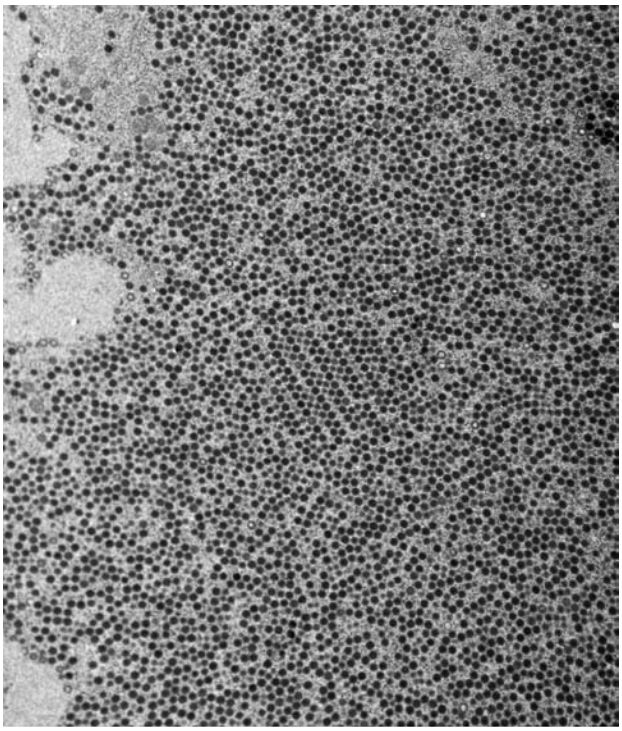

*3-4. Skin, bluegill. The cytoplasm of a fibroblast contains numerous hexagonal viral particles which are arranged in paracrystalline arrays. Electron micrograph courtesy of US Army Medical Research Institute of Infectious Diseases, ATTN: MCMR-UIP, 1425 Porter Street, Fort Detrick, MD 21702 donald.k.nichols@amedd.army.mil.*

control the disease in the remaining group of fish: 1) the fish were closely examined and each one with visible lymphocystis lesions was removed and euthanized; 2) water flow through the holding tank was increased to flush out any viral particles in the tank; and 3) the temperature of the water in the tank was increased to 25°C to enhance the immune function of the fish and inhibit virus "survival" in the tank environment. These control measures were successful; no additional cases of lymphocystis have since been identified in these fish.

**AFIP Diagnosis:** Scaled skin: Fibroblast hypertrophy, nodular, focal with karyomegaly, basophilic cytoplasmic inclusions and moderate lymphoplasmacytic dermatitis

**Conference Comment:** The contributor did an outstanding job of covering all the salient features of lymphocystis. Viruses in the family *Iridoviridae* generally affect fish, amphibians and invertebrates. Within the family there are 5 genera: 1) *Iridovirus* (the iridoviruses); 2) *Chloriridovirus* (large iridescent insect viruses); 3) *Ranavirus* (frog iridoviruses); 4) *Lymphocystivirus* (lymphocystis viruses of fish); and 5) unnamed (goldfish iridoviruses). African swine fever was once considered part of the *Iridoviridae* family, but it has recently been recategorized into its own family.

**Contributing Institution:** US Army Medical Research Institute of Infectious Diseases, Pathology Division, 1425 Porter Street, Fort Detrick, MD , http://www.usamriid.army.mil/

**References:**

1. Anders K: Lymphocystis disease of fishes. *In:* Viruses of Lower Vertebrates, eds. Ahne W, Kurstak E, pp. 141-160. Springer-Verlag, New York, NY, 1989
2. Dunbar CE, Wolf K: The cytological course of experimental lymphocystis in the bluegill. J Infect Dis **116**:466-472, 1966
3. ICTVdB Management (2006). 00.036. Iridoviridae. In: ICTVdB - The Universal Virus Database, version 3, Büchen-Osmond, C. (Ed), Columbia University, New York, NY http://www.ncbi.nlm.nih.gov/ICTVdb/ICTVdB/
4. Murphy, FA: Virus taxonomy. *In:* Fundamental Virology, eds. Fields BN, Knipe DM, Howley PM, 3rd ed., pp. 47-48. Lippincott–Raven Publishers, Philadelphia, PA, 1996
5. Roberts RJ: The virology of teleosts. *In:* Fish Pathology, 2nd ed., pp. 192-195. Bailliere Tindall, London, UK, 1989

**CASE IV – 48928 (AFIP 3026807)**

**Signalment:** Five-year-old, captive hatched, male tentacled snake (*Erpeton tentaculatum*)

**History:** One of a group of tentacled snakes with a 3 or 4 month history of skin lesions. Six snakes died despite treatment.

**Gross Pathology:** Numerous 2-4 mm diameter irregular slightly depressed rough tan lesions are scattered in the skin of the entire body.

**Laboratory Results:** Fungal culture of skin grew *Chrysosprorium* anamorph of *Nannizziopsis vriesii*

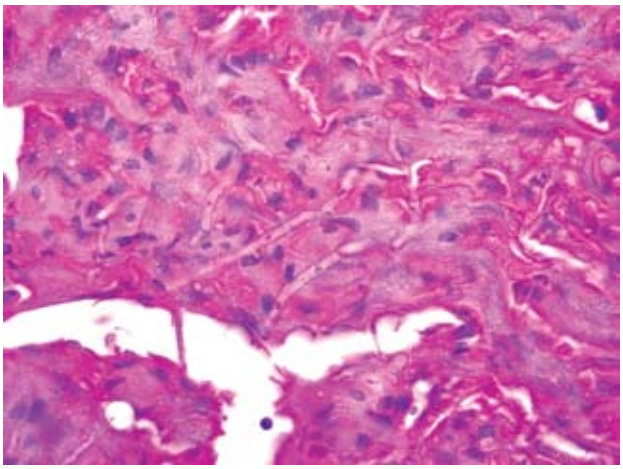

*4-1. Skin, tentacled snake. Multifocally, the epidermis is replaced by a necrotic coagulum which contains numerous branching septate fungal hyphae. (HE 1000X)*

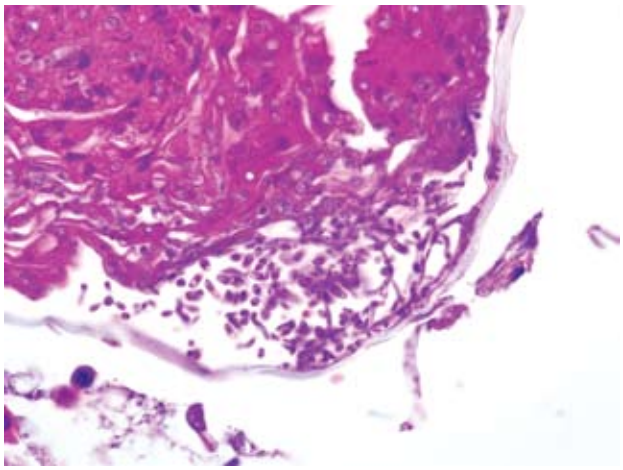

*4-2. Skin, tentacled snake. Rarely admixed with the fungal hyphae are numerous arthroconidia. (HE 1000X)*

**Histopathologic Description:** Multifocally, there is full-thickness epidermal necrosis with invasion and expansion of the necrotic tissue by numerous branching, septate fungal hyphae **(Fig. 4-1)** and rare arthroconidia **(Fig. 4-2)**. In some affected areas, myriads of mixed bacteria are also present. Heterophils multifocally infiltrate the epidermis and dermis and are especially abundant in the dermis in areas where there is separation or loss (ulceration) of the necrotic epithelium. Less affected epidermis is diffusely mildly hyperplastic. Spongiosis and cytoplasmic vacuolation are common.

**Contributor's Morphologic Diagnosis:** Skin: Severe multifocal ulcerative and necrotizing dermatitis with intralesional fungi (etiology: *Chrysosprorium* anamorph of *Nannizziopsis vriesii*)

**Contributor's Comment:** The *Chrysosporium* anamorph of *Nannizziopsis vriesii* (CANV) has relatively recently been recognized as a pathogenic fungus that can cause significant morbidity and mortality in some species of reptiles.[2,4,6] In previous reports, dermatomycoses in snakes and lizards have been ascribed to several different species of fungi including dermatophytes such as *Geotrichium* sp., *Trichosporon* sp., and numerous other soil fungi (e.g., *Aspergillus, Candida, Cladosporium, Fusarium*, and *Mucor*).[2,4,6] It is proposed that in many of these cases the fungus was misidentified and infection was due to the CANV.[2,4] *Nannizziopsis vriesii* is a sexually reproductive keratinophilic species in the phylum Ascomycota, order Onygenales, that was originally isolated from the tissues of a lizard (*Ameiva* sp.).[4,6] Sexual fruiting bodies are formed on nutrient-poor medium at 30 degrees C. The asexual (mitotic) state seen in histologic lesions is typical of *Chrysosporium* and produces solitary conidia (aleurioconidia) and arthroconidia. Although culture is necessary to definitively identify the CANV from lesions in affected reptiles, the characteristic appearance of the arthroconidia in histologic section is a key diagnostic feature. The CANV was cultured from the skin of the snake submitted for this conference **(Fig. 1)**. Arthroconidia were not seen histologically in this snake but were seen in the skin lesions of other snakes in this group **(Fig. 2)**. The origin of infection with the CANV in this and other cases is unknown. An extensive survey of skin samples from healthy reptiles did not recover any of the CANV.[7] Thus, *N. vriesii* does not appear to be a common constituent of the microflora of healthy reptiles. An environmental source is postulated but has not been demonstrated. Factors that might predispose a reptile to infection and disease are also not known.

**AFIP Diagnosis:** Scaled skin: Epidermitis, necrotizing and ulcerative, multifocal, marked with intralesional fungi

**Conference Comment:** Within the last 10 years, CANV has been identified as the causative agent of dermatomycosis in several reptilian species to include green iguanas, bearded dragons, brown tree snakes, a salt-water crocodile, and veiled chameleons as well as tentacled snakes.[1,2,3,4,5,8] A necrotizing and granulomatous dermatitis is commonly seen in these species with some species variation.[1,2,3,4,5,8] One of the bearded dragons infected with CANV also had a granulomatous hepatitis with intralesional hyphae.[3] Histologically, CANV is

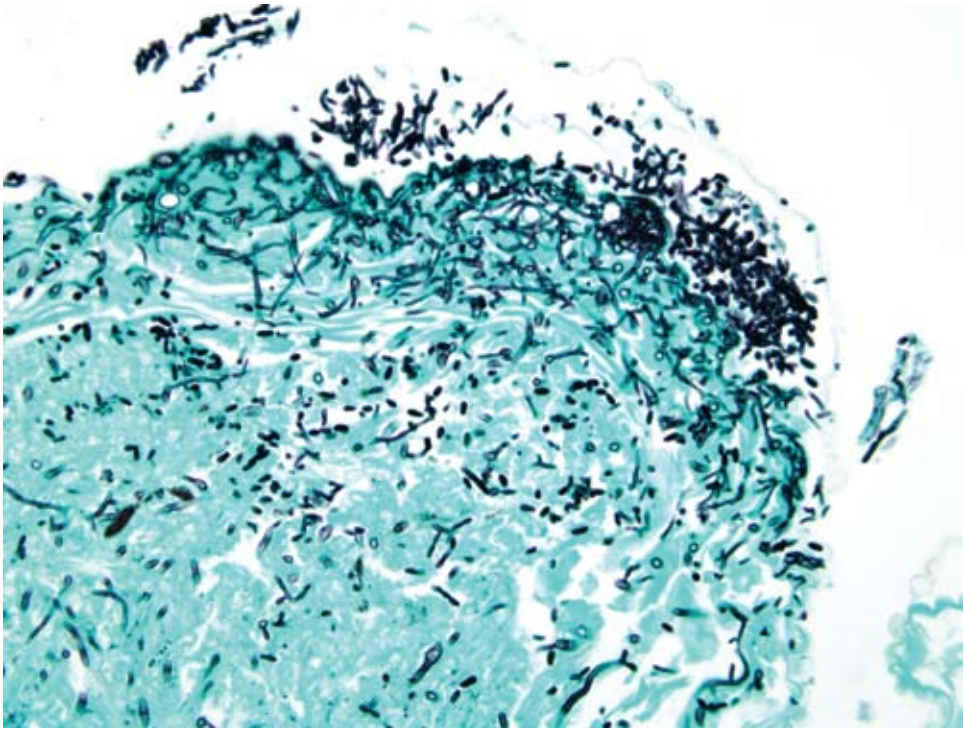

*4-3. Skin, tentacled snake. GMS positive branching fungal hyphae within the necrotic epidermis. (GMS 400X)*

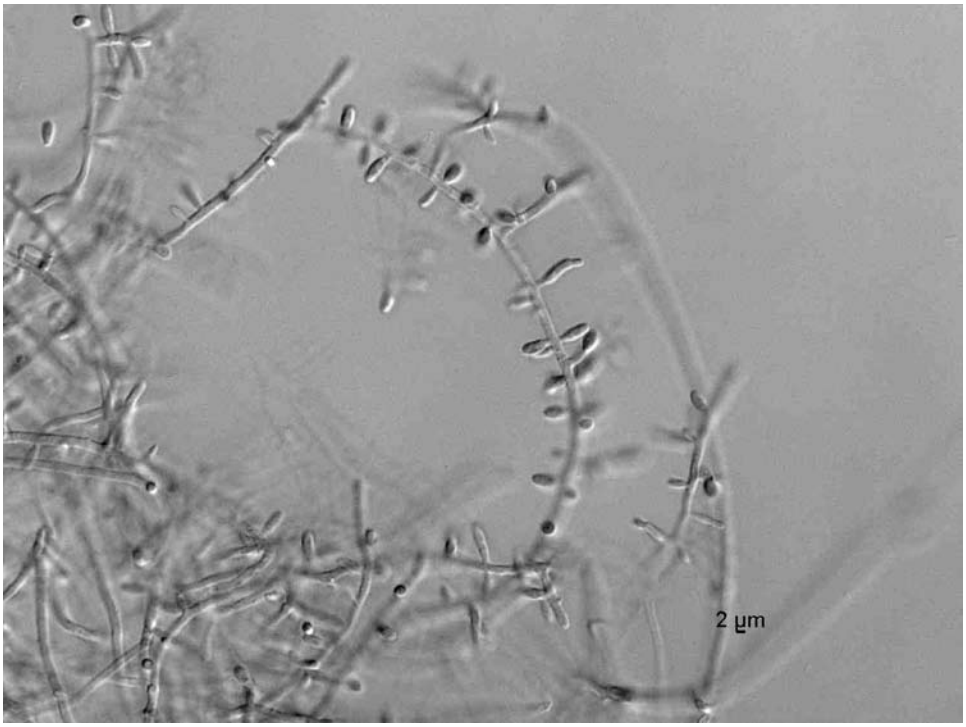


*4-4. Skin, tentacled snake. Fungal arthroconidia isolated from culture.*
*Photograph courtesy of Zoolocial Society of San Diego, P.O. Box 120551, San Diego, CA 92112-055, pathology@sandiegozoo.org.*

found in necrotic lesions and appears as hyaline, septate, branching hyphae often 2-4 um in width with characteristic arthroconidia.[2]

In the case of the tentacled snakes, it was speculated by the author of the article that failure to maintain an acidic environment predisposed these snakes to skin infection. These snakes normally inhabit slow moving acidic streams at a pH of 6-6.5, and the affected snakes were kept in water at a pH of > 8.[2] Snakes kept in water at a pH of 7 did not

develop lesions.[2]

The morphologic features of CANV in tissue section are best demonstrated with special stains such as GMS **(Fig. 4-3)**. The contributor submitted a superb image of hyphae and arthroconidia growing in culture **(Fig. 4-4)**.

**Contributing Institution:** Zoological Society of San Diego, Department of Pathology, P.O. Box 120551, San Diego, CA, http://cres.sandiegozoo.org/

**References:**

1. Abarca ML, Martorell J, Castellia G, Ramis A, Cabanes FJ: Cutaneous hyalohyphomycosis caused by Bhrysosporiuim species related to *Nannizziopsis vriesii* in two green iguanas (Iguana iguana). Med Mycol. 46(4):349-354, 2008

2. Bertelsen MF, Crawshaw GJ, Sigler L, Smith DA: Fatal cutaneous mycosis in tentacled snakes (*Erpeton tentaculatum*) caused by the *Chrysosporium* anamorph of *Nannizziopsis vriesii*. J Zoo Wild Med **36**(1): 82-87, 2005

3. Bowman MR, Pare JA, Sigler L, Naeser JP, Sladky KK, Hanley CS, Helmer P, Phillips LA, Brower A, Porter R: Deep fungal dermatitis in three inland bearded dragons (*Pogona vitticeps*) caused by the *Chrysosporium* anamorph of *Nannizziopsis vriesii*. Med Mycol. **45**(4) 371-376, 2007

4. Nichols DK, Weyant RS, Lamirande EW, Sigler L, Mason RT: Fatal mycotic dermatitis in captive brown tree snakes (*Boiga irregularis*). J Zoo Wildl Med **30**(1): 111-118, 1999

5. Pare A, Coyle KA, Sigler L, Maas AK, Mitchell RL: Pathogenicity of the *Chrysosporium* anamorph of *Nannizziopsis* for veiled chameleons (*Chamaeleo calyptratus*). Med Mycol **44**(1):25-31, 2006

6. Paré JA, Sigler L, Hunter DB, Summerbell RC, Smith DA, Machin KL: Cutaneous mycoses in chameleons caused by the *Chrysosporium* anamorph of *Nannizziopsis vriesii* (Apinis) Currah. J Zoo Wildl Med **28**(4): 443-453, 1997

7. Paré JA, Sigler L, Rypien K, Gibas CF, Hoffman TL: Cutaneous fungal microflora of healthy squamate reptiles and prevalence of the *Chyrsosporium* anamorph of *Nannizziopsis vriesii*: Proc AAZV, AAWV, ARAV NAZWV Joint Conf. pp. 36-38, 2001

8. Thomas AD, Sigler L, Peucker S, Norton JH, Nielan A: *Chrysosporium* anamorph of *Nannizziopsis vriesii* asso ciated with fatal cutaneous mycoses in the salt-water crocodile (*Crocodylus porosus*). Med Mycol **40**(2):143-151, 2002

The Armed Forces Institute of Pathology
Department of Veterinary Pathology

*Conference Coordinator:*
Todd M. Bell, DVM

WEDNESDAY SLIDE CONFERENCE 2008-2009

# Conference 24

6 May 2009

**Conference Moderator:**

**Dr. Thomas P. Lipscomb, DVM, Diplomate ACVP**

## CASE I – 06N802 (AFIP 3105941)

**Signalment:** 3-year-old, gelding, quarter horse, (*Equus caballus*) equine

History: The patient presented with muscle fasciculations, hyperhidrosis, tachycardia (88 bpm) and tachypnea. The temperature was within normal limits and capillary refill time was prolonged. ECG revealed sinus tachycardia. Laboratory abnormalities included mild thrombocytopenia, azotemia (creatine 4.8), hyperglycemia (glucose 483), hypokalemia (K 3.0), hyponatremia (Na 120), hypochloremia (Cl 81), hyperbilirubinemia (4.6) and elevated CK (5050) and AST (927).

**Gross Pathology:** An adult quarter horse gelding (500 kg) in good flesh with mild postmortem autolysis is presented for necropsy. The cranioventral lungs, representing approximately 20% of the lung parenchyma, are sharply demarcated, dark green, and consolidated with marked expansion of the interlobular spaces by edema and yellow friable material (fibrin). The trachea and bronchial airways are filled with white foam; clear fluid oozes from the cut section. The remaining lung tissue is rubbery and partially collapsed. The cranioventral pulmonary pleura is covered by a thin layer of brown friable material (fibrin). The pericardial sac contains ~ 200 mls of dark yellow fluid. There is pale tan streaking throughout the myocardium of the ventricular free wall and the interventricular septum; the left ventricular free wall appears most severely affected. This discoloration affects greater than 40% of the myocardium. The liver is mildly firm and has an accentuated lobular pattern. There are several dozen subcapsular hemorrhages in both kidneys. Approximately 40% of the glandular stomach is thickened and hyperemic; about half of this area is covered by a fibrinous pseudomembrane. The stomach contains grain and hay/grass ingesta. The small colon contains formed feces. Urine is clear and yellow. There is mild edema of the lamina of P3 in the right front and left rear feet.

**Laboratory Results:**
Mild thrombocytopenia
Azotemia (creatinine 4.8)
Hyperglycemia (glucose 483)
Hypokalemia (K 3.0)
Hyponatremia (Na 120)
Hypochloremia (Cl 81)
Hyperbilirubinemia (4.6)
Elevated CK (5070)
Elevated AST (927)

*Sponsored by the American Veterinary Medical Association, the American College of Veterinary Pathologists, and the C. L. Davis Foundation.

**Histopathologic Description:** Heart: Multifocal myocardial degeneration and necrosis are present within multiple sections of heart, affecting approximately 25% of the myocardium. The change is characterized by loss of myocardial cross striations, fragmentation, and vacuolation of myocardial cytoplasm, and nuclear pyknosis and karyolysis **(Fig. 1-1)**. Sarcolemmal sheaths are collapsed, satellite cell nuclei are plump and closely arranged, and there are moderate numbers of macrophages with fewer lymphocytes and occasional neutrophils in the affected areas. Perivascular supporting tissues and tissues surrounding Purkinje cells are expanded by edema fluid or finely granular, basophilic, loose mucinous material.

**Contributor's Morphologic Diagnosis:** Heart: Myocardial degeneration and necrosis, severe, multifocal to coalescing, subacute, quarter horse, *Equus caballus*

**Contributor's Comment:** This horse is one of several that died or were euthanized after being given clenbuterol. In addition to the myocardial necrosis, the horse had varying degrees of skeletal muscle necrosis in different muscle groups. High levels of clenbuterol were found in this horse's serum the day after dosing, and clenbuterol overdose is believed to be responsible for the clinical signs of muscle fasciculation, tachycardia, and hyperhydrosis seen at presentation, as well as for the skeletal and cardiac muscle degeneration and necrosis seen grossly and histologically.

Clenbuterol is a beta-2 sympathomimetic, with most of the pharmacologic activity coming from the levo form.[4] The drug is used as a bronchodilator in horses and non-lactating cattle at a recommended dosage of 0.8 micrograms per kilogram of body weight.[4] Excretion is primarily via urine as unmetabolized clenbuterol. Four studies have shown that clenbuterol induces myocardial necrosis in laboratory rats [1, 2], although a recent study of the relative myotoxicity of clenbuterol versus other beta agonists showed that clenbuterol is less myotoxic than fenoterol, another beta-2 sympathomimetic.[3]

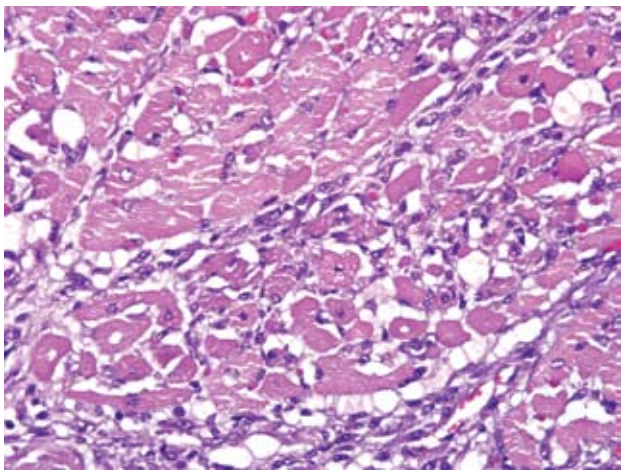

*1-1. Myocardium, horse. Multifocally, cardiac myocytes are degenerative or necrotic, and are often replaced by moderate numbers of histiocytes, lymphocytes, and fibroblasts. (HE 400X)*

In this case, further history revealed a questionable source of clenbuterol that, when tested at the LSU Analytical Systems Laboratory, contained 67.4 times the FDA approved level of the drug. The bottle was labeled "Clenbuterol HCl, 72.5 mcg/ml, 0.5 ml/100lb," but actually contained 5.0 mg/ml instead of the labeled 72.5 mcg/ml, or 0.0725 mg/ml. The horse was given clenbuterol from this bottle five days prior to euthanasia.

**AFIP Diagnosis:** Heart, left ventricle: Myocardial degeneration and necrosis, multifocally extensive, moderate, with histiocytic and lymphocytic myocarditis and fibroplasia

**Conference Comment:** Catecholamines and catecholamine receptor agonists are believed to cause myocardial necrosis in various settings including "brain-heart syndrome," pheochromocytoma and sympathomimetic drug overdoses. Numerous toxins cause myocardial necrosis as well.

Ionophore toxicity occurs in horses and other monogastrics that are mistakenly fed coccidiostats used in ruminant and poultry feed.[4]

Cardiac glycosides are found in several different plants in various parts of the world, and ingestion often causes death within a few hours with little to no gross or histologic footprint.[4] These glycosides inhibit the sodium-potassium ATPase pump causing a disruption in ion concentration and membrane potential leading to muscle necrosis.[4] Diagnosis is often based on discovery of the offending plant in the gastrointestinal system or circumstantial evidence.[4]

Some toxic alcohols, such as gossypol and tremetol, can cause myocardial necrosis. Gossypol, often found in cottonseed meal used as a protein supplement in feed, causes myocardial necrosis in young ruminants, pigs, and dogs.[4] Tremetol is the toxic principal in *Eupatorium rugosum* (white snakeroot).[4]

Horses ingest blister beetles in dried hay, and the canthardin present in the insects causes gastric lesions, hemorrhagic cystitis, enterocolitis, and myocardial necrosis.[4] Hairy vetch (*Vicia villosa*) can also cause myocardial lesions

in cattle but not horses. Histologic lesions consist of monocytes, lymphocytes, plasma cells, and giant cells. In cattle, eosinophils are also present.[5]

**Contributing Institution:** Louisiana State University School of Veterinary Medicine, Skip Bertman Drive, Baton Rouge, LA 70803, http://www.vetmed.lsu.edu/

**References:**

1. Burniston JG, Chester N, Clark WA, Tan LB, Goldspink DF: Dose-dependent apoptotic and necrotic myocyte death induced by the beta2-adrenergic receptor agonist, clenbuterol. Muscle Nerve **32**:767-774, 2005
2. Burniston JG, Ng Y, Clark WA, Colyer J, Tan LB, Goldspink DF: Myotoxic effects of clenbuterol in the rat heart and soleus muscle. J Appl Physiol **93**:1824-1832, 2002
3. Burniston JG, Tan LB, Goldspink DF: Relative myotoxic and haemodynamic effects of the beta-agonists fenoterol and clenbuterol measured in conscious unrestrained rats. Exp Physiol **91**:1041-1049, 2006
4. EMEA: Clenbuterol Hyodrochloride Summary Report (1), ed. Products CfVM. European Agency for the Evaluation of Medicinal Products, Veterinary Medicines and Information Technology Unit, 2000
5. Ginn, PE, Mansell JEKL, Rakich PM: Skin and appendages. *In:* Jubb, Kennedy, and Palmer's Pathology of Domestic Animals, vol. 1 ed. Maxie MG, pp. 619-620. Elsevier Limited, Philadelphia, PA, 2007
6. Maxie MG, Robinson WF: Cardiovascular system. *In:* Jubb, Kennedy and Palmer's Pathology of Domestic Animals, vol. 3 ed. Maxie MG, 5th ed., pp. 32-33. Elsevier, Philadelphia, PA, 2007

## CASE II – A07-11068-4 (AFIP 3103240)

**Signalment:** 15-year-old, castrated male, mixed breed, (*Canis familiaris*) dog

**History:** A 15-year-old castrated male mongrel dog developed a mass in the left hemimandible around the first molar tooth. The owner reported that the dog pawed at its mouth. Two 1 cm x 2 cm incisional biopsy specimens from the buccal and lingual aspects of the mass were processed en toto for histologic examination by a reference laboratory; the diagnosis was osteosarcoma. One month later, the dog was admitted to the Purdue University Veterinary Teaching Hospital for total left hemimandibulectomy.

**Gross Pathology:** A left hemimandibular surgical specimen containing the entire mass had its margins painted prior to immersion in 10% neutral buffered formalin and submission to the Purdue University Animal Disease Diagnostic Laboratory (ADDL), where the specimen was transferred to a formic acid decalcifying solution. A firm to hard fibrous and bony mandibular mass surrounded the neck and roots of the first molar tooth and measured about 2.5 cm from rostral to caudal margins and 2 cm from medial to lateral aspects **(Figs. 2-1, 2-2)**. The mass on cross-section consisted mostly of hard, white tissue that infiltrated alveolar and cortical bone and adjacent soft tissue **(Fig. 2-3)**.

**Laboratory Results:** No abnormalities were detected in the available lateral radiographic view of the skull because of superimposition of the hemimandibles. However, in the computed tomographic (CT) scan, an expansile and lytic lesion, about 1.8 cm in width and 2 cm from rostral to caudal borders, was evident in the dorsal aspect of the left hemimandible, surrounding the neck and roots of the first molar tooth **(Fig. 2-4)**. The mass destroyed alveolar and cortical bone, but had well-defined borders with a short transition zone. There was slight swelling, but no post-contrast enhancement of adjacent soft tissues. Thoracic and abdominal radiographs were within normal limits and free of evidence of metastatic neoplasia.

**Histopathologic Description:** The tumor consisted of a spindle-cell proliferation resembling periodontal stroma that appeared to be centered midway between the neck of the tooth and its apex. At its apparent site of origin, the tumor had provoked osteoclastic destruction of alveolar bone, adjacent cortical compacta, periodontal ligament and bone of the alveolar crest. Symmetric growth of the mass expanded the lingual and buccal borders of the hemimandible, again by stimulating osteoclastic removal of the cortical compacta at a rate that allowed development of a thin, incomplete shell of periosteal new bone that partially contained the tumor. At the gingival sulcus, the incomplete and partially resorbed periosteal shell of reactive bone nearly abutted the junctional gingival epithelium. Upward expansion of the tumor into gingival lamina propria led to ulceration and granulation tissue formation. On the buccal surface, the tumor was also partially bound by a thin periosteal shell of reactive bone that ended at the former level of the alveolar crest, which had been replaced by neoplastic tissue. Here, the tumor extended above the level of the periosteal reaction into the gingiva. Neoplastic tissue was composed of fusiform cells in scanty fibrous stroma with light but diffuse infiltration by neutrophils. The fusiform cells had an elongated oval nucleus, small nucleolus, no mitotic figures in 15 high-power fields, and scanty pale

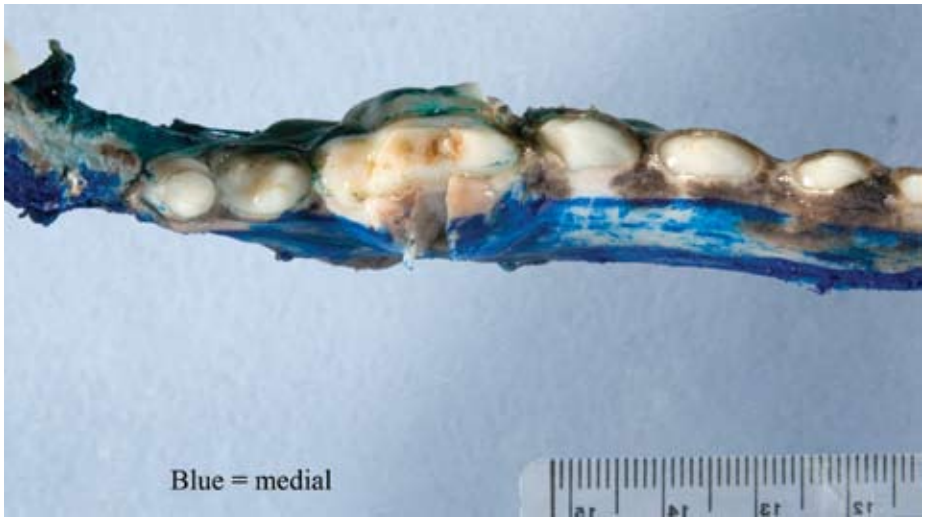


*2-1, 2-2, 2-3 (From top on left). Mandible, dog. A 2.0 x 2.5 cm firm fibrous and bony mass surrounds the neck and roots of the first molar.* *Photographs courtesy of the Animal Disease Diagnostic Laboratory, 406 S. University Street, Purdue University, West Lafayette, IN 47907, pegmiller@purdue.edu.*

*2-4. Mandible, dog (Below). Effacing alveolar and cortical bone, surrounding the neck and roots of the first molar tooth, and expanding gingival soft tissues at the dorsal aspect of the left hemimandible is a well defined mass.* *Computed tomograph courtesy of the Animal Disease Diagnostic Laboratory, 406 S. University Street, Purdue University, West Lafayette, IN 47907, pegmiller@purdue.edu.*

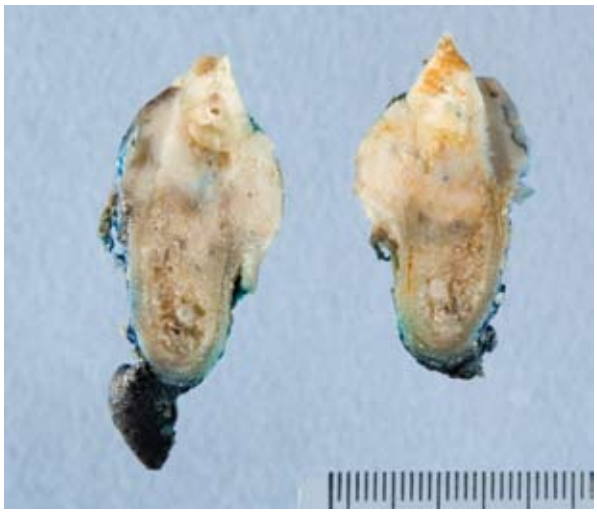

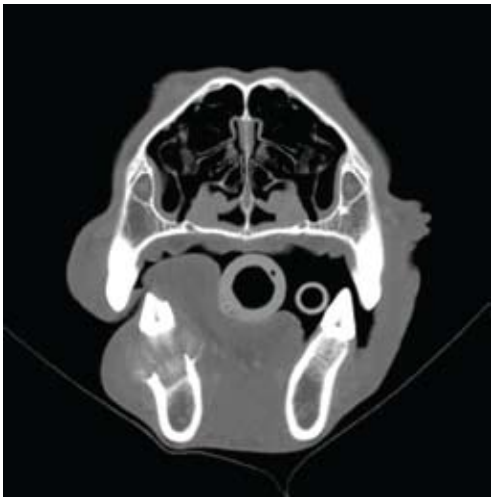

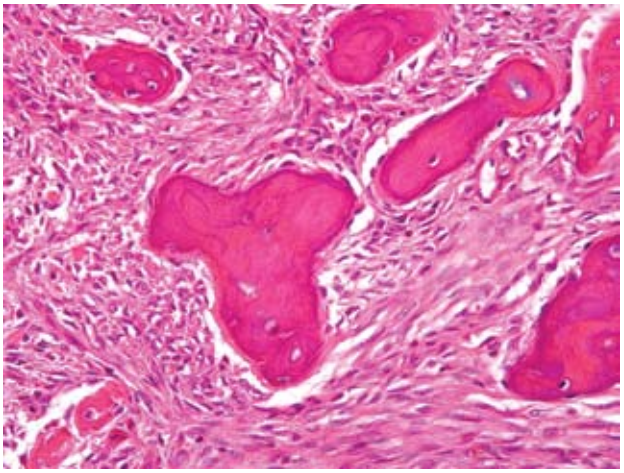

*2-5. Mandible, dog. Ossifying fibroma. Effacing periodontal ligament and alveolar bone is a neoplasm composed of fusiform cells admixed with low numbers of neutrophils on a scant fibrous matrix. Within the neoplasm are islands of woven bone lined by a single layer of osteoblasts which are distinct from the neoplastic cell population. (HE 400X)*

eosinophilic cytoplasm with indistinct cell borders **(Fig. 2-5)**. The stroma was moderately vascular with numerous irregular trabeculae of osteoid and partially mineralized woven bone. Bony trabeculae were bordered by one layer of osteoblasts. A few osteoclasts were adjacent to bony spicules. There was little fibrous collagen in tumoral stroma; most of the Masson's trichrome-stained collagen was in the bony trabeculae. A preliminary diagnosis of ossifying fibroma was reported with the final diagnosis to follow examination of remaining (central) tissue.

Sections of the fully decalcified central portion of the tumor were histologically similar to the initial peripheral sections, except that 1 to 3 mitotic figures were found per ten high-power fields. Neoplastic tissue was not found in soft tissue ventral to the hemimandible or in mandibular or soft tissue caudal to the mass. Histologic impression was complete excision of an ossifying fibroma.

**Contributor's Morphologic Diagnosis:** Mandibular ossifying fibroma

**Contributor's Comment:** The case was reported as a brief communication in Vet Pathol.[1] Benign fibro-osseous proliferations of bone in veterinary species include ossifying fibroma, osteoma, and fibrous dysplasia.[2,3] Osteomas are typically solitary osteosclerotic lesions that arise from the surface of bones of the jaw or skull; trabeculae of woven bone constitute the bulk of the tumor, are rimmed by one layer of well-differentiated osteoblasts and, in many cases, are oriented perpendicular to the surface of the tumor.[3] Fibrous dysplasia [3] is a tumor-like lesion that can involve one or multiple bones, often in young animals. It arises within the bone, rather than from the periosteal surface, and its ample fibrous stroma contains only thin, curved trabeculae of woven bone. The bony trabeculae are generally not rimmed by osteoblasts, which distinguishes it from ossifying fibroma or osteoma, and are regularly spaced but without orientation relative to the periosteal surface.

Ossifying fibroma has histologic features that are intermediate between those of osteoma and fibrous dysplasia, although there can be overlap among the three entities.[2] Ossifying fibroma is an expansile, lytic, and invasive mass that develops within the bone, particularly the mandible. Its bony trabeculae are rimmed by osteoblasts as in osteoma, but are arranged haphazardly and contribute relatively less to the fibro-osseous stroma.

Importantly, from a prognostic perspective, ossifying fibroma must be differentiated from malignant tumors, such as osteosarcoma. That distinction can be based on the lower cellularity, bland cytologic features, and low mitotic index of ossifying fibroma. Furthermore, bony trabeculae of ossifying fibroma tend to be better developed than in osteosarcoma and are bordered by a single layer of osteoblasts that are distinct from the tumor cells. However, histologic examination of excisional biopsy specimens and knowledge of the anatomic location of the tumor may be necessary for accurate diagnosis.

**AFIP Diagnosis:** Gingiva, tooth, and alveolar and cortical bone: Ossifying fibroma

**Conference Comment:** Ossifying fibromas are most commonly reported in young horses, generally less than one year of age, and usually present as a protruding mass from the rostral mandible.[4] There have also been reported cases in cats, dogs, and sheep.[4] In horses, the differential diagnosis for ossifying fibroma includes fibrous osteodystrophy, fibrous dysplasia, osteoma, and osteosarcoma.[4] Fibrous osteodystrophy presents as a symmetrical, bilateral lesion with numerous osteoclasts.[4] In fibrous dysplasia, bone spicules are not rimmed by osteoblasts and are more uniform.[4] Osteomas are composed of more normal appearing bone, while osteosarcomas have invasive, pleomorphic cells with a higher mitotic index.[4] Osteomas are most common in horses and cattle and have been reported as large as 14 cm in diameter.[3]

Many tumors diagnosed as osteomas in dogs are actually multilobular tumors of bone.[3] Histologically, the multilobular tumor of bone consists of multiple vari-shaped nodules of bone and/or cartilage at various stages of

differentiation separated by a fibrovascular stroma.[2,4] These tumors are slow growing but can be invasive and may metastasize.[4] They have been reported in dogs, cats, and horses.[4] Osteomas are dense masses of well-differentiated bone that protrude from bone surfaces.

**Contributing Institution:** Purdue University, Animal Disease Diagnostic Laboratory, url: http://www.addl.purdue.edu/; Department of Comparative Pathobiology, http://www.vet.purdue.edu/cpb/

**References:**

1. Miller MA, Towle HAM, Heng HG, Greenberg CB, Pool RR: Mandibular ossifying fibroma in a dog. Vet Pathol **45**:203-206, 2008
2. Slayter MV, Boosinger TR, Pool RR, Dämmrich K, Misdorp W, Larsen S: Benign tumors. *In:* Histological Classification of Bone and Joint Tumors of Domestic Animals, 2nd series, vol. 1, p. 5-7. Armed Forces Institute of Pathology, Washington, DC, 1994
3. Thomson KG, Pool RR: Benign tumors of bone. *In:* Tumors in Domestic Animals, ed. Meuten DJ, 4th ed., pp. 248-255. Iowa State Press, Ames, IA, 2002
4. Thompson K: Bones and joints. In: Jubb, Kennedy and Palmer's Pathology of Domestic Animals, vol 1 ed. Maxie MG, 5th ed., pp.110-124. Elsevier, Philadelphia, PA, 2007

## CASE III – APO7-2381 (AFIP 3103604)

**Signalment:** 11-month-old, male castrated, dachshund, canine, (*Canis familiaris*)

**History:** This dog was presented to the North Carolina State University College of Veterinary Medicine Neurology Service for a 3-month history of stumbling and falling which had progressed to severe vestibular ataxia, nystagmus, and possible seizure activity. This dog had been treated previously with antibiotics and there was no response.

**Gross Pathology:** The necropsy was limited to the head only. Bilaterally, the meninges of the caudal part of the temporal, parietal lobe and the occipital lobe were fluctuant and markedly thickened, up to 6 mm. Serosanginous fluid and dark red soft clots were found within the subdural space (subdural hematoma). On the cut surface, the arachnoid space was markedly dilated due to marked cerebral atrophy which was most prominent in the left occipital lobe. The lateral ventricles were asymmetrical with the left lateral ventricle smaller than the right lateral ventricle **(Fig. 3-1)**. The third ventricle was slightly enlarged ventrodorsally and the interthalamic adhesion was moderately thinned.

**Laboratory Results:**

***MRI findings***

Moderate ventricular asymmetry is present with the right lateral ventricle being somewhat larger than the left. The third ventricle is also enlarged. There is a large accumulation of fluid peripheral to the cerebral cortex (extra-axial) most apparent from the level of the optic chiasm caudally **(Fig. 3-2)**. This fluid accumulation does not suppress on the FLAIR sequence as does the fluid within the ventricles and is slightly T1 hyperintense relative to fluid within the ventricles. The interthalamic adhesion is noticeably small and asymmetrical. The cerebellum has an irregular margin and the folia within the cerebellum have increased conspicuity. Post contrast medium administration, there is florid enhancement of the meninges surrounding the cerebral cortex and falx. There is no abnormal parenchymal enhancement. There is no evidence of increased intracranial pressure.

**Histopathologic Description:** Cerebrum: Diffusely in the cerebral cortical gray matter, approximately 60% of the neurons contain abundant, eosinophilic to amphophilic, granular to globular, cytoplasmic pigment, which occasionally displaces the nuclei peripherally **(Fig. 3-4)**. The cytoplasmic pigment stains positively with the PAS reaction and Sudan black and more obviously, but less frequently, with LFB stain **(Fig. 3-5)**. Moderate numbers of neurons are shrunken, rounded or angular, and hypereosinophilic, with hyperchromatic or pyknotic nuclei, interpreted as neuronal degeneration and necrosis. The dura and arachnoid mater are markedly thickened up to 5 times normal by fibroblasts, moderate multifocal angiogenesis and additional connective tissue matrix. Multifocally, there is a moderate amount of subarachnoid hemorrhage. Under U.V. illumination the pigment is autofluorescent. Ultrastructurally, the neurons have intracytoplasmic storage bodies which consist of curvilinear forms **(Figs. 3-5, 3-6)**.

Other sections examined: Cerebellum: There is moderate depletion of Purkinje cells and marked depletion of granular cells accompanied by marked narrowing of the granular layer and the molecular layer of the cerebellar cortex. Purkinje cells also contain eosinophilic cytoplasmic pigment which stains with PAS and LFB.

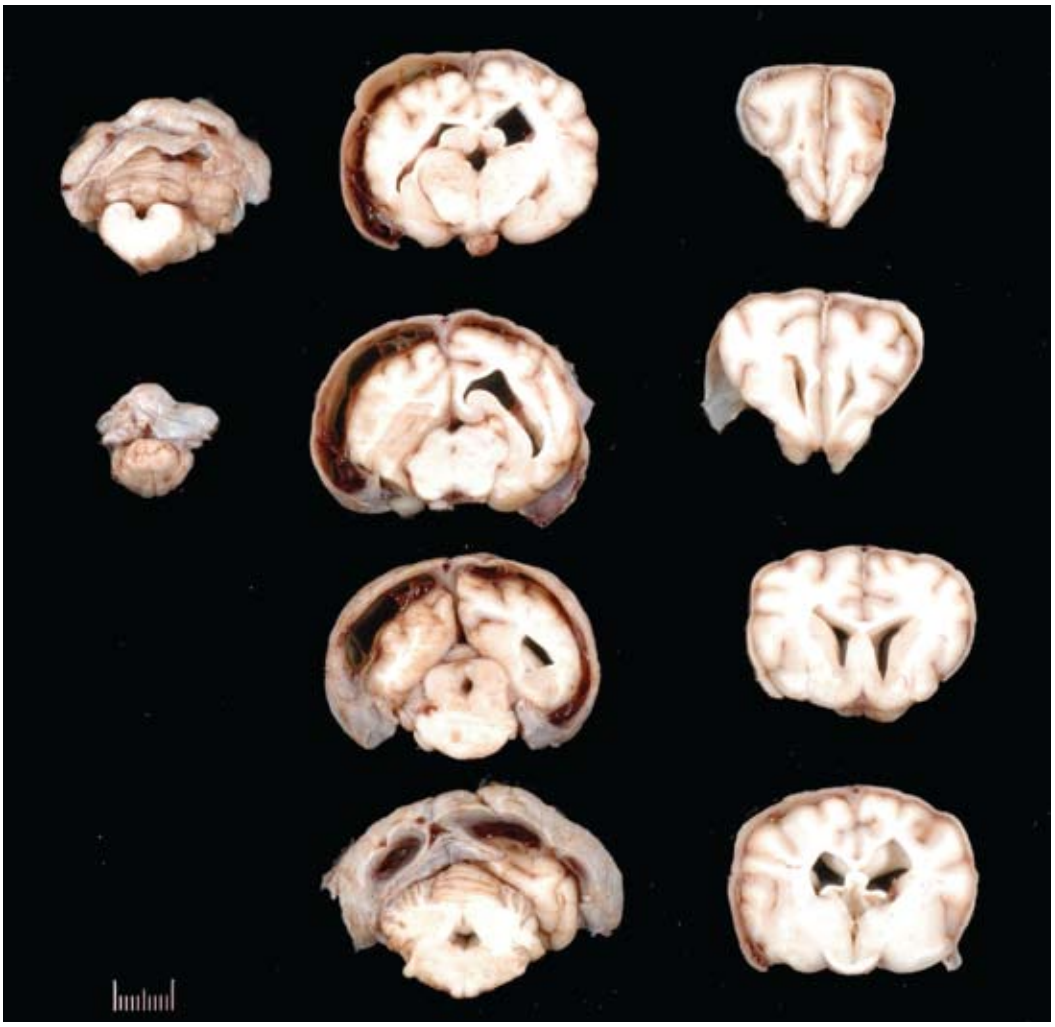

*3-1. Brain, dog. Bilaterally, the meninges are thickened up to 6 mm. The subarachnoid space is markedly dilated, most notably on the left side, and the lateral ventricles are asymmetrical with the left lateral ventricle smaller than the right, and the third ventricle is mildly enlarged.*
*Photograph courtesy of the College of Veterinary Medicine, North Carolina State University, 4700 Hillsborough Street, Raleigh, NC 27606, Sandra_horton@ncsu.edu.*

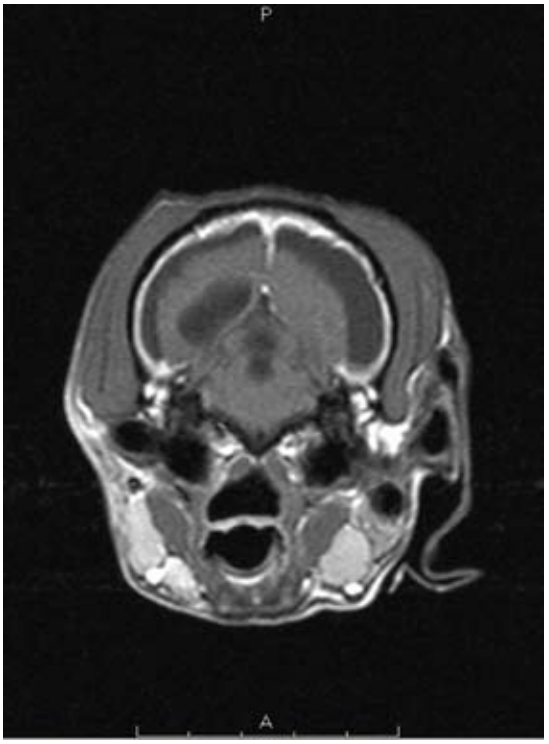


*3-2. Cranium, dog. Lateral ventricles are markedly asymmetrical, with the left lateral ventricle smaller than the right, and the third ventricle is moderately enlarged. There is an accumulation of fluid peripheral to the cerebral cortex which is more prominent over the left hemisphere.*
*Computed tomography courtesy of the College of Veterinary Medicine, North Carolina State University, 4700 Hillsborough Street, Raleigh, NC 27606, Sandra_horton@ncsu.edu.*

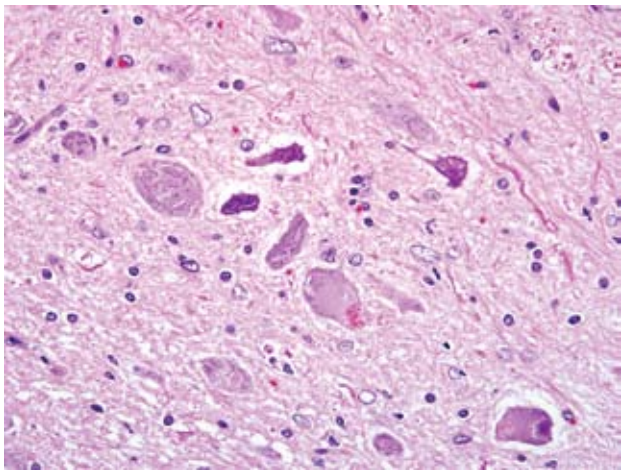

*3-3. Cerebrum, dog. Multifocally within the cerebral cortical gray matter, there are low numbers of necrotic neurons, occasional satelitosis, and numerous neurons which contain globular eosinophilic cytoplasmic inclusion material. (HE 400X)*

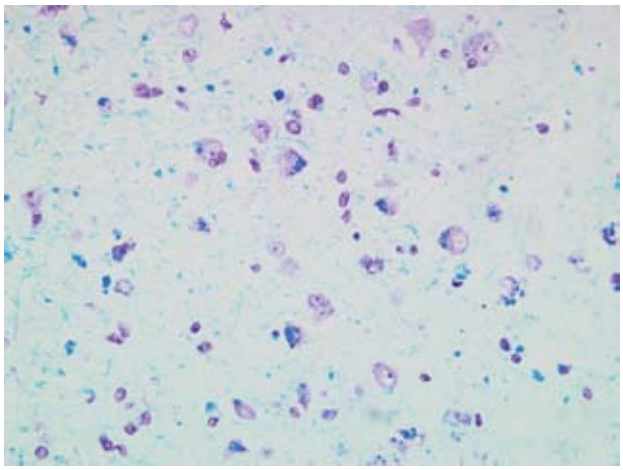

*3-4. Cerebrum, dog. Neuronal inclusion material staining with luxol fast blue. (LUXOL FAST BLUE 400X)*

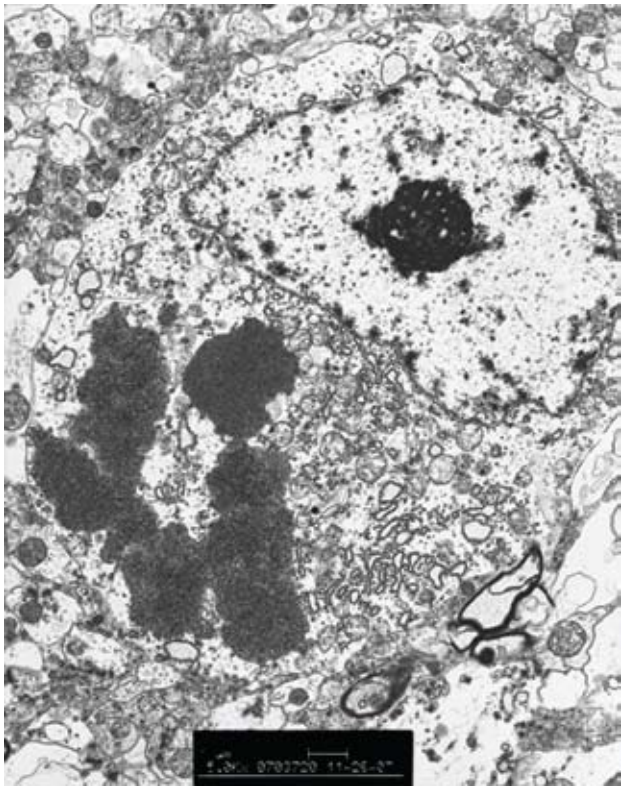

*3-5. Neuron, dog. Electron dense ceroid lipofuscin intracytoplasmic inclusions. Electron micrograph courtesy of the College of Veterinary Medicine, North Carolina State University, 4700 Hillsborough Street, Raleigh, NC 27606, Sandra_horton@ncsu.edu.*

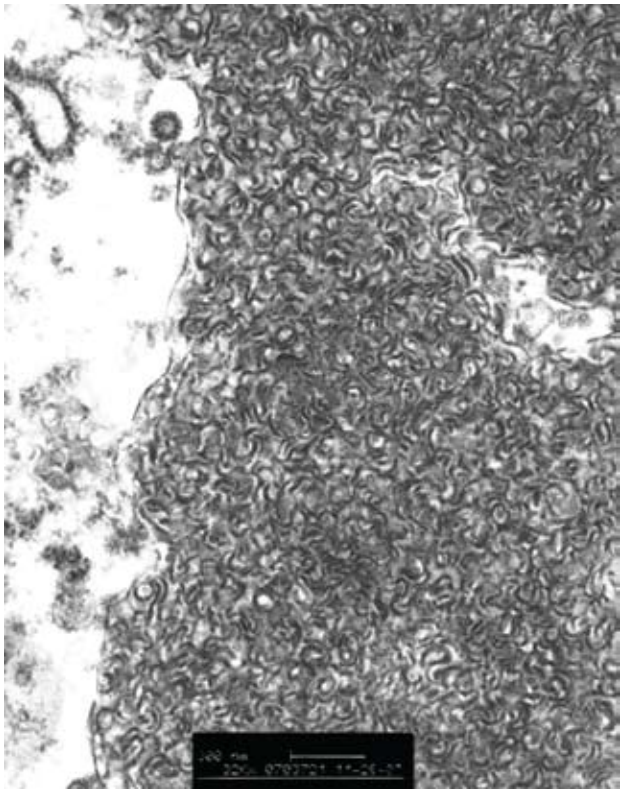

*3-6. Neuron, dog. Ceroid lipofuscin inclusions composed of many curvilinear bodies. t*

Eye: Bilaterally, there is mild depletion of the ganglion cells in the retina. There are a few ganglion cells with intracytoplasmic granules which stain with LFB. There is multifocal detachment of the retina with mild hypertrophy and hyperplasia of the pigmented epithelium (tombstone change).

**Contributor's Morphologic Diagnosis:** Diffuse, moderate, neuronal degeneration and necrosis and abundant neuronal intracytoplasmic granular pigment with cerebral atrophy

**Contributor's Comment:** The neuronal ceroid lipofuscinoses (NCLs) are inherited lysosomal storage diseases characterized by progressive neuropathy and accumulation of autofluorescent lipopigment in neurons and other cells.[3] NCLs have been described in human beings, cattle, sheep, goats, cats and in several breeds of dogs.[1,4] Human NCLs are classified into several forms based on the age of clinical onset, causative gene and ultrastructure of the accumulating lysosomal storage bodies.[3] The causative mutations in dogs have been reported in English setters (a missense mutation in *CLN 8*), border collies (a nonsense mutation in *CLN5*), bulldogs (a missense mutation in *CTSD*) and juvenile dachshund (a frame shift mutation in canine *TPP1*: the ortholog of human *CLN2*). The canine *TPP1* gene encodes a lysosomal enzyme called tripeptidyl 1 peptidase [1] and is known as the causative gene of infantile neuronal ceroid lipofuscinosis in humans and when mutated leads to accumulation of curvilinear-appearing cytosomes in neurons as well.[3]

The major accumulating protein in this breed is unknown, but subunit C of mitochondrial ATP is reported in English setters, border collies and Tibetan terriers, and sphingolipid activator proteins A and D have been identified in some types of human NCLs.[1,3,4] The cerebral and cerebellar cortex atrophy with cytoplasmic eosinophilic pigmen, which stained with PAS and LFB stain in neurons, is consistent with ceroid lipofuscinosis. The autofluorescence and ultrastructure of the accumulating pigment in this dog are very similar to the previous reports of juvenile ceroid lipofuscinosis in this breed. The dilated subdural space is considered to be secondary to the cerebral cortical atrophy.

**AFIP Diagnosis:** Cerebrum: Neuronal degeneration, necrosis and loss, extensive, with gliosis, cerebral atrophy, meningeal fibrosis, subdural hemorrhage, and eosinophilic neuronal cytoplasmic bodies

**Conference Comment:** Neuronal ceroid-lipofuscinosis, also known as Batten disease, has been reported in several domestic species and was recently reported in a Vietnamese pot-bellied pig.[2] The mode of inheritance is thought to be autosomal recessive for this type of storage disease.[5] Although accumulation of intracytoplasmic storage material can be found in many organs, the most prominent pathologic manifestations of these diseases are seen in the retina, cerebral cortex, andcerebellum.[5]

Gross lesions can vary from being nearly imperceptible to marked cerebral atrophy. The earlier the onset of the disease the more severe the brain atrophy.[4] Ultrastructurally, ceroid-lipofuscinosis can take on many different structural forms including curvilinear bodies, fingerprint bodies, and laminated stacks of membranes.[5] Areas of cerebral atrophy often appear to have a brown tinge.[5] The subdural hematoma in the present case is suspected to have resulted from trauma associated with motor disturbances.

Veterinary research into affected sheep resulted in a major contribution to understanding the human and animal ceroid lipofuscinoses by demonstrating that the stored material is predominantly protein (subunit C of mitochondrial ATP synthase) rather than lipid, as had been believed. Further research showed that in some forms of the disease, sphingolipid activator proteins are accumulated. Thus, "ceroid lipofuscinosis" is actually a misnomer.

**Contributing Institution:** College of Veterinary Medicine, North Carolina State University, http://www.cvm.ncsu.edu/

**References:**

1. Awano T, Katz LM, Brein PD, Sohar I, Lobel P, Coates RJ, Johnson CG, Giger U and Jonson SG: A frame shift mutation in canine TPP1 (the ortholog of human CLN2) in a juvenile Dachshund with neuronal Ceroid lipofuscinosis. Mol Genet Metab **89**:254260, 2006
2. Cesta MF, Mozzachil K, Little PB, Olby NJ, Sills RC, Brown TT: Neuronal ceroid lipofuscinosis in a Vietnamese pot-bellied pig (*Sus scrofa*). Vet Pathol **43**:556-560, 2006
3. Haltia M: The neuronal ceroid-lipofusinoses: From past to present, review. Biochamica et Biophysica **1762**:850-856, 2006
4. Jolly DR, Palmer ND, Studdert PV, Sutton HR, Kelly RW, Koppang N, Dahme G, Hartley JW, Patterson SJ and Riis CR: Canine ceroid-lipofusinoses: A review and classification. J Small Anim Prac **35**:299-306, 1994
5. Maxie MG, Youssef S: Nervous system. *In:* Jubb, Kennedy and Palmer's Pathology of Domestic Animals, vol. 1 ed. Maxie MG, 5th ed., pp.329-330. Elsevier, Philadelphia, PA, 2007

## CASE IV – 07 0284-54 (AFIP 3065568)

**Signalment:** Male, 8-year-old, dog, Shar Pei (*Canis familiaris*)

**History:** This dog was dysorectic for 15 days and showed poor condition and severe weight loss. Examination by clinician revealed a caudal abdominal mass, pain at palpation and corneal edema of the right eye. No micturitional troubles were reported. Prostatic abscesses were suspected. Urinary analysis revealed inflammatory cells and macrophages according to the clinician. The dog was euthanized for humane reasons.

**Gross Pathology:** Along with dramatic cachexia, the dog showed a severely enlarged (20 cm diameter), white, multilobulated and cystic prostate. Numerous white, firm, sometimes umbilicated masses were encountered in lungs, kidneys, spleen and tracheo-bronchial lymph nodes. Three ulcers were detected in proximal duodenum. Urinary bladder exhibited muscular hypertrophy.

**Laboratory Results:**

***Urinary analysis***

| Parameter | Value |
|---|---|
| Density | 1.026 |
| Blood | +++ |
| pH | 6 |
| Bilirubin | + |
| Leukocytes | + |
| Macrophages | +++ |

***Blood analysis***

| Parameter | Value | *Normal value* |
|---|---|---|
| Urea | 0.64 g/L | *0.2-0.6 g/L* |
| Creat | 13 mg/L | *< 12 mg/L* |
| PAL | 76 UI/L | *< 200 UI/L* |
| ALAT | 24 UI/L | *< 80 UI/L* |
| TP | 47 g/L | *55-80 g/L* |
| Glucose | 0.87 g/L | *0.6-1.1 g/L* |
| $Na^+$ | 138 mmol/L | *140-150 mmol/L* |
| $K^+$ | 4.4 mmol/L | *3.8-5.2 mmol/L* |
| $HCO_3^-$ | 22 mmol/L | *25 mmol/L* |

**Histopathologic Description:** Prostate: Multifocal and very infiltrative cell proliferations are effacing normal prostatic architecture. They are poorly encapsulated, highly cellular and contain discrete amount of connective tissue. Cells are round-to-oval with a 15-µm diameter, not jointed, contain variable amounts of eosinophilic cytoplasm sometimes microvacuolated, have a highly vesicular and irregular nucleus showing prominent nucleoli **(Fig. 4-1)**. Multinucleated cells, mitoses and abnormal mitotic figures are very frequent. Phagocytosis (erythrophagocytosis) is sometimes observed. Some areas of liquefaction necrosis are noted. Multifocal and discrete infiltrations by lymphocytes, plasma cells and neutrophils are observed. Tumoral cells can be found in the lumen of the prostatic glands. Immunohistochemical phenotype is: Vimentin-positive, cytokeratin-negative, CD3-negative, CD79a-negative.

**Contributor's Morphologic Diagnosis:**
Prostate: Malignant histiocytosis, Shar Pei, dog
Lung, kidney, duodenum, spleen (not submitted): Malignant histiocytosis, Shar Pei, dog

**Contributor's Comment:** Histiocytic disorders have been reported in many species, mainly in humans, dogs and rats, rarely in cats.[1,2,3,4,6] They arise from the large family of antigen-presenting cells (APC) originated from the bone marrow. The different APC cell types along with their immunophenotypes are presented in **Table 1**.

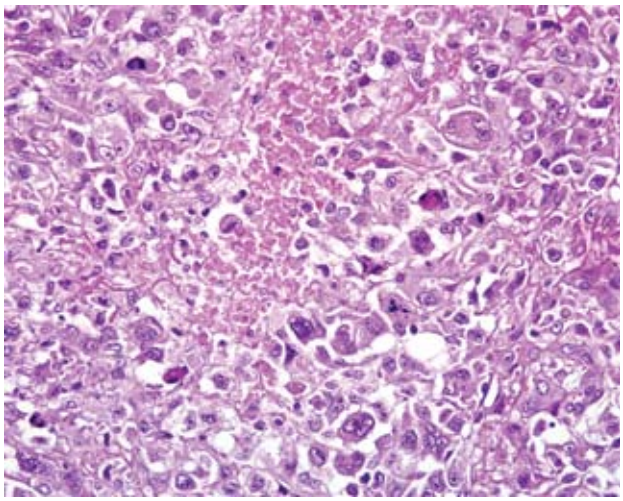

*4-1. Prostate gland, dog. Histiocytic sarcoma. Neoplastic cells are highly pleomorphic spindle to round cells with moderate anisocytosis and anisokaryosis, multinucleate cells, and bizarre mitoses. (HE 400X)*

**Table 1: Immunophenotypes of the different antigen-presenting cells [2]**

| Multipotent bone marrow stem cells | | | |
|---|---|---|---|
| CD34 +<br>CLA + | CD34 +<br>CLA- | | CD34+<br>IL-3R |
| Langerhans cells<br>(epithelial dendritic cells) | Interstitial dendritic cells | Macrophages/<br>Histiocytes | Dendritic cells of<br>lymphoid organs |
| CD1+<br>CD14-<br>CD11c+<br>MHCII<br>Birbeck granules+ | CD1+<br>CD14-<br>CD11c+<br>MHCII+<br>Thy-1+ | CD1-<br>CD14+<br>MHCII+<br>CD11c-<br>CD11b+ | IL-3R<br>MHCII+<br>CD45RA+<br>CD4+ |

Origin lineage of histiocytic disorders in dogs is the subject of many debates. In humans, they tend to arise from both macrophages/histiocytes and dendritic cells whereas in rats, they are of macrophagic origin. In dogs and cats, they are believed to be mostly of dendritic origin.[2]

In dogs, the main histiocytic disorders are: cutaneous histiocytoma, cutaneous histiocytosis, systemic histiocytosis, histiocytic sarcoma (HS) and malignant histiocytosis (MH).[4] Whereas cutaneous and systemic histiocytosis are non-neoplastic proliferations of activated dendritic cells, the others are classified as true neoplasms. There is a lot of confusion concerning the terms HS and MH. HS should be used when the lesion is solitary or has metastasized. MH defines a multicentric proliferation. Thus, a disseminated histiocytic sarcoma could be undistinguishable from a malignant histiocytosis. Bernese mountain dogs (BMD) show particular susceptibility to histiocytic disorders and neoplasms.[6] Properties of these histiocytic disorders are summarized in **Table 2**. Concerning HS/MH, respiratory symptoms are the most frequent cause of consultations. Anemia can be observed as part of a regenerative hemolytic process or a non-regenerative anemia caused by bone marrow invasion and erythrophagocytosis. Hypercalcemia can be observed as a paraneoplastic syndrome. On histopathologic examination, there is proliferation of round-to-oval cells with abundant eosinophilic cytoplasm, nuclear atypia, numerous mitoses, multinucleation, phagocytosis and some infiltration by lymphocytes, plasma cells and neutrophils.[4] On immunohistochemistry, along with markers of **Table 1**, cells are positive for lysozyme, vimentin, and negative for cytokeratin A.[3] Differential diagnosis includes: anaplastic carcinoma or lymphoma, rhabdomyosarcoma, and lymphomatoid granulomatosis. This case showed original features. Indeed, MH has only been reported in two Shar Peis and prostate involvement was only reported once.[2] Furthermore, no infiltration of the liver was observed, both at gross and microscopic examination. This feature is uncommon as the liver is one of the three most frequently involved organs.[2]

**Table 2: Properties of histiocytic disorders in dogs**

| Diseases | Concerned breeds | Mean age | Cytonuclear atypias | Involved organs | Metastatic potential | Prognosis |
|---|---|---|---|---|---|---|
| Cutaneous histiocytoma | All, predisposition of Boxer, dachshund, cocker spaniel, Great Dane, Shetland | Mostly young dogs | Rare | Skin (mainly solitary lesion). Draining lymph nodes involvement is exceptional | None | Good |

| | | | | | | |
|---|---|---|---|---|---|---|
| Cutaneous histiocytosis | All, predisposition of golden retriever and German shepherd | Mostly young dogs | Rare | Skin (multiple lesions), sometimes lymph nodes | Rare | Good |
| Systemic histiocytosis | BMD, golden retriever, Dobermann pinscher, rottweiler | Adults Mean age is 7 for BMD | Moderate | Skin (multiple lesions), lymph nodes, sometimes ocular tissues | Moderate | Guarded |
| Histiocytic sarcoma | | Adults Mean age is 6 for BMD | Severe | Subcutaneous tissues or internal organs | Elevated, to draining lymph nodes | Guarded |
| Malignant histiocytosis | | | Severe | Rapid multicentric dissemination (lungs, liver, spleen) | Elevated | Poor |

**AFIP Diagnosis:** Prostate gland: Histiocytic sarcoma

**Conference Comment:** On additional immunohistochemical testing, the neoplastic cells were positive for CD18 and CD45 and negative for muscle actin. The diagnosis of histiocytic sarcoma was based on characteristic histopathologic and immunohistochemical findings.

Canine malignant histiocytosis/histiocytic sarcoma was first reported in Bernese mountain dogs and has since been reported in various dog breeds, cats, and other species.[4] Malignant histiocytosis implies multicentric origin of the neoplasm. In cases of widespread disease, it is unclear whether the neoplasm arose multicentrically or metastasized widely from a single primary site. Since conference participants were only aware of the neoplasm in the prostate, histiocytic sarcoma was considered the most appropriate diagnosis. Given the presence of widespread disease, disseminated histiocytic sarcoma is preferred. These tumors are composed of pleomorphic histiocyte-like cells that are often multinucleated or may contain phagocytized material. Two major patterns have been described: round cell predominant and spindle cell predominant.[4] In the round cell variant, neoplastic cells often have abundant eosinophilic cytoplasm and round to reniform nuclei.[4,5] The spindle cell variant is often composed of plump spindle cells and these tumors often resemble other sarcomas.[4] Organs most commonly affected include the liver, lung, kidney, spleen, lymph node, and bones. Almost any organ may be affected by this neoplasm.[5] Canine histiocytic sarcomas are of dendritic antigen presenting cell origin and express CD18, CD1, CD11c, ICAM-1 and MHC II; CD45 expression is variable. For immunohistochemistry on formalin-fixed, paraffin-embedded tissues, CD18 positivity and negative findings for CD3 and CD79a combined with characteristic histomorphology is considered diagnostic.

A variety of other histiocytic proliferative diseases have been described in dogs. Histiocytomas generally occur in dogs four years of age or younger, are extremely common and have a predilection for the head and ears. These tumors are of Langerhans cell origin and express CD1, CD11c, MHC II, and E-cadhedrin.[7] At the subgross level, these tumors often appear dome shaped with aggregates of lymphocytes and plasma cells at the periphery. There is often superficial dermal edema, and tumor cells infiltrate the epidermis in a fashion similar to Pautrier's microabscesses of epitheliotropic lymphoma. Neoplastic cells form sheets and generally lack a discernable stroma. Neoplastic cells have oval to reniform nuclei with a moderate to abundant amount of eosinophilic cytoplasm and mitotic figures are frequent. There is little cellular atypia.[5] Multiple, persistent and recurring histiocytomas have also been described. Such tumors may progress to a malignancy characterized by dissemination to various organs. This condition has been designated Langerhans cell histiocytosis. Cutaneous histiocytosis is a non-neoplastic, reactive condition characterized by nodules of histiocytic cells that express CD45, CD18, CD1, CD11c, MHC II and E-cadherin. Mature lymphocytes and neutrophils are often scattered amongst the histiocytic cells. The mitotic rate is variable. Systemic histiocytosis is generally similar to cutaneous histiocytosis but has a more extensive distribution. The immunohistochemical profile is the same. Sites most commonly affected include lymph nodes, eyelids, sclera, nasal cavities, lungs, spleen and bone marrow.

**Contributing Institution:** Ecole Nationale Veterinaire D'Alfort, Unité d'Histologie etd'Anatomie Pathologique 7, avenue du Général de Gaulle, 94704 Maisons-Alfort Cedex, France

**References:**

1. Affolter VK, Moore PF: *In:* Proceedings for ESVD Workshop on immunodermatology 2000: from the laboratory to the clinic, advances in the diagnosis and pathogenesis of animal skin diseases, Saint-Paul de Vence, 2000
2. Affolter VK, Moore PF: Localized and disseminated histiocytic sarcoma of dendritic cell origin in the dog. Vet. Pathol **39**,74-83, 2002
3. Azakami D, Bonkobara M, Washizu T, et al: Establishment and biological characterization of canine histiocytic sarcoma cell lines. J Vet Med Sci **68**(12):1343-1346, 2006
4. Gross TL, Ihrke P, Walder EJ, Affolter VK: Histiocytic tumors. *In:* Skin diseases of the dog and cat, 2nd edition, pp. 848-851, 2005
5. Hendrick MJ, Mahaffey EA, Moore FM, Vos JH, Walder EJ: Histological classification of mesenchymal tumors of skin and soft tissues of domestic animals. In: World Health Organization Histological Classification of Tumors of Domestic Animals, ed. Schulman FY, Second Series, vol. 2, pp. 29-31, 58-59. Armed Forces Institute of Pathology,Washington, DC, 1999
6. Moore PF., Rosin A.: Malignant histiocytosis of Bernese Mountain dogs. Vet Pathol **23**:1-10, 1986
7. Moore PF: Canine histiocytosis. At: http://www.histiocytosis.ucdavis.edu/

**NOTES:**

**The Armed Forces Institute of Pathology**
**Department of Veterinary Pathology**

*Conference Coordinator:*
**Todd M. Bell, DVM**

## WEDNESDAY SLIDE CONFERENCE 2008-2009

# Conference 25

**13 May 2009**

*Conference Moderator:*

Jo Lynne Raymond, DVM, Diplomate ACVP

### CASE I – 07-59363 (AFIP 3121220)

**Signalment:** 4-year-old, male castrated, Italian greyhound breed canine (*Canis familiaris*)

**History:** This dog presented to the critical care service with a primary complaint from the referring veterinarian of possible toxicity and/or multi-organ failure. The owner reported that the night before presentation, the dog had vomited 18 times, and that since then the dog was listless and weak, and had not urinated since the onset of clinical signs. The dog was housed with three other dogs, including one who exhibited vomiting and diarrhea three days prior to this dog's illness but had recovered uneventfully.

**Gross Pathology:** Autolysis was moderate. The right and left kidneys were diffusely purple-black, and the urinary bladder contained approximately 1 ml of dark red urine. Petechial hemorrhages were present on visceral pleural surfaces of all lung lobes, and there was mild pulmonary edema. The peritoneal cavity contained approximately 150 ml of serosanguineous fluid. The entire gastrointestinal tract from stomach to rectum contained scant, tenacious, brown-black material resembling digested blood. The spleen was contracted, with an absence of blood in the red pulp.

**Laboratory Results:** At presentation to the teaching hospital the dog's hematocrit was 5% (37-55), white blood cell count was 51.7 x$10^3$/ul (6-17) (95% neutrophils, no bands), hemolysis index 2567 (3-56), creatinine was 6.9 mg/dl (0.6-1.4), and blood urea nitrogen was 185 mg/dl (12-26). The dog was anuric, and no urine was available for diagnostic testing. A Coomb's test was not performed on this patient.

**Histopathologic Description:** Diffusely, most cortical distal tubules, collecting ducts, and medullary tubules contain extensive intraluminal casts **(Fig. 1-1)**. Fewer casts are present in cortical proximal tubules. The majority of casts consist of amorphous to elongate crystalline, brightly eosinophilic material (hemoglobin casts) with fewer casts composed of eosinophilic, amorphous, globular or granular material variably admixed with sloughed epithelial cells (hyaline, cellular or granular casts). Less severely affected tubules within the cortex contain globular proteinaceous debris. When viewed with polarized light, casts contain small numbers of refractile, white, acicular, 5um x 20-30um crystals. The epithelium lining these tubules is in various stages of degeneration, necrosis, and early regeneration, characterized by cells that are markedly attenuated, hypereosinophilic with pyknotic or karyorrhectic nuclei,

*Sponsored by the American Veterinary Medical Association, the American College of Veterinary Pathologists, and the C. L. Davis Foundation.

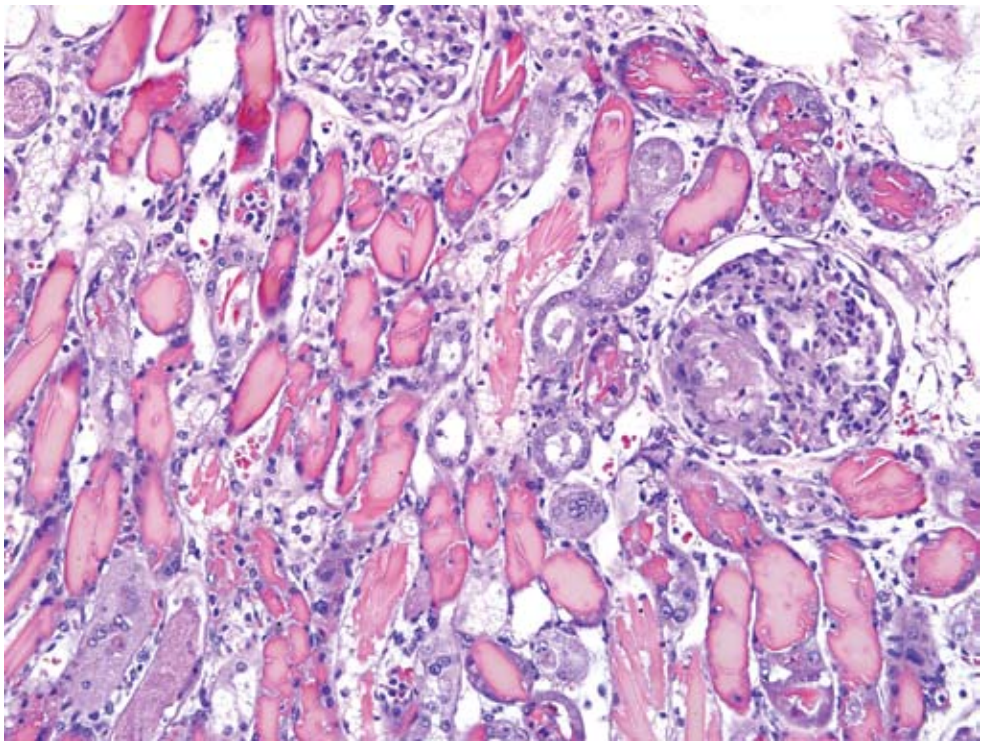

*1-1. Kidney, dog. Multifocally occluding tubules are numerous red-orange hyaline casts and fewer eosinophilic granular casts. Tubular epithelium is multifocally degenerative, necrotic, or regenerative. Capillary loops within glomeruli are occasionally occluded by fibrin thrombi and there is mild membranoproliferative glomerulonephritis. The cortical interstitium is multifocally expanded by edema. (HE 200X)*

or sloughed into the tubular lumen (degeneration and necrosis). Some cells display anisocytosis, anisokaryosis, aggregation, hyperchromatic nuclei and occasional mitoses (regeneration). Scattered tubular epithelial cells contain brown granular cytoplasmic pigment. The tubular basement membrane is multifocally disrupted, and the adjacent interstitium is mildly edematous and has a mild interstitial infiltrate of neutrophils. Glomeruli diffusely have moderate amounts of proteinaceous material within Bowman's space. Within the vasa recta, there is variable congestion and neutrophilic leukostasis.

**Contributor's Morphologic Diagnosis:** Tubular epithelial degeneration and necrosis, acute, diffuse, severe, with regeneration, and marked intratubular hemoglobin, hyaline, and granular cast formation, consistent with hemoglobinuric nephrosis, kidney, Italian greyhound breed canine

**Contributor's Comment:** Clinical pathology data for this patient suggests an acute intravascular hemolysis, likely secondary to autoimmune mechanisms. The proximal tubular necrosis, in conjunction with the dramatic, widespread accumulation of obstructive hemoglobin casts, is consistent with peracute primary hemoglobin toxicity. Primary hemoglobin nephrotoxicity has a controversial role in veterinary medicine, although it is widely recognized in human medicine as a common and serious postoperative complication following cardiopulmonary bypass [1] and, less commonly, in certain envenomations. Two diverging theories hold that hemoglobin is 1) not a direct nephrotoxin, but rather induces renal damage by a combination of hemoglobin-induced hypotension, increased vascular resistance, and disseminated intravascular coagulation resulting in renal ischemia; or 2) that hemoglobin is not directly toxic, but is converted to toxic byproducts within the urinary space, thereby inducing tubular necrosis.[3] In experimental studies utilizing intravenously administered purified hemoglobin in rats, Zager et. al. [3] concluded that hemoglobin can act as a primary nephrotoxin only in the presence of aciduria, and that the likely mechanism for this is aciduria-dependent conversion of hemoglobin to methemoglobin, the latter of which precipitates within distal tubule segments and forms casts. Unlike hemoglobin, once methemoglobin forms its precipitation can occur under either aciduric or alkalinuric conditions, and is more toxic than hemoglobin under either condition. Furthermore, distal tubular obstruction can lead to enhanced "upstream" uptake of hemoglobin and its metabolites by proximal tubules.[3] Tubular damage in this case likely resulted from both local and systemic contributing factors, including massive, widespread tubular obstruction and attendant tubular epithelial necrosis, hypoxia secondary to the markedly decreased hematocrit, and hemoglobin-induced vasoconstriction via activation of the renin-angiotensin and sympathetic nervous system.[2]

The patient had mildly to moderately elevated D-dimers and partial thromboplastin time, but normal prothrombin time and no clinical evidence of bleeding. Calculation of the lipemia, free hemoglobin, and bilirubin is performed on a clinical chemistry analyzer by passing light of different wavelengths through the serum or plasma and calculating the amount of each interfering substance based on the light absorption of the sample. The amount of free hemoglobin is reported as the hemolysis index in units of mg/dL. Elevations as high as those present in this case can falsely decrease bicarbonate, GGT, amylase, and alkaline phosphatase, and can falsely increase AST, CK, iron, phosphate, triglycerides, magnesium, and total protein.

**AFIP Diagnosis:** Kidney: Tubular degeneration, necrosis, and regeneration, diffuse, marked with hemoglobin and granular casts and rare glomerular fibrin thrombi

**Conference Comment:** Acute renal failure is often caused by acute tubular necrosis. Acute tubular necrosis is usually caused by either nephrotoxic agents from the bloodstream, ischemia, or complete urinary outflow obstruction. The anatomic locations most susceptible to acute tubular necrosis are the proximal convoluted tubule and the thick ascending limb of the loop of Henle. This is in direct correlation to their high metabolic activity thus making them more susceptible to damage and necrosis.[2]

Ischemic tubular necrosis usually follows profound shock, and the extreme decrease in blood flow to the kidney results in renal cortical necrosis. The histologic hallmark of ischemic acute tubular necrosis is necrosis of the proximal, and to a lesser extent, distal tubules with disruption of tubular basement membranes and plugging of tubular lumina by casts. If the basement membrane is extensively damaged, then regeneration is impossible and the prognosis becomes grave.[2]

Nephrotoxic acute tubular necrosis causes necrosis of the proximal convoluted tubule because of the PCT's exposure to more toxin than the rest of the nephron as well as its high metabolic activity. The basement membrane is normally preserved in cases of nephrotoxic acute tubular necrosis providing scaffolding for cells to regenerate thus making the prognosis much more favorable than ischemic acute tubular necrosis.[2]

During the conference, several causes of tubular necrosis were discussed. Aminoglycosides, tetracyclines, sulfonamides, and the antifungal agent amphotericin B can cause tubular necrosis in domestic animals.[2] Ethylene glycol is also a common cause of tubular necrosis in dogs and cats. Oxalate containing plants including *Halgeton glomeratus* (halogeton), *Sarcobatus vermiculatas* (greasewood), *Rheum rhaponticum* (rhubarb) are a few of the oxalate containing plants that cause poisoning in sheep and cattle.[2] Other plants that cause tubular necrosis include Easter lily in cats, *Quercus* spp. (oak) in ruminants, and *Amaranthus retroflexus* (pigweed) in pigs and cattle.[2] *Apergillus niger* and *flavus* can also produce enough oxalates to cause renal damage when ingested with feedstuffs.[2] Grapes and raisins cause tubular necrosis in dogs.[2]

**Contributing Institution:** Auburn University College of Veterinary Medicine (Dr. Koehler: jaw0007@auburn.edu)

**References:**

1. Haase M, Haase-Fielitz A, Bagshaw SM, Ronco C, Bellomo R: Cardiopulmonary bypass-associated acute kidney injury: a pigment nephropathy? Contrib Nephrol **156**:340-353, 2007
2. Schlafer DH, Miller, RB: Inflammatory Diseases of the Uterus. *In:* Jubb, Kennedy, and Palmer's Pathology of Domestic Animals, ed. Maxie, MG, 5th ed., vol. 2, pp 466-469. Elsevier, Philadelphia, USA, 2007
3. Zager RA, Gamelin LM: Pathogenetic mechanisms in experimental hemoglobinuric acute renal failure. Am J Physiol **256**:F446-F455, 1989

## CASE II – Rabbit 2008 (AFIP 3106178)

**Signalment:** Female rabbit (*Orytolagus cuniculus*), adult (unknown age)

**History:** The rabbit was found outdoors with a mammary mass (sub-Q mass about 5-6 cm diameter) in the caudal ventral abdomen that turned out to be a malignant hair follicle tumor. The uterus was removed at a later date because an abdominal mass was palpated and to spay the rabbit.

**Gross Pathology:** Firm pale masses, thickened friable mucosa, and multiple mucosal cysts.

**Laboratory Results:** NA

**Histopathologic Description:** Histologically, there are two distinctly different masses present within the same section adjacent to the mesometrial insertion;

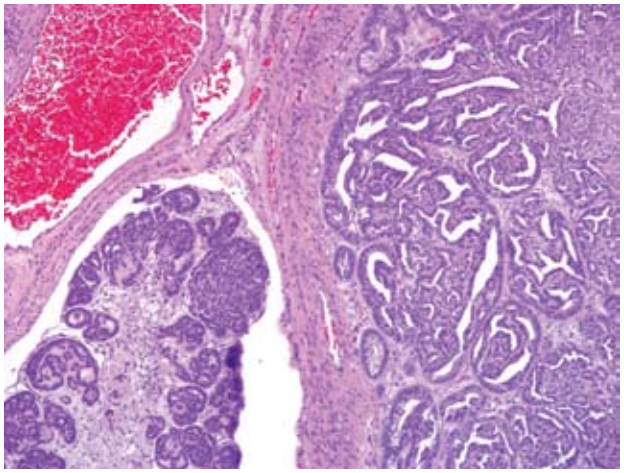

*2-1. Uterus, rabbit. Adenocarcinoma. Expanding the endometrium and infiltrating the myometrium is a neoplasm composed of polygonal cells arranged in tubules and papillary projections. Multifocally, there is lymphatic invasion by the neoplastic cells. (HE 200X)*

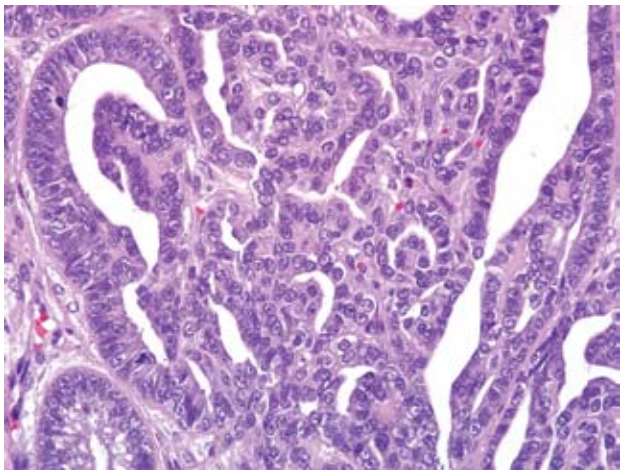

*2-2. Uterus, rabbit. Adenocarcinoma. Neoplastic cells are arranged on a fine fibrovascular stroma. Mitoses average 1 per 400X field. (HE 400X)*

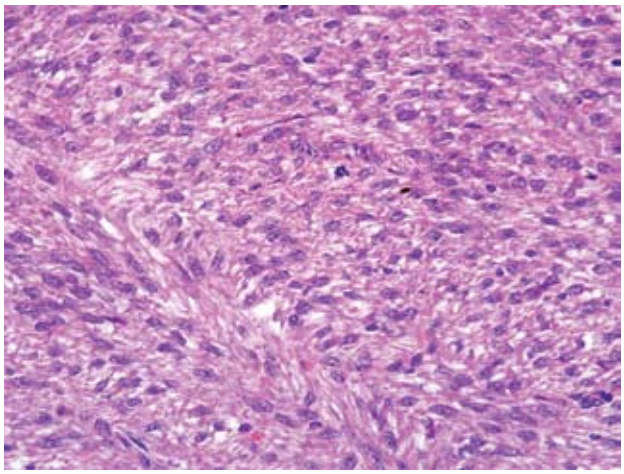

*2-3. Uterus, rabbit. Leiomyosarcoma. Expanding the myometrium is a neoplasm composed of spindled cells arranged in short interlacing streams and bundles on a fine fibrovascular stroma. Mitoses average 2 per 400X field, and there are rare multinucleate neoplastic cells. (HE 400X)*

the first located in the endometrium, the second located within the myometrium. The masses are located adjacent to one another and in some areas are in direct contact. The endometrial mass is multilobulated and well demarcated but unencapsulated. It is composed of thick papillary projections expanding into the uterine lumen, as well as lobules of densely packed tubular and glandular structures infiltrating into the subjacent myometrium **(Fig. 2-1)**. Within the papillary projections and lobules, cuboidal to columnar neoplastic epithelial cells form a single, albeit crowded, layer supported by variable amounts of loose vascular collagenous stroma **(Fig. 2-2)**. Lobules are separated by moderate amounts of loose collagenous or myxomatous stroma, while within lobules, cells are supported by scant stroma. The neoplastic population has moderate anisocytosis and anisokaryosis. There are 1-3 mitotic figures per 400X field. Minimal amounts of sloughed cells, inflammation and necrosis are present within the mass. In some sections there are lobules of neoplastic cells within uterine lymphatic vessels covered by a layer of endothelium. Microscopic features of this mass are consistent with an adenocarcinoma.[2]

Microscopically, the second mass, located in the myometrium, is multilobulated, unencapsulated, poorly demarcated in some areas and infiltrative. It is composed of densely cellular, broad interlacing fascicles of medium sized spindloid cells **(Fig. 2-3)**. These neoplastic cells have indistinct cytoplasmic borders, moderate amounts of vacuolated or fibrillar eosinophilic cytoplasm, a blunt-ended oval nucleus with finely granulated chromatin and a single eosinophilic nucleolus. In general, there is slight anisocytosis and anisokaryosis, however, rare karyomegalic and multinucleated cells are present. Mitotic figures are uncommon (1 per ten 400X fields). There are several large areas of necrosis with hemorrhage present within the mass (not present in all sections, Images 1 and 2). Although the mitotic rate is low and the neoplastic cells are well-differentiated, the presence of areas of necrosis is consistent with a diagnosis of leiomyosarcoma rather than leiomyoma.[2]

### Contributor's Morphologic Diagnosis:

Uterus: Adenocarcinoma

Uterus: Leiomyosarcoma

**Contributor's Comment:** In contrast to other domestic species where uterine adenocarcinomas are a rare occurrence, the incidence of uterine adenocarcinomas has been reported to be up to 79% in female rabbits over the age of five years, with variation in breed predisposition. In fact, this tumor type is the most common tumor of Orytolagus cuniculus overall.[6] Uterine adenocarcinomas in rabbits are often multicentric and affect both uterine horns.[1] Most are slow growing and present with bloody discharge and/or decreased fertility in breeding animals.[5,6] The pathogenesis of these tumors is unclear and appears to be different from those occurring in humans, although there is controversy over this subject in the literature. Uterine leiomyosarcomas are much less common than adenocarcinomas with reported incidences of 1% in aging Dutch rabbits, and 2% in rabbits presenting to veterinarians with uterine disorders.[1,5] The submitted case represents a simultaneous occurrence of two spontaneous uterine tumors in a female rabbit. Recently a similar case of concurrent adenocarcinoma and leiomyoma in an individual animal was reported by Kurotaki et al.[4] The case report describes two endometrial adenocarcinomas, one of which was closely associated with a myometrial leiomyoma. These cases are similar in the presence of both primary epithelial and mesenchymal tumors within the uterus, with a close physical association between the two. They are different in that the smooth muscle tumor is malignant in the submitted case.

**AFIP Diagnosis:**
Uterus: Adenocarcinoma
Uterus: Leiomyosarcoma

**Conference Comment:** The cow is the only other domesticated animal that commonly gets uterine adenocarcinomas. This tumor is often seen in abbatoirs and grossly appears as single or multiple firm masses in the wall of the uterus.[3] These tumors are often umbilicated and are known to metastasize to the internal iliac lymph nodes and lungs.[3] Histologically, this tumor often causes an intense fibrous response with numerous mitoses, cellular pleomorphism, and vascular and lymphatic invasion.[3]

Other differentials for a neoplastic growth in the uterus of domesticated animals include adenoma, fibroma, leiomyoma, and leiomyosarcoma as mentioned by the contributor. Adenomas are generally rare in domesticated species and can be difficult to distinguish from focal endometrial hyperplasia.[3] Fibromas are generally firm, white, expansile masses that histologically appear as very bland, sparsely cellular, densely collagenous growths.[3] Fibromas are seen most commonly in dogs and cattle, but they are not prevalent tumors.[3] Leiomyomas are composed of interwoven bundles of smooth muscle originating in the myometrium. The amount of connective tissue can be highly variable.[3] These tumors are seen in dogs, cats, and cattle.[3]

**Contributing Institution:** Eli Lilly and Company, Greenfield IN

**References:**
1. Baba N, von Haam E: Animal Model: Spontaneous adenocarcinoma in aged rabbits. Am J Path **68**:653-656, 1972
2. Cooper BJ, Valentine BA: Tumors of Muscle. *In:* Tumors of Domestic Animals, ed Meuten DJ, 4th ed., 319-363, 2002
3. Kennedy PC, Cullen JM, Edwards JF, Goldschmidt MH, Larsen S, Munson L, Nielsen S: Histological classification of tumors of the genital system of domestic animals. *In:* World Health Organization Histological Classification of Tumors of Domestic Animals, ed. Schulman FY, Second Series, vol. 4, pp. 32-33, 72. Armed Forces Institute of Pathology,Washington, DC, 1999
4. Kurotaki T, Kokoshima H, Kitamori F, Kitamori T, Tsuchitani M: A case of adenocarcinoma of the endometrium extending into the leiomyoma of the uterus in a rabbit. J Vet Med Sci **69**:981-984, 2007
5. Saito K, Nakanishi M, Hasegawa A: Uterine disorders diagnosed by ventrotomy in 47 rabbits. J Vet Med Sci **64**(6)495-497, 2002
6. Weisbroth SH: Neoplastic Diseases. *In:* The Biology of the Laboratory Rabbit, eds. Manning PJ, Ringler DH, Newcomer CE, 2nd ed., 259–292, Academic Press, New York, NY, 1994

## CASE III – 07-59363 (AFIP 3121220)

**Signalment:** 6-month-old, male, domestic ferret (*Mustela putorius furo*)

**History:** This 6-month-old, male domestic ferret presented to the referring veterinarian with a 1-2 week history of diarrhea and lethargy. On physical exam, the animal was assessed as being moderately dehydrated. The abdomen was moderately distended. Abdominal ultrasound showed marked enlargement of the spleen, multifocal areas of hyperechogenicity in the liver, and markedly enlarged mesenteric lymph nodes. Over the next week, diarrhea

continued and the ferret became anorexic, lost weight, and developed a mild cough despite symptomatic treatment. Euthanasia was elected and the animal was submitted to the Diagnostic Center for Population and Animal Health, Lansing, MI for necropsy.

**Gross Pathology:** On gross necropsy, the animal was in fair to poor body condition with no visible fat stores and increased prominence of bony protuberances. Dehydration was marked as evinced by retraction of the eyes into the orbits and tackiness of visceral surfaces. The abdomen was prominently distended due to marked enlargement of the spleen and mesenteric lymph nodes. The spleen was approximately 10 times normal size, dark black and diffusely meaty. There were 7-8 relatively indistinct, poorly circumscribed, pale white, semi-firm, nodular foci dispersed throughout the splenic parenchyma. These foci ranged from 0.5-1.5 cm in maximum diameter, and the capsular surface of the spleen overlying few of these areas was slightly raised. The liver was diffusely mottled dark red and tan, and was mildly enlarged with slightly rounded borders. There were 10-12 slightly raised, occasionally coalescing, pale white, firm, slightly nodular plaques ranging from 0.5-1 cm in diameter randomly distributed on the capsular surface of the liver. The mesenteric lymph nodes were markedly enlarged being approximately 5-8 times normal size. The capsular surfaces of lymph nodes were irregular due to dozens of 2-5 mm in diameter, slightly raised white nodules. On cut surface, the normal nodal architecture was obliterated by pale tan to white, firm tissue **(Fig. 3-1)**. The mesentery was irregularly thickened by dozens of coalescing pale white, firm nodules and irregular plaques. Similar white nodules and plaques were segmentally distributed across the serosal surfaces of the jejunum, ileum and to a lesser degree colon. In few areas, sections of intestinal loops were adhered to each other and to adjacent mesenteric lymph nodes by both fibrinous and fibrous adhesions. The visceral pleural surfaces of the lung were focally raised 1-3 mm by similar irregularly shaped, pale white, poorly demarcated, firm plaques that ranged from .2-1.5 cm in diameter. No other significant lesions were noted grossly.

**Laboratory Results:** PCR for Aleutian mink disease virus was negative.

**Histopathologic Description:** The submitted slides represent small intestine and/or lymph node.

In the wall of the small intestine, there are multifocal to coalescing areas of granulomatous to pyogranulomatous inflammation. These areas are most prominent on the serosal surfaces of the intestine, but also extend into the underlying tunic muscularis and more rarely into the submucosa and mucosa. Granulomas and pyogranulomas are characterized by variable central necrosis and infiltrates of degenerate neutrophils surrounded by thick dense bands of plump epithelioid macrophages and rare multinucleated foreign body type giant cells. Varying rings of lymphocytes, plasma cells, and dense maturing fibrosis surround granulomas. Granulomatous inflammation is generally randomly distributed, but

*3-1. Mesenteric lymph node, ferret. Lymph nodes are markedly enlarged and nodal architecture on cut surface is obliterated by pale tan to white firm tissue.* *Photograph courtesy of Diagnostic Center for Population & Animal Health, 4125 Beaumont Road, Lansing, MI 48910, fitzgerald@dcpah.msu.edu.*

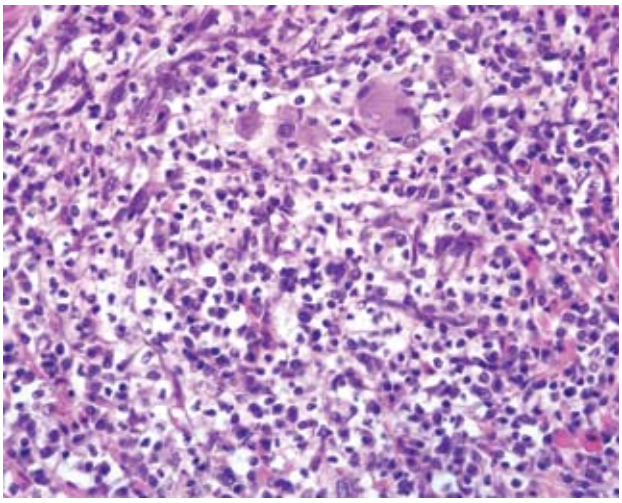

*3-2. Mesenteric lymph node, ferret. Nodal architecture is effaced by pyogranulomatous inflammation with few multinucleate giant cells and scattered fibroblasts. (HE 400X)*

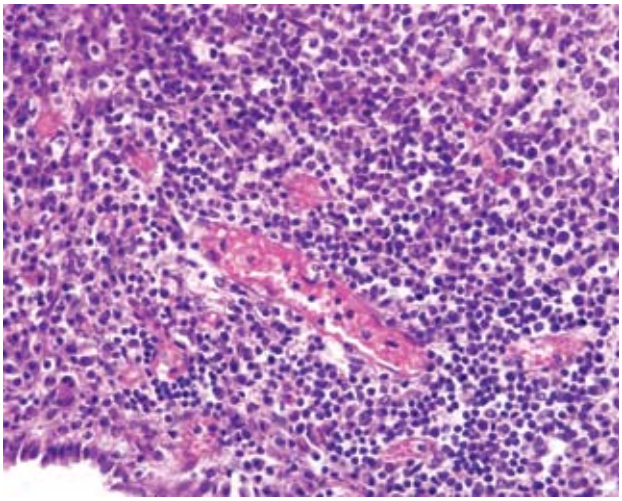

*3-3. Small intestine, ferret. Multifocally surrounding vasculature near areas of pyogranulomatous inflammation are large numbers of lymphocytes and plasma cells and fewer histiocytes. (HE 400X)*

occasionally is associated with vasculature. In sections of lymph node, nodal architecture is expanded and ablated by multifocal and coalescing granulomas and pyogranulomas similar to those described in the small intestine **(Fig. 3-2)**. Granulomatous inflammation extensively extends through the capsule into the surrounding perinodal adipose tissue. Similar foci of granulomatous to occasionally pyogranulomatous inflammation expand the serosal surfaces of the liver and lung, and focally obliterate the normal parenchyma of the lung and spleen. In rare areas, the meninges overlying the cerebral cortex are expanded by granulomatous inflammation. Vasculature within tissue surrounding foci of granulomatous inflammation in the liver, lung, and cerebral cortex is segmentally surrounded by moderate cuffs of lymphocytes, plasma cells, and fewer histiocytes **(Fig. 3-3)**. Immunohistochemistry using a generic antibody against Group 1 coronaviruses on sections of small intestine, lymph node, lung, and spleen demonstrated strong positive, intracytoplasmic immunoreactivity within macrophages at the center of granulomas. A generic coronavirus RT-PCR yielded amplification of a 650 base pair fragment. Sequencing of this segment suggests that the amplified virus is distinct from feline coronavirus (FeCoV). The amplified virus appears to be most closely related to ferret enteric coronavirus (FECV) that reportedly causes epizootic catarrhal enteritis (ECE) in ferrets.

**Contributor's Morphologic Diagnosis:** Small intestine: Severe chronic segmental granulomatous to pyogranulomatous enteritis and peritonitis
Lymph node: Severe chronic multifocal and coalescing granulomatous to pyogranulomatous lymphadenitis

**Contributor's Comment:** This case presentation represents a disease that has been termed granulomatous inflammatory syndrome (GIS) or ferret systemic coronavirus infection (FSCV).[1,4] This is an emerging disease in ferrets that was first reported in the veterinary literature in 2006 and closely resembles the clinical, gross and microscopic features of feline infectious peritonitis.[1,2,4]

The exact etiopathogenesis of this lesion is unclear at this point, but appears to be related to infection with a group 1 coronavirus. Immunohistochemistry using monoclonal antibodies against feline coronavirus (FCoV) has been reported to demonstrate immunoreactivity in macrophages within lesions.[1,2] This antibody is not specific for FCoV as it has been shown to detect other group 1 coronaviruses including ferret enteric coronavirus (FECV) that has been implicated as the cause of epizootic catarrhal enteritis (ECE).[5,6] Electron microscopy confirmed the presence of coronavirus-like particles within macrophages.[1] RT-PCR using primers that detect a broad array of group 1 coronaviruses yielded amplification of a 599bp sequence that showed significant similarity to FECV (77% homology) and to other group 1 coronaviruses.[1] Whether this virus represents a novel virus or variation within an already described coronavirus is unclear. The exact mechanism by which this virus causes the described lesions is unknown. Further characterization of the virus is required.

**AFIP Diagnosis:** Small intestine: Enteritis and peritonitis, pyogranulomatous, multifocal to coalescing, moderate
Lymph node: Lymphadenitis, pyogranulomatous, multifocal to coalescing, moderate

**Conference Comment:** Coronaviruses are single-stranded RNA viruses of major importance in domestic animals.[3] Coronaviruses are currently split into 3 serogroups. Group 1 includes transmissible gastroenteritis of swine (TGEV), canine coronavirus (CCV), feline coronavirus (FCoV), and human coronavirus 229E. Mouse hepatitis virus, sialodacryoadenitis of rats, turkey coronavirus ("bluecomb"), and bovine coronavirus are the major viruses recognized in group 2.[1,3] Group 3 comprises the avian viruses and includes infectious bronchitis virus.[1,3] As the contributor mentioned, ferret systemic coronavirus infection (FSCV) has an almost identical gross and histologic appearance as FIP in domestic cats. Juvenile and young adult ferrets seem to be the most susceptible to this disease.[1] Gross lesions consist of widespread nodular foci on multiple serosal surfaces that closely resemble similar foci seen in clinical cases of FIP.[1] Involvement of mesenteric lymph nodes is also reminiscent of FIP in cats. FSCV closely resembles the dry form of FIP.[1] Histologic lesions are identical to what is seen in cats with FIP and consist of pyogranulomatous inflammation with vasculitis and perivasculitis.[1] Relevant clinical pathologic findings in these ferrets included a mild non-regenerative anemia (anemia of chronic disease), thrombocytopenia and hyperproteinemia.[1] The thrombocytopenia was attributed to DIC secondary to vasculitis, while the hyperproteinemia occurred due to hyperglobulinemia.[1]

**Contributing Institution:** Michigan State University, Diagnostic Center for Population and Animal Health, 4125 Beaumont Rd, Lansing, MI 48910 www.animalhealth.msu.edu

**References:**

1. Garner MM, Ramsell K, Morera N, Juan-Sallés C, Jiménez J, Ardiaca M, Montesinos A, Teifke JP, Löhr CV, Evermann JF, Baszler TV, Nordhausen RW, Wise AG, Maes RK, Kiupel M. Clinicopathologic features of a systemic coronavirus-associated disease resembling feline infectious peritonitis in the domestic ferret (*Mustela putorius*). Vet Pathol **45**(2):236-46, 2008
2. Martínez J, Ramis AJ, Reinacher M, Perpiñán D. Detection of feline infectious peritonitis virus-like antigen in ferrets. Vet Rec **158**:523, 2006
3. Murphy FA, Gibbs EPJ, Horzinek MC, Studdert MJ: Coronaviridae. *In:* Veterinary Virology, 3rd ed., pp. 495-508. Academic Press, San Diego, California, 1999
4. Perpiñán D, López C. Clinical aspects of systemic granulomatous inflammatory syndrome in ferrets (*Mustela putorius furo*). Vet Rec **162**(6):180-185, 2008
5. Williams B, Kiupel M, West K, Raymond JT, Grant CK, Glickmann LT, Coronavirus associated enzootic catarrhal enteritis (ECE) in ferrets (*Mustela putorius furo*): a review of 120 cases (1993-1998) JAVMA 217: 526-530, 2000
6. Wise AG, Kiupel M, Maes RK. A novel coronavirus associated with epizootic catarrhal enteritis (ECE) in ferrets. Virol **349**:164-174, 2006

## CASE IV – S08-0692 (AFIP 3103039)

**Signalment:** 10-year-old, female, (*Lama pacos*) Alpaca

**History:** The animal was presented to the clinicians of the Institute of Farm Animals of the University of Zurich because of cachexia and weakness although it seemed to be eating normally. Clinical findings were intensified breathing, weakness and loss of gastrointestinal motility. The sonografic picture of the liver showed multifocal, echogenic, round to sickle-shaped unencapsulated structures of about 1 to 3 cm in diameter.

**Gross Pathology:** Firm, whitish nodules in size from 1 to 7 centimeters in diameter were found in the liver, lung, mediastinum, pleura, and omentum **(Figs. 4-1, 4-2)**. In the cut surface some of the nodules showed fine whitish to grey beige spikes which were arranged in radial patterns **(Fig. 4-3)**, other nodules showed centrally located homogenous grey beige caseous material with multifocal white gritty spots **(Fig. 4-4)**.

**Laboratory Results:** Acid-fast stain (Ziehl-Neelson stain) revealed myriads of acid-fast bacteria in epithelioid macrophages and the PCR analysis resulted in *Mycobacterium kansasii*.

**Histopathologic Description:** Liver: Up to 70% of the parenchyma is replaced by multifocal to coalescing granulomas characterized by an amorphous, eosinophilic necrosis material surrounded by a smaller layer of elongated macrophages with light eosinophilic cytoplasm, a centrally located oval nucleus and indistinct cell boarders (epithelioid cells) and rarely of large cells with eosinophilic cytoplasm and numerous nuclei located

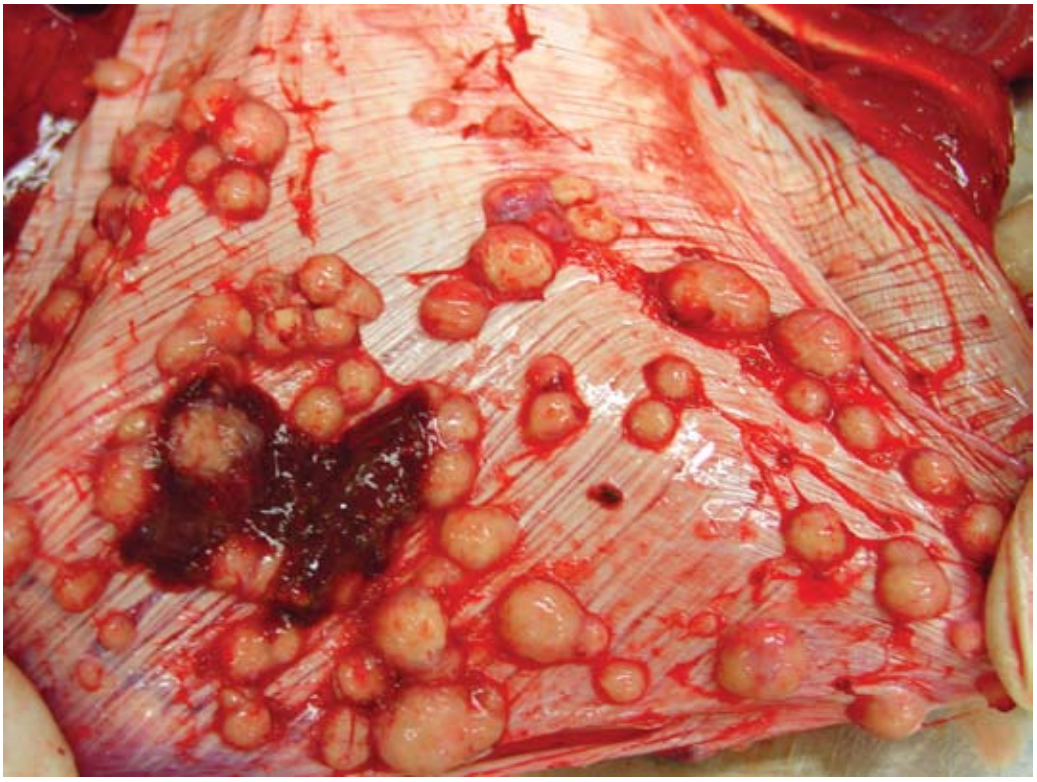

*4-1. Pleura, alpaca. Adherent to the pleura are multiple granulomas.* *Photograph courtesy of Institute of Veterinary Pathology, Winterhurerstrasse 268, 8057 Zuerich, Switzerland, grest@vetpath.uzh.ch.*

in the periphery of the cell (multinucleated giant cells, Langhans-type) which are once again surrounded by a rim of lymphocytes, plasma cells, macrophages, fibroblasts embedded in a small amount of collagen fibers and to a lesser extend neutrophils **(Fig. 4-5)**. Multifocally necrotic areas contain dark basophilic granular material (dystrophic calcification). The liver parenchyma is diffusely infiltrated with a moderate amount of lymphocytes and neutrophils.

**Contributor's Morphologic Diagnosis:** Liver, granulomatous hepatitis, multifocal and coalescing, severe, chronic, with central caseous necrosis and myriads of acid-fast intrahistiocytic rod shaped bacteria **(Fig. 4-6)** (*Mycobacteria kansasii*)

**Contributor's Comment:** *Mycobacterium kansasii* is classified in Runion's Group 1 and belongs to the nontuberculous mycobacteria (NTM); or mycobacteria other than tuberculosis (MOTT)). It is a saprophyte which is found in soil and water. *M. kansasii* is very heterogeneous as 5 well-defined different types (I-V) exist of which type I is frequently isolated from humans, type II from humans and the environment and III-V were present mostly in the environment and only rarely in humans sources.[2] *M. kansasii* infection is described in cattle to cause lesions similar to bovine tuberculosis (BTB) although it seems to be exceedingly rare.[5,6] In slaughtered cattle in Great Britain an incidence of 0.8% NTM was found and the majority of these belong to the M. avium complex.[5] In Northern Ireland *M. kansasii* could be detected in 14 tissue specimens of 16,506 cattle, which demonstrates the rareness of the disease in cattle. Nevertheless, it is not known how many animals that are exposed to *M. kansasii* do not develop disease. It was also found that *M. kansasii* could be isolated from humans without disease.[5] However, *M. kansasii* can cause pulmonary or disseminated disease in humans with an estimated 300 times higher incidence in HIV- patients.[2] Experimental infection of healthy cattle failed to cause disease or pathologic changes but it did induce immune responses in TB tests.[6] Since, some NTM and specifically *M. kansasii* do share some diagnostic antigens with *Mycobacterium bovis* complex bacteria [4, 5] there can be cross-reactions in traditional TB tests, which complicates the control and eradication of BTB.

**AFIP Diagnosis:** Liver: Granulomas, multifocal to coalescing, with mild hepatocellular degeneration

**Conference Comment:** Mycobacteria are gram-positive bacteria with high lipid content within their cell wall. This makes traditional gram staining largely ineffective, but mycobacteria do stain with carbol-fuschin and resist decoloration by inorganic acids giving them their "acid-fast" staining characteristic.[3] Mycolic acid

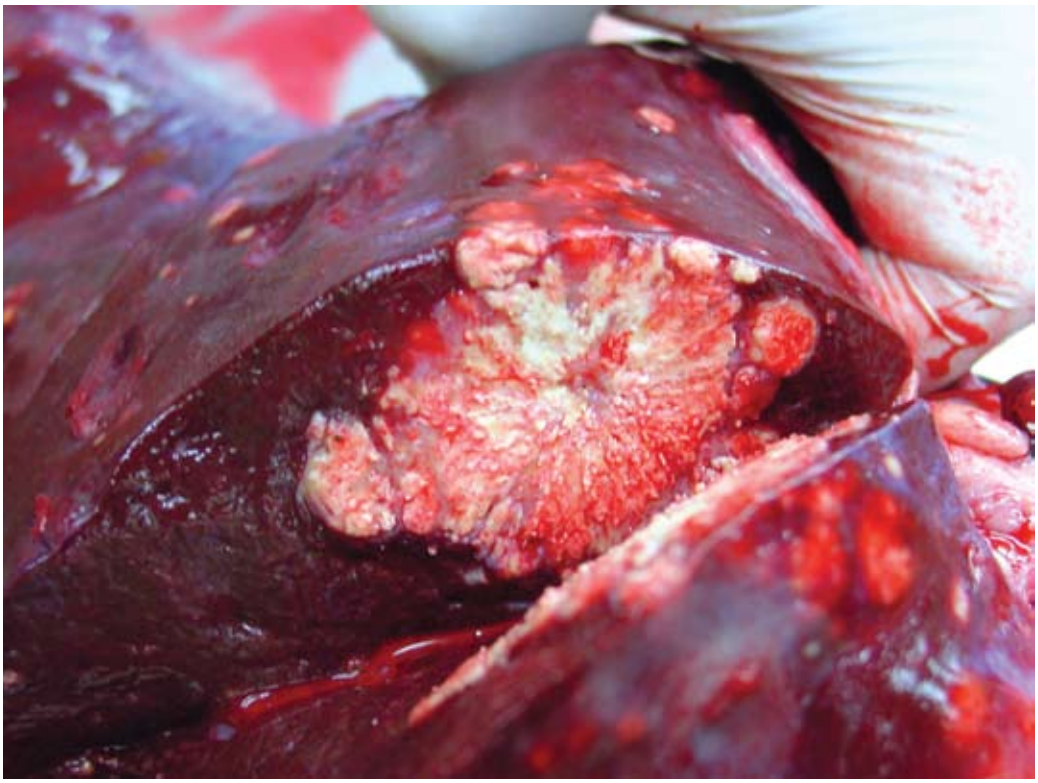

*4-2., 4-3. Liver, alpaca. Expanding the hepatic parenchyma are multifocal to coalescing granulomas. On cut surface, granulomas have radiating streaks of mineral which surround a central area of necrosis.* *Photographs courtesy of Institute of Veterinary Pathology, Winterhurerstrasse 268, 8057 Zuerich, Switzerland, grest@vetpath.uzh.ch.*

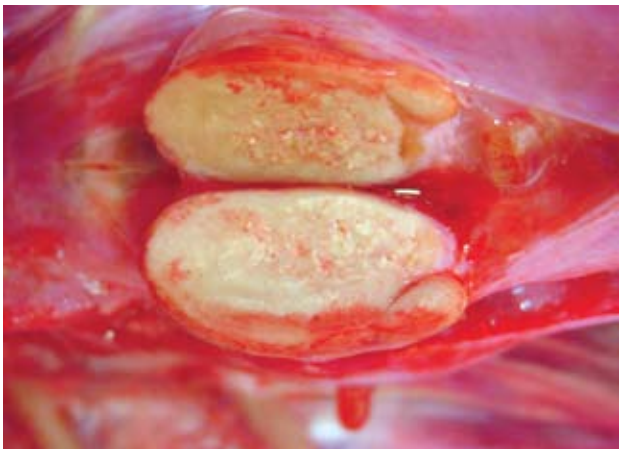

*4-4. Lymph node, alpaca. Normal nodal architecture is effaced by a large granuloma which contains granular foci of mineral.* *Photograph courtesy of Institute of Veterinary Pathology, Winterhurerstrasse 268, 8057 Zuerich, Switzerland, grest@vetpath.uzh.ch.*

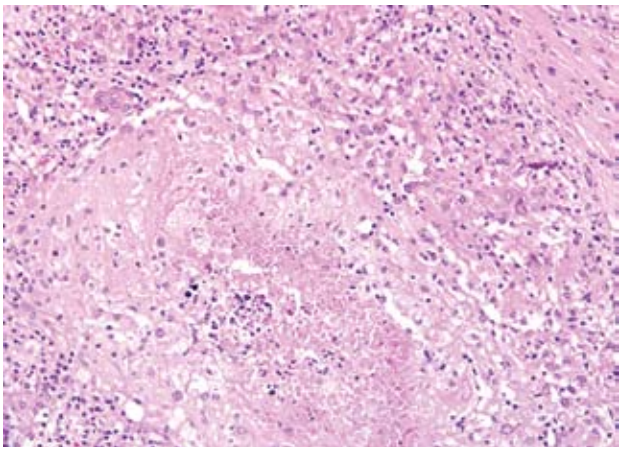

*4-5. Liver, alpaca. Granulomas are composed of a central core of necrosis and mineral which are bounded by moderate numbers of epithelioid macrophages and fewer multinucleate giant cells, further bounded by lymphocytes and plasma cells admixed with few fibroblasts. (HE 400X)*

spacing within the bacterial cell wall is key to these bacteria being acid-fast.[3] These same mycolic acids are hydrophobic accounting for the environmental hardiness and antimicrobial resistance of these troublesome bacteria.[3] During the conference, Colonel Raymond questioned the participants about the classifications of mycobacteria and then the mechanistic basis of tuberculin skin testing. These bacteria cause a type IV hypersensitivity reaction, or delayed type hypersensitivity, as demonstrated by the tuberculin test. Histologically this manifests as aggregates of mononuclear cells around small veins and venules, or perivascular inflammation and cuffing.[1] Important cytokines involved in delayed type hypersensitivity reactions include IL-12, IL-2, IFN-gamma, and TNF. IL-12 is critical in propagating a Th1 response, IL-2 causes an autocrine and paracrine proliferation of T cells, and IFN-gamma is a potent macrophage activator.[1] TNF is an important cytokine that acts on endothelial cells to cause vasodilation and facilitates the process of adhesion and extravasation of lymphocytes and monocytes.[1]

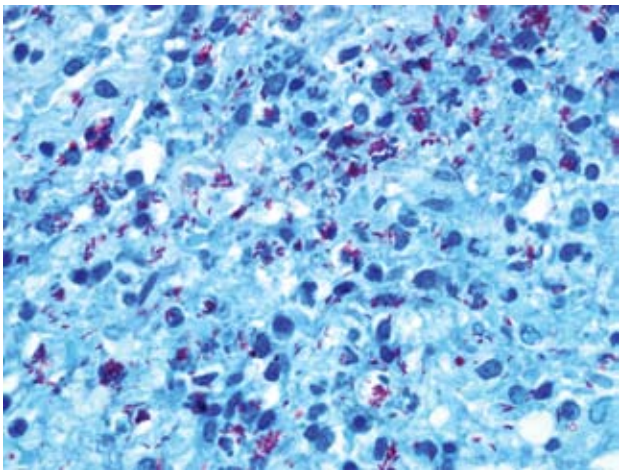

*4-6. Liver, alpaca. Within granulomas are numerous free and intrahistiocytic, 1x3 um, filamentous, acid fast bacteria. (Fite-Faraco 1000X)*

**Contributing Institution:** Institute of Veterinary Pathology, University of Zürich, Winterthurerstrasse 268, CH-8057 Zürich, Switzerland.

**References:**

1. Abbas, Abul K: Disease of Immunity. *In:* Robins and Cotran Pathologic Basis of Diseases, ed. Kumar VK, Abbas AK, Fausto N, 7th ed., pp. 216-218. Elsevier, Philadelphia, Pennsylvania, 2005

2. Alcaide F, Richter I, Bernasconi C, Springer B, Hagenau C, Schulze-Röbbecke R, Tortoli E, Martin R, Böttger EC, Telenti A: Heterogeneity and clonality among isolates of *Mycobacterium kansasii*: implications for epidemiological and pathogenicity studies. J Clin Microbiol 35(8):1959-64, 1997

3. Caswell JL, Williams KJ: Respiratory system. *In:* Jubb, Kennedy and Palmer's Pathology of Domestic Animals, ed. Maxie MG, 5th ed., pp. 632. Elsevier, Philadelphia, Pennsylvania, 2007

4. Huges MS, Ball NW, McCarroll J, Erskine M, Taylor MJ, Pollock JM, Skuce RA, Neill SD: Molecular analysis of mycobacteria other than the *M. tuberculosis* complex isolated from Northern Ireland cattle. Vet microbiol **108**:101-112, 2005

5. Vordermeier HM, Brown J, Cockle OJ, Franken WPJ,

Arend SM, Ottenhoff THM, Jahans K, Hewinson RG: Assessment of cross-reactivity between *Mycobacterium bovis* and *M. kansasii* ESAT-6 and CFP-10 at the T-cell epitope level. Clin Vaccine Immunol **14**(9):1203-9, 2007

6. Waters WR, Palmer MV, Thacker TC, Payeur JB, Harris NB, Minion FC, Greenwald R, Esfandiari J, Andersen P, McNair J, Pollock JM, Lyashchenko KP: Immune responses do defined antigens of *Mycobacterium bovis* in cattle experimentally infected with *Mycobacterium kansasii*. Clin Vaccine Immunol **13**:611-9, 2006